frontiers | Research Topics

Innate lymphoid cells: Characterization and classification

Edited by
Carolina Jancic, Carmelo Luci and Rachel Golub

Published in
Frontiers in Immunology

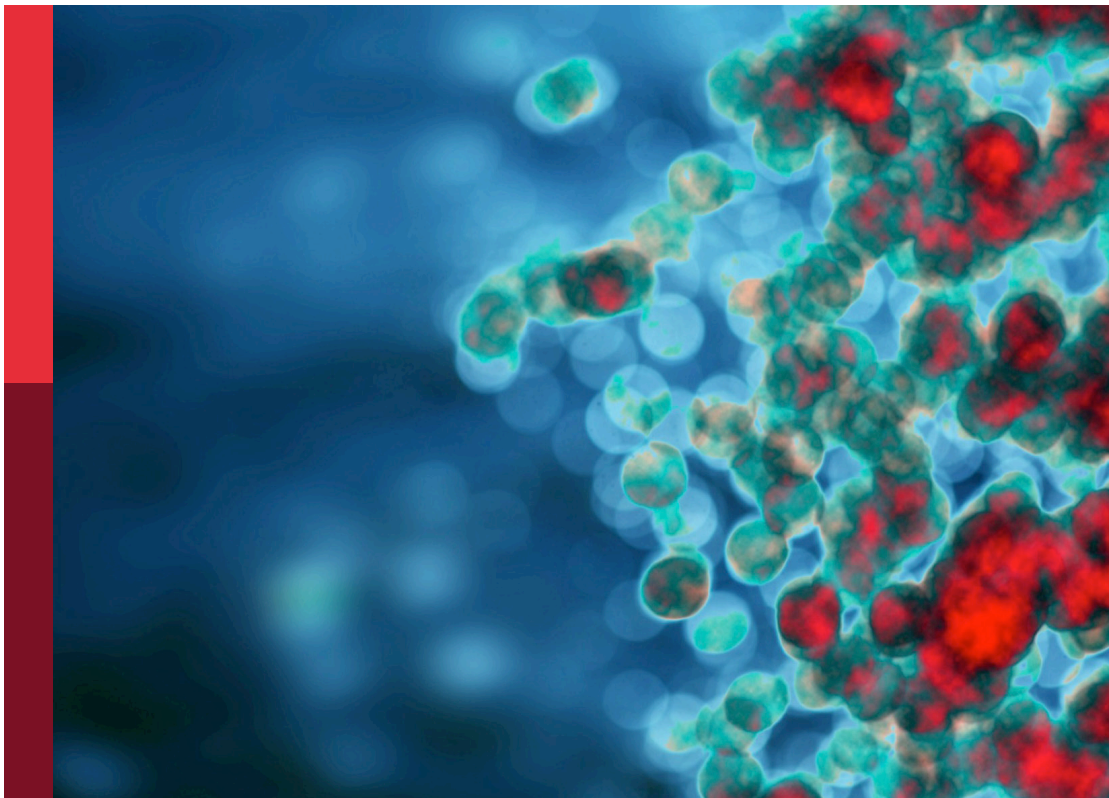

ISSN 1664-8714
ISBN 978-2-8325-4086-2
DOI 10.3389/978-2-8325-4086-2

About Frontiers

Frontiers is more than just an open access publisher of scholarly articles: it is a pioneering approach to the world of academia, radically improving the way scholarly research is managed. The grand vision of Frontiers is a world where all people have an equal opportunity to seek, share and generate knowledge. Frontiers provides immediate and permanent online open access to all its publications, but this alone is not enough to realize our grand goals.

Frontiers journal series

The Frontiers journal series is a multi-tier and interdisciplinary set of open-access, online journals, promising a paradigm shift from the current review, selection and dissemination processes in academic publishing. All Frontiers journals are driven by researchers for researchers; therefore, they constitute a service to the scholarly community. At the same time, the *Frontiers journal series* operates on a revolutionary invention, the tiered publishing system, initially addressing specific communities of scholars, and gradually climbing up to broader public understanding, thus serving the interests of the lay society, too.

Dedication to quality

Each Frontiers article is a landmark of the highest quality, thanks to genuinely collaborative interactions between authors and review editors, who include some of the world's best academicians. Research must be certified by peers before entering a stream of knowledge that may eventually reach the public - and shape society; therefore, Frontiers only applies the most rigorous and unbiased reviews. Frontiers revolutionizes research publishing by freely delivering the most outstanding research, evaluated with no bias from both the academic and social point of view. By applying the most advanced information technologies, Frontiers is catapulting scholarly publishing into a new generation.

What are Frontiers Research Topics?

Frontiers Research Topics are very popular trademarks of the *Frontiers journals series*: they are collections of at least ten articles, all centered on a particular subject. With their unique mix of varied contributions from Original Research to Review Articles, Frontiers Research Topics unify the most influential researchers, the latest key findings and historical advances in a hot research area.

Find out more on how to host your own Frontiers Research Topic or contribute to one as an author by contacting the Frontiers editorial office: frontiersin.org/about/contact

Innate lymphoid cells: Characterization and classification

Topic editors

Carolina Jancic — National Scientific and Technical Research Council (CONICET), Argentina

Carmelo Luci — Institut National de la Santé et de la Recherche Médicale (INSERM), France

Rachel Golub — Université Paris Cité, France

Citation

Jancic, C., Luci, C., Golub, R., eds. (2023). *Innate lymphoid cells: Characterization and classification*. Lausanne: Frontiers Media SA. doi: 10.3389/978-2-8325-4086-2

Table of contents

frontiers | Frontiers in Immunology

TYPE Editorial
PUBLISHED 24 November 2023
DOI 10.3389/fimmu.2023.1338463

OPEN ACCESS

EDITED AND REVIEWED BY
Christoph Siegfried Niki Klose,
Charité University Medicine Berlin,
Germany

*CORRESPONDENCE
Carolina C. Jancic
cjancic@fmed.uba.ar

RECEIVED 14 November 2023
ACCEPTED 17 November 2023
PUBLISHED 24 November 2023

CITATION
Luci C, Golub R and Jancic CC (2023) Editorial: Innate lymphoid cells: characterization and classification. *Front. Immunol.* 14:1338463. doi: 10.3389/fimmu.2023.1338463

Editorial: Innate lymphoid cells: characterization and classification

Carmelo Luci[1], Rachel Golub[2] and Carolina C. Jancic[3,4]*

[1]Université Côte d'Azur, INSERM U1065, Centre Méditerranéen de Médecine Moléculaire, Nice, France, [2]Institut Pasteur, Université Paris Cité, INSERM U1223, Paris, France, [3]Instituto de Medicina Experimental–Consejo Nacional de Investigaciones Científicas y Técnicas (CONICET)–Academia Nacional de Medicina, Buenos Aires, Argentina, [4]Departamento de Microbiología, Parasitología e Inmunología, Facultad de Medicina, Universidad de Buenos Aires, Buenos Aires, Argentina

KEYWORDS

innate lymphoid cells, health, disease, classification, development

Editorial on the Research Topic
Innate lymphoid cells: characterization and classification

Innate lymphoid cells (ILCs) are lymphocytes lacking the rearranged antigen receptors and mainly localized at epithelial surfaces, where they maintain tissue homeostasis, and provide a rapid response to pathogen assaults (1). ILCs share similarities with conventional T cells and are divided into 5 subsets based on cell surface markers, transcription factor requirement and ability to produce type 1, type 2 and Th17 cell-associated cytokines: conventional Natural Killer (NK) cells, helper ILC1, ILC2, ILC3 and Lymphocytes Tissue-Inducers (LTi) cells. They are endowed with a plasticity that allows them to modify their phenotype and their functionality to adapt to the microenvironment in which they are located (2). ILCs are considered resident cells in different peripheral tissues but they can also be present in lymph and peripheral blood as it is the case for NK cells (3). The description of the ILCs are complex and discordant since distinctive markers are either not supported in few tissues or across species and after inflammatory conditions. Today, to better understand the origin and classification of ILCs as a whole, and its participation in the immune response, it is necessary to unify criteria and nomenclature after comparing human and mouse recent studies (4).

The goal of this Research Topic was to deepen our knowledge on the origin, classification and activity of ILCs, by focusing on:

- ILCs classification depending on developmental and functional studies.
- ILCs characterization and enlargement to humans.
- How much of ILCs biology is transposable between mice and humans?
- ILCs identity and plasticity during an immune response.
- Diversity in renewal of ILCs subsets during an immune response.
- New functions of specific ILCs subsets (kidney, joints, brain, etc.).

This Research Topic brings together original articles and reviews related to different aspects of ILCs behavior, ranging from their development to their tissue dynamic, including their role in health and diseases. Since the discovery of ILCs, there has been a steady increase

in the knowledge about their physiology, which includes their impact on maintaining tissue homeostasis, and their involvement in protection against pathogens and tumors. However, much remains to learn about ILCs, in fields such as ontogenesis, differentiation, migration, among others. Zhang et al. by an integrative analysis of RNA, using scRNA-seq algorithms, identify two gene sets that predominantly differentiate ILCs from $CD4^+$ Th subsets, as well as three gene sets that distinguish various immune responses. Authors observe that ILCs and Th subsets are under differential transcriptional regulation. Besides the similarities in effector functions, in ILCs and Th subsets, the underlying regulatory mechanisms exhibit substantial distinctions, supporting the unique roles played by each cell type during immune responses. Additionally, Koprivica et al. focus on the discrepancies in the phenotypic characterization of human and mouse ILC3. The authors analyzed in depth the molecular markers used to identify this population. They discuss the need to unify the definition, isolation, and propagation of ILC3 to increase the possibility of a confluent interpretation of the role of ILC3 in immunity. Calvi et al. provide an overview of the current knowledge about NK cells and helper ILC ontogenesis in humans. They focus on the circulating ILC subsets with killing properties, the unconventional $CD56^{dim}$ NK cells and cytotoxic helper ILCs, and discuss their contribution in both physiological and pathological conditions. Concerning diseases, Roberts et al. summarize the current evidence for the pathological and protective roles of ILCs in cardiovascular disease and its associated risk factor, obesity. Likewise, Wang and Pavert address the steady-state involvement of ILCs in the central nervous system and their participation in major neurological diseases such as ischemic stroke, Alzheimer's disease, and multiple sclerosis. Concerning the ability of ILC2s to circulate between different organs during inflammation and their potential functions in organs, Mathä et al. review recent findings on ILC2 migration, including their traffic within, into and out of tissues during inflammation, analyzing their roles in mediating multiple type 2 diseases.

A key function of ILCs is their ability to act as a first line of defense during infection, as well as contribute to tissue repair. This is due in part, to their location in the epithelial barriers, skin and mucosa (intestine and lung among others) (5). As a consequence, they may have a pivotal role in the regulation of intestinal homeostasis and in the orchestration of the inflammatory responses. In this Research Topic, and focusing on Inflammatory Bowel disease (IBD), Coman et al. discuss what is currently understood about the roles of helper-like ILC1 in the progression of IBD pathogenesis. As well, authors summarize the published data on helper-like ILC1 plasticity and in their classification in murine and human models. Of note, ILC1s are not the only ILCs involved in gut pathologies, Irie et al. analyze ILC2s, which are mainly associated with parasites immune defense, by studying the global gene expression of ILC2s in health and in colitic conditions using dextran sodium sulfate-induced colitis. Authors reveal the potential roles of type I interferon (T1IFN) in ILC2s during colitis manifestation as T1IFN-stimulated genes were up-regulated in ILC2s. In a similar model of induced colitis, Schroeder et al. reveal the unexpected results that CD90 is not constitutively expressed by functional ILCs in the gut. The authors show that $CD90^{negative/low}$ $CD127^+$ ILCs were a potential source of IL-13, IFN-γ and IL-17A at steady state and upon dysbiosis- and dextran sulphate sodium-elicited colitis and could contribute in disease progression. Furthermore, Shi et al. observe that Daikenchuto, one of the most widely used Japanese herbal formulae for various gastrointestinal disorders, restore the reduced colonic ILC3s, mainly RORγthigh-ILC3 in dextran sulphate sodium-elicited colitis model. This herbal formulae attenuates the severity of experimental colitis and maintain the symbiotic microbiota in the colon suggesting that ILC3s play a protective function on colonic inflammation. In accordance with the ability of ILCs to respond to microenvironmental stimuli, Song et al. demonstrate that ILCs are deeply imprinted by their organ of residence, and the conditions specific to healthy or pathological tissues. In the hepatocellular carcinoma microenvironment, authors identified intermediate c-kit^+ILC2 population, and lin-$CD127^-$ NK-like cells that expressed markers of cytotoxicity. Additionally, $CD127+CD94^+$ ILC1 were preferentially enriched in inflamed ileum from patients with Crohn's disease. These analyses provided a baseline for studies focused on tissue-specific ILC-mediated immunity. Notably, there are non-pathologic processes in certain organs, such as in the uterus that require a fine regulation of the immune responses. Interestingly, uterine natural killer cells (uNK) play an important role in promoting successful pregnancy. uNK cells can be divided into three subsets, which may have different roles in pregnancy, and Whettlock et al. establish how uNK frequency and function change dynamically across the healthy reproductive cycle suggesting their implications for the study of subfertility, recurrent miscarriage, and related conditions.

As in many cells, regulation of transcription factors expression needs to be finely controlled to allow ILC development. Conserved non-coding sequences (CNSs) are regulatory cis-acting elements critically controlling gene expression via interaction with various trans-acting factors. The cis-regulatory mechanisms controlling *Rorc* transcription in ILC3s remain unclear. In their study, Chang et al. discover that the deficiency in the conserved noncoding sequence 9 (CNS9) located in *Rorc* gene, selectively decreases RORγt expression in ILC3s. Accordingly, this alters ILC3 gene expression features and promotes cell intrinsic generation of $CD4^+$NKp46+ ILC3 subset. This study points CNS9 as an essential cis-regulatory element controlling the lineage stability and plasticity. Contributing to the evidence on the dependence between phenotype and cell localization, Gao et al. uncovered subset-specific differences in the proliferative status between vascular and tissue ILCs within lymphoid and non-lymphoid organs by employing MISTRG humanized mice as an *in vivo* model to study human ILCs. Authors show the proliferative topography of human ILCs, linking cell migration and spatial compartmentalization with cell division. Noticeable, Kabil et al. remark about the plasticity of ILCs, which is controversial due to several confounding caveats that include, among others, the independent large-scale recruitment of new ILC subsets from distal sites and the local, in situ, differentiation of uncommitted resident precursors. To clarify this point, authors detail current methodologies used to study ILC plasticity in mice and review the mechanisms that drive and regulate functional ILC plasticity in response to polarizing signals in their microenvironment.

Collectively, the variety of original papers and reviews presented in this Research Topic have provided a comprehensive overview on

ILC physiology and on their behavior in diseases. The insights described here are expected to help understand their role as a key effector in the immune response and their relationship to different pathologies and conditions.

Author contributions

CL: Writing – review & editing. RG: Writing – review & editing. CJ: Writing – original draft, Writing – review & editing.

Funding

The author(s) declare that no financial support was received for the research, authorship, and/or publication of this article.

Conflict of interest

The authors declare that the research was conducted in the absence of any commercial or financial relationships that could be construed as a potential conflict of interest.

Publisher's note

References

1. Vivier E, Artis D, Colonna M, Diefenbach A, Di Santo JP, Eberl G, et al. Innate lymphoid cells: 10 years on. *Cell* (2018) 174(5):1054–66. doi: 10.1016/j.cell.2018.07.017

2. Bal SM, Golebski K, Spits H. Plasticity of innate lymphoid cell subsets. *Nat Rev Immunol* (2020) 20(9):552–65. doi: 10.1038/s41577-020-0282-9

3. Meininger I, Carrasco A, Rao A, Soini T, Kokkinou E, Mjösberg J. Tissue-specific features of innate lymphoid cells. *Trends Immunol* (2020) 41(10):902–17. doi: 10.1016/J.IT.2020.08.009

4. Scoville SD, Freud AG, Caligiuri MA. Cellular pathways in the development of human and murine innate lymphoid cells. *Curr Opin Immunol* (2019) 56:100–6. doi: 10.1016/j.coi.2018.11.003

5. Klose CS, Artis D. Innate lymphoid cells as regulators of immunity, inflammation and tissue homeostasis. *Nat Immunol* (2016) 17(7):765–74. doi: 10.1038/ni.3489

frontiers in Immunology

REVIEW
published: 03 February 2022
doi: 10.3389/fimmu.2022.837250

Innate Lymphoid Cells in the Central Nervous System

*Shuaiwei Wang and Serge A. van de Pavert**

Aix-Marseille Université, Centre National de la Recherche Scientifique (CNRS), Institut National de la Santé et de la Recherche Médicale (INSERM), Centre d'Immunologie de Marseille-Luminy (CIML), Marseille, France

Immune cells are present within the central nervous system and play important roles in neurological inflammation and disease. As relatively new described immune cell population, Innate Lymphoid Cells are now increasingly recognized within the central nervous system and associated diseases. Innate Lymphoid Cells are generally regarded as tissue resident and early responders, while conversely within the central nervous system at steady-state their presence is limited. This review describes the current understandings on Innate Lymphoid Cells in the central nervous system at steady-state and its borders plus their involvement in major neurological diseases like ischemic stroke, Alzheimer's disease and Multiple Sclerosis.

Keywords: NK, ILC1, ILC2, ILC3, ischemic stroke, Alzheimer's disease, multiple sclerosis, glioma

OPEN ACCESS

Edited by:
Carmelo Luci, Institut National de la Santé et de la Recherche Médicale (INSERM), France

Reviewed by:
Marina Cella, Washington University School of Medicine in St. Louis, United States
Christoph Siegfried Niki Klose, Charité Universitätsmedizin Berlin, Germany

***Correspondence:**
Serge A. van de Pavert
vandepavert@ciml.univ-mrs.fr

Specialty section:
This article was submitted to NK and Innate Lymphoid Cell Biology, a section of the journal Frontiers in Immunology

Received: *16 December 2021*
Accepted: *17 January 2022*
Published: *03 February 2022*

Citation:
Wang S and van de Pavert SA (2022) Innate Lymphoid Cells in the Central Nervous System. Front. Immunol. 13:837250. doi: 10.3389/fimmu.2022.837250

INTRODUCTION

The central nervous system (CNS) is a highly sensitive organ and requires protection. Physical protection to the CNS is provided by three meningeal layers. These three layers are the dura mater, adjacent to the skull, the pia mater, located just above the CNS parenchyma, and the arachnoid mater, in between the dura and pia mater (1) (**Figure 1**). Besides the physical protection of the brain, the dura mater layer also harbor a variety of immune cells, whereas arachnoid- and pia mater contain fewer (2). Moreover, dural myeloid and lymphoid cells are replenished from skull or vertebrae bone-marrow in steady-state and inflammatory conditions (3–6). Within the dura mater the superior sagittal sinus and the transverse sinus collect blood from the veins of the brain, meninges and skull and transport this towards the internal jugular veins. The sinuses in the dura mater are the neuro-immunological interface where CNS-derived antigens accumulate and the local antigen presenting cells (APCs) prime patrolling T cells (7). Dural lymphatic vessels lining the sinuses collect CSF from the subarachnoid space and interstitial fluid (ISF) from the brain and drain *via* connections through the nasal-cribriform plate into the nasopharynx lymphatic vasculature (8) towards the mandibular and deep cervical lymph nodes (dcLN) (9, 10). Therefore, the meninges is a critical neuro-immunological interface where immune cells are situated to sense threatening factors such as pathogens and antigens (7). During steady-state, migration of immune cells and macromolecules into the brain parenchyma is restricted by the presence of the blood brain barrier (BBB) around the blood vessels (11), made up of endothelial cells connected by tight junctions (12, 13). Within the CNS, there are immune cells present within the choroid plexus (CP), a villous structure located within brain ventricles comprised of a continuous single layer of epithelium surrounding stroma. The major role of the CP is to produce the cerebral spinal fluid

(CSF) (14). Blood vessels with fenestrated endothelium vascularize the CP stroma to enable entry of peripheral leukocytes *via* interactions with blood vessel selectins, integrin ligands and chemokines. Subsequently, recruited leukocytes are able to migrate through the epithelial monolayer into the CSF, mediated by the chemokines in the choroid plexus (15).

A variety of innate and adaptive immune cell subsets including mast cells, dendritic cells (DCs), monocytes, macrophages, T cells and B cells are located in the meninges and CP under steady-state conditions (3, 7, 14, 16–20). The detection of the relative newly described Innate Lymphoid Cells (ILCs) (21) at the CNS borders under steady-state conditions and damaged parenchyma gained increased attention in recent years. ILCs are the innate counterparts of T cells but lack antigen receptor rearrangement. The first ILC subset to be described was the conventional natural killer (cNK) cell in 1975 (22, 23). Later, Lymphoid Tissue Inducer (LTi) cells were described (24), followed by ILC1, ILC2 and ILC3 members (24–32). NK cells are considered to be the innate counterpart of $CD8^+$ T lymphocytes. The other ILCs share the characteristics of helper $CD4^+$ T cells, and are hence named helper-ILCs. The $CD4^+$ helper T cell populations Th1, 2 and 17 share transcription factors and cytokines with their analogous ILC counterparts, respectively ILC1, 2 and 3. As ILCs lack T cell receptor, their activation does not rely on specific antigens and co-stimulation, but rather requires cytokines and signals usually provided by their tissue of residence. Therefore, they are early and immediate responders to a microenvironmental challenge. ILCs distribute to lymphoid and non-lymphoid tissues, including lymph nodes, intestine, liver, lung, skin, uterus and decidua (21, 33). They have been described as tissue-resident, being maintained and expanding locally (34). Other data suggest that a proportion of the ILCs are migratory (35). The CNS parenchyma is almost devoid of ILCs under steady-state condition due to the presence of brain barriers such as the blood-brain barrier (BBB), meningeal barrier, blood-cerebrospinal fluid (CSF) barrier and the ventricular barrier (3, 36). This raises questions on the presence of supposedly tissue resident ILCs within the immune privileged CNS, and what occurs with ILCs upon an inflammation within the CNS. Here, we provide an overview of the ILC presence within the CNS, including the meninges, during steady-state plus their involvement and function in major neurological diseases.

ILCs IN THE CNS AT STEADY-STATE

NK and ILC1

NK cells (NKs) and type 1 innate lymphoid cells (ILC1s) commonly express NK1.1 and are defined as $Lin^-CD45^+NK1.1^+$ $NKp46^+$ lymphocytes, with a notable difference in NKs which express transcription factor Eomes and T-bet while in general ILC1s express transcription factor T-bet exclusively (37, 38). Although both NKs and ILC1s produce the principle cytokine IFN-γ, they display different roles. NKs are cytotoxic, whereas ILC1s are generally non-cytotoxic due to the lower expression of perforin and granzyme B production (39).

CD49a and CD49b are used to distinguish NK from ILC1s in some tissues, such as liver, skin and bone marrow, but not in salivary glands (21). Within the CNS, $CD45^{high}CD3^-NK1.1^+$ $CD49a^-CD49b^+$ cells are $Eomes^+T\text{-}bet^+$, thus NKs. $CD45^{high}CD3^-NK1.1^+CD49a^+CD49b^-$ cells are $Eomes^-T\text{-}bet^+$, thus ILC1s (38). NKs have been described to convert into intermediate ILC1s (intILC1s) by TGFβ, and notably express CD49a, CD49b and Eomes within a tumor microenvironment (40, 41). $CD49a^+CD49b^+Eomes^+$ intILC1s are also present within the meninges (38). However, about 40% of the $CD49a^+CD49b^+$ intILC1s in the meninges have been described not to express Eomes. Whether the $CD49a^+CD49b^+Eomes^-$ intILC1s are unique meningeal resident cells and are functionally different remains unknown. Both NKs and ILC1s have been observed within the meninges during steady-state conditions (3, 38, 42, 43) (**Figure 1**). Moreover, these two populations recirculate through peripheral lymphoid tissues (35), raising the question whether NKs and ILC1s within the meninges are migratory or resident. Compared to the NKs in blood, NKs found in the dura mater express higher levels of CD62L and CD27, which are critical for the maturation- and effector- function of NKs (44, 45) and provide a faster and stronger protection against challenges to the CNS. It has been reported that neurons express chemokine CX3CL1 to recruit $CX3CR1^+$ NKs to the brain parenchyma, which is associated with a better prognosis against e.g. glioma (46). NKs found in the dura mater also express higher level of CX3CR1 compared to NKs in blood (3), suggesting that NKs patrol the CNS in the homeostatic state and could rapidly be involved in the reaction to pathological conditions. Moreover, meningeal resident NKs are the main contributors for IFN-γ production which transmigrates through the arachnoid and pia mater to induce the death receptor-ligand TRAIL expression in astrocytes. Subsequently, activation of the death receptor on T-cells limits their numbers and inhibits neuroinflammation (42) (**Figure 1**). These findings suggest that regulating the plasticity of NKs in the meninges might be a potential therapy against neurological diseases. Compared to meninges, fewer $CD45^+CD3^-NK1.1^+$ lymphocytes have been observed within the choroid plexus (CP) at steady state, most of which are ILC1s but not NKs nor intILC1s (38). However, the role of ILC1s in the CP at steady state is currently unknown.

ILC2

Type 2 innate lymphoid cells (ILC2s) do not only protect against helminth parasites that infect CNS and lead to aggressive neurological diseases (47), but can also promote tissue repair (48). Neurotransmitter receptors such as neuromedin U receptor (NMUR1) and vasoactive intestinal peptide receptor 2 (VIPR2) expressed by ILC2s mediate the crosstalk between the peripheral nervous system (PNS) and ILC2s (49). Neuromedin U (NMU) secreted by neurons positively regulate activation, proliferation and cytokine production of $NMUR1^+$ ILC2s (50, 51) to provide a rapid tissue protection against helminth infection. IL-5 produced by immune cells, including ILC2s, promotes release of vasoactive intestinal peptide (VIP) by sensory neurons. In return, VIP stimulates $VIPR2^+$ ILC2s to secret IL-5 (52, 53), providing a strong auto-regulatory loop. Neurotransmitter receptor expression by CNS-resident ILC2s has not been reported yet.

The transmembrane receptor RET (REarranged during Transfection) tyrosine kinase in ILC2s is activated by glial-derived neutrotrophic factor (GDNF) and induces IL-5 and IL-13 expression (54). Neurons within the CNS express GDNF, and thus the expression of these cytokines in CNS residing ILC2s could be indicative of a neuronal-ILC2 communication (55). ILC2s have been shown mainly within the dural meninges, but not within the leptomeninges (arachnoid mater and pia mater) at steady-state (56, 57) (**Figure 1**). Although few ILC2s have been detected within the choroid plexus in a healthy young brain, an abundance of this population has been found in the aged brain. The increase of ILC2s in the aged brain is probably due to an accumulation of CNS-resident ILC2s since they do not re-enter circulation (56). Transcriptional plasticity analysis show that NK cells and ILC1s could differentiate into ILC2s within the aged brain (58), suggesting that the shift of other ILCs contribute to the ILC2 increase. Interestingly, the ILC2s in the choroid plexus and meninges from aged mice can be divided into three subsets, with different capabilities to proliferate and produce cytokines. ILC2s in the choroid plexus contain more $Arg1^{+}Il13^{+}$ ILC2s which mediate type 2 inflammation, whereas the meningeal ILC2s contained more *Csf2* (encoding GM-CSF) expressing ILC2s. Since ILC2-derived GM-CSF induces differentiation of hematopoietic stem and progenitor cells (HSPC) (59, 60), these ILC2s could improve treatment efficacy when transplanting HSPC during neurodegenerative disease treatments. The heterogeneity of ILC2s in the CNS suggests that the distinctive ILC2 subsets only respond to their corresponding stimulation upon a specific inflammation.

ILC3

Group 3 ILCs share the expression of transcription factor RORγt and are divided into two main populations, the NCR^{-} and the NCR^{+} ILC3s. The NCR^{-} population includes LTi cells which are generated before birth and LTi-like cells generated after birth (61). ILC3s play critical roles before and after birth (61). NCR^{-} ILC3s are essential for the formation of lymph nodes and Peyer's patches in the embryo, while both NCR^{-} and NCR^{+} ILC3s regulate mucosal immunity. There have been several examples described on neuro-ILC3 crosstalk. Circadian circuits regulate stability of enteric ILC3s that express circadian clock genes (62–64). Disruption of these genes in ILC3s cause impaired microbiome homeostasis and increase susceptibility to inflammatory bowel disease. VIP produced by enteric neurons is recognized as a regulator for enteric VIPR2-expressing ILC3s, even though the results about regulation of VIP on IL-22 production by these ILC3s remain controversial (65–67). Relatively little is known about the presence and roles for ILC3s within the CNS. Heterogeneous ILC3 subsets LTi/LTi-like cells and NCR^{+} ILC3s have been observed in the healthy meninges (68) (**Figure 1**). Although ILC1s and ILC2s are present within the choroid plexus, barely any ILC3s are detected within the CNS (56).

ILCs IN NEUROLOGICAL DISEASES

NK and ILC1

The global burden of neurological diseases is increasing (69). Recent advancements in neuroimmunology indicate that developing immunotherapies against neurological diseases are beneficial in improving clinical treatment. Therefore, a better understanding of the roles for ILCs could benefit development of immunotherapies. We will restrict the discussion on ILCs in major neurological diseases such as cerebrovascular disease ischemic stroke, demyelinating disease multiple sclerosis (MS), Alzheimer's disease (AD) and glioma.

Stroke is a major cause of disability and death worldwide and classified into ischemic stroke and hemorrhagic stroke. Innate and adaptive immune cells including microglia, neutrophils, monocytes and lymphocytes play multiphasic roles in ischemic stroke and impact the pathogenesis of ischemic brain

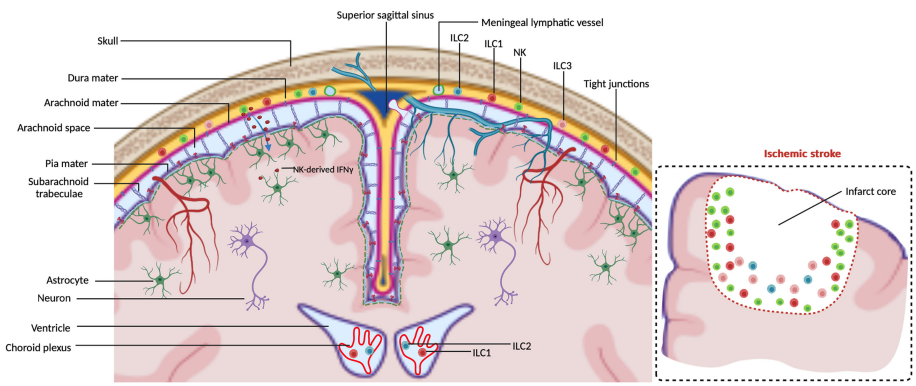

FIGURE 1 | ILCs in the CNS borders at steady-state. Meninges consist of the dura mater, arachnoid mater and pia mater. Dural lymphatic vessels lining the sinuses absorb CSF from the subarachnoid space. Arachnoid- and pia mater are impermeable to immune cells due to tight junctions. NK cells are observed within the meninges to regulate astrocytes by secreting IFN-γ which diffuses into the brain parenchyma. ILC1s are observed to reside in both meninges and choroid plexus. ILC2s and ILC3s are mainly observed within the meninges. The insert illustrates that in an ischemic stroke ILCs accumulate at the lesion border, the majority being NK cells.

injury (70–73). NK cells have been detected in the brain parenchyma of stroke patients and mouse models with induced ischemic stroke (43, 74, 75). We observed that the robust accumulation of NK cells in the stroke lesion is caused by progressive migration rather than *in situ* proliferation (43). The main chemotaxis described thus far for controlling migration of NKs towards the lesion are the CX3CL1/CX3CR1 and CXCL12/CXCR4 axis (43, 74). The roles for NK cells in ischemic stroke are contradictionary. To establish the role of NKs, anti-NK1.1 treatment has been frequently used to deplete NKs and ILC1s. However, it is important to note that NK1.1 is expressed on a subset of (ex)ILC3s, which are NKp46^{+}T-bet^{+}RORyt^{+} (76), and thus anti-NK1.1 treatment can affect this population. However, it has been shown that there are no NK1.1^{+} (ex)ILC3 within the CNS by using the *RORc*^{GFP} fate mapping reporter mouse model (38). Moreover, the presence of the RORγt^{+} ILC population is very limited in ischemic stroke brain when compared to the NK cells and ILC1 (43). Therefore, studies using anti-NK1.1 to mediate depletion affect most likely only NKs and ILC1s, but not ILC3s within the CNS. Depletion of NK cells using anti-NK1.1 decreases infarction size and neurological deficits in MCAO (middle cerebral artery occlusion) stroke model (74). However, we have observed that CXCR4^{+} NK cells protect motor behavioral functions in the photothrombotic stroke model by using anti-NK1.1 mediated depletion. Also, blocking migration towards the lesion by *Cxcr4* deletion specifically in NKs and ILC1s protects motor-behavior after stroke ischemic induction (43). The contradiction in the effects of the NKs between these studies can partly be attributed to differences in behavioral test applied. In the study by Gan et al. a less precise Bederson score testing forelimb flexion has been used, which basically measures resistance to lateral push and circling behavior (77). In our study where we have observed a protective effect, we have used beam-walk assay testing foot slips when mice cross an elevated beam to analyze the motor-behavioral deficits. Indeed, using the *Rag1*$^{-/-}$ mice, in which all T cells are absent, but not ILCs or NK cells, an improvement of the motor behavior has also been observed in the tMCAO stroke model (78). These findings on the protective nature of NK cells fit with the recent study by Sanmarco et al. reporting that IFNy from NK cells induced TRAIL expression in LAMP^{+} astrocytes to limit the T cell presence and hence prevent inflammation in EAE (42). The protective IFN-γ production by meningeal NK cells, positively regulating the protective role of LAMP^{+}TRAIL^{+} astrocytes, has been shown to be induced by the intestinal microbiome (42). Therefore, another explanation for the contradictionary findings is a possible difference in commensal microbes within the intestines of the mice used in the different labs. Intriguingly, clinical studies showed that dysbiosis of gut microbiota has been correlated with the severity of acute ischemic stroke and mice receiving fecal transplantation of ischemic stroke patients with significant dysbiosis develop more severe brain injury (79, 80). To better understand the role of NK cells in the stroke brain, additional studies on how microbiota affect the regulation of NK cells on stroke brain recovery are required.

Multiple sclerosis (MS) is an autoimmune disease of the central nervous system, with a hallmark of nerve fiber demyelination. The pathological role of Th17 cells in MS and its animal model experimental autoimmune encephalomyelitis (EAE) has been described before (81). Anti-NK1.1 mediated depletion of mainly NK and ILC1s suppress Th17-mediated neuroinflammation in EAE (82). Moreover, specifically deletion of NKs and ILC1s using the *Tbx21*$^{-/-}$ (encoding T-Bet) and *Tbx21*$^{f/f}$ NKp46-Cre^{+} model indicate the importance of these cells in the onset of the Th17 mediated inflation as well (83) (**Table 1**). Indeed, several other studies indicate the protective role of NK cells in neuroinflammation, notably in EAE and MS patients (42, 86–89). NKp44 is only expressed on activated NK cells and mediates both activating and inhibitory signals to NK cells (90). NKp44 ligand (NKp44L) is expressed by astrocytes and the interaction of astrocytes with NK cells is mediated by NKp44L-NKp44 interaction. This interaction activates NK cells function and leads to NK mediated astrocyte cell death (91). Therefore, NKs and ILC1s can either inhibit or enhance inflammation in EAE depending on signaling pathways used.

ILC1s in the CP of the CNS maintain stable expression of IFN-γ and TNF-α in EAE, which could synergistically regulate the levels of IFN-γR and TNF-R1 expressed by the choroid plexus endothelium (38, 92). IFN-γ upregulates a wide array of trafficking molecules expressed by the choroid plexus epithelium, such as vascular cell adhesion molecule 1 (VCAM1), intercellular adhesion molecule 1 (ICAM1) and chemokines (CCL2, CCL5, CXCL9, CXCL10, CX3CL1), which contribute to the trafficking across of CP epithelial barriers by immune cells (92). Thus, ILC1s in the choroid plexus probably act as a gatekeeper for the entry of neuroinflammation-induced immune cells into the CNS.

TABLE 1 | Overview of ILCs localization in steady-state and neurological diseases.

	NK	ILC1	ILC2	ILC3
Steady-state	Meninges (3, 42, 43)	Meninges and CP (3, 38, 42, 43)	Meninges and CP (56)	Meninges (68)
Stroke	BP (43, 74)	BP (43)	BP (43)	BP (43)
AD	CSF (84)	N.D.	N.D.	N.D.
MS (EAE)	SCP (82, 83)	BP (38)	N.D.	BP and SCP (68)
	Meninges (83)	Meninges (83)		Meninges (68)
SCI	N.D.	N.D.	Meninges and SCP (57)	N.D.
Glioma	TME (85)	N.D.	N.D.	N.D.

There are no ILCs found within the brain parenchyma (BP) at steady-state.

AD, Alzheimer's disease; EAE, Experimental autoimmune encephalomyelitis; SCI, Spinal cord injury; SCP, Spinal cord parenchyma; TME, Tumor microenvironment; N.D., Not Determined.

Alzheimer's disease (AD) is a neurodegenerative disorder and research on AD focusses on the two well-established hallmarks, amyloid beta (Aβ) plaques and neurofibrillary tangles (NFT) (93, 94). Bioinformatical experimental and clinical studies indicate that the immune system plays an indispensable role in AD pathology (95–98). NK cells have been also reported in the CSF from AD patients (84). However, the role of NK cells in AD patients and the underlying mechanism mediating the migration of NK cells towards the plaques and interaction with the plaques is unknown. Therefore, it remains to be established if NK cells are present in, or near, the plaques, and with which cells they interact. Since IL7Rα is expressed by the majority of ILC1s and hardly on NK cells in the adult, some IL7Rα$^+$ NK cells detected in the CSF of Alzheimer's disease are most likely ILC1s (21, 84). It does not exclude the possibility that the CP-resident ILC1s enter the CSF to patrol the Alzheimer's brain. In order to distinguish ILC1s from NK cells in the CSF from Alzheimer's disease in future studies, CD49a and CD49b can be used. CD49a promote the persistence of CD8$^+$ T cells within the skin and increases this population after local antigen challenge (99). In analogy to skin CD8$^+$ T cells, the CD49a-expressing ILC1s might also protect brain parenchyma from AD and viral or bacterial infections by promoting the persistence of CD8$^+$ cells within the CNS.

Glioma is the most prevalent tumor of the CNS with a high mortality rate (100). High heterogeneity of gliomas indicates the complexity of immune landscape within glioma tumor microenvironment (101). The involvement of microglia, macrophage, effector- and regulatory T cells in glioma is described in detail elsewhere (102–104). NK cells are present within the glioma tumor microenvironment (85) and are attracted towards the tumor by neuronal expressed chemokine CX3CL1. The attraction of the CX3CR1$^+$ NK cells is associated with a better prognosis in glioma patients (46). The role of NK cells and NK cell immunotherapy against malignant CNS tumors is discussed in detail elsewhere (105). Summarized, activated NK cells are associated with improved prognosis and survival of glioma patients and therefore strategies to enhance NK cell mediated anti-glioma function could improve clinical outcomes.

We propose that NK cells are involved in regulating CNS diseases in a multiphasic manner. NK cells can be activated at the onset of the disease and secret cytokines to regulate its progression. When NK cells arrive at the focal zone, they are capable of directly interacting with some targets such as neurons, microglia and astrocytes. Natural cytotoxicity receptors (NCR) expressed by NK cells recognize a variety of ligands derived from cells, viruses, bacteria and parasites, which affect the activation or inhibition of NK cells (106). Experimental data support the interaction between NK cells and motor neuron (MN) within the CNS, mediated by NCR NKG2D on NK cells, promoting MN degeneration and impairment (107). IL-2-activated NK cells rapidly form synapses with human microglia, mediated by NKG2D and NKp46. This interaction results in killing of the resting microglia and modulate the innate and adaptive immune responses within the CNS (108). Knowledge about ILC1s in neurological diseases is limited since they were previously mis-characterized as closely related conventional NK cells. The recent ILC1 characterization open new areas of investigations into CNS diseases.

ILC2

Meningeal ILC2 cell numbers increase after spinal cord injury (SCI) (57). Intriguingly, lung-derived ILC2s present within the meninges have been shown beneficial for the recovery after SCI (57), suggesting that they share some characteristics with meningeal ILC2s. ILC2s in other tissues such as lung and gut express the neurotransmitter receptors NMUR1 and VIPR2. Meningeal ILC2s upregulate the gene encoding the receptor for calcitonin gene-related peptide (CGRP) (57), which implies that they are not only activated by cytokine IL-33 but possibly also by CGRP, a neurotransmitter secreted by nociceptive neurons after SCI (**Table 1**). Whether meningeal ILC2s also express other neurotransmitter receptors involved in ILC2s-neuron communication remains to be established. After SCI induction, *in situ* proliferating ILC2s are capable of positively regulating Th2 cell response by IL-13, which could promote axonal regrowth (109, 110).

ILC2s are also detected in the lesion of mouse stroke model (43), meaning that they are potential candidates to regulate the regeneration of affected neurons within the CNS.

Meningeal ILC2 are mainly present within the dural sinuses which have been shown as a critical site for local antigen presentation and immune cell interactions in the CNS (7, 57). The transfer of bone marrow-derived ILC2s into *Cd132*$^{-/-}$ (IL2Rγ) mouse model induces CNS demyelination upon CNS viral infection, indicating this process is ILC2-dependent (111). However, using a more specific ILC2 knock-out model is required to establish the exact role of ILC2s in demyelination, as in the *Cd132* knock-out also other ILCs are deleted which can potentially bias the conclusion. Demyelination causes a variety of problems including diminished memory, impaired vision, slurred speech and trouble walking. Identifying the cytokines secreted by meningeal ILC2s and the targeted immune cells which promote demyelination after viral infection will be beneficial for understanding the role of ILC2s in CNS diseases and beneficial to use in treatments to inhibit CNS demyelination caused by viral infections.

Female MS patients show symptoms at a younger age and exhibit more severe disease-course than males in general, the reason of which is not fully understood (112, 113). A possible explanation is that testosterone has been shown to increase IL-33 expression which activates ILC2s, induces Th2 responses and involved in limited Th17-dominated demyelination (114). Therefore, increased IL33 levels in males could lead to an increased ILC2 activation and inhibition of MS related symptoms. Also, since ILC2s play a vital role in suppressing tumor growth and metastasis (115), the gender bias in IL-33 secretion could also contribute to differences in glioma incidence and evolution (116, 117).

ILC3

LTi cells are part of the ILC3 subset and essential for the development of secondary lymphoid organs (SLOs). A critical step in this process is mediated through the lymphotoxin (LT)

α1β2 signaling pathway (118), and the cells are involved in formation of some tertiary lymphoid organs (TLOs) (119, 120). LTi cells are attracted by CXCL13 during embryonic lymph node formation (121) and in analogy, increased CXCL13 levels in the CSF of MS patients attract $CXCR5^+$ LTi cells towards the CNS (122). Indeed, detection of $ROR\gamma t^+CD3^-$ (ILC3) cells in the sub-meningeal B cell follicles suggest the involvement of LTi cells in MS patients (123). Also in relapsing-remitting MS patients, LTi cells have been observed in blood (124) and associate with a specific lesion tomography. On the contrary, in the mouse experimental model for MS, EAE, LTi cells have not been found in TLO's within the cerebellum parenchyma, but instead Lymphotoxin expressing B-cells have been suggested as inducers of the TLO (125). In another study on EAE, an increase of $OX40L^+$ and $CD30L^+$ ILC3s in the meninges has been observed, but these are not associated with TLO's (68). Since LTi cells in adult mice are known to express OX40L and CD30L, these ILC3 within the meninges could very well be LTi cells (126) (**Table 1**). Combined, results from patients and mouse models suggest that the peripheral LTi cells could organize meningeal lymphoid follicles in specific circumstances in MS or EAE, while in other cases their function would be taken over by other cells expressing lymphotoxin.

ILC3s are essential in CNS inflammation, as deletion of $MHC\text{-}II^+$ ILC3s cells results in loss of symptoms associated with EAE. In this neuroinflammatory model, ILC3's are capable of presenting antigen to autoimmune T cells in focal lesions and thereby mediate neuroinflammation within the CNS parenchyma (83, 127). Similarly, MHC-II expression by some LTi cells (24, 128) suggests that LTi cells could also promote inflammation in EAE by initiating circulating inflammatory T cells. How antigens are obtained by these ILCs and present it on their MHC-II remains unknown, as they have not been shown to be phagocytic. Accumulated ILC3s, including LTi cells and other ILC3s, are capable of producing pro-inflammatory cytokines such as IFN-γ, IL-17 and GM-CSF, which are responsible for chronic inflammation (68, 83). Besides cytokines, ILC3s could regulate the function and survival of memory $CD4^+$ T cells by expressing CD30L and OX40L (129). OX40L expressed by ILC3s is reported to regulate the homeostasis of intestinal Treg cells (130). The existence of Treg cells and ILC3s in the stroke lesion (43, 131) indicates a crosstalk between ILC3s and Treg cells in this disease.

CONCLUDING REMARKS

Although the presence of ILCs in the meninges and choroid plexus in steady-state has been shown, their origin and maintenance remain unknown. Circulating ILC progenitors in the blood might replenish these subsets as was shown in human (132). Previously shown for CNS B-cell and myeloid cell renewal, the contribution of skull and vertebral bone marrow to ILC maintenance has not been investigated (4). Brain barriers prevent the migration of ILC into brain parenchyma at steady-state. It has been shown that neurological diseases cause break down of BBB and meningeal integrity (133–135). The permeability of the BBB is notably increased in stroke and glioma during which the vasculature bed is completely remodeled and re-constructed (136, 137). Also, tight junctions within the BBB are disrupted by molecules such as matrix metalloproteinases (MMPs) in ischemic stroke model (138). Similar as in the BBB, tight junctions in the arachnoid and pia mater might also be disrupted in the inflammatory conditions. These processes could lead to a massive invasion of immune cells, and ILCs, towards the brain lesion. In this model, the ILCs are absent within the brain parenchyma in steady-state conditions but infiltrate the lesion from the dural meninges and local blood vessels upon insult and loss of meningeal- and blood-brain- barrier function.

Considering the importance of ILCs in neurological diseases, such as NK cells in ischemic stroke as well as ILC2s and ILC3s in EAE, knowing the origin and maintenance could aid inducing and culturing these cells *in vitro*. Subsequently, these cells can contribute to developing therapies. The interaction of ILCs with other immune cells such as T cells in the CNS tissues remains to be studied. This knowledge will enhance our understanding of pathological or protective immune responses. Research on ILCs and neuroimmunology has gained much attention in the last few years, whereas the knowledge of ILC-CNS crosstalk remains to be improved. The description of ILC-neuron circuits in peripheral tissues such as lung and intestine (50, 51, 54, 66, 139) raise the question of whether ILCs could also directly communicate with neurons within the CNS.

AUTHOR CONTRIBUTIONS

SW and SP wrote the manuscript. SP supervised the project. All authors contributed to the article and approved the submitted version.

ACKNOWLEDGMENTS

We wish to thank Rejane Rua for her valuable comments. The authors received funding from ANR (ANR-17-CE13-0029). **Figure 1** was made using BioRender.com.

REFERENCES

1. Dias MC, Mapunda JA, Vladymyrov M, Engelhardt B. Structure and Junctional Complexes of Endothelial, Epithelial and Glial Brain Barriers. *Int J Mol Sci* (2019) 20:5372. doi: 10.3390/ijms20215372
2. Van Hove H, Martens L, Scheyltjens I, De Vlaminck K, Pombo Antunes AR, De Prijck S, et al. A Single-Cell Atlas of Mouse Brain Macrophages Reveals Unique Transcriptional Identities Shaped by Ontogeny and Tissue Environment. *Nat Neurosci* (2019) 22:1021–35. doi: 10.1038/s41593-019-0393-4
3. Korin B, Ben-Shaanan TL, Schiller M, Dubovik T, Azulay-Debby H, Boshnak NT, et al. High-Dimensional, Single-Cell Characterization of the Brain's Immune Compartment. *Nat Neurosci* (2017) 20:1300–9. doi: 10.1038/nn.4610

4. Cugurra A, Mamuladze T, Rustenhoven J, Dykstra T, Beroshvili G, Greenberg ZJ, et al. Skull and Vertebral Bone Marrow Are Myeloid Reservoirs for the Meninges and CNS Parenchyma. *Science (80-)* (2021) 373:eabf7844. doi: 10.1126/science.abf7844
5. Brioschi S, Le WW, Peng V, Wang M, Shchukina I, Greenberg ZJ, et al. Heterogeneity of Meningeal B Cells Reveals a Lymphopoietic Niche at the CNS Borders. *Science (80-)* (2021) 373:eabf9277. doi: 10.1126/science.abf9277
6. Wang Y, Chen D, Xu D, Huang C, Xing R, He D, et al. Early Developing B Cells Undergo Negative Selection by Central Nervous System-Specific Antigens in the Meninges. *Immunity* (2021) 54:2784–94. doi: 10.1016/j.immuni.2021.09.016
7. Rustenhoven J, Drieu A, Mamuladze T, de Lima KA, Dykstra T, Wall M, et al. Functional Characterization of the Dural Sinuses as a Neuroimmune Interface. *Cell* (2021) 184:1000–16. doi: 10.1016/j.cell.2020.12.040
8. Decker Y, Krämer J, Xin L, Müller A, Scheller A, Fassbender K, et al. Magnetic Resonance Imaging of Cerebrospinal Fluid Outflow After Low-Rate Lateral Ventricle Infusion in Mice. *JCI Insight* (2021):e150881. doi: 10.1172/jci.insight.150881
9. Louveau A, Harris TH, Kipnis J. Revisiting the Mechanisms of CNS Immune Privilege. *Trends Immunol* (2015) 36:569–77. doi: 10.1016/j.it.2015.08.006
10. Aspelund A, Antila S, Proulx ST, Karlsen TV, Karaman S, Detmar M, et al. A Dural Lymphatic Vascular System That Drains Brain Interstitial Fluid and Macromolecules. *J Exp Med* (2015) 212:991–9. doi: 10.1084/jem.20142290
11. Muldoon LL, Alvarez JI, Begley DJ, Boado RJ, Del Zoppo GJ, Doolittle ND, et al. Immunologic Privilege in the Central Nervous System and the Blood-Brain Barrier. *J Cereb Blood Flow Metab* (2013) 33:13–21. doi: 10.1038/jcbfm.2012.153
12. Abbott NJ, Patabendige AAK, Dolman DEM, Yusof SR, Begley DJ. Structure and Function of the Blood-Brain Barrier. *Neurobiol Dis* (2010) 37:13–25. doi: 10.1016/j.nbd.2009.07.030
13. Förster C. Tight Junctions and the Modulation of Barrier Function in Disease. *Histochem Cell Biol* (2008) 130:55–70. doi: 10.1007/s00418-008-0424-9
14. Baruch K, Schwartz M. CNS-Specific T Cells Shape Brain Function *via* the Choroid Plexus. *Brain Behav Immun* (2013) 34:11–6. doi: 10.1016/j.bbi.2013.04.002
15. Ransohoff RM, Kivisäkk P, Kidd G. Three or More Routes for Leukocyte Migration Into the Central Nervous System. *Nat Rev Immunol* (2003) 3:569–81. doi: 10.1038/nri1130
16. Arac A, Grimbaldeston MA, Nepomuceno ARB, Olayiwola O, Pereira MP, Nishiyama Y, et al. Evidence That Meningeal Mast Cells can Worsen Stroke Pathology in Mice. *Am J Pathol* (2014) 184:2493–504. doi: 10.1016/j.ajpath.2014.06.003
17. McMenamin PG. Distribution and Phenotype of Dendritic Cells and Resident Tissue Macrophages in the Dura Mater, Leptomeninges, and Choroid Plexus of the Rat Brain as Demonstrated in Wholemount Preparations. *J Comp Neurol* (1999) 405:553–62. doi: 10.1002/(SICI)1096-9861(19990322)405:4<553::AID-CNE8>3.0.CO;2-6
18. Lewitus GM, Cohen H, Schwartz M. Reducing Post-Traumatic Anxiety by Immunization. *Brain Behav Immun* (2008) 22:1108–14. doi: 10.1016/j.bbi.2008.05.002
19. Quintana E, Fernández A, Velasco P, de Andrés B, Liste I, Sancho D, et al. DNGR-1+ Dendritic Cells Are Located in Meningeal Membrane and Choroid Plexus of the Noninjured Brain. *Glia* (2015) 63:2231–48. doi: 10.1002/glia.22889
20. Goldmann T, Wieghofer P, Jordão MJC, Prutek F, Hagemeyer N, Frenzel K, et al. Origin, Fate and Dynamics of Macrophages at Central Nervous System Interfaces. *Nat Immunol* (2016) 17:797–805. doi: 10.1038/ni.3423
21. Vivier E, Artis D, Colonna M, Diefenbach A, Di Santo JP, Eberl G, et al. Innate Lymphoid Cells: 10 Years on. *Cell* (2018) 174:1054–66. doi: 10.1016/j.cell.2018.07.017
22. Kiessling R, Klein E, Wigzell H. "Natural" Killer Cells in the Mouse. I. Cytotoxic Cells With Specificity for Mouse Moloney Leukemia Cells. Specificity and Distribution According to Genotype. *Eur J Immunol* (1975) 5:112–7. doi: 10.1002/eji.1830050208
23. Herberman RB, Nunn ME, Lavrin DH. Natural Cytotoxic Reactivity of Mouse Lymphoid Cells Against Syngeneic and Allogeneic Tumors. I. Distribution of Reactivity and Specificity. *Int J Cancer* (1975) 16:216–29. doi: 10.1002/ijc.2910160204
24. Mebius RE, Rennert P, Weissman IL. Developing Lymph Nodes Collect CD4+CD3- LTbeta+ Cells That Can Differentiate to APC, NK Cells, and Follicular Cells But Not T or B Cells. *Immunity* (1997) 7:493–504. doi: 10.1016/S1074-7613(00)80371-4
25. Satoh-Takayama N, Vosshenrich CAJ, Lesjean-Pottier S, Sawa S, Lochner M, Rattis F, et al. Microbial Flora Drives Interleukin 22 Production in Intestinal NKp46+ Cells That Provide Innate Mucosal Immune Defense. *Immunity* (2008) 29:958–70. doi: 10.1016/j.immuni.2008.11.001
26. Price AE, Liang H, Sullivan BM, Reinhardt RL, Eisley CJ, Erle DJ. Systemically Dispersed Innate IL-13 – Expressing Cells in Type 2 Immunity. *Proc Natl Acad Sci USA* (2010) 107:11489–94. doi: 10.1073/pnas.1003988107
27. Moro K, Yamada T, Tanabe M, Takeuchi T, Ikawa T, Kawamoto H, et al. Innate Production of TH2 Cytokines by Adipose Tissue-Associated C-Kit+Sca-1+ Lymphoid Cells. *Nature* (2010) 463:540–4. doi: 10.1038/nature08636
28. Neill DR, Wong SH, Bellosi A, Flynn RJ, Daly M, Langford TKA, et al. Nuocytes Represent a New Innate Effector Leukocyte That Mediates Type-2 Immunity. *Nature* (2010) 464:1367–70. doi: 10.1038/nature08900
29. Luci C, Reynders A, Ivanov II, Cognet C, Chiche L, Chasson L, et al. Influence of the Transcription Factor RORgammat on the Development of NKp46+ Cell Populations in Gut and Skin. *Nat Immunol* (2009) 10:75–82. doi: 10.1038/ni.1681
30. Cella M, Fuchs A, Vermi W, Facchetti F, Otero K, Lennerz JKM, et al. A Human Natural Killer Cell Subset Provides an Innate Source of IL-22 for Mucosal Immunity. *Nature* (2009) 457:722–5. doi: 10.1038/nature07537
31. Sanos SL, Bui VL, Mortha A, Oberle K, Heners C, Johner C, et al. RorγT and Commensal Microflora Are Required for the Differentiation of Mucosal Interleukin 22–Producing NKp46+ Cells. *Nat Immunol* (2009) 10:83–91. doi: 10.1038/ni.1684
32. Fuchs A, Vermi W, Lee JS, Lonardi S, Gilfillan S, Newberry RD, et al. Intraepithelial Type 1 Innate Lymphoid Cells Are a Unique Subset of Il-12- and Il-15-Responsive Ifn-γ-Producing Cells. *Immunity* (2013) 38:769–81. doi: 10.1016/j.immuni.2013.02.010
33. Miller D, Motomura K, Garcia-Flores V, Romero R, Gomez-Lopez N. Innate Lymphoid Cells in the Maternal and Fetal Compartments. *Front Immunol* (2018) 9:2396. doi: 10.3389/fimmu.2018.02396
34. Gasteiger G, Fan X, Dikiy S, Lee SY, Rudensky AY. Tissue Residency of Innate Lymphoid Cells in Lymphoid and Nonlymphoid Organs. *Science* (2015) 350:981–5. doi: 10.1126/science.aac9593
35. Dutton EE, Gajdasik DW, Willis C, Fiancette R, Bishop EL, Camelo A, et al. Peripheral Lymph Nodes Contain Migratory and Resident Innate Lymphoid Cell Populations. *Sci Immunol* (2019) 4:eaau8082. doi: 10.1126/sciimmunol.aau8082
36. Palmer AM. The Role of the Blood-CNS Barrier in CNS Disorders and Their Treatment. *Neurobiol Dis* (2010) 37:3–12. doi: 10.1016/j.nbd.2009.07.029
37. Daussy C, Faure F, Mayol K, Viel S, Gasteiger G, Charrier E, et al. T-Bet and Eomes Instruct the Development of Two Distinct Natural Killer Cell Lineages in the Liver and in the Bone Marrow. *J Exp Med* (2014) 211:563–77. doi: 10.1084/jem.20131560
38. Romero-Suárez S, Del Rio Serrato A, Bueno RJ, Brunotte-Strecker D, Stehle C, Figueiredo CA, et al. The Central Nervous System Contains ILC1s That Differ From NK Cells in the Response to Inflammation. *Front Immunol* (2019) 10:2337. doi: 10.3389/fimmu.2019.02337
39. Bernink JH, Peters CP, Munneke M, Te Velde AA, Meijer SL, Weijer K, et al. Human Type 1 Innate Lymphoid Cells Accumulate in Inflamed Mucosal Tissues. *Nat Immunol* (2013) 14:221–9. doi: 10.1038/ni.2534
40. Gao Y, Souza-Fonseca-Guimaraes F, Bald T, Ng SS, Young A, Ngiow SF, et al. Tumor Immunoevasion by the Conversion of Effector NK Cells Into Type 1 Innate Lymphoid Cells. *Nat Immunol* (2017) 18:1004–15. doi: 10.1038/ni.3800
41. Cortez VS, Ulland TK, Cervantes-Barragan L, Bando JK, Robinette ML, Wang Q, et al. SMAD4 Impedes the Conversion of NK Cells Into ILC1-Like Cells by Curtailing Non-Canonical TGF-β Signaling. *Nat Immunol* (2017) 18:995–1003. doi: 10.1038/ni.3809
42. Sanmarco LM, Wheeler MA, Gutiérrez-Vázquez C, Polonio CM, Linnerbauer M, Pinho-Ribeiro FA, et al. Gut-Licensed Ifnγ+ NK Cells

Drive LAMP1+TRAIL+ Anti-Inflammatory Astrocytes. *Nature* (2021) 590:473–9. doi: 10.1038/s41586-020-03116-4
43. Wang S, de Fabritus L, Ashok Kumar P, Werner Y, Siret C, Simic M, et al. Brain Endothelial CXCL12 Attracts Protective Natural Killer Cells During Ischemic Stroke. *bioRxiv* (2021). doi: 10.1101/2021.02.18.431426. 2021.02.18.431426.
44. Hayakawa Y, Smyth MJ. CD27 Dissects Mature NK Cells Into Two Subsets With Distinct Responsiveness and Migratory Capacity. *J Immunol* (2006) 176:1517–24. doi: 10.4049/jimmunol.176.3.1517
45. Peng H, Sun R, Tang L, Wei H, Tian Z. CD62L Is Critical for Maturation and Accumulation of Murine Hepatic NK Cells in Response to Viral Infection. *J Immunol* (2013) 190:4255–62. doi: 10.4049/jimmunol.1202395
46. Ren F, Zhao Q, Huang L, Zheng Y, Li L, He Q, et al. The R132H Mutation in IDH1 Promotes the Recruitment of NK Cells Through CX3CL1/CX3CR1 Chemotaxis and Is Correlated With a Better Prognosis in Gliomas. *Immunol Cell Biol* (2019) 97:457–69. doi: 10.1111/imcb.12225
47. Herbert DR, Douglas B, Zullo K. Group 2 Innate Lymphoid Cells (ILC2): Type 2 Immunity and Helminth Immunity. *Int J Mol Sci* (2019) 20:2276. doi: 10.3390/ijms20092276
48. Rak GD, Osborne LC, Siracusa MC, Kim BS, Wang K, Bayat A, et al. IL-33-Dependent Group 2 Innate Lymphoid Cells Promote Cutaneous Wound Healing. *J Invest Dermatol* (2016) 136:487–96. doi: 10.1038/JID.2015.406
49. Chu C, Artis D, Chiu IM. Neuro-Immune Interactions in the Tissues. *Immunity* (2020) 52:464–74. doi: 10.1016/j.immuni.2020.02.017
50. Cardoso V, Chesné J, Ribeiro H, García-Cassani B, Carvalho T, Bouchery T, et al. Neuronal Regulation of Type 2 Innate Lymphoid Cells *via* Neuromedin U. *Nature* (2017) 549:277–81. doi: 10.1038/nature23469
51. Klose CSN, Mahlakõiv T, Moeller JB, Rankin LC, Flamar A-L, Kabata H, et al. The Neuropeptide Neuromedin U Stimulates Innate Lymphoid Cells and Type 2 Inflammation. *Nature* (2017) 549:282–6. doi: 10.1038/nature23676
52. Nussbaum JC, Van Dyken SJ, Von Moltke J, Cheng LE, Mohapatra A, Molofsky AB, et al. Type 2 Innate Lymphoid Cells Control Eosinophil Homeostasis. *Nature* (2013) 502:245–8. doi: 10.1038/nature12526
53. Talbot S, Abdulnour REE, Burkett PR, Lee S, Cronin SJF, Pascal MA, et al. Silencing Nociceptor Neurons Reduces Allergic Airway Inflammation. *Neuron* (2015) 87:341–54. doi: 10.1016/j.neuron.2015.06.007
54. Cardoso F, Klein Wolterink RGJ, Godinho-Silva C, Domingues RG, Ribeiro H, da Silva JA, et al. Neuro-Mesenchymal Units Control ILC2 and Obesity *via* a Brain–Adipose Circuit. *Nature* (2021) 597:410–4. doi: 10.1038/s41586-021-03830-7
55. Duarte Azevedo M, Sander S, Tenenbaum L. GDNF, A Neuron-Derived Factor Upregulated in Glial Cells During Disease. *J Clin Med* (2020) 9:456. doi: 10.3390/jcm9020456
56. Fung ITH, Sankar P, Zhang Y, Robison LS, Zhao X, D'Souza SS, et al. Activation of Group 2 Innate Lymphoid Cells Alleviates Aging-Associated Cognitive Decline. *J Exp Med* (2020) 217:e20190915. doi: 10.1084/jem.20190915
57. Gadani SP, Smirnov I, Wiltbank AT, Overall CC, Kipnis J. Characterization of Meningeal Type 2 Innate Lymphocytes and Their Response to CNS Injury. *J Exp Med* (2017) 214:285–96. doi: 10.1084/jem.20161982
58. Golomb SM, Guldner IH, Zhao A, Wang Q, Palakurthi B, Aleksandrovic EA, et al. Multi-Modal Single-Cell Analysis Reveals Brain Immune Landscape Plasticity During Aging and Gut Microbiota Dysbiosis. *Cell Rep* (2020) 33:108438. doi: 10.1016/j.celrep.2020.108438
59. Altarche-Xifro W, di Vicino U, Muñoz-Martin MI, Bortolozzi A, Bové J, Vila M, et al. Functional Rescue of Dopaminergic Neuron Loss in Parkinson's Disease Mice After Transplantation of Hematopoietic Stem and Progenitor Cells. *EBioMedicine* (2016) 8:83–95. doi: 10.1016/j.ebiom.2016.04.016
60. Sudo T, Motomura Y, Okuzaki D, Hasegawa T, Yokota T, Kikuta J, et al. Group 2 Innate Lymphoid Cells Support Hematopoietic Recovery Under Stress Conditions. *J Exp Med* (2021) 218:e20200817. doi: 10.1084/jem.20200817
61. van de Pavert SA, Vivier E. Differentiation and Function of Group 3 Innate Lymphoid Cells, From Embryo to Adult. *Int Immunol* (2016) 28:35–42. doi: 10.1093/intimm/dxv052
62. Teng F, Goc J, Zhou L, Chu C, Shah MA, Eberl G, et al. A Circadian Clock Is Essential for Homeostasis of Group 3 Innate Lymphoid Cells in the Gut. *Sci Immunol* (2019) 4:eaax1215. doi: 10.1126/sciimmunol.aax1215
63. Godinho-silva C, Domingues RG, Rendas M, Raposo B. Light-Entrained and Brain-Tuned Circadian Circuits Regulate ILC3 and Gut Homeostasis. *Nature* (2019) 574:254–8. doi: 10.1038/s41586-019-1579-3.Light-entrained
64. Wang Q, Robinette ML, Billon C, Collins PL, Bando JK, Fachi JL, et al. Circadian Rhythm-Dependent and Circadian Rhythm-Independent Impacts of the Molecular Clock on Type 3 Innate Lymphoid Cells. *Sci Immunol* (2019) 4:eaay7501. doi: 10.1126/sciimmunol.aay7501
65. Seillet C, Luong K, Tellier J, Jacquelot N, Shen RD, Hickey P, et al. The Neuropeptide VIP Confers Anticipatory Mucosal Immunity by Regulating ILC3 Activity. *Nat Immunol* (2020) 21:168–77. doi: 10.1038/s41590-019-0567-y
66. Talbot J, Hahn P, Kroehling L, Nguyen H, Li D, Littman DR. Feeding-Dependent VIP Neuron–ILC3 Circuit Regulates the Intestinal Barrier. *Nature* (2020) 579:575–80. doi: 10.1038/s41586-020-2039-9
67. Yu HB, Yang H, Allaire JM, Ma C, Graef FA, Mortha A, et al. Vasoactive Intestinal Peptide Promotes Host Defense Against Enteric Pathogens by Modulating the Recruitment of Group 3 Innate Lymphoid Cells. *Proc Natl Acad Sci USA* (2021) 118:e2106634118. doi: 10.1073/pnas.2106634118
68. Hatfield JK, Brown MA. Group 3 Innate Lymphoid Cells Accumulate and Exhibit Disease-Induced Activation in the Meninges in EAE. *Cell Immunol* (2015) 297:69–79. doi: 10.1016/j.cellimm.2015.06.006
69. Feigin VL, Nichols E, Alam T, Bannick MS, Beghi E, Blake N, et al. Global, Regional, and National Burden of Neurological Disorders, 1990–2016: A Systematic Analysis for the Global Burden of Disease Study 2016. *Lancet Neurol* (2019) 18:459–80. doi: 10.1016/S1474-4422(18)30499-X
70. Garcia JH, Liu KF, Yoshida Y, Lian J, Chen S, Del Zoppo GJ. Influx of Leukocytes and Platelets in an Evolving Brain Infarct (Wistar Rat). *Am J Pathol* (1994) 144:188–99.
71. Eldahshan W, Fagan SC, Ergul A. Inflammation Within the Neurovascular Unit: Focus on Microglia for Stroke Injury and Recovery. *Pharmacol Res* (2019) 147:104349. doi: 10.1016/j.phrs.2019.104349
72. Werner Y, Mass E, Ashok Kumar P, Ulas T, Händler K, Horne A, et al. Cxcr4 Distinguishes HSC-Derived Monocytes From Microglia and Reveals Monocyte Immune Responses to Experimental Stroke. *Nat Neurosci* (2020) 23:351–62. doi: 10.1038/s41593-020-0585-y
73. Gelderblom M, Leypoldt F, Steinbach K, Behrens D, Choe CU, Siler DA, et al. Temporal and Spatial Dynamics of Cerebral Immune Cell Accumulation in Stroke. *Stroke* (2009) 40:1849–57. doi: 10.1161/STROKEAHA.108.534503
74. Gan Y, Liu Q, Wu W, Yin JX, Bai XF, Shen R, et al. Ischemic Neurons Recruit Natural Killer Cells That Accelerate Brain Infarction. *Proc Natl Acad Sci USA* (2014) 111:2704–9. doi: 10.1073/pnas.1315943111
75. Liu Q, Jin W-N, Liu Y, Shi K, Sun H, Zhang F, et al. Brain Ischemia Suppresses Immunity in the Periphery and Brain *via* Different Neurogenic Innervations. *Immunity* (2017) 46:474–87. doi: 10.1016/j.immuni.2017.02.015
76. Klose CSN, Flach M, Möhle L, Rogell L, Hoyler T, Ebert K, et al. Differentiation of Type 1 ILCs From a Common Progenitor to All Helper-Like Innate Lymphoid Cell Lineages. *Cell* (2014) 157:340–56. doi: 10.1016/j.cell.2014.03.030
77. Bederson JB, Pitts LH, Tsuji M, Nishimura MC, Davis RL, Bartkowski H. Rat Middle Cerebral Artery Occlusion: Evaluation of the Model and Development of a Neurologic Examination. *Stroke* (1986) 17:472–6. doi: 10.1161/01.STR.17.3.472
78. Kleinschnitz C, Schwab N, Kraft P, Hagedorn I, Dreykluft A, Schwarz T, et al. Early Detrimental T-Cell Effects in Experimental Cerebral Ischemia Are Neither Related to Adaptive Immunity Nor Thrombus Formation. *Blood* (2010) 115:3835–42. doi: 10.1182/blood-2009-10-249078
79. Yin J, Liao SX, He Y, Wang S, Xia GH, Liu FT, et al. Dysbiosis of Gut Microbiota With Reduced Trimethylamine-N-Oxide Level in Patients With Large-Artery Atherosclerotic Stroke or Transient Ischemic Attack. *J Am Heart Assoc* (2015) 4:1–12. doi: 10.1161/JAHA.115.002699
80. Xia GH, You C, Gao XX, Zeng XL, Zhu JJ, Xu KY, et al. Stroke Dysbiosis Index (SDI) in Gut Microbiome Are Associated With Brain Injury and Prognosis of Stroke. *Front Neurol* (2019) 10:397. doi: 10.3389/fneur.2019.00397
81. Kaskow BJ, Baecher-Allan C. Effector T Cells in Multiple Sclerosis. *Cold Spring Harb Perspect Med* (2018) 8:a029025. doi: 10.1101/cshperspect.a029025
82. Hao J, Liu R, Piao W, Zhou Q, Vollmer TL, Campagnolo DI, et al. Central Nervous System (CNS)-Resident Natural Killer Cells Suppress Th17

Responses and CNS Autoimmune Pathology. *J Exp Med* (2010) 207:1907–21. doi: 10.1084/jem.20092749
83. Kwong B, Rua R, Gao Y, Flickinger J, Wang Y, Kruhlak MJ, et al. Lazarevic V. T-Bet-Dependent NKp46 + Innate Lymphoid Cells Regulate the Onset of T H 17-Induced Neuroinflammation. *Nat Immunol* (2017) 18:1117–27. doi: 10.1038/ni.3816
84. Gate D, Saligrama N, Leventhal O, Yang AC, Unger MS, Middeldorp J, et al. Clonally Expanded CD8 T Cells Patrol the Cerebrospinal Fluid in Alzheimer ' s Disease. *Nature* (2020) 577:399–404. doi: 10.1038/s41586-019-1895-7
85. Friebel E, Kapolou K, Unger S, Núñez NG, Utz S, Rushing EJ, et al. Single-Cell Mapping of Human Brain Cancer Reveals Tumor-Specific Instruction of Tissue-Invading Leukocytes. *Cell* (2020) 181:1626–42. doi: 10.1016/j.cell.2020.04.055
86. Infante-Duarte C, Weber A, Krätzschmar J, Prozorovski T, Pikol S, Hamann I, et al. Frequency of Blood CX 3 CR1-Positive Natural Killer Cells Correlates With Disease Activity in Multiple Sclerosis Patients. *FASEB J* (2005) 19:1902–4. doi: 10.1096/fj.05-3832fje
87. Bielekova B, Catalfamo M, Reichert-Scrivner S, Packer A, Cerna M, Waldmann TA, et al. Regulatory CD56bright Natural Killer Cells Mediate Immunomodulatory Effects of IL-2rα-Targeted Therapy (Daclizumab) in Multiple Sclerosis. *Proc Natl Acad Sci USA* (2006) 103:5941–6. doi: 10.1073/pnas.0601335103
88. Chanvillard C, Millward JM, Lozano M, Hamann I, Paul F, Zipp F, et al. Mitoxantrone Induces Natural Killer Cell Maturation in Patients With Secondary Progressive Multiple Sclerosis. *PLoS One* (2012) 7:e39625. doi: 10.1371/journal.pone.0039625
89. Gross CC, Schulte-Mecklenbeck A, Rünzi A, Kuhlmann T, Posevitz-Fejfár A, Schwab N, et al. Impaired NK-Mediated Regulation of T-Cell Activity in Multiple Sclerosis Is Reconstituted by IL-2 Receptor Modulation. *Proc Natl Acad Sci USA* (2016) 113:E2973–82. doi: 10.1073/pnas.1524924113
90. Morse RHA, Séguin R, McCrea EL, Antel JP. NK Cell-Mediated Lysis of Autologous Human Oligodendrocytes. *J Neuroimmunol* (2001) 116:107–15. doi: 10.1016/S0165-5728(01)00289-2
91. Bowen KE, Mathew SO, Borgmann K, Ghorpade A, Mathew PA. A Novel Ligand on Astrocytes Interacts With Natural Cytotoxicity Receptor NKp44 Regulating Immune Response Mediated by NK Cells. *PLoS One* (2018) 13:1–12. doi: 10.1371/journal.pone.0193008
92. Kunis G, Baruch K, Rosenzweig N, Kertser A, Miller O, Berkutzki T, et al. IFN-γ-Dependent Activation of the Brain's Choroid Plexus for CNS Immune Surveillance and Repair. *Brain* (2013) 136:3427–40. doi: 10.1093/brain/awt259
93. Panza F, Solfrizzi V, Frisardi V, Imbimbo BP, Capurso C, D'Introno A, et al. Beyond the Neurotransmitter-Focused Approach in Treating Alzheimer's Disease: Drugs Targeting β-Amyloid and Tau Protein. *Aging Clin Exp Res* (2009) 21:386–406. doi: 10.1007/BF03327445
94. Deture MA, Dickson DW. The Neuropathological Diagnosis of Alzheimer's Disease. *Mol Neurodegener* (2019) 14:1–18. doi: 10.1186/s13024-019-0333-5
95. Tarkowski E, Andreasen N, Tarkowski A, Blennow K. Intrathecal Inflammation Precedes Development of Alzheimer's Disease. *J Neurol Neurosurg Psychiatry* (2003) 74:1200–5. doi: 10.1136/jnnp.74.9.1200
96. Cribbs DH, Berchtold NC, Perreau V, Coleman PD, Rogers J, Tenner AJ, et al. Extensive Innate Immune Gene Activation Accompanies Brain Aging, Increasing Vulnerability to Cognitive Decline and Neurodegeneration: A Microarray Study. *J Neuroinflamm* (2012) 9:1–18. doi: 10.1186/1742-2094-9-179
97. Zhang B, Gaiteri C, Bodea LG, Wang Z, McElwee J, Podtelezhnikov AA, et al. Integrated Systems Approach Identifies Genetic Nodes and Networks in Late-Onset Alzheimer's Disease. *Cell* (2013) 153:707–20. doi: 10.1016/j.cell.2013.03.030
98. Bis JC, Jian X, Kunkle BW, Chen Y, Hamilton-Nelson KL, Bush WS, et al. Whole Exome Sequencing Study Identifies Novel Rare and Common Alzheimer's-Associated Variants Involved in Immune Response and Transcriptional Regulation. *Mol Psychiatry* (2020) 25:1859–75. doi: 10.1038/s41380-018-0112-7
99. Bromley SK, Akbaba H, Mani V, Mora-Buch R, Chasse AY, Sama A, et al. CD49a Regulates Cutaneous Resident Memory CD8+ T Cell Persistence and Response. *Cell Rep* (2020) 32:108085. doi: 10.1016/j.celrep.2020.108085
100. Aldape K, Amin SB, Ashley DM, Barnholtz-Sloan JS, Bates AJ, Beroukhim R, et al. Glioma Through the Looking GLASS: Molecular Evolution of Diffuse Gliomas and the Glioma Longitudinal Analysis Consortium. *Neuro Oncol* (2018) 20:873–84. doi: 10.1093/neuonc/noy020
101. Suzuki H, Aoki K, Chiba K, Sato Y, Shiozawa Y, Shiraishi Y, et al. Mutational Landscape and Clonal Architecture in Grade II and III Gliomas. *Nat Genet* (2015) 47:458–68. doi: 10.1038/ng.3273
102. Hussain SF, Yang D, Suki D, Aldape K, Grimm E, Heimberger AB. The Role of Human Glioma-Infiltrating Microglia/Macrophages in Mediating Antitumor Immune Responses. *Neuro Oncol* (2006) 8:261–79. doi: 10.1215/15228517-2006-008
103. Lohr J, Ratliff T, Huppertz A, Ge Y, Dictus C, Ahmadi R, et al. Effector T-Cell Infiltration Positively Impacts Survival of Glioblastoma Patients and Is Impaired by Tumor-Derived TGF-β. *Clin Cancer Res* (2011) 17:4296–308. doi: 10.1158/1078-0432.CCR-10-2557
104. Fecci PE, Mitchell DA, Whitesides JF, Xie W, Friedman AH, Archer GE, et al. Increased Regulatory T-Cell Fraction Amidst a Diminished CD4 Compartment Explains Cellular Immune Defects in Patients With Malignant Glioma. *Cancer Res* (2006) 66:3294–302. doi: 10.1158/0008-5472.CAN-05-3773
105. Sedgwick AJ, Ghazanfari N, Constantinescu P, Mantamadiotis T, Barrow AD. The Role of NK Cells and Innate Lymphoid Cells in Brain Cancer. *Front Immunol* (2020) 11:1549. doi: 10.3389/fimmu.2020.01549
106. Kruse PH, Matta J, Ugolini S, Vivier E. Natural Cytotoxicity Receptors and Their Ligands. *Immunol Cell Biol* (2014) 92:221–9. doi: 10.1038/icb.2013.98
107. Garofalo S, Cocozza G, Porzia A, Inghilleri M, Scavizzi F, Aronica E, et al. Natural Killer Cells Modulate Motor Neuron-Immune Cell Cross Talk in Models of Amyotrophic Lateral Sclerosis. *Nat Commun* (2020) 11:1773. doi: 10.1038/s41467-020-15644-8
108. Lünemann A, Lünemann JD, Roberts S, Messmer B, da Silva RB, Raine CS, et al. Human NK Cells Kill Resting But Not Activated Microglia *via* NKG2D- and NKp46-Mediated Recognition. *J Immunol* (2008) 181:6170–7. doi: 10.4049/jimmunol.181.9.6170
109. Halim TYF, Hwang YY, Scanlon ST, Zaghouani H, Garbi N, Fallon PG, et al. Group 2 Innate Lymphoid Cells License Dendritic Cells to Potentiate Memory TH2 Cell Responses. *Nat Immunol* (2016) 17:57–64. doi: 10.1038/ni.3294
110. Walsh JT, Hendrix S, Boato F, Smirnov I, Zheng J, Lukens JR, et al. MHCII-Independent CD4+ T Cells Protect Injured CNS Neurons *via* IL-4. *J Clin Invest* (2015) 125:699–714. doi: 10.1172/JCI76210
111. Hirose S, Jahani PS, Wang S, Jaggi U, Tormanen K, Yu J, et al. Type 2 Innate Lymphoid Cells Induce CNS Demyelination in an HSV-IL-2 Mouse Model of Multiple Sclerosis. *iScience* (2020) 23:101549. doi: 10.1016/j.isci.2020.101549
112. Koch-Henriksen N, Sørensen PS. The Changing Demographic Pattern of Multiple Sclerosis Epidemiology. *Lancet Neurol* (2010) 9:520–32. doi: 10.1016/S1474-4422(10)70064-8
113. Khalid R. Contributing Factors in Multiple Sclerosis and the Female Sex Bias. *Immunol Lett* (2014) 162:223–32. doi: 10.1016/j.imlet.2014.09.004
114. Russi AE, Ebel ME, Yang Y, Brown MA. Male-Specific IL-33 Expression Regulates Sex-Dimorphic EAE Susceptibility. *Proc Natl Acad Sci USA* (2018) 115:E1520–9. doi: 10.1073/pnas.1710401115
115. Saranchova I, Han J, Zaman R, Arora H, Huang H, Fenninger F, et al. Type 2 Innate Lymphocytes Actuate Immunity Against Tumours and Limit Cancer Metastasis. *Sci Rep* (2018) 8:1–17. doi: 10.1038/s41598-018-20608-6
116. Ostrom QT, Gittleman H, Xu J, Kromer C, Wolinsky Y, Kruchko C, et al. CBTRUS Statistical Report: Primary Brain and Other Central Nervous System Tumors Diagnosed in the United States in 2009-2013. *Neuro Oncol* (2016) 18:v1–v75. doi: 10.1093/neuonc/now207
117. De Boeck A, Ahn BY, D'Mello C, Lun X, Menon SV, Alshehri MM, et al. Glioma-Derived IL-33 Orchestrates an Inflammatory Brain Tumor Microenvironment That Accelerates Glioma Progression. *Nat Commun* (2020) 11:4997. doi: 10.1038/s41467-020-18569-4
118. van de Pavert SA. Lymphoid Tissue Inducer (LTi) Cell Ontogeny and Functioning in Embryo and Adult. *BioMed J* (2021) 44:123–32. doi: 10.1016/j.bj.2020.12.003
119. Luo S, Zhu R, Yu T, Fan H, Hu Y, Mohanta SK, et al. Chronic Inflammation: A Common Promoter in Tertiary Lymphoid Organ Neogenesis. *Front Immunol* (2019) 10:2938. doi: 10.3389/fimmu.2019.02938
120. Shields JD, Kourtis IC, Tomei A a, Roberts JM, Swartz MA. Induction of Lymphoidlike Stroma and Immune Escape by Tumors That Express the Chemokine CCL21. *Science (80-)* (2010) 328:749–52. doi: 10.1126/science.1185837

121. van de Pavert SA, Olivier BJ, Goverse G, Vondenhoff MF, Greuter M, Beke P, et al. Chemokine CXCL13 Is Essential for Lymph Node Initiation and Is Induced by Retinoic Acid and Neuronal Stimulation. *Nat Immunol* (2009) 10:1193–9. doi: 10.1038/ni.1789
122. Ragheb S, Li Y, Simon K, Vanhaerents S, Galimberti D, De Riz M, et al. Multiple Sclerosis: BAFF and CXCL13 in Cerebrospinal Fluid. *Mult Scler J* (2011) 17:819–29. doi: 10.1177/1352458511398887
123. Serafini B, Rosicarelli B, Veroni C, Zhou L, Reali C, Aloisi F. Rorγt Expression and Lymphoid Neogenesis in the Brain of Patients With Secondary Progressive Multiple Sclerosis. *J Neuropathol Exp Neurol* (2016) 75:877–88. doi: 10.1093/jnen/nlw063
124. Gross CC, Schulte-Mecklenbeck A, Hanning U, Posevitz-Fejfár A, Korsukewitz C, Schwab N, et al. Distinct Pattern of Lesion Distribution in Multiple Sclerosis Is Associated With Different Circulating T-Helper and Helper-Like Innate Lymphoid Cell Subsets. *Mult Scler J* (2017) 23:1025–30. doi: 10.1177/1352458516662726
125. Schropp V, Rohde J, Rovituso DM, Jabari S, Bharti R, Kuerten S. Contribution of LTi and TH17 Cells to B Cell Aggregate Formation in the Central Nervous System in a Mouse Model of Multiple Sclerosis. *J Neuroinflamm* (2019) 16:111. doi: 10.1186/s12974-019-1500-x
126. Kim M-Y, Anderson G, White A, Jenkinson E, Arlt W, Martensson I-L, et al. OX40 Ligand and CD30 Ligand Are Expressed on Adult But Not Neonatal CD4 + CD3 – Inducer Cells: Evidence That IL-7 Signals Regulate CD30 Ligand But Not OX40 Ligand Expression. *J Immunol* (2005) 174:6686–91. doi: 10.4049/jimmunol.174.11.6686
127. Grigg JB, Shanmugavadivu A, Regen T, Parkhurst CN, Ahmed A, Joseph AM, et al. Antigen-Presenting Innate Lymphoid Cells Orchestrate Neuroinflammation. *Nature* (2021) 600:707–12. doi: 10.1038/s41586-021-04136-4
128. Simic M, Manosalva I, Spinelli L, Gentek R, Shayan RR, Siret C, et al. Distinct Waves From the Hemogenic Endothelium Give Rise to Layered Lymphoid Tissue Inducer Cell Ontogeny. *Cell Rep* (2020) 32:108004. doi: 10.1016/j.celrep.2020.108004
129. Withers DR, Gaspal FM, Bekiaris V, McConnell FM, Kim M, Anderson G, et al. OX40 and CD30 Signals in CD4(+) T-Cell Effector and Memory Function: A Distinct Role for Lymphoid Tissue Inducer Cells in Maintaining CD4(+) T-Cell Memory But Not Effector Function. *Immunol Rev* (2011) 244:134–48. doi: 10.1111/j.1600-065X.2011.01057.x
130. Deng T, Suo C, Chang J, Yang R, Li J, Cai T, et al. ILC3-Derived OX40L Is Essential for Homeostasis of Intestinal Tregs in Immunodeficient Mice. *Cell Mol Immunol* (2020) 17:163–77. doi: 10.1038/s41423-019-0200-x
131. Ito M, Komai K, Mise-Omata S, Iizuka-Koga M, Noguchi Y, Kondo T, et al. Brain Regulatory T Cells Suppress Astrogliosis and Potentiate Neurological Recovery. *Nature* (2019) 565:246–50. doi: 10.1038/s41586-018-0824-5
132. Lim AI, Li Y, Lopez-Lastra S, Stadhouders R, Paul F, Casrouge A, et al. Systemic Human ILC Precursors Provide a Substrate for Tissue ILC Differentiation. *Cell* (2017) 168:1086–100.e10. doi: 10.1016/j.cell.2017.02.021
133. Moretti R, Pansiot J, Bettati D, Strazielle N, Ghersi-Egea JF, Damante G, et al. Blood-Brain Barrier Dysfunction in Disorders of the Developing Brain. *Front Neurosci* (2015) 9:40. doi: 10.3389/fnins.2015.00040
134. Derk J, Jones HE, Como C, Pawlikowski B, Siegenthaler JA. Living on the Edge of the CNS: Meninges Cell Diversity in Health and Disease. *Front Cell Neurosci* (2021) 15:703944. doi: 10.3389/fncel.2021.703944
135. Ichikawa H, Itoh K. Blood-Arachnoid Barrier Disruption in Experimental Rat Meningitis Detected Using Gadolinium-Enhancement Ratio Imaging. *Brain Res* (2011) 1390:142–9. doi: 10.1016/j.brainres.2011.03.035
136. Yang Y, Torbey MT. Angiogenesis and Blood-Brain Barrier Permeability in Vascular Remodeling After Stroke. *Curr Neuropharmacol* (2020) 18:1250–65. doi: 10.2174/1570159x18666200720173316
137. Wang Y, Zhang F, Xiong N, Xu H, Chai S, Wang H, et al. Remodelling and Treatment of the Blood-Brain Barrier in Glioma. *Cancer Manag Res* (2021) 13:4217–32. doi: 10.2147/CMAR.S288720
138. Abdullahi W, Tripathi D, Ronaldson PT. Blood-Brain Barrier Dysfunction in Ischemic Stroke: Targeting Tight Junctions and Transporters for Vascular Protection. *Am J Physiol - Cell Physiol* (2018) 315:C343–56. doi: 10.1152/ajpcell.00095.2018
139. Wallrapp A, Riesenfeld SJ, Burkett PR, Abdulnour R-EE, Nyman J, Dionne D, et al. The Neuropeptide NMU Amplifies ILC2-Driven Allergic Lung Inflammation. *Nature* (2017) 549:351–6. doi: 10.1038/nature24029

Conflict of Interest: The authors declare that the research was conducted in the absence of any commercial or financial relationships that could be construed as a potential conflict of interest.

frontiers | Frontiers in Immunology

MINI REVIEW
published: 29 April 2022
doi: 10.3389/fimmu.2022.877005

Tissue Resident and Migratory Group 2 Innate Lymphoid Cells

Laura Mathä[1], *Fumio Takei*[2,3] *and Itziar Martinez-Gonzalez*[1]*

[1] Department of Microbiology, Tumor and Cell Biology, Karolinska Institutet, Solna, Sweden, [2] Terry Fox Laboratory, British Columbia Cancer, Vancouver, BC, Canada, [3] Department of Pathology and Laboratory Medicine, University of British Columbia, Vancouver, BC, Canada

Group 2 innate lymphoid cells (ILC2s) are present in both mouse and human mucosal and non-mucosal tissues and implicated in initiating type 2 inflammation. ILC2s are considered to be tissue resident cells that develop in the perinatal period and persist throughout life with minimal turning over in adulthood. However, recent studies in animal models have shown their ability to circulate between different organs during inflammation and their potential functions in the destined organs, suggesting their roles in mediating multiple type 2 diseases. Here, we review recent findings on ILC2 migration, including migration within, into and out of tissues during inflammation.

Keywords: group 2 innate lymphoid cells, type 2 inflammation, tissue residency, recruitment, migration

OPEN ACCESS

Edited by:
Carmelo Luci,
Institut National de la Santé et de la Recherche Médicale (INSERM), France

Reviewed by:
Kenta Shinoda,
Pfizer, United States
Lei Shen,
Shanghai Jiao Tong University, China

***Correspondence:**
Itziar Martinez-Gonzalez
itziar.martinez.gonzalez@ki.se

Specialty section:
This article was submitted to NK and Innate Lymphoid Cell Biology, a section of the journal Frontiers in Immunology

Received: *16 February 2022*
Accepted: *08 April 2022*
Published: *29 April 2022*

Citation:
Mathä L, Takei F and Martinez-Gonzalez I (2022) Tissue Resident and Migratory Group 2 Innate Lymphoid Cells. Front. Immunol. 13:877005. doi: 10.3389/fimmu.2022.877005

INTRODUCTION – TISSUE RESIDENCY OF ILC2S

ILC2s reside at barrier surfaces, such as the skin, lung and intestine and are activated by cytokines released upon tissue damage, such as IL-33, IL-25 and thymic stromal lymphopoietin (TSLP) (1). They potently produce type 2 cytokines, IL-5 and IL-13, and initiate a cascade of reactions leading to type 2 inflammation. Owing to their ability to produce copious amounts of type 2 cytokines, they have been implicated in various type 2 inflammatory diseases, such as asthma and atopic dermatitis (2). The tissue resident nature of ILC2s was initially reported using parabiosis mouse models, where congenic mice were surgically joined together to investigate migratory capacity of cells. Gasteiger et al. demonstrated that more than 95% of ILCs in small intestine (SI), salivary gland, lung and liver are tissue resident with minimal trafficking at homeostasis (3). Interestingly, there was a slight increase in ILC2s derived from the paired parabiont in a long-term parabiosis experiment (3), suggesting some degree of ILC2 replenishment from hematogenous sources, but to a much lesser extent compared to circulatory lymphocytes, such as NK, T and B cells. They also demonstrated tissue residency of ILC2s in inflammatory conditions by using a mouse model of *Nippostrongylus brasiliensis* (Nb) infection in parabiotic mice. During acute Nb infection, ILC2s locally expanded and very little influx of ILC2s derived from the other parabiont was observed. In contrast, minor but significant recruitment of ILC2s was observed during the chronic infections. Moro et al. also reported local expansion of tissue resident ILC2s in fat-associated lymphoid clusters (FALC), lung and bronchoalveolar lavage fluid (BALF) during respiratory inflammation induced by intratracheal IL-33 administration into parabiotic mice (4). Many other groups also used parabiosis models and confirmed ILC2 tissue residency at homeostasis and during inflammation (5–8).

TISSUE SEEDING AND ADAPTATION TO THE TISSUE ENVIRONMENT

ILC precursors and ILC2s can be detected in the fetal intestine, lung and skin during embryonic development in mice (7, 9), while the majority of adult ILC2s seems to be neonatally derived (**Figure 1A**). Several studies showed that ILC2s are rare in mouse lungs right after birth, but they gradually increase in number, reaching a peak around two weeks after birth (10–12). Knock out mouse studies and antibody blocking showed that this ILC2 expansion is dependent on IL-33 and IL-7 signaling (7, 11, 12). The defect in ILC2 expansion in the absence of IL-33 signals is likely due to the impairment of ILC2 progenitor (ILC2P) egress from the bone marrow (BM), as ST2 deficient mice have increased numbers of ILC2P in the BM in parallel with reduced number of ILC2s in the lung 2 weeks after birth (6). The neonatal wave of ILC2 proliferation and activation is not only limited to the lung but seems systemic as high percentages

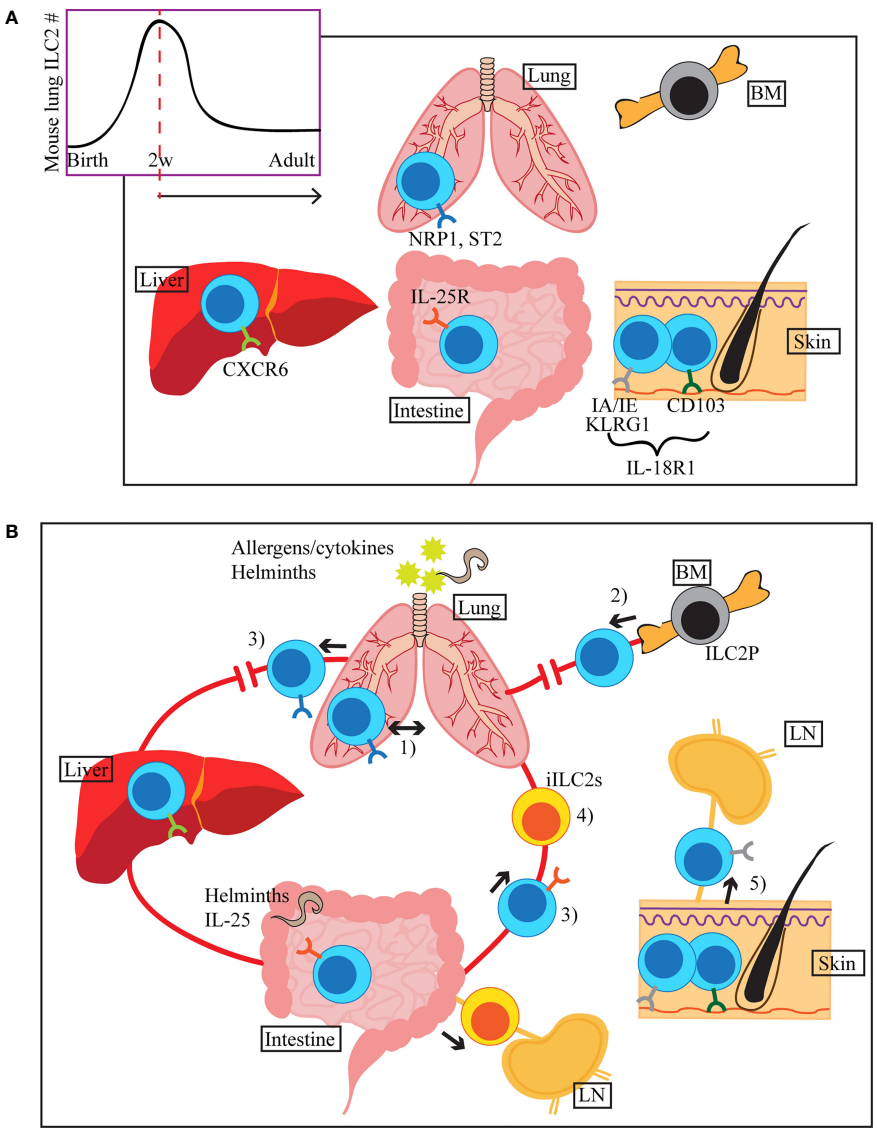

FIGURE 1 | **(A)** ILC2s seed tissues early during the neonatal period, with a peak of ILC2 accumulation around 2 weeks after birth (mouse lung). Once in tissues, they receive environmental cues and adapt tissue specific phenotypes, indicated by different colours of the surface receptors in the figure. Common ILC2 markers in each tissue are shown, but they can also be expressed in other organs. **(B)** ILC2s migrate within the lung upon i.n. IL-33 or Aa treatment (1). During allergen-induced respiratory inflammation or tissue disruption, ILC2s are recruited from hematogenous sources (2). When activated by allergens/cytokines or helminth infection, some of the lung and small intestinal ILC2s appear in the peripheral blood (3). Stimulation by i.n. IL-33 or papain induces migration of a subset of lung ILC2s to the liver, where they contribute to the regulation of local immunity (3). Upon helminth infection or i.p. IL-25 stimulation, small intestine-derived inflammatory ILC2s (iILC2s) appear in circulation and accumulate in the lung, liver, mesenteric LN and spleen (4). iILC2s ultimately become conventional ILC2s in the lung. Tissue resident and circulating ILC2s are present in the skin. During atopic dermatitis-like inflammation, circulatory ILC2s migrate to the draining LN (5).

of Ki67$^+$ and IL-5$^+$ ILC2s were observed in the SI and skin as well (7). Schneider et al. used tamoxifen-inducible Cre approach to irreversibly label prenatal and postnatal ILC2s and showed that the majority of adult lung, visceral adipose tissue and ST2$^+$ SI ILC2s develop in the neonatal period while a small fraction of prenatally-derived ILC2s contributes to the adult pool of ILC2s (7). In contrast, the proportion of the neonatally-derived skin, BM and IL-25R$^+$ SI ILC2s rapidly declined, suggesting that the turnover rate of ILC2s differs depending on the tissue environment (7). Overall, this and our own studies detected very few ILC2s slowly turning over in adult mice (7, 13, 14).

Once in peripheral tissues, ILC2s are phenotypically and functionally adapted to the tissue specific environment of the residing organs. This was shown by single cell RNA sequencing (scRNAseq) analyses of ILC2s isolated from various adult mouse organs, which revealed tissue-specific transcriptomic signature of ILC2s (15). For instance, intestinal ILC2s have enhanced expression of *Il17rb* and *Ikzf3* (encodes Aiolos) and lung ILC2s express *Nrp1*, while skin ILC2s highly express *Il18r1* (15, 16). Interestingly, ILC2 turnover is strikingly different depending on their residing tissues, further supporting tissue specific dynamics of these cells. The ILC2 pool is relatively stable in the lung, SI and adipose tissues, whereas ILC2s are quickly replenished by newly generated pool of ILC2s in the skin and BM (7). It is possible that each tissue has its specific ILC precursor populations that contribute to the maintenance of ILC2 pool at homeostasis and ILC2-poiesis during inflammation. Indeed, recent work has identified the presence of IL-18R1$^+$ ST2$^-$ tissue ILC precursors in mouse lung (17, 18).

It is important to note that tissue distribution of ILC2s differ depending on the species. In the human system, helper ILCs, including ILC2s, are underrepresented in the non-mucosal compared to the mucosal tissues due to the abundance of NK cells, similar to mice (19). However, ILC2s are relatively rare in human SI (20), whereas they are one of the major ILC populations in mouse SI (8, 21).

ILC2 RECRUITMENT DURING INFLAMMATION AND TISSUE DISRUPTION

Although Gasteiger et al. demonstrated ILC2 tissue residency under steady-state and acute inflammatory conditions using parabiotic mice, they did observe significant infiltration of donor-derived ILC2s during chronic Nb infections (3). These data suggested potential recruitment of ILC2s from hematogenous sources in chronic inflammatory conditions. Karta et al. showed that ILC2 numbers were reduced in the BM after intranasal (i.n.) treatment of mice with the fungal allergen, *Alternaria alternata* (Aa). In parallel, they observed ILC2 increase in the blood and lung, suggesting that ILC2s emigrate from the BM, circulate and are recruited to the lung during airway inflammation (22). This recruitment was mediated by β2 integrin. Stier et al. similarly used Aa induced lung inflammation model to show elevated IL-33 levels in the serum, and IL-33 dependent egress of ILC2P from the BM (6). Moreover, systemic treatment of mice with intravenous IL-33 injections caused egress of ILC2P from the BM partially through downregulation of CXCR4 (6). These data suggest that, in Aa induced inflammation, ILC2P may be mobilized in response to IL-33 release by regulating β2 integrin and CXCR4 expressions.

In the same study, Stier and colleagues used the parabiotic system, where one parabiont was irradiated before parabiosis surgery, to model tissue disruption (6). ILC2s derived from non-irradiated parabiont readily reconstituted the irradiated parabiont, illustrating the ability of ILC2s to migrate and fill the empty niche. A similar observation has been made in the human system, where ILC2 reconstitution occurred in severe combined immunodeficiency (SCID) patients who underwent hematopoietic stem cell transplantation (HSCT) in myeloablative conditions (23). This suggests that ILC2 recruitment to an empty niche may occur upon tissue disruption, which likely provides signals for ILC2-poiesis and recruitment. However, it is unclear whether ILC2s can repopulate the empty niches under homeostatic condition. When parabiotic mice were generated between ILC2 sufficient and deficient (*Il7r*$^{-/-}$, also deficient in T and B cells) mice, ILC2s did not efficiently reconstitute the deficient host (7).

The idea of ILC recruitment is supported by some human studies. CD117$^+$ ILCs in human peripheral blood have been described as circulating ILC precursors that can give rise to all ILC subsets *in vitro* and *in vivo* upon transfer into immunodeficient mice (24). Authors suggested that these ILC precursors can generate tissue ILCs when required in steady-state or during inflammation. In another study, scRNAseq of blood and tissue ILC2s demonstrated that blood ILC2s express cell trafficking associated genes, such as *S1PR2* and *CCR2*, whereas lung ILC2s have activation-related phenotype characterized by the expression of the receptors for ILC2 activating cytokines, *IL1RL1* and *IL17RB* (25). This observation led authors to hypothesize that blood ILC2s may be recruited to the lung, where they become responsive to epithelium-derived cytokines. Stimulation of blood ILC2s with ILC2-activating cytokines indeed induced IL-1RL1 (IL-33 receptor) and IL-17RB (IL-25 receptor) expression in blood ILC2s, which resemble the phenotype of lung ILC2s. It has also been shown, in asthmatic patients, that ILC2s accumulate in BALF after allergen challenge, whereas circulating ILC2 numbers decrease at the same time, suggesting that ILC2s are recruited from circulation into the lung during inflammation (26).

Overall, despite their tissue resident nature, existing data indicate that ILC2s can be *de novo* generated and recruited to tissues to meet the production demand, during inflammation and tissue disruption. The disparity between the reports demonstrating local expansion of ILC2s and those that show ILC2 recruitment during inflammation can be on account of several factors. First of all, the majority of the studies that demonstrated tissue residency of ILC2s were in mouse models of Nb infection or IL-33 treatment in parabiosis mice (3–5, 8), whereas those that showed recruitment were Aa model in non-parabiotic mice, where ILC2 recruitment was determined based

on decrease in ILC2P/ILC2 in the BM (6, 22). Stier et al. saw an increase in IL-33 in the serum after Aa treatment (6), while we did not detect it after i.n. IL-33 treatment (8), indicating that the inflammatory events that occur upon the initiation of immune responses can greatly differ depending on the model. The strain of mice and identification of ILC2s are also inconsistent among these papers, and consequently, we cannot directly compare different studies. Lastly, the time point of the analyses is determined by the models and thus differs in each study. Therefore, considering all of the potential variables among these reports, it is likely that recruitment and local expansion of ILC2s are not mutually exclusive events during inflammation but rather they may occur sequentially or concurrently. It is also possible that in some cases, local expansion of ILC2s dominate, while recruited ILC2s are the primary responders in other cases.

ILC2 MIGRATION DURING INFLAMMATION

As the first line of defense in barrier tissues, ILC2s exhibit dynamic behaviour within tissues upon exposure to damage signals. Recent evidence also suggests that a subset of ILC2s may leave their residing tissues, circulate and migrate to a different organ(s) once activated (**Figure 1B**).

ILC2 Migration Within Organs

ILC2s in multiple organs, including the lung, liver, brain meninges and adipose tissue, reside in perivascular adventitial cuff spaces (27, 28). In the lung, the majority of the ILC2s are in proximity to adventitial stromal cells, which produce IL-33 and TSLP (27). However, i.n. IL-33 or Aa treatment in mice induces ILC2 motility around blood vessels and airways, where ILC2s exhibit amoeboid-like movement (29). Interestingly, ILC2s present much more motile behaviour compared to $CD4^+$ T cells in these models. Intra-organ motility and activation of lung ILC2s are dependent on chemotactic signal through CCR8 in IL-33 treated mice, whereas its ligand CCL8 also induces migration of human ILC2s. TGF-β has also previously been shown to increase the basal motility of ILC2s in mice (30). The induction of ILC2 motility during IL-33 mediated inflammation was, at least in part, due to collagen I in the extracellular matrix (ECM), which provides signals to alter ILC2 shape towards pro-migratory phenotype with polarized F-actin arrangement (29).

Dahlgren et al. previously reported that ILC2s primarily remain in the adventitial cuff spaces during inflammation induced by Nb infection, papain treatment or systemic IL-33 injections, while a small proportion of them also expands in the parenchyma (27). In the recent report by Cautivo et al., the authors closely examined the topographic distributions of ILC2s during mixed inflammation induced by exogenous IL-33 + IFNγ treatment or Nb + *Listeria monocytogenes* infections (28). Although the majority of ILC2s reside near the adventitial space in steady state, type 2 inflammation induced their expansion in the parenchyma. In the mixed inflammation models, IFNγ restricted parenchymal ILC2 expansion and promoted their cell death. RNAseq analyses revealed that IFNγ suppressed cell survival and movement associated pathways. Moreover, IL-33 repressed ILC2 retention-associated genes, such as *Cd44* and *Cd69*, while it induced cell trafficking-related genes, including *S1pr1*, *S1pr4*, chemokine receptors and integrins. The authors suggest two potential mechanisms by which ILC2s traffic to the parenchyma. They either migrate from the adventitia to parenchyma, or they enter directly from circulation into parenchymal areas, which requires further investigation. However, lung and liver ILC2 accumulation in the parenchyma was inhibited by blockade of S1PRs, suggesting that the latter may be the dominant mechanism.

ILC2 Emigration to Other Organs Upon Activation

Although ILC2s are rare in naïve mouse blood, they are readily detectable in healthy human peripheral blood (19, 20). Circulating ILC2s in healthy human blood are considered naïve as they express the CD45RA isoform of the CD45 receptor (31), which is expressed by naïve T cells (32). Previous studies reported that the frequency of ILC2s is elevated in the peripheral blood of patients with allergic diseases, such as asthma (33). Therefore, it is possible that these ILC2s are in circulation en route to the site of inflammation as described earlier. However, it is also likely that these ILC2s have left their residing tissues after being activated. Indeed, several recent mouse studies have described activation induced migratory behaviour of ILC2s. Intraperitoneal (i.p.) injections of mice with IL-25 induces an expansion of $KLRG1^+ST2^-$ ILC2s, also known as inflammatory ILC2s (iILC2s), in the lung, liver, mesenteric LN and spleen (34). These cells are rare in naïve mice but are elicited by IL-25 stimulation and Nb infection. They are transient cells appearing at an early stage of inflammation and eventually become $ST2^+$ conventional ILC2s in tissues. In a later study by the same group, it was found that iILC2s are circulatory cells that originate in the intestine and migrate in a sphingosine 1 phosphate (S1P) dependent manner upon IL-25 stimulation or Nb infection (5). It is important to note that a human equivalent of mouse iILC2s has recently been identified in the nasal polyps (NP) of the patients with chronic rhinosinusitis with nasal polyps (CRSwNP) (31). These ILC2s exhibited activated gene expression profiles and were marked by the expression of CD45RO, which is a well-established marker of activated T cells (32). $CD45RO^+$ ILC2 were enriched in the gene signature of mouse iILC2s (31). Interestingly, these $CD45RO^+$ ILC2s were not only present in the inflamed tissues, but also increased in the peripheral blood of the CRSwNP patients compared to healthy controls, suggesting that they may have migrated out of the inflamed nasal tissue.

Ricardo-Gonzalez et al. investigated ILC2s that appear in circulation upon Nb infections in mice (35). Circulatory ILC2s elicited after Nb infections exhibited two distinct phenotypes at different time points during the course of infection. The first circulatory ILC2 wave, which appears on day 5 after infection, was accounted for by IL-25 dependent SI ILC2s. In contrast, the

second wave on day 12 was due to IL-33 dependent lung ILC2s. Migration of ILC2s was S1P dependent. These results indicated the potential of ILC2s residing in various organs to invade circulation upon activation and propagate local immune response to systemic type 2 immunity.

Nakatani-Kusakabe et al. recently performed scRNAseq of skin and draining LN of IL-33 transgenic (IL33tg) mice (36). These mice express IL-33 under the control of keratin 14 promoter and spontaneously develop atopic dermatitis (AD)-like skin inflammation (37). They identified two clusters, cluster 1 and 2, of ILC2s in the skin, while only cluster 1 was present in the draining LN. They hypothesized that only cluster 1 is migratory, and thus named the two clusters "circulating" and "resident" ILC2s, respectively (36). To track ILC2s, they crossed IL33tg mice with photoconvertible KikGR knock in mice, which upon exposure to violet light, undergo irreversible photoconversion from green to red fluorescence (38). Using these mice, they labeled skin cells and analyzed skin-derived and LN ILC2s in the LN by scRNAseq (36). Interestingly, skin (red) and LN (green) ILC2s shared gene signatures, suggesting that LN ILC2s are a single subset of migratory ILC2s that have migrated from the skin, while skin ILC2s consists of resident and migratory ILC2s. The "circulating" ILC2s uniquely expressed IA/IE and KLRG1, while only skin "resident" ILC2s expressed CD103, which is a known marker of skin ILC2s (39). While both subsets can produce type 2 cytokines, skin "resident" ILC2s have a higher capacity to produce them compared to the "circulating" subset.

We recently followed lung ILC2s after activation by i.n. administration of IL-33 or the protease allergen papain to determine the destination of migratory ILC2s (8). Similar to the studies described above, ILC2s quickly appeared in circulation after activation in the lung and their migration was dependent on S1P signaling. ILC2 numbers also increased in the spleen and liver, but not in the SI. Interestingly, liver ILC2 numbers remained higher than those in naïve mice even a month after initial activation in the lung. Lung-derived ILC2s promoted fibrotic inflammation in the liver in an IL-33 induced type 2 inflammation model, whereas they exerted protective effects in concanavalin A induced acute hepatitis model (8). Based on the phenotypic analyses, we determined that the migratory ILC2s are a subset of ILC2s which expresses the chemokine receptor CXCR6, a surface molecule readily detected on the liver resident ILC2s. In contrast, they lack the expression of CD103, which is highly expressed by the activated lung ILC2s (8). ILC2s that accumulated in the liver after i.n. IL-33 treatment also produced more IL-6 compared to lung ILC2s. This study highlighted the possibility of migratory ILC2s to mediate inflammatory events in two different organs and potential connections between various allergic diseases. However, the physiological contribution of the migratory ILC2s in linking several human diseases is currently unclear and requires further investigation.

CONCLUSION AND FUTURE PERSPECTIVE

ILC2s are widely accepted as tissue resident lymphocytes under steady-state and inflammatory conditions. Hence, the majority of the studies in the field has focused on the pathological or protective roles of ILC2s in the sites where they reside. However, recent evidence in mouse models highlight the capacity of ILC2s to circulate and migrate between tissues upon activation, which is supported by evidence from human studies. This opens up a whole new avenue of research investigating connections between various type 2 immune mediated diseases, which is currently lacking. Understanding the mechanisms by which ILC2s traffic between tissues, heterogeneity among tissue resident and migratory ILC2s and their functions will be key areas of investigation in the future research, which may lead to the development of therapies specifically targeting the migratory populations of ILC2s.

AUTHOR CONTRIBUTIONS

LM wrote and edited the manuscript and generated the figure. FT and IM-G reviewed the drafts, provided critical input, and edited the manuscript and figure. All authors contributed to the article and approved the submitted version.

FUNDING

This work was supported by grants from the Canadian Institutes of Health Research (GR018902) and the Knut and Alice Wallenberg Foundation (2019.0221).

REFERENCES

1. Martinez-Gonzalez I, Steer CA, Takei F. Lung ILC2s Link Innate and Adaptive Responses in Allergic Inflammation. *Trends Immunol* (2015) 36:189–95. doi: 10.1016/j.it.2015.01.005
2. Halim TYF. Group 2 Innate Lymphoid Cells in Disease. *Int Immunol* (2016) 28:13–22. doi: 10.1093/intimm/dxv050
3. Gasteiger G, Fan X, Dikiy S, Lee SY, Rudensky AY. Tissue Residency of Innate Lymphoid Cells in Lymphoid and Nonlymphoid Organs. *Science* (2015) 350:981–5. doi: 10.1126/science.aac9593
4. Moro K, Kabata H, Tanabe M, Koga S, Takeno N, Mochizuki M, et al. Interferon and IL-27 Antagonize the Function of Group 2 Innate Lymphoid Cells and Type 2 Innate Immune Responses. *Nat Immunol* (2016) 17:76–86. doi: 10.1038/ni.3309
5. Huang Y, Mao K, Chen X, Sun MA, Kawabe T, Li W, et al. S1P-Dependent Interorgan Trafficking of Group 2 Innate Lymphoid Cells Supports Host Defense. *Science* (2018) 359:114–9. doi: 10.1126/science.aam5809
6. Stier MT, Zhang J, Goleniewska K, Cephus JY, Rusznak M, Wu L, et al. IL-33 Promotes the Egress of Group 2 Innate Lymphoid Cells From the Bone Marrow. *J Exp Med* (2018) 215:263–81. doi: 10.1084/jem.20170449
7. Schneider C, Lee J, Koga S, Ricardo-Gonzalez RR, Nussbaum JC, Smith LK, et al. Tissue-Resident Group 2 Innate Lymphoid Cells Differentiate by Layered Ontogeny and *In Situ* Perinatal Priming. *Immunity* (2019) 50:1425–38.e5. doi: 10.1016/j.immuni.2019.04.019

8. Mathä L, Romera-Hernández M, Steer CA, Yin YH, Orangi M, Shim H, et al. Migration of Lung Resident Group 2 Innate Lymphoid Cells Link Allergic Lung Inflammation and Liver Immunity. *Front Immunol* (2021) 12:679509. doi: 10.3389/fimmu.2021.679509
9. Bando JK, Liang H-E, Locksley RM. Identification and Distribution of Developing Innate Lymphoid Cells in the Fetal Mouse Intestine. *Nat Immunol* (2015) 16:153–60. doi: 10.1038/ni.3057
10. de Kleer IM, Kool M, de Bruijn MJW, Willart M, van Moorleghem J, Schuijs MJ, et al. Perinatal Activation of the Interleukin-33 Pathway Promotes Type 2 Immunity in the Developing Lung. *Immunity* (2016) 45:1285–98. doi: 10.1016/j.immuni.2016.10.031
11. Steer CA, Martinez-Gonzalez I, Ghaedi M, Allinger P, Mathä L, Takei F. Group 2 Innate Lymphoid Cell Activation in the Neonatal Lung Drives Type 2 Immunity and Allergen Sensitization. *J Allergy Clin Immunol* (2017) 140:593–5.e3. doi: 10.1016/j.jaci.2016.12.984
12. Saluzzo S, Gorki AD, Rana BMJ, Martins R, Scanlon S, Starkl P, et al. First-Breath-Induced Type 2 Pathways Shape the Lung Immune Environment. *Cell Rep* (2017) 18:1893–905. doi: 10.1016/j.celrep.2017.01.071
13. Martinez-Gonzalez I, Mathä L, Steer CA, Ghaedi M, Poon GFT, Takei F. Allergen-Experienced Group 2 Innate Lymphoid Cells Acquire Memory-Like Properties and Enhance Allergic Lung Inflammation. *Immunity* (2016) 45:198–208. doi: 10.1016/j.immuni.2016.06.017
14. Ghaedi M, Steer CA, Martinez-Gonzalez I, Halim TYF, Abraham N, Takei F. Common-Lymphoid-Progenitor-Independent Pathways of Innate and T Lymphocyte Development. *Cell Rep* (2016) 15:471–80. doi: 10.1016/j.celrep.2016.03.039
15. Ricardo-Gonzalez RR, van Dyken SJ, Schneider C, Lee J, Nussbaum JC, Liang HE, et al. Tissue Signals Imprint ILC2 Identity With Anticipatory Function. *Nat Immunol* (2018) 19:1093–9. doi: 10.1038/s41590-018-0201-4
16. Qiu J, Zhang J, Ji Y, Sun H, Gu Z, Sun Q, et al. Tissue Signals Imprint Aiolos Expression in ILC2s to Modulate Type 2 Immunity. *Mucosal Immunol* (2021) 14:1306–22. doi: 10.1038/s41385-021-00431-5
17. Ghaedi M, Shen ZY, Orangi M, Martinez-Gonzalez I, Wei L, Lu X, et al. Single-Cell Analysis of Rorα Tracer Mouse Lung Reveals ILC Progenitors and Effector ILC2 Subsets. *J Exp Med* (2020) 217:jem.20182293. doi: 10.1084/jem.20182293
18. Zeis P, Lian M, Fan X, Herman JS, Hernandez DC, Gentek R, et al. *In Situ* Maturation and Tissue Adaptation of Type 2 Innate Lymphoid Cell Progenitors. *Immunity* (2020) 53:775–792.e9. doi: 10.1016/j.immuni.2020.09.002
19. Simoni Y, Fehlings M, Kløverpris HN, McGovern N, Koo SL, Loh CY, et al. Human Innate Lymphoid Cell Subsets Possess Tissue-Type Based Heterogeneity in Phenotype and Frequency. *Immunity* (2017) 46:148–61. doi: 10.1016/j.immuni.2016.11.005
20. Mjösberg JM, Trifari S, Crellin NK, Peters CP, van Drunen CM, Piet B, et al. Human IL-25- and IL-33-Responsive Type 2 Innate Lymphoid Cells are Defined by Expression of CRTH2 and CD161. *Nat Immunol* (2011) 12:1055–62. doi: 10.1038/ni.2104
21. Burrows K, Chiaranunt P, Ngai L, Mortha A. Rapid Isolation of Mouse ILCs From Murine Intestinal Tissues. *Methods Enzymol* (2020) 631:305–27. doi: 10.1016/bs.mie.2019.10.001
22. Karta MR, Rosenthal PS, Beppu A, Vuong CY, Miller M, Das S, et al. β2integrins Rather Than β1integrins Mediate Alternaria-Induced Group 2 Innate Lymphoid Cell Trafficking to the Lung. *J Allergy Clin Immunol* (2018) 141:329–38.e12. doi: 10.1016/j.jaci.2017.03.010
23. Vély F, Barlogis V, Vallentin B, Neven B, Piperoglou C, Ebbo M, et al. Evidence of Innate Lymphoid Cell Redundancy in Humans. *Nat Immunol* (2016) 17:1291–9. doi: 10.1038/ni.3553
24. Lim AI, Li Y, Lopez-Lastra S, Stadhouders R, Paul F, Casrouge A, et al. Systemic Human ILC Precursors Provide a Substrate for Tissue ILC Differentiation. *Cell* (2017) 168:1086–1100.e10. doi: 10.1016/j.cell.2017.02.021
25. Mazzurana L, Czarnewski P, Jonsson V, Wigge L, Ringnér M, Williams TC, et al. Tissue-Specific Transcriptional Imprinting and Heterogeneity in Human Innate Lymphoid Cells Revealed by Full-Length Single-Cell RNA-Sequencing. *Cell Res* (2021) 31:554–68. doi: 10.1038/s41422-020-00445-x
26. Winkler C, Hochdörfer T, Israelsson E, Hasselberg A, Cavallin A, Thörn K, et al. Activation of Group 2 Innate Lymphoid Cells After Allergen Challenge in Asthmatic Patients. *J Allergy Clin Immunol* (2019) 144:61–69.e7. doi: 10.1016/j.jaci.2019.01.027
27. Dahlgren MW, Jones SW, Cautivo KM, Dubinin A, Ortiz-Carpena JF, Farhat S, et al. Adventitial Stromal Cells Define Group 2 Innate Lymphoid Cell Tissue Niches. *Immunity* (2019) 50:707–22.e6. doi: 10.1016/j.immuni.2019.02.002
28. Cautivo KM, Matatia PR, Lizama CO, Mroz NM, Dahlgren MW, Yu X, et al. Interferon Gamma Constrains Type 2 Lymphocyte Niche Boundaries During Mixed Inflammation. *Immunity* (2022) 55:254–71.e7. doi: 10.1016/j.immuni.2021.12.014
29. Puttur F, Denney L, Gregory LG, Vuononvirta J, Oliver R, Entwistle LJ, et al. Pulmonary Environmental Cues Drive Group 2 Innate Lymphoid Cell Dynamics in Mice and Humans. *Sci Immunol* (2019) 4:eaav7638. doi: 10.1126/sciimmunol.aav7638
30. Denney L, Byrne AJ, Shea TJ, Buckley JS, Pease JE, Herledan GMF, et al. Pulmonary Epithelial Cell-Derived Cytokine TGF-β1 Is a Critical Cofactor for Enhanced Innate Lymphoid Cell Function. *Immunity* (2015) 43:945–58. doi: 10.1016/j.immuni.2015.10.012
31. van der Ploeg EK, Golebski K, van Nimwegen M, Fergusson JR, Heesters BA, Martinez-Gonzalez I, et al. Steroid-Resistant Human Inflammatory ILC2s are Marked by CD45RO and Elevated in Type 2 Respiratory Diseases. *Sci Immunol* (2021) 6:eabd3489. doi: 10.1126/sciimmunol.abd3489
32. Hermiston ML, Xu Z, Weiss A. CD45: A Critical Regulator of Signaling Thresholds in Immune Cells. *Annu Rev Immunol* (2003) 21:107–37. doi: 10.1146/annurev.immunol.21.120601.140946
33. Bartemes KR, Kephart GM, Fox SJ, Kita H. Enhanced Innate Type 2 Immune Response in Peripheral Blood From Patients With Asthma. *J Allergy Clin Immunol* (2014) 134:671–8.e4. doi: 10.1016/j.jaci.2014.06.024
34. Huang Y, Guo L, Qiu J, Chen X, Hu-Li J, Siebenlist U, et al. IL-25-Responsive, Lineage-Negative KLRG1 Hi Cells are Multipotential "Inflammatory" Type 2 Innate Lymphoid Cells. *Nat Immunol* (2015) 16:161–9. doi: 10.1038/ni.3078
35. Ricardo-Gonzalez RR, Schneider C, Liao C, Lee J, Liang H-E, Locksley RM. Tissue-Specific Pathways Extrude Activated ILC2s to Disseminate Type 2 Immunity. *J Exp Med* (2020) 217:e20191172. doi: 10.1084/jem.20191172
36. Nakatani-Kusakabe M, Yasuda K, Tomura M, Nagai M, Yamanishi K, Kuroda E, et al. Monitoring Cellular Movement With Photoconvertible Fluorescent Protein and Single-Cell RNA Sequencing Reveals Cutaneous Group 2 Innate Lymphoid Cell Subtypes, Circulating ILC2 and Skin-Resident Ilc2. *JID Innovations* (2021) 1:100035. doi: 10.1016/j.xjidi.2021.100035
37. Imai Y, Yasuda K, Sakaguchi Y, Haneda T, Mizutani H, Yoshimoto T, et al. Skin-Specific Expression of IL-33 Activates Group 2 Innate Lymphoid Cells and Elicits Atopic Dermatitis-Like Inflammation in Mice. *Proc Natl Acad Sci U.S.A.* (2013) 110:13921–6. doi: 10.1073/pnas.1307321110
38. Tomura M, Hata A, Matsuoka S, Shand FHW, Nakanishi Y, Ikebuchi R, et al. Tracking and Quantification of Dendritic Cell Migration and Antigen Trafficking Between the Skin and Lymph Nodes. *Sci Rep* (2015) 4:6030. doi: 10.1038/srep06030
39. Roediger B, Kyle R, Yip KH, Sumaria N, Guy TV, Kim BS, et al. Cutaneous Immunosurveillance and Regulation of Inflammation by Group 2 Innate Lymphoid Cells. *Nat Immunol* (2013) 14:564–73. doi: 10.1038/ni.2584

Conflict of Interest: The authors declare that the research was conducted in the absence of any commercial or financial relationships that could be construed as a potential conflict of interest.

frontiers | Frontiers in Immunology

MINI REVIEW
published: 11 May 2022
doi: 10.3389/fimmu.2022.903678

Heartbreakers or Healers? Innate Lymphoid Cells in Cardiovascular Disease and Obesity

Luke B. Roberts[1*], *Graham M. Lord*[1,2] *and Jane K. Howard*[3]

[1] School of Immunology and Microbial Sciences, King's College London, London, United Kingdom, [2] Faculty of Biology, Medicine and Health, University of Manchester, Manchester, United Kingdom, [3] School of Cardiovascular and Metabolic Medicine & Sciences, King's College London, London, United Kingdom

Cardiovascular diseases (CVDs) are responsible for most pre-mature deaths worldwide, contributing significantly to the global burden of disease and its associated costs to individuals and healthcare systems. Obesity and associated metabolic inflammation underlie development of several major health conditions which act as direct risk factors for development of CVDs. Immune system responses contribute greatly to CVD development and progression, as well as disease resolution. Innate lymphoid cells (ILCs) are a family of helper-like and cytotoxic lymphocytes, typically enriched at barrier sites such as the skin, lung, and gastrointestinal tract. However, recent studies indicate that most solid organs and tissues are home to resident populations of ILCs - including those of the cardiovascular system. Despite their relative rarity, ILCs contribute to many important biological effects during health, whilst promoting inflammatory responses during tissue damage and disease. This mini review will discuss the evidence for pathological and protective roles of ILCs in CVD, and its associated risk factor, obesity.

Keywords: ILCs, innate lymphoid cells, cardiovascular disease, obesity, heart

OPEN ACCESS

Edited by:
Carolina Jancic,
Consejo Nacional de Investigaciones Científicas y Técnicas (CONICET), Argentina

Reviewed by:
Marek Wagner,
University of Bergen, Norway
Yi Ding,
National Cancer Institute (NIH), United States

****Correspondence:***
Luke B. Roberts
luke.roberts@kcl.ac.uk

Specialty section:
This article was submitted to NK and Innate Lymphoid Cell Biology, a section of the journal Frontiers in Immunology

Received: *24 March 2022*
Accepted: *19 April 2022*
Published: *11 May 2022*

Citation:
Roberts LB, Lord GM and Howard JK (2022) Heartbreakers or Healers? Innate Lymphoid Cells in Cardiovascular Disease and Obesity. Front. Immunol. 13:903678. doi: 10.3389/fimmu.2022.903678

INTRODUCTION

Cardiovascular diseases (CVDs) are the major global cause of premature human death. Obesity and associated metabolic inflammation underlie the development of several major health issues including type 2 diabetes (T2DM), insulin resistance, hypertension, dyslipidaemia, and increased expression of inflammatory mediators - all of which are risk factors for CVDs. Tackling obesity therefore remains a key goal the effort to reduce the increasing burden of CVDs worldwide.

Five major subsets of Innate lymphoid cells (ILCs) are acknowledged: cytotoxic natural killer cells (NKs), lymphoid tissue inducers (LTi) and helper-like ILC1s, ILC2s and ILC3s (1). ILC1s depend on the transcription factor (TF) T-bet for their development (2) and peripheral maintenance (3). They produce IFNγ, tumor necrosis factor (TNF) (4, 5), and TGF-β under some contexts (6). ILC2s are regulated by a suite of TFs including GATA3 and RORα, express type 2 cytokines including interleukin (IL)-4, IL-5, IL-9 and IL-13, and tissue repair factors including amphiregulin. LTi and helper-like ILC3s express TF RORγt and produce IL-17, IL-22, and TNF-superfamily members, including lymphotoxins. ILCs are activated by environmental signals including cytokines, tissue-derived danger signals, metabolites, neurotransmitters, and neuropeptides (1, 7).

While NKs are predominantly circulatory, helper-like ILCs reside in tissues and are enriched at barrier mucosal sites such as the lung and intestinal tract. However, since their discovery, almost all organs have been found to play host to ILC subsets, including tissues of the cardiovascular system (8). Cardiovascular-associated ILCs (cILCs) reside in the pericardium and pericardial fluid (9), in the adventitia of arteries including the aorta (10), and in fat-associated lymphoid clusters (FALC) (11) of perivascular (12) and pericardial adipose tissue (13). The majority of cILCs are ILC2s or ILC2-commited precursors, with minimal presence of ILC1s and ILC3s (14, 15). As observed in other tissues, cILC2 populations are dependent on IL-33 signalling for their development as well as their activation and function. cILC2s may even be more responsive to IL-33 signalling than counterparts at barrier sites such as the lungs, due to unique phenotypic attributes including greater expression of GATA3 (15). Cardiac fibroblasts are a main source of IL-33 in the heart, responsible for ILC2 homeostasis and activity (9), while adventitial stromal cells provide IL-33 and thymic stromal lymphopoietin (TSLP) to ILC2s in arteries and FALC, providing a tissue supportive niche for their development and activation (16). Developmental, adoptive transfer, and parabiosis studies in mice suggest that, similarly to ILCs from barrier sites (17–19), cILC populations are tissue-resident cells, seeded during early embryonic development and shortly after birth, sustaining themselves through local renewal, even during cardiac inflammation (14, 15).

This mini review will summarise the known protective and pathological actions of ILCs in the context of CVDs. As a major cardiometabolic risk factor, obesity, and its relatedness to ILC activity will also be discussed. **Figure 1** summarises the information presented. **Table 1** provides a list of the abbreviations used throughout.

PROTECTIVE AND REPARATIVE ROLES OF ILCS IN CVD

NK Cells

Viral myocarditis is predominantly caused by infection with Coxsackievirus B3. NKs limit viral replication primarily through their potent cytotoxicity, among other protective mechanisms (20). NKs are recruited to the infected heart by cardiomyocyte upregulation of CXCL10, a chemokine ligand of the NK-expressed receptor CXCR3 (21). Expression of CXCL10 is promoted by NK-derived IFNγ - a feed-forward mechanism, driven by NKs for further expansion of the population with in the tissue (21).

Observational studies linking decreased NK numbers and activities, with low grade inflammation and increased disease severity, implicate a protective role for NK cells in atherosclerosis (AS) and coronary artery disease (CAD) (46–48). These effects may be related to NK apoptosis (49) and increased expression of inhibitory molecules (50). However, results from murine models complicate interpretation of these findings, suggesting either pro-atherogenic roles for NKs (51), or conversely, no impact on AS development (52).

NKs may also serve cardioprotective functions during eosinophilic myocarditis, restricting eosinophil influx and survival. Anti-asialo GM1-mediated NK depletion in an anti-MHC (myosin heavy chain) immunisation model of experimental autoimmune myocarditis (EAM) resulted in worsened disease outcome and enhanced eosinophilic influx, accompanied by greater cardiac tissue fibrosis (53). NKs may defend against eosinophilic inflammation directly, by promoting eosinophil apoptosis (36, 53, 54), and indirectly by suppressing fibroblast production of the eosinophil recruiting chemokine eotaxin-1 (CCL11). Furthermore, CXCL10 is an inhibitor of eosinophil recruitment *via* antagonism of the eosinophil trafficking receptor CCR3 (53, 55). IFNγ also restricts ILC2 cytokine expression and limits the active niche in which ILC2s can exert their effects (56, 57). As will be discussed, ILC2s may promote pathological recruitment of eosinophils in the setting of cardiac inflammation (9). IFNγ production by NKs may therefore also act to inhibit cardiac ILC2 activity.

ILC2s

Apolipoprotein E deficient mice (*Apoe*$^{-/-}$) display defective lipoprotein clearance and accrue abnormal levels of low-density lipids, making them prone to development of AS. IL-25 administration limits initiation and progression of AS in high fat diet (HFD)-fed *Apoe*$^{-/-}$ mice. This is concomitant with expansion of splenic ILC2 populations and enhanced IL-5 production (42, 43). Furthermore, IL-25 treatment increases levels of circulating anti-phosphorylcholine (PC) IgM, dependent on intact IL-5 expression, indicative of an atheroprotective effect of ILC2 activation by IL-25. The PC epitope is a component of oxidised low-density lipoprotein (ox-LDL), strongly associated with AS development. Anti-PC IgM is produced by B-1a cells – an atheroprotective, innate-like B cell subtype. B-1a cells expand following IL-25 treatment (43), and depend on IL-5 for their survival and maturation to produce natural IgM antibodies (58, 59). Transfer of IL-25-expanded, wild type ILC2s to *Apoe*$^{-/-}$ mice reduces the lipid content of AS lesions and augments B-1a cells and anti-PC IgM, suggestive of a therapeutic avenue to tackle AS (42). Of note, the ILC2/IL-5/B-1a axis is critically dependent on ILC2 expression of the helix loop-helix TF, ID3 (60). As an ID3 single nucleotide polymorphism (rs11574) is associated with increased carotid intimal media thickness, this may link ILC2 dysfunction in humans with enhanced AS risk (61).

HFD feeding also reduces peripheral ILC2 numbers and alters their functional cytokine responses in AS-prone mouse strains - linking defective ILC2 activity with disease (12). Low-density lipoprotein receptor deficient mice (*Ldlr*$^{-/-}$) share a similar functional defect in lipid clearance as *Apoe*$^{-/-}$ mice and are similarly AS-prone. *Ldlr*$^{-/-}$ mice reconstituted with bone marrow from ILC2 deficient mice (^{Staggerer}/*Rora*^{Flox} x *Il7ra*^{Cre}) displayed accelerated AS plaque lesion development. This was associated with reduced collagen deposition found in larger plaques (indicative of increased plaque destabilisation) and altered plaque immune cell composition, dependent on loss of

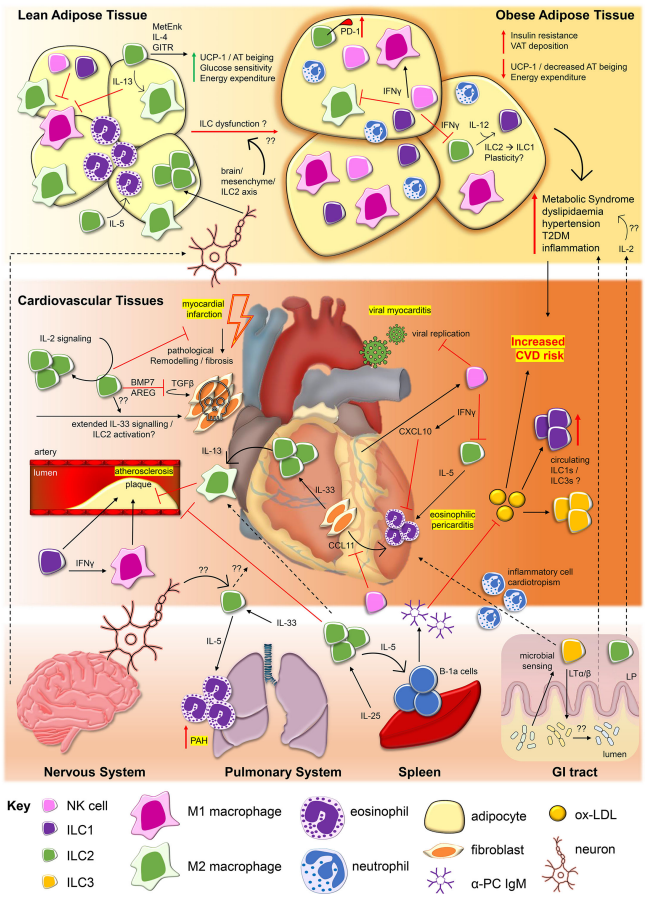

FIGURE 1 | Innate lymphoid cells contribute to protective and pathological processes in cardiovascular diseases and obesity. During viral myocarditis caused by agents such as Coxsackie virus B3 (*CV-B3*), NKs restrict viral replication (20) and are recruited to cardiac tissues by cardiomyocyte production of C-X-C motif chemokine ligand 10 (*CXCL10*), itself promoted by NK-derived interferon gamma (*IFNγ*) (21). IFNγ may also restrict ILC2 activity, influencing ILC2 capacity to drive inflammation associated with eosinophilic pericarditis. Interleukin (*IL*)-33 derived from cardiac fibroblasts drives cardiac ILC2 proliferation and along with fibroblast production of eotaxins (i.e. eotaxin-1/*CCL11*), ILC2 production of IL-5 may facilitate recruitment of eosinophils to the pericardium (9). ILC2 production of IL-13 can also promote polarisation of M2 macrophages, which may serve protective roles in *atherosclerosis* (12, 22). Conversely, ILC1s and promotion of classically activated proinflammatory M1 macrophages may promote atherosclerotic plaque formation (23–25). ILC2s, regulated by IL-2 signalling, may also serve protective roles for cardiac tissue repair following major adverse events such as myocardial infarction, *via* the production of amphiregulin (AREG) and bone morphogenic protein 7 (*BMP7*), inhibiting pathological tissue remodelling and fibrosis (26). The impact of prolonged activation of ILC2s by factors such as IL-33 on the outcome of ILC2 repair responses in this context require further study (27). In the circulation, increased frequencies of ILC1s and ILC3s are associated with major cardiovascular and cerebrovascular events including ST-elevated myocardial infarction (STEMI) and acute cerebrovascular infarction (ACI/Stroke) (28, 29). This may be related to increased circulating levels of oxidised low-density lipoproteins (*ox-LDL*) in patients, but the impact of these alterations to ILC subset frequencies inpatients remain to be elucidated. *Obesity*, and its associated metabolic inflammation is associated with major risk factors for the development of CVDs, including type 2 diabetes mellitus (*T2DM*), dyslipidaemia, hypertension, and inflammation. As observed in cardiovascular tissues, ILC2s are the dominant ILC subtype found within *lean adipose tissue*. ILC2s promote alternatively activated M2 macrophage phenotypes and eosinophils within adipose tissue *via* their production of IL-5 and IL-13, contributing to lean adipose tissue homeostasis (30–33). ILC2 expression of methionine enkephalin (*MetEnk*) (31) and IL-4 (34), in addition to signaling *via* Glucocorticoid-induced TNFR-related protein (*GITR*) (32) can protect from obesity by promoting beiging of white adipose tissue, linked to upregulation of mitochondrial uncoupling protein 1 (UCP-1), increasing glucose sensitivity and energy expenditure. In *obese adipose tissue* ILC2 numbers and functions are impaired, contributing to increased visceral adipose tissue (*VAT*) depots, insulin resistance and decreased beiging. Upregulation of inhibitory receptor PD-1 by ILC2s (35), negative regulation by IFNγ derived from ILC1s and natural killer cells (NKs) (36, 37), and ILC2 to ILC1 conversion (38) may be among the mechanisms which result in ILC2 dysfunction in obesity. NKs and ILC1s numbers are also altered in obesity, potentially impacting upon the ratio between inflammatory M1 and anti-inflammatory M2 macrophages (33, 39). Influences from physiological signals and ILCs present in other tissues may also impact upon CVDs and obesity pathogenesis. The *nervous system* can regulate ILC2 activity within lean adipose tissue *via* a brain/mesenchymal/ILC2 axis (40). Dysregulation of this axis may contribute to development of obesity, however, broader effects of neuronal signalling on ILCs in the context of CVDs requires further study. In the induction of pulmonary arterial hypertension (*PAH*), IL-5 derived from *pulmonary system* ILC2s are responsible for tissue eosinophilia which may drive arterial damage (41). IL-25 drives ILC2 proliferation in the *spleen*, promoting atheroprotective effects, IL-5-dependent B-1a expansion and production of anti- phosphorylcholine (PC) Immunoglobulin M (*IgM*) which targets ox-LDL (42, 43). In the *gastrointestinal (GI) tract*, sensing of microbial composition by ILC3s may influence inflammatory cell cardiotropism in the context of myocarditis (44), while ILC2s and ILC3s within the intestinal lamina propria (LP) may also contribute to processes driving obesity, through factors such as production of IL-2 (45).

TABLE 1 | Meanings of abbreviations used in this article.

Abbreviation	Meaning
ACI	Acute cerebrovascular infarction
AS	Atherosclerosis
AT	Adipose tissue
AT1-ILCs	Group 1 adipose tissue innate lymphoid cells
ATM	Adipose tissue macrophage
BAT	Brown adipose tissue
cILCs	Cardiovascular-associated innate lymphoid cells
CVD/CVDs	Cardiovascular disease/s
DCM	Dilated cardiomyopathy
DIO	Diet-induced obesity
EAM	Experimental autoimmune myocarditis
FALC	Fat-associated lymphoid tissue
HFD	High fat diet
ILC/ILCs	Innate lymphoid cell/innate lymphoid cells
ILC1/ILC1s	Helper-like type 1 innate lymphoid cell/s
ILC2/ILC2s	Helper-like type 2 innate lymphoid cell/s
ILC3/ILC3s	Helper-like type 3 innate lymphoid cell/s
LTi	Lymphoid tissue inducer cell
MI	Myocardial infarction
NK/NKs	Natural killer cell/natural killer cells
ox-LDL	Oxidised low-density lipoprotein
PAH	Pulmonary arterial hypertension
PBMCs	Peripheral blood mononuclear cells
PC	phosphorylcholine
STEMI	ST-elevation myocardial infarction
T2DM	Type 2 Diabetes mellitus
TF/TFs	Transcription factor/s
TSLP	Thymic stromal lymphopoietin
WAT	White adipose tissue

ILC2-derived IL-13. Plaque macrophage phenotypes were disrupted by ILC2 loss, with reduced arginase-1 expression suggestive of a restricted capacity for tissue repair. This supports work identifying IL-13 as an atheroprotective cytokine, acting *via* induction of alternatively activated (M2) macrophages (22), potentially supporting the augmentation of ILC2 responses as a novel therapeutic strategy for AS. Indeed, expansion of $CD25^+$ ILC2s by IL-2/anti-IL-2 complexes reduces circulating ox-LDL and AS lesion development in HFD-fed lymphopenic $Rag^{-/-}Ldlr^{-/-}$ mice (10), indicating that IL-2 therapy may be a novel treatment option in some forms of CVD. Supportive of this, genetic ablation of ILC2s in a murine model of myocardial infarction (MI) delayed recovery of cardiac function. MI-protective functions of ILC2s were associated with an upstream regulatory IL-2 signalling axis (13). Furthermore, analysis of peripheral blood from patients recruited to a placebo-controlled, double-blind trial designed to assess the safety of Low-dose InterLeukin-2 treatment in patients with stable ischaemic heart disease and Acute Coronary Syndromes [LILACS trial (62)], revealed a short-term increase in circulating ILC2s, serum IL-5, and eosinophil counts (13). This indicates that IL-2 therapy activates human ILC2s *in vivo*. However, putative protective roles of ILC2s in this context remain to be fully investigated. Post-cardiac injury, augmentation of ILC2 repair responses may also be an attractive therapeutic option, inhibiting TGF-β1-driven pathological fibrosis and remodelling by cardiac fibroblasts which can lead to terminal heart failure (26).

ILC3s

ILC3 associated cytokines IL-17A and IL-22 have been linked to CVDs, but may be protective under certain contexts (63–65). ILC3s might also be protective during hepatic (66) and intestinal (67) ischemia-reperfusion-injury (IRI), suggestive, potentially, of similar roles during reperfusion following MI. However, in both the liver and the intestinal tract, ILC3s are far more populous than in cardiovascular tissues, where Th17 cells are also more likely to be the major source of ILC3-associated effector cytokines. Whether ILC3s serve protective roles in CVDs requires further investigation.

ILCS AND CVD PATHOGENESIS

ILC1s

ILC1s constitute only a minor population of the ILCs identified within murine cardiovascular tissues (14, 15). Despite this, $Ldlr^{-/-}$ and $Apoe^{-/-}$ models combining genetic knockout of T-bet or IL-12, implicate roles for ILC1s in development of HFD-induced AS (23, 24). However, these models also deplete other cells important in AS pathogenesis, including Th1 and NKs (68). ILC1s have been more specifically linked to AS plaque development using adaptive lymphocyte deficient $Rag^{-/-}Apoe^{-/-}$ models. Anti-NK1.1 or anti-IL-15R antibodies were used to deplete ILC1s and/or NK cells respectively, followed by adoptive transfer of splenic ILC1s, identifying a possible role for ILC1s in aggravation of AS (25).

Involvement of ILC1s in the pathology of major cardiovascular and cerebrovascular adverse events has been proposed, based on correlations between disease severity and circulating frequency of these cells. Total number and proportions of ILCs among circulating leukocytes were increased in acute ST-segment elevation myocardial infarction (STEMI) patients, compared to healthy controls (28). This was accounted for by a specific increase in ILC1s, while numbers of ILC2s and ILC3s remained unaltered, indicating an expansion of ILC1s rather than ILC subset plasticity towards the ILC1 phenotype (69, 70). Similar observations were made in acute cerebral infarction (ACI) patients (29). A significantly increased proportion of ILC1s among total circulating ILCs, profiled at the time of admission, was observed compared to healthy controls. Concomitant with this was a decrease in the proportion of ILC2s and no impact on circulating ILC3s. However, as total number of ILCs among leukocytes was not reported, whether alterations to subset prevalence among total ILCs represents phenotypic plasticity between ILC2s to ILC1s (38, 71–73) in the context of ACI, or reflects a specific expansion of ILC1s, remains unclear.

ILC2s

ILC2s may drive the recruitment of eosinophils to the pericardium *via* production of IL-5 and promotion of cardiac fibroblast-derived eotaxins (9). Choi et al., utilised repeated IL-33 administration to induce eosinophilic pericarditis in mice, finding that pericardial $IL\text{-}33R^+$ ($ST2^+$) ILC2s greatly expanded in response to treatment (9). IL-5 deficiency prevented pericardial eosinophil infiltration, however $Il13^{-/-}$ mice

displayed a similar level of pericarditis to WT mice. Furthermore, total ILCs were enriched in the pericardial fluid of pericarditis patients, relative to patients with other heart diseases or healthy controls. However, deeper analysis of ILC subsets was not reported, impeding specific association of human pericarditis with ILC2s. ILC2-derived IL-5 also promotes eosinophil accumulation around pulmonary arteries, following chronic activation by IL-33 (41). This accumulation resulted in severe arterial occlusion and pulmonary arterial hypertrophy (PAH). This was ablated in IL-5 deficient and eosinophil deficient mice, but not in *Rag*$^{-/-}$ mice, supporting an ILC2/IL-5/eosinophil dependent axis in the aetiology of PAH. Furthermore, PAH has previously been associated with vascular remodelling driven by IL-33 (74). Despite eosinophilia and other abnormalities in IL-5 overexpressing mice, pulmonary arteries in these animals do not appear to be affected (75). Therefore, while the ILC2/eosinophil axis plays a role, other factors also contribute to PAH development. Prolonged IL-33/ST2 signalling may also contribute to poorer cardiac remodelling and promote heart failure following MI (27), despite augmenting ILC2-driven type 2 immune activity, which may be protective or reparative of ventricular function in the acute phase post-MI (57). ILC2s therefore act as a "double-edged sword" (37), the activity of which must be precisely balanced to provide protection, while limiting pathological outcomes.

ILC3s

Few studies have investigated ILC3s in CVD pathogenesis. During EAM, differential disease susceptibility in mice from different sources has been associated with intestinal ILC3s and specific microbiome profiles (44). Anti-CD90 antibody mediated depletion of ILCs restricted inflammatory leukocyte trafficking to the heart during EAM, indicating that microbial sensing *via* ILC3s plays a role in development of inflammatory heart diseases *via* cardiotropic immune cell chemotaxis. Additionally, a study investigating ILC3s in axial spondyloarthritis (axSpA) indirectly suggests ILC3 differentiation is promoted by risk factors driving CVD (76). Patients with inflammatory joint conditions, including axSpA, have an increased risk of developing CVD (77). Therefore, clinical management of CVD risk factors, including dyslipidaemia, is important. Circulating IL-22^{+} ILC3s were increased in axSPa patients with dyslipidaemia compared to patients without dyslipidaemia or healthy controls. Furthermore, ox-LDL promoted IL-22^{+} and IL-17^{+} ILC3 differentiation from axSPa patient peripheral blood mononuclear cells (PBMCs) (76) and ILC3s expressed the ox-LDL receptor CD36, blockade of which prevented ox-LDL-mediated differentiation of the cells (76). This indicates that ox-LDL affects ILC3 generation, similar to observations made for ILC1 differentiation from ACI patient PBMCs (29). Although in that study, no effect of ox-LDL stimulation on ILC3s was observed, suggestive of other disease-specific effects of ox-LDL signalling on ILCs. ILC3s are regulated by hypoxia, acting *via* hypoxia inducible factor (HIF)-1α (78). Tissue hypoxia can be induced by, and contribute to CVDs (79). Hypoxia-driven ILC3 responses might therefore also play a role in some forms of CVD.

ILCs, Adipose Tissue and Obesity

Lean adipose tissue (AT) contains populations of immune cells important for maintaining metabolic homeostasis, including regulatory T cells (T_{REGs}), eosinophils and M2 macrophages. These cells are regulated by ILC2s resident in AT-depots in mice and humans (30–33) and these functions are reliant on IL-33 signalling (30, 33). Disruption of IL-33 signalling in mice reduces ILC2s in white AT (WAT), increasing visceral fat depots, impairing glucose homeostasis, and disrupting energy metabolism by prevention of WAT beiging (33). Beiging converts white adipocytes, or adipogenic precursors within WAT, to brown-like AT and is associated with the upregulation of mitochondrial uncoupling protein 1 (UCP1). This increases thermogenesis - raising body heat and calorific expenditure, protecting from obesity, at least in mice. Mechanistically, IL-33-mediated beiging is dependent on the ILC2-expressed opioid peptide methionine enkephalin, which acts on WAT to induce UCP1 expression (31), similarly to the actions of other ILC2-associated molecules like IL-4 (34) and activation of Glucocorticoid-induced TNFR-related protein (GITR), expressed by both human and murine AT ILC2s (32).

During obesity in humans and in murine diet-induced obesity (DIO) models, AT ILC2 frequencies are reduced, and their functions become dysregulated. This may negatively impact the homeostatic, immunometabolic roles of ILC2s, such as restricting differentiation of obesity-protective M2 AT macrophages (ATM) (30). The mechanisms responsible for reduction of ILC2 responses during obesity are likely multifaceted and remain under study. Recent developments suggest they include the upregulation and activation of inhibitory co-stimulatory receptor PD-1 on ILC2s during obesity (35), and dysregulation of brain-AT circuits, which modulate ILC2 activation indirectly *via* neuro-mesenchymal interactions (40). Furthermore, as human and murine AT is also populated by group 1 ILCs (AT1-ILCs), including mature and immature NKs, and non-NK ILC1s, AT ILC2 activities may be affected by aberrant IFNγ signaling, which restrains ILC2 responses (30, 56). An increase in AT ILC1s during DIO has been reported by some studies. This might drive ATM M1 polarization *via* IFNγ production, promoting insulin resistance and metabolic dysfunction in a manner dependent on IL-12 and downstream STAT4 signalling (80). IL-12-mediated plasticity of AT ILC2s to ILC1-like cells may further contribute to these effects (38). ATM M1 responses may also be promoted by increased WAT expression of CD36 in the context of defective ILC2 functions, resulting in enhanced absorption of saturated fatty acids by adipocytes, driving M1 polarisation (33). Conversely, Boulenouar and colleagues report that obesity is associated with a decrease in the number and cytotoxicity of AT1-ILCs. This may contribute to ATM accumulation and alterations to the ratio of proinflammatory M1 to anti-inflammatory M2, thereby impacting insulin resistance and metabolic dysfunction (39). The contribution of AT1-ILC responses and their roles in AT homeostasis and during obesity is an area that requires further investigation.

While AT ILC2s have emerged as important metabolic regulators which promote AT homeostasis, ILC2s from other tissues may also act to promote obesity. In the setting of

lymphopenic DIO murine models, adoptive transfer of small intestinal ILC2s, but not WAT ILC2s, promotes obesity *via* an axis dependent on their production of IL-2 (45) – supportive of a role for this cytokine in obesity induction (81). Intestinal ILC3s also moderately contributed to DIO (45). Currently, few studies have investigated the roles of ILC3s in obesity. However, increased frequency of circulating ILC3s in children who are overweight and asthmatic (compared to children who are asthmatic but not-overweight) suggests that obesity may be an independent risk-factor for promotion of ILC3 differentiation (82). Furthermore, the lymphotoxin pathway may promote DIO by driving a pro-obesity intestinal microbiota (83). As LTi and helper-ILC3s produce lymphotoxins, this potentially implicates these cells in obesity pathogenesis.

CONCLUSIONS AND FUTURE PERSPECTIVES

CVD and obesity are major global health concerns. ILCs are emerging as cells capable of both driving or protecting from CVD pathology. As the field expands, it will shed light on current gaps in our knowledge – for instance, whether ILC1s or ILC3s serve any CVD protective functions. Studies which investigate whether and how cILCs are regulated by factors known to control ILC activity in other tissues and disease states are also required. This may include investigation of cILC regulation by neurotransmitters and neuropeptides (1, 84), post-transcriptional regulation by non-coding RNAs (85–87), and effects of metabolic dysfunction, such as lactic acidosis (88) - a known indicator of cardiac stress. Further studies which compare functions and transcriptional profiles of cILCs with more widely studied barrier ILC populations would also be useful. This would facilitate understanding of similarities and unique differences between these populations, related to the pressures and requirements exerted by the disparate tissue environments these cells function within. Such work may inform new, tissue-specific therapeutic strategies. Encouragingly, there are now several studies which demonstrate how modification of ILC responses might show promise for therapeutic intervention of CVD and obesity in humans. However, most of our mechanistic knowledge about ILC activity is still derived from murine models. As these models are often lymphopenic in nature, the potential translational meaning of these observations to immunocompetent human disease settings is somewhat confounded. Future research should continue to explore and unravel cardiovascular-associated ILC responses, particularly focusing on their roles in the context of human disease.

AUTHOR CONTRIBUTIONS

LR conceptualised the manuscript's theme. LR researched and wrote the manuscript. LR designed and created the figures. GL and JH advised on content and edited the manuscript. All authors contributed to the article and approved the submitted version.

FUNDING

LR is supported by the National Institute for Health Research (NIHR) Biomedical Research Centre based at Guy's and St Thomas' NHS Foundation Trust and King's College London. JH is supported by the Medical Research Council (grant MR/K002996/1). GL is supported by the Wellcome Trust (grant number 091009), the British Heart Foundation (award number PG/12/36/29444), the MRC (grant number MR/M003493/1), and the NIHR at Guy's & St Thomas' NHS Foundation Trust in partnership with King's College London and King's College Hospital NHS Foundation Trust.

ACKNOWLEDGMENTS

The authors thank Joana F. Neves (King's College London) for critically reading the manuscript and providing useful feedback, and Andy Forest for the creation of heart and organ graphics used in **Figure 1**.

REFERENCES

1. Vivier E, Artis D, Colonna M, Diefenbach A, Di Santo JP, Eberl G, et al. Innate Lymphoid Cells: 10 Years on. *Cell* (2018) 174:1054–66. doi: 10.1016/j.cell.2018.07.017
2. Klose CSN, Flach M, Möhle L, Rogell L, Hoyler T, Ebert K, et al. Differentiation of Type 1 ILCs From a Common Progenitor to All Helper-Like Innate Lymphoid Cell Lineages. *Cell* (2014) 157:340–56. doi: 10.1016/j.cell.2014.03.030
3. Schroeder JH, Roberts LB, Meissl K, Lo JW, Hromadová D, Hayes K, et al. Sustained Post-Developmental T-Bet Expression Is Critical for the Maintenance of Type One Innate Lymphoid Cells *In Vivo*. *Front Immunol* (2021) 12:760198. doi: 10.3389/fimmu.2021.760198
4. Daussy C, Faure F, Mayol K, Viel S, Gasteiger G, Charrier E, et al. T-Bet and Eomes Instruct the Development of Two Distinct Natural Killer Cell Lineages in the Liver and in the Bone Marrow. *J Exp Med* (2014) 211:563–77. doi: 10.1084/jem.20131560
5. Fuchs A, Vermi W, Lee JS, Lonardi S, Gilfillan S, Newberry RD, et al. Intraepithelial Type 1 Innate Lymphoid Cells Are a Unique Subset of IL-12- and IL-15-Responsive IFN-γ-Producing Cells. *Immunity* (2013) 38:769–81. doi: 10.1016/j.immuni.2013.02.010
6. Jowett GM, Norman MDA, Yu TTL, Rosell Arévalo P, Hoogland D, Lust ST, et al. ILC1 Drive Intestinal Epithelial and Matrix Remodelling. *Nat Mater* (2020) 20:250–9. doi: 10.1038/s41563-020-0783-8
7. McGinty JW, von Moltke J. A Three Course Menu for ILC and Bystander T Cell Activation. *Curr Opin Immunol* (2020) 62:15–21. doi: 10.1016/j.coi.2019.11.005
8. Murphy JM, Ngai L, Mortha A, Crome SQ. Tissue-Dependent Adaptations and Functions of Innate Lymphoid Cells. *Front Immunol* (2022) 13. doi: 10.3389/fimmu.2022.836999
9. Choi HS, Won T, Hou X, Chen G, Bracamonte-Baran W, Talor MV, et al. Innate Lymphoid Cells Play a Pathogenic Role in Pericarditis. *Cell Rep* (2020) 30:2989–3003.e6. doi: 10.1016/j.celrep.2020.02.040
10. Engelbertsen D, Foks AC, Alberts-Grill N, Kuperwaser F, Chen T, Lederer JA, et al. Expansion of CD25+ Innate Lymphoid Cells Reduces Atherosclerosis. *Arterioscler Thromb Vasc Biol* (2015) 35:2526–35. doi: 10.1161/ATVBAHA.115.306048
11. Moro K, Yamada T, Tanabe M, Takeuchi T, Ikawa T, Kawamoto H, et al. Innate Production of T(H)2 Cytokines by Adipose Tissue-Associated C-Kit(+)Sca-1(+) Lymphoid Cells. *Nature* (2010) 463:540–4. doi: 10.1038/nature08636

12. Newland SA, Mohanta S, Clément M, Taleb S, Walker JA, Nus M, et al. Type-2 Innate Lymphoid Cells Control the Development of Atherosclerosis in Mice. *Nat Commun* (2017) 8:1–11. doi: 10.1038/ncomms15781
13. Yu X, Newland SA, Zhao TX, Lu Y, Sage AS, Sun Y, et al. Innate Lymphoid Cells Promote Recovery of Ventricular Function After Myocardial Infarction. *J Am Coll Cardiol* (2021) 78:1127–42. doi: 10.1016/j.jacc.2021.07.018
14. Bracamonte-Baran W, Chen G, Hou X, Talor MV, Choi HS, Davogustto G, et al. Non-Cytotoxic Cardiac Innate Lymphoid Cells Are a Resident and Quiescent Type 2-Commited Population. *Front Immunol* (2019) 10:634. doi: 10.3389/fimmu.2019.00634
15. Deng Y, Wu S, Yang Y, Meng M, Chen X, Chen S, et al. Unique Phenotypes of Heart Resident Type 2 Innate Lymphoid Cells. *Front Immunol* (2020) 11:802. doi: 10.3389/fimmu.2020.00802
16. Dahlgren MW, Jones SW, Cautivo KM, Dubinin A, Ortiz-Carpena JF, Farhat S, et al. Adventitial Stromal Cells Define Group 2 Innate Lymphoid Cell Tissue Niches. *Immunity* (2019) 50:707–722.e6. doi: 10.1016/j.immuni.2019.02.002
17. Bando JK, Liang H-E, Locksley RM. Identification and Distribution of Developing Innate Lymphoid Cells in the Fetal Mouse Intestine. *Nat Immunol* (2015) 16:153–60. doi: 10.1038/ni.3057
18. Zeis P, Lian M, Fan X, Herman JS, Hernandez DC, Gentek R, et al. *In Situ* Maturation and Tissue Adaptation of Type 2 Innate Lymphoid Cell Progenitors. *Immunity* (2020) 53:775–792.e9. doi: 10.1016/j.immuni.2020.09.002
19. Ghaedi M, Shen ZY, Orangi M, Martinez-Gonzalez I, Wei L, Lu X, et al. Single-Cell Analysis of Rorα Tracer Mouse Lung Reveals ILC Progenitors and Effector ILC2 Subsets. *J Exp Med* (2020) 217:1–19. doi: 10.1084/jem.20182293
20. Ong S, Rose NR, Čiháková D. Natural Killer Cells in Inflammatory Heart Disease. *Clin Immunol* (2017) 175:26–33. doi: 10.1016/j.clim.2016.11.010
21. Yuan J, Liu Z, Lim T, Zhang H, He J, Walker E, et al. CXCL10 Inhibits Viral Replication Through Recruitment of Natural Killer Cells in Coxsackievirus B3-Induced Myocarditis. *Circ Res* (2009) 104:628–38. doi: 10.1161/CIRCRESAHA.108.192179
22. Cardilo-Reis L, Gruber S, Schreier SM, Drechsler M, Papac-Milicevic N, Weber C, et al. Interleukin-13 Protects From Atherosclerosis and Modulates Plaque Composition by Skewing the Macrophage Phenotype. *EMBO Mol Med* (2012) 4:1072–86. doi: 10.1002/emmm.201201374
23. Buono C, Binder CJ, Stavrakis G, Witztum JL, Glimcher LH, Lichtman AH. T-Bet Deficiency Reduces Atherosclerosis and Alters Plaque Antigen-Specific Immune Responses. *Proc Natl Acad Sci USA* (2005) 102:1596–601. doi: 10.1073/pnas.0409015102
24. Davenport P, Tipping PG. The Role of Interleukin-4 and Interleukin-12 in the Progression of Atherosclerosis in Apolipoprotein E-Deficient Mice. *Am J Pathol* (2003) 163:1117–25. doi: 10.1016/S0002-9440(10)63471-2
25. Wu C, He S, Liu J, Wang B, Lin J, Duan Y, et al. Type 1 Innate Lymphoid Cell Aggravation of Atherosclerosis Is Mediated Through TLR4. *Scand J Immunol* (2018) 87:1–14. doi: 10.1111/sji.12661
26. Chen WY, Wu YH, Tsai TH, Li RF, Lai ACY, Li LC, et al. Group 2 Innate Lymphoid Cells Contribute to IL-33-Mediated Alleviation of Cardiac Fibrosis. *Theranostics* (2021) 11:2594–611. doi: 10.7150/THNO.51648
27. Ghali R, Habeichi NJ, Kaplan A, Tannous C, Abidi E, Bekdash A, et al. IL-33 Induces Type-2-Cytokine Phenotype But Exacerbates Cardiac Remodeling Post-Myocardial Infarction With Eosinophil Recruitment, Worsened Systolic Dysfunction, and Ventricular Wall Rupture. *Clin Sci* (2020) 134:1191–218. doi: 10.1042/CS20200402
28. Li J, Wu J, Zhang M, Zheng Y. Dynamic Changes of Innate Lymphoid Cells in Acute ST-Segment Elevation Myocardial Infarction and Its Association With Clinical Outcomes. *Sci Rep* (2020) 10:1–12. doi: 10.1038/s41598-020-61903-5
29. Li Q, Liu M, Fu R, Cao Q, Wang Y, Han S, et al. Alteration of Circulating Innate Lymphoid Cells in Patients With Atherosclerotic Cerebral Infarction. *Am J Transl Res* (2018) 10:4322–30.
30. Molofsky AB, Nussbaum JC, Liang HE, Dyken SJV, Cheng LE, Mohapatra A, et al. Innate Lymphoid Type 2 Cells Sustain Visceral Adipose Tissue Eosinophils and Alternatively Activated Macrophages. *J Exp Med* (2013) 210:535–49. doi: 10.1084/jem.20121964
31. Brestoff JR, Kim BS, Saenz SA, Stine RR, Monticelli LA, Sonnenberg GF, et al. Group 2 Innate Lymphoid Cells Promote Beiging of White Adipose Tissue and Limit Obesity. *Nature* (2015) 519:242–6. doi: 10.1038/nature14115
32. Galle-Treger L, Sankaranarayanan I, Hurrell BP, Howard E, Lo R, Maazi H, et al. Costimulation of Type-2 Innate Lymphoid Cells by GITR Promotes Effector Function and Ameliorates Type 2 Diabetes. *Nat Commun* (2019) 10:1–14. doi: 10.1038/s41467-019-08449-x
33. Okamura T, Hashimoto Y, Mori J, Yamaguchi M, Majima S, Senmaru T, et al. ILC2s Improve Glucose Metabolism Through the Control of Saturated Fatty Acid Absorption Within Visceral Fat. *Front Immunol* (2021) 12:669629. doi: 10.3389/fimmu.2021.669629
34. Qiu Y, Nguyen KD, Odegaard JI, Cui X, Tian X, Locksley RM, et al. Eosinophils and Type 2 Cytokine Signaling in Macrophages Orchestrate Development of Functional Beige Fat. *Cell* (2014) 157:1292–308. doi: 10.1016/j.cell.2014.03.066
35. Oldenhove G, Boucquey E, Taquin A, Acolty V, Bonetti L, Ryffel B, et al. PD-1 Is Involved in the Dysregulation of Type 2 Innate Lymphoid Cells in a Murine Model of Obesity. *Cell Rep* (2018) 25:2053–2060.e4. doi: 10.1016/j.celrep.2018.10.091
36. Awad A, Yassine H, Barrier M, Vorng H, Marquillies P, Tsicopoulos A, et al. Natural Killer Cells Induce Eosinophil Activation and Apoptosis. *PloS One* (2014) 9:1–9. doi: 10.1371/journal.pone.0094492
37. Duan Z, Liu M, Yuan L, Du X, Wu M, Yang Y, et al. Innate Lymphoid Cells Are Double-Edged Swords Under the Mucosal Barrier. *J Cell Mol Med* (2021) 25:8579–87. doi: 10.1111/jcmm.16856
38. Lim AI, Menegatti S, Bustamante J, Le Bourhis L, Allez M, Rogge L, et al. IL-12 Drives Functional Plasticity of Human Group 2 Innate Lymphoid Cells. *J Exp Med* (2016) 213:569–83. doi: 10.1084/jem.20151750
39. Boulenouar S, Michelet X, Duquette D, Alvarez D, Hogan AE, Dold C, et al. Adipose Type One Innate Lymphoid Cells Regulate Macrophage Homeostasis Through Targeted Cytotoxicity. *Immunity* (2017) 46:273–86. doi: 10.1016/j.immuni.2017.01.008
40. Cardoso F, Klein Wolterink RGJ, Godinho-Silva C, Domingues RG, Ribeiro H, da Silva JA, et al. Neuro-Mesenchymal Units Control ILC2 and Obesity *via* a Brain–Adipose Circuit. *Nature* (2021) 597:410–4. doi: 10.1038/s41586-021-03830-7
41. Ikutani M, Tsuneyama K, Kawaguchi M, Fukuoka J, Kudo F, Nakae S, et al. Prolonged Activation of IL-5-Producing ILC2 Causes Pulmonary Arterial Hypertrophy. *JCI Insight* (2017) 2:e90721. doi: 10.1172/jci.insight.90721
42. Mantani PT, Dunér P, Ljungcrantz I, Nilsson J, Björkbacka H, Fredrikson GN. ILC2 Transfers to Apolipoprotein E Deficient Mice Reduce the Lipid Content of Atherosclerotic Lesions. *BMC Immunol* (2019) 20:1–13. doi: 10.1186/s12865-019-0330-z
43. Mantani PT, Dunér P, Bengtsson E, Alm R, Ljungcrantz I, Söderberg I, et al. IL-25 Inhibits Atherosclerosis Development in Apolipoprotein E Deficient Mice. *PloS One* (2015) 10:1–18. doi: 10.1371/journal.pone.0117255
44. Barin JG, Talor MV, Diny NL, Ong SF, Schaub JA, Gebremariam E, et al. Regulation of Autoimmune Myocarditis by Host Responses to the Microbiome. *Exp Mol Pathol* (2017) 103:141–52. doi: 10.1016/j.yexmp.2017.08.003
45. Sasaki T, Moro K, Kubota T, Kubota N, Kato T, Ohno H, et al. Innate Lymphoid Cells in the Induction of Obesity. *Cell Rep* (2019) 28:202–217.e7. doi: 10.1016/j.celrep.2019.06.016
46. Hak Ł, Mysśliwska J, Wieckiewicz J, Szyndler K, Trzonkowski P, Siebert J, et al. NK Cell Compartment in Patients With Coronary Heart Disease. *Immun Ageing* (2007) 4:1–8. doi: 10.1186/1742-4933-4-3
47. Jonasson L, Backteman K, Ernerudh J. Loss of Natural Killer Cell Activity in Patients With Coronary Artery Disease. *Atherosclerosis* (2005) 183:316–21. doi: 10.1016/j.atherosclerosis.2005.03.011
48. Backteman K, Ernerudh J, Jonasson L. Natural Killer (NK) Cell Deficit in Coronary Artery Disease: No Aberrations in Phenotype But Sustained Reduction of NK Cells Is Associated With Low-Grade Inflammation. *Clin Exp Immunol* (2014) 175:104–12. doi: 10.1111/cei.12210
49. Szymanowski A, Li W, Lundberg A, Evaldsson C, Nilsson L, Backteman K, et al. Soluble Fas Ligand Is Associated With Natural Killer Cell Dynamics in Coronary Artery Disease. *Atherosclerosis* (2014) 233:616–22. doi: 10.1016/j.atherosclerosis.2014.01.030
50. Hou N, Zhao D, Liu Y, Gao L, Liang X, Liu X, et al. Increased Expression of T Cell Immunoglobulin- and Mucin Domain-Containing Molecule-3 on Natural Killer Cells in Atherogenesis. *Atherosclerosis* (2012) 222:67–73. doi: 10.1016/j.atherosclerosis.2012.02.009
51. Selathurai A, Deswaerte V, Kanellakis P, Tipping P, Toh BH, Bobik A, et al. Natural Killer (NK) Cells Augment Atherosclerosis by Cytotoxic-Dependent Mechanisms. *Cardiovasc Res* (2014) 102:128–37. doi: 10.1093/cvr/cvu016

52. Nour-Eldine W, Joffre J, Zibara K, Esposito B, Giraud A, Zeboudj L, et al. Genetic Depletion or Hyperresponsiveness of Natural Killer Cells Do Not Affect Atherosclerosis Development. *Circ Res* (2018) 122:47–57. doi: 10.1161/CIRCRESAHA.117.311743
53. Ong S, Ligons DL, Barin JG, Wu L, Talor MV, Diny N, et al. Natural Killer Cells Limit Cardiac Inflammation and Fibrosis by Halting Eosinophil Infiltration. *Am J Pathol* (2015) 185:847–61. doi: 10.1016/j.ajpath.2014.11.023
54. Barnig C, Cernadas M, Dutile S, Liu X, Perrella MA, Kazani S, et al. Lipoxin A4 Regulates Natural Killer Cell and Type 2 Innate Lymphoid Cell Activation in Asthma. *Sci Transl Med* (2013) 5:174ra26. doi: 10.1126/scitranslmed.3004812
55. Xanthou G, Duchesnes CE, Williams TJ, Pease JE. CCR3 Functional Responses Are Regulated by Both CXCR3 and Its Ligands CXCL9, CXCL10 and CXCL11. *Eur J Immunol* (2003) 33:2241–50. doi: 10.1002/eji.200323787
56. Molofsky AB, Van Gool F, Liang H-E, Van Dyken SJ, Nussbaum JC, Lee J, et al. Interleukin-33 and Interferon-γ Counter-Regulate Group 2 Innate Lymphoid Cell Activation During Immune Perturbation. *Immunity* (2015) 43:161–74. doi: 10.1016/j.immuni.2015.05.019
57. Cautivo KM, Matatia PR, Lizama CO, Mroz NM, Dahlgren MW, Yu X, et al. Interferon Gamma Constrains Type 2 Lymphocyte Niche Boundaries During Mixed Inflammation. *Immunity* (2022) 55:254–271.e7. doi: 10.1016/j.immuni.2021.12.014
58. Moon B, Takaki S, Miyake K, Takatsu K. The Role of IL-5 for Mature B-1 Cells in Homeostatic Proliferation, Cell Survival, and Ig Production. *J Immunol* (2004) 172:6020–9. doi: 10.4049/jimmunol.172.10.6020
59. Baumgarth N. The Double Life of a B-1 Cell: Self-Reactivity Selects for Protective Effector Functions. *Nat Rev Immunol* (2011) 11:34–46. doi: 10.1038/nri2901
60. Perry HM, Oldham SN, Fahl SP, Que X, Gonen A, Harmon DB, et al. Helix-Loop-Helix Factor Inhibitor of Differentiation 3 Regulates Interleukin-5 Expression and B-1a B Cell Proliferation. *Arterioscler Thromb Vasc Biol* (2013) 33:2771–9. doi: 10.1161/ATVBAHA.113.302571
61. Doran AC, Lehtinen AB, Meller N, Lipinski MJ, Slayton RP, Oldham SN, et al. Id3 Is a Novel Atheroprotective Factor Containing a Functionally Significant Single-Nucleotide Polymorphism Associated With Intima-Media Thickness in Humans. *Circ Res* (2010) 106:1303–11. doi: 10.1161/CIRCRESAHA.109.210294
62. Zhao TX, Kostapanos M, Griffiths C, Arbon EL, Hubsch A, Kaloyirou F, et al. Low-Dose Interleukin-2 in Patients With Stable Ischaemic Heart Disease and Acute Coronary Syndromes (LILACS): Protocol and Study Rationale for a Randomised, Double-Blind, Placebo-Controlled, Phase I/II Clinical Trial. *BMJ Open* (2018) 8. doi: 10.1136/bmjopen-2018-022452
63. Robert M, Miossec P. Effects of Interleukin 17 on the Cardiovascular System. *Autoimmun Rev* (2017) 16:984–91. doi: 10.1016/j.autrev.2017.07.009
64. Luo JW, Hu Y, Liu J, Yang H, Huang P. Interleukin-22: A Potential Therapeutic Target in Atherosclerosis. *Mol Med* (2021) 27. doi: 10.1186/s10020-021-00353-9
65. Che Y, Su Z, Xia L. Effects of IL-22 on Cardiovascular Diseases. *Int Immunopharmacol* (2020) 81:106277. doi: 10.1016/j.intimp.2020.106277
66. Eggenhofer E, Sabet-Rashedi M, Lantow M, Renner P, Rovira J, Koehl GE, et al. Rorγt+ IL-22-Producing NKp46+ Cells Protect From Hepatic Ischemia Reperfusion Injury in Mice. *J Hepatol* (2016) 64:128–34. doi: 10.1016/j.jhep.2015.08.023
67. Geha M, Tsokos MG, Bosse RE, Sannikova T, Iwakura Y, Dalle Lucca JJ, et al. IL-17a Produced by Innate Lymphoid Cells Is Essential for Intestinal Ischemia-Reperfusion Injury. *J Immunol* (2017) 199:2921–9. doi: 10.4049/jimmunol.1700655
68. Mallat Z, Taleb S, Ait-Oufella H, Tedgui A. The Role of Adaptive T Cell Immunity in Atherosclerosis. *J Lipid Res* (2009) 50:364–9. doi: 10.1194/jlr.R800092-JLR200
69. Colonna M. Innate Lymphoid Cells: Diversity, Plasticity, and Unique Functions in Immunity. *Immunity* (2018) 48:1104–17. doi: 10.1016/j.immuni.2018.05.013
70. Bal SM, Golebski K, Spits H. Plasticity of Innate Lymphoid Cell Subsets. *Nat Rev Immunol* (2020) 20:552–65. doi: 10.1038/s41577-020-0282-9
71. Ohne Y, Silver JS, Thompson-Snipes LA, Collet MA, Blanck JP, Cantarel BL, et al. IL-1 Is a Critical Regulator of Group 2 Innate Lymphoid Cell Function and Plasticity. *Nat Immunol* (2016) 17:646–55. doi: 10.1038/ni.3447
72. Silver JS, Kearley J, Copenhaver AM, Sanden C, Mori M, Yu L, et al. Inflammatory Triggers Associated With Exacerbations of COPD Orchestrate Plasticity of Group 2 Innate Lymphoid Cells in the Lungs. *Nat Immunol* (2016) 17:626–35. doi: 10.1038/ni.3443
73. Bal SM, Bernink JH, Nagasawa M, Groot J, Shikhagaie MM, Golebski K, et al. IL-1β, IL-4 and IL-12 Control the Fate of Group 2 Innate Lymphoid Cells in Human Airway Inflammation in the Lungs. *Nat Immunol* (2016) 17:636–45. doi: 10.1038/ni.3444
74. Kumar R, Graham B. IL-33-Hif1α Axis in Hypoxic Pulmonary Hypertension. *EBioMedicine* (2018) 33:8–9. doi: 10.1016/j.ebiom.2018.07.004
75. Lee JJ, McGarry MP, Farmer SC, Denzler KL, Larson KA, Carrigan PE, et al. Interleukin-5 Expression in the Lung Epithelium of Transgenic Mice Leads to Pulmonary Changes Pathognomonic of Asthma. *Pneumologie* (1998) 52(6). doi: 10.1084/jem.185.12.2143
76. Min HK, Moon J, Lee S, Lee AR, Lee CR, Lee J, et al. Expanded IL-22 + Group 3 Innate Lymphoid Cells and Role of Oxidized LDL-C in the Pathogenesis of Axial Spondyloarthritis With Dyslipidaemia. *Immune Netw* (2021) 21:e43. doi: 10.4110/in.2021.21.e43
77. Agca R, Heslinga SC, Rollefstad S, Heslinga M, McInnes IB, Peters MJL, et al. EULAR Recommendations for Cardiovascular Disease Risk Management in Patients With Rheumatoid Arthritis and Other Forms of Inflammatory Joint Disorders: 2015/2016 Update. *Ann Rheum Dis* (2016) 76:17–28. doi: 10.1136/annrheumdis-2016-209775
78. Fachi JL, Pral LP, dos Santos JAC, Codo AC, de Oliveira S, Felipe JS, et al. Hypoxia Enhances ILC3 Responses Through HIF-1α-Dependent Mechanism. *Mucosal Immunol* (2021) 14:828–41. doi: 10.1038/s41385-020-00371-6
79. Liu M, Galli G, Wang Y, Fan Q, Wang Z, Wang X, et al. Novel Therapeutic Targets for Hypoxia-Related Cardiovascular Diseases: The Role of HIF-1. *Front Physiol* (2020) 11:774. doi: 10.3389/fphys.2020.00774
80. O'Sullivan TE, Rapp M, Fan X, Weizman O-E, Bhardwaj P, Adams NM, et al. Adipose-Resident Group 1 Innate Lymphoid Cells Promote Obesity-Associated Insulin Resistance. *Immunity* (2016) 45:428–41. doi: 10.1016/j.immuni.2016.06.016
81. Kochumon S, Al Madhoun A, Al-Rashed F, Thomas R, Sindhu S, Al-Ozairi E, et al. Elevated Adipose Tissue Associated IL-2 Expression in Obesity Correlates With Metabolic Inflammation and Insulin Resistance. *Sci Rep* (2020) 10:1–13. doi: 10.1038/s41598-020-73347-y
82. Wu Y, Yue J, Wu J, Zhou W, Li D, Ding K, et al. Obesity may Provide Pro-ILC3 Development Inflammatory Environment in Asthmatic Children. *J Immunol Res* (2018) 2018. doi: 10.1155/2018/1628620
83. Upadhyay V, Poroyko V, Kim T, Devkota S, Fu S, Liu D, et al. Lymphotoxin Regulates Commensal Responses to Enable Diet-Induced Obesity. *Nat Immunol* (2012) 13:947–53. doi: 10.1038/ni.2403
84. Roberts LB, Schnoeller C, Berkachy R, Darby M, Pillaye J, Oudhoff MJ, et al. Acetylcholine Production by Group 2 Innate Lymphoid Cells Promotes Mucosal Immunity to Helminths. *Sci Immunol* (2021) 6(57). doi: 10.1126/sciimmunol.abd0359
85. Berrien-Elliott MM, Sun Y, Neal C, Ireland A, Trissal MC, Sullivan RP, et al. MicroRNA-142 Is Critical for the Homeostasis and Function of Type 1 Innate Lymphoid Cells. *Immunity* (2019) 51:479–490.e6. doi: 10.1016/j.immuni.2019.06.016
86. Roberts LB, Jowett GM, Read E, Zabinski T, Berkachy R, Selkirk ME, et al. MicroRNA-142 Critically Regulates Group 2 Innate Lymphoid Cell Homeostasis and Function. *J Immunol* (2021) 206(11):2725–39. doi: 10.4049/jimmunol.2000647
87. Grimaldi A, Pietropaolo G, Stabile H, Kosta A, Capuano C, Gismondi A, et al. The Regulatory Activity of Noncoding Rnas in Ilcs. *Cells* (2021) 10:1–15. doi: 10.3390/cells10102742
88. Wagner M, Ealey KN, Tetsu H, Kiniwa T, Motomura Y, Moro K, et al. Tumor-Derived Lactic Acid Contributes to the Paucity of Intratumoral ILC2s. *Cell Rep* (2020) 30:2743–2757.e5. doi: 10.1016/j.celrep.2020.01.103

Conflict of Interest: The authors declare that the research was conducted in the absence of any commercial or financial relationships that could be construed as a potential conflict of interest.

this article, or claim that may be made by its manufacturer, is not guaranteed or endorsed by the publisher.

frontiers | Frontiers in Immunology

REVIEW
published: 26 May 2022
doi: 10.3389/fimmu.2022.914266

Development of Human ILCs and Impact of Unconventional Cytotoxic Subsets in the Pathophysiology of Inflammatory Diseases and Cancer

Michela Calvi[1], *Clara Di Vito*[2], *Alessandro Frigo*[1], *Sara Trabanelli*[3,4], *Camilla Jandus*[3,4] *and Domenico Mavilio*[1,2*]

[1] Department of Medical Biotechnologies and Translational Medicine (BioMeTra), University of Milan, Milan, Italy, [2] Unit of Clinical and Experimental Immunology, IRCCS Humanitas Research Hospital, Milan, Italy, [3] Department of Pathology and Immunology, Faculty of Medicine, University of Geneva, Geneva, Switzerland, [4] Ludwig Institute for Cancer Research, Lausanne, Switzerland

OPEN ACCESS

Edited by:
Rachel Golub,
Université Paris Diderot, France

Reviewed by:
Marina Cella,
Washington University in St. Louis, United States
Kamel Benlagha,
INSERM U1160 Alloimmunité Transplantation, France

***Correspondence:**
Domenico Mavilio
domenico.mavilio@unimi.it

Specialty section:
This article was submitted to NK and Innate Lymphoid Cell Biology, a section of the journal Frontiers in Immunology

Received: 06 April 2022
Accepted: 28 April 2022
Published: 26 May 2022

Citation:
Calvi M, Di Vito C, Frigo A, Trabanelli S, Jandus C and Mavilio D (2022) Development of Human ILCs and Impact of Unconventional Cytotoxic Subsets in the Pathophysiology of Inflammatory Diseases and Cancer. Front. Immunol. 13:914266. doi: 10.3389/fimmu.2022.914266

Innate lymphoid cells (ILCs) were firstly described by different independent laboratories in 2008 as tissue-resident innate lymphocytes mirroring the phenotype and function of T helper cells. ILCs have been subdivided into three distinct subgroups, ILC1, ILC2 and ILC3, according to their cytokine and transcriptional profiles. Subsequently, also Natural Killer (NK) cells, that are considered the innate counterpart of cytotoxic CD8 T cells, were attributed to ILC1 subfamily, while lymphoid tissue inducer (LTi) cells were attributed to ILC3 subgroup. Starting from their discovery, significant advances have been made in our understanding of ILC impact in the maintenance of tissue homeostasis, in the protection against pathogens and in tumor immune-surveillance. However, there is still much to learn about ILC ontogenesis especially in humans. In this regard, NK cell developmental intermediates which have been well studied and characterized prior to the discovery of helper ILCs, have been used to shape a model of ILC ontogenesis. Herein, we will provide an overview of the current knowledge about NK cells and helper ILC ontogenesis in humans. We will also focus on the newly disclosed circulating ILC subsets with killing properties, namely unconventional $CD56^{dim}$ NK cells and cytotoxic helper ILCs, by discussing their possible role in ILC ontogenesis and their contribution in both physiological and pathological conditions.

Keywords: innate lymphoid cells (ILCs), natural killer (NK) cells, ILC-poiesis, cytotoxicity, unconventional subsets, inflammation, cancer

1 INTRODUCTION

Starting from 2008, several independent laboratories around the world identified new players of innate immunity in both humans and mice (1–4). These cells, named innate lymphoid cells (ILCs), are a heterogeneous group of lymphocytes lacking recombination-activating gene (RAG)-dependent rearranged antigen-specific receptors.

ILCs originate from the common lymphoid progenitor (CLP) and require the common γ chain of the interleukin (IL)-2 receptor and the transcriptional repressor ID2 for their development (2–4). They are considered the innate counterpart of adaptive T lymphocytes: ILCs share with T cells the transcription factors governing their differentiation and the same cytokines in response to inflammatory insults (5, 6), which allows the classification of ILCs into different subsets. Indeed, the ILC1, ILC2 and ILC3 subsets produce T helper (Th) 1-, Th2- and Th17/22-cytokines, respectively. Furthermore, given their phenotypic, developmental and functional similarities, Natural Killer (NK) cells, the innate counterpart of cytotoxic T lymphocytes, are now grouped together with ILC1s, whereas lymphoid tissue inducer (LTi) cells, belong now to group 3 ILCs (5, 7, 8).

Despite these similarities, ILCs arise from distinct developmental pathways and display unique epigenetic and transcriptional programs with respect to T cells, thus suggesting nonredundant roles of ILCs in immunity (9).

Differently from NK cells, that are mainly circulating lymphocytes, helper ILCs are primarily tissue resident cells and have been found in both lymphoid and non-lymphoid tissues. Indeed, they are particularly enriched at the mucosal surfaces of several organs, such as gut, lungs and skin, where they play a pivotal role in tissue homeostasis and disease, by promoting immune responses, inflammation, tissue repair and tolerance to commensal microbiota (10–12). Despite being a rare population in peripheral blood (PB), several lines of evidence indicate that circulating helper ILCs are characterized by a unique pattern of cytokine receptors, thus suggesting that they are not exclusively tissue resident (9, 13). Moreover, given their innate nature, ILCs represent one of the primary sources of pro- and anti-inflammatory cytokines during the early stages of the immune responses (14–17).

Although progresses have been made in understanding the role of ILCs in the maintenance of tissue homeostasis, in immune-defense and in tumor immune-surveillance, there is still much to learn concerning ILCs, especially in humans.

In this review we will summarize the principal features of ILCs, focusing mainly on circulating subsets. Moreover, we will provide an overview on ILC development in humans. In this context, we will focus on the newly disclosed circulating ILC subsets with cytotoxic properties, namely $CD56^{dim}CD16^{neg}$ NK cells and cytotoxic helper ILCs, by discussing their possible role in ILC ontogenesis and their contribution in both physiological and pathological conditions.

2 GENERAL FEATURES OF ILCs

ILCs are subdivided into three main groups based on the cytokine production, genetic signature and transcription factors involved in their development (**Figure 1A**).

Total circulating ILCs, which comprises helper ILCs and NK cells, are identified as lineage (CD3, CD14, CD15, CD19, CD20, CD33, CD34, CD203c and FcεRI) negative lymphocytes (**Figure 1B**) (17). This lineage markers can be used also to identify tissue resident ILCs, with the exception of human tonsil ILC3s which express CD33 (18). Total helper ILCs are defined as $CD16^{neg}$ cells that constitutively express the IL-7 receptor-α chain (CD127) and the different subsets are identified according to the expression of CRTH2, cKit (CD117) and CD56: ILC1s are $CRTH2^{neg}CD117^{neg}CD56^{neg}$, ILC2s are $CRTH2^{pos}CD117^{pos/neg}CD56^{neg}$ and ILC3s $CRTH2^{neg}CD117^{pos}CD56^{pos/neg}$ (**Figure 1B**) (5, 17, 19). However, it has been shown that ILC2s, in some cases, can express CD56 (20). In addition, among lineage negative cells, NK cell subsets are identified according to the differential expression of CD56 and CD16 (**Figure 1B**) (21).

Despite the phenotype of the different ILC subsets is well defined, their precise distribution across organs and species needs to be refined. Indeed, ILC subset distribution and cytokine production profiles are impacted by environmental cues, that enable a prompt response in case of inflammatory insults without the *de novo* recruitment of ILC subsets (22, 23).

2.1 Group 1 ILCs

NK cells and ILC1s have been grouped together in group 1 ILCs. Indeed, both subsets are characterized by the production of interferon-γ (IFN-γ) and tumor necrosis factor α (TNF-α) in response to IL-12 and IL-18 (5, 7, 24). Moreover, IL-15 is required for the differentiation, homeostasis, and function of both NK cells and ILC1s (25). Similarly to NK cells, ILC1s express natural cytotoxicity receptors (NCRs) (26) and the T-box transcription factor expressed in T cells (T-bet) (25, 27). In addition, both ILC1s and NK cells require the expression of HOBIT TFs, encoded by *Zfp683*, for their differentiation and functional programs (28–30).

Despite their overlapping features, NK cells and ILC1s are two phenotypically and functionally distinct immune cell subsets. Indeed, while ILC1s require T-bet for their development, NK cells need T-bet expression only for maturation and require the expression of the transcription factor Eomesodermin (Eomes) for differentiation (25, 27). Moreover, ILC1s are fundamentally tissue-resident lymphocytes, whereas NK cells can circulate across lymphoid organs *via* the bloodstream and lymphatic system to act as immune sentinels. Indeed, NK cells are unique in their ability to recognize and kill virally infected and malignantly transformed cells, through the balance of the signaling that NK cells receive from their repertoire of activating and inhibitory NK cell receptors (31, 32).

Circulating NK cells comprise two main subsets, a cytotoxic $CD56^{dim}$ and a regulatory $CD56^{bright}$ NK cell subset. $CD56^{dim}$ NK cell subset accounts for up to the 90% of circulating NK cells. They show high baseline perforin expression and are endowed with cytotoxic abilities against target cells not expressing or downregulating the major histocompatibility complex (MHC) class I molecules on their surface. They preferentially produce cytokines in response to direct target cell interactions rather than *via* monocyte-derived cytokines stimulation (33). On the other hand, $CD56^{bright}$ NK cells represent the 10% of circulating NK cells, while they are enriched in peripheral and lymphoid tissues (34). Differently from $CD56^{dim}$ NK cells, and similarly to ILC1s, $CD56^{bright}$ NK cells are poorly cytotoxic, can rapidly secrete

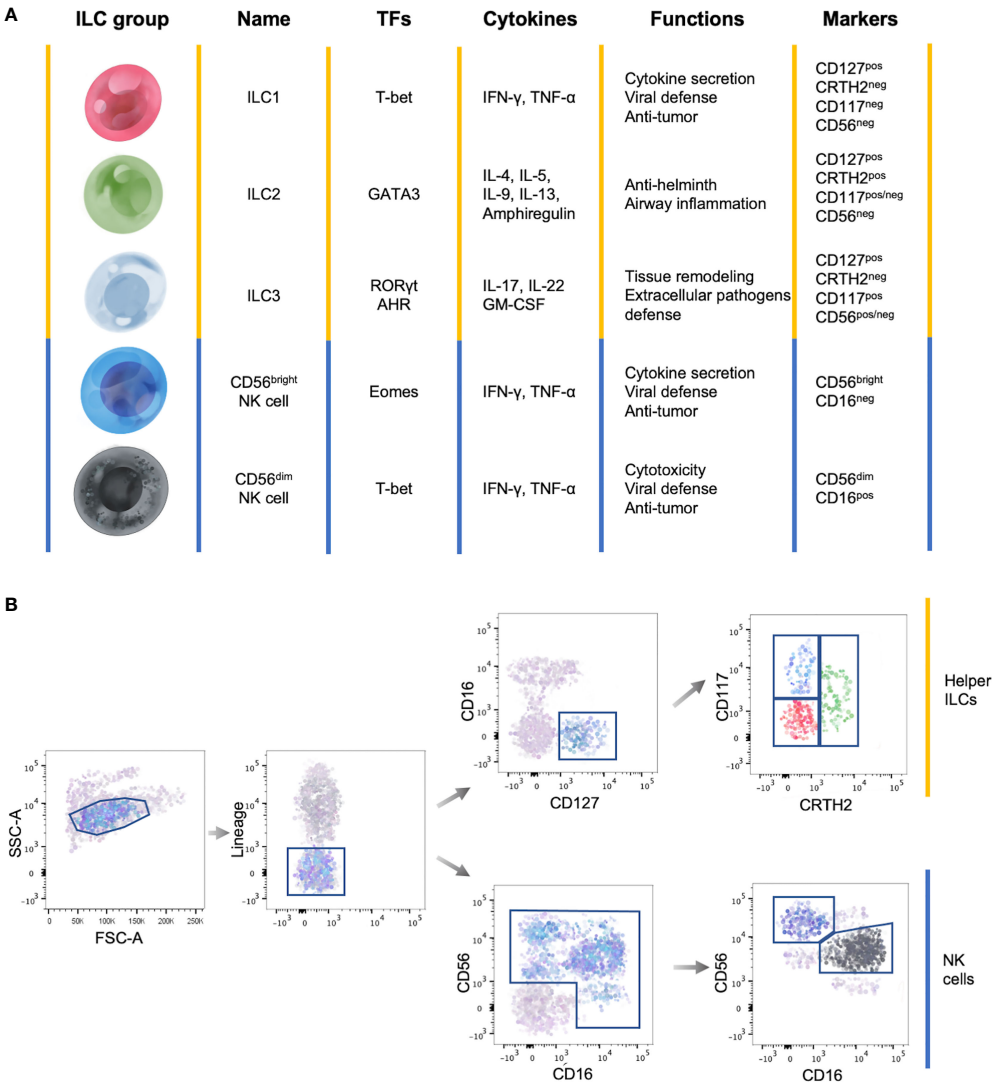

FIGURE 1 | General features of ILC subsets. **(A)** Summary table showing the main transcription factors (TFs) governing the development, the cytokine production, the functions and marker expression in the different ILC subsets. **(B)** Representative flow cytometry gating strategy to identify circulating ILC subsets among Lineage^{neg} lymphocytes. Yellow lines identify helper ILCs, while the blue lines identify NK cells.

cytokines, including IFN-γ, following stimulation by monocyte-derived cytokines (35).

2.2 Group 2 ILCs

Group 2 ILCs are involved in several processes, including lipid metabolism, protection against parasites and accumulate during type 2 inflammation in the airways (36). Among all ILCs, ILC2s express the highest level of the transcription factor GATA3 and are characterized by the production of Th2-associated cytokines, such as IL-4, IL-5, IL-9, IL-13 and amphiregulin (AREG) in response to IL-25, IL-33 and thymic stromal lymphopoietin (TSLP). Hence, they are considered the innate counterpart of Th2 cells (37–39). Of note, several lines of evidence indicate that ILC2s can produce higher levels of cytokine than T cells, thus suggesting their primary role in the innate local immunity against infections in different organs (40). Indeed, they have been described in a variety of human tissues, including tonsils, bone marrow (BM), spleen, skin, adenoids, adipose tissue, lung lymph nodes (LNs) (41).

ILC2s are characterized by the expression of the transcription factor BCL11B which controls their identity (42), the prostaglandin D2 receptor 2 (CRTH2), the IL-33 receptor (IL1RL1 also referred as ST2) and by variable levels of c-Kit (43), all involved in ILC2 localization and function (43–46). More recently, it has been shown that ILC2s are further characterized by the expression of the killer cell lectin-like receptor subfamily G member 1 (KLRG1), a co-inhibitory receptor previously reported in T and NK cells that binds to

the members of the cadherin family and is upregulated during infection in response to IL-25 (20, 47).

2.3 Group 3 ILCs

Group 3 ILCs, consisting of ILC3s as well as LTis, share features with Th17 cells, including the expression of the transcription factor retinoic acid orphan receptor isoform γt (RORγt), required for their development and function, and the aryl hydrocarbon receptor (AHR) (7, 48). Group 3 ILCs are capable of producing IL-17, IL-22 and granulocyte-macrophage colony-stimulating factor (GM-CSF) in response to IL-23, IL-1β, or natural cytotoxicity receptor ligands (NCR-L), thus mirroring Th17 response (5, 49). Regardless of the functional association with ILC3s, LTis are considered a separate ILC lineage (49, 50). Indeed, LTis are involved in the secondary lymphoid organ formation during embryogenesis and adulthood and in their restoration following infection (51), whereas ILC3s mainly contribute to the immune responses against specific extracellular pathogens and in the maintenance of tissue homeostasis at mucosal sites, where they are mainly localized (48).

ILC3s can be further subdivided according to the expression of the NCR NKp44: human NKp44^{pos} ILC3s, largely co-expressing NKp46, are the majority in adult tonsil and intestine and represent an exclusive source of IL-22, while NKp44^{neg} ILC3s are the major population in fetal LNs and preferentially express IL-17 transcripts (48).

Differently from tissues, ILC3s are under-represented in the circulating lymphocyte pool. However, recently, a subpopulation of cells phenotypically resembling to NKp44^{neg} ILC3s has been described in cord and adult PB. However, most peripheral-blood CD127^{pos}CD117^{pos} ILCs express low levels of RORγt, do not produce any of the ILC cytokine signatures following stimulation with IL-1β and IL-23 and their transcriptome is different from that of mature ILC3s present in secondary lymphoid organs (52, 53). Circulating CD127^{pos}CD117^{pos} ILCs are instead multi-potent ILC precursors (ILCPs) that retain the ability to give rise to functionally mature helper ILC subsets, as well as to Eomes^{pos} NK cells, after *in vitro* culture with appropriate cytokine mix or after transfer *in vivo* into immunodeficient mice (49, 53).

3 ILC DEVELOPMENT

ILC-poiesis has been a topic of ardent research in the last several years. Although many issues remain to be disclosed, including the transcriptional regulators that dictate the choice of mature ILC subset fate, the ILC differentiation in mouse has been deeply investigated, thanks to genetically modified rodent models. On the contrary, the study of the human ILC differentiation is still in its infancy because of different reasons. Firstly, the lack of comparable genetic and tracing tools that are available in animal models of lymphoid development. Secondly, the heterogeneity of the studies conducted in terms of definition of progenitor, identification of lineages based solely on cytokine secretion or on few surrogate markers.

Despite these limitations, over the past years a map of human ILC development has been under construction (**Figure 2**) by taking advantage of both murine ILC-developmental model and the pre-existing model of human NK cell development, based on the identification and characterization of human NK cell developmental intermediates (NKDIs) prior to the discovery of helper ILCs (54).

3.1 Human NK Cell Development

Since their discovery in 1970s, NKDIs have been well characterized in both mice and humans as well as the site for NK cell development.

Human NK cells were originally thought to develop strictly within the BM (33, 55). Indeed, CD34^{pos}CD45RA^{pos} precursors with *ex vivo* potential for NK cell differentiation were firstly identified in the BM, and then were also found in PB and in extramedullary tissues, including thymus, secondary lymphoid tissues (SLTs), liver, and uterus, at steady state conditions (56–58). Noteworthy, IL-15-responsive CD34^{pos}CD45RA^{pos} precursors comprise a relatively higher proportion of total CD34^{pos} progenitor cells (5-10%) in the blood compared to bone marrow (<1%), and in SLT they comprise the major subset of CD34^{pos} progenitor cells (>90%) (59, 60). In this regard, several lines of evidence demonstrated that CD34^{pos}CD45RA^{pos} precursors originate in the BM and traffic to extramedullary tissues where later stages of NK cell differentiations can take place, giving rise to tissue-specific and functionally distinct mature NK cell subsets. In particular, tonsils, spleen, and lymph nodes are considered those SLTs hosting the main extra-medullary sites of NK cell development and maturation (57, 59–62).

Originally, five main sequential stages of NK cell maturation were identified: NK cell progenitors (NKPs, stage 1), pre-NK cells (stage 2), immature NK cells (iNK, stage 3) (63–65) and the mature CD56^{bright} (stage 4) and CD56^{dim} (stage 5) NK cell subsets [reviewed in (62)].

Briefly, NKPs and pre-NK cells still express CD34 and retain the ability to differentiate into T cells, dendritic cells (DCs) and other ILCs. Subsequently, the expression of CD122 (IL-2Rβ), together with the downregulation of CD34, marks the irreversible fate decision into NK cell lineage. The commitment of NKPs towards pre-NK cells also required the acquisition of CD117 expression (64, 66). Recently, the stage 2 has been further subdivided into two additional stages: the IL-1R1^{neg} stage 2a, mainly enriched in SLTs and PB, that still retains the ability to give rise to T cells and DCs, and the IL-1R1^{pos} stage 2b, with a commitment restricted to the generation of ILCs, including NK cells (62, 67). IL-1R1^{pos} stage 2b give rise to iNKs whose features, including AHR, CD127, RORγt, IL-1R1, and IL-22 expression, mirror those of Group 3 ILCs (5, 68, 69). Indeed, it is not yet clear if iNKs and ILC3s are entirely overlapping at least in their phenotypic characteristics and further investigation is needed.

The final transition of iNK into mature NK cell subsets is marked by the appearance of CD56 expression and the main functional properties, including cytokine secretion (i.e. TNF, IL-8, GM-CSF, CXCL12 and IL-13, together with IL-22), IFN-γ release and then cytolytic activity (58, 70–72). Two distinct stages 4 CD56^{bright} NK cells have been described: the NKp80^{neg} stage 4a

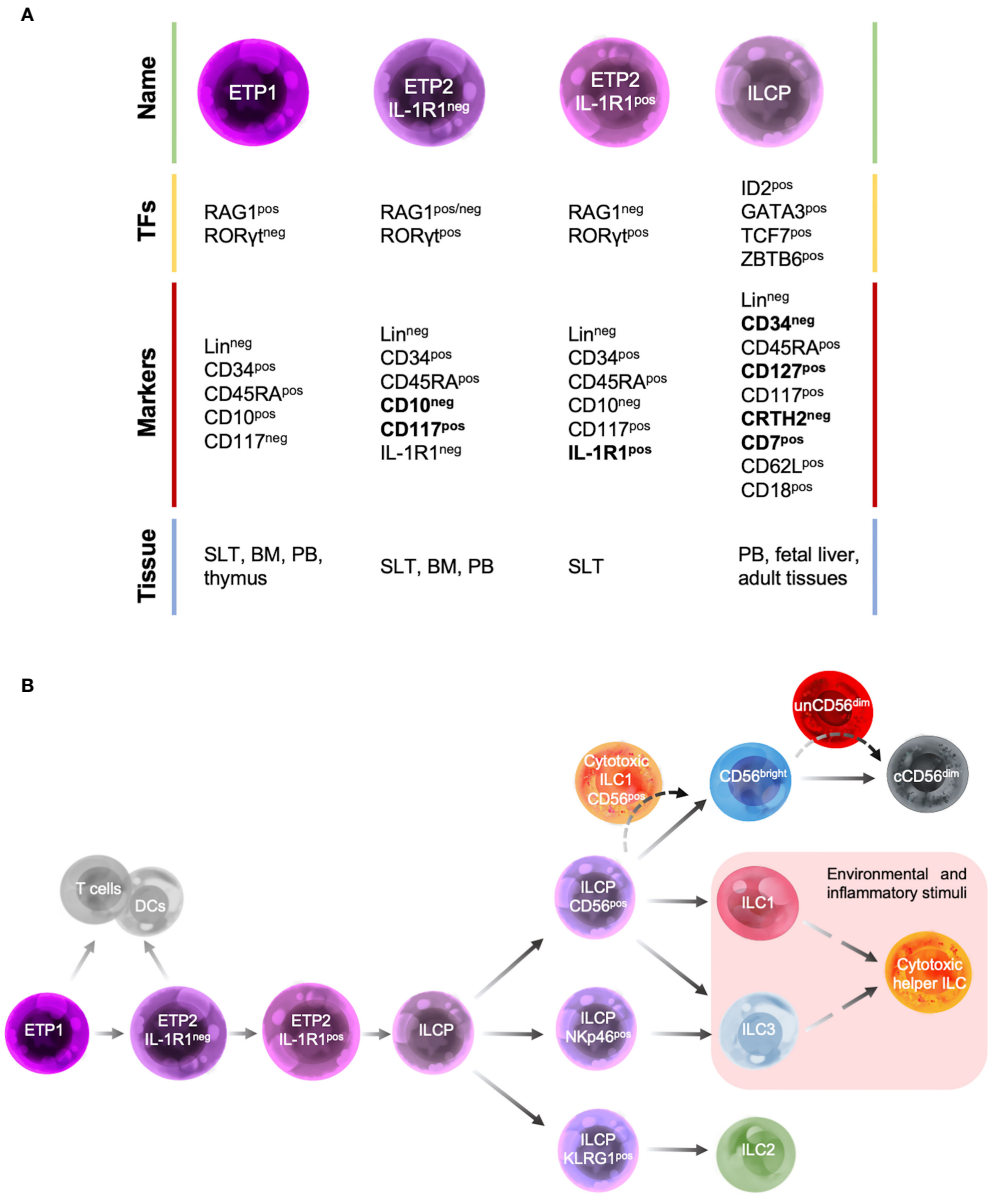

FIGURE 2 | Human ILC developmental stages. **(A)** Summary table of the main transcription factors (TFs), marker expression and tissue localization of common precursors/progenitors. **(B)** Schematic representation of different stages of human ILC-poiesis starting from the early tonsillar progenitors (ETPs), that still retain the ability to give rise to T cells and dendritic cells (DCs), to ILC precursor (ILCPs) that branches into progenitors with restricted differentiation potential and give rise to different mature ILC subsets. Dashed lines indicate the hypothetic developmental pathways of unconventional cytotoxic ILC subsets.

cells, that, despite the bright expression of CD56, are more similar to iNKs cells due to their higher expression of transcription factors RORγt and AHR, their higher production of IL-22 and their preferential localization in SLTs, the NKp80^{pos} stage 4b cells, expressing higher levels of T-bet and Eomes and producing IFN-γ (73). Subsequently, through the acquisition of CD16, Killer Immunoglobulin-like receptors (KIRs) and cytotoxic granules, the fully mature CD56^{dim} NK cells, endowed with cytolytic potential and able to perform antibody-dependent cell-mediated cytotoxicity (ADCC) are generated.

Despite the process of NK cell-poiesis is well defined, with the identification and characterization of other subtypes of ILCs, the old model of NK cell ontogenesis needs to be reassessed and refined in the context of new data about helper ILCs (74).

3.2 Murine ILC Development

Murine ILC differentiation is regulated by a wide range of transcription factors, including *Id2*, *Nfil3*, *Zbtb16*, *Tcf7*, *Gata3*, *Ets1*, and *Tox* [reviewed in (75)].

Two distinct progenitors downstream of the murine CLP have been identified, each with restricted ILC potential. These include the CXCR6$^{pos}\alpha_4\beta_7^{pos}$CD127^{pos} α-lymphoid precursor (αLP) and the Lin^{neg}Thy1.2^{neg}CD127$^{neg}\alpha_4\beta_7^{pos}$ early innate lymphoid progenitor (EILCP) that along with the other downstream progenitors are most prevalent in murine BM (54, 76). The transcription factor *Nfil3* is required for the generation of αLP. Indeed, *Nfil3* knock out mouse models lack mature ILCs, including NK cells (76–78).

On the other hand, EILCPs, requires the transcription factor *Tcf7* (79). Given the drastic reduction of αLPs together with EILCPs in *Tcf7*-deficient mice, it has been also proposed that αLP could constitute an intermediate stage of maturation between CLP and EILCP (76).

Two additional EILCP subsets with different commitment potential have been identified: the early-stage EILCPs (EILP1s), that can give rise to DCs as well as cytotoxic and helper ILCs, and the committed EILPs (cEILCP) expressing TCF-1 and losing the ability to differentiate in DCs (80).

The EILCP can further differentiate in *Id2*-dependent Lin^{neg}Id2^{pos}IL-7R^{pos}IL-2Rα^{neg}α4β7^{pos} common helper-like ILC progenitors (CHILPs), which can give rise to helper-like ILCs (ILC1s, ILC2s, and ILC3s) and LTis but not to NK cells (79, 81) or in *Id2*-independent NK1.1^{neg}IL-2Rβ^{pos} NKPs (82, 83).

CHILPs can be separated into two different subsets based on the expression of *Zbtb16*. The Zbtb16^{neg} common ILC precursor (CILCP) which can no longer produce LTi cells (83, 84) and the *Zbtb16^{pos}* ILC precursor (ILCP) capable of potentially giving rise to conventional NK cells, ILC1s and ILC2s, but with a reduced ability to differentiate into ILC3s (83–86).

3.3 Human ILC Development

According to NK cell developmental model, the most immature ILC progenitors identified in humans are mainly localized in SLTs and were originally described as stage 1 and stage 2 NKIDs and are now defined as early tonsillar progenitors (ETPs) in the context of ILC-poiesis (**Figure 2A**). In particular, ETPs are subdivided into Lin^{neg}CD34^{pos}CD10^{pos}CD117^{neg} ETP1 and Lin^{neg}CD34^{pos}CD10^{neg}CD117^{pos} ETP2 (54, 63). Both ETP1s and ETP2s are multipotent and could also give rise to T cells and DCs *in vitro* (54, 63). ETP2s are heterogeneous in terms of IL-1R1 expression. IL-1R1^{neg} ETP2s have a residual T-cell and DC potential, whereas IL-1R1^{pos} ETP2s are ILC restricted. These population are also characterized by a unique transcription factor signature: ETP1 are RAG1^{pos} and express low levels of ID2 and RORγt, IL-1R1^{neg} ETP2s are ID2^{pos}RORγt^{pos} and retain a low expression of RAG1, whereas IL-1R1^{pos} ETP2s are ID2^{pos}RORγt^{pos}RAG1^{neg} (**Figures 2A, B**) (67). Hence, IL-1R1^{pos}ETP2s are the earliest committed human CILCP identified to date.

In addition, a Lin^{neg}CD34^{neg}CD7^{pos}CD127^{pos}CD117^{pos} CRTH2^{neg} ILC progenitor (ILCP), with phenotypic features that overlap those of stage 3 NKIDs endowed with a restricted potential for ILC generation, has been recently identified in human cord and adult PB as well as fetal liver and several adult tissues. Upon *in vitro* culture with an appropriate cytokine environment or after transfer *in vivo* to immunodeficient mice, these human ILCPs demonstrate their potential for generating all mature helper- and cytotoxic-ILCs (53).

Consistent with their differentiation potential, ILCPs express high levels of transcription factors that have been shown to be essential for mouse ILC development, such as ID2, GATA3, TCF-7 and ZBTB16 (**Figure 2A**). In contrast, moderate to low levels of the lineage-determining transcription factors RORγt, T-bet, Eomes, cytokine receptors (including IL-1R1), and signature cytokines have been found (53). ILCPs show a migratory profile including the expression of L-selectin (CD62L) and β2-integrin (CD18), which would allow these cells to populate the mucosal tissues where they terminally differentiate into mature ILCs in response to local and environmental triggers, during both homeostatic and inflammatory conditions (54, 87, 88). Consistent with this idea, ILCPs were found at mucosal sites where they mature (53).

In light of this evidence, ILCPs might be the equivalents of naïve CD4^{pos} T cells. Indeed, they both express CD45RA and CD62L and the development of ILC subsets from ILCP parallels that of CD4^{pos} T cell subsets from naive CD4^{pos} T cells, with similar polarizing cytokines and transcription factors being required for their differentiation, although the differentiation of naïve CD4^{pos} T cell subsets also depends on TCR signaling and CD28 co-stimulation (22).

Different ILCP populations with a restricted differentiation potential have been recently described and can be identified based on the expression of CD56, NKp46 and KLRG1. CD56^{pos} ILCPs show a restricted potential for NK cells, ILC1s and ILC3s, NKp46^{pos} ILCP predominantly differentiate into ILC3s, whereas KLRG1^{pos} ILC precursors mostly develop into ILC2s (**Figure 2B**) (88, 89).

Adding complexity to this scenario there is the so called ILC plasticity phenomenon. Indeed, it has been demonstrated in both humans and mice, that ILC subsets can switch into another subset depending on the presence of cytokines and NOTCH ligands in their environment. This process is regulated by a complex network of transcription factors. Briefly, ILC2s and ILC3s transdifferentiate into ILC1s in response to IL-1β and IL-12, whereas IL-1β and IL-23 can drive the plasticity of ILC1s and ILC2s towards ILC3s. Despite ILC2s lack the expression of IL-23 receptor, IL-1 β is known to induce ILC2s responsiveness to IL-23 by STAT3 phosphorylation (90). The transdifferentiation of ILC2s into ILC1s or ILC3s can be reversed by IL-4. ILC2s requires TGF-β in addition to IL-1β and IL-23 to differentiate into ILC3s (22). Moreover, NK cells, in a TGF-β-rich tumor environment, transdifferentiate into ILC1-like cells devoid of cytotoxic activity (91, 92). Likely, the plasticity of ILCs is the mechanism of tissue-resident ILCs to dynamically adapt to a given stimulus, such as an inflamed state (23).

4 KILLER ILC SUBSETS

Until recently, NK cells were considered the only cytotoxic innate lymphocytes, being functionally associated with CD8 T cells (7). However, owing to the highly plastic nature of ILCs,

increasing evidence shows that beside their ability to transdifferentiate between helper subpopulations, these cells can also acquire cytotoxic capacities upon defined environmental conditions (93). Indeed, it has been recently reported that, upon exposure to cytokine cocktails, ILC3s or ILC1s, isolated from human tonsils, secondary lymphoid organs (e.g., spleen) and intestinal tissues of humanized mice, give rise to cytotoxic lymphocytes resembling stage 4a NK cells (94, 95). In particular, hallmark NK cell genes, such as *NCAM-1*, *KLRD1, KLRC1, CD2, CD226* have been reported to be significantly upregulated in ILC3s or ILC1s exposed to IL-12/IL-15, and to be paralleled by the acquisition of cell surface expression of at least some of these markers (e.g. NKG2A, NKG2C, CD2). Moreover, these cells show a weak IFN-γ secretion in response to K562, but an efficient perforin- and granzyme-dependent cytotoxicity, primarily mediated by the $Eomes^{pos}T\text{-}bet^{pos}$ fraction of stimulated ILC3s. Nevertheless, these cytotoxic responses remain weaker and of slower kinetics as compared to that of conventional NK cells.

Phenotypically, the distinction between human cytotoxic helper ILCs and NK cells is complicated by the fact that many markers are shared, including CD56, CD161, NKp44 and NKp46. The same stands for mouse ILCs and NK cells that share the expression of NKp46 and NK1.1. Possible discriminators to distinguish cytotoxic helper ILCs, or helper ILCs in general, from NK cells include CD127, which is constitutively expressed by both human and murine helper ILC subsets but not by terminally-differentiated $CD56^{dim}$ NK cells (67) and only at intermediate levels on human peripheral blood $CD56^{bright}$ NK cells (96). Noteworthy, in mice, ILCs with cytotoxic potential were also described within $NK1.1^{pos}CD49a^{pos}$ cells, lacking CD127 expression (26).

Another marker enabling the discrimination between helper ILCs and NK cells might be the inhibitory receptor CD200R1. The expression of CD200R1 has been described to be specific for ILCs in human blood and tonsils (20), and in mice (84, 97). However, intestinal NK cells have been recently described to express CD200R1, although at lower levels as compared to conventional ILCs (95). Inversely, CD200R1 is poorly expressed by intraepithelial ILC1s in the small intestine, lamina propria and visceral adipose tissue (98). Overall, these results highlight the difficulty to identify a universal marker enabling ultimate discrimination between helper ILCs, including cytotoxic ones, and NK cells. Nevertheless, despite potential overlapping phenotypes and functions, the distinct anatomic distribution of cytotoxic helper ILCs and NK cells argues for complementary roles in the protection against infections or emerging malignancies.

Evidence of *in vivo* ability of helper ILCs to acquire cytotoxic features has been recently shown in different districts, as detailed in the next paragraphs.

4.1 Unconventional $CD56^{dim}$ NK Cells

In the context of NK cell development, an additional NK cell subset has been recently identified. This subset, named unconventional NK cells ($unCD56^{dim}$), displays a $CD56^{dim}CD16^{neg}/CD56^{low}CD16^{low}$ phenotype. Barely detectable in the PB, this NK cell subset is mainly enriched in the BM (99, 100). On the other hand, their presence in extramedullary tissues has not been investigated so far.

$UnCD56^{dim}$ NK cell subset expresses surface markers of mature NK cells, such as NKG2D and NKp30 (99). Moreover, this NK cell subset is equipped with lytic molecules, thus suggesting its putative role in mediating cytotoxic responses.

However, their phenotype and transcriptional profile suggest that $unCD56^{dim}$ NK cells are a *bona fide* NK cell subset distinct from activated $CD56^{dim}$ that underwent CD16 shedding mediated by the metalloproteinase-17 (101). Indeed, compared to $CD56^{dim}$ NK cells, $unCD56^{dim}$ NK cells show higher levels of CD27, whose expression was described to decline during NK cell development in mice, and lower levels of markers of terminally differentiated and licensed NK cells, namely CD57 and KIRs, which are acquired at late stages of NK cell differentiation (100). Moreover, $unCD56^{dim}$ NK cells display higher levels of CD25, CD122 and CD127, the receptor chains for IL-2, IL-15 and IL-7 cytokines, which play a major role in controlling NK cell development, homeostasis, survival and activation (100). The chemokine receptor expression pattern of $unCD56^{dim}$ is consistent with a less differentiated phenotype compared to $CD56^{dim}$ NK cells. Indeed, they are characterized by undetectable *CX3CR1* expression, which is usually acquired during NK cell development, and by a higher expression of *CXCR4* compared to the other conventional NK cell subsets, in line with their preferential BM localization (100).

In the context of the lymphopenic environment of patients affected by hematologic malignancies and which underwent haploidentical hematopoietic stem cell transplantation (haplo-HSCT), others and we reported that $unCD56^{dim}$ NK cells are by far the largest subset of NK cells immune-reconstituting in the first 2-4 weeks after the transplant, compensating the low frequency of the conventional cytotoxic $CD56^{dim}$ NK cells (99, 102). These data, together with the transcriptional and phenotypic characteristics of $unCD56^{dim}$ NK cells, intermediate between that of $CD56^{bright}$ and $CD56^{dim}$ NK cells, suggest that this subset could represent an additional or alternative stage of NK cell differentiation that drives the NK cell maturation process (**Figure 2B**) (99, 100).

In vitro experimental evidence also suggests that $unCD56^{dim}$ NK cells possess multifunctional ability and superior effector-functions. Indeed, despite poorly present under homeostatic conditions in the PB, they are endowed with potent cytotoxicity, significantly higher than that of $CD56^{dim}$, and an IFN-γ producing capability comparable to that of $CD56^{bright}$ in response to cytokine stimulation (99, 100, 103). On the contrary, immune-reconstituting $unCD56^{dim}$ NK cells, highly expanded early after haplo-HSCT, are anergic due to a high expression of CD94/NKG2A, an inhibitory receptor involved in NK cell differentiation and education, thus further supporting the assumption of $unCD56^{dim}$ NK cells as a distinct NK cell subset and highlighting their key role in NK cell development. Moreover, this observation allowed us to develop a phase II clinical trial (ONC-2020-001) by using an anti-NKG2A humanized monoclonal antibody (humZ270 mAb, IPH2201, monalizumab, AstraZeneca) to block this inhibitory checkpoint, unleashing alloreactive $unCD56^{dim}$ NK cells, thus

potentially improving the clinical outcome of haplo-HSCT early after transplant (99, 104, 105).

4.2 Cytotoxic Helper ILCs

4.2.1 Tonsillar Cytotoxic ILCs

The *ex vivo* analysis of human tonsil ILCs has shown the existence of a population of CD94^{pos} cells, that co-expressed CD200R1, while negative for CD16, NKp80 and KIRs. In terms of transcriptomic profiles, these cells cluster close to NKp44^{pos} ILC3s, sharing with them the expression of *RORγt*, but being distinct in terms of cytotoxic gene expression (e.g., *Eomes*, *Granzymes*, *Granulysin*) (106). This gene expression pattern has been also correlated with direct cytotoxic activity against the target cell line K562, which is predominant for the CD94^{pos}NKp44^{neg} ILC3 subpopulation. Additional evidence of the *in vivo* generation of cytotoxic helper ILCs in human inflamed tonsils has been recently reported by combining bulk and single cell RNA sequencing (scRNAseq), flow- and mass-cytometry studies (107). In particular, it has been demonstrated that ILC3s and ILC1s reside at the terminal ends of a differentiation spectrum. Between these two extremes, four ILC3-ILC1 intermediates, with a NKp44^{pos}CD56^{pos} phenotype, emerge by RNA velocity analyses. These intermediates are characterized by the gradual acquisition of genes expressed in conventional NK cells, such as *KLRD1*, *KLRC2*, *GZMB* and *GZMK*, loss of *RORG*, *CD200R1*, *KIT*, *IL7R* and upregulation of *Tbx21* and *IKZF3*.

4.2.2 Circulating Cytotoxic ILCs

We recently identified a CD56-expressing subset of circulating ILCs with high cytotoxic potential that belong to conventional ILC1s, being characterized by the lack of lineage markers, the expression of CD127 and the absence of CD117 and CRTH2 (108). RNA-sequencing analysis revealed a transcriptional profile closer to ILCPs and NK cells rather than ILC1s. These CD56^{pos}ILC1-like cells showed distinct nutrient uptake and mitochondrial activity in comparison to helper ILCs and NK cells, low expression of NKp46 and the capacity to produce IL-8, beside IFN-γ, when stimulated with IL-12, IL-15 and IL-18. Through comparison with NK developmental intermediates in terms of phenotype (73), by verifying their presence in patients with severe combined immunodeficiency, in human fetal tissues and during immune reconstitution in humanized mice, and by assessing their capacity to differentiate into conventional ILCs/NKs when cultured on OP9 mouse stromal cells, we concluded that they are related to the developmental stage 4a of NK cells. The cytotoxic machinery of CD56^{pos}ILC1-like ILCs comprised DNAM-1, NKp30, NKp80 and TRAIL, as well as the ability to produce perforin, granzyme A, B, K, M and granulysin. Functionally, CD56^{pos}ILC1-like ILCs can kill both the MHC-I^{neg} K562 cell line and MHC-I^{pos} cell lines, such as BJAB and U937, in accordance with the absence of KIRs. Their cytotoxic capacity is dependent on the expression of NKp30, NKp80 and TRAIL, since the addition of specific blocking antibodies can inhibit their killing ability. We further investigated their presence and function in acute myeloid leukemia (AML), a hematologic malignancy characterized by a dysfunctional helper ILC compartment (109, 110). The data obtained demonstrated that in AML patients at diagnosis, the cytotoxic machinery of CD56^{pos}ILC1-like ILCs is completely impaired, resulting in their inability to kill target cells, either K562 or autologous blasts. On the other hand, AML patients that achieved remission showed a completely restored function of CD56^{pos}ILC1-like cells. Interestingly, CD56^{pos}ILC1-like ILCs but not conventional NK cells from AML patients at diagnosis had a reduced expression of TRAIL, NKp80 and granulysin, thus suggesting that despite their relatedness they are distinct populations able to differentially react to the microenvironment. Further studies are needed to determine whether this population is an intermediate between helper ILCs and NK cells, or a specific cytotoxic circulating helper ILC subset.

4.2.3 Intestinal Cytotoxic ILCs

In a recent study aimed at creating a high-dimensional tissue map of human NK cells across multiple tissues, cytotoxic helper ILCs have been also identified (111). Indeed, CD56^{pos}CD3^{neg} cells expressing CD127, CD56 and CD161 have been found to be enriched in the intestine, as well as in lung-draining lymph nodes and mesenteric lymph nodes. These cells secreted IFN-γ upon stimulation and upregulated CD107a when co-cultured with MHC-I^{neg} targets, suggesting that they might represent either immature NK cells or tissue-resident cytotoxic helper ILC3s, present at selected anatomical sites. These cells might be key in maintaining intestinal homeostasis by cytokine secretion. In that regard, intraepithelial cytotoxic ILCs, very much resembling NK cells, have also been identified by others in the intestinal mucosa (26). These cells are characterized by the expression of CD56, Eomes, T-bet, variable levels of NKp44 and CD103, low levels of CD94 and CD127. This phenotype has not been observed in other anatomic locations, suggesting a selective localization of this subset in the mucosal epithelium of the gut. *In vitro* characterization of these cells revealed that they are able to respond to IL-12 and IL-15 stimulation by secreting IFN-γ, to produce Granzyme B and to express CD107a when exposed to cell targets. Studies in mice showed that these intraepithelial cytotoxic ILCs rely on *Nfil3*- and *Tbx21*-transcription factors, while IL-15 is dispensable for their development, suggesting that, at least in mice, they are distinct from conventional NK cells. The investigation of their putative role in gut inflammation revealed that their frequency is increased in patients with Crohn's disease as well as in *in vivo* models of colitis, arguing for a direct involvement in pathology. In a more recent study, amplified CD94^{pos}CD127^{pos} ILCs has been reported in the intestinal lamina propria in adults, but not in the epithelium, as opposed to the previous study (95). scRNAseq analysis of healthy and Chron's disease patients' tissue specimens revealed the existence of two clusters of lamina propria CD94^{pos}CD127^{pos} cells, with cytotoxic attributes. These cells express Eomes and CD200R1, but lacked CD16 expression. Heterogeneity was observed in terms of CD161, CD117, CD18, cytotoxic molecules (e.g., granzymes and perforin) and granulysin expression. Specifically, the granulysin^{high} perforin^{high} subpopulation is highly amplified in Chron's disease patients, arguing for its induction during the inflammatory process. This hypothesis is supported by the observation that CD94^{pos}CD127^{pos} ILCs are absent in fetal intestine, where instead NK cells are abundant. The activation of these CD94^{pos}CD127^{pos} ILC1-like

ILCs in patients with bowel inflammation might have opposite effects: sustain inflammation on the one hand and fulfill bactericidal activities on the other hand. However, additional experimental investigations are needed to confirm this hypothesis. Given the localization of ILC3s at mucosal barriers, these *in vitro* observations argue for a potential role of cytokine-induced NK-cell like ILC3s in providing cytotoxic protection at mucosal sites, where NK cells are low abundant. If and how this NK cell-like activity of ILC3s could be exploited in vaccination settings against viruses or cancer remains to be studied (94).

4.2.4 Liver Cytotoxic ILCs

A very recent work, investigating the immune phenotype of ILCs in hepatocellular carcinoma by scRNAseq, has demonstrated the existence of a cluster of liver-resident ILC1s endowed with cytotoxic potential (112). This cluster is characterized by the expression of cytolytic effector genes, including *FGFBP2*, *FCGR3A*, *CX3CR1*, *GZMB*, *GZMH*, and *PRF1*. Moreover, these cytotoxic ILC1s are mainly enriched in non-tumor tissues, while in tumor samples ILC1s are characterized by higher levels of exhaustion markers, such as *LAG3*, thus suggesting that ILC1s could undergo functional conversion during liver cancer progression. Further, a high accessibility to the granzyme C gene locus and high *GrzmC* transcripts were recently observed in ILC1s purified from murine liver and salivary glands. Granzyme C^{pos} ILC1 could be differentiated from ILC precursors, are ontogenetically distinct from NK cells and do not convert into ILC2 or ILC3. Granzyme C expression is dependent on T-bet, while sustained TGF-β signaling is required for the maintenance of granzyme C^{pos} ILC1 in the salivary gland, but not in the liver. Using the PyMT breast carcinoma model, the authors show that these cells expand and contribute to tumor anti-tumor functions in a TGF-β-dependent manner. If a similar ILC1 subset exists in humans remains to be tested (113).

Overall, cytotoxic helper ILCs have been so far identified within the ILC1 and/or the ILC3/ILCP subsets, but not within ILC2 compartment (**Figure 2B**). However, $CD56^{pos}$ (89), $CD94^{pos}$ (20) and $NKG2D^{pos}$ (114) ILC2s have been reported in different settings, either *in vitro* upon cytokine exposure or *in vivo* in human peripheral blood. It remains to be verified if these cells have direct cytotoxic functions, like their cytotoxic ILC1 and ILC3 counterparts.

5 CONCLUDING REMARKS

Since their discovery, many efforts have been done to characterize the origin, the function and identity of different ILC subsets. The knowledge regarding ILC biology is continuing to expand and includes the identification and characterization of progenitors, the refinement of mature ILC identities as well as the definition of additional ILC subsets. However, it is of utmost importance to understand if these novel ILC subsets coincide to additional developmental intermediate stages or they are the result of ILC plasticity to adapt to environmental stimuli. Furthermore, emerging evidence highlights the existence of circulating and tissue-resident helper ILCs endowed with cytotoxic potential. These cells, with a phenotype resembling to ILC1s and/or ILC3s/Ps but not ILC2s, most likely are a consequence of environmental and/or inflammatory triggers and could provide early innate defenses against different pathogens, particularly in mucosal tissues, where NK cells are underrepresented.

In the present review, we gave an overview of the current knowledge of ILC biology, mainly focusing on their developmental process. We further summarized the possible developmental pathways of the unconventional cytotoxic ILC subsets recently identified (**Figure 2B**).

Nevertheless, further studies are also needed to deeper characterize the pathways of human ILC development and to understand the differences and similarities with murine ILC-poiesis. In this context, studying the immune-reconstitution of ILC subsets after HSCT certainly represents an important strategy to shedding light on the *in vivo* ILC developmental trajectories at least in periphery. Moreover, the understanding of ILC-poiesis and homeostatic mechanisms driving donor-derived ILC immune-reconstitution as well as determining the acquisition of cytotoxic features, could be of clinical utility. Indeed, it will allow the development of protocols to ameliorate the HSCT outcome based either on adoptive ILC transfer therapies of *ex vivo* generated alloreactive ILCs or on systemic cytokine infusion/blocking antibodies to boost *in vivo* ILC effector-functions. Moreover, given the important role of helper ILCs in tissue immune-surveillance, these novel therapeutic options will find application in the management of solid as well as hematologic cancers and of inflammatory disorders.

AUTHOR CONTRIBUTIONS

MC, CDV, AF, ST, CJ, and DM wrote and critically reviewed the manuscript. AF and MC draw the figures. All authors gave the final approval to the manuscript.

FUNDING

This work was supported by Associazione Italiana per la Ricerca sul Cancro (IG 2018-21567 to DM), Intramural Research Funding of Istituto Clinico Humanitas (to DM), the Italian Ministry of Health (Bando Ricerca Finalizzata PE-2016-02363915 to DM), SNSF PRIMA fellowship (PR900P3_17972729 to CJ), the Swiss Cancer Research Foundation (KFS 5250-02-2021 to CJ) and the Geneva Cancer League (GCL, 2007 to CJ). MC is a recipient of the Leonelli AIRC fellowship (26580). MC and AF are recipients of competitive fellowships awarded from the PhD program of Experimental Medicine from University of Milan. ST is recipient of a Dr Henri Dubois-Ferrière Dinu Lipatti Foundation research fellowship. We also thank the financial support from Fondazione Romeo ed Enrica Invernizzi.

REFERENCES

1. Kiessling R, Klein E, Pross H, Wigzell H. "Natural" Killer Cells in the Mouse. Ii. Cytotoxic Cells With Specificity for Mouse Moloney Leukemia Cells. Characteristics of the Killer Cell. *Eur J Immunol* (1975) 5(2):117–21. doi: 10.1002/eji.1830050209
2. Mebius RE, Rennert P, Weissman IL. Developing Lymph Nodes Collect Cd4 +Cd3- Ltbeta+ Cells That Can Differentiate to Apc, Nk Cells, and Follicular Cells But Not T or B Cells. *Immunity* (1997) 7(4):493–504. doi: 10.1016/s1074-7613(00)80371-4
3. Spits H, Di Santo JP. The Expanding Family of Innate Lymphoid Cells: Regulators and Effectors of Immunity and Tissue Remodeling. *Nat Immunol* (2011) 12(1):21–7. doi: 10.1038/ni.1962
4. Vivier E. The Discovery of Innate Lymphoid Cells. *Nat Rev Immunol* (2021) 21(10):616. doi: 10.1038/s41577-021-00595-y
5. Spits H, Artis D, Colonna M, Diefenbach A, Di Santo JP, Eberl G, et al. Innate Lymphoid Cells–a Proposal for Uniform Nomenclature. *Nat Rev Immunol* (2013) 13(2):145–9. doi: 10.1038/nri3365
6. Vivier E, van de Pavert SA, Cooper MD, Belz GT. The Evolution of Innate Lymphoid Cells. *Nat Immunol* (2016) 17(7):790–4. doi: 10.1038/ni.3459
7. Vivier E, Artis D, Colonna M, Diefenbach A, Di Santo JP, Eberl G, et al. Innate Lymphoid Cells: 10 Years on. *Cell* (2018) 174(5):1054–66. doi: 10.1016/j.cell.2018.07.017
8. Shih HY, Sciume G, Poholek AC, Vahedi G, Hirahara K, Villarino AV, et al. Transcriptional and Epigenetic Networks of Helper T and Innate Lymphoid Cells. *Immunol Rev* (2014) 261(1):23–49. doi: 10.1111/imr.12208
9. Ercolano G, Wyss T, Salome B, Romero P, Trabanelli S, Jandus C. Distinct and Shared Gene Expression for Human Innate Versus Adaptive Helper Lymphoid Cells. *J Leukoc Biol* (2020) 108(2):723–37. doi: 10.1002/JLB.5MA0120-209R
10. Panda SK, Colonna M. Innate Lymphoid Cells in Mucosal Immunity. *Front Immunol* (2019) 10:861. doi: 10.3389/fimmu.2019.00861
11. Mjosberg J, Spits H. Human Innate Lymphoid Cells. *J Allergy Clin Immunol* (2016) 138(5):1265–76. doi: 10.1016/j.jaci.2016.09.009
12. Ebbo M, Crinier A, Vely F, Vivier E. Innate Lymphoid Cells: Major Players in Inflammatory Diseases. *Nat Rev Immunol* (2017) 17(11):665–78. doi: 10.1038/nri.2017.86
13. Gasteiger G, Fan X, Dikiy S, Lee SY, Rudensky AY. Tissue Residency of Innate Lymphoid Cells in Lymphoid and Nonlymphoid Organs. *Science* (2015) 350(6263):981–5. doi: 10.1126/science.aac9593
14. Mebius RE. Organogenesis of Lymphoid Tissues. *Nat Rev Immunol* (2003) 3 (4):292–303. doi: 10.1038/nri1054
15. Tait Wojno ED, Artis D. Innate Lymphoid Cells: Balancing Immunity, Inflammation, and Tissue Repair in the Intestine. *Cell Host Microbe* (2012) 12(4):445–57. doi: 10.1016/j.chom.2012.10.003
16. Diefenbach A, Colonna M, Koyasu S. Development, Differentiation, and Diversity of Innate Lymphoid Cells. *Immunity* (2014) 41(3):354–65. doi: 10.1016/j.immuni.2014.09.005
17. Trabanelli S, Gomez-Cadena A, Salome B, Michaud K, Mavilio D, Landis BN, et al. Human Innate Lymphoid Cells (Ilcs): Toward a Uniform Immune-Phenotyping. *Cytometry B Clin Cytom* (2018) 94(3):392–9. doi: 10.1002/cyto.b.21614
18. Cella M, Otero K, Colonna M. Expansion of Human Nk-22 Cells With Il-7, Il-2, and Il-1beta Reveals Intrinsic Functional Plasticity. *Proc Natl Acad Sci USA* (2010) 107(24):10961–6. doi: 10.1073/pnas.1005641107
19. Sonnenberg GF, Mjosberg J, Spits H, Artis D. Snapshot: Innate Lymphoid Cells. *Immunity* (2013) 39(3):622–e1. doi: 10.1016/j.immuni.2013.08.021
20. Nagasawa M, Heesters BA, Kradolfer CMA, Krabbendam L, Martinez-Gonzalez I, de Bruijn MJW, et al. Correction: Klrg1 and Nkp46 Discriminate Subpopulations of Human Cd117(+)Crth2(-) Ilcs Biased Toward Ilc2 or Ilc3. *J Exp Med* (2019) 216(9):2221–2. doi: 10.1084/jem.2019049007302019c
21. Fan YY, Yang BY, Wu CY. Phenotypically and Functionally Distinct Subsets of Natural Killer Cells in Human Pbmcs. *Cell Biol Int* (2008) 32(2):188–97. doi: 10.1016/j.cellbi.2007.08.025
22. Bal SM, Golebski K, Spits H. Plasticity of Innate Lymphoid Cell Subsets. *Nat Rev Immunol* (2020) 20(9):552–65. doi: 10.1038/s41577-020-0282-9
23. Murphy JM, Ngai L, Mortha A, Crome SQ. Tissue-Dependent Adaptations and Functions of Innate Lymphoid Cells. *Front Immunol* (2022) 13:836999. doi: 10.3389/fimmu.2022.836999
24. Juelke K, Romagnani C. Differentiation of Human Innate Lymphoid Cells (Ilcs). *Curr Opin Immunol* (2016) 38:75–85. doi: 10.1016/j.coi.2015.11.005
25. Daussy C, Faure F, Mayol K, Viel S, Gasteiger G, Charrier E, et al. T-Bet and Eomes Instruct the Development of Two Distinct Natural Killer Cell Lineages in the Liver and in the Bone Marrow. *J Exp Med* (2014) 211 (3):563–77. doi: 10.1084/jem.20131560
26. Fuchs A, Vermi W, Lee JS, Lonardi S, Gilfillan S, Newberry RD, et al. Intraepithelial Type 1 Innate Lymphoid Cells Are a Unique Subset of Il-12- and Il-15-Responsive Ifn-Gamma-Producing Cells. *Immunity* (2013) 38 (4):769–81. doi: 10.1016/j.immuni.2013.02.010
27. Gordon SM, Chaix J, Rupp LJ, Wu J, Madera S, Sun JC, et al. The Transcription Factors T-Bet and Eomes Control Key Checkpoints of Natural Killer Cell Maturation. *Immunity* (2012) 36(1):55–67. doi: 10.1016/j.immuni.2011.11.016
28. Post M, Cuapio A, Osl M, Lehmann D, Resch U, Davies DM, et al. The Transcription Factor Znf683/Hobit Regulates Human Nk-Cell Development. *Front Immunol* (2017) 8:535. doi: 10.3389/fimmu.2017.00535
29. Friedrich C, Taggenbrock R, Doucet-Ladeveze R, Golda G, Moenius R, Arampatzi P, et al. Effector Differentiation Downstream of Lineage Commitment in Ilc1s Is Driven by Hobit Across Tissues. *Nat Immunol* (2021) 22(10):1256–67. doi: 10.1038/s41590-021-01013-0
30. Yomogida K, Bigley TM, Trsan T, Gilfillan S, Cella M, Yokoyama WM, et al. Hobit Confers Tissue-Dependent Programs to Type 1 Innate Lymphoid Cells. *Proc Natl Acad Sci USA* (2021) 118(50):e2117965118. doi: 10.1073/pnas.2117965118
31. Lanier LL. Nk Cell Recognition. *Annu Rev Immunol* (2005) 23:225–74. doi: 10.1146/annurev.immunol.23.021704.115526
32. Vivier E, Raulet DH, Moretta A, Caligiuri MA, Zitvogel L, Lanier LL, et al. Innate or Adaptive Immunity? The Example of Natural Killer Cells. *Science* (2011) 331(6013):44–9. doi: 10.1126/science.1198687
33. Caligiuri MA. Human Natural Killer Cells. *Blood* (2008) 112(3):461–9. doi: 10.1182/blood-2007-09-077438
34. Melsen JE, Lugthart G, Lankester AC, Schilham MW. Human Circulating and Tissue-Resident Cd56(Bright) Natural Killer Cell Populations. *Front Immunol* (2016) 7:262. doi: 10.3389/fimmu.2016.00262
35. Cooper MA, Fehniger TA, Caligiuri MA. The Biology of Human Natural Killer-Cell Subsets. *Trends Immunol* (2001) 22(11):633–40. doi: 10.1016/s1471-4906(01)02060-9
36. Kim BS, Artis D. Group 2 Innate Lymphoid Cells in Health and Disease. *Cold Spring Harb Perspect Biol* (2015) 7(5):a016337. doi: 10.1101/cshperspect.a016337
37. Neill DR, Wong SH, Bellosi A, Flynn RJ, Daly M, Langford TK, et al. Nuocytes Represent a New Innate Effector Leukocyte That Mediates Type-2 Immunity. *Nature* (2010) 464(7293):1367–70. doi: 10.1038/nature08900
38. Moro K, Kabata H, Tanabe M, Koga S, Takeno N, Mochizuki M, et al. Interferon and Il-27 Antagonize the Function of Group 2 Innate Lymphoid Cells and Type 2 Innate Immune Responses. *Nat Immunol* (2016) 17(1):76–86. doi: 10.1038/ni.3309
39. Monticelli LA, Osborne LC, Noti M, Tran SV, Zaiss DM, Artis D. Il-33 Promotes an Innate Immune Pathway of Intestinal Tissue Protection Dependent on Amphiregulin-Egfr Interactions. *Proc Natl Acad Sci USA* (2015) 112(34):10762–7. doi: 10.1073/pnas.1509070112
40. Fonseca W, Lukacs NW, Elesela S, Malinczak CA. Role of Ilc2 in Viral-Induced Lung Pathogenesis. *Front Immunol* (2021) 12:675169. doi: 10.3389/fimmu.2021.675169
41. Meininger I, Carrasco A, Rao A, Soini T, Kokkinou E, Mjosberg J. Tissue-Specific Features of Innate Lymphoid Cells. *Trends Immunol* (2020) 41 (10):902–17. doi: 10.1016/j.it.2020.08.009
42. Califano D, Cho JJ, Uddin MN, Lorentsen KJ, Yang Q, Bhandoola A, et al. Transcription Factor Bcl11b Controls Identity and Function of Mature Type 2 Innate Lymphoid Cells. *Immunity* (2015) 43(2):354–68. doi: 10.1016/j.immuni.2015.07.005
43. Hochdorfer T, Winkler C, Pardali K, Mjosberg J. Expression of C-Kit Discriminates Between Two Functionally Distinct Subsets of Human Type

2 Innate Lymphoid Cells. *Eur J Immunol* (2019) 49(6):884–93. doi: 10.1002/eji.201848006
44. Oyesola OO, Duque C, Huang LC, Larson EM, Fruh SP, Webb LM, et al. The Prostaglandin D2 Receptor Crth2 Promotes Il-33-Induced Ilc2 Accumulation in the Lung. *J Immunol* (2020) 204(4):1001–11. doi: 10.4049/jimmunol.1900745
45. Stier MT, Zhang J, Goleniewska K, Cephus JY, Rusznak M, Wu L, et al. Il-33 Promotes the Egress of Group 2 Innate Lymphoid Cells From the Bone Marrow. *J Exp Med* (2018) 215(1):263–81. doi: 10.1084/jem.20170449
46. Hernandez DC, Juelke K, Muller NC, Durek P, Ugursu B, Mashreghi MF, et al. An in Vitro Platform Supports Generation of Human Innate Lymphoid Cells From Cd34(+) Hematopoietic Progenitors That Recapitulate Ex Vivo Identity. *Immunity* (2021) 54(10):2417–32.e5. doi: 10.1016/j.immuni.2021.07.019
47. Huang Y, Guo L, Qiu J, Chen X, Hu-Li J, Siebenlist U, et al. Il-25-Responsive, Lineage-Negative Klrg1(Hi) Cells Are Multipotential 'Inflammatory' Type 2 Innate Lymphoid Cells. *Nat Immunol* (2015) 16(2):161–9. doi: 10.1038/ni.3078
48. Montaldo E, Juelke K, Romagnani C. Group 3 Innate Lymphoid Cells (Ilc3s): Origin, Differentiation, and Plasticity in Humans and Mice. *Eur J Immunol* (2015) 45(8):2171–82. doi: 10.1002/eji.201545598
49. An Z, Flores-Borja F, Irshad S, Deng J, Ng T. Pleiotropic Role and Bidirectional Immunomodulation of Innate Lymphoid Cells in Cancer. *Front Immunol* (2019) 10:3111. doi: 10.3389/fimmu.2019.03111
50. Ishizuka IE, Chea S, Gudjonson H, Constantinides MG, Dinner AR, Bendelac A, et al. Single-Cell Analysis Defines the Divergence Between the Innate Lymphoid Cell Lineage and Lymphoid Tissue-Inducer Cell Lineage. *Nat Immunol* (2016) 17(3):269–76. doi: 10.1038/ni.3344
51. van de Pavert SA. Lymphoid Tissue Inducer (Lti) Cell Ontogeny and Functioning in Embryo and Adult. *BioMed J* (2021) 44(2):123–32. doi: 10.1016/j.bj.2020.12.003
52. Bar-Ephraim YE, Cornelissen F, Papazian N, Konijn T, Hoogenboezem RM, Sanders MA, et al. Cross-Tissue Transcriptomic Analysis of Human Secondary Lymphoid Organ-Residing Ilc3s Reveals a Quiescent State in the Absence of Inflammation. *Cell Rep* (2017) 21(3):823–33. doi: 10.1016/j.celrep.2017.09.070
53. Lim AI, Li Y, Lopez-Lastra S, Stadhouders R, Paul F, Casrouge A, et al. Systemic Human Ilc Precursors Provide a Substrate for Tissue Ilc Differentiation. *Cell* (2017) 168(6):1086–100.e10. doi: 10.1016/j.cell.2017.02.021
54. Scoville SD, Freud AG, Caligiuri MA. Cellular Pathways in the Development of Human and Murine Innate Lymphoid Cells. *Curr Opin Immunol* (2019) 56:100–6. doi: 10.1016/j.coi.2018.11.003
55. Colucci F, Caligiuri MA, Di Santo JP. What Does It Take to Make a Natural Killer? *Nat Rev Immunol* (2003) 3(5):413–25. doi: 10.1038/nri1088
56. Chinen H, Matsuoka K, Sato T, Kamada N, Okamoto S, Hisamatsu T, et al. Lamina Propria C-Kit+ Immune Precursors Reside in Human Adult Intestine and Differentiate Into Natural Killer Cells. *Gastroenterology* (2007) 133(2):559–73. doi: 10.1053/j.gastro.2007.05.017
57. Moroso V, Famili F, Papazian N, Cupedo T, van der Laan LJ, Kazemier G, et al. Nk Cells Can Generate From Precursors in the Adult Human Liver. *Eur J Immunol* (2011) 41(11):3340–50. doi: 10.1002/eji.201141760
58. Vacca P, Vitale C, Montaldo E, Conte R, Cantoni C, Fulcheri E, et al. Cd34+ Hematopoietic Precursors Are Present in Human Decidua and Differentiate Into Natural Killer Cells Upon Interaction With Stromal Cells. *Proc Natl Acad Sci USA* (2011) 108(6):2402–7. doi: 10.1073/pnas.1016257108
59. Freud AG, Becknell B, Roychowdhury S, Mao HC, Ferketich AK, Nuovo GJ, et al. A Human Cd34(+) Subset Resides in Lymph Nodes and Differentiates Into Cd56bright Natural Killer Cells. *Immunity* (2005) 22(3):295–304. doi: 10.1016/j.immuni.2005.01.013
60. Yu J, Freud AG, Caligiuri MA. Location and Cellular Stages of Natural Killer Cell Development. *Trends Immunol* (2013) 34(12):573–82. doi: 10.1016/j.it.2013.07.005
61. Male V, Hughes T, McClory S, Colucci F, Caligiuri MA, Moffett A. Immature Nk Cells, Capable of Producing Il-22, Are Present in Human Uterine Mucosa. *J Immunol* (2010) 185(7):3913–8. doi: 10.4049/jimmunol.1001637
62. Di Vito C, Mikulak J, Mavilio D. On the Way to Become a Natural Killer Cell. *Front Immunol* (2019) 10:1812. doi: 10.3389/fimmu.2019.01812
63. Freud AG, Yokohama A, Becknell B, Lee MT, Mao HC, Ferketich AK, et al. Evidence for Discrete Stages of Human Natural Killer Cell Differentiation in Vivo. *J Exp Med* (2006) 203(4):1033–43. doi: 10.1084/jem.20052507
64. Freud AG, Caligiuri MA. Human Natural Killer Cell Development. *Immunol Rev* (2006) 214:56–72. doi: 10.1111/j.1600-065X.2006.00451.x
65. Grzywacz B, Kataria N, Sikora M, Oostendorp RA, Dzierzak EA, Blazar BR, et al. Coordinated Acquisition of Inhibitory and Activating Receptors and Functional Properties by Developing Human Natural Killer Cells. *Blood* (2006) 108(12):3824–33. doi: 10.1182/blood-2006-04-020198
66. McClory S, Hughes T, Freud AG, Briercheck EL, Martin C, Trimboli AJ, et al. Evidence for a Stepwise Program of Extrathymic T Cell Development Within the Human Tonsil. *J Clin Invest* (2012) 122(4):1403–15. doi: 10.1172/JCI46125
67. Scoville SD, Mundy-Bosse BL, Zhang MH, Chen L, Zhang X, Keller KA, et al. A Progenitor Cell Expressing Transcription Factor Rorgammat Generates All Human Innate Lymphoid Cell Subsets. *Immunity* (2016) 44(5):1140–50. doi: 10.1016/j.immuni.2016.04.007
68. Hughes T, Becknell B, Freud AG, McClory S, Briercheck E, Yu J, et al. Interleukin-1beta Selectively Expands and Sustains Interleukin-22+ Immature Human Natural Killer Cells in Secondary Lymphoid Tissue. *Immunity* (2010) 32(6):803–14. doi: 10.1016/j.immuni.2010.06.007
69. Cella M, Fuchs A, Vermi W, Facchetti F, Otero K, Lennerz JK, et al. A Human Natural Killer Cell Subset Provides an Innate Source of Il-22 for Mucosal Immunity. *Nature* (2009) 457(7230):722–5. doi: 10.1038/nature07537
70. Lanier LL, Le AM, Phillips JH, Warner NL, Babcock GF. Subpopulations of Human Natural Killer Cells Defined by Expression of the Leu-7 (Hnk-1) and Leu-11 (Nk-15) Antigens. *J Immunol* (1983) 131(4):1789–96.
71. Loza MJ, Perussia B. Final Steps of Natural Killer Cell Maturation: A Model for Type 1-Type 2 Differentiation? *Nat Immunol* (2001) 2(10):917–24. doi: 10.1038/ni1001-917
72. Ahn YO, Blazar BR, Miller JS, Verneris MR. Lineage Relationships of Human Interleukin-22-Producing Cd56+ Rorgammat+ Innate Lymphoid Cells and Conventional Natural Killer Cells. *Blood* (2013) 121(12):2234–43. doi: 10.1182/blood-2012-07-440099
73. Freud AG, Keller KA, Scoville SD, Mundy-Bosse BL, Cheng S, Youssef Y, et al. Nkp80 Defines a Critical Step During Human Natural Killer Cell Development. *Cell Rep* (2016) 16(2):379–91. doi: 10.1016/j.celrep.2016.05.095
74. Scoville SD, Freud AG, Caligiuri MA. Modeling Human Natural Killer Cell Development in the Era of Innate Lymphoid Cells. *Front Immunol* (2017) 8:360. doi: 10.3389/fimmu.2017.00360
75. Serafini N, Vosshenrich CA, Di Santo JP. Transcriptional Regulation of Innate Lymphoid Cell Fate. *Nat Rev Immunol* (2015) 15(7):415–28. doi: 10.1038/nri3855
76. Seillet C, Mielke LA, Amann-Zalcenstein DB, Su S, Gao J, Almeida FF, et al. Deciphering the Innate Lymphoid Cell Transcriptional Program. *Cell Rep* (2016) 17(2):436–47. doi: 10.1016/j.celrep.2016.09.025
77. Yu X, Wang Y, Deng M, Li Y, Ruhn KA, Zhang CC, et al. The Basic Leucine Zipper Transcription Factor Nfil3 Directs the Development of a Common Innate Lymphoid Cell Precursor. *Elife* (2014) 3:e04406. doi: 10.7554/eLife.04406
78. Guia S, Narni-Mancinelli E. Helper-Like Innate Lymphoid Cells in Humans and Mice. *Trends Immunol* (2020) 41(5):436–52. doi: 10.1016/j.it.2020.03.002
79. Harly C, Cam M, Kaye J, Bhandoola A. Development and Differentiation of Early Innate Lymphoid Progenitors. *J Exp Med* (2018) 215(1):249–62. doi: 10.1084/jem.20170832
80. Yang Q, Li F, Harly C, Xing S, Ye L, Xia X, et al. Tcf-1 Upregulation Identifies Early Innate Lymphoid Progenitors in the Bone Marrow. *Nat Immunol* (2015) 16(10):1044–50. doi: 10.1038/ni.3248
81. Harly C, Kenney D, Ren G, Lai B, Raabe T, Yang Q, et al. The Transcription Factor Tcf-1 Enforces Commitment to the Innate Lymphoid Cell Lineage. *Nat Immunol* (2019) 20(9):1150–60. doi: 10.1038/s41590-019-0445-7
82. Renoux VM, Zriwil A, Peitzsch C, Michaelsson J, Friberg D, Soneji S, et al. Identification of a Human Natural Killer Cell Lineage-Restricted Progenitor in Fetal and Adult Tissues. *Immunity* (2015) 43(2):394–407. doi: 10.1016/j.immuni.2015.07.011

83. Xu W, Cherrier DE, Chea S, Vosshenrich C, Serafini N, Petit M, et al. An Id2 (Rfp)-Reporter Mouse Redefines Innate Lymphoid Cell Precursor Potentials. *Immunity* (2019) 50(4):1054–68.e3. doi: 10.1016/j.immuni.2019.02.022
84. Walker JA, Clark PA, Crisp A, Barlow JL, Szeto A, Ferreira ACF, et al. Polychromic Reporter Mice Reveal Unappreciated Innate Lymphoid Cell Progenitor Heterogeneity and Elusive Ilc3 Progenitors in Bone Marrow. *Immunity* (2019) 51(1):104–18.e7. doi: 10.1016/j.immuni.2019.05.002
85. Constantinides MG, McDonald BD, Verhoef PA, Bendelac A. A Committed Precursor to Innate Lymphoid Cells. *Nature* (2014) 508(7496):397–401. doi: 10.1038/nature13047
86. Klose CSN, Flach M, Mohle L, Rogell L, Hoyler T, Ebert K, et al. Differentiation of Type 1 Ilcs From a Common Progenitor to All Helper-Like Innate Lymphoid Cell Lineages. *Cell* (2014) 157(2):340–56. doi: 10.1016/j.cell.2014.03.030
87. Bar-Ephraim YE, Koning JJ, Burniol Ruiz E, Konijn T, Mourits VP, Lakeman KA, et al. Cd62l Is a Functional and Phenotypic Marker for Circulating Innate Lymphoid Cell Precursors. *J Immunol* (2019) 202(1):171–82. doi: 10.4049/jimmunol.1701153
88. Mazzurana L, Czarnewski P, Jonsson V, Wigge L, Ringner M, Williams TC, et al. Tissue-Specific Transcriptional Imprinting and Heterogeneity in Human Innate Lymphoid Cells Revealed by Full-Length Single-Cell Rna-Sequencing. *Cell Res* (2021) 31(5):554–68. doi: 10.1038/s41422-020-00445-x
89. Chen L, Youssef Y, Robinson C, Ernst GF, Carson MY, Young KA, et al. Cd56 Expression Marks Human Group 2 Innate Lymphoid Cell Divergence From a Shared Nk Cell and Group 3 Innate Lymphoid Cell Developmental Pathway. *Immunity* (2018) 49(3):464–76.e4. doi: 10.1016/j.immuni.2018.08.010
90. Golebski K, Ros XR, Nagasawa M, van Tol S, Heesters BA, Aglmous H, et al. Il-1beta, Il-23, and Tgf-Beta Drive Plasticity of Human Ilc2s Towards Il-17-Producing Ilcs in Nasal Inflammation. *Nat Commun* (2019) 10(1):2162. doi: 10.1038/s41467-019-09883-7
91. Gao Y, Souza-Fonseca-Guimaraes F, Bald T, Ng SS, Young A, Ngiow SF, et al. Tumor Immunoevasion by the Conversion of Effector Nk Cells Into Type 1 Innate Lymphoid Cells. *Nat Immunol* (2017) 18(9):1004–15. doi: 10.1038/ni.3800
92. Cortez VS, Ulland TK, Cervantes-Barragan L, Bando JK, Robinette ML, Wang Q, et al. Smad4 Impedes the Conversion of Nk Cells Into Ilc1-Like Cells by Curtailing Non-Canonical Tgf-Beta Signaling. *Nat Immunol* (2017) 18(9):995–1003. doi: 10.1038/ni.3809
93. Krabbendam L, Bernink JH, Spits H. Innate Lymphoid Cells: From Helper to Killer. *Curr Opin Immunol* (2021) 68:28–33. doi: 10.1016/j.coi.2020.08.007
94. Raykova A, Carrega P, Lehmann FM, Ivanek R, Landtwing V, Quast I, et al. Interleukins 12 and 15 Induce Cytotoxicity and Early Nk-Cell Differentiation in Type 3 Innate Lymphoid Cells. *Blood Adv* (2017) 1 (27):2679–91. doi: 10.1182/bloodadvances.2017008839
95. Krabbendam L, Heesters BA, Kradolfer CMA, Haverkate NJE, Becker MAJ, Buskens CJ, et al. Cd127+ Cd94+ Innate Lymphoid Cells Expressing Granulysin and Perforin Are Expanded in Patients With Crohn's Disease. *Nat Commun* (2021) 12(1):5841. doi: 10.1038/s41467-021-26187-x
96. Romagnani C, Juelke K, Falco M, Morandi B, D'Agostino A, Costa R, et al. Cd56brightcd16- Killer Ig-Like Receptor- Nk Cells Display Longer Telomeres and Acquire Features of Cd56dim Nk Cells Upon Activation. *J Immunol* (2007) 178(8):4947–55. doi: 10.4049/jimmunol.178.8.4947
97. Weizman OE, Adams NM, Schuster IS, Krishna C, Pritykin Y, Lau C, et al. Ilc1 Confer Early Host Protection at Initial Sites of Viral Infection. *Cell* (2017) 171(4):795–808.e12. doi: 10.1016/j.cell.2017.09.052
98. McFarland AP, Yalin A, Wang SY, Cortez VS, Landsberger T, Sudan R, et al. Multi-Tissue Single-Cell Analysis Deconstructs the Complex Programs of Mouse Natural Killer and Type 1 Innate Lymphoid Cells in Tissues and Circulation. *Immunity* (2021) 54(6):1320–37.e4. doi: 10.1016/j.immuni.2021.03.024
99. Roberto A, Di Vito C, Zaghi E, Mazza EMC, Capucetti A, Calvi M, et al. The Early Expansion of Anergic Nkg2a(Pos)/Cd56(Dim)/Cd16(Neg) Natural Killer Represents a Therapeutic Target in Haploidentical Hematopoietic Stem Cell Transplantation. *Haematologica* (2018) 103(8):1390–402. doi: 10.3324/haematol.2017.186619
100. Stabile H, Nisti P, Morrone S, Pagliara D, Bertaina A, Locatelli F, et al. Multifunctional Human Cd56 Low Cd16 Low Natural Killer Cells Are the Prominent Subset in Bone Marrow of Both Healthy Pediatric Donors and Leukemic Patients. *Haematologica* (2015) 100(4):489–98. doi: 10.3324/haematol.2014.116053
101. Lajoie L, Congy-Jolivet N, Bolzec A, Gouilleux-Gruart V, Sicard E, Sung HC, et al. Adam17-Mediated Shedding of Fcgammariiia on Human Nk Cells: Identification of the Cleavage Site and Relationship With Activation. *J Immunol* (2014) 192(2):741–51. doi: 10.4049/jimmunol.1301024
102. Stabile H, Nisti P, Peruzzi G, Fionda C, Pagliara D, Brescia PL, et al. Reconstitution of Multifunctional Cd56(Low)Cd16(Low) Natural Killer Cell Subset in Children With Acute Leukemia Given Alpha/Beta T Cell-Depleted Hla-Haploidentical Haematopoietic Stem Cell Transplantation. *Oncoimmunology* (2017) 6(9):e1342024. doi: 10.1080/2162402X.2017.1342024
103. Vulpis E, Stabile H, Soriani A, Fionda C, Petrucci MT, Mariggio E, et al. Key Role of the Cd56(Low)Cd16(Low) Natural Killer Cell Subset in the Recognition and Killing of Multiple Myeloma Cells. *Cancers (Basel)* (2018) 10(12):473. doi: 10.3390/cancers10120473
104. Zaghi E, Calvi M, Marcenaro E, Mavilio D, Di Vito C. Targeting Nkg2a to Elucidate Natural Killer Cell Ontogenesis and to Develop Novel Immune-Therapeutic Strategies in Cancer Therapy. *J Leukoc Biol* (2019) 105(6):1243–51. doi: 10.1002/JLB.MR0718-300R
105. Locatelli F, Pende D, Mingari MC, Bertaina A, Falco M, Moretta A, et al. Cellular and Molecular Basis of Haploidentical Hematopoietic Stem Cell Transplantation in the Successful Treatment of High-Risk Leukemias: Role of Alloreactive Nk Cells. *Front Immunol* (2013) 4:15. doi: 10.3389/fimmu.2013.00015
106. Krabbendam L, Heesters BA, Kradolfer CMA, Spits H, Bernink JH. Identification of Human Cytotoxic Ilc3s. *Eur J Immunol* (2021) 51(4):811–23. doi: 10.1002/eji.202048696
107. Cella M, Gamini R, Secca C, Collins PL, Zhao S, Peng V, et al. Subsets of Ilc3-Ilc1-Like Cells Generate a Diversity Spectrum of Innate Lymphoid Cells in Human Mucosal Tissues. *Nat Immunol* (2019) 20(8):980–91. doi: 10.1038/s41590-019-0425-y
108. Salome B, Gomez-Cadena A, Loyon R, Suffiotti M, Salvestrini V, Wyss T, et al. Cd56 as a Marker of an Ilc1-Like Population With Nk Cell Properties That Is Functionally Impaired in Aml. *Blood Adv* (2019) 3(22):3674–87. doi: 10.1182/bloodadvances.2018030478
109. Trabanelli S, Curti A, Lecciso M, Salome B, Riether C, Ochsenbein A, et al. Cd127+ Innate Lymphoid Cells Are Dysregulated in Treatment Naive Acute Myeloid Leukemia Patients at Diagnosis. *Haematologica* (2015) 100(7):e257–60. doi: 10.3324/haematol.2014.119602
110. Munneke JM, Bjorklund AT, Mjosberg JM, Garming-Legert K, Bernink JH, Blom B, et al. Activated Innate Lymphoid Cells Are Associated With a Reduced Susceptibility to Graft-Versus-Host Disease. *Blood* (2014) 124 (5):812–21. doi: 10.1182/blood-2013-11-536888
111. Dogra P, Rancan C, Ma W, Toth M, Senda T, Carpenter DJ, et al. Tissue Determinants of Human Nk Cell Development, Function, and Residence. *Cell* (2020) 180(4):749–63.e13. doi: 10.1016/j.cell.2020.01.022
112. He Y, Luo J, Zhang G, Jin Y, Wang N, Lu J, et al. Single-Cell Profiling of Human Cd127(+) Innate Lymphoid Cells Reveals Diverse Immune Phenotypes in Hepatocellular Carcinoma. *Hepatology* (2022). doi: 10.1002/hep.32444
113. Nixon BG, Chou C, Krishna C, Dadi S, Michel AO, Cornish AE, et al. Cytotoxic Granzyme C-Expressing Ilc1s Contribute to Antitumor Immunity and Neonatal Autoimmunity. *Sci Immunol* (2022) 7(70):eabi8642. doi: 10.1126/sciimmunol.abi8642
114. Gomez-Cadena A, Spehner L, Kroemer M, Khelil MB, Bouiller K, Verdeil G, et al. Severe Covid-19 Patients Exhibit an Ilc2 Nkg2d(+) Population in Their Impaired Ilc Compartment. *Cell Mol Immunol* (2021) 18(2):484–6. doi: 10.1038/s41423-020-00596-2

Conflict of Interest: The authors declare that the research was conducted in the absence of any commercial or financial relationships that could be construed as a potential conflict of interest.

this article, or claim that may be made by its manufacturer, is not guaranteed or endorsed by the publisher.

frontiers | Frontiers in Immunology

ORIGINAL RESEARCH
published: 02 June 2022
doi: 10.3389/fimmu.2022.903459

A Japanese Herbal Formula, Daikenchuto, Alleviates Experimental Colitis by Reshaping Microbial Profiles and Enhancing Group 3 Innate Lymphoid Cells

Zhengzheng Shi[1,2], *Tadashi Takeuchi*[1], *Yumiko Nakanishi*[1,3], *Tamotsu Kato*[1,3], *Katharina Beck*[1], *Ritsu Nagata*[1,3], *Tomoko Kageyama*[1,3], *Ayumi Ito*[1,3], *Hiroshi Ohno*[1,2,3] *and Naoko Satoh-Takayama*[1,3]*

[1] *Laboratory for Intestinal Ecosystem, RIKEN Center for Integrative Medical Sciences, Yokohama, Japan,* [2] *Laboratory for Immune Regulation, Graduate School of Medical and Pharmaceutical Sciences, Chiba University, Chiba, Japan,* [3] *Immunobiology Laboratory, Graduate School of Medical Life Science, Yokohama City University, Yokohama, Japan*

Daikenchuto (DKT) is one of the most widely used Japanese herbal formulae for various gastrointestinal disorders. It consists of *Zanthoxylum Fructus* (Japanese pepper), *Zingiberis Siccatum Rhizoma* (processed ginger), *Ginseng radix*, and maltose powder. However, the use of DKT in clinical settings is still controversial due to the limited molecular evidence and largely unknown therapeutic effects. Here, we investigated the anti-inflammatory actions of DKT in the dextran sodium sulfate (DSS)-induced colitis model in mice. We observed that DKT remarkably attenuated the severity of experimental colitis while maintaining the members of the symbiotic microbiota such as family Lactobacillaceae and increasing levels of propionate, an immunomodulatory microbial metabolite, in the colon. DKT also protected colonic epithelial integrity by upregulating the fucosyltransferase gene *Fut2* and the antimicrobial peptide gene *Reg3g*. More remarkably, DKT restored the reduced colonic group 3 innate lymphoid cells (ILC3s), mainly RORγt^{high}-ILC3s, in DSS-induced colitis. We further demonstrated that ILC3-deficient mice showed increased mortality during experimental colitis, suggesting that ILC3s play a protective function on colonic inflammation. These findings demonstrate that DKT possesses anti-inflammatory activity, partly *via* ILC3 function, to maintain the colonic microenvironment. Our study also provides insights into the molecular basis of herbal medicine effects, promotes more profound mechanistic studies towards herbal formulae and contributes to future drug development.

Keywords: Japanese herbal medicine (Kampo medicine), Daikenchuto (DKT), biomolecular functions of herbal medicine, experimental colitis, Lactobacillaceae, gut microbiota, colonic homeostasis, group 3 innate lymphoid cells (ILC3s)

OPEN ACCESS

Edited by:
Carolina Jancic,
Consejo Nacional de Investigaciones Científicas y Técnicas (CONICET), Argentina

Reviewed by:
Yue Wang,
Second Hospital of Anhui Medical University, China
Chen Lina,
Nanjing Medical University, China
Pengfei Xu,
University of Pittsburgh, United States

****Correspondence:***
Naoko Satoh-Takayama
naoko.satoh@riken.jp

Specialty section:
This article was submitted to NK and Innate Lymphoid Cell Biology, a section of the journal Frontiers in Immunology

Received: *24 March 2022*
Accepted: *04 May 2022*
Published: *02 June 2022*

Citation:
Shi Z, Takeuchi T, Nakanishi Y, Kato T, Beck K, Nagata R, Kageyama T, Ito A, Ohno H and Satoh-Takayama N (2022) A Japanese Herbal Formula, Daikenchuto, Alleviates Experimental Colitis by Reshaping Microbial Profiles and Enhancing Group 3 Innate Lymphoid Cells. Front. Immunol. 13:903459. doi: 10.3389/fimmu.2022.903459

INTRODUCTION

Traditional Japanese herbal medicine, or Kampo medicine, originated in ancient China and was introduced to Japan and practiced since approximately the 6th century. Kampo medicine has evolved over the centuries and has been successfully integrated into the modernized medical system in Japan (1). In the 1980s, Japanese medical insurance approved 148 herbal preparations as prescribed medicines (1, 2). These preparations are mainly derived from several ancient Chinese medicine textbooks dated 2,000 years ago (1, 2). This management system guarantees the quality, purity, and safety of herbal medicines, providing preconditions for scientific research (1, 3). The management also makes herbal formulae more affordable and accessible to patients in need.

Herbal medicine also gained popularity in European countries and the U.S. three decades ago (4, 5). Approximately 20% of the U.S. population consumes herbal products (5). In addition, to date, herbal therapies still dominate primary health care in developing countries (6). However, the efficacy of herbal medicine is controversial due to the limited scientific evidence.

Daikenchuto (DKT) is one of the most frequently prescribed Kampo preparations for various digestive disorders (1, 3). It consists of *Zanthoxylum Fructus* (Japanese pepper), *Zingiberis Siccatum Rhizoma* (processed ginger), *Ginseng radix*, and maltose powder. Initially, DKT served as a prokinetic agent to improve gut motility in several clinical settings. A number of clinical trials have suggested that DKT enhanced the intestinal transit in patients who underwent abdominal surgeries and mechanical ventilation (7–9). In addition, clinical observations have indicated that oral intake of DKT for several months prevents the need for reoperation in patients with a subtype of inflammatory bowel disease (IBD) (10). Later reports have proposed that the herbal formula's prokinetic actions may be due to its anti-inflammatory actions (11). More recently, several animal studies have revealed that DKT exerts anti-inflammatory activities by suppressing Akt and NF-κB pathways and interleukin (IL)-6 and enhancing adrenomedullin in gut epithelial cells (12–14). DKT has also been studied in the dextran sulfate sodium (DSS)-induced colitis models. Matsunaga *et al.* found that DKT resulted in higher serum hemoglobin concentrations and IL-10 levels compared with DSS-treated mice (15). DKT also reduced visceral pain and eosinophilic infiltration into the colon in a rat DSS colitis model (16). U.S. researchers have also developed considerable interest in DKT (17, 18). Additionally, a multi-center clinical trial of DKT has been performed, aiming for the FDA approval (ClinicalTrials.gov Identifier: NCT01607307).

IBD, which encompasses Crohn's disease and ulcerative colitis, is a chronic gut inflammatory disorder thought to be caused by inappropriate immune responses. It is usually a life-long condition that can be treated with several medications, although it is difficult to achieve a complete cure. IBD has become a global health concern as we have seen a large surge in its prevalence in North America and northern Europe. IBD morbidity is also on the rise in newly industrialized regions such as Asia, the Middle East, South America, and Africa. The number of individuals with IBD worldwide almost doubled in the last twenty years, increasing from 3.7 million to 6.8 million by 2017 (19, 20). Drugs for IBD include 5-aminosalicylic acid (5-ASA) compounds, antibiotics, systemic corticosteroids, immunosuppressors, monoclonal antibodies, and inhibitors of tumor necrosis factor. Although these drugs have tremendously improved the outcome of IBD treatment, individual responses vary, and adverse events and the high cost of several of these medications are still problematic (20, 21). Hence, new therapeutic options balancing cost-effectiveness and potent anti-inflammatory effects for IBD are desired (20, 21).

Intestinal tissue-resident innate lymphoid cells (ILCs) are key mediators in gut homeostasis and might serve as novel therapeutic targets in IBD management (22). For instance, group 1 ILCs (ILC1s) contribute to the pathogenesis of IBD in humans and mice by producing interferon-γ (22). Group 3 ILCs (ILC3s) are potent immune cells for pathogen clearance in the intestine by secreting cytokines IL-22 and IL-17, although their role in IBD is still elusive (23, 24).

Previous observations in human and animal disease models imply that DKT resolves local inflammation in the gut by several mechanisms (10, 14). Thus, it leads us to speculate that DKT can serve as another anti-inflammatory agent complementary to the standard IBD therapies. Nevertheless, the studies regarding DKT were inconclusive due to the lack of molecular evidence. In particular, in-depth immunological insights into DKT and its therapeutic effects on colitis are largely undetermined yet.

Here, we investigated the impacts of DKT on the DSS-induced colitis model, with particular emphasis on its effects on gut microbiota and immune cell profiles. We demonstrated that DKT accelerated the recovery from experimental colitis in mice, accompanied by improvements in several colitis-associated features of gut microbiota, their metabolites, and the colonic ILC3 population. Our study highlights previously unrecognized effects of DKT on the immune-microbiota axis in colitis, and our work opens a future therapeutic opportunity for IBD patients.

RESULTS

DKT Contributes to a Swift Recovery of DSS-Induced Colitis

We first evaluated the efficacy of DKT on DSS-induced colitis. To this end, we set the following four experimental groups: a normal chow diet group (Control), a group given 5% DKT extracts mixed in a normal chow diet (DKT), a 2.5% DSS-induced colitis group (DSS), and a group of 2.5% DSS colitis mice that treated with 5% DKT (DSS+DKT) (**Figure 1A**). The body weight of the DSS group dropped sharply after two days of the DSS challenge until the day of sacrifice (day 15), whereas the DSS+DKT group almost maintained the starting body weight (**Figure 1B**). As expected, the body weight of the Control and DKT groups increased slightly throughout the experiments. The DSS+DKT group displayed a significantly longer colon than the DSS-treated mice (**Figures 1C, D**). Consistently, the DSS+DKT group showed significantly lower clinical colitis scores (**Figure 1E**). Histological analysis indicated that the DSS+DKT group had less epithelial damage than the DSS group, although hyperplasia was

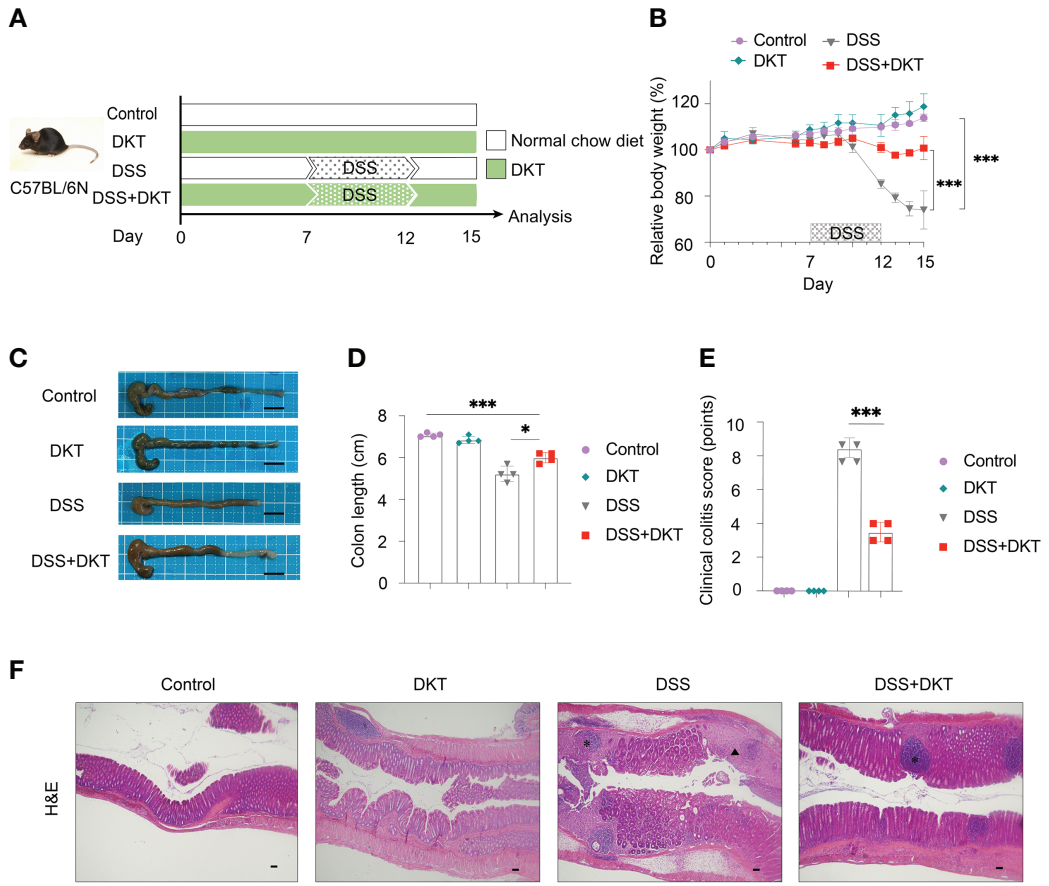

FIGURE 1 | DKT alleviates the symptoms and pathology of dextran sodium sulfate (DSS)-induced acute colitis. **(A)** Experimental schematic: C57BL/6 mice were divided into four groups: a normal chow diet group (Control), a group given 5% DKT extract mixed in normal chow diet (DKT), a 2.5% DSS-induced colitis group (DSS), and a group of 2.5% DSS-colitis mice fed the same diet as the DKT group (DSS+DKT). 2.5% DSS in drinking water was administered beginning on day 7 and continued for 5 days, followed by a three-day DSS-free period. The mice were sacrificed on day 15. **(B)** Body weight changes over the course of the experiment (N=4 per group). **(C)** Representative macroscopic images of the colon post-mortem (N=4 per group). Scale bars represent 1 cm. **(D)** Colon lengths were measured from the proximal colon to the rectum post-mortem (N=4 per group). **(E)** Clinical colitis scores of the four experimental groups on day 15, measured in a blind fashion (N=4 per group). **(F)** Representative histology of H&E-stained longitudinal sections of the rectal colon (Control N=4, DKT N=4, DSS N=5, DSS+DKT N=5). Scale bars represent 100 μm. *indicates the isolated lymphoid follicles. The triangle indicates the ulceration. Each symbol **(D, E)** represents data from an individual mouse. Results are representative of two or three independent experiments with three to four mice in each experimental group. Graph **(B, D, E)** show means ± SEM; *p<0.05, and ***p<0.001. Statistical analysis was performed using One-way ANOVA with Tukey's multiple comparisons test.

slightly presented in this group (**Figure 1F**). By contrast, the DSS group showed severe mucosa damage, such as multiple ulcerations, hyperplasia, edema, and inflammatory cell infiltration into the submucosa region. No apparent changes in the colon were observed in the Control and DKT groups. Overall, these results suggest that DKT treatment significantly prevents colonic damage in DSS-induced colitis; these observations prompted us to further interrogate the underlying molecular basis for the anti-inflammatory activities of DKT in colitis.

DKT Ameliorates Colonic Dysbiosis by Increasing Lactobacillaceae and Propionate

Previous evidence suggested that gut microbiota plays a pivotal role in DSS-induced colitis as it affects the sensitivity of DSS-induced colitis (25). In addition, short-chain fatty acids (SCFAs), the most abundant gut microbial metabolites, are deeply involved in the pathogenesis of colitis (26). We, therefore, asked whether DKT could impact the gut microbiota and their metabolites to alleviate the DSS-induced colitis. We first analyzed the gut microbiota composition by 16S rRNA amplicon sequencing. Both DSS and DSS+DKT groups showed lower taxonomic diversity represented by Chao1 index after colitis induction (**Figure 2A**), suggesting that DKT did not restore the loss of bacterial diversity that accompanies DSS colitis. However, the bacterial landscape of the four groups displayed unique features, as shown in the principal coordinates analysis of Bray-Curtis dissimilarity (**Figure 2B**). Dietary DKT itself did not affect the bacterial compositions compared to the Control group, while the DSS challenge

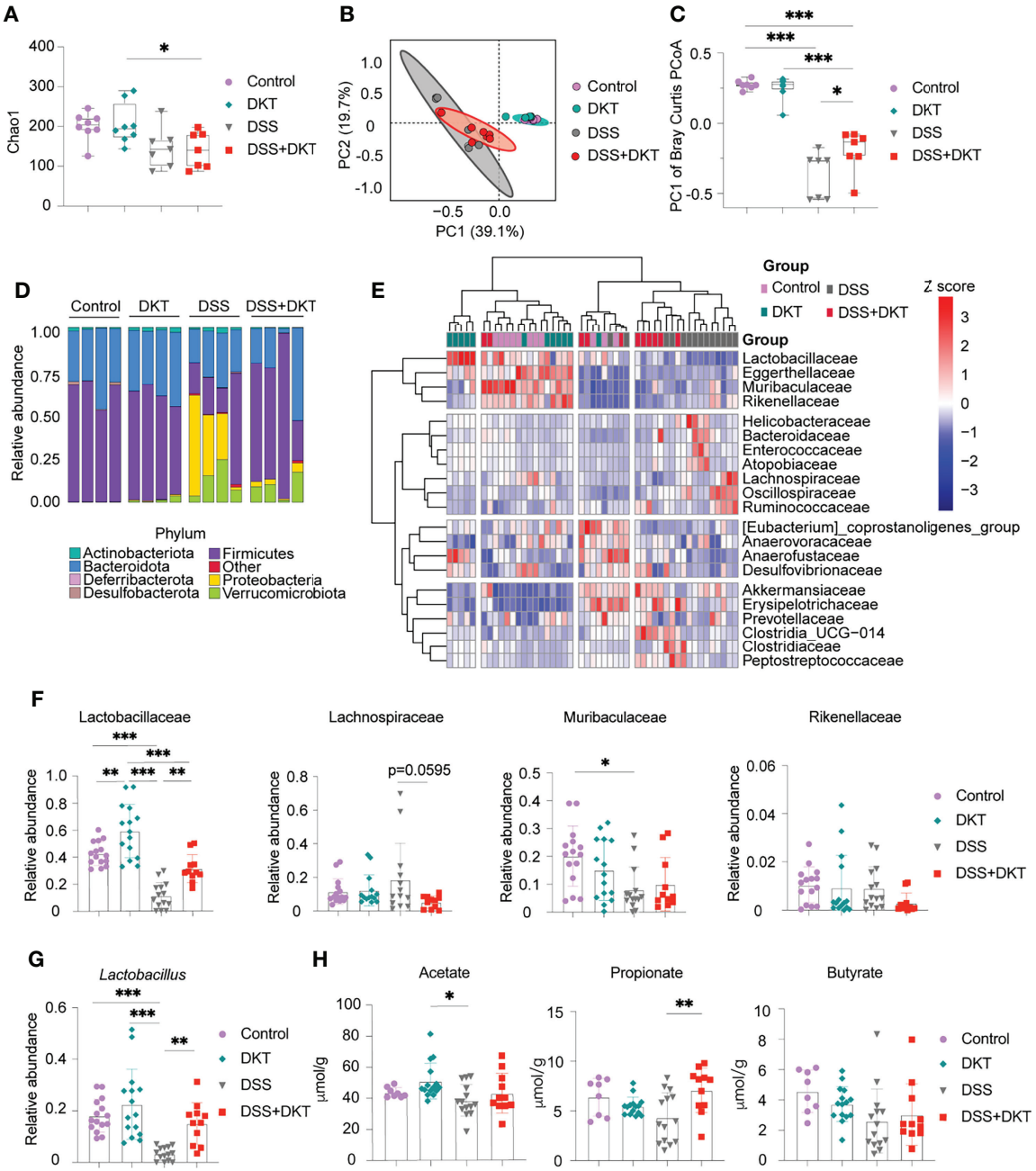

FIGURE 2 | DKT alters the colonic microbiota composition and metabolites in DSS-induced acute colitis. **(A)** Chao1 alpha diversity of the colonic microbiota on day 15 (Control N=8, DKT N=8, DSS N=7, DSS+DKT N=7). **(B)** Principal coordinates analysis (PCoA) of the Bray Curtis distances between samples; day 15 samples are shown (Control N=8, DKT N=8, DSS N=7, DSS+DKT N=7). The ellipses indicate 95% confidence levels for the four groups. **(C)** PC1 of the Bray-Curtis PCoA among the four groups (Control N=8, DKT N=8, DSS N=7, DSS+DKT N=7). **(D)** The bacteria composition in the colonic contents at the phylum level on day 15 (N=4 per group). **(E)** Heatmap showing the top 21 highly abundant family-level bacteria on day 15 among the four groups. The microbial composition data at the family level were scaled and clustered based on the Ward-linkage method (Control N=11, DKT N=12, DSS N=14, DSS+DKT N=11). **(F)** Relative abundance of the family-level bacteria Lactobacillaceae, Lachnospiraceae, Muribaculaceae and Rikenellaceae on day 15 are shown (Control N=15, DKT N=15, DSS N=14, DSS+DKT N=11). **(G)** Relative abundance of the genus-level bacteria *Lactobacillus* on day 15 among the four groups (Control N=15, DKT N=15, DSS N=14, DSS+DKT N=11). **(H)** The concentration of three short-chain fatty acids (SCFAs), acetate, propionate and butyrate, on day 15 in the colonic contents are shown (Control N=8, DKT N=15, DSS N=14, DSS+DKT N=11). The SCFAs were measured by a GCMS platform. Results are pooled from two or three independent experiments with three to five mice in each experimental group. Each symbol **(A–C** and **F–H)** represents data from an individual mouse. Graphs **(A, C**, and **F–H)** display means ± SEM; *p<0.05, **p<0.01, and ***p<0.001. Statistical analysis was performed using One-way ANOVA with Tukey's multiple comparisons test.

shifted the colonic bacterial community apart from these two groups negatively along PC1. Although DSS and DSS+DKT groups were not clearly separated, the DSS+DKT group was closer to the non-colitis groups along PC1 (**Figure 2C**). In line with this result, taxonomic microbiota profiles at the phylum level showed that DKT restored the abundance of Firmicutes to levels similar to the non-DSS groups. In addition, Proteobacteria, the well-known pathobionts that facilitate colitis (27), were enriched in the DSS group while they were substantially reduced in the DSS+DKT group (**Figure 2D**). We next used the unsupervised hierarchical clustering based on Ward's method to further characterize the similarities of the microbiota composition at the family-level among the four experimental groups (**Figure 2E**). Although the groups were not perfectly separated, the DSS group was distantly located from the non-DSS groups; the DSS+DKT group was largely located between the DSS and non-DSS samples. These findings imply that DSS administration vigorously altered the gut bacterial community and DKT blunted such alterations.

In the heatmap (**Figure 2E**), the top cluster of family-level bacteria, including Lactobacillaceae, Eggerthellaceae, Muribaculaceae, and Rikenellaceae, were the most prominently reduced by DSS administration. We further found that Lactobacillaceae, which belongs to the phylum Firmicutes and exerts various beneficial effects on the host physiology, including attenuation of gut inflammation (28), showed substantial alterations among the four experimental groups (**Figure 2F**, left panel). DSS challenge suppressed Lactobacillaceae while DKT administration partially restored their abundance. Consistently, DKT administration restored the abundance of *Lactobacillus*, a major genus-level bacteria of Lactobacillaceae, to levels similar to the non-DSS groups (**Figure 2G**). Of note, dietary DKT increased Lactobacillaceae compared to the control group (**Figure 2F**, left panel). In addition to the effects on Lactobacillaceae, the DSS+DKT group displayed a tendency of decreased Lachnospiraceae, which also belongs to the Firmicutes phylum and is the third most abundant family in the non-DSS groups, compared with the DSS group (**Figure 2F**). Lachnospiraceae plays a controversial role in human physiology and is known to contribute to the onset of inflammation and several metabolic disorders (29, 30). We did not observe any apparent alterations in other families (**Figure 2F** and **Supplementary Figure 1**).

We next performed a fecal metabolome analysis with particular emphasis on SCFAs. Notably, propionate, a major SCFA derived from the colonic bacteria, was significantly higher in the DSS+DKT group than the DSS group, and its concentration was comparable to the two healthy groups (**Figure 2H**). DKT did not affect acetate or butyrate. Collectively, these data reveal that DKT restores several critical features of DSS-induced colitis in terms of gut microbiota and their metabolites.

DKT Preserves the Integrity of the Colonic Epithelial Barrier by Restoring Goblet Cells and Promoting Antimicrobial Peptides

Once colitis strikes the community of microorganisms, it impairs mucus properties, and the microorganisms may reach the epithelium and affect its barrier function (31). MUC2 mucin, secreted by goblet cells, is a critical component of the gastrointestinal mucus layer to protect the epithelium (32). Previous studies also suggested that *Lactobacillus* could upregulate the MUC2 mucin (33, 34). Since we found that DKT maintained *Lactobacillus* under the DSS challenge, we asked how the MUC2 mucin and goblet cells were affected. We found that *Muc2* expression in colonic epithelial cells tended to be higher in the DSS+DKT group than in the DSS group (**Figure 3A**). Immunohistochemistry analysis of MUC2 showed no apparent differences between the two healthy groups, while the DSS+DKT group appeared to have restored MUC2 compared to the DSS group (**Figure 3B**). Goblet cells in the DSS+DKT group also appeared to increase due to the hyperplasia of the colonic glands, whereas DSS-treated mice showed significantly depleted and disrupted goblet cells (**Figure 3B**).

In addition to the mucus layer, antimicrobial peptides and fucosylation are other critical regulators in maintaining intestinal homeostasis and are deeply involved in the pathogenesis of colitis (35, 36). In this regard, we observed that a representative antimicrobial peptide gene *Reg3g* and an essential epithelial fucosylation gene *Fut2* mRNAs were significantly upregulated in the DSS+DKT group compared with the DSS group (**Figure 3C**).

Altogether, these findings reveal that DKT improves epithelial integrity in DSS-induced colitis, which may explain the ameliorated colitis symptoms in the DSS+DKT group.

DKT Enhances ILC3 to Promote the Host Defense Against Experimental Colitis

It has been previously reported that secretion of antimicrobial peptides and fucosylation on epithelial cells are regulated by IL-22 (37, 38), which is secreted by several types of lymphocytes from the adaptive and innate immune systems, such as effector $CD4^+$ T lymphocytes, particularly Th17 cells, and ILC3s (39, 40). The observed upregulation of *Reg3g* and *Fut2* by DKT in the colonic epithelial cells (**Figure 3C**) prompted us to interrogate the involvement of IL-22 in DKT-mediated amelioration of colitis. We first examined Th17 cell and ILC3 populations by flow cytometry. Colitis significantly increased the Th17 numbers and there was no difference between the DSS and DSS+DKT groups (**Figure 4A**). By contrast, the population of tissue-resident ILC3s tended to increase in the DSS+DKT group compared to the DSS group (**Figure 4B**). We further noted that DSS treatment suppressed the ROR-related orphan receptor gamma t (RORγt) intensity, as its expression level was lower than the other three experimental groups (**Figure 4C**). DSS decreased the $ROR\gamma t^{high}$ expressing ILC3s, while DKT treatment significantly restored the frequency and cell numbers of $ROR\gamma t^{high}$-ILC3s to levels similar to the non-DSS groups (**Figures 4C, D**: upper panel). There were no differences in $ROR\gamma t^{low}$-ILC3s between the DSS and non-DSS groups (**Figure 4D**: lower panel). Moreover, DKT did not impact other subtypes of ILCs, such as ILC1s/natural killer (NK) cells or ILC2s (**Supplementary Figure 2B**). Although DSS-induced colitis led to the expansion of $CD4^+$ T cells, B cells, and macrophages, DKT did not influence these populations (**Supplementary Figure 2C**). And conventional dendritic cells (DCs) remained unchanged among the four groups (**Supplementary Figure 2C**).

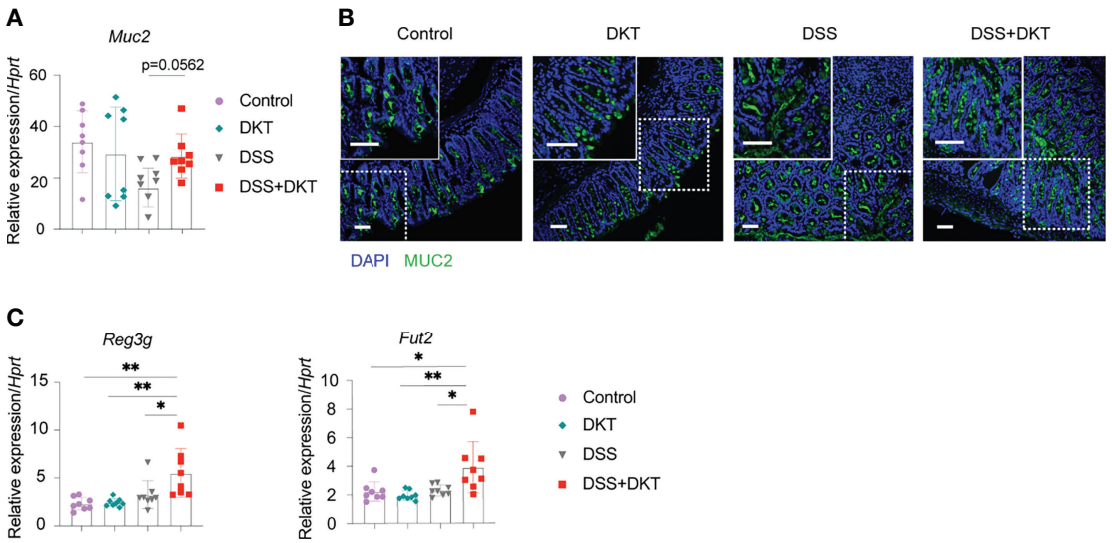

FIGURE 3 | DKT protects the integrity of colonic epithelium by upregulating *Muc2*, the antimicrobial peptide gene *Reg3* and the fucosyltransferase gene *Fut2*. **(A)** *Muc2* mRNA expression in the colonic enterocytes after colitis induction (N=8 per group). **(B)** Immunofluorescence images of MUC2 expression (green) and DAPI (blue) staining in the rectal colonic tissue (Control N=3, DKT N=3, DSS N=4, DSS+DKT N=4). Scale bars represent 50 μm, inset scale bars represent 50 μm. **(C)** *Reg3g* and *Fut2* mRNA expression in the colonic enterocytes after colitis induction (N=8 per group). Each symbol **(A, C)** represents data from an individual mouse. **(A, C)**, results are pooled from two independent experiments with four mice in each experimental group and show means ± SEM; *p<0.05, **p<0.01. Statistical analysis was performed using One-way ANOVA with Tukey's multiple comparisons test.

ILC3s have been reported to be quite heterogeneous and to encompass at least two major subsets. One subgroup expresses the surface marker NKp46, termed natural cytotoxicity receptor $(NCR)^+$ ILC3s (40). The other subset expresses the chemokine receptor CCR6, as well as CD4 and MHCII, and these cells are termed lymphoid tissue inducer (LTi)-like cells (41, 42). Of note, differences in RORγt expression levels have been previously suggested to correlate with the different subtypes of ILC3s in the mouse small intestine (43). In order to further characterize the $ROR\gamma t^{high}$-ILC3s in the mouse colon, which was significantly different between the DSS and DSS+DKT groups (**Figures 4C, D**), we next assessed the expression of surface markers such as CCR6, MHCII, NKp46, and CD4 to discriminate the ILC3 subgroups among naïve cells. $ROR\gamma t^{high}$-ILC3s predominantly expressed CCR6, MHCII, and CD4, while $ROR\gamma t^{low}$-ILC3s showed a higher level of NKp46 expression (**Figure 4E**). Taken together, these observations indicate that a large proportion of $ROR\gamma t^{high}$-ILC3s primarily consists of the LTi-like phenotype, while the $ROR\gamma t^{low}$-ILC3s mainly comprise NCR^+ ILC3s.

We next assessed IL-22 and IL-17A-producing colonic ILC3s in $Rorc^{GFP/+}$ mice (**Figure 4F**). In steady-state, ILC3s produced a certain level of IL-22, although they barely produced IL-17A (**Figure 4G**). Despite the increase in $IL\text{-}22^+$-ILC3s under the colitis condition, the cell number remained comparable between the DSS and DSS+DKT groups. $IL\text{-}17A^+$-ILC3s did not differ among the four experimental groups. Similarly, *Il22* and *Il17a* mRNA levels in $ROR\gamma t^{high}$-ILC3s in $Rorc^{GFP/+}$ mice were unchanged in all four groups (**Supplementary Figure 2D**).

SCFAs act as ligands for G-protein coupled receptors (GPCRs), including GPR41, GPR43, and GPR109A, to activate signaling cascades that exert anti-inflammatory activities in IBD (44). We, therefore, qPCR-quantified the expression of mRNAs encoding these GPCRs in the sorted $ROR\gamma t^{high}$-ILC3s. We detected GPR43-encoding *Ffar2* mRNA in $ROR\gamma t^{high}$-ILC3s in steady-state, and DSS treatment upregulated *Ffar2* expression, although there was no difference between the DSS and DSS+DKT groups (**Supplementary Figure 2E**). By contrast, the expression of GPR41-encoding *Ffar3* and GPR109a-encoding *Hcar2* was barely detected (comparing the scale of Y-axes in **Supplementary Figure 2E**), and the expression of *Ffar3* and *Hcar2* was unchanged regardless of DKT or DSS treatment (**Supplementary Figure 2E**).

Taken together, these data provide evidence that DKT impacts the colonic immune system, particularly by increasing the $ROR\gamma t^{high}$-ILC3 subpopulation in DSS-induced colitis. We also show that this $ROR\gamma t^{high}$-ILC3 population phenotypically resembles LTi-like cells, although their effector functions remain to be investigated.

ILC3 Is a Critical Protective Immunoregulator in Experimental Colitis

The above-described increase in $ROR\gamma t^{high}$-ILC3s prompted us to test if these cells are involved in DKT-mediated alleviation of DSS-induced colitis. We took advantage of ILC3-specific knockout (KO) mice, generated by crossing CD127-Cre and $Rorc^{fl/fl}$ mice. While ILC3-sufficient wildtype (WT) mice survived DSS treatment regardless of DKT, ILC3 ablation resulted in a mortality rate of 83.3% in DSS-induced colitis. On the contrary, DKT treatment strikingly reduced the mortality to 16.7% (**Figure 5A**). Since under the experimental colitis condition,

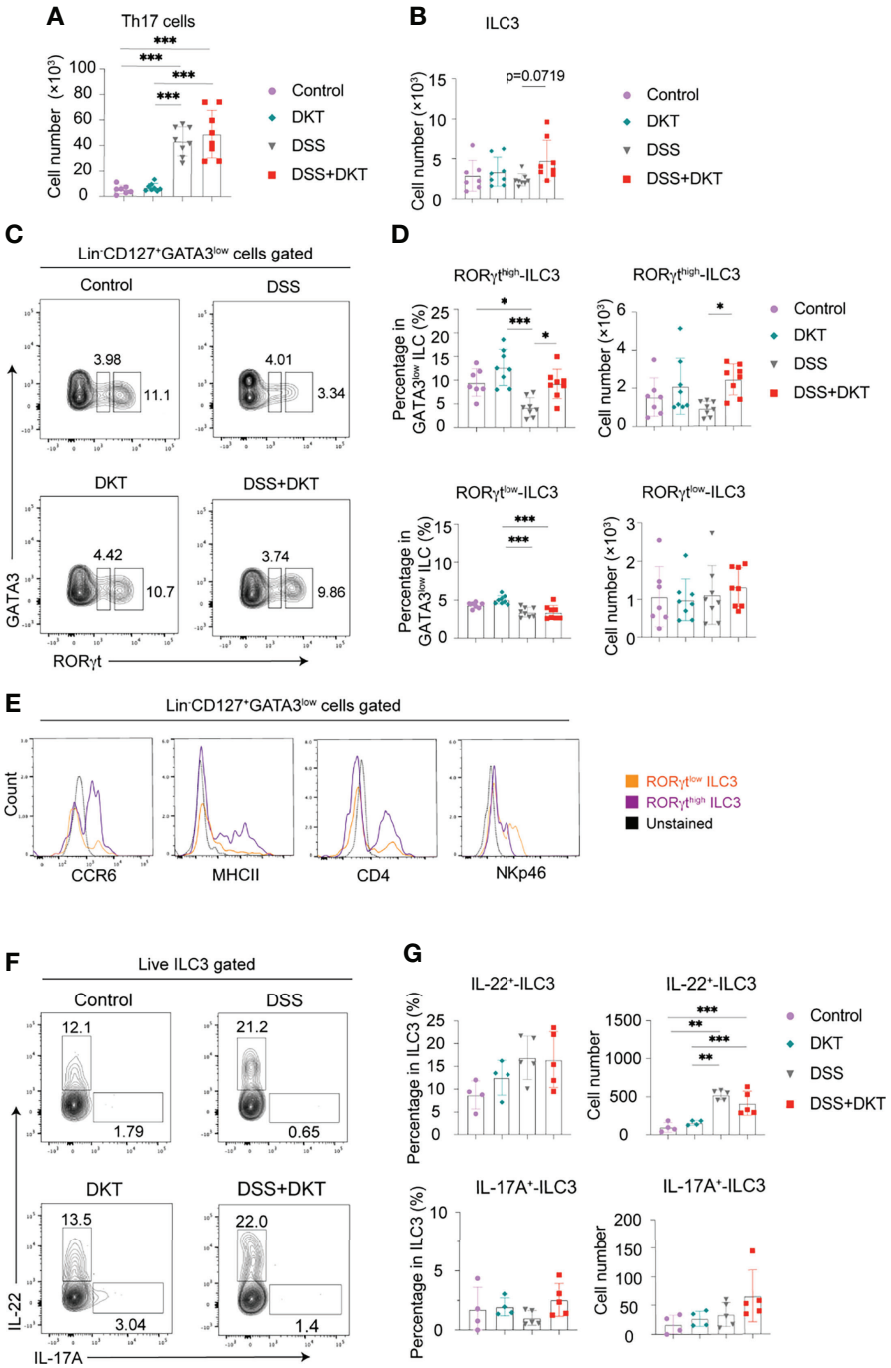

FIGURE 4 | DKT significantly increases colonic RORγt^{high}-ILC3 which resembles CCR6^{+} ILC3. **(A)** Absolute cell numbers of colonic Th17 cells isolated from the lamina propria region (Control N=7, DKT N=8, DSS N=8, DKT+DSS N=8). **(B)** Absolute cell numbers of colonic ILC3s isolated from the lamina propria region (Control N=7, DKT N=8, DSS N=8, DKT+DSS N=8). **(C)** Representative flow cytometry plots for gating colonic ILC3, and the two subpopulations of RORγt^{low} and RORγt^{high}-ILC3s based on the intensity of the transcription factor RORγt. See **Supplementary Figure 2A** for details on the gating strategy. **(D)** Frequency and absolute cell numbers of RORγt^{high} and RORγt^{low}-ILC3s (Control N=7, DKT N=8, DSS N=8, DKT+DSS N=8). **(E)** Representative histogram plots showing the expression of the surface markers CCR6, MHCII, CD4, and NKp46 by naive colonic ILC3s to discriminate the two ILC3 subpopulations, NKp46^{+} ILC3 (or NCR^{+} ILC3) and CCR6^{+} ILC3 (or LTi-like cell) (N=6). **(F)** Representative flow cytometry plots for IL-22^{+}- and IL-17A^{+}-producing ILC3s of the four experimental groups using *Rorc*$^{GFP/+}$ mice. **(G)** Frequency and absolute cell numbers of IL-22^{+}- and IL-17A^{+}-producing ILC3s (Control N=4, DKT N=4, DSS N=5, DKT+DSS N=5). Each symbol **(A, B, D, G)** represents data from an individual mouse. **(A–D)**, results are pooled from two independent experiments with three to four mice in each experimental group. Graphs **(A, B, D, G)** show means SEM; *p<0.05, **p<0.01, and ***p<0.001. Statistical analysis was performed using One-way ANOVA with Tukey's multiple comparisons test.

ILC3 KO mice started to die on day 13, we analyzed the body weight on day 13 instead of day 15 in this experimental setting. DSS-treated ILC3 KO mice showed a significantly lower body weight than their WT littermates (**Figure 5B**). The beneficial effect of DKT on DSS-induced body weight loss was, albeit partially, cancelled in the absence of ILC3, since the body weight loss of ILC3 KO mice upon DKT treatment was not as severe as that without DKT treatment (**Figure 5B**). Consistently, DKT treatment partially improved the clinical colitis score in ILC3 KO mice, although those mice suffered from more severe colitis symptoms than their WT littermates (**Figures 5C, D**). Collectively, these observations suggest that ILC3s play a critical role in attenuating DSS colitis and that DKT could ameliorate the severity of colitis at least partly through ILC3s.

DISCUSSION

The current study revealed novel biomedical functions of DKT extracts. We show that DKT significantly blunts DSS-induced acute experimental colitis by altering gut bacterial composition, increasing SCFAs, and sustaining colonic RORγt^{high}-ILC3s, which could collaboratively maintain epithelial integrity (illustrated in **Supplementary Figure 3**). To the best of our knowledge, this is the most comprehensive study to characterize the molecular basis of the anti-inflammatory actions of DKT. The role of ILC3s in IBD has remained controversial, as they have been shown to exhibit both protective and pathogenic effects in the development of colitis (45). Our study thus provides a rationale for further clinical studies of DKT as a promising therapeutic option for IBD patients.

We found that DKT increased Lactobacillaceae and its genus-level bacteria *Lactobacillus*, which is beneficial to human health as it exhibits antimicrobial actions and promotes nutrient acquisition (46). *Lactobacillus* has also been shown to be an immunoregulator to resolve experimental colitis and can inhibit several pathogens *in vitro* (47, 48). Furthermore, DKT enhanced the microbial-derived SCFA propionate in the colon. This is consistent with previous studies showing that *Lactobacillus*, together with several other bacteria, contributes to intestinal

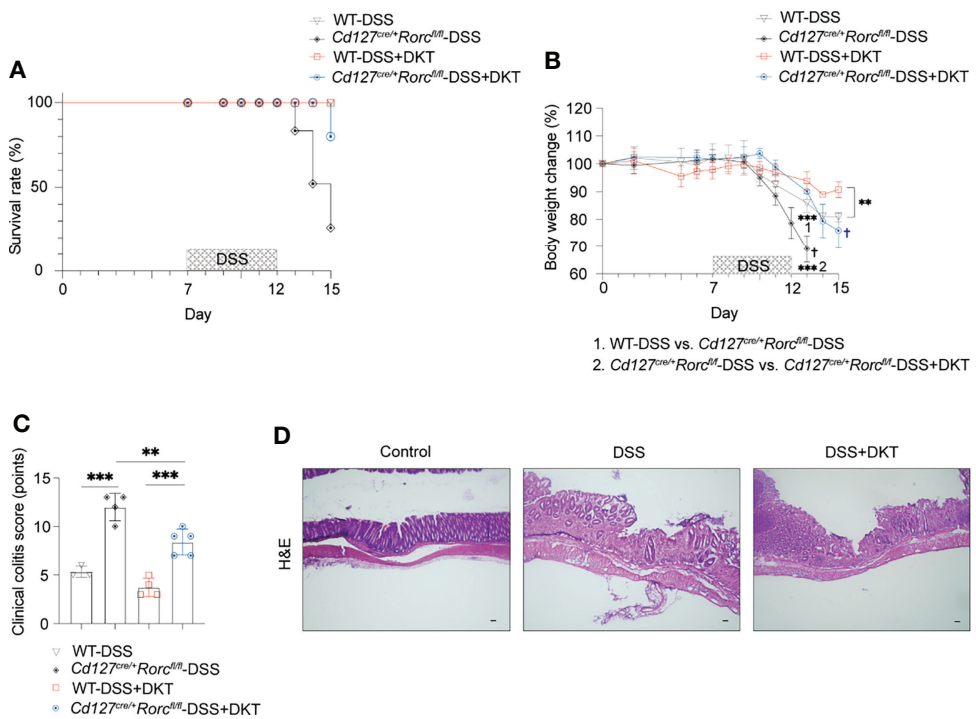

FIGURE 5 | ILC3 knockout (KO) leads to a high fatality rate from DSS-induced colitis that could be partially blunted by DKT. **(A)** *Cd127*$^{cre/+}$*Rorc*$^{fl/fl}$ mice, or ILC3 KO mice and their corresponding *Cd127*$^{+/+}$*Rorc*$^{fl/fl}$, or wildtype (WT) littermates underwent DSS treatment as described in **Figure 1A**. The survival rate for the four experimental groups is shown (WT-DSS N=3, *Cd127*$^{cre/+}$*Rorc*$^{fl/fl}$-DSS N=4, WT-DSS+DKT N=4, *Cd127*$^{cre/+}$*Rorc*$^{fl/fl}$-DSS+DKT N=5). **(B)** Body weight changes of the four experimental groups (WT-DSS N=3, *Cd127*$^{cre/+}$*Rorc*$^{fl/fl}$-DSS N=4, WT-DSS+DKT N=4, *Cd127*$^{cre/+}$*Rorc*$^{fl/fl}$-DSS+DKT N=5). "1" refers to the significantly lower body weight in the ILC3 KO mice compared to their WT littermates after DSS treatment on day 13. "2" indicates that the body weight of the DSS-treated ILC3 KO mice was significantly lower relative to the ILC3 KO mice treated with DSS+DKT on day 13. † indicates death of the mice. **(C)** Clinical colitis scoring of the four experimental groups on day 13 (WT-DSS N=3, *Cd127*$^{cre/+}$*Rorc*$^{fl/fl}$-DSS N=4, WT-DSS+DKT N=4, *Cd127*$^{cre/+}$*Rorc*$^{fl/fl}$-DSS+DKT N=5). **(D)** Representative light micrographs of colon sections of the ILC3 KO mice on day 15 that stained with H&E (Control N=2, DSS N=1, DSS+DKT N=4). Scale bars, 100 μm. Each symbol in graph **(C)** represents data from an individual mouse. Graphs **(B, C)** show means ± SEM; **p<0.01, and ***p<0.001. Statistical analysis was performed using One-way ANOVA with Tukey's multiple comparisons test.

fermentation and increases gut metabolites, including acetate, propionate, and lactate (49, 50). Together, these findings imply that the effects of DKT on experimental colitis are partly attributable to the promotion of colonic microbe symbiosis and enhancement of beneficial metabolites.

Our experiments further uncovered fundamental immune functions that DKT exerts to ameliorate experimental colitis. We conducted an extensive examination of the immune cell profiles in the colon, including both innate and adaptive immune cells. We found that only the RORγt^{high}-ILC3 subset was significantly higher in the DSS+DKT group than the DSS group. These findings revealed that DKT ameliorates experimental colitis partially by modulating the ILC3 subset. The importance of ILC3s in colitis was corroborated by the experiment using ILC3 KO mice, where DSS induced a higher mortality in the KO mice compared to WT littermates. Meanwhile, DKT significantly reduced the mortality rate of ILC3 KO mice treated with DSS. This result also indicated that DKT ameliorates DSS colitis partly in an ILC3-independent manner. However, the underlying mechanisms are unknown and await further studies.

ILC3s are highly abundant in the gastrointestinal tract and promote metabolic and immune homeostasis by sensing and conveying cues from the luminal microbial community to the lamina propria (41). Nevertheless, their functions in colitis have not been well characterized (51). In this regard, our results show that colonic ILC3 plays an essential role in regulating the immune responses during colitis, supporting the hypothesis that ILC3 may serve as a potential therapeutic target to overcome intestinal inflammations (51). However, our data did not show significant differences in IL-22 or IL-17A production by ILC3s in DKT-treated mice. This is possibly due to our experimental scheme of evaluating the ILC3 phenotypes in the recovery phase rather than in the acute inflammatory phase and the transiently altered cytokine productions cannot be captured (52).

ILC3s are a heterogeneous population whose biological functions are highly tissue-specific (41). Our data demonstrate that DSS challenge suppressed the RORγt expression in ILC3s, whereas DKT administration reversed this phenomenon. Furthermore, this RORγt^{high}-ILC3 subpopulation shares similarities with CCR6^{+} ILC3s, the predominant ILC3 subset in the colon (41). Based on our observations and a previous study (43), we extrapolate that the different RORγt expression levels may represent different ILC3 subpopulations, as RORγt^{high}-ILC3s may consist of a large proportion of CCR6^{+} ILC3s and RORγt^{low}-ILC3s contain mainly NCR^{+} ILC3s. This finding may further link the RORγt expression level to the unique effector functions of the two ILC3 subsets (53). The characteristics of RORγt^{high}-ILC3s and their specific role in ameliorating colitis merit exploration in future studies. Additionally, we observed a higher propionate level in the DSS+DKT group compared to the DSS group and an unchanged propionate concentration upon DSS administration compared to the healthy controls. Taken together with the upregulation of GPR43-encoding *Ffar2* mRNA among the SCFA-sensing GPCRs, it raises the possibility that GPR43 might be involved in the propionate-mediated anti-inflammatory functions through RORγt^{high}-ILC3s in experimental colitis.

Unlike western medicine, herbal formulae are conventionally considered multi-target medicines as they comprise numerous chemically diverse compounds (3, 6). Besides ILC3s, our analyses suggest that DKT might be capable of directly modulating colonic epithelial cells and intraepithelial lymphocytes to protect the barrier functions. Our finding also adds more convincing evidence to previous *in vitro* experiments, which suggested that DKT enhances endogenous adrenomedullin production in intestinal epithelial cells (14). Thus, investigating the bioactive ingredients in DKT that interact with ILC3s, epithelial cells, and intraepithelial lymphocytes and identifying the DKT-activated receptors on those cells are of particular interest for future studies. In addition, experiments using germ-free and gnotobiotic animals to study the biomedical effects of DKT in experimental colitis may expand our understanding on the causative roles of gut microbiota and their metabolites.

In summary, we show that DKT blunts the severity of experimental colitis in mice by reshaping gut microbiota, enhancing propionate, and maintaining the RORγt^{high}-ILC3 population. Our findings highlight novel effects of DKT on the microbiota-immune cell axis in experimental colitis. Our work provides immunological insights into DKT, serving as an anti-inflammatory agent that complements the standard western medicine-based treatment of IBD. Our study also suggests that ILC3 may serve as a potential therapeutic target for IBD. Although the biological evaluation of herbal medicine is complicated and challenging due to the lack of appropriate evaluation methods (6), our work provides a rationale and basis for future mechanistic studies of herbal medicines.

METHODS

Mice

C57BL/6N female mice at 6-7 weeks of age were purchased from CLEA Japan, Inc. Mice were acclimatized with a normal chow diet CA-1 (CLEA Japan Inc.) for three weeks under specific-pathogen-free (SPF) conditions in the animal facility of RIKEN Yokohama Branch before the experiments. *Rorc*$^{fl/fl}$ mice were purchased from Jackson Laboratory. *Rorc*$^{GFP/+}$ mice from Dr. D. Littman (54) and CD127-Cre mice from Dr. HR. Rodewald (55) were kindly provided by the indicated investigators. To obtain specific depletion of ILC3, *Rorc*$^{fl/fl}$ mice were bred with CD127-Cre transgenic mice at the RIKEN animal facility and two parental littermates were used for the experiments. *Rorc*$^{GFP/+}$ mice were bred on a C57BL/6J background at the RIKEN SPF animal facility. For ILC3 cell sorting and cytokine detection, sex-matched littermates of *Rorc*$^{GFP/+}$ mice were used. All the transgenic mice were used at 8-12 weeks of age. The SPF facility of RIKEN is maintained in a 12-hour light, 12-hour dark cycle at 23 ± 2 °C with a humidity of 50 ± 10%, and food and water available *ad libitum*. All experimental procedures were

approved by and conducted in accordance with, the Institutional Animal Care and Use Committee (IACUC) of the RIKEN Yokohama Branch.

Dietary DKT Administration and Induction of DSS-Colitis

DKT extract granules were obtained from TSUMURA & Co. (Tokyo, Japan). We determined the final dosage of dietary DKT based on the literature (14, 56) and adjusted the human equivalent dosage to the mouse dosage based on the animal surface area (57, 58). As for the preparation of dietary DKT, we mixed the autoclaved DKT extracts and filtered maltose monohydrate powder (Wako) and blended them in a ratio of 1:8 based on previous reports (14). We then mixed them with the CA-1 powder at a defined quantity of 50g DKT powder/Kg (5% wt/wt).

For colitis experiments, mice were administered dietary DKT (DKT and DSS+DKT group) or CA-1 diet (Control and DSS group) with drinking water *ad libitum* for 6 days prior to colitis induction and continued throughout the experiments. 2.5% DSS (36,000-50,000mw; M.P. Biomedicals) was subsequently added to their drinking water and continued for five consecutive days, followed by three days of DSS-free period (**Figure 1A**). We repeated most of the experiments at least twice but mainly three times, and three to five mice were used in each experimental group. We monitored the clinical parameters during the experiments, including body weight loss, stool formation, rectal bleeding, total behavior, conditions of the fur, and survival rate until the mice were sacrificed. The severity of colitis was judged based on the previously described clinical colitis scoring system of DSS-induced colitis (59) (**Table 1**). All clinical scorings were conducted in a blinded manner. Post-mortem, the colon was dissected from cecum to anus, and the colon length was measured.

Histological and Immunohistochemistry

For histological analysis, 0.5 cm distal colon was fixed in Zinc Formalin (Polyscience Inc.) for 3 hours and then embedded in paraffin blocks. We then prepared 5 μm paraffin cross-sections, which were used for hematoxylin and eosin (H&E) staining (Mayer's Hematoxylin solution, 1% Eosin Solution, Wako) following standard procedures. The histological images were captured using the BX51-P Polarizing microscope (Olympus) and processed with the Olympus D.P. Controller 2002 software.

TABLE 1 | Clinical colitis scoring system (59).

Clinical parameters		Score
Stool consistency	Normal, soft, soft with blood	0-2
Posture	Normal to hunched	0-2
Spontaneous behavior	Normal to no activity (without disturbing)	0-2
Provoked behavior	Normal to no activity (after disturbing)	0-2
Evaluation of the eyes	Clearness, openness	0-3
Evaluation of the fur	Cleanliness, gloss, smoothness	0-3
General appearance	Not, mildly, moderately, severely disturbed	0-3
Total highest score		17

For immunohistochemistry analysis, 0.5 cm distal colon was fixed overnight in 4% paraformaldehyde (PFA) (Wako) at 4°C and mounted in embedding medium Tissue-Tek O.C.T Compound (Sakura). The tissues were cut into 8 μm sections and permeabilized with 0.2% saponin (Nacalai Tesque) in PBS. The sections were then blocked with 5% goat serum (Wako) for Mucin 2 detection. Subsequently, the sections were stained with anti-Mucin2 (1:200, rabbit, clone: H-300, Santa Cruz Biotechnology) at 4°C overnight. For the second antibody, Alexa Fluor 488 conjugated donkey anti-rabbit IgG antibody (1:400, Thermo Fisher Scientific) was used with DAPI (1:1000, Dojindo). The sections were assessed using the Leica TCS SP8 (Leica Microsystems).

Analysis of the Microbiota Composition in Mice Colonic Contents

The colonic contents were collected from the mice post-mortem after the colon had been removed and cut open longitudinally. Bacterial DNA was extracted as previously described with minor modifications (60). For 16S amplicon sequencing, the V4 region of 16S rRNA genes was amplified by PCR with dual barcoded primers, as previously reported (61). Sequencing of the 16s rRNA was performed on a MiSeq instrument (Illumina, 2 × 250-bp paired-end reads). Sequence data were demultiplexed using bcl2fastq v.1.8.4, then subjected to microbiome informatics using QIIME v2021-2. Taxonomy was assigned to amplicon sequence variants (ASVs) using the Silva rRNA database. For detailed analyses, ASV tables were rarefied to 20,000 reads per sample or the lowest reads within the examined dataset. Relative abundance, Bray Curtis distances, and permutational MANOVA (Adonis) were calculated with the QIIME 2 and R package qiime2R v 0.99.5, phyloseq v2, vegan v2.5-7 by RStudio v1.4.1106.

Isolation of Colonic Epithelial Cells and Immune Cells From the Lamina Propria Region

Colons were dissected and fat tissue was removed. Colons were cut open longitudinally and washed with cold RPMI-1640 medium (Sigma Aldrich) to remove luminal contents and debris, then incubated in RPMI-1640 medium containing 5mM EDTA and 2% fetal bovine serum (FBS) for 15 mins at 37°C, followed by 2% FBS in RPMI-1640 medium for another cycle. After vigorously shaking for 15s, the dissociated cells were collected as colonic epithelial cells. The epithelial cells were then passed through a 40 μm cell strainer (B.D. Biosciences) and cell pellets were stored after being washed with cold PBS. For the immune cell isolation from the lamina propria region, the remaining colonic tissues were cut into small pieces and digested with 1.0 mg/ml collagenase (Sigma) suspended in RPMI-1640 medium for 15 min at 37°C. The resultant supernatants from the collagenase digestion were collected and passed through a 100 μm cell strainer after 3 cycles of these steps. The cells were subjected to Percoll (G.E. Healthcare) gradient separation and lymphocytes in the interphase were collected and proceeded for the flow cytometric analysis.

Flow Cytometric Analysis and Cell Sorting

Single-cell suspensions (1×10^6 cells/sample) were stained with the indicated antibodies at 4°C after blocking Fc receptors with the 2.4G2 mAb (BD Pharmingen) and dead cells were stained with LIVE/DEAD fixable Aqua Dead Cell Stain (Thermo Fisher). For detection of ILC3, $CD4^+$ T cells, B cells, DCs and macrophages, we used fluorochrome-conjugated antibodies, all from BioLegend, against combinations, indicated below, of the following surface antigens: CD45.2 (PerCP/Cyanine5.5, clone:104), CD3ϵ (FITC or BV605, clone: 145-2C11), TCR β (FITC or BV605, clone: H57-597), CD4 (APC/Cyanine7, clone: GK1.5), CD19 (BV605, clone: 6D5), CD127 (PE/Cyanine7, clone: A7R34), NKp46 (FITC, clone: 29A1.4), MHC class II (FITC or BV421, M5/114.15.2), F4/80 (FITC, clone: BM8), CD103 (PE/Cyanine7, clone: 2E7), CD11b (APC, M1/70), Ly6C (APC/Cyanine7, clone: HK1.4). We also used CCR6 (PE, Clone: 140706, R&D Systems) and CD11c (PE, clone: HL3, BD). $CD4^+$ T cells were identified as $CD45.2^+CD3\epsilon^+TCR\beta^+CD4^+CD19^-$; B cells were gated as $CD45.2^+CD3^-TCR\beta^-CD19^+$; conventional DCs were gated as $CD45.2^+CD11b\epsilon^+CD11c^{high}MHCII^+$; macrophages were gated as $CD45.2^+CD11c^-CD11b^+F4/80^{inter}Ly6C^{low}CD64^+MHCII^+$.

For transcription factor staining, after staining with antibodies to surface antigens as described above, the lymphocytes were then fixed and permeabilized with Foxp3/Transcription Factor Buffer set (Thermo Fisher Scientific) according to the manufacturer's instructions and stained with T-bet (APC, clone: 4B10, BioLegend), GATA3 (PE, clone: 16E10A23, BioLegend) and RORγt (BV421, clone: Q31-378, BD). ILC1/NK cells were gated as $CD45.2^+CD3\epsilon^-TCR\beta^-CD19^-CD127^+GATA3^-ROR\gamma t^-T\text{-}bet^+$; ILC2 were gated as $CD45.2^+CD3\epsilon^-TCR\beta^-CD19^-CD127^+GATA3^{high}ROR\gamma t^-$: ILC3 were gated as $CD45.2^+CD3\epsilon^-TCR\beta^-CD19^-CD127^+GATA3^{low}ROR\gamma t^+$; Th17 were gated as $CD45.2^+CD3\epsilon^+TCR\beta^+CD19^-CD4^+ROR\gamma t^+$.

For the measurement of intracellular cytokine production, cells were cultured for 3 hr at 37°C in the presence of GolgiPlug (BD Biosciences). The cells were subsequentially stained with IL-22 (PE, clone: Poly5164, BioLegend) and IL-17A (APC, clone: TC11-18H10.1, BioLegend) antibodies after being fixed with 4% PFA.

For colonic ILC3 sorting, $Rorc^{GFP/+}$ mice were used. $CD45.2^+CD3\epsilon^-TCR\beta^-CD19^-CD127^+Rorc^{GFP\text{-}high}$ expressing ILC3s were gated and sorted to detect cytokines and GPCR mRNAs by qPCR.

All stained cells were analyzed or sorted on a BD FACSAriaIII. For all lymphocyte analysis by flow cytometry, lymphocytes were first strictly defined by forward scatter (FSC), and side scatter (SSC) intensity and then carefully gated based on CD45 expression. The data were analyzed with FlowJo v10.8.0.

RNA Extraction and Quantitative PCR Analysis of Colonic Epithelial Cells and ILC3

The epithelial cells were lysed in RLT buffer (QIAGEN) with 2-mercaptoethanol (Nacalai Tesque) after washing with PBS. The RNeasy Mini Kit (QIAGEN) was used for total RNA extraction following the manufacturer's instructions. cDNA was synthesized through reverse transcription PCR with SuperScript IV Reverse Transcriptase (Thermo Fisher Scientific) using random hexamer primer (Thermo Fisher Scientific).

For the colonic ILC3 sorting, 200-500 colonic ILC3 isolated from $Rorc^{GFP/+}$ mice were directly sorted into RLT buffer with 2-mercaptoethanol (Nacalai Tesque). Total RNA from sorted ILC3 was extracted with RNeasy Micro Kit (QIAGEN) following the manufacturer's instructions. The extracted RNA was subsequentially subjected to amplification with a SuperScript™ IV Single Cell/Low Input cDNA PreAmp Kit (Thermo Fisher Scientific).

Real-time PCR for epithelial cells and ILC3s was performed with SYBR Premix Ex Taq (Takara) on a LightCycler 480 (Roche). The primers were used for the analyses are shown in **Table 2**.

Quantification of Fecal SCFAs

SCFAs and other metabolites were extracted and measured as previously described (60). In brief, 5 mg of feces or colonic contents were lyophilized. Dried samples were added to 5 µl Milli-Q water containing internal standards (2.2 mM [1,2-13C2] acetate, 2.2 mM [2H7]butyrate and 2.2 mM crotonate), 50 µl HCl and 200 µl diethyl ether. After centrifugation, 80 µl of the organic layer was transferred to a glass vial and then 16 µl of N-tert-butyldimethylsilyl-N-trifluoroacetamide (Sigma-Aldrich) was added to derivatize the samples. The vials were incubated at 80°C or 20 min and allowed to stand for 48h before injection. The analysis was performed using a gas chromatography-tandem mass spectrometry (GCMS) platform on a Shimadzu GCMS-TQ8040 triple quadrupole mass spectrometer (Shimadzu) with a capillary column (BPX5) (SGE Analytical Science). The program of GCMS analysis is described in a previously published paper (60). The GCMS data were processed, and concentrations were calculated by LabSolutions Insight (Shimadzu).

TABLE 2 | Primers used in the study.

Primer	sequence
Hprt	Forward, 5'-TCAGTCAACGGGGGACATAAA-3'
	Reverse, 5'-GGGGCTGTACTGCTTAACCAG-3'
Muc2	Forward, 5'-TCAGCACACCAACCAAAACC-3'
	Reverse, 5'-CACTTCAGCGGCACAATCTC-3'
Reg3g	Forward, 5'-ACCTAGCCACAAGCAAGATCCCA-3'
	Reverse, 5'- ATGAGAGGAGGGAAGGGCCA-3'
Fut2	Forward, 5'-GAGTCAAGGGGAGGGAGAAC-3'
	Reverse, 5'-AACTTGGTGAGGGGACTGTG-3'
Il-22	Forward, 5'-CATGCAGGAGGTGGTACCTT-3'
	Reverse, 5'-CAGACGCAAGCATTTCTCAG-3'
Il17a	Forward, 5'-TCCAGAAGGCCCTCAGACTA-3'
	Reverse, 5'-TGAGCTTCCCAGATCACAGA-3'
Ffar2(Gpr43)	Forward, 5'-CTTGATCCTCACGGCCTACAT-3'
	Reverse, 5'-CCAGGGTCAGATTAAGCAGGAG-3'
Ffar3 (Gpr41)	Forward, 5' -ACCTGACCATTTCGGACCT-3'
	Reverse, 5'-CCATCTCATGCCACATGC-3'
Hcar2 (Gpr109a)	Forward, 5' -ATGGCGAGGCATATCTGTGTAGCA-3'
	Reverse, 5'-TCCTGCCTGAGCAGAACAAGATGA-3'

Statistical Analysis

Multiple sample comparisons were performed by one-way ANOVA with Tukey's *post hoc* test. All statistical analyses were performed using Prism version 8 and 9 (GraphPad Software, USA). $P < 0.05$ and FDR adjusted $P < 0.05$ were considered statistically significant.

Diagram

Created with BioRender.com, as shown in **Supplementary Figure 3**.

DATA AVAILABILITY STATEMENT

The data presented in the study are deposited in the DDBJ repository, accession number: DRA013869, run: DRR359766-DDR359820. The data can be found at the link: https://ddbj.nig.ac.jp/resource/sra-submission/DRA013869.

ETHICS STATEMENT

The animal study was reviewed and approved by the Institutional Animal Care and Use Committee (IACUC) of the RIKEN Yokohama Branch.

AUTHOR CONTRIBUTIONS

ZS, NS-T and HO conceived the study. ZS designed, performed the experiments and data analyses and co-wrote the manuscript. TT contributed to the microbiota data analyses and data interpretation. YN quantified the SCFA concentrations in the mouse colons using GCMS. TKato performed 16S rRNA gene sequencing for the mouse colonic contents. KB and RN contributed to the experiments and helped to interpret the data. TKageyama contributed to the flow cytometry analyses and cell sorting. AI assisted with the SCFA analyses. NS-T and HO directed the research, provided essential materials and co-wrote the manuscript. All authors contributed to the article and approved the submitted version.

FUNDING

ZS, TT and RN are recipients of RIKEN Junior Research Associate (JRA) Program. KB was supported by Deutsche Forschungsgemeinschaft (DFG; BE 6909/1-1). NS-T was supported by the Japan Society for the Promotion of Science KAKENHI (20KK0360), the Japan Agency for Medical Research and Development AMED-PRIME and Yakult Bio-Science foundation. HO was supported by the Japan Society for the Promotion of Science KAKENHI (19H01030, 19F19785).

ACKNOWLEDGMENTS

We thank Tsumura & Co. for providing Daikenchuto extract granules. We thank Prof. Peter D. Burrows for his critical comments and proofreading of the manuscript.

SUPPLEMENTARY MATERIAL

The Supplementary Material for this article can be found online at: https://www.frontiersin.org/articles/10.3389/fimmu.2022.903459/full#supplementary-material

Supplementary Figure 1 | The relative abundance of several family-level bacteria in the four experimental groups. The relative abundance of fecal Akkermanciaceae, Clostridiaceae, Bacteriodaceae, and Eggerthellaceae (Control N=15, DKT N=15, DSS N=14, DSS+DKT N=11). Each symbol represents data from an individual mouse. Data are pooled from 3 independent experiments with three to five mice in each experimental group. Graphs show means ± SEM; *p<0.05, **p<0.01, and ***p<0.001. Statistical analysis was performed using One-way ANOVA with Tukey's multiple comparisons test.

Supplementary Figure 2 | DKT treatment does not affect ILC1, ILC2, T and B lymphocytes, macrophages, or DCs. **(A)** Gating strategy for colonic ILC3. For flow cytometry analyses, lymphocytes were firstly gated on SSC-A vs. FSC-A and doublets were excluded by gating on SSC-W vs. SSC-H. Live immune cells were further gated as Zombie dye negative and CD45 positive cells. CD127 expression was used to gate the ILC population. **(B)** The absolute cell number of colonic ILC, ILC1/NK cells and ILC2 (Control N=7, DKT N=8, DSS N=8, DKT+DSS N=8). **(C)** The absolute cell number of colonic $CD4^+$ T cells, B cells, macrophages, and DCs (Control N=7, DKT N=8, DSS N=8, DKT+DSS N=8). **(D)** Relative expression of *Il22* and *Il17a* in $ROR\gamma t^{high}$-ILC3s using $Rorc^{GFP/+}$ mice (Control N=4, DKT N=4, DSS N=5, DSS+DKT N=4). **(E)** Relative expression of G-protein coupled receptors (GPCRs), *Ffar2, Ffar3* and *Hcar2* mRNAs in $ROR\gamma t^{high}$-ILC3s using $Rorc^{GFP/+}$ mice (Control N=4, DKT N=5, DSS N=5, DSS+DKT N=5). Each symbol **(B–E)** represents data from an individual mouse. Graphs **(A–C)**, Results are pooled from two independent experiments with three to four mice in each experimental group. Graph **(E)**, results are representative of three independent experiments. Graphs **(B–E)** display means ± SEM; *p<0.05, **p<0.01, and ***p<0.001. Statistical analysis was performed using One-way ANOVA with Tukey's multiple comparisons test.

Supplementary Figure 3 | Graphical abstract summarizing the observations described in this paper. DKT treatment sustains colonic homeostasis by changing the activities of luminal microbes, enhancing $ROR\gamma t^{high}$-ILC3s and protecting barrier function.

REFERENCES

1. Watanabe K, Matsuura K, Gao P, Hottenbacher L, Tokunaga H, Nishimura K, et al. Traditional Japanese Kampo Medicine: Clinical Research Between Modernity and Traditional Medicine-The State of Research and Methodological Suggestions for the Future. *Evid Based Complement Alternat Med* (2011) 2011:513842. doi: 10.1093/ecam/neq067
2. Katayama K, Yoshino T, Munakata K, Yamaguchi R, Imoto S, Miyano S, et al. Prescription of Kampo Drugs in the Japanese Health Care Insurance Program. *Evid Based Complement Alternat Med* (2013) 2013:576973. doi: 10.1155/2013/576973
3. Kono T, Shimada M, Yamamoto M, Kaneko A, Oomiya Y, Kubota K, et al. Complementary and Synergistic Therapeutic Effects of Compounds Found in Kampo Medicine: Analysis of Daikenchuto. *Front Pharmacol* (2015) 6:159. doi: 10.3389/fphar.2015.00159
4. Eardley S, Bishop FL, Prescott P, Cardini F, Brinkhaus B, Santos-Rey K, et al. A Systematic Literature Review of Complementary and Alternative Medicine Prevalence in EU. *Forsch Komplementmed* (2012) 19 Suppl 2:18–28. doi: 10.1159/000342708

5. Bent S. Herbal Medicine in the United States: Review of Efficacy, Safety, and Regulation: Grand Rounds at University of California, San Francisco Medical Center. *J Gen Intern Med* (2008) 23(6):854–9. doi: 10.1007/s11606-008-0632-y
6. Ekor M. The Growing Use of Herbal Medicines: Issues Relating to Adverse Reactions and Challenges in Monitoring Safety. *Front Pharmacol* (2014) 4:177. doi: 10.3389/fphar.2013.00177
7. Ohbe H, Jo T, Matsui H, Fushimi K, Yasunaga H. Effect of Daikenchuto for Mechanically Ventilated Patients With Enteral Feeding Intolerance: A Propensity Score-Matched Analysis Using a Nationwide Administrative Inpatient Database. *JPEN J Parenter Enteral Nutr* (2021) 45(8):1703–13. doi: 10.1002/jpen.2076
8. Oyama F, Futagami M, Shigeto T, Miura R, Osawa Y, Oishi M, et al. Preventive Effect of Daikenchuto, a Traditional Japanese Herbal Medicine, on Onset of Ileus After Gynecological Surgery for Malignant Tumors. *Asia Pac J Clin Oncol* (2020) 16(4):254–8. doi: 10.1111/ajco.13329
9. Yoshikawa K, Shimada M, Wakabayashi G, Ishida K, Kaiho T, Kitagawa Y, et al. Effect of Daikenchuto, a Traditional Japanese Herbal Medicine, After Total Gastrectomy for Gastric Cancer: A Multicenter, Randomized, Double-Blind, Placebo-Controlled, Phase II Trial. *J Am Coll Surg* (2015) 221(2):571–8. doi: 10.1016/j.jamcollsurg.2015.03.004
10. Kanazawa A, Sako M, Takazoe M, Tadami T, Kawaguchi T, Yoshimura N, et al. Daikenchuto, a Traditional Japanese Herbal Medicine, for the Maintenance of Surgically Induced Remission in Patients With Crohn's Disease: A Retrospective Analysis of 258 Patients. *Surg Today* (2014) 44 (8):1506–12. doi: 10.1007/s00595-013-0747-6
11. Endo M, Hori M, Ozaki H, Oikawa T, Hanawa T. Daikenchuto, a Traditional Japanese Herbal Medicine, Ameliorates Postoperative Ileus by Anti-Inflammatory Action Through Nicotinic Acetylcholine Receptors. *J Gastroenterol* (2014) 49(6):1026–39. doi: 10.1007/s00535-013-0854-6
12. Ueno N, Hasebe T, Kaneko A, Yamamoto M, Fujiya M, Kohgo Y, et al. TU-100 (Daikenchuto) and Ginger Ameliorate Anti-CD3 Antibody Induced T Cell-Mediated Murine Enteritis: Microbe-Independent Effects Involving Akt and NF-kappaB Suppression. *PloS One* (2014) 9(5):e97456. doi: 10.1371/journal.pone.0097456
13. Shinyama S, Kaji T, Mukai M, Nakame K, Matsufuji H, Takamatsu H, et al. The Novel Preventive Effect of Daikenchuto (TJ-100), a Japanese Herbal Drug, Against Neonatal Necrotizing Enterocolitis in Rats. *Pediatr Surg Int* (2017) 33(10):1109–14. doi: 10.1007/s00383-017-4145-9
14. Kono T, Kaneko A, Hira Y, Suzuki T, Chisato N, Ohtake N, et al. Anti-Colitis and -Adhesion Effects of Daikenchuto *via* Endogenous Adrenomedullin Enhancement in Crohn's Disease Mouse Model. *J Crohns Colitis* (2010) 4 (2):161–70. doi: 10.1016/j.crohns.2009.09.006
15. Matsunaga T, Hashimoto S, Yamamoto N, Kawasato R, Shirasawa T, Goto A, et al. Protective Effect of Daikenchuto on Dextran Sulfate Sodium-Induced Colitis in Mice. *Gastroenterol Res Pract* (2017) 2017:1298263. doi: 10.1155/2017/1298263
16. Kogure Y, Kanda H, Wang S, Hao Y, Li J, Yamamoto S, et al. Daikenchuto Attenuates Visceral Pain and Suppresses Eosinophil Infiltration in Inflammatory Bowel Disease in Murine Models. *JGH Open* (2020) 4 (6):1146–54. doi: 10.1002/jgh3.12410
17. Iturrino J, Camilleri M, Wong BS, Linker Nord SJ, Burton D, Zinsmeister AR. Randomised Clinical Trial: The Effects of Daikenchuto, TU-100, on Gastrointestinal and Colonic Transit, Anorectal and Bowel Function in Female Patients With Functional Constipation. *Aliment Pharmacol Ther* (2013) 37(8):776–85. doi: 10.1111/apt.12264
18. Acosta A, Camilleri M, Linker-Nord S, Busciglio I, Iturrino J, Szarka LA, et al. A Pilot Study of the Effect of Daikenchuto on Rectal Sensation in Patients With Irritable Bowel Syndrome. *J Neurogastroenterol Motil* (2016) 22 (1):69–77. doi: 10.5056/jnm15120
19. Ng SC, Shi HY, Hamidi N, Underwood FE, Tang W, Benchimol EI, et al. Worldwide Incidence and Prevalence of Inflammatory Bowel Disease in the 21st Century: A Systematic Review of Population-Based Studies. *Lancet* (2017) 390(10114):2769–78. doi: 10.1016/S0140-6736(17)32448-0
20. Collaborators GBDIBD. The Global, Regional, and National Burden of Inflammatory Bowel Disease in 195 Countries and Territories, 1990-2017: A Systematic Analysis for the Global Burden of Disease Study 2017. *Lancet Gastroenterol Hepatol* (2020) 5(1):17–30. doi: 10.1016/S2468-1253(19)30333-4
21. Misselwitz B, Juillerat P, Sulz MC, Siegmund B, Brand SSwiss Ibdnet. Emerging Treatment Options in Inflammatory Bowel Disease: Janus Kinases, Stem Cells, and More. *Digestion* (2020) 101 Suppl 1:69–82. doi: 10.1159/000507782
22. Goldberg R, Prescott N, Lord GM, MacDonald TT, Powell N. The Unusual Suspects–Innate Lymphoid Cells as Novel Therapeutic Targets in IBD. *Nat Rev Gastroenterol Hepatol* (2015) 12(5):271–83. doi: 10.1038/nrgastro.2015.52
23. Geremia A, Arancibia-Carcamo CV, Fleming MP, Rust N, Singh B, Mortensen NJ, et al. IL-23-Responsive Innate Lymphoid Cells Are Increased in Inflammatory Bowel Disease. *J Exp Med* (2011) 208(6):1127–33. doi: 10.1084/jem.20101712
24. Zeng B, Shi S, Ashworth G, Dong C, Liu J, Xing F. ILC3 Function as a Double-Edged Sword in Inflammatory Bowel Diseases. *Cell Death Dis* (2019) 10 (4):315. doi: 10.1038/s41419-019-1540-2
25. Brinkman BM, Becker A, Ayiseh RB, Hildebrand F, Raes J, Huys G, et al. Gut Microbiota Affects Sensitivity to Acute DSS-Induced Colitis Independently of Host Genotype. *Inflamm Bowel Dis* (2013) 19(12):2560–7. doi: 10.1097/MIB.0b013e3182a8759a
26. Maslowski KM, Vieira AT, Ng A, Kranich J, Sierro F, Yu D, et al. Regulation of Inflammatory Responses by Gut Microbiota and Chemoattractant Receptor GPR43. *Nature* (2009) 461(7268):1282–6. doi: 10.1038/nature08530
27. Mukhopadhya I, Hansen R, El-Omar EM, Hold GL. IBD-What Role Do Proteobacteria Play? *Nat Rev Gastroenterol Hepatol* (2012) 9(4):219–30. doi: 10.1038/nrgastro.2012.14
28. Jang YJ, Kim WK, Han DH, Lee K, Ko G. Lactobacillus Fermentum Species Ameliorate Dextran Sulfate Sodium-Induced Colitis by Regulating the Immune Response and Altering Gut Microbiota. *Gut Microbes* (2019) 10 (6):696–711. doi: 10.1080/19490976.2019.1589281
29. Kostic AD, Gevers D, Siljander H, Vatanen T, Hyotylainen T, Hamalainen AM, et al. The Dynamics of the Human Infant Gut Microbiome in Development and in Progression Toward Type 1 Diabetes. *Cell Host Microbe* (2015) 17(2):260–73. doi: 10.1016/j.chom.2015.01.001
30. Vacca M, Celano G, Calabrese FM, Portincasa P, Gobbetti M, De Angelis M. The Controversial Role of Human Gut Lachnospiraceae. *Microorganisms* (2020) 8(4). doi: 10.3390/microorganisms8040573
31. Jakobsson HE, Rodriguez-Pineiro AM, Schutte A, Ermund A, Boysen P, Bemark M, et al. The Composition of the Gut Microbiota Shapes the Colon Mucus Barrier. *EMBO Rep* (2015) 16(2):164–77. doi: 10.15252/embr.201439263
32. Johansson ME, Larsson JM, Hansson GC. The Two Mucus Layers of Colon are Organized by the MUC2 Mucin, Whereas the Outer Layer is a Legislator of Host-Microbial Interactions. *Proc Natl Acad Sci USA* (2011) 108 Suppl 1:4659–65. doi: 10.1073/pnas.1006451107
33. Subramani DB, Johansson ME, Dahlen G, Hansson GC. Lactobacillus and Bifidobacterium Species Do Not Secrete Protease That Cleaves the MUC2 Mucin Which Organises the Colon Mucus. *Benef Microbes* (2010) 1(4):343–50. doi: 10.3920/BM2010.0039
34. Mattar AF, Teitelbaum DH, Drongowski RA, Yongyi F, Harmon CM, Coran AG. Probiotics Up-Regulate MUC-2 Mucin Gene Expression in a Caco-2 Cell-Culture Model. *Pediatr Surg Int* (2002) 18(7):586–90. doi: 10.1007/s00383-002-0855-7
35. Ho S, Pothoulakis C, Koon HW. Antimicrobial Peptides and Colitis. *Curr Pharm Des* (2013) 19(1):40–7. doi: 10.2174/13816128130108
36. Wang Y, Huang D, Chen KY, Cui M, Wang W, Huang X, et al. Fucosylation Deficiency in Mice Leads to Colitis and Adenocarcinoma. *Gastroenterology* (2017) 152(1):193–205.e10. doi: 10.1053/j.gastro.2016.09.004
37. Qiu J, Heller JJ, Guo X, Chen ZM, Fish K, Fu YX, et al. The Aryl Hydrocarbon Receptor Regulates Gut Immunity Through Modulation of Innate Lymphoid Cells. *Immunity* (2012) 36(1):92–104. doi: 10.1016/j.immuni.2011.11.011
38. Goto Y, Obata T, Kunisawa J, Sato S, Ivanov II, Lamichhane A, et al. Innate Lymphoid Cells Regulate Intestinal Epithelial Cell Glycosylation. *Science* (2014) 345(6202):1254009. doi: 10.1126/science.1254009
39. Liang SC, Tan XY, Luxenberg DP, Karim R, Dunussi-Joannopoulos K, Collins M, et al. Interleukin (IL)-22 and IL-17 Are Coexpressed by Th17 Cells and Cooperatively Enhance Expression of Antimicrobial Peptides. *J Exp Med* (2006) 203(10):2271–9. doi: 10.1084/jem.20061308
40. Satoh-Takayama N, Vosshenrich CA, Lesjean-Pottier S, Sawa S, Lochner M, Rattis F, et al. Microbial Flora Drives Interleukin 22 Production in Intestinal NKp46+ Cells That Provide Innate Mucosal Immune Defense. *Immunity* (2008) 29(6):958–70. doi: 10.1016/j.immuni.2008.11.001

41. Withers DR, Hepworth MR. Group 3 Innate Lymphoid Cells: Communications Hubs of the Intestinal Immune System. *Front Immunol* (2017) 8:1298. doi: 10.3389/fimmu.2017.01298
42. Hepworth MR, Monticelli LA, Fung TC, Ziegler CG, Grunberg S, Sinha R, et al. Innate Lymphoid Cells Regulate CD4+ T-Cell Responses to Intestinal Commensal Bacteria. *Nature* (2013) 498(7452):113–7. doi: 10.1038/nature12240
43. Satoh-Takayama N, Lesjean-Pottier S, Vieira P, Sawa S, Eberl G, Vosshenrich CA, et al. IL-7 and IL-15 Independently Program the Differentiation of Intestinal CD3-NKp46+ Cell Subsets From Id2-Dependent Precursors. *J Exp Med* (2010) 207(2):273–80. doi: 10.1084/jem.20092029
44. Parada Venegas D, de la Fuente MK, Landskron G, Gonzalez MJ, Quera R, Dijkstra G, et al. Short Chain Fatty Acids (SCFAs)-Mediated Gut Epithelial and Immune Regulation and Its Relevance for Inflammatory Bowel Diseases. *Front Immunol* (2019) 10:277. doi: 10.3389/fimmu.2019.00277
45. Hueber W, Sands BE, Lewitzky S, Vandemeulebroecke M, Reinisch W, Higgins PD, et al. Secukinumab, a Human Anti-IL-17A Monoclonal Antibody, for Moderate to Severe Crohn's Disease: Unexpected Results of a Randomised, Double-Blind Placebo-Controlled Trial. *Gut* (2012) 61 (12):1693–700. doi: 10.1136/gutjnl-2011-301668
46. Vieco-Saiz N, Belguesmia Y, Raspoet R, Auclair E, Gancel F, Kempf I, et al. Benefits and Inputs From Lactic Acid Bacteria and Their Bacteriocins as Alternatives to Antibiotic Growth Promoters During Food-Animal Production. *Front Microbiol* (2019) 10:57. doi: 10.3389/fmicb.2019.00057
47. Kim DH, Kim S, Ahn JB, Kim JH, Ma HW, Seo DH, et al. Lactobacillus Plantarum CBT LP3 Ameliorates Colitis *via* Modulating T Cells in Mice. *Int J Med Microbiol* (2020) 310(2):151391. doi: 10.1016/j.ijmm.2020.151391
48. Chen CC, Lai CC, Huang HL, Huang WY, Toh HS, Weng TC, et al. Antimicrobial Activity of Lactobacillus Species Against Carbapenem-Resistant Enterobacteriaceae. *Front Microbiol* (2019) 10:789. doi: 10.3389/fmicb.2019.00789
49. El Hage R, Hernandez-Sanabria E, Calatayud Arroyo M, Props R, Van de Wiele T. Propionate-Producing Consortium Restores Antibiotic-Induced Dysbiosis in a Dynamic *In Vitro* Model of the Human Intestinal Microbial Ecosystem. *Front Microbiol* (2019) 10:1206. doi: 10.3389/fmicb.2019.01206
50. Derrien M, van Hylckama Vlieg JE. Fate, Activity, and Impact of Ingested Bacteria Within the Human Gut Microbiota. *Trends Microbiol* (2015) 23 (6):354–66. doi: 10.1016/j.tim.2015.03.002
51. Meininger I, Carrasco A, Rao A, Soini T, Kokkinou E, Mjosberg J. Tissue-Specific Features of Innate Lymphoid Cells. *Trends Immunol* (2020) 41 (10):902–17. doi: 10.1016/j.it.2020.08.009
52. Kupcova Skalnikova H, Cizkova J, Cervenka J, Vodicka P. Advances in Proteomic Techniques for Cytokine Analysis: Focus on Melanoma Research. *Int J Mol Sci* (2017) 18(12). doi: 10.3390/ijms18122697
53. Melo-Gonzalez F, Hepworth MR. Functional and Phenotypic Heterogeneity of Group 3 Innate Lymphoid Cells. *Immunology* (2017) 150(3):265–75. doi: 10.1111/imm.12697
54. Eberl G, Marmon S, Sunshine MJ, Rennert PD, Choi Y, Littman DR. An Essential Function for the Nuclear Receptor RORgamma(t) in the Generation of Fetal Lymphoid Tissue Inducer Cells. *Nat Immunol* (2004) 5(1):64–73. doi: 10.1038/ni1022
55. Schlenner SM, Madan V, Busch K, Tietz A, Laufle C, Costa C, et al. Fate Mapping Reveals Separate Origins of T Cells and Myeloid Lineages in the Thymus. *Immunity* (2010) 32(3):426–36. doi: 10.1016/j.immuni.2010.03.005
56. Miyoshi J, Nobutani K, Musch MW, Ringus DL, Hubert NA, Yamamoto M, et al. Time-, Sex-, and Dose-Dependent Alterations of the Gut Microbiota by Consumption of Dietary Daikenchuto (TU-100). *Evid Based Complement Alternat Med* (2018) 2018:7415975. doi: 10.1155/2018/7415975
57. Nair AB, Jacob S. A Simple Practice Guide for Dose Conversion Between Animals and Human. *J Basic Clin Pharm* (2016) 7(2):27–31. doi: 10.4103/0976-0105.177703
58. Bachmanov AA, Reed DR, Beauchamp GK, Tordoff MG. Food Intake, Water Intake, and Drinking Spout Side Preference of 28 Mouse Strains. *Behav Genet* (2002) 32(6):435–43. doi: 10.1023/A:1020884312053
59. Hager C, Keubler LM, Biernot S, Dietrich J, Buchheister S, Buettner M, et al. Time to Integrate to Nest Test Evaluation in a Mouse DSS-Colitis Model. *PloS One* (2015) 10(12):e0143824. doi: 10.1371/journal.pone.0143824
60. Takeuchi T, Miyauchi E, Kanaya T, Kato T, Nakanishi Y, Watanabe T, et al. Acetate Differentially Regulates IgA Reactivity to Commensal Bacteria. *Nature* (2021) 595(7868):560–4. doi: 10.1038/s41586-021-03727-5
61. Kozich JJ, Westcott SL, Baxter NT, Highlander SK, Schloss PD. Development of a Dual-Index Sequencing Strategy and Curation Pipeline for Analyzing Amplicon Sequence Data on the MiSeq Illumina Sequencing Platform. *Appl Environ Microbiol* (2013) 79(17):5112–20. doi: 10.1128/AEM.01043-13

Conflict of Interest: The authors declare that the research was conducted in the absence of any commercial or financial relationships that could be construed as a potential conflict of interest.

frontiers | Frontiers in Immunology

ORIGINAL RESEARCH
published: 16 June 2022
doi: 10.3389/fimmu.2022.880438

Dynamic Changes in Uterine NK Cell Subset Frequency and Function Over the Menstrual Cycle and Pregnancy

Emily M. Whettlock†, *Ee Von Woon*†, *Antonia O. Cuff*, *Brendan Browne*, *Mark R. Johnson* and *Victoria Male**

Department of Metabolism, Digestion and Reproduction, Institute of Reproductive and Developmental Biology, Imperial College London, London, United Kingdom

OPEN ACCESS

Edited by:
Carolina Jancic, Consejo Nacional de Investigaciones Científicas y Técnicas (CONICET), Argentina

Reviewed by:
Federico Jensen, University of Buenos Aires, Argentina
Thomas Vauvert Hviid, Zealand University Hospital, Denmark
Gendie Lash, Guangzhou Medical University, China

***Correspondence:**
Victoria Male
v.male@imperial.ac.uk

†*These authors have contributed equally to this work and share first authorship*

Specialty section:
This article was submitted to NK and Innate Lymphoid Cell Biology, a section of the journal Frontiers in Immunology

Received: *21 February 2022*
Accepted: *04 May 2022*
Published: *16 June 2022*

Citation:
Whettlock EM, Woon EV, Cuff AO, Browne B, Johnson MR and Male V (2022) Dynamic Changes in Uterine NK Cell Subset Frequency and Function Over the Menstrual Cycle and Pregnancy. Front. Immunol. 13:880438. doi: 10.3389/fimmu.2022.880438

Uterine natural killer cells (uNK) play an important role in promoting successful pregnancy by regulating trophoblast invasion and spiral artery remodelling in the first trimester. Recently, single-cell RNA sequencing (scRNAseq) on first-trimester decidua showed that uNK can be divided into three subsets, which may have different roles in pregnancy. Here we present an integration of previously published scRNAseq datasets, together with novel flow cytometry data to interrogate the frequency, phenotype, and function of uNK1–3 in seven stages of the reproductive cycle (menstrual, proliferative, secretory phases of the menstrual cycle; first, second, and third trimester; and postpartum). We found that uNK1 and uNK2 peak in the first trimester, but by the third trimester, the majority of uNK are uNK3. All three subsets are most able to degranulate and produce cytokines during the secretory phase of the menstrual cycle and express KIR2D molecules, which allow them to interact with HLA-C expressed by placental extravillous trophoblast cells, at the highest frequency during the first trimester. Taken together, our findings suggest that uNK are particularly active and able to interact with placental cells at the time of implantation and that uNK1 and uNK2 may be particularly involved in these processes. Our findings are the first to establish how uNK frequency and function change dynamically across the healthy reproductive cycle. This serves as a platform from which the relationship between uNK function and impaired implantation and placentation can be investigated. This will have important implications for the study of subfertility, recurrent miscarriage, pre-eclampsia, and pre-term labour.

Keywords: NK cells, innate lymphocytes, decidua, endometrium, pregnancy, single-cell analysis

INTRODUCTION

Uterine natural killer cells (uNK) are NK-like cells that are found in the lining of the uterus (called "decidua" in pregnancy and "endometrium" outside of pregnancy). They are distinct from peripheral blood NK (pNK) cells in both phenotype and function. Unlike pNK, uNK are only weakly cytotoxic and instead produce factors that are pro-angiogenic and that attract foetal derived placental cells called extravillous trophoblast (EVT) (1–6). uNK are most prominent in the first trimester of pregnancy, at which time they account for 70%–80% of immune cells in the decidua (7).

Their prominence at the time of implantation, and their production of factors that are predicted to promote trophoblast invasion and spiral artery remodelling, indicates they are likely to have a role in placental implantation.

Further evidence for the role of uNK in implantation comes from their expression of high levels of killer-cell immunoglobulin-like receptors (KIRs), CD94/NKG2 (8, 9), and LILRB1 (9), which allows them to recognise the human leukocyte antigens (HLAs) expressed by EVT: HLA-C, HLA-E, and HLA-G, respectively (10–12). A number of immunogenetic studies have demonstrated that combinations of HLA and KIR that lead to lower activation are associated with disorders of insufficient implantation such as pre-eclampsia, foetal growth restriction, and recurrent miscarriage, suggesting that uNK activation *via* KIR is important for implantation (13–20), although it is important to note that not all studies have been able to find this association (21). The increased expression of KIRs by uNK around the time of implantation provides additional support for this idea (22).

CD107a staining is a proxy for degranulation, and previous studies have shown that this acts as a reliable measure of overall uNK activation (23). Uterine NK cells have been reported to produce IL-8 and granulocyte-macrophage colony-stimulating factor (GM-CSF): IL-8 is postulated to stimulate EVT invasion, whereas GM-CSF has been found to attract EVT (6, 23). On the other hand, the cytokines characteristically produced by pNK cells, TNFα and IFNγ, inhibit invasion of EVT cells and display increased production at later stages of early pregnancy, between 12 and 14 weeks (24, 25). However, there is some evidence that IFNγ may also be involved in spiral artery remodelling in early gestation (26).

Until recently, it was thought that uNK formed a single population, but single-cell RNA sequencing (scRNAseq) has now demonstrated three subpopulations of uNK in first-trimester decidua (27). These were originally called decidual NK (dNK) 1, 2, and 3, but they have now also been found in non-pregnant endometrium (28). Here, we call these subsets "uNK1," "uNK2," and "uNK3" in recognition of the finding that they are not confined to the decidua. uNK1 express higher levels of KIRs and LILRB1, indicating they may be specialised to communicate with EVT (27, 29). uNK2 and uNK3 produced more cytokines upon stimulation, indicating that their role may be immune defence (29). However, several questions remain open. Are these three subpopulations still present at the end of pregnancy? Do the subpopulations change in prominence and/or activity over the reproductive cycle? The answers to these questions could elucidate which subpopulations are important in implantation, parturition, and immune protection throughout the reproductive cycle.

Here, we show that the proportions of the uNK subpopulations remain stable through the menstrual cycle, but all three are more active and express higher levels of KIR around the time of implantation. uNK1 are more prominent in the first trimester of pregnancy, potentially indicating a requirement for this subset in the mediation of implantation, whereas uNK3 are the most prominent at the end of pregnancy. Overall, we outline how the three uNK subpopulations change in proportion, phenotype, and function throughout the reproductive cycle.

MATERIALS AND METHODS

Primary Tissue

The collection of human tissue was approved by London—Chelsea Research Ethics Committee (study numbers: 10/H0801/45 and 11/LO/0971).

We examined tissues and collected data at seven stages of the reproductive cycle. In the menstrual cycle, there are three stages: menstrual (when the lining of the uterus is shed), proliferative (prior to ovulation), and secretory (after ovulation). Pregnancy is divided into three trimesters: first (1–12 weeks), second (12–28 weeks), and third (28 – 40 weeks). We also examined postpartum samples (up to 16 weeks post-delivery). During the menstrual cycle stages, the uterine tissue we examined is known as the endometrium. During pregnancy, this tissue undergoes a process called decidualisation and results in three tissues known as the decidua basalis (DB) (which lines the maternal side of the placenta), decidua parietalis (DP) (which lines the rest of the uterus), and decidua capsularis (which lines the embryo on the luminal side). When taking samples from first-trimester tissue, it is not possible to differentiate between the different decidual tissues. During the second trimester, the decidua capsularis fuses with the DP. When taking samples from third-trimester tissue, it is possible to dissect distinct samples from the DB and the DP.

A total of 29 endometrial samples were taken by Pipelle biopsy before insertion of an intrauterine device for contraception. Samples taken on a day of bleeding were assigned as a menstrual phase. Other samples were categorised into proliferative or secretory phase by date of last menstrual period and serum progesterone level: samples obtained before day 14 were assigned as proliferative phase and after day 14 as a secretory phase with retrospective confirmation by serum progesterone level, according to previously published reference range (30). We collected 8 menstrual, 7 proliferative, and 10 secretory phase samples and 4 samples from postpartum participants, up until 16 weeks postpartum.

A total of 10 decidual samples were taken from participants undergoing surgical management of elective termination of pregnancy between 6 and 13 weeks of pregnancy and 16 from participants undergoing elective caesarean sections, over 37 weeks of pregnancy and not in labour. For labouring data, a further 9 samples were taken from participants in the early stages of labour (1–3-cm cervical dilation and regular contractions) who had a caesarean section, and 9 samples were taken from participants after vaginal birth. Matched peripheral venous blood was obtained from all patients at the time of obtaining endometrial or decidual samples. Patient characteristics are summarised in **Supplementary Tables 1, 2**.

Lymphocytes were extracted from peripheral blood by layering onto Histopaque (Sigma-Aldrich, St. Louis, MO, USA), spinning down (700 ×*g*, 20 min, 21°C), and retrieving the interface, which was washed twice with Dulbecco's

Phosphate-Buffered Saline (PBS) (Life Technologies, Carlsbad, CA, USA) (500 ×*g*, 10 min, 4°C). Briefly, endometrial tissue was passed through a 100-µm cell strainer, pelleted (700 ×*g*, 10 min, 4°C), resuspended in Dulbecco's PBS supplemented by 10% Foetal Calf Serum (FCS) (Sigma-Aldrich), passed through a 70-µm strainer, and layered on Histopaque as above.

For first-trimester samples, decidua compacta was extracted from products of conception and stirred for 20 min to remove blood before mincing with a scalpel followed by gentleMACS dissociation (Miltenyi, Bergisch Gladbach, Germany). Minced tissue was passed through a 75-µm sieve, pelleted (500 ×*g*, 10 min, 4°C), and resuspended in PBS/1% FCS before passing through a 100-µm strainer. The filtrate was layered on Histopaque as above.

For third-trimester DB samples, small sections were cut from the maternal side of the placenta and washed using a magnetic stirrer in Mg^{2+}- and Ca^{2+}-free PBS (Gibco, Grand Island, NY, USA) for 20 min. Blood clots, vessels, and placental tissue were physically removed, and cleaned decidual tissue was placed in new Mg^{2+}- and Ca^{2+}-free PBS. The tissue was spun (400 ×*g*, 5 mins 21°C), and PBS was removed. The tissue was resuspended in Accutase (Invitrogen, Carlsbad, CA, USA), mechanically digested in C tubes using a gentleMACS dissociater, and placed in a 37°C shaking water bath for 45 min. Minced tissue was passed through a 70-µm strainer and resuspended in PBS/1% FCS/2 mM EDTA. The filtrate was layered on Histopaque as above. For the third-trimester DP samples, 10 cm × 10 cm sections of the foetal membrane were dissected, and the decidua was removed using a cell scraper (Sarstedt, Nümbrecht, Germany). The tissue underwent enzymatic and mechanical digestion as described in the DB protocol.

Extracted lymphocytes were counted by light microscopy (Leica, Wetzlar, Germany) with a haemocytometer. A total of 0.2×10^6 to 1×10^6 cells per condition were allocated for phenotype and functional assessment.

Stimulation With PMA/Ionomycin

A total of 21 endometrial, all first-trimester and all third-trimester samples were used for functional assessment. Endometrial lymphocytes were stimulated immediately after isolation, and decidual lymphocytes were stimulated after 12 to 20 h of rest at 37°C. Optimisation experiments showed no difference between cells stimulated fresh and after rest (**Supplementary Figure 1**).

For functional assessment, cells were suspended in Roswell Park Memorial Institute (RPMI) enriched with antibiotics, EDTA, and sodium pyruvate and divided into unstimulated and stimulated wells. Anti-CD107a BV605 (100 µl/ml), Brefeldin (10 µg/ml), and Monensin (2 µM/ml) were added to all wells and phorbol 12-myristate 13-acetate (PMA) (50 ng/ml) and ionomycin (1 µg/ml) into the stimulated wells only. Cells were incubated for 4 h at 37°C and then stained with antibodies. For third-trimester samples, cells were incubated for 6 h with anti-CD107a, PMA, and ionomycin, with Brefeldin and Monensin added 2 h into the incubation.

Single-Cell RNA Sequencing Data Analysis

For the scRNAseq data, 5 stages of the reproductive cycle were examined: proliferative (n = 3), secretory (n = 3), first trimester (n = 5), second trimester (n = 1), and third trimester (term in labour (TNL) = 3). R (31) was used for the majority of the analysis. This included the use of the package Seurat (32), designed for analysis of scRNAseq data, and various data manipulation and visualisation packages (33–40).

A scRNAseq dataset from the non-pregnant uterus (available at www.reproductivecellatlas.org/) was converted from a Python format into an R Seurat object. The object was a subset of cells that had been classified as "Lymphoid" or "Myeloid" under "Cell.type" in the metadata.

A scRNAseq dataset from the first-trimester uterus (available at Array Express E-MTAB-6701) was converted from.txt into an R seurat object. The object was a subset of cells that had been designated an immune cell type, e.g., "dNK1" under "Annotation," in the metadata. Cells originating from the placenta or blood were removed, so only decidual cells remained. Data from one donor were removed from the analysis due to their NK cells clustering independently of all other NK cells.

The scRNAseq dataset (dbGaP phs001886.v1.p1, reanalysed with permission of the NIH, project ID 26528) contained samples from one second-trimester accreta case, which is therefore pathological, and 9 third-trimester participants. Both datasets were filtered, aligned, and quantified using Cell Ranger software (version 5.0.1, 10x Genomics). h19 was used as a human genome reference. Downstream analyses were performed using the R package Seurat (version 4.0.2) (32). Cells with fewer than 200 genes and genes that were expressed in less than 10 cells were removed. Furthermore, cells where the gene content was greater than 10% mitochondrial genes were removed. Clusters were identified using "FindClusters" algorithm. The "FindAllMarkers" algorithm was used to identify the immune clusters and subset the object to immune cells. Cells from placental tissue were removed. TIL and PTL samples were not included in the analysis observing uNK across the reproductive cycle. PTL samples were not included in the term labouring analysis.

The four datasets were integrated based on a previously published workflow (41). Clusters that appeared to be non-immune cells were removed, and the remaining cells were reanalysed using the same workflow. The integrated dataset contained 2,180 cells from non-pregnant endometrium, 18,243 cells from first-trimester decidua, 3,900 from second-trimester decidua, and 6,077 from third-trimester decidua. The algorithm "FindConservedMarkers" was used to identify the clusters uNK1, uNK2, and uNK3. This was confirmed by the metadata column "annotation" from the first-trimester dataset. For visualisation of clusters and gene expression across the reproductive cycle, each dataset was downsampled so that the total number of cells displayed was equal in each dataset.

Flow Cytometry

The following anti-human antibodies were used: anti-CD56 Brilliant Violet (BV) 650 (clone NCAM 16.2, BD Biosciences, San Jose, CA, USA), anti-CD39 BV421 (clone A1, BioLegend, San Diego, CA, USA), anti-CD3 BV711 (clone SK7, BioLegend), anti-CD103 BV785 (clone Ber-ACT8, BioLegend), anti-CD16 Alexa Fluor(AF)700 (clone 3G8, BioLegend), anti-CD9

phycoerythrin(PE)/Dazzle 594 (clone HI9a, BioLegend), anti-CD49a PE/Cy7 (clone TS2/7, BioLegend), anti-CD45 allophycocyanin (APC) (clone HI30, BioLegend), anti-CD94 PE (clone HP-3D9, BD Biosciences), anti-CD158a/h (KIR2DL1/DS1) VioBright 515 (clone REA1010, Miltenyi Biotec, Bergisch Gladbach, Germany), anti-CD158b (KIR2DL2/DL3) APC vio 770 (clone REA 1006, Miltenyi Biotec), CD85j (ILT2 or CD94) Peridinin chlorophyll protein (PerCP)-eFluor 710 (clone HP-F1, Thermo Fisher Scientific, Waltham, MA, USA) and anti-CD107a BV605 (clone H4A3, BioLegend) for surface antigens, and anti-IL-8 PE (clone G265-8, BD Biosciences), anti-IFN-γ APCvio770 (clone REA600, Miltenyi Biotec), anti-GM-CSF PERCP/Cyanine 5.5 (clone BVD2-21C11, BioLegend), and anti-TNFα fluorescein isothiocyanate (FITC) (clone MAb11, BioLegend) for intracellular staining.

Cells were first incubated with fixable viability dye (Live/Dead Fixable Aqua Dead Cell stain kit, Life Technologies) (15 min, 4°C) followed by incubation with surface antibodies (15 min, 4°C). For intracellular staining, human FoxP3 buffer (BD Biosciences) was used according to the manufacturer's instructions before staining with intracellular antibodies (30 min, 4°C). For third-trimester samples, fixable viability dye was included with the surface staining antibodies (20 min, RT) and intracellular staining using the Cytofix/Cytoperm kit (BD Biosciences) according to the manufacturer's instructions. Excess antibodies were washed off (5 min, 500 ×*g*, 4°C) between each incubation and twice after the final incubation with intracellular antibodies.

Statistical Analysis

Data were acquired on a BD Fortessa and analysed using FlowJo (Tree Star, Ashland, OR, USA). Application settings were used to ensure reproducible results. Statistical analysis was performed using PRISM (GraphPad Software Inc.). Data were assessed for normality using Shapiro–Wilk tests to determine whether a parametric or a non-parametric statistical test was appropriate. The appropriate statistical test was used to compare subsets as specified in figure legends. $p < 0.05$ was considered significant.

RESULTS

uNK1, uNK2, and uNK3 Are Present Throughout the Human Reproductive Cycle and Vary in Frequency

scRNAseq analysis has previously identified that three subpopulations of uNK, uNK1, uNK2, and uNK3, are present in first-trimester decidua (27) and non-pregnant endometrium (28). Previous analysis of scRNAseq data from third-trimester decidua identified only a single cluster within the uNK population (42), and our reanalysis of the third-trimester dataset alone confirmed this. However, when the third-trimester data were integrated with data from the non-pregnant uterus, first- and second-trimester, the third-trimester uNK cells did form three clusters (**Figures 1A, B**).

In the first trimester, uNK can be distinguished from circulating NK cells by their expression of CD49a and CD9; the subsets are then defined by their expression of CD39 and CD103 (27). We confirmed the presence of CD49a+ uNK in the endometrium and in the first- and third-trimester decidua and that the three subpopulations uNK1, uNK2, and uNK3 can be identified using CD39 and CD103 (**Figure 2A**). However, in third-trimester samples, there was a significant CD49a+CD9− population. A comparison of CD49a+CD9+ and CD49a+ CD9− detected no phenotypic differences between these two populations, suggesting that CD49a alone can be used to identify uNK cells in the third trimester (**Supplementary Figure 2**). For consistency of gating strategy, we therefore also identified uNK cells by their expression of CD49a alone in the endometrial, first-trimester, and postpartum samples.

In line with previous reports (7), we observed a peak in total uNK, as a proportion of total CD45+ lymphocytes, in first-trimester pregnancy by both scRNAseq and flow cytometry (**Figures 1C**, **2B**). We observed a similar proportion of total uNK in the proliferative and secretory phases (**Figures 1C**, **2C**). Additionally, we analysed CD56+CD49a− cells (which represent pNK cells) as a proportion of total CD56+ NK cells in endometrium/decidua and found this to be significantly higher in third- compared to first-trimester decidua; however, no difference was noted through the menstrual cycle [median (interquartile range (IQR)) for menstrual, 27.7 (38.1); proliferative, 23.8 (20.7); secretory, 22.3 (19.1); first trimester, 8.1 (5.0); third trimester DB 26.7 (12.4); third trimester DP 38.2 (22.6), postpartum, 13.6 (12.3)]. This highlights the importance of using tissue-specific immune cell markers, particularly when examining third-trimester decidua.

Next, we examined uNK1, uNK2, and uNK3 frequency expressed as a proportion of either total CD45+ lymphocytes or total uNK. We observed an increase in the frequency of uNK1 when transitioning from the secretory phase to first-trimester pregnancy, but this was not sustained into the third trimester. This observation applied to uNK1 as a percentage of both CD45+ lymphocytes and the percentage of total NK cells (**Figures 1C**, **2B**), and the change was significant when measured by flow cytometry.

The variation of uNK2 frequency was similar to that observed for uNK1, with a peak in the first trimester observed by scRNAseq, and flow cytometry when the frequency was measured as a percentage of CD45+ lymphocytes (**Figures 1C**, **2B**). For the latter, uNK2 was significantly higher in the first trimester, compared to the third. Further, there was an upward trend of uNK2 when transitioning from third-trimester decidua to postpartum endometrium when measured as a proportion of total NK (**Figure 2C**).

For uNK3, there was no change in frequency through the menstrual cycle. When measured as a percentage of CD45+ lymphocytes, there was a reduction in uNK3 in third-trimester DP, compared to both first-trimester decidua and third-trimester DB. This was significant when measured by flow cytometry. When measuring uNK3 as a percentage of total uNK, there was a dip in the first trimester and a peak in both types of the third-trimester decidua. This was significant when measured by flow cytometry. The discrepancy between the proportions when expressed as a percentage of CD45+ lymphocytes or total uNK

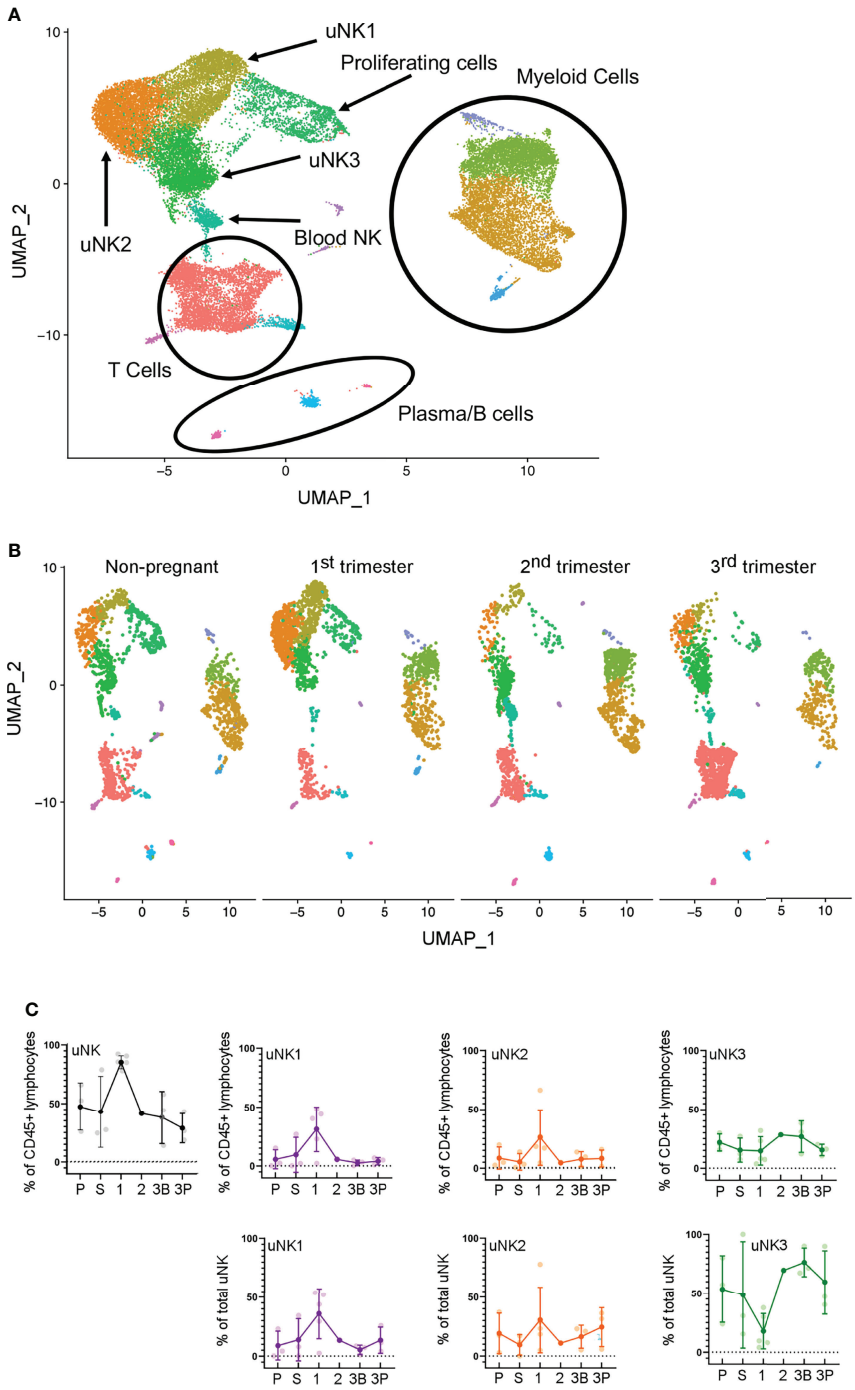

FIGURE 1 | uNK1, uNK2, and uNK3 are present throughout the human reproductive cycle, by scRNAseq. **(A)** Integrated immune cells from non-pregnant endometrium, and first-, second-, and third-trimester decidua, visualised by Uniform Manifold Approximation and Projection (UMAP). Colours are indicative of clusters and are identified with appropriate immune cell types. n = 12 (non-pregnant), n = 5 (1T), n = 1 (2T), n = 3 (3T). uNK, uterine natural killer. **(B)** Immune cells from each of the four stages in the reproductive cycle subset to 2,200 cells. Immune cells separated by stage and then visualised by UMAP. Colours are indicative of clusters. **(C)** Using the scRNAseq dataset, graphs show frequency of total NK from CD45+ lymphocytes and then frequency of each uNK subset (uNK1, uNK2, and uNK3) as both a proportion of CD45+ lymphocytes and a proportion of total uNK cells. Means and SDs are shown for n = 3 (proliferative), n = 3 (secretory) n = 5 (first trimester), n = 1 (second trimester), n = 3 (third-trimester decidua basalis), and n = 3 (third-trimester decidua parietalis). P, proliferative phase; S, secretory phase; 1, first trimester; 2, second trimester; 3B, third-trimester decidua basalis; 3P, third-trimester decidua parietalis.

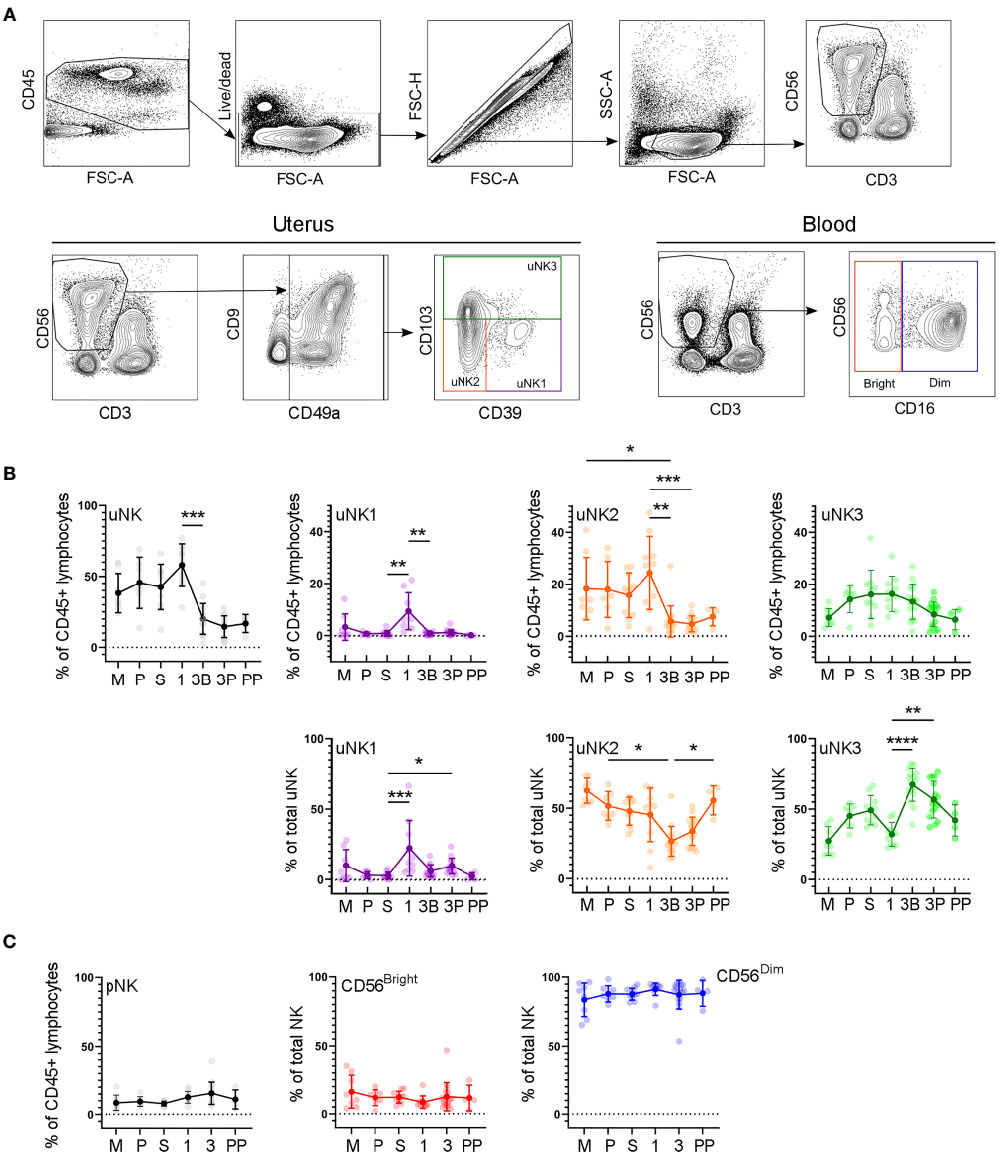

FIGURE 2 | uNK1, -2 and -3 are present throughout the human reproductive cycle, by flow cytometry. **(A)** FACs gating strategy used to identify three uNK subsets and pNK (representative example shown). Coloured boxes in final plot indicate colour used for that subset in subsequent graphs. **(B)** Using flow cytometry data, graphs show frequency of total NK from CD45+ lymphocytes and then frequency of each uNK subset (uNK1, -2 -3) both as a proportion of CD45+ lymphocytes and proportion of total uNK cells. Means and standard deviations are shown for n = 8 (menstrual), n = 7 (proliferative), n = 10 (secretory) n= 10 (first trimester), n= 16 (third trimester decidua basalis), n = 16 (third trimester decidua parietalis), n = 4 (postpartum). Statistical testing was done using Kruskal Wallis with a post-hoc Dunn test *p < 0.05, **p < 0.01, ***p < 0.001, ****p< 0.0001. **(C)** Using flow cytometry data, graphs show frequency of total NK from CD45+ lymphocytes and then frequency of each pNK subset ($CD56^{Bright}$ and $CD56^{Dim}$) as a proportion of total pNK. Sample numbers for each group are the same as B. M, menstrual phase; P, proliferative phase; S, secretory phase; 1, first trimester; 3B, third trimester decidua basalis; 3P, third trimester decidua parietalis; PP, post-partum.

cells is likely due to the change in frequency of total uNK, as a proportion of CD45+ lymphocytes.

Within the third-trimester decidua, the uNK2 population appeared greater as a proportion of total uNK in the DP compared to the DB in both scRNAseq and flow cytometry, although this did not reach significance for either (**Figure 1C**, **2B**). The uNK3 population appeared greater in the DB, compared to the DP, which was significant when measured by flow cytometry as a percentage of CD45+ lymphocytes (**Figure 1C**, **2B**).

Peripheral Blood NK Cell Frequency Does Not Vary Over the Reproductive Cycle or Correlate With uNK Frequency

We also examined $CD56^{Bright}$ and $CD56^{Dim}$ NK cells in matched peripheral blood, using a conventional gating strategy to identify

these populations (**Figure 2C**). Unlike uNK, there was no variation in total CD56+ pNK, $CD56^{Bright}$, or $CD56^{Dim}$ in peripheral blood when transitioning through different phases of the reproductive cycle. Furthermore, there was no significant correlation in levels of pNK and uNK subsets when expressed as either a proportion of CD45+ live lymphocytes or total NK cells (**Supplementary Figure 3**).

uNK Subsets Upregulate KIR and LILRB1 During Transition From Non-Pregnant Endometrium to First-Trimester Decidua

We next examined uNK expression of receptors that interact with trophoblast cells: KIR2DL1 and KIR2DL2/3 recognise HLA-C, LILRB1 recognises HLA-G, and CD94 recognises HLA-E (**Figure 3A**) (43).

In line with earlier findings on first-trimester uNK (27, 29), we observed that uNK1 expressed higher levels of KIR than uNK2 and uNK3 (**Figures 3B, C**). We also found that all three uNK subsets expressed increased KIR in the first trimester of pregnancy, compared to non-pregnant endometrium and third-trimester decidua (**Figures 3B, C**). Similar to KIR, LILRB1 protein expression peaked in the first trimester, although this was only statistically significant in uNK2 and uNK3 (**Figure 3B**). *LILRB1* transcript expression followed a similar trend, although in contrast to our findings at the protein level, *LILRB1* mRNA was not detectable in the DB (**Figure 3C**). At the transcript and protein levels, CD94 was expressed at a higher level on uNK2 and -3 compared to uNK1 (**Figures 3B, C**). There was a slight reduction in CD94 transcript (*KLRD1*) towards the end of pregnancy, but this was not observed at the protein level (**Figures 3B, C**).

In line with our finding that pNK did not change in frequency over the reproductive cycle, examination of NK cells from matched blood showed no change in the frequency at which KIR, LILRB1, and CD94 are expressed in these cells (**Figure 3B**).

uNK Are the Most Active at the Time of Implantation

We next assessed functional responses with and without stimulation with PMA and ionomycin (**Figure 4A**). Degranulation in unstimulated conditions declined during the proliferative phase, slightly in uNK2, and significantly in uNK3, compared to the other two phases of the menstrual cycle (**Figure 4B**). At the end of pregnancy, degranulation was significantly lower in the third-trimester DP compared to DB in uNK1, but this was not replicated in the other subsets (**Figure 4B**). In stimulated cells, there was a reduction in degranulation in uNK2 and uNK3 in both third-trimester decidua compared to first-trimester decidua (**Figure 4B**).

For TNFα, IFNγ, and IL-8, we observed peaks in cytokine production across all stimulated uNK subsets during the secretory phase, compared to the proliferative phase and first trimester, although this did not reach statistical significance in all cases (**Figure 4B**). For IL-8 in uNK3, this peak was maintained into first-trimester pregnancy. This trend was also present in unstimulated cells for IL-8 (**Figure 4B**).

Third-trimester uNK produced less cytokine than first-trimester uNK, although this only reached significance in IL-8 production from uNK3. This reduction in cytokine production through pregnancy was also seen at the mRNA level for IL-8 (**Figure 4C**). In contrast, GM-CSF protein production was consistently low in the menstrual cycle, including the secretory phase, but increased significantly in the first trimester of pregnancy in unstimulated uNK1 and stimulated uNK3 (**Figure 4B**).

For examination of NK cells from matched peripheral blood, data from $CD56^{Bright}$ and ^{Dim} NK cells are shown together due to downregulation of CD16 after stimulation. Aside from a significant decline in CD107a expression in unstimulated cells when transitioning from the secretory phase to first-trimester pregnancy, there was no distinct trend in either stimulated or unstimulated cells (**Figure 4B**).

The mRNA expression of other NK cell proteins of interest across the reproductive cycle, such as granzymes, that were not included in the flow cytometry panel, can be seen in **Supplementary Figures 4**, **5**.

uNK Phenotype and Function Do Not Change in Labour

In line with previous findings (44, 45), we did not observe any change in the proportion of total uNK in labouring compared to non-labouring decidua (**Figure 5B**). The proportion of uNK in non-labouring decidua was lower in the DP compared to the DB (**Figure 5B**). We next examined the uNK subpopulations in non-labour compared to early labour and established labour samples. We observed no change in the frequency of any of the uNK or pNK subsets across the spectrum of these samples (**Figures 5A, B**). The receptors examined were also stably expressed during labour (**Supplementary Figure 6**), an observation that suggests that EVT cross-talk with uNK is not a major participant in labour. Similarly, for those markers examined, the function of uNK and pNK subsets remains stable during labour, although we did observe that, regardless of labouring state, the uNK1 population in the DB is significantly more active than the population in the DP (**Figure 5** and **Supplementary Figure 7**). This is supported by the low number of differentially expressed genes across all three uNK subsets in the scRNAseq data compared with non-labour to labour samples (**Supplementary Table 3**).

DISCUSSION

To our knowledge, this is the first study to track the three uNK subpopulations throughout the reproductive cycle, examining their frequency, phenotypes, and functions, although one limitation is the small sample size in several of the groups, which should be taken into consideration during interpretation of these results. In line with previous studies, we found that the total uNK population peaked during the first trimester of pregnancy (7, 46). We discovered that uNK1 and uNK2 peak in this period but that uNK3 peaks towards the end of pregnancy. This aligns with a recent report that KIR+CD39+ uNK (mostly

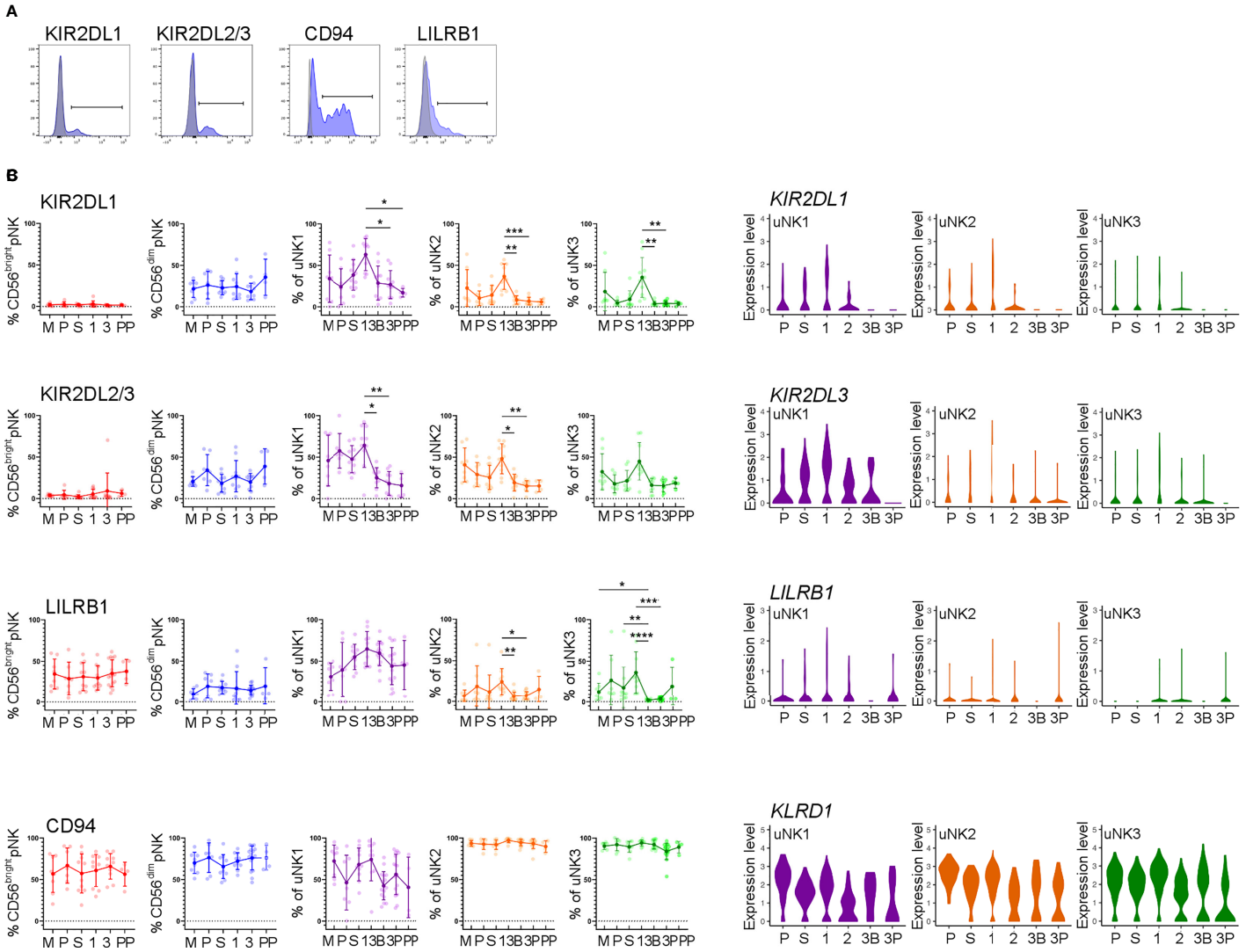

FIGURE 3 | uNK upregulate expression of KIR and LILRB1 in first trimester. **(A)** Uterine and peripheral NK cells taken at different stages of the reproductive cycle were freshly stained for phenotypic markers. Representative staining from CD56dim pNK is shown in blue alongside FMO controls in grey. **(B)** Graphs showing frequencies of KIR2DL1, KIR2DL2/3, LILRB1 and CD94 on pNK and uNK subsets. Means and standard deviations are shown for n = 8 (menstrual), n = 7 (proliferative), n = 10 (secretory) n= 10 (first trimester), n= 16 (third trimester decidua basalis), n = 16 (third trimester decidua parietalis), n = 4 (postpartum). Statistical testing was done using Kruskal Wallis with a post-hoc Dunn test *p < 0.05, **p < 0.01, ***p < 0.001, ****p< 0.0001. **(C)** Violin plots showing corresponding mRNA expression in uNK subsets over the reproductive cycle as determined by scRNAseq. M, menstrual phase; P, proliferative phase; S, secretory phase; 1, first trimester; 2, second trimester; 3, third trimester; 3B, third trimester decidua basalis; 3P, third trimester decidua parietalis.

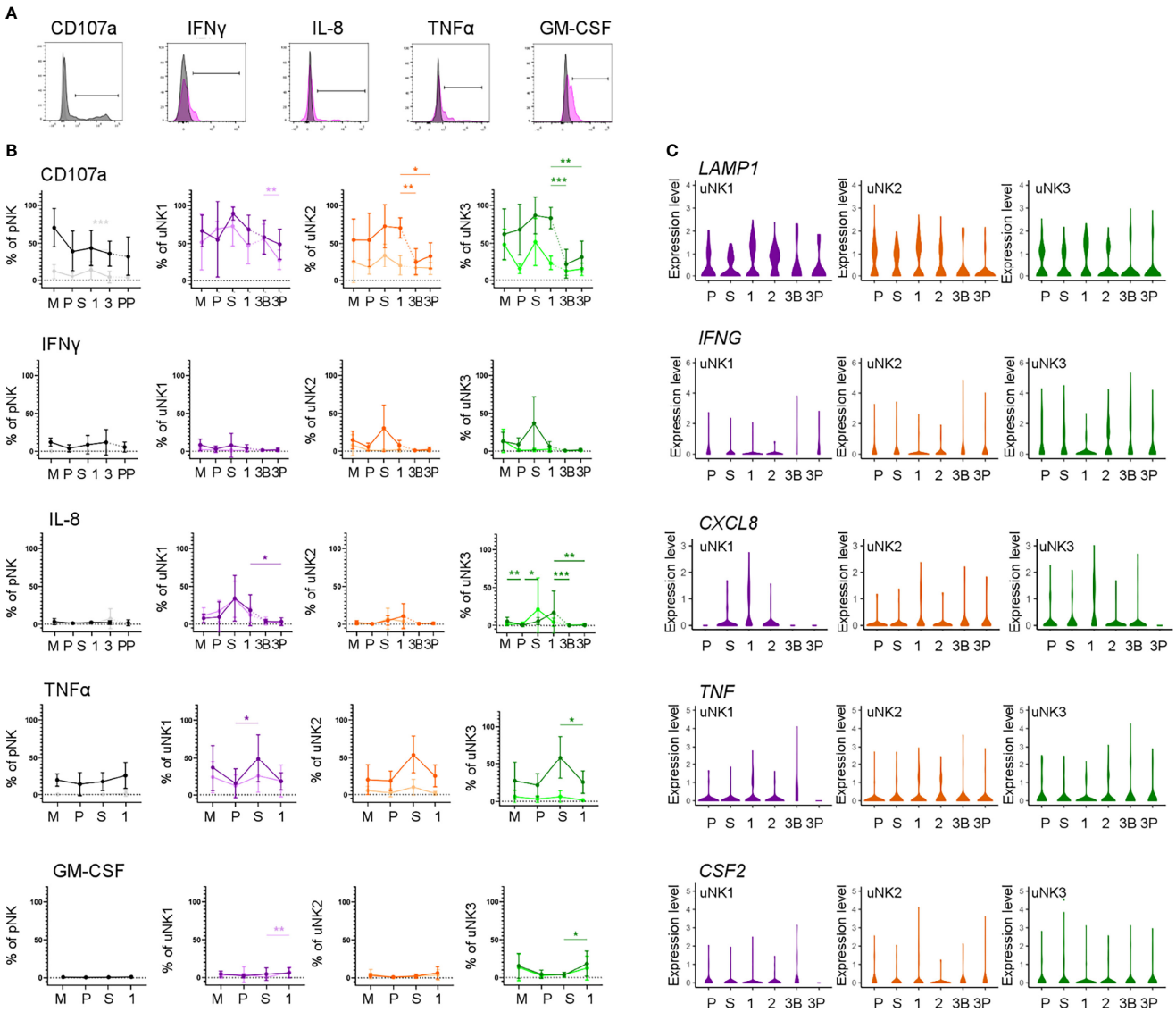

FIGURE 4 | uNK are most active at the time of implantation. **(A)** Uterine and peripheral NK cells taken at different stages of the reproductive cycle were cultured with or without PMA and ionomycin stimulation and assessed for degranulation (CD107a) and production of IFNγ, IL-8, TNFα and GM-CSF. Representative staining of CD107a on total pNK is shown in black, alongside FMO controls in light grey. Representative staining from secretory phase uNK1 is shown for the cytokines in pink, alongside internal negative controls in grey. The positive gates were set by reference to FMO controls. **(B)** Graphs showing frequencies of CD107a, IFNγ, IL-8, TNFα and GM-CSF on pNK and uNK subsets. Unstimulated cells are represented by lighter lines and stimulated cells by darker lines. Means and standard deviations are shown for n = 5 (menstrual), n = 6 (proliferative), n = 10 (secretory) n= 10 (first trimester), n= 16 (third trimester decidua basalis), n = 16 (third trimester decidua parietalis). Statistical testing was done using Kruskal Wallis with a post-hoc Dunn test *p < 0.05, **p < 0.01, ***p < 0.001, and ****p < 0.0001. **(C)** Violin plots showing corresponding mRNA expression in uNK subsets over the reproductive cycle as determined by scRNAseq. M, menstrual phase; P, proliferative phase; S, secretory phase; 1, first trimester; 2, second trimester; 3, third trimester; 3B, third trimester decidua basalis; 3P, third trimester decidua parietalis.

representing uNK1) and KIR+CD39− (mostly representing uNK2) increase in frequency towards the end of the menstrual cycle and remain elevated in early pregnancy (47). Both these reports support the proposal that uNK1 communicate with EVTs in early pregnancy (27, 29) but may also point to a role for uNK2 in this process.

Although previous studies have agreed that uNK fluctuate over the menstrual cycle, there has been some disagreement about precisely how. Studies using immunohistochemistry showed an increase in numbers of CD56+ cells in the secretory compared to the proliferative phase (48–51). This finding was borne out by one study that demonstrated a significant increase in CD3−CD56+ NK cells as a proportion of CD45+ cells in the early secretory compared to the late proliferative stage by flow cytometry (52), but two others were unable to detect this difference (49, 53). In our study, which used CD49a to remove

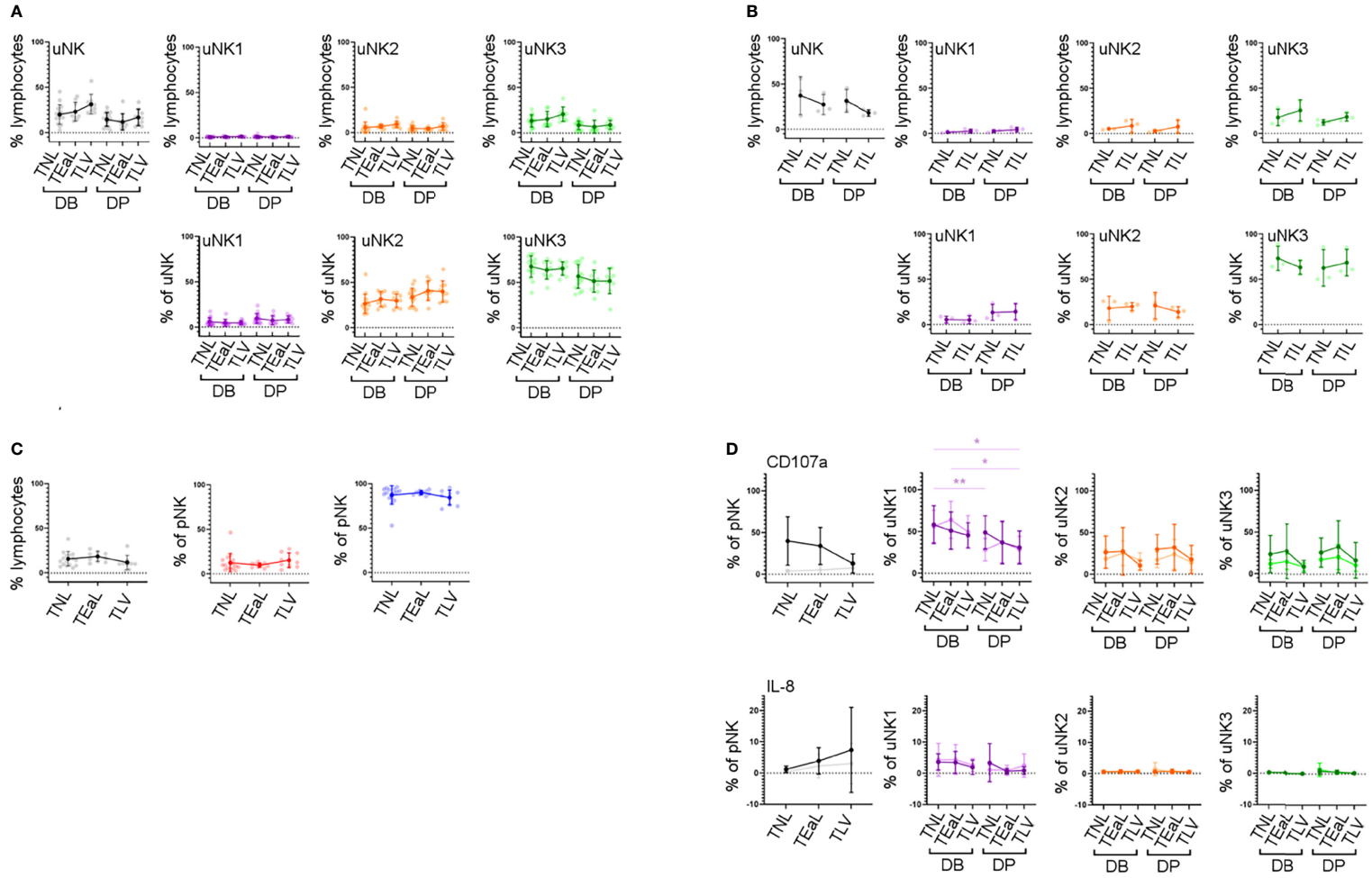

FIGURE 5 | uNK phenotype and function do not change in labour. **(A)** The FACs gating strategy shown in **Figure 2A** was used to identify the three uNK subsets. Graphs show frequency of total NK from CD45+ lymphocytes and then frequency of each uNK subset (uNK1, uNK2, and uNK3) as both a proportion of CD45+ lymphocytes and proportion of total uNK cells. Graphs are divided to show results from both decidua basalis and decidua parietalis. Means and SDs are shown for n = 16 (TNL), n = 9 (TEaL), and n = 9 (TLV). Statistical testing was done using Kruskal–Wallis with a *post-hoc* Dunn test: * $p < 0.05$, and ** $p < 0.01$. **(B)** Using the scRNAseq dataset, graphs show frequency of total NK from CD45+ lymphocytes and then frequency of each uNK subset (uNK1, uNK2, and uNK3) as both a proportion of CD45+ lymphocytes and proportion of total uNK cells. Graphs are divided to show results from both decidua basalis and decidua parietalis. Means and SDs are shown for n = 3 (TNL) and n = 3 (TIL). **(C)** The FACs gating strategy shown in **Figure 2C** was used to identify the two pNK subsets. Using flow cytometry data, graphs show frequency of total NK from CD45+ lymphocytes and then frequency of each pNK subset ($CD56^{Bright}$ and $CD56^{Dim}$) from total NK. Sample numbers for each group are the same as in panel **(A, D)** Uterine and peripheral NK cells were cultured as described in **Figure 4A**. Graphs showing frequencies of CD107a and IL-8 on pNK and uNK subsets. Unstimulated cells are represented by lighter lines and stimulated cells by darker lines. n, numbers for each group are the same as in panel **(A)** Statistical testing was done using Kruskal–Wallis with a *post-hoc* Dunn test: * $p < 0.05$, and ** $p < 0.01$. DB, decidua basalis; DP, decidua parietalis; TNL, term non-labouring; TEaL, term early labouring; TLV, term vaginal birth; TIL, term in labour.

pNK from the analysis thereby giving a true reflection of tissue-resident uNK, we were also unable to detect a change in the proportion of uNK through the menstrual cycle. However, a possible limitation is that we did not classify our secretory phase samples into early, mid, and late, which may have limited our ability to detect differences observed in studies with sufficient samples to use this more rigorous classification.

Compared to pNK, uNK cells are biased towards the expression of KIR2D expression: one previous study using tissue samples found this bias only in first-trimester decidua (22), whereas a more recent study also detected this bias in uNK isolated from menstrual blood, and therefore originating in the non-pregnant uterus (54). Here, we find a clear peak in the expression of KIR2D expression specifically in the first trimester, among all three uNK subsets. A similar trend was seen for LILRB1. This suggests that all uNK subpopulations increase their ability to recognise EVT, *via* HLA-C and HLA-G, in the first trimester. In comparison, CD94 expression was higher on uNK2 and uNK3 subsets compared to uNK1. This is in contrast with previous findings (29). However, the earlier study measured marker intensity on recovered cryopreserved cells, whereas we report a percentage of CD94+ fresh cells. It is possible that the freezing process preferentially killed CD94− uNK1 cells or that uNK1 have a lower percentage of cells expressing CD94 but a higher expression per cell: either of these could explain the disparity in our results. Other markers that may be of interest, which were not examined in our study, are KIR2DL4, which has been suggested to be a receptor for HLA-G and HLA-F (55, 56).

By examining degranulation as a proxy for uNK cell activation (23), we found that uNK were typically most active around the time of implantation, in the secretory phase of the menstrual cycle and the first trimester of pregnancy. This is in line with previous findings that first-trimester uNK are more able to degranulate in response to HCMV-infected targets than those at term, although the same study found that, following IL-15 stimulation, term uNK are better able to degranulate in response to PMA and ionomycin than first-trimester cells (9). Without stimulation, uNK produce little IFNγ, IL-8, TNFα, and GM-CSF. However, after stimulation with PMA and ionomycin, uNK have the highest ability to produce most of these cytokines during the secretory phase. This may be in line with a previous report suggesting that endometrial NK cells are more transcriptionally active than decidual NK cells (57). The exception was GM-CSF, whose production peaks in the first trimester. Previous studies suggest that the ability of uNK to produce growth factors and cytokines evolves as pregnancy progresses, with production predominantly of pro-angiogenic and growth factors at 8–10 weeks, and predominantly cytokines at 12–14 weeks (58). We did not collect sufficient first-trimester samples to undertake an analysis stratified by gestational age, but nonetheless, our finding that the timing of maximum activation coincides with the window of implantation is interesting because it suggests that uNK may have a role in coordinating successful implantation.

Cumulative evidence indicates an important physiological role for uNK in first-trimester pregnancy, but there is conflicting evidence on their role in reproductive failure. Our findings and those of others (27, 29) point to uNK1 as the uNK subset more likely to mediate placental implantation in early pregnancy. Future studies focusing specifically on this subset may be able to elucidate differences that were previously masked due to the examination of uNK as a bulk population. A recent study using scRNAseq suggests that there is a reduction of uNK1 in pathological pregnancies (59); however, these findings should be interpreted with caution because the pathological samples were collected after pregnancy loss, making it difficult to discern if changes seen in immune cells are a cause or an effect of pregnancy loss, due to inflammatory changes that typically occur after foetal demise. To overcome this, future studies could interrogate uNK during the window of implantation (60) or from elective termination of pregnancy samples stratified to low and high risk by uterine artery Doppler ultrasound, which has high specificity in predicting the risk of pre-eclampsia and intrauterine growth restriction (61).

In the third trimester, we found a greater proportion of uNK in the DB compared to DP. This is in contrast to a previous report that found a higher frequency of $CD56B^{right}$ NK cells in the parietalis than in the basalis (62). However, the lack of tissue-specific markers in this earlier study means that it is difficult to be sure if these all represent uNK. In both decidual tissues in the third trimester, the majority of uNK cells are uNK3, which express low levels of KIRs and LILRB1. This could suggest that, in contrast to early pregnancy, the major role of uNK in late pregnancy does not involve interactions with EVTs. Similarly, the expression of the functional markers we examined was lower in the third trimester. This could indicate that, if these cells have a role at the end of pregnancy, it is *via* a different mechanism of action. The resemblance of uNK3 to intra-epithelial ILC1 (29) could suggest that their role is in mucosal homeostasis, and this is likely to be important throughout pregnancy, in line with the relative constancy of uNK3, compared to uNK1 and uNK2. Intriguingly, by scRNAseq, uNK3 were the subset that differed the most, transcriptionally, between non-labouring and labouring states, suggesting they may have a role in labour that is yet to be defined. It would be interesting to do a broader analysis of the potential functions of these cells or examine their roles in pathological cases such as pre-eclampsia or preterm birth.

In conclusion, we show here how uNK subset number, expression of receptors, and function change dynamically across the healthy reproductive cycle. This provides evidence of their physiological role in implantation but will also provide an important platform from which the relationship between uNK function and pathologies of pregnancy associated with impaired implantation and placentation can be investigated.

DATA AVAILABILITY STATEMENT

The datasets presented in this study can be found in online repositories. The names of the repository/repositories and accession number(s) can be found below: www.reproductivecellatlas.org/, https://cellgeni.cog.sanger.ac.uk/vento/reproductivecellatlas/endometrium_all.h5ad; https://www.ncbi.nlm.nih.gov/projects/gap/cgi-bin/study.cgi?study_id=phs001886.

v1.p1; and https://osf.io/wkxyz/, https://osf.io/wkxyz/. Code is available from https://github.com/ewhettlock/reproductive_cycle.

ETHICS STATEMENT

The collection of human tissue was approved by London—Chelsea Research Ethics Committee (study numbers: 10/H0801/45 and 11/LO/0971). The patients/participants provided their written informed consent to participate in this study.

AUTHOR CONTRIBUTIONS

EMW, EVW, and VM designed the study, analysed the results, and wrote the manuscript. EMW, EVW, and AC carried out the experiments. EVW, BB, and MJ obtained patients' consent and collected the clinical samples. All others contributed to editing the manuscript. All authors listed have made a substantial, direct, and intellectual contribution to the work and approved it for publication.

FUNDING

This study was funded by Borne. Study phs001886.v1.p1 was, in part, supported by the Perinatology Research Branch, Division of Obstetrics and Maternal-Fetal Medicine, Division of Intramural Research, Eunice Kennedy Shriver National Institute of Child Health and Human Development, National Institutes of Health, U.S. Department of Health and Human Services (NICHD/NIH/DHHS). This study was also, in part, supported with Federal funds from NICHD/NIH/DHHS under Contract No. HHSN275201300006C. Dr. Gomez-Lopez is also supported by the Perinatal Initiative of the Wayne State University School of Medicine.

ACKNOWLEDGMENTS

We would like to thank all the people from Chelsea and Westminster Hospital, West Middlesex University Hospital, and John Hunter Clinic (London, UK), who contributed samples to this study. We would also like to thank Dr Pei Lai, Dr Nishel Shah, Miss Sharmista Guha, and all the clinical staff who helped in the collection of samples.

SUPPLEMENTARY MATERIAL

The Supplementary Material for this article can be found online at: https://www.frontiersin.org/articles/10.3389/fimmu.2022.880438/full#supplementary-material

REFERENCES

1. Abadía-Molina AC, Ruiz C, Montes MJ, King A, Loke YW, Olivares EG. Immune Phenotype and Cytotoxic Activity of Lymphocytes From Human Term Decidua Against Trophoblast. *J Reprod Immunol* (1996) 31(1-2):109–23. doi: 10.1016/0165-0378(96)00965-5
2. King A, Birkby C, Loke YW. Early Human Decidual Cells Exhibit NK Activity Against the K562 Cell Line But Not Against First Trimester Trophoblast. *Cell Immunol* (1989) 118(2):337–44. doi: 10.1016/0008-8749(89)90382-1
3. Koopman LA, Kopcow HD, Rybalov B, Boyson JE, Orange JS, Schatz F, et al. Human Decidual Natural Killer Cells are a Unique NK Cell Subset With Immunomodulatory Potential. *J Exp Med* (2003) 198(8):1201–12. doi: 10.1084/jem.20030305
4. Kopcow HD, Allan DS, Chen X, Rybalov B, Andzelm MM, Ge B, et al. Human Decidual NK Cells Form Immature Activating Synapses and are Not Cytotoxic. *Proc Natl Acad Sci USA.* (2005) 102(43):15563–8. doi: 10.1073/pnas.0507835102
5. Siewiera J, El Costa H, Tabiasco J, Berrebi A, Cartron G, Le Bouteiller P, et al. Human Cytomegalovirus Infection Elicits New Decidual Natural Killer Cell Effector Functions. *PloS Pathog* (2013) 9(4):e1003257. doi: 10.1371/journal.ppat.1003257
6. Hanna J, Goldman-Wohl D, Hamani Y, Avraham I, Greenfield C, Natanson-Yaron S, et al. Decidual NK Cells Regulate Key Developmental Processes at the Human Fetal-Maternal Interface. *Nat Med* (2006) 12(9):1065–74. doi: 10.1038/nm1452
7. Williams PJ, Searle RF, Robson SC, Innes BA, Bulmer JN. Decidual Leucocyte Populations in Early to Late Gestation Normal Human Pregnancy. *J Reprod Immunol* (2009) 82(1):24–31. doi: 10.1016/j.jri.2009.08.001
8. King A, Hiby SE, Verma S, Burrows T, Gardner L, Loke YW. Uterine NK Cells and Trophoblast HLA Class I Molecules. *Am J Reprod Immunol* (1997) 37(6):459–62. doi: 10.1111/j.1600-0897.1997.tb00260.x
9. de Mendonça Vieira R, Meagher A, Crespo >Â, Kshirsagar SK, Iyer V, Norwitz ER, et al. Human Term Pregnancy Decidual NK Cells Generate Distinct Cytotoxic Responses. *J Immunol* (2020) 204(12):3149–59. doi: 10.4049/jimmunol.1901435
10. King A, Boocock C, Sharkey AM, Gardner L, Beretta A, Siccardi AG, et al. Evidence for the Expression of HLAA-C Class I mRNA and Protein by Human First Trimester Trophoblast. *J Immunol* (1996) 156(6):2068–76. Available at: https://www.jimmunol.org/content/156/6/2068.long
11. King A, Allan DS, Bowen M, Powis SJ, Joseph S, Verma S, et al. HLA-E is Expressed on Trophoblast and Interacts With CD94/NKG2 Receptors on Decidual NK Cells. *Eur J Immunol* (2000) 30(6):1623–31. doi: 10.1002/1521-4141(200006)30:6<1623::AID-IMMU1623>3.0.CO;2-M
12. Kovats S, Main EK, Librach C, Stubblebine M, Fisher SJ, DeMars R. A Class I Antigen, HLA-G, Expressed in Human Trophoblasts. *Science.* (1990) 248(4952):220–3. doi: 10.1126/science.2326636
13. Hiby SE, Regan L, Lo W, Farrell L, Carrington M, Moffett A. Association of Maternal Killer-Cell Immunoglobulin-Like Receptors and Parental HLA-C Genotypes With Recurrent Miscarriage. *Hum Reprod* (2008) 23(4):972–6. doi: 10.1093/humrep/den011
14. Johnsen GM, Størvold GL, Drabbels JJM, Haasnoot GW, Eikmans M, Spruyt-Gerritse MJ, et al. The Combination of Maternal KIR-B and Fetal HLA-C2 is Associated With Decidua Basalis Acute Atherosis in Pregnancies With Preeclampsia. *J Reprod Immunol* (2018) 129:23–9. doi: 10.1016/j.jri.2018.07.005
15. Moffett A, Chazara O, Colucci F, Johnson MH. Variation of Maternal KIR and Fetal HLA-C Genes in Reproductive Failure: Too Early for Clinical Intervention. *Reprod BioMed Online* (2016) 33(6):763–9. doi: 10.1016/j.rbmo.2016.08.019
16. Cartwright JE, Fraser R, Leslie K, Wallace AE, James JL. Remodelling at the Maternal-Fetal Interface: Relevance to Human Pregnancy Disorders. *Reproduction.* (2010) 140(6):803–13. doi: 10.1530/REP-10-0294
17. Hiby SE, Walker JJ, O'shaughnessy KM, Redman CW, Carrington M, Trowsdale J, et al. Combinations of Maternal KIR and Fetal HLA-C Genes Influence the Risk of Preeclampsia and Reproductive Success. *J Exp Med* (2004) 200(8):957–65. doi: 10.1084/jem.20041214
18. Hiby SE, Apps R, Sharkey AM, Farrell LE, Gardner L, Mulder A, et al. Maternal Activating KIRs Protect Against Human Reproductive Failure

Mediated by Fetal HLA-C2. *J Clin Invest*. (2010) 120(11):4102–10. doi: 10.1172/JCI43998
19. Kennedy PR, Chazara O, Gardner L, Ivarsson MA, Farrell LE, Xiong S, et al. Activating KIR2DS4 Is Expressed by Uterine NK Cells and Contributes to Successful Pregnancy. *J Immunol* (2016) 197(11):4292–300. doi: 10.4049/jimmunol.1601279
20. Nakimuli A, Chazara O, Hiby SE, Farrell L, Tukwasibwe S, Jayaraman J, et al. A KIR B Centromeric Region Present in Africans But Not Europeans Protects Pregnant Women From Pre-Eclampsia. *Proc Natl Acad Sci USA*. (2015) 112 (3):845–50. doi: 10.1073/pnas.1413453112
21. Larsen TG, Hackmon R, Geraghty DE, Hviid TVF. Fetal Human Leukocyte Antigen-C and Maternal Killer-Cell Immunoglobulin-Like Receptors in Cases of Severe Preeclampsia. *Placenta* (2019) 75:27–33. doi: 10.1016/j.placenta.2018.11.008
22. Male V, Sharkey A, Masters L, Kennedy PR, Farrell LE, Moffett A. The Effect of Pregnancy on the Uterine NK Cell KIR Repertoire. *Eur J Immunol* (2011) 41(10):3017–27. doi: 10.1002/eji.201141445
23. Xiong S, Sharkey AM, Kennedy PR, Gardner L, Farrell LE, Chazara O, et al. Maternal Uterine NK Cell-Activating Receptor KIR2DS1 Enhances Placentation. *J Clin Invest* (2013) 123(10):4264–72. doi: 10.1172/JCI68991
24. Lash GE, Otun HA, Innes BA, Kirkley M, De Oliveira L, Searle RF, et al. Interferon-Gamma Inhibits Extravillous Trophoblast Cell Invasion by a Mechanism That Involves Both Changes in Apoptosis and Protease Levels. *FASEB J* (2006) 20(14):2512–8. doi: 10.1096/fj.06-6616com
25. Otun HA, Lash GE, Innes BA, Bulmer JN, Naruse K, Hannon T, et al. Effect of Tumour Necrosis Factor-α in Combination With Interferon-γ on First Trimester Extravillous Trophoblast Invasion. *J Reprod Immunol* (2011) 88 (1):1–11. doi: 10.1016/j.jri.2010.10.003
26. Robson A, Harris LK, Innes BA, Lash GE, Aljunaidy MM, Aplin JD, et al. Uterine Natural Killer Cells Initiate Spiral Artery Remodeling in Human Pregnancy. *FASEB J* (2012) 26(12):4876–85. doi: 10.1096/fj.12-210310
27. Vento-Tormo R, Efremova M, Botting RA, Turco MY, Vento-Tormo M, Meyer KB, et al. Single-Cell Reconstruction of the Early Maternal-Fetal Interface in Humans. *Nature* (2018) 563(7731):347–53. doi: 10.1038/s41586-018-0698-6
28. Garcia-Alonso L, Handfield L-F, Roberts K, Nikolakopoulou K, Fernando RC, Gardner L, et al. Mapping the Temporal and Spatial Dynamics of the Human Endometrium *In Vivo* and *In Vitro*. *Nat Genet* (2021), 53(12):1698-711. doi: 10.1038/s41588-021-00972-2
29. Huhn O, Ivarsson MA, Gardner L, Hollinshead M, Stinchcombe JC, Chen P, et al. Distinctive Phenotypes and Functions of Innate Lymphoid Cells in Human Decidua During Early Pregnancy. *Nat Commun* (2020) 11(1):381. doi: 10.1038/s41467-019-14123-z
30. Stricker R, Eberhart R, Chevailler MC, Quinn FA, Bischof P. Establishment of Detailed Reference Values for Luteinizing Hormone, Follicle Stimulating Hormone, Estradiol, and Progesterone During Different Phases of the Menstrual Cycle on the Abbott ARCHITECT Analyzer. *Clin Chem Lab Med* (2006) 44(7):883–7. doi: 10.1515/CCLM.2006.160
31. Team RC. *R: A Language and Environment for Statistical Computing*. Vienna, Austria: R Foundation for Statistical Computing. (2020).
32. Hao Y, Hao S, Andersen-Nissen E, Mauck WM, Zheng S, Butler A, et al. Integrated Analysis of Multimodal Single-Cell Data. *Cell* (2021) 184 (13):3573–87.e29. doi: 10.1016/j.cell.2021.04.048
33. Hadley W, Romain F, Lionel H, Kirill M. *Dplyr: A Grammar of Data Manipulation*. (2021). Available at: https://github.com/tidyverse/dplyr
34. Wickham H. *Ggplot2: Elegant Graphics for Data Analysis*. Verlag New York: Springer (2016).
35. Wickham H. *Tidyr: Tidy Messy Data*. (2021). Available at: https://github.com/tidyverse/tidyr
36. Chan C-h, Chan GC, Leeper TJ, Becker J. *Rio: A Swiss-Army Knife for Data File I/O*. (2021). Available at: https://github.com/leeper/rio
37. Fischer B, Smith M, Pau G. *Rhdf5: R Interface to HDF5*. (2020). Available at: https://github.com/grimbough/rhdf5.
38. Pedersen TL. *Patchwork: The Composer of Plots*. (2020).
39. Schauberger P, Walker A. *Openxlsx: Read, Write and Edit Xlsx Files*. (2020). Available at: https://github.com/ycphs/openxlsx
40. Ushey K, Allaire J, Tang Y. *Reticulate: Interface to 'Python'*. (2021). Available at: https://github.com/rstudio/reticulate
41. Stuart T, Butler A, Hoffman P, Hafemeister C, Papalexi E, Mauck WM, et al. Comprehensive Integration of Single-Cell Data. *Cell* (2019) 177(7):1888–902.e21. doi: 10.1016/j.cell.2019.05.031
42. Pique-Regi R, Romero R, Tarca AL, Sendler ED, Xu Y, Garcia-Flores V, et al. Single Cell Transcriptional Signatures of the Human Placenta in Term and Preterm Parturition. *Elife* (2019) 8:e52004. doi: 10.7554/eLife.52004
43. Parham P. NK Cells and Trophoblasts: Partners in Pregnancy. *J Exp Med* (2004) 200(8):951–5. doi: 10.1084/jem.20041783
44. Hamilton S, Oomomian Y, Stephen G, Shynlova O, Tower CL, Garrod A, et al. Macrophages Infiltrate the Human and Rat Decidua During Term and Preterm Labor: Evidence That Decidual Inflammation Precedes Labor. *Biol Reprod* (2012) 86(2):39. doi: 10.1095/biolreprod.111.095505
45. Rinaldi SF, Makieva S, Saunders PT, Rossi AG, Norman JE. Immune Cell and Transcriptomic Analysis of the Human Decidua in Term and Preterm Parturition. *Mol Hum Reprod* (2017) 23(10):708–24. doi: 10.1093/molehr/gax038
46. Pace D, Morrison L, Bulmer JN. Proliferative Activity in Endometrial Stromal Granulocytes Throughout Menstrual Cycle and Early Pregnancy. *J Clin Pathol* (1989) 42(1):35–9. doi: 10.1136/jcp.42.1.35
47. Strunz B, Bister J, Jönsson H, Filipovic I, Crona-Guterstam Y, Kvedaraite E, et al. Continuous Human Uterine NK Cell Differentiation in Response to Endometrial Regeneration and Pregnancy. *Sci Immunol* (2021) 6(56): eabb7800. doi: 10.1126/sciimmunol.abb7800
48. King A, Wellings V, Gardner L, Loke YW. Immunocytochemical Characterization of the Unusual Large Granular Lymphocytes in Human Endometrium Throughout the Menstrual Cycle. *Hum Immunol* (1989) 24 (3):195–205. doi: 10.1016/0198-8859(89)90060-8
49. Manaster I, Mizrahi S, Goldman-Wohl D, Sela HY, Stern-Ginossar N, Lankry D, et al. Endometrial NK Cells are Special Immature Cells That Await Pregnancy. *J Immunol* (2008) 181(3):1869–76. doi: 10.4049/jimmunol.181.3.1869
50. Klentzeris LD, Bulmer JN, Warren A, Morrison L, Li TC, Cooke ID. Endometrial Lymphoid Tissue in the Timed Endometrial Biopsy: Morphometric and Immunohistochemical Aspects. *Am J Obstet Gynecol* (1992) 167(3):667–74. doi: 10.1016/S0002-9378(11)91568-3
51. Bulmer JN, Morrison L, Longfellow M, Ritson A, Pace D. Granulated Lymphocytes in Human Endometrium: Histochemical and Immunohistochemical Studies. *Hum Reprod* (1991) 6(6):791–8. doi: 10.1093/oxfordjournals.humrep.a137430
52. Flynn L, Byrne B, Carton J, Kelehan P, O'Herlihy C, O'Farrelly C. Menstrual Cycle Dependent Fluctuations in NK and T-Lymphocyte Subsets From Non-Pregnant Human Endometrium. *Am J Reprod Immunol* (2000) 43(4):209–17. doi: 10.1111/j.8755-8920.2000.430405.x
53. Ho HN, Chao KH, Chen CK, Yang YS, Huang SC. Activation Status of T and NK Cells in the Endometrium Throughout Menstrual Cycle and Normal and Abnormal Early Pregnancy. *Hum Immunol* (1996) 49(2):130–6. doi: 10.1016/0198-8859(96)00120-6
54. Ivarsson MA, Stiglund N, Marquardt N, Westgren M, Gidlöf S, Björkström NK. Composition and Dynamics of the Uterine NK Cell KIR Repertoire in Menstrual Blood. *Mucosal Immunol* (2017) 10(2):322–31. doi: 10.1038/mi.2016.50
55. Djurisic S, Skibsted L, Hviid TV. A Phenotypic Analysis of Regulatory T Cells and Uterine NK Cells From First Trimester Pregnancies and Associations With HLA-G. *Am J Reprod Immunol* (2015) 74(5):427–44. doi: 10.1111/aji.12421
56. Persson G, Jørgensen N, Nilsson LL, Andersen LHJ, Hviid TVF. A Role for Both HLA-F and HLA-G in Reproduction and During Pregnancy? *Hum Immunol* (2020) 81(4):127–33. doi: 10.1016/j.humimm.2019.09.006
57. Kopcow HD, Eriksson M, Mselle TF, Damrauer SM, Wira CR, Sentman CL, et al. Human Decidual NK Cells From Gravid Uteri and NK Cells From Cycling Endometrium are Distinct NK Cell Subsets. *Placenta* (2010) 31 (4):334–8. doi: 10.1016/j.placenta.2010.01.003
58. Lash GE, Naruse K, Innes BA, Robson SC, Searle RF, Bulmer JN. Secretion of Angiogenic Growth Factors by Villous Cytotrophoblast and Extravillous Trophoblast in Early Human Pregnancy. *Placenta* (2010) 31(6):545–8. doi: 10.1016/j.placenta.2010.02.020
59. Wang F, Jia W, Fan M, Shao X, Li Z, Liu Y, et al. Single-Cell Immune Landscape of Human Recurrent Miscarriage. *Genomics Proteomics Bioinf* (2021). doi: 10.1101/2020.09.16.300939
60. Tuckerman E, Mariee N, Prakash A, Li TC, Laird S. Uterine Natural Killer Cells in Peri-Implantation Endometrium From Women With Repeated

Implantation Failure After IVF. *J Reprod Immunol* (2010) 87(1-2):60–6. doi: 10.1016/j.jri.2010.07.001
61. Fraser R, Whitley GS, Thilaganathan B, Cartwright JE. Decidual Natural Killer Cells Regulate Vessel Stability: Implications for Impaired Spiral Artery Remodelling. *J Reprod Immunol* (2015) 110:54–60. doi: 10.1016/j.jri.2015.04.003
62. Sindram-Trujillo A, Scherjon S, Kanhai H, Roelen D, Claas F. Increased T-Cell Activation in Decidua Parietalis Compared to Decidua Basalis in Uncomplicated Human Term Pregnancy. *Am J Reprod Immunol* (2003) 49 (5):261–8. doi: 10.1034/j.1600-0897.2003.00041.x

Conflict of Interest: The authors declare that the research was conducted in the absence of any commercial or financial relationships that could be construed as a potential conflict of interest.

frontiers | Frontiers in Immunology

MINI REVIEW
published: 23 June 2022
doi: 10.3389/fimmu.2022.903688

Helper-Like Type-1 Innate Lymphoid Cells in Inflammatory Bowel Disease

Diana Coman[1†], *Isabelle Coales*[1†], *Luke B. Roberts*[2] *and Joana F. Neves*[1*]

[1] Centre for Host Microbiome Interactions, King's College London, London, United Kingdom, [2] School of Immunology and Microbial Sciences, King's College London, London, United Kingdom

Inflammatory bowel disease (IBD) is an idiopathic condition characterized by chronic relapsing inflammation in the intestine. While the precise etiology of IBD remains unknown, genetics, the gut microbiome, environmental factors, and the immune system have all been shown to contribute to the disease pathophysiology. In recent years, attention has shifted towards the role that innate lymphoid cells (ILCs) may play in the dysregulation of intestinal immunity observed in IBD. ILCs are a group of heterogenous immune cells which can be found at mucosal barriers. They act as critical mediators of the regulation of intestinal homeostasis and the orchestration of its inflammatory response. Despite helper-like type 1 ILCs (ILC1s) constituting a particularly rare ILC population in the intestine, recent work has suggested that an accumulation of intestinal ILC1s in individuals with IBD may act to exacerbate its pathology. In this review, we summarize existing knowledge on helper-like ILC1 plasticity and their classification in murine and human settings. Moreover, we discuss what is currently understood about the roles that ILC1s may play in the progression of IBD pathogenesis.

Keywords: innate lymphocyte cells, intestine, inflammatory bowel disease, inflammation, natural killer cell, type 1 innate lymphoid cells

OPEN ACCESS

Edited by:
Carolina Jancic, Consejo Nacional de Investigaciones Científicas y Técnicas (CONICET), Argentina

Reviewed by:
Sabrina B. Bennstein, Heinrich Heine University of Düsseldorf, Germany
Iona Schuster, Monash University, Australia

***Correspondence:**
Joana F. Neves
joana.pereira_das_neves@kcl.ac.uk

[†]*These authors have contributed equally to this work*

Specialty section:
This article was submitted to NK and Innate Lymphoid Cell Biology, a section of the journal Frontiers in Immunology

Received: *24 March 2022*
Accepted: *17 May 2022*
Published: *23 June 2022*

Citation:
Coman D, Coales I, Roberts LB and Neves JF (2022) Helper-Like Type-1 Innate Lymphoid Cells in Inflammatory Bowel Disease. Front. Immunol. 13:903688. doi: 10.3389/fimmu.2022.903688

INTRODUCTION

Inflammatory bowel disease (IBD) primarily describes two idiopathic conditions characterized by chronic relapsing inflammation in the intestine: ulcerative colitis (UC) and Crohn's disease (CD). Despite many similarities between the two, UC and CD are differentiated based upon their histopathological features, the primary affected anatomical location, and their associated symptoms. Within the gastrointestinal tract, UC is exclusively colorectal, with mucosal inflammation found continuously extending from the rectum throughout the length of the colon (1). In contrast, individuals with CD exhibit discontinuous pockets of transmural inflammation which can be found scattered along the length of the gastrointestinal tract (2). In comparison to the relatively superficial legions of UC, CD is destructive, with around half of all patients exhibiting complications such as strictures or fistulae, within 10 years of being diagnosed (2). Yet while the precise etiology of IBD remains unknown, its progression has been shown to be influenced by complex interactions between genetic predispositions (3), perturbations to the gut microbiome and its associated metabolites (4–8), and the dysregulation of innate and adaptive immune responses (2, 9). Recently, attention has shifted towards the role that innate lymphoid cells (ILCs) may play in the pathophysiology of IBD. ILCs are a highly heterogenous family of lymphocytes which are considered the innate counterpart of adaptive T cells. Broadly, they have been split into 5

subtypes based on their development, transcription factor expression, and effector functions; these comprise natural killer (NK) cells, lymphoid tissue inducer, and the helper-like type 1, 2 and 3 ILCs (ILC1, ILC2, and ILC3, respectively) (10).

As extensively reviewed elsewhere, the abundance and phenotype of ILCs were shown to vary substantially across tissues (11). However, in contrast to other mucosal sites, such as the salivary gland and liver, ILC1s constitute an extremely rare ILC population in the intestine. Despite this, recent work suggests that they may play a critical role in the pathology of IBD (12–16). However, due to their substantial phenotypic overlap with NK cells, the identification and characterization of intestinal ILC1 remains under debate. Here we will discuss the complexities surrounding the differentiation of ILC1s from NK cells, with a focus on those found in the intestine, and highlight the potential roles of ILC1s in the exacerbation of IBD pathogenesis and its associated complications.

MURINE INTESTINAL ILC1

In mice, both ILC1s and NK cells can be identified by their shared co-expression of the activating receptors NK1.1 and NKp46 in the absence of other cell lineage (Lin^-)-defining markers, including CD3, CD14, CD19, and T cell receptor proteins (17) (**Table 1**). Additionally, they share the expression of T-bet, a canonical master transcriptional regulator of type 1 immunity which includes the production of IFN-γ in lymphocytes (19). Within the murine intestine, four distinct populations of Lin^- $NK1.1^+$ $NKp46^+$ cells have been described, which were differentiated based on their anatomical location, transcription factor expression, cell surface marker profile, and effector functions (10). These are comprised of conventional NK (cNK) cells, lamina propria (LP) ILC1s, intra-epithelial ILC1s (ieILC1), and a population of ILC1-like ex-ILC3s.

TABLE 1 | NK cell and ILC1 Markers.

Mouse				Human				
	LP ILC1	**ieILC1**	**cNK cells**		**LP ILC1**	**ieILC1**	**cytotoxic ILC1 / trNK cells**	**cNK cells**
NK1.1	+	+	+	**CD161**	+	lo	+/lo	–
NKp46	+	+	+	**NKp46**	+/-	+	+/lo	+
T-bet	+	+	+	**T-bet**	+/-	+/-	+	+
Eomes	–	+	+ ↓	**Eomes**	–	+	+/-	+
CD127	+	–	–	**CD127**	+	–	+/-	–
CD49a	+/-	+	- ↑	**CD49a**	–	+	+	–
c-Kit (CD117)	+	+	–	**c-Kit (CD117)**	–	–	+/-	–
CD49b (DX5)	–	–	+ ↓	**NKp44**	–	+	+/-	–
CD90 (Thy1)	+	lo	- ↑	**CD94**	+/-	lo	+/-	+
KLRG1	-/lo	–	+	**KLRG1**	+	nd	+	+
CD103	–	+	–	**CD103**	–	+	+/-	–
CXCR6	+	+	-/lo	**CXCR6**	nd	+	lo/-	–
Ly49D/H	-/lo	–	+/-	**KIR**	–	+	+/-	+
Ly6C	-/lo	-	+	**NKG2A**	–	+	lo	lo
CD160	lo	+	- ↑	**CD160**	–	+/-	–	- ↑
CD200r1	+/-	+/-	–	**CD200r1**	+	lo	+*	–
Tcf-7	–	–	-/lo	**CD56**	–	+	+	+
CD11b	-	-	+	**CD11b**	–	+/lo	lo	+
HOBIT	+	+	–	**HOBIT**	+	+	–	–
TRAIL	nd	nd	- ↑	**IKZF3 (Aiolos)**	+	+	+	+
CD122	lo	nd	+	**CD122**	lo	+	+	+
CD61	+	nd	- ↑	**CD16**	nd	–	+/-	- ↑
CD69	+	+	- ↑	**CD69**	+/-	+	+	-/lo
Granzyme	–	+	+	**Granzyme**	–	+	+	+
Perforin	–	+	+	**Perforin**	–	+	+	+

*Markers which may be used to identify and discriminate between NK cells and ILC1sin mice with a C57BL/6 background, and human tissues. Mouse LP ILC1 and ieILC1 markers shown here are those which have been determined in the intestine and these markers may vary between tissues. For both mouse and human cNK cells and iNK cells, these are primarily circulating cells and so these markers were predominantly identified from cells isolated from the blood. Human cytotoxic ILC1s/trNK cells are exclusive to those identified in the intestine; however, due to the limited information on human intestinal LP ILC1s and ieILC1 populations, these markers additionally include those found in human tonsils, where the majority of research into human ILC1s has been performed, and which have been shown to exhibit substantial overlap with those found in the intestine (12–14). Abbreviations: Lamina propria (LP), intra-epithelial ILC1s (ieILC1), tissue-resident (tr)- , conventional (c)-, and immature (i)-NK cells. Annotations: (+) positive expression; (-) not expressed; (+/-) heterogenous expression; (lo) expressed, but to a low level; (nd) not determined in the specific tissue/s examined; ↑ can be regulated following activation; ↓ can be downregulated following activation; * only observed in the $CD127^+$ ILC1-like population (18).*

Predominantly found circulating in the blood or residing in the bone marrow and lymphoid organs, cNK cells are critical for the recognition and elimination of virus-infected and transformed cells, mediated *via* their secretion of cytotoxic effector molecules, such as perforin and granzyme B, and of proinflammatory cytokines, principally that of IFN-γ (10). In contrast, ILC1s are primarily a tissue-resident population of cells (20, 21). Within the LP, ILC1s harbor little to no cytotoxic capacity but exhibit significantly greater IFN-γ secretion than cNK cells, coupled to the production of TNFα upon their activation (12, 22, 23). Moreover, they lack the characteristic expression of Eomes found in cNK cells, instead expressing the IL-7 receptor subunit CD127, a marker of all helper-like ILC lineages (12, 22, 24–26). In the intestine, homeostatic cNK cells and LP ILC1s have further been shown to exhibit a dichotomous expression of cell surface markers including CD49a, CD49b, CXCR6, and CD200r1 and the inhibitory Ly49 family of receptors (21, 27, 28). Consequentially, under steady-state conditions, murine ILC1s and cNK cells form distinct clusters following global analyses of both their chromatin and transcriptional landscapes (21, 27, 29). However, none of those cited above acts alone as a population-defining marker. The advent of single-cell RNA sequencing technologies has highlighted the complex tissue-specific expression patterns of ILC1s and revealed that, even within tissues, ILC1 populations exhibit substantial transcriptional, functional, and developmental heterogeneity (11, 21, 27, 28, 30). Consequentially, many markers previously proposed to define ILC1s, including CD49a, TRAIL, Ly6C, CD103, CD200r1, and CD127 (10, 11), have been found inconsistently expressed within ILC1 populations and/or have been found expressed in immature NK cells and their progenitors (17, 21). This is exemplified by Eomes. While only cNK cells depend on the expression of Eomes for their maturation (31), a lack of Eomes is insufficient as a marker for ILC1s, as it is not expressed on immature NK cells (26). To complicate matters further, activated cNK cells have been shown to downregulate Eomes expression and upregulate ILC1 markers (32–34), resulting in increasingly blurred boundaries between the cell types under inflammatory conditions—for example, NK cells have recently been shown to be able to transition towards an ILC1-like phenotype ($Eomes^-$ $CD49a^+$ $Ly6C^+$) as a consequence of IL-12 s following infection with *Toxoplasma gondii* (32), or in response to TGF-β signaling in the tumor microenvironment (35), in a manner which may be mediated *via* STAT4 signaling (36). Consequentially, no universal cell surface marker that is able to conclusively distinguish ILC1s from NK cells has been identified.

As with the ability of cNK cells to differentiate to ILC1s, there is substantial and convincing evidence demonstrating a high level of plasticity between the helper-like ILCs in mice (37), particularly among ILC3s and ILC1s (23, 27, 28, 38, 44). In homeostasis, ILC3s form the major ILC population in the intestine, characterized *via* a high expression of the transcription factor RORγt and secretion of the cytokine IL-22 (10). However, in response to an infection or IL-12 signaling, ILC3s can downregulate RORγt while upregulating the expression of T-bet (38–42, 44), of which ILC1s are completely dependent upon for their differentiation (10) and post-developmental maintenance (43). Consequentially, the IL-22-expressing population of intestinal ILC3s is depleted, replaced by an expansion of IFN-γ-producing cells exhibiting a phenotype indistinguishable from ILC1s. Notably, using RORγt fate mapping analysis, an accumulation of these ILC1-like ex-ILC3s (Lin^- $Eomes^-$ $NK1.1^-$ $IFN\gamma^+$ $T\text{-}bet^+$) was shown to be the principal driver of *Campylobacter jejuni*-induced intestinal pathology (44).

Finally, the remaining Lin^- $NK1.1^+$ $NKp46^+$ population described in mice are $CD103^+$ ILC1s, resembling the well-characterized ieILC1s in the human intestine (27).

INTESTINAL ILC1 IN HUMANS

Two distinct types of ILC1s have been described in the human intestine (**Table 1**). Intestinal LP Lin^- $c\text{-}Kit^-$ $NKp44^-$ $NKp46^+$ $CD127^+$ $CD161^+$ ILC1s exhibit T-bet expression and produce IFNγ in response to inflammation, resemblant of cNK cells (12). However, human LP ILC1s are $Eomes^-$ and do not express perforin or granzyme B or other markers typically seen in cNK cells in humans with cNK cells, including the expression of KIR3DL1, CD56, and/or IL1R1 (12, 13). These intestinal LP ILC1s are resemblant of ILC1s identified within other human mucosal tissues, such as the tonsils (45) where the majority of research into human ILCs have been performed. The second ILC1 subtype is a cytotoxic population found within the intra-epithelial lymphocyte compartment, characterized by their high expression of CD103 relative to other local ILC populations (13, 14). Contrasting those found in the LP, human $CD103^+$ ILC1s are $NKp46^+$ $CD56^+$ $Eomes^+$ $CD127^-$ $CD161^{low}$, thus exhibiting a transcriptional and effector function signature reflecting that of both cNK cells and LP ILC1s (13, 14, 46).

Importantly, while the presence of $NK1.1^+$ $NKp46^+$ $CD127^+$ ILC1s within the intestinal LP is consistently observed in mice, a question remains as to the existence of their $NKp46^+$ $CD127^+$ $CD161^+$ LP ILC1 counterparts within the non-inflamed human intestine (30, 47, 48). Critically, the level of T-bet expression is heterogeneous in both ILC1 and NK cell populations in human tissues (46, 49), and a lack of T-bet in a putative ILC1 population (Lin^- $c\text{-}Kit^-$ $NKp44^-$ $CD45^+$ $CD127^+$) has led some to question the very existence of ILC1s themselves (47). In contrast, the presence of cytotoxic populations of ILC1s, comparable to ieILC1s ($CD103^{+/-}$ $T\text{-}bet^+$ $Eomes^+$ $CD56^+$ $NKp46^+$ $CD49a^+$ $CD127^-$), is more consistently observed in various human tissues (13, 14, 47, 50, 51). However, these constitute highly heterogenous populations of cells which have been proposed to resemble cNK cells more closely than other helper-like ILC lineages (46, 47, 49). Accordingly, they are often instead classed as tissue-resident NK (trNK) cells.

While the subpopulations of LP ILC1, ieILC1, cytotoxic/trNK cells, and cNK cells exhibit highly overlapping phenotypes, a direct transition between these populations in the intestine has yet to be demonstrated. However, as described in mice, ILC3 to ILC1 phenotypic plasticity may also be present in human intestinal tissues (13, 15, 47, 52, 53)—for example, $CD14^+$ dendritic cells from CD resection specimens have been found to promote the

differentiation of ILC3s into ILC1s *in vitro* (13). Moreover, human tonsillar ILC3s have shown that they are able to convert to ILC1-like ex-ILC3s in a manner which may be driven, in part, by TGF-β and IL-23 acting coordinately to regulate the expression of the transcription factors Aiolos, T-bet, and RORγt (15, 53). These transitionary cells were also identified in the ileum of both individuals with CD and non-disease controls (15), suggesting that it is not a tissue-specific phenomenon. In the absence of fate mapping within human tissues, this plasticity acts to further complicate the identification of *bona fide* human ILC1s.

The consequence of their overlapping transcriptional phenotypes and the plasticity between populations result in a lack of consistently used nomenclature to define and differentiate between ILC1 and NK cells, particularly within human intestinal tissues. Until markers which conclusively discriminate between the two are identified, this remains a major challenge to the field.

ILC1 IN INTESTINAL INFLAMMATION

LP ILC1s act in the first line of defense to external pathogens, rapidly inducing cytokine secretion upon their activation and promoting the recruitment of other immune cells to the site of inflammation (10) (**Figure 1**). Most studies addressing the potential roles of LP ILC1s in murine intestinal inflammation are primarily focused on their secretion of pro-inflammatory cytokines, namely, IFN-γ and TNFα (14, 18, 33, 38, 39, 44, 54). While these have been shown to aid the clearance of infections, such as mouse cytomegalovirus (33), *Toxoplasma gondii* (23), and *Clostridium difficile* (54), the excess production of IFN-γ and TNFα is highly disruptive to intestinal homeostasis, inhibiting proliferation and inducing apoptosis of local epithelial cells (55, 56). Consequentially, signaling *via* these pro-inflammatory cytokines has been shown to exacerbate IBD-associated

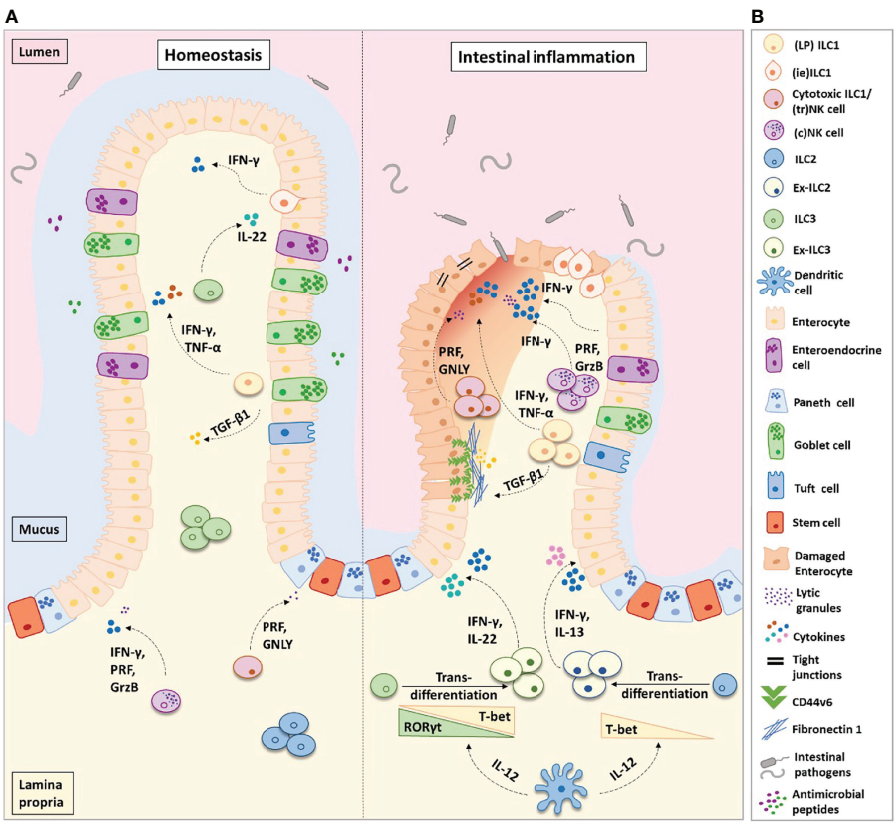

FIGURE 1 | Helper-like type 1 ILCs (ILC1s) in homeostasis and intestinal inflammation. **(A)** ILC1s comprise of lamina propria (LP) ILC1s, intra-epithelial (ie) ILC1s, and cytotoxic ILC1s/tissue-resident (tr) natural killer cells. In the healthy intestinal microenvironment, ILC1s are the least frequent ILC population. In inflammatory bowel disease (IBD), the frequency of ILC1s is increased at the expense of ILC3s and ILC2s. ILC3s and ILC2s transdifferentiate into ILC1s aided by the secretion of IL-12 from dendritic cells. Ex-ILC3s can secrete both IFN-γ and IL-22 upon stimulation, while ex-ILC2s can produce both IFN-γ and IL-13. The increase in ILC1 frequency leads to an increase in pro-inflammatory cytokine secretion and augmented levels of ILC1-derived TGF-β1. TGF-β1 has been shown to increase CD44v6^{+} expression in epithelial and mesenchymal cells. In homeostasis, this may aid wound healing; however, in IBD this is associated with enhanced fibronectin-1 deposition and extracellular matrix degradation, consequently promoting tissue scarring. Abundant levels of IFN-γ disrupt the epithelial tight junctions, leading to increased epithelial permeability. This allows commensal, pathogenic, and opportunistic bacterial species (such as *Bacteroides fragilis*, *Escherichia coli*, *Mycobacterium avium* subsp. *paratuberculosis*, and *C. difficile*) to penetrate the lamina propria, thus perpetuating the inflammation. **(B)** Figure key illustrating the different cell types and molecules participating in intestinal inflammation. IFN-γ, interferon-gamma; IL-22, interleukin-22; IL-17, interleukin-17; IL-13, interleukin-13; IL-12, interleukin-12; TGF-β1, transforming growth factor-beta 1; TNF-α, tumor necrosis factor-alpha; PRF, perforin; GrzB, granzyme-B; GNLY, granulysin.

pathology in response to infection with *Helicobacter typhlonius* and in mouse models of dextran sulfate sodium (DSS)-induced colitis (12, 25, 43, 55, 57–59)—for example, in response to DSS treatment, IFN-γ disrupts the vascular barrier integrity by altering the adherens junction protein VE-cadherin. As a result, this drives an increase in vascular permeability and an accumulation of immune cells at the site of inflammation, enabling the migration of intestinal bacteria into the blood and other organs (55). Concordantly, the depletion of LP ILC1s and/or their associated cytokines have been shown to significantly attenuate the symptoms of colitis *in vivo* (43, 57, 59).

As observed in mice, VE-cadherin-mediated disruption of the intestinal vascular barrier by IFN-γ has additionally been described in human IBD patients, suggesting a direct causative role of IFN-γ in the pathogenicity of the disease (55). Moreover, an accumulation of ILC1s in the inflamed intestine has repeatedly been identified in patients with IBD (12–14, 18, 52, 60). This was first observed by Bernink *et al.*, who demonstrated an accumulation of *IFNG*-expressing c-Kit$^-$ NKp44$^-$ CD127$^+$ ILC1s in the intestinal LP of Crohn's disease patients and following DSS-induced colitis in mice with a humanized immune system (12). Subsequently, these results have been confirmed in larger patient groups (15, 60) and have been shown not to be restricted to LP ILC1s but to include an increase in the proportions of cytotoxic ieILC1s/trNK cells and ILC1-like cells (CD127$^+$ CD94$^+$) in individuals with CD (14, 18). However, it is not currently clear whether an increase in the frequencies of ILC1s is a universal feature of IBD. Recent investigations into ILC1s in the mucosal tissue of patients newly diagnosed with CD and UC found that while LP ILC1 proportions increased at the sites of active inflammation in CD, ILC2s instead accumulated in patients with UC (48). This finding supports the controversial Th1/Th2 paradigm, in which CD is a Th1-mediated disease and UC a Th2-mediated disease (61). In contrast, using cytometry by time-of-flight analysis, the presence of NK cells and ILC1s (Lin$^-$ CD161$^+$ T-bet$^+$ CD56^{lo-}) has been demonstrated in the mucosa of UC patients, albeit to a lesser extent than was present in individuals with CD (62).

In patients with active IBD, perturbations in the ILC compartment may not be restricted to the intestine, with a small increase in the frequency of c-Kit$^-$ NKp44$^-$ CD127$^+$ CD161$^+$ ILC1s identified in their peripheral blood (63). However, this finding is not universal with earlier reports demonstrating no alterations in circulating ILC subtypes between IBD patients and/or healthy controls (48, 62). Recently, in the absence of changes in the total frequencies of helper-like ILCs, an expansion of those exhibiting putative markers of activation was observed, including HLR-DR$^+$ ILC1s and both HLR-DR$^+$ and FMALF1$^+$ ILC2s (64). This suggested that existing peripheral ILC populations may be switching from a homeostatic to an activated phenotype. While a question remains as to what extent this may impact IBD pathogenesis (65), it is notable that such a switch was additionally observed in the population of ILC precursors (ILCp); an increase in NKp44$^+$ and CD56$^+$ ILCp was detected in CD patients, coupled to a decrease in their corresponding naïve CD45RA$^+$ ILCp (64). However, while circulating human ILCp has been shown to contribute to the pool of ILCs in tissues (66), the extent to which perturbations in peripheral ILCp in IBD patents may impact the ILC compartment within the intestinal mucosae remains to be determined—for example, recent research has shown that CD45RA$^+$ ILCp exhibits tissue-specific differentiation potential (67). Moreover, the authors demonstrated an accumulation of a CD62L$^-$ subpopulation of CD45RA$^+$ ILCp in the inflamed mucosa of patients with both UC and CD. The expansion of CD26L$^-$ ILCp was found to be inversely proportional to the frequency of NKp44$^+$ ILC3s, suggesting that disruptions to ILCp compartments may act to promote the disequilibrium of ILCs observed in IBD (67).

A ROLE FOR ILC1-DERIVED TGF-β IN IBD PATHOGENESIS?

The lack of long-term treatment options for IBD brings into question the principal role of pro-inflammatory cytokines as key drivers of the disease pathology—for example, the current gold-standard treatment is the use of TNF-α blockers (*e.g.*, infliximab, adalimumab, certolizumab pegol, and golimumab), yet while this has dramatically improved the IBD outcomes for both CD and UC patients (68), only 1 in 3 initially responded to the drug, and in 30–50% of these patients, the efficacy of treatment decreases over time (69). Furthermore, despite IFN-γ signaling being shown to drive colitis in mice, a lack of efficacy was observed in treatments aimed at suppressing signaling by this pro-inflammatory cytokine in humans (70, 71). However, recent work within our laboratory has demonstrated an alternative signaling method by which ILC1s may act to exacerbate IBD-associated pathology. Using both human and murine intestinal organoids co-cultured with ILC1s, it was shown that LP ILC1-derived TGF-β can drive the degradation of the extracellular matrix, enhance fibronectin deposition, and induce the non-specific expansion of intestinal epithelial cells (16). While in homeostasis these pathways may drive epithelial regeneration and wound healing, under conditions of chronic inflammation, they have the potential to be pathological (15)—for example, TGF-β has previously been characterized as an upstream regulator of fibrosis in CD (72, 73). Notably, despite the organoids used here being genetically, epigenetically, and environmentally identical, pathological matrix remodeling was only observed in the hyper-proliferative ILC1s isolated from the inflamed tissue of CD patients (16). This concurred with previous research in 2019 by Cella et al., who observed a significant increase in a population of proliferative ILC1s in the ileum of individuals with CD (15). These data together highlight a novel non-canonical function of ILC1 in the exacerbation of IBD, in which their augmented expansion may be coupled to enhanced TGF-β signaling, consequentially driving the inflamed tissues toward fibrotic scar tissue formation and/or promoting the growth of epithelial tumors during chronic inflammation, two life-threatening sequalae of IBD (74).

Interestingly, Cella et al. additionally identified a transitionary population of ILC3–ILC1 cells in both CD patients and non-disease controls. As with the conversion of NK cells to ILC1s in

the TGF-β-rich tumor microenvironment (35), this transition was demonstrated to be mediated *via* TGF-β signaling in both mice and humans (15, 42). Considering that the accumulation of ILC1s in IBD is coupled to a decrease in the frequency of ILC3s (12, 48, 60), a question remains as to what extent this is reflective of an expansion of the existing ILC1 population or an increased conversion of other ILC subtypes to an "ILC1-like" phenotype or both. Moreover, TGF-β has also been shown to impair NK cell activity (75), and the presence of dysregulated NK cells has been observed in the blood of IBD patients (76). Thus, while these data do not show a direct relationship to intestinal inflammation, they highlight the need for further investigations into the pleiotropic role of TGF-β signaling in the dysregulated immune compartment found within IBD.

CONCLUDING REMARKS AND FUTURE DIRECTIONS OF RESEARCH

ILC1s represent a minor fraction of the innate cell population in the intestinal LP of healthy individuals. When present in small numbers, ILC1-derived TGF-β may contribute to the maintenance of epithelial regeneration (16). However, the expansion of their population at sites of active intestinal inflammation may indicate their potential role as inducer and/or driver of IBD pathogenicity, which is linked to the development of IBD sequelae such as fibrosis and cancer (16). Critically, there are still many key questions that need to be addressed regarding their presence in inflamed tissues. Do ILC1s accumulate in the intestinal lamina propria of CD patients as a cause or consequence of inflammation? Does the pro-inflammatory microenvironment lead to the augmented plasticity of ILC2s and ILC3s, driving their transition towards ILC1s? Or does it promote ILC1 survival and expansion *via* the secretion of the cytokines and growth factors that they depend on? To what extent may perturbed blood ILC compartments impact or reflect on those observed within the intestine? Does the inflamed microenvironment observed in CD imprint a highly proliferative state on ILC1s? Are the effects on ILC1s a result of "trained" immunity as recently reported for murine ILC3 (77)?

The development of new experimental techniques, such as the co-culture of human organoids with ILCs (78, 79) and single-cell multiomics, provides new avenues to address these questions. Such studies will lead to a better understanding of the role of ILC1 in IBD. Importantly, they will contribute to the development of new therapeutic approaches to revert the pathogenic accumulation of ILC1s in inflamed tissues.

AUTHOR CONTRIBUTIONS

JN and DC conceptualized the manuscript's theme. DC, IC, LR, and JN designed and reviewed the manuscript. DC and IC researched and wrote the manuscript. DC designed the figure. IC constructed the table. All authors contributed to the article and approved the submitted version.

ACKNOWLEDGMENTS

DC acknowledges a Ph.D. studentship from the National Institute of Health and Care Research (NIHR) Biomedical Research Centre (BRC) based at Guy's and St Thomas' (GSTT) NHS Foundation Trust and King's College London (KCL), and LR is also supported by NIHR BRC based at GSTT and KCL. The views expressed are those of the authors and not necessarily those of the NHS, the NIHR, or the Department of Health and Social Care. We apologize to authors whose papers we could not include due to space and scope limitations.

REFERENCES

1. Kobayashi T, Siegmund B, le Berre C, Wei SC, Ferrante M, Shen B, et al. Ulcerative Colitis. *Nat Rev Dis Primers* (2020) 6(1):1–20. doi: 10.1038/s41572-020-0205-x
2. Roda G, Chien Ng S, Kotze PG, Argollo M, Panaccione R, Spinelli A, et al. Crohn's Disease. *Nat Rev Dis Primers* (2020) 6(1):1–19. doi: 10.1038/s41572-020-0156-2
3. Graham DB, Xavier RJ. Pathway Paradigms Revealed From the Genetics of Inflammatory Bowel Disease. *Nature* (2020) 578(7796):527–39. doi: 10.1038/s41586-020-2025-2
4. Ungaro F, Massimino L, Furfaro F, Rimoldi V, Peyrin-Biroulet L, D'Alessio S, et al. Metagenomic Analysis of Intestinal Mucosa Revealed a Specific Eukaryotic Gut Virome Signature in Early-Diagnosed Inflammatory Bowel Disease. *Gut Microbes* (2019) 10:149–58. doi: 10.1080/19490976.2018.1511664
5. Lloyd-Price J, Arze C, Ananthakrishnan AN, Schirmer M, Avila-Pacheco J, Poon TW, et al. Multi-Omics of the Gut Microbial Ecosystem in Inflammatory Bowel Diseases. *Nature* (2019) 569(7758):655–62. doi: 10.1038/s41586-019-1237-9
6. Jostins L, Ripke S, Weersma RK, Duerr RH, McGovern DP, Hui KY, et al. Host–microbe Interactions Have Shaped the Genetic Architecture of Inflammatory Bowel Disease. *Nature* (2012) 491(7422):119–24. doi: 10.1038/nature11582
7. Caruso R, Lo BC, Núñez G. Host–microbiota Interactions in Inflammatory Bowel Disease. *Nat Rev Immunol* (2020) 20(7):411–26. doi: 10.1038/s41577-019-0268-7
8. Ma Y, Zhang Y, Xiang J, Xiang S, Zhao Y, Xiao M, et al. Metagenome Analysis of Intestinal Bacteria in Healthy People, Patients With Inflammatory Bowel Disease and Colorectal Cancer. *Front Cell Infect Microbiol* (2021) 11. doi: 10.3389/FCIMB.2021.599734
9. Zhang M, Sun K, Wu Y, Yang Y, Tso P, Wu Z, et al. Interactions Between Intestinal Microbiota and Host Immune Response in Inflammatory Bowel Disease. *Front Immunol* (2017) 8:942. doi: 10.3389/fimmu.2017.00942
10. Vivier E, Artis D, Colonna M, Diefenbach A, di Santo JP, Eberl G, et al. Innate Lymphoid Cells: 10 Years on. *Cell* (2018) 174:1054–66. doi: 10.1016/j.cell.2018.07.017
11. Meininger I, Carrasco A, Rao A, Soini T, Kokkinou E, Mjösberg J, et al. Tissue-Specific Features of Innate Lymphoid Cells. *Trends Immunol* (2020) 41:902–17. doi: 10.1016/j.it.2020.08.009
12. Bernink JH, Peters CP, Munneke M, te Velde AA, Meijer SL, Weijer K, et al. Human Type 1 Innate Lymphoid Cells Accumulate in Inflamed Mucosal Tissues. *Nat Immunol* (2013) 14(3):221–9. doi: 10.1038/ni.2534
13. Bernink JH, Krabbendam L, Germar K, de Jong E, Gronke K, Kofoed-Nielsen M, et al. Interleukin-12 and -23 Control Plasticity of CD127+ Group 1 and Group 3 Innate Lymphoid Cells in the Intestinal Lamina Propria. *Immunity* (2015) 43:146–60. doi: 10.1016/j.immuni.2015.06.019

14. Fuchs A, Vermi W, Lee JS, Lonardi S, Gilfillan S, Newberry RD, et al. Intraepithelial Type 1 Innate Lymphoid Cells are a Unique Subset of Il-12- and Il-15-Responsive Ifn-γ-Producing Cells. *Immunity* (2013) 38:769–81. doi: 10.1016/j.immuni.2013.02.010
15. Cella M, Gamini R, Sécca C, Collins PL, Zhao S, Peng V, et al. Subsets of ILC3–ILC1-Like Cells Generate a Diversity Spectrum of Innate Lymphoid Cells in Human Mucosal Tissues. *Nat Immunol* (2019) 20(8):980–91. doi: 10.1038/s41590-019-0425-y
16. Jowett GM, Norman MDA, Yu TTL, Rosell Arévalo P, Hoogland D, Lust ST , et al. ILC1 Drive Intestinal Epithelial and Matrix Remodelling. *Nat Mater* (2021) 20(2):250–9. doi: 10.1038/s41563-020-0783-8
17. Riggan L, Freud AG, O'Sullivan TE. True Detective: Unraveling Group 1 Innate Lymphocyte Heterogeneity. *Trends Immunol* (2019) 40:909–21. doi: 10.1016/j.it.2019.08.005
18. Krabbendam L, Heesters BA, Kradolfer CMA, Haverkate NJE, Becker MAJ, Buskens CJ, et al. CD127+ CD94+ Innate Lymphoid Cells Expressing Granulysin and Perforin Are Expanded in Patients With Crohn's Disease. *Nat Commun* (2021) 12(1):1–11. doi: 10.1038/s41467-021-26187-x
19. Mohamed R, Lord GM. T-Bet as a Key Regulator of Mucosal Immunity. *Immunology* (2016) 147:367–76. doi: 10.1111/imm.12575
20. Gasteiger G, Fan X, Dikiy S, Lee SY, Rudensky AY. Tissue Residency of Innate Lymphoid Cells in Lymphoid and Nonlymphoid Organs. *Science* (2015) 350:981–5. doi: 10.1126/science.aac9593
21. McFarland AP, Yalin A, Wang SY, Cortez VS, Landsberger T, Sudan R, et al. Multi-Tissue Single-Cell Analysis Deconstructs the Complex Programs of Mouse Natural Killer and Type 1 Innate Lymphoid Cells in Tissues and Circulation. *Immunity* (2021) 54:1320–37.e4. doi: 10.1016/j.immuni.2021.03.024
22. Vosshenrich CAJ, García-Ojeda ME, Samson-Villéger SI, Pasqualetto V, Enault L, Goff le OR, et al. A Thymic Pathway of Mouse Natural Killer Cell Development Characterized by Expression of GATA-3 and CD127. *Nat Immunol* (2006) 7(11):1217–24. doi: 10.1038/ni1395
23. Klose CSN, Flach M, Möhle L, Rogell L, Hoyler T, Ebert K, et al. Differentiation of Type 1 ILCs From a Common Progenitor to All Helper-Like Innate Lymphoid Cell Lineages. *Cell* (2014) 157:340–56. doi: 10.1016/j.cell.2014.03.030
24. Takeda K, Hayakawa Y, Smyth MJ, Kayagaki N, Yamaguchi N, Kakuta S, et al. Involvement of Tumor Necrosis Factor-Related Apoptosis-Inducing Ligand in Surveillance of Tumor Metastasis by Liver Natural Killer Cells. *Nat Med* (2001) 7(1):94–100. doi: 10.1038/83416
25. Cortez VS, Fuchs A, Cella M, Gilfillan S, Colonna M. Cutting Edge: Salivary Gland NK Cells Develop Independently of Nfil3 in Steady-State. *J Immunol* (2014) 192:4487–91. doi: 10.4049/jimmunol.1303469
26. Sojka DK, Plougastel-Douglas B, Yang L, Pak-Wittel MA, Artyomov MN, Ivanova Y, et al. Tissue-Resident Natural Killer (NK) Cells are Cell Lineages Distinct From Thymic and Conventional Splenic NK Cells. *Elife* (2014) 3: e01659. doi: 10.7554/eLife.01659
27. Robinette ML, Fuchs A, Cortez VS, Lee JS, Wang Y, Durum SK, et al. Transcriptional Programs Define Molecular Characteristics of Innate Lymphoid Cell Classes and Subsets. *Nat Immunol* (2015) 16(3):306–17. doi: 10.1038/ni.3094
28. Gury-BenAri M, Thaiss CA, Serafini N, Winter DR, Giladi A, Lara-Astiaso D, et al. The Spectrum and Regulatory Landscape of Intestinal Innate Lymphoid Cells Are Shaped by the Microbiome. *Cell* (2016) 166:1231–46.e13. doi: 10.1016/j.cell.2016.07.043
29. Shih HY, Sciumè G, Mikami Y, Guo L, Sun HW, Brooks SR, et al. Developmental Acquisition of Regulomes Underlies Innate Lymphoid Cell Functionality. *Cell* (2016) 165:1120–33. doi: 10.1016/j.cell.2016.04.029
30. Mazzurana L, Czarnewski P, Jonsson V, Wigge L, Ringnér M, Williams TC, et al. Tissue-Specific Transcriptional Imprinting and Heterogeneity in Human Innate Lymphoid Cells Revealed by Full-Length Single-Cell RNA-Sequencing. *Cell Res* (2021) 31(5):554–68. doi: 10.1038/s41422-020-00445-x
31. Gordon SM, Chaix J, Rupp LJ, Wu J, Madera S, Sun JC, et al. The Transcription Factors T-Bet and Eomes Control Key Checkpoints of Natural Killer Cell Maturation. *Immunity* (2012) 36:55–67. doi: 10.1016/j.immuni.2011.11.016
32. Park E, Patel S, Wang Q, Andhey P, Zaitsev K, Porter S, et al. Toxoplasma Gondii Infection Drives Conversion of NK Cells Into ILC1-Like Cells. *Elife* (2019) 8. doi: 10.7554/eLife.47605
33. Weizman O, Adams NM, Schuster IS, Krishna C, Pritykin Y, Lau C, Degli-Esposti MA, et al, et al. ILC1 Confer Early Host Protection at Initial Sites of Viral Infection. *Cell* (2017) 171:795–808.e12. doi: 10.1016/j.cell.2017.09.052
34. Bezman NA, Kim CC, Sun JC, Min-Oo G, Hendricks DW, Kamimura Y, et al. Molecular Definition of the Identity and Activation of Natural Killer Cells. *Nat Immunol* (2012) 13. doi: 10.1038/ni.2395
35. Gao Y, Souza-Fonseca-Guimaraes F, Bald T, Ng SS, Young A, Ngiow SF, et al. Tumor Immunoevasion by the Conversion of Effector NK Cells Into Type 1 Innate Lymphoid Cells. *Nat Immunol* (2017) 18(9):1004–15. doi: 10.1038/ni.3800
36. Cortez VS, Ulland TK, Cervantes-Barragan L, Bando JK, Robinette ML, Wang Q, et al. SMAD4 Impedes the Conversion of NK Cells Into ILC1-Like Cells by Curtailing non-Canonical TGF-β Signaling. *Nat Immunol* (2017) 18(9):995–1003. doi: 10.1038/ni.3809
37. Bal SM, Golebski K, Spits H. Plasticity of Innate Lymphoid Cell Subsets. *Nat Rev Immunol* (2020) 20(9):552–65. doi: 10.1038/s41577-020-0282-9
38. Vonarbourg C, Mortha A, Bui VL, Hernandez PP, Kiss EA, Hoyler T, et al. Regulated Expression of Nuclear Receptor Rorγt Confers Distinct Functional Fates to NK Cell Receptor-Expressing Rorγt+ Innate Lymphocytes. *Immunity* (2010) 33:736–51. doi: 10.1016/j.immuni.2010.10.017
39. Klose CSN, Kiss EA, Schwierzeck V, Ebert K, Hoyler T, D'Hargues Y, et al. A T-Bet Gradient Controls the Fate and Function of CCR6–Rorγt+ Innate Lymphoid Cells. *Nature* (2013) 494(7436):261–5. doi: 10.1038/nature11813
40. Rankin LC, Groom JR, Chopin M, Herold MJ, Walker JA, Mielke LA, et al. The Transcription Factor T-Bet is Essential for the Development of NKp46+ Innate Lymphocytes *via* the Notch Pathway. *Nat Immunol* (2013) 14:389–95. doi: 10.1038/ni.2545
41. Tizian C, Lahmann A, Hölsken O, Cosovanu C, Kofoed-Branzk M, Heinrich F, et al. C-Maf Restrains T-Bet-Driven Programming of CCR6-Negative Group 3 Innate Lymphoid Cells. *Elife* (2020) 9:e52549. doi: 10.7554/eLife.52549
42. Viant C, Rankin LC, Girard-Madoux MJH, Seillet C, Shi W, Smyth MJ, et al. Transforming Growth Factor-β and Notch Ligands Act as Opposing Environmental Cues in Regulating the Plasticity of Type 3 Innate Lymphoid Cells. *Sci Signaling* (2016) 9:426. doi: 10.1126/scisignal.aaf2176
43. Schroeder JH, Roberts LB, Meissl K, Lo JW, Hromadová D, Hayes K, et al. Sustained Post-Developmental T-Bet Expression Is Critical for the Maintenance of Type One Innate Lymphoid Cells *In Vivo*. *Front Immunol* (2021) 12:4446. doi: 10.3389/fimmu.2021.760198
44. Muraoka WT, Korchagina AA, Xia Q, Shein SA, Jing X, Lai Z, et al. Campylobacter Infection Promotes Ifnγ-Dependent Intestinal Pathology *via* ILC3 to ILC1 Conversion. *Mucosal Immunol* (2021) 14:703–16. doi: 10.1038/s41385-020-00353-8
45. Björklund AK, Forkel M, Picelli S, Konya V, Theorell J, Friberg D, et al. The Heterogeneity of Human CD127+ Innate Lymphoid Cells Revealed by Single-Cell RNA Sequencing. *Nat Immunol* (2016) 17(4):451–60. doi: 10.1038/ni.3368
46. Sagebiel AF, Steinert F, Lunemann S, Körner C, Schreurs RRCE, Altfeld M, et al. Tissue-Resident Eomes+ NK Cells are the Major Innate Lymphoid Cell Population in Human Infant Intestine. *Nat Commun* (2019) 10(1):1–13. doi: 10.1038/s41467-018-08267-7
47. Simoni Y, Fehlings M, Kløverpris HN, McGovern N, Koo SL, Loh CY, et al. Human Innate Lymphoid Cell Subsets Possess Tissue-Type Based Heterogeneity in Phenotype and Frequency. *Immunity* (2017) 46:148–61. doi: 10.1016/j.immuni.2016.11.005
48. Forkel M, VanTol S, Höög C, Michaëlsson J, Almer S, Mjösberg J, et al. Distinct Alterations in the Composition of Mucosal Innate Lymphoid Cells in Newly Diagnosed and Established Crohn's Disease and Ulcerative Colitis. *J Crohn's Colitis* (2019) 13:67–78. doi: 10.1093/ecco-jcc/jjy119
49. Yudanin NA, Schmitz F, Flamar AL, Thome JJC, Tait Wojno E, Moeller JB, et al. Spatial and Temporal Mapping of Human Innate Lymphoid Cells Reveals Elements of Tissue Specificity. *Immunity* (2019) 50:505–19.e4. doi: 10.1016/j.immuni.2019.01.012
50. Koues OI, Collins PL, Cella M, Robinette ML, Porter SI, Pyfrom SC, et al. Distinct Gene Regulatory Pathways for Human Innate Versus Adaptive Lymphoid Cells. *Cell* (2016) 165:1134–46. doi: 10.1016/j.cell.2016.04.014
51. Collins PL, Cella M, Porter SI, Li S, Gurewitz GL, Hong HS, et al. Gene Regulatory Programs Conferring Phenotypic Identities to Human NK Cells. *Cell* (2019) 176:348–60.e12. doi: 10.1016/j.cell.2018.11.045

52. Cella M, Otero K, Colonna M. Expansion of Human NK-22 Cells With IL-7, IL-2, and IL-1β Reveals Intrinsic Functional Plasticity. *Proc Natl Acad Sci USA* (2010) 107:10961–6. doi: 10.1073/pnas.1005641107
53. Mazzurana L, Forkel M, Rao A, van Acker A, Kokkinou E, Ichiya T, et al. Suppression of Aiolos and Ikaros Expression by Lenalidomide Reduces Human ILC3–ILC1/NK Cell Transdifferentiation. *Eur J Immunol* (2019) 49:1344–55. doi: 10.1002/eji.201848075
54. Abt MC, Lewis BB, Caballero S, Xiong H, Carter RA, Susac B, et al. Innate Immune Defenses Mediated by Two ILC Subsets Are Critical for Protection Against Acute Clostridium Difficile Infection. *Cell Host Microbe* (2015) 18:27–37. doi: 10.1016/j.chom.2015.06.011
55. Langer V, Vivi E, Regensburger D, Winkler TH, Waldner MJ, Rath T, et al. IFN-γ Drives Inflammatory Bowel Disease Pathogenesis Through VE-Cadherin-Directed Vascular Barrier Disruption. *J Clin Invest* (2019) 129:4691–707. doi: 10.1172/JCI124884
56. Nava P, Koch S, Laukoetter MG, Lee WY, Kolegraff K, Capaldo CT, et al. Interferon-Gamma Regulates Intestinal Epithelial Homeostasis Through Converging Beta-Catenin Signaling Pathways. *Immunity* (2010) 32:392–402. doi: 10.1016/j.immuni.2010.03.001
57. Ito R, Shin-Ya M, Kishida T, Urano A, Takada R, Sakagami J, et al. Interferon-Gamma Is Causatively Involved in Experimental Inflammatory Bowel Disease in Mice. *Clin Exp Immunol* (2006) 146:330–8. doi: 10.1111/j.1365-2249.2006.03214.x
58. Powell N, Walker AW, Stolarczyk E, Canavan JB, Gökmen MR, Marks E, et al. The Transcription Factor T-Bet Regulates Intestinal Inflammation Mediated by Interleukin-7 Receptor+ Innate Lymphoid Cells. *Immunity* (2012) 37:674–84. doi: 10.1016/j.immuni.2012.09.008
59. Xiao YT, Yan WH, Cao Y, Yan JK, Cai W. Neutralization of IL-6 and TNF-α Ameliorates Intestinal Permeability in DSS-Induced Colitis. *Cytokine* (2016) 83:189–92. doi: 10.1016/j.cyto.2016.04.012
60. Li J, Doty AL, Tang Y, Berrie D, Iqbal A, Tan SA, et al. Enrichment of IL-17a + IFN-γ + and IL-22 + IFN-γ + T Cell Subsets is Associated With Reduction of NKp44 + ILC3s in the Terminal Ileum of Crohn's Disease Patients. *Clin Exp Immunol* (2017) 190:143–53. doi: 10.1111/cei.12996
61. Li J, Ueno A, Gasia MF, Luider J, Wang T, Hirota C, et al. Profiles of Lamina Propria T Helper Cell Subsets Discriminate Between Ulcerative Colitis and Crohn's Disease. *Inflamma Bowel Dis* (2016) 22:1779–92. doi: 10.1097/MIB.0000000000000811
62. Mitsialis V, Wall S, Liu P, Ordovas-Montanes J, Parmet T, Vukovic M, et al. Single-Cell Analyses of Colon and Blood Reveal Distinct Immune Cell Signatures of Ulcerative Colitis and Crohn's Disease. *Gastroenterology* (2020) 159:591–608.e10. doi: 10.1053/J.GASTRO.2020.04.074
63. Creyns B, Jacobs I, Verstockt B, Cremer J, Ballet V, Vandecasteele R, et al. Biological Therapy in Inflammatory Bowel Disease Patients Partly Restores Intestinal Innate Lymphoid Cell Subtype Equilibrium. *Front Immunol* (2020) 11:1847. doi: 10.3389/fimmu.2020.01847
64. Mazzurana L, Bonfiglio F, Forkel M, D'Amato M, Halfvarson J, Mjösberg J, et al. Crohn's Disease Is Associated With Activation of Circulating Innate Lymphoid Cells. *Inflamma Bowel Dis* (2021) 27:1128–38. doi: 10.1093/ibd/izaa316
65. Farber DL. Tissues, Not Blood, are Where Immune Cells Function. *Nature* (2021) 593(7860):506–9. doi: 10.1038/d41586-021-01396-y
66. Lim AI, Li Y, Lopez-Lastra S, Stadhouders R, Paul F, Casrouge A, et al. Systemic Human ILC Precursors Provide a Substrate for Tissue ILC Differentiation. *Cell* (2017) 168:1086–100.e10. doi: 10.1016/j.cell.2017.02.021
67. Kokkinou E, Pandey RV, Mazzurana L, Gutierrez-Perez I, Tibbitt CA, Weigel W, et al. CD45RA+CD62L– ILCs in Human Tissues Represent a Quiescent Local Reservoir for the Generation of Differentiated ILCs. *Sci Immunol* (2022) 7:8301. doi: 10.1126/sciimmunol.abj8301
68. Vulliemoz M, Brand S, Juillerat P, Mottet C, Ben-Horin S, Michetti P, et al. TNF-Alpha Blockers in Inflammatory Bowel Diseases: Practical Recommendations and a User's Guide: An Update. *Digestion* (2020) 101 Suppl 1:16–26. doi: 10.1159/000506898
69. Bank S, Andersen PS, Burisch J, Pedersen N, Roug S, Galsgaard J, et al. Genetically Determined High Activity of IL-12 and IL-18 in Ulcerative Colitis and TLR5 in Crohns Disease Were Associated With Non-Response to Anti-TNF Therapy. *Pharmacogenom J* (2018) 18:87–97. doi: 10.1038/tpj.2016.84
70. Hommes DW, Mikhajlova TL, Stoinov S, Štimac D, Vucelic B, Lonovics J, et al. Fontolizumab, a Humanised Anti-Interferon Gamma Antibody, Demonstrates Safety and Clinical Activity in Patients With Moderate to Severe Crohn's Disease. *Gut* (2006) 55:1131–7. doi: 10.1136/gut.2005.079392
71. Reinisch W, de Villiers W, Bene L, Simon L, Rácz I, Katz S, et al. Fontolizumab in Moderate to Severe Crohn's Disease: A Phase 2, Randomized, Double-Blind, Placebo-Controlled, Multiple-Dose Study. *Inflammation Bowel Dis* (2010) 16:233–42. doi: 10.1002/ibd.21038
72. Meng XM, Nikolic-Paterson DJ, Lan HY. TGF-β: The Master Regulator of Fibrosis. *Nat Rev Nephrol* (2016) 12(6):325–38. doi: 10.1038/nrneph.2016.48
73. Györfi AH, Matei AE, Distler JHW. Targeting TGF-β Signaling for the Treatment of Fibrosis. *Matrix Biol* (2018) 68–69:8–27. doi: 10.1016/j.matbio.2017.12.016
74. Shimshoni E, Yablecovitch D, Baram L, Dotan I, Sagi I. ECM Remodelling in IBD: Innocent Bystander or Partner in Crime? The Emerging Role of Extracellular Molecular Events in Sustaining Intestinal Inflammation. *Gut* (2015) 64:367–72. doi: 10.1136/gutjnl-2014-308048
75. Viel S, Marçais A, Guimaraes FSF, Loftus R, Rabilloud J, Grau M, Degouve S, et al, et al. TGF-β Inhibits the Activation and Functions of NK Cells by Repressing the mTOR Pathway. *Sci Signaling* (2016) 9:415. doi: 10.1126/scisignal.aad1884
76. Zaiatz Bittencourt V, Jones F, Tosetto M, Doherty GA, Ryan EJ. Dysregulation of Metabolic Pathways in Circulating Natural Killer Cells Isolated From Inflammatory Bowel Disease Patients. *J Crohn's Colitis* (2021) 15:1316–25. doi: 10.1093/ecco-jcc/jjab014
77. Serafini N, Jarade A, Surace L, Goncalves P, Sismeiro O, Varet H, et al. Trained ILC3 Responses Promote Intestinal Defense. *Science* (2022) 375:859–63. doi: 10.1126/science.aaz8777
78. Read E, Jowett GM, Coman D, Neves JF. Co-Culture of Murine Small Intestine Epithelial Organoids With Innate Lymphoid Cells. *JoVE (Journal Visualized Experiments)* (2022) 181:e63554. doi: 10.3791/63554
79. Jowett GM, Coales I, Neves JF. Organoids as a Tool for Understanding Immune-Mediated Intestinal Regeneration and Development. *Development* (2022) 149:8. doi: 10.1242/DEV.199904

Conflict of Interest: The authors declare that the research was conducted in the absence of any commercial or financial relationships that could be construed as a potential conflict of interest.

Publisher's Note: All claims expressed in this article are solely those of the authors and do not necessarily represent those of their affiliated organizations, or those of the publisher, the editors and the reviewers. Any product that may be evaluated in this article, or claim that may be made by its manufacturer, is not guaranteed or endorsed by the publisher.

frontiers | Frontiers in Immunology

TYPE Original Research
PUBLISHED 27 July 2022
DOI 10.3389/fimmu.2022.902881

OPEN ACCESS

EDITED BY
Carmelo Luci,
Institut National de la Santéet de la Recherche Médicale (INSERM), France

REVIEWED BY
Aharon Freud,
The Ohio State University, United States
Marieke Lavaert,
National Institutes of Health (NIH), United States

*CORRESPONDENCE
Tim Willinger
tim.willinger@ki.se

†PRESENT ADDRESS
Imran Mohammad, Department of Otolaryngology-Head and Neck Surgery, Stanford Cancer Institute, Institute for Stem Cell Biology and Regenerative Medicine, Stanford University School of Medicine, Stanford, CA, United States

‡These authors have contributed equally to this work

SPECIALTY SECTION
This article was submitted to NK and Innate Lymphoid Cell Biology, a section of the journal Frontiers in Immunology

RECEIVED 23 March 2022
ACCEPTED 04 July 2022
PUBLISHED 27 July 2022

CITATION
Gao Y, Alisjahbana A, Boey DZH, Mohammad I, Sleiers N, Dahlin JS and Willinger T (2022) A single-cell map of vascular and tissue lymphocytes identifies proliferative TCF-1$^+$ human innate lymphoid cells.
Front. Immunol. 13:902881.
doi: 10.3389/fimmu.2022.902881

A single-cell map of vascular and tissue lymphocytes identifies proliferative TCF-1$^+$ human innate lymphoid cells

Yu Gao[1‡], Arlisa Alisjahbana[1‡], Daryl Zhong Hao Boey[2], Imran Mohammad[1†], Natalie Sleiers[1], Joakim S. Dahlin[2] and Tim Willinger[1*]

[1]Center for Infectious Medicine, Department of Medicine Huddinge, Karolinska Institutet, Karolinska University Hospital, Stockholm, Sweden, [2]Department of Medicine Solna, Karolinska Institutet, Karolinska University Hospital, Stockholm, Sweden

Innate lymphoid cells (ILCs) play important roles in tissue homeostasis and host defense, but the proliferative properties and migratory behavior of especially human ILCs remain poorly understood. Here we mapped at single-cell resolution the spatial distribution of quiescent and proliferative human ILCs within the vascular versus tissue compartment. For this purpose, we employed MISTRG humanized mice as an *in-vivo* model to study human ILCs. We uncovered subset-specific differences in the proliferative status between vascular and tissue ILCs within lymphoid and non-lymphoid organs. We also identified CD117$^-$CRTH2$^-$CD45RA$^+$ ILCs in the spleen that were highly proliferative and expressed the transcription factor TCF-1. These proliferative ILCs were present during the neonatal period in human blood and emerged early during population of the human ILC compartment in MISTRG mice transplanted with human hematopoietic stem and progenitor cells (HSPCs). Single-cell RNA-sequencing combined with intravascular cell labeling suggested that proliferative ILCs actively migrated from the local vasculature into the spleen tissue. Collectively, our comprehensive map reveals the proliferative topography of human ILCs, linking cell migration and spatial compartmentalization with cell division.

KEYWORDS

innate lymphoid cells, proliferation, migration, tissue residency, ontogeny, spleen, humanized mice, single-cell RNA-sequencing

Abbreviations: HSPCs, human hematopoietic stem and progenitor cells; IFNγ, interferon gamma; IL, interleukin; ILCs, innate lymphoid cells; ILCPs, innate lymphoid cell precursors; IV, intravenous; Lin, lineage; NK, natural killer; TCF-1, T cell factor-1; UMAP, Uniform Manifold Approximation and Projection.

Introduction

ILCs belong to a new lineage of immune cells of lymphoid origin that has innate properties, such as rapid effector function (1–6). Similar to T lymphocytes, ILCs are classified into distinct subsets that express lineage-defining transcription factors and effector molecules: (i) Cytotoxic natural killer (NK) cells expressing the signature transcription factors EOMES and T-BET; (ii) ILC1s expressing T-BET and the signature cytokine interferon gamma (IFNγ); (iii) ILC2s expressing GATA3 and the cytokines interleukin-5 (IL-5) and IL-13; (iv) ILC3s expressing RORγt and the effector cytokines IL-17 and/or IL-22. Surface expression of IL-7Rα (CD127) is generally used to distinguish helper-like $CD127^+$ ILC1s, ILC2s, and ILC3s from $CD127^-$ $CD94^+$ human NK cells (7).

ILCs inhabit various organs where they are strategically positioned to help maintain organ homeostasis and to participate in host defense. ILCs are considered to be mainly tissue-resident at steady state, at least in mice (8). However, ILCs actively migrate during their ontogeny and tissue injury (9–19) and the function of ILCs is linked to their localization within tissues (20, 21). The relative frequency of human ILC subsets differs between organs (22, 23). Moreover, differences in ILC compartmentalization between mice and humans have been reported (23). However, the distribution of human ILCs between the vascular and tissue space is unknown due to the difficulty of studying human ILCs *in vivo*.

ILCs lack antigen-specific receptors but expand in response to locally produced cytokines. Recently, the concept that mature ILCs differentiate locally from systemic ILC precursors (ILCPs) that enter tissues has been established (11, 24–26). However, the mechanisms of ILC proliferation, especially in the human context, are not completely understood. For example, it is unclear where ILCs proliferate and whether ILC proliferation is spatially compartmentalized. We hypothesized that ILCs differ in their proliferative status and that it is linked to their anatomical location. To test this hypothesis, we used a humanized mouse model to investigate human ILCs *in vivo* because human ILC studies are largely restricted to *ex-vivo* and *in-vitro* experiments. This model named "MISTRG" expresses human cytokines (27–29) and supports the development of human NK cells and all types of ILCs after transplantation with human hematopoietic stem and progenitor cells (30, 31). Therefore, this model allows studying human ILCs directly in their surrounding tissue microenvironment and to investigate their ontogeny, migration, and proliferation *in vivo*.

Here, we comprehensively resolved the spatial distribution of quiescent and proliferating human ILCs in bone marrow, spleen, liver, and lung of MISTRG mice transplanted with human $CD34^+$ HSPCs. Intravascular labeling to distinguish vascular from tissue ILCs revealed that human ILCs have a specific proliferative topology within lymphoid and non-lymphoid organs. Moreover, we identified a specific population of $CD117^-CRTH2^-CD45RA^+$ ILCs with high proliferative potential that expressed the transcription factor TCF-1, emerged early during ontogeny, and acquired tissue residency in the spleen. Our findings support the notion that ILCs residing in the local organ vasculature are primed for proliferation before entering the extravascular (tissue) compartment.

Materials and methods

Human blood

We obtained human tissues through Karolinska University Hospital Huddinge after informed consent was given by all tissue donors following verbal and written information. Umbilical cord blood was obtained from Caesarean sections. Buffy coats were provided by the local Blood Bank. Approval for the use of human tissues was obtained from the Ethical Review Board at Karolinska Institutet (#2006/229-31/3, 2015/1368-31/4, 2015/2122-32, 2016/1415-32, 2019-03863). The study was conducted according to the Declaration of Helsinki.

Generation of mice with a human immune system

To study human ILCs *in vivo*, we used MISTRG mice as in our recent study (31). MISTRG mice on the *Rag2*$^{-/-}$*Il2rg*$^{-/-}$ background were previously described (27, 32) and express human genes encoding the proteins M-CSF, IL-3/GM-CSF, SIRPα, and TPO through gene knock-in. For the experiments, we used both male and female MISTRG mice that were heterozygous for *SIRPA* and homozygous for all other human genes. MISTRG mice were housed under specific pathogen-free conditions and did not receive any prophylactic antibiotics. Human $CD34^+$ cells containing HSPCs were purified from umbilical cord blood (pooled from several donors) with the $CD34^+$ microbead kit (Miltenyi Biotec) as previously described (31). Newborn MISTG mice that were 3-5 days old were then injected with 1 x 10^5 human $CD34^+$ cells (pooled from several donors) *via* the intrahepatic route as described (31, 33). Mice did not receive any irradiation as pre-conditioning before transplantation except for the experiments shown in Supplementary Figure 4 and for the single-cell RNA-sequencing of spleen ILCs. In these cases, mice were irradiated once with 100 cGy before HSPC transplantation. Successful engraftment with human $CD45^+$ hematopoietic cells was confirmed by flow cytometry of blood collected from MISTRG mice at ~6-8 weeks post-transplantation. In general, HSPC-engrafted MISTRG mice were used for experiments 7-12 weeks after injection with human $CD34^+$ cells, except for the kinetics experiments where mice were analyzed also at 3-5 weeks post-transplantation. All mouse experiments were approved by the Linköping Animal Experimentation Ethics

Committee (ethical permits #29-15 and #03127-2020). The use of MISTRG mice requires Material Transfer Agreements with Regeneron Pharmaceuticals and Yale University.

Labeling of intravascular ILCs in MISTRG mice

Human $CD45^+$ hematopoietic cells in the blood and the organ vasculature of HSPC-engrafted MISTRG mice were labeled as previously described (31). For this purpose, 2 µg of a phycoerythrin (PE)-conjugated anti-human CD45 antibody (Biolegend, clone HI30) was injected intravenously (IV) 5 minutes before organ harvest without any prior perfusion. After isolation from various organs (bone marrow, spleen, liver, lung), cells were stained *ex vivo* with an APC-Cy7-conjugated anti-human CD45 antibody and other cell surface antibodies to determine the frequency of intravascular (IV $CD45\text{-}PE^+$) and extravascular (IV $CD45\text{-}PE^-$) ILCs by flow cytometry. Blood was also analyzed by flow cytometry to confirm successful intravascular labelling, defined as >90% IV $CD45\text{-}PE^+$ human cells in blood.

Isolation of human ILCs from MISTRG mice and from human blood

Lung, liver, spleen, and bone marrow harvested from MISTRG mice were processed as described in (31). Briefly, small lung pieces were digested at 37°C for 1 hour in RPMI 1640 with 5% FCS, 0.2 mg/mL collagenase IV (Sigma) and 0.02 mg/mL DNAse I (Sigma). Digested lung pieces were mashed using a syringe plunger to mechanically dissociate the cells and passed through a 70 µm filter. Lung lymphocytes were then further purified by density gradient centrifugation with Lymphoprep (Fisher Scientific). Like the lungs, crushed liver pieces were digested at 37°C for 1 hour in digestion media (see above) and then washed with RPMI 1640/5% FCS. To remove hepatocytes, digested livers were centrifuged at 300 rpm for 3 minutes at 4°C. Then, leukocytes in the supernatant were pelleted by centrifugation (1,700 rpm for 10 minutes at 4°C) before further purification by density gradient centrifugation with 27.5% Optiprep (Abbott Rapid Diagnostics). Spleen were mechanically dissociated with a syringe plunger before passing through a 70 µm filter. For bone marrow, hind legs harvested from MISTRG mice were cleaned, cut at both ends, and bone marrow cells flushed from the bone with a syringe and 25G needle. Cells isolated from all four organs were treated with red blood cell lysis buffer (from Karolinska University Hospital), washed with RPMI 1640, and counted prior to staining for flow cytometry. Blood was obtained from HSPC-engrafted MISTRG mice by cardiac puncture and red blood cell lysis performed before staining cells for flow cytometry. Density gradient centrifugation was used to isolate peripheral blood mononuclear cells from human cord blood and buffy coats. The $CD34^-$ fraction from cord blood (after immunomagnetic selection) was used for flow cytometry of ILCs.

Flow cytometry of human ILCs

Surface staining of immune cells isolated from human blood or from HSPC-engrafted MISTRG mice was performed essentially as previously described (31). Briefly, suspensions of single cells were incubated with the fluorochrome- or biotin-conjugated antibodies listed in Supplementary Table 1 in 100 µl FACS buffer (PBS/2% FCS) for 1 hour at room temperature. After washing, cells were incubated with streptavidin-Brilliant Violet 711 (BD Biosciences) for 30 minutes on ice. Then, surface-stained cells were incubated with fixable viability dye-eFluor506 (eBioscience) for 15 minutes on ice. For detection of Ki67 and transcription factors, cells were fixed and permeabilized with the Foxp3/Transcription Factor Staining kit (eBioscience) after surface and viability staining. Fixed and permeabilized cells were then stained with antibodies against transcription factors or Ki67 as well as matched isotype control antibodies. For cell cycle analysis, Ki67-stained cells were incubated with 20 µl propidium iodide (PI) (eBioscience) per 5 x 10^6 cells for 30 minutes at room temperature in 100 µl Cytoperm buffer (BD Biosciences) containing RNase A. Intracellular staining for IFNγ was performed with the Cytofix/Cytoperm kit (BD Biosciences) as described (31) after 6 hours of stimulation with phorbol 12-myristate 13-acetate (PMA) (Sigma) and ionomycin (Sigma). After cell acquisition on a LSR II Fortessa flow cytometer (BD Biosciences), FlowJoV10 software was used for data analysis. ILCs were gated as viable human $CD45^+CD127^+CD94^-CD3^-TCR\alpha\beta^-$ cells that were negative for Lineage (Lin) markers (CD11c, CD14, CD19, CD123, FceRI) as well as lacking human CD34 and mouse CD45 as indicated.

Single-cell RNA-sequencing of ILCs

Cells for single-cell RNA-sequencing were isolated from the spleens of two months-old irradiated and HSPC-engrafted MISTRG mice after intravascular cell labeling was performed with IV-injected anti-CD45-PE antibody (see above). To obtain sufficient cells, spleen cells were pooled from ten MISTRG mice, engrafted with three pooled batches of human $CD34^+$ cells to reduce the impact of HSPC donor variability. ILCs were then purified as live $CD45^+CD127^+CD94^-CD3^-TCR\alpha\beta^-Lin^-CD34^-$ lymphocytes and divided into intravascular (IV-$CD45\text{-}PE^+$) and extravascular (IV-$CD45\text{-}PE^-$) ILCs. Lin markers included CD11c, CD14, CD19, CD123, FceRI. Single-cell libraries were prepared using the 10x Genomics Single Cell 3' Library v2 kit

according to the manufacturer's instructions. Libraries were sequenced on a Nextseq 550 (Illumina) and mapped to the human GRCh38 reference genome using the Cell Ranger 3.0.1 pipeline (10x Genomics). Both extravascular and intravascular samples were analyzed using Seurat 4.1.1, with cut-offs applied for genes expressed in a minimum of 3 cells, and cells expressing a minimum of 200 genes. The samples were then merged into a single Seurat object using the merge function. Further quality control selected cells with > 100 genes, < 4,000 genes, and < 5 percent mitochondrial genes, using the subset function on the merged dataset. Log normalization to 10,000 counts was next applied to the remaining 5,853 cells. The FindVariableFeatures function was applied to select 2,000 highly variable genes, followed by ScaleData, which was then used to produce a PCA and neighborhood graph (10 principal components). Louvain clustering was applied with the FindClusters function with resolution 0.45, resulting in 11 clusters (Supplementary Figure 5A). The FindAllMarkers function (min.pct=0.25, logfc.threshold=0.25) function was applied to identify marker genes for each cluster, pct.1 represents the fraction of cells expressing the gene in the specified cluster being tested, while pct.2 represents the remaining cells. To better represent the main ILC populations we applied the subset function to extract clusters containing ILCs (Clusters 0-5), resulting in 4,936 remaining cells (2,704 vascular and 2,232 tissue cells). PCA, neighborhood graph (10 principal components), and Louvain clustering (resolution 0.44) was reapplied to the new Seurat object, resulting in 8 clusters. This was the Seurat object used for all further analysis. Uniform Manifold Approximation and Projection (UMAP) embedding was produced using 10 principal components (Figure 7B). The FindAllMarkers function (min.pct=0.25, logfc.threshold=0.25) function was applied to identify marker genes for each cluster in the final object. Violin and feature plots were produced using the VlnPlot and FeaturePlot function, respectively. Cell cycle analysis of ILC clusters was performed with the CellCycleScoring function. To identify biological processes over-represented within the gene signature of *MKI67*-ILCs, WebGestalt (http://webgestalt.org/) was employed using default parameters.

Statistical analysis

For statistical comparisons between two groups Student's *t* test was used. One-way ANOVA was employed to determine statistical significance between multiple groups. ANOVA *post hoc* testing was done with Tukey' Multiple Comparison Test. Results were considered statistically significant with α= 0.05. Mean and standard error of the mean (SEM) are shown in the figures. The number of biological replicates and independent experiments are stated in the figure legends. GraphPad Prism 8 was used to perform statistical analysis and create graphs.

Cartoons to illustrate experimental outlines

The cartoons in Figures 1A, 2A, 7A, and S6 were prepared using images from Mind the Graph (http://mindthegraph.com).

Results

Proliferative status of human ILCs in lymphoid and non-lymphoid organs

We first asked in which organs ILC proliferation takes place. To investigate the link between human ILC localization and proliferation, we used MISTRG mice transplanted with human CD34$^+$ HSPCs (Figure 1A) as in our previous studies (27, 31, 33). MISTRG mice were not pre-conditioned by irradiation before HSPC transplantation. ILCs derived from human HSPCs were gated as CD45$^+$CD127$^+$CD94$^-$ cells that lacked T cell markers (CD3, TCRαβ) and other Lin markers (CD11c, CD14, CD19, CD123, FceRI) (Supplementary Figure 1). Then the cell division status of human ILCs and NK cells (CD45$^+$CD127$^-$CD94$^+$CD3$^-$TCRαβ$^-$Lin$^-$) was determined by intracellular staining for the proliferation marker Ki67 in hematopoietic (bone marrow), lymphoid (spleen), and non-lymphoid organs (lung, liver). Flow cytometry analysis revealed a high frequency of Ki67$^+$ ILCs in bone marrow, while in peripheral organs the highest frequency of proliferating ILCs was found in the spleen (Figures 1B, C). In contrast, proliferating NK cells (Figures 1B, C) and T cells (Supplementary Figures 2A, B) were mostly located in non-lymphoid organs (lung and liver) as well as in the bone marrow. These results indicate that ILCs have an organ-specific proliferative hierarchy that is distinct from that of NK cells and T lymphocytes.

Spatial distribution of quiescent and proliferative ILCs within vascular and tissue compartments

The above findings suggested that human ILC proliferation may be spatially compartmentalized and prompted us to determine the localization of proliferating ILCs within vascular and tissue compartments. To distinguish vascular from tissue-resident Ki67$^+$ ILCs, we employed intravascular labeling of human CD45$^+$ hematopoietic cells by the IV injection of a PE-conjugated anti-human CD45 antibody (Figure 2A), as we did previously (31, 33). This experimental approach allowed us to distinguish four different ILC populations (Figure 2A): (i) quiescent tissue-resident (Q-R) ILCs (Ki67$^-$ IVCD45-PE$^-$), (ii) quiescent intravascular (Q-IV) ILCs (Ki67$^-$ IVCD45-PE$^+$), (iii) proliferative tissue-resident (P-R) ILCs (Ki67$^+$ IVCD45-PE$^-$), and (iv) proliferative intravascular (P-IV) ILCs (Ki67$^+$ IVCD45-

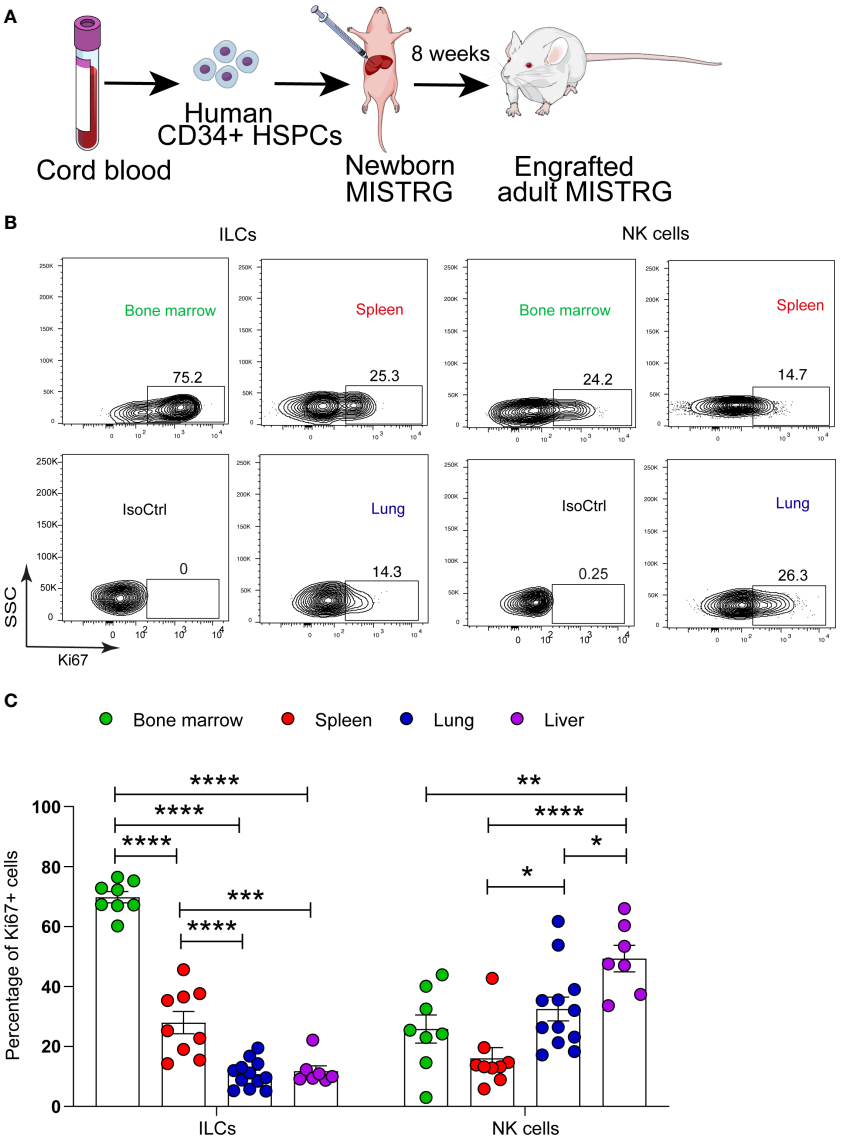

FIGURE 1
Proliferative status of human ILCs in lymphoid and non-lymphoid organs of HSPC-engrafted MISTRG mice. **(A)** Transplantation of newborn MISTRG mice with human CD34$^+$ cord blood HSPCs. **(B, C)** Intracellular Ki67 expression by human ILCs and NK cells as determined by flow cytometry. Isotype control (IsoCtrl) staining is shown for the lung. ILCs were gated as human CD45$^+$CD127$^+$CD94$^-$CD3$^-$TCRαβ$^-$Lin$^-$ cells and NK cells were gated as human CD45$^+$CD127$^-$CD94$^+$CD3$^-$TCRαβ$^-$Lin$^-$ cells as in Supplementary Figure 1. For bone marrow analysis, ILCs and NK cells were also gated as CD34$^-$ cells. Frequencies of Ki67$^+$ ILCs and NK cells in the indicated organs of HSPC-engrafted MISTRG mice (n = 7-12) are shown in **(C)**. *, P <0.05; **, *P* <0.01; ***, P <0.001; ****, *P* <0.0001 by one-way ANOVA, Tukey's post-test. Data are represented as mean ± SEM. Data are from two independent experiments using MISTRG mice engrafted with different pools of HSPCs. (A) was created with Mind the Graph.

PE$^+$). The distribution of these four populations differed among ILC subsets (CD117$^-$CRTH2$^-$ ILC1s, CRTH2$^+$ ILC2s, CD117$^+$CRTH2$^-$ ILCPs/ILC3s) in different organs (Figures 2B, C). ILC2s were mostly quiescent and intravascular in spleen, lung, and liver (Figures 2B, C). NK cells (Supplementary Figures 3A, B) and T lymphocytes (Supplementary Figure 3C, D) showed a similar pattern, but with more proliferating cells within the lung and liver vasculature than ILC2s. ILC3s and CD117$^+$ ILCPs were largely quiescent in spleen, lung, and liver, whereas in the bone marrow they were proliferative and tissue-resident (Figures 2B, C). In the spleen ILC3s and CD117$^+$ ILCPs were located preferentially within the tissue compartment, whereas they mostly had an intravascular localization in the lung and liver (Figures 2B, C). CD117$^-$CRTH2$^-$ ILC1s on the other hand were more proliferative than the other ILC subsets, especially in the spleen (Figures 2B, C). Moreover, Ki67$^+$ ILC1s

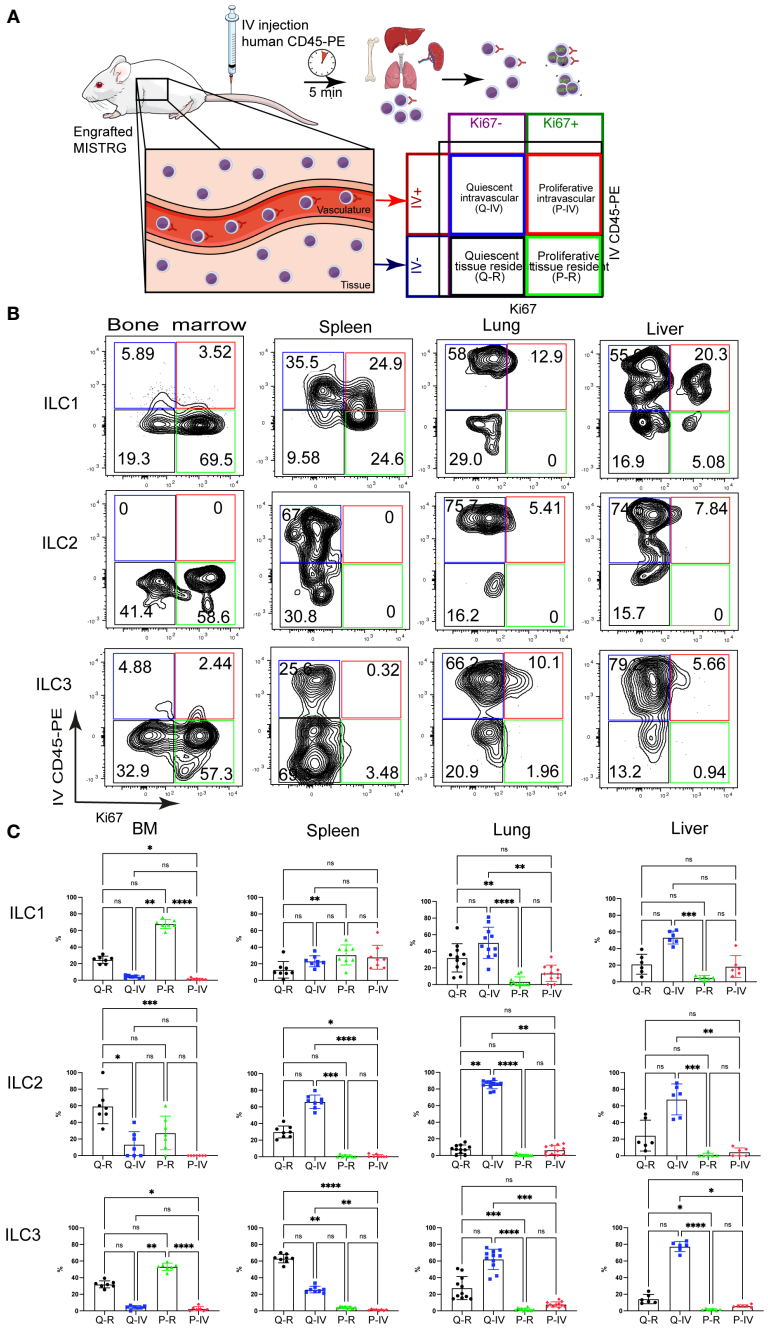

FIGURE 2
Spatial distribution of quiescent and proliferative ILCs within vascular and tissue compartments. **(A)** Experimental outline. Intracellular Ki67 staining of human ILCs was performed in HSPC-engrafted MISTRG mice after (IV) injection of anti-human CD45-PE antibody to label intravascular human hematopoietic cells. Human cells in the organ vasculature are stained by the IV-injected anti-CD45 antibody (IV CD45-PE), whereas cells residing in the tissue are not stained. Following intravascular labeling, cells were surface-stained *ex vivo* and stained intracellularly with an antibody against Ki67. Then quiescent ($Ki67^-$) and proliferative ($Ki67^+$) as well as intravascular ($IVCD45\text{-}PE^+$) and extravascular ILCs within tissue ($IVCD45\text{-}PE^-$) were distinguished by flow cytometry. **(B)** Flow cytometry analysis of intravascular versus extravascular and quiescent versus proliferative $CD117^-CRTH2^-$ ILC1s, $CRTH2^+$ ILC2s, and $CD117^+$ ILC3s in the indicated organs of HSPC-engrafted MISTRG mice. ILCs were gated as human $CD45^+CD127^+CD94^-CD3^-TCR\alpha\beta^-Lin^-$ cells as in Supplementary Figure 1 and as $CD34^-$ cells. **(C)** Frequencies of quiescent tissue-resident (Q-R), quiescent intravascular (Q-IV), proliferative tissue-resident (P-R), and proliferative intravascular (P-IV) human ILC1s, ILC2s, and ILC3s in the indicated organs (n = 6-11) as determined in (B). n.s., not significant; *, P <0.05; **, *P* <0.01; ***, P <0.001; ****, *P* <0.0001 by one-way ANOVA, Tukey's post-test. Data represent mean ± SEM and are representative of two independent experiments using MISTRG mice engrafted with different pools of HSPCs. (A) was created with Mind the Graph.

were present in the local vasculature of peripheral organs (spleen, lung, liver), whereas in the bone marrow they mostly resided in the extravascular space (Figures 2B, C). Combined, these data suggest that human ILC subsets differ in their proliferative state and spatial compartmentalization within organs.

CD117$^-$CRTH2$^-$CD45RA$^+$ ILCs in the spleen are highly proliferative

Having discovered discrete subsets of Ki67$^+$ ILCs, we further examined the proliferation of ILCs with an ILC1 surface phenotype (CD117$^-$CRTH2$^-$). For this purpose, we divided ILC1s into two subsets based on surface expression of CD45RA, a marker for immature ILCs (24, 34, 35), although it is also uniformly expressed by mature NK cells. Ki67$^+$ cells among CD117$^-$CRTH2$^-$ ILCs mostly expressed CD45RA on their cell surface in all organs examined (Figure 3A). Moreover, there was a large population of CD117$^-$CRTH2$^-$ CD45RA$^+$ ILCs in the spleen that was Ki67$^+$ and present in both the intravascular and extravascular compartment of the spleen (Figures 3B, C). Intravascular Ki67$^+$ CD45RA$^+$ ILC1s were also present in lung and liver, whereas proliferating CD45RA$^+$ ILC1s were predominantly extravascular in the bone marrow (Figures 3B, C). Further flow cytometric analysis revealed that proliferative CD117$^-$CRTH2$^-$CD45RA$^+$ ILCs in the spleen were mostly in G1 phase of the cell cycle (Figure 3D). We conclude that proliferative CD117$^-$CRTH2$^-$ ILCs have an immature surface phenotype and mostly reside within both the vascular and tissue compartment of the spleen.

Proliferative CD117$^-$CRTH2$^-$CD45RA$^+$ ILCs express the transcription factor TCF-1

To further elucidate the features of proliferating CD117$^-$ CRTH2$^-$CD45RA$^+$ ILCs, we examined the expression of transcription factors that define ILC lineages. As expected, CD117$^-$CRTH2$^-$CD45RA$^+$ ILCs from the spleen of HSPC-engrafted MISTRG mice lacked expression of EOMES and RORγt (Figure 4A). In addition, the majority of splenic CD117$^-$CRTH2$^-$CD45RA$^+$ ILCs did not express intracellular T-BET protein, the signature transcription factor for ILC1s, whereas NK cells were uniformly T-BET$^+$ (Figure 4A). The observation that most CD117$^-$CRTH2$^-$ ILCs were Ki67$^+$ but lacked intracellular T-BET protein, suggested that CD117$^-$ CRTH2$^-$ ILCs contained proliferating immature ILCs. To further explore this possibility, we determined expression of the transcription factor TCF-1 that is associated with proliferative potential (11, 24, 36, 37). We also assessed the expression of PLZF, another transcription factor associated with ILC development (38–41). CD117$^-$CRTH2 CD45RA$^+$ ILCs expressed high amounts of intracellular TCF-1 protein, but not PLZF, which was expressed by the other ILC subsets including NK cells (Figure 4B). CD117$^+$CRTH2$^-$ ILCPs/ILC3s also highly expressed TCF-1 but with only few Ki67$^+$ cells, in contrast to CD117$^-$CRTH2$^-$CD45RA$^+$ ILCs that were TCF-1^{hi}Ki67$^+$ (Figure 4B). Therefore, two populations of ILCs with high TCF-1 expression could be distinguished, namely proliferative CD117$^-$CRTH2$^-$CD45RA$^+$ ILCs and quiescent CD117$^+$ ILCPs/ILC3s. The lack of T-BET expression indicated that splenic CD117$^-$CRTH2$^-$CD45RA$^+$ ILCs do not represent *bona-fide* ILC1s. To further corroborate this notion, we examined production of IFNγ, the signature cytokine produced by ILC1s. As expected, most human NK cells expressed intracellular IFNγ protein in response to stimulation with PMA and ionomycin *in vitro* (Figure 4C). In contrast, neither human ILCs from the spleen of HSPC-engrafted MISTRG mice nor human ILCs from umbilical cord blood produced IFNγ after stimulation (Figure 4C). In summary, we found that CD117$^-$ CRTH2$^-$ ILCs in the spleen contain a proliferative population that expressed TCF-1 and had features of functionally immature ILCs.

Proliferative CD117$^-$CRTH2$^-$CD45RA$^+$ ILCs are present in the circulation and in human umbilical cord blood

We next asked whether proliferative CD117$^-$CRTH2$^-$ CD45RA$^+$ ILCs resided in local vascular compartments and/or circulated between organs. The latter predicted that Ki67$^+$ CD117$^-$ CRTH2$^-$CD45RA$^+$ ILCs were present in the systemic circulation. Consistent with this prediction, we found that circulating human CD117$^-$CRTH2$^-$ ILCs in HSPC-engrafted MISTRG mice were mostly CD45RA$^+$ (Figure 5A). Umbilical cord blood also contained a substantial proportion of CD117$^-$CRTH2$^-$CD45RA$^+$ ILCs, whereas CD117$^-$CRTH2$^-$CD45RA$^+$ ILCs were present in adult blood at a lower frequency (Figure 5A). Furthermore, we detected CD117$^-$CRTH2$^-$CD45RA$^+$ ILCs in the blood of HSPC-engrafted MISTRG mice that were Ki67$^+$ (Figure 5B). Ki67$^+$ ILC2s and ILC3s/CD117+ ILCPs were also present in the blood of HSPC-engrafted MISTRG mice (Figure 5B), despite being less abundant in the local vasculature of the spleen, lung, and liver than Ki67$^+$ CD45RA$^+$ ILC1s (Figure 2C and 3C). This suggested that Ki67$^+$ ILC2s and ILC3s/CD117+ ILCPs mostly recirculate through organs, whereas Ki67$^+$ CD117$^-$CRTH2$^-$CD45RA$^+$ ILCs may marginate and accumulate in the local vasculature, especially in the spleen. We next investigated whether proliferative CD117$^-$ CRTH2$^-$CD45RA$^+$ ILCs could also be detected in human blood. Ki67$^+$ CD45RA$^+$ ILC1s, as well as Ki67$^+$ ILC2s and ILC3s/CD117 + ILCPs were rare in the blood of adult humans, consistent with a previous report (22), but more prevalent in umbilical cord blood, although less frequent than in the blood of HSPC-engrafted

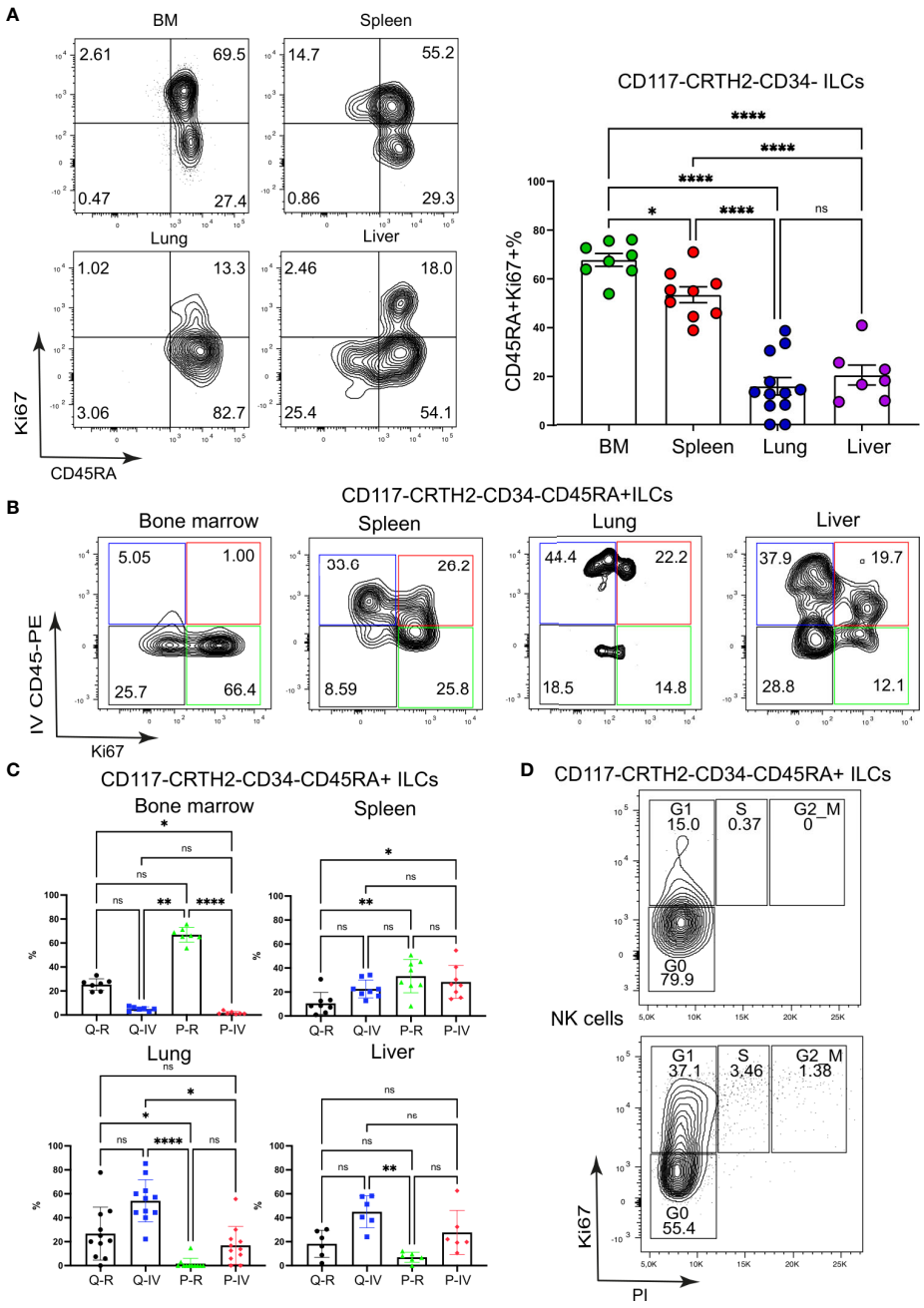

FIGURE 3
CD117$^-$CRTH2$^-$CD45RA$^+$ ILCs in the spleen are highly proliferative. **(A)** Frequencies of proliferating CD117$^-$CRTH2$^-$CD34$^-$ ILCs according to CD45RA surface expression in various organs of HSPC-engrafted MISTRG mice (n = 7-12). ILCs were gated as human CD45$^+$CD127$^+$CD94$^-$CD3$^-$ TCRαβ$^-$Lin$^-$ cells as in Supplementary Figure 1 and then gated as CD117$^-$CRTH2$^-$CD34$^-$ ILCs. **(B)** Flow cytometry analysis of intravascular versus extravascular and quiescent versus proliferative CD117$^-$CRTH2$^-$CD34$^-$ ILCs in the indicated organs of HSPC-engrafted MISTRG mice. ILCs were gated as human CD45$^+$CD127$^+$CD94$^-$CD3$^-$TCRαβ$^-$Lin$^-$ cells as in Supplementary Figure 1 and then gated as CD117$^-$CRTH2$^-$CD34$^-$ ILCs. **(C)** Frequencies of quiescent tissue-resident (Q-R), quiescent intravascular (Q-IV), proliferative tissue-resident (P-R), and proliferative intravascular (P-IV) CD117$^-$CRTH2$^-$CD34$^-$ ILCs in the indicated organs (n = 6-11) as determined in **(B)**. **(D)** Cell cycle status of CD117$^-$CRTH2$^-$CD45RA$^+$ ILCs and NK cells from the spleen of HSPC-engrafted MISTRG mice (n = 4). n.s., not significant; *, P <0.05; **, *P* <0.01; ***, P <0.001; ****, *P* <0.0001 by one-way ANOVA, Tukey's post-test. Data represent mean ± SEM and are representative of two independent experiments using MISTRG mice engrafted with different pools of HSPCs. **(A)** was created with Mind the Graph.

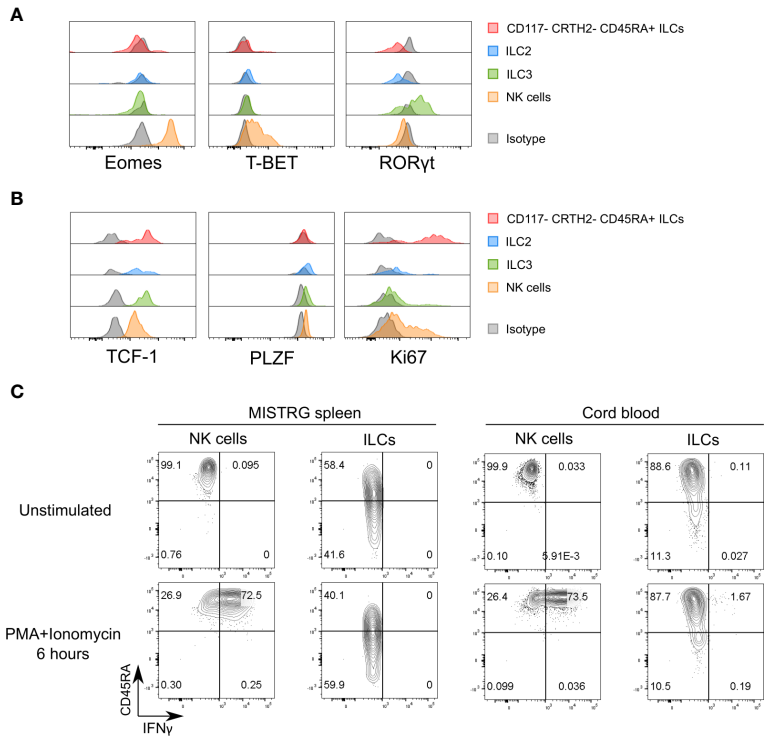

FIGURE 4
Proliferative CD117$^-$CRTH2$^-$CD45RA$^+$ ILCs express the transcription factor TCF-1. **(A)** Intracellular expression of signature transcription factors (Eomes, T-BET, RORγt) in human CD117$^-$CRTH2$^-$CD45RA$^+$ ILCs, CRTH2$^+$ ILC2s, CD117$^+$CRTH2$^-$ ILC3s, and NK cells isolated from the spleen of HSPC-engrafted MISTRG mice (n = 5). Matched isotype antibodies were used as controls. **(B)** Intracellular expression of transcription factors (TCF-1, PLZF) and Ki67 in human CD117$^-$CRTH2$^-$CD45RA$^+$ ILCs, CRTH2$^+$ ILC2s, CD117$^+$CRTH2$^-$ ILC3s, and NK cells isolated from the spleen of HSPC-engrafted MISTRG mice (n = 6). Matched isotype antibodies were used as controls. **(C)** Intracellular IFNγ expression by human ILCs and NK cells in the spleen of HSPC-engrafted MISTRG mice and in umbilical cord blood (n = 4). Cells were either unstimulated or stimulated with PMA and ionomycin for 6 hours. ILCs were gated as human CD45$^+$CD127$^+$CD94$^-$CD3$^-$TCRαβ$^-$Lin$^-$ cells and NK cells were gated as human CD45$^+$CD127$^-$CD94$^+$CD3$^-$TCRαβ$^-$Lin$^-$ cells as in Supplementary Figure 1. ILC subsets and NK cells were also gated as CD34$^-$ cells. Data represent mean ± SEM and are representative of two **(B, C)** or three (A) independent experiments.

MISTRG mice (Figures 5B, C). Taken together, these findings indicate that CD117$^-$CRTH2$^-$CD45RA$^+$ ILCs distribute *via* the vascular system and that they represent a conserved population in humans during early life.

CD117$^-$CRTH2$^-$CD45RA$^+$ ILCs appear early during ontogeny

Their presence during the neonatal period suggested that CD117$^-$CRTH2$^-$CD45RA$^+$ ILCs represented circulating immature cells that may seed various organs. To further explore the ontogeny of CD117$^-$CRTH2$^-$CD45RA$^+$ ILCs, we examined the kinetics of human ILC reconstitution in MISTRG mice after transplantation with CD34$^+$ HSPCs. CRTH2$^-$CD117$^-$ ILCs were present in all organs including the spleen, lung, and liver (Figures 6A, B). At 3 weeks post-transplantation, CD117$^-$CRTH2$^-$ ILCs were the prevalent ILC subset in peripheral organs (spleen, liver, lung) when compared to ILC2s and ILC3s (Figure 6A). These data support the notion that CD117$^-$CRTH2$^-$ ILCs appeared early before other ILC subsets during development. In the spleen, the frequency of CD45RA$^+$ cells within CD117$^-$CRTH2$^-$ ILCs decreased over time (Figures 6C, D), indicating a potential conversion of CD45RA$^+$ into CD45RA$^-$ CD117$^-$CRTH2$^-$ ILCs.

Next, we investigated the developmental niche occupied by CD117$^-$CRTH2$^-$CD45RA$^+$ ILCs in different organs of HSPC-engrafted MISTRG mice. We found that the frequency of CD117$^-$CRTH2$^-$CD45RA$^+$ ILCs was the same whether MISTRG mice were irradiated or not before transplantation with human CD34$^+$ HSPCs (Supplementary Figures 4A, B). This result suggested that clearing of their anatomical niche by irradiation is not required for the development of CD117$^-$CRTH2$^-$CD45RA$^+$ ILCs in MISTRG mice. These results are in line with human data showing that reconstitution of CD117$^-$CRTH2$^-$ ILC1s after hematopoietic stem cell transplantation

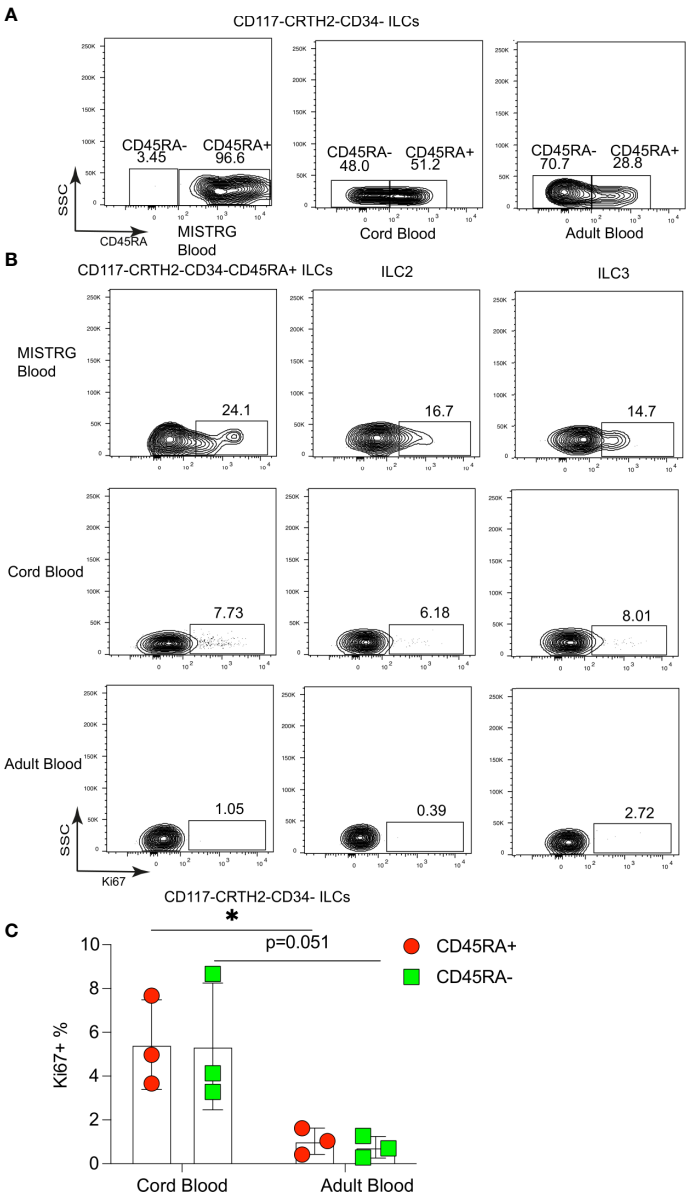

FIGURE 5
Proliferative CD117$^-$CRTH2$^-$CD45RA$^+$ ILCs are present in the circulation and in human umbilical cord blood. **(A)** CD45RA surface expression by CD117$^-$CRTH2$^-$ ILCs from the blood of HSPC-engrafted MISTRG mice, human umbilical cord blood, and human adult blood (n = 3). **(B)** Flow cytometry analysis of intracellular Ki67 expression by human CD117$^-$CRTH2$^-$CD34$^-$CD45RA$^+$ ILCs, CRTH2$^+$ ILC2s, and CD117$^+$CRTH2$^-$ ILC3s from the blood of HSPC-engrafted MISTRG mice as well as from human cord blood and human adult blood (n = 3). ILCs were gated as human CD45$^+$CD127$^+$CD94$^-$CD3$^-$TCRαβ$^-$Lin$^-$ cells as in Supplementary Figure 1. **(C)** Frequencies of Ki67$^+$ human CD117$^-$CRTH2$^-$CD34$^-$CD45RA$^+$ and CD117$^-$CRTH2$^-$CD34$^-$CD45RA$^-$ ILCs in human cord blood and adult blood (n = 3). *, P <0.05 by Student's *t* test. Data represent mean ± SEM and are from three independent experiments.

occurs in the absence of myeloablation (42). Collectively, these data demonstrate that CD117$^-$CRTH2$^-$CD45RA$^+$ ILCs appear early during development and inhabit a radio-insensitive developmental niche. These features indicate that CD117$^-$CRTH2$^-$CD45RA$^+$ ILCs may contribute to the expanding ILC compartment in early life.

Heterogeneity of vascular and tissue ILCs in the spleen defined by single-cell RNA-sequencing

To further define the heterogeneity of human ILCs located in the intra- and extravascular compartments of the spleen, we

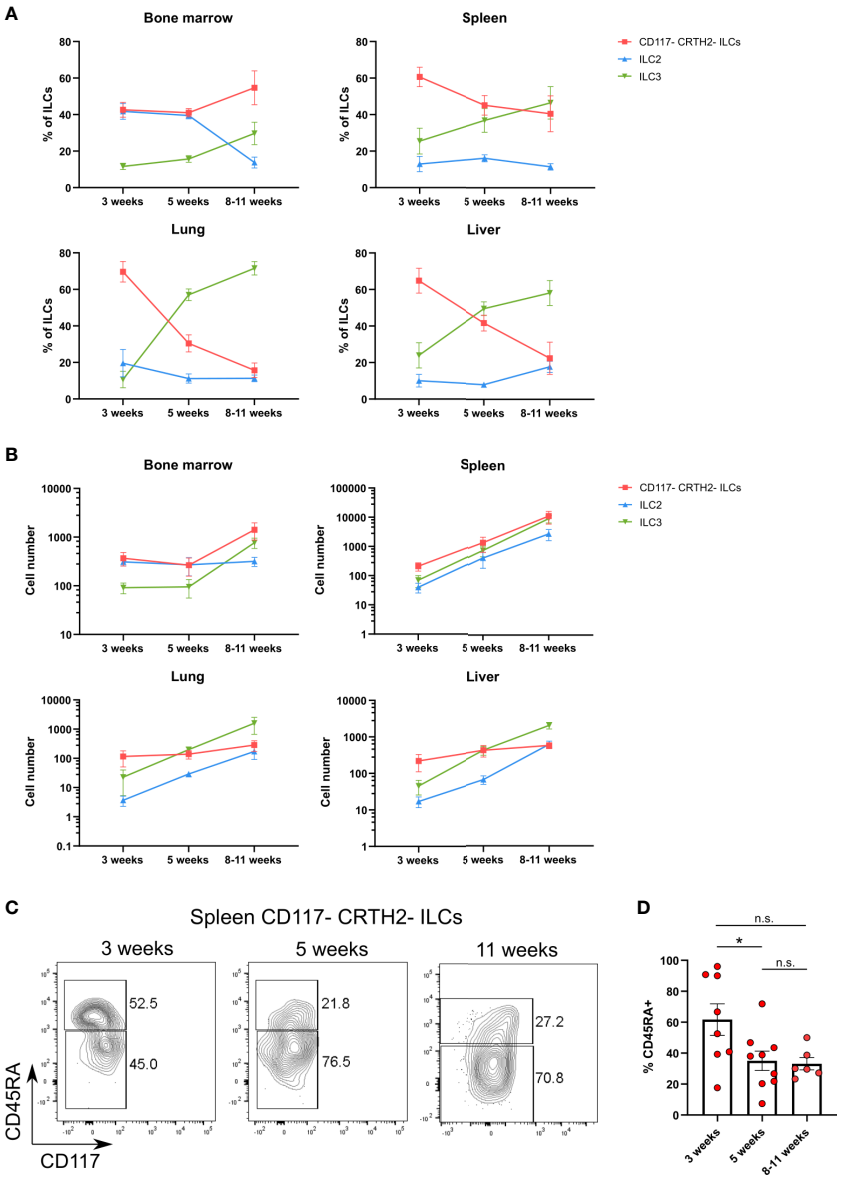

FIGURE 6
CD117$^-$CRTH2$^-$CD45RA$^+$ ILCs appear early during ontogeny in HSPC-engrafted MISTRG mice. **(A, B)** Frequencies **(A)** and numbers **(B)** of human CD117$^-$CRTH2$^-$ ILCs, CRTH2$^+$ ILC2s, and CD117$^+$CRTH2$^-$ ILC3s in bone marrow, spleen, lung, and liver at 3 weeks, 5 weeks, and 8-11 weeks after transplantation of MISTRG mice with human CD34$^+$ HSPCs (n = 6-9 per time-point). ILCs were gated as human CD45$^+$CD127$^+$CD94$^-$CD3$^-$ TCRαβ$^-$Lin$^-$ cells as in Supplementary Figure 1 and as CD34$^-$ cells. **(C)** Flow cytometry analysis of human CD117$^-$CRTH2$^-$ ILCs in the spleen of MISTRG mice at 3, 5, and 11 weeks after transplantation with human CD34$^+$ HSPCs (n = 6-9 per time-point). ILCs were gated as human CD45$^+$CD127$^+$CD94$^-$CD3$^-$TCRαβ$^-$Lin$^-$ cells as in Supplementary Figure 1 and as CD34$^-$ cells. **(D)** Frequency of CD45RA$^+$ cells among human CD117$^-$CRTH2$^-$ ILCs in the spleen of MISTRG mice at 3, 5, and 11 weeks after transplantation with human CD34$^+$ HSPCs (n = 6-9 per time-point). n.s., not significant; *, P <0.05 by one-way ANOVA, Tukey's post-test. Data represent mean ± SEM and are from two independent experiments.

employed single-cell RNA-sequencing using the 10x Genomics platform (Figure 7A). For this purpose, human ILCs were purified from the spleens of HSPC-engrafted MISTRG mice by cell sorting. Before spleen harvest, intravascular cell labeling with IV CD45-PE antibody was performed to isolate ILCs from the intravascular (IV CD45-PE$^+$) and extravascular space (IV CD45-PE$^-$) for single-cell RNA-sequencing. 11 transcriptionally different clusters could be distinguished after unsupervised clustering of cells by UMAP (Supplementary Figure 5A). After removal of minor contaminating clusters consisting of myeloid cells and red blood

cells, 8 clusters consisting of 4,936 lymphocytes remained for further analysis (Figure 7B). Cluster 7 corresponded to B lymphocytes (*JCHAIN, CD79A, HLA-DPA1*) and cluster 5 was identified as T lymphocytes or T cell progenitors (*CD3D, CD3G, TRBC1, RAG1, CD1B, CD1E, CD8B, LEF1*) that lacked TCRαβ and CD3 surface expression (Supplementary Table 2).

We then focused our analysis on the six remaining ILC clusters. Cells in cluster 4 mostly had an intravascular localization (Figure 7C) and were identified as ILC1s (and/or possibly $CD127^{+}CD94^{-}$ NK cells) based on genes expressed by ILC1s in human spleen (23), such lytic granule molecules (*GZMK, GNLY, NKG7*) and the chemokine *CCL5* (Figure 7D and Supplementary Table 2). Cluster 6 expressed genes characteristic of ILC2s, such as the signature transcription factor *GATA3*, transcripts for the ILC2 surface markers *KLRB1* (encoding CD161) and *KLRG1*, as well as the ILC2 signature genes *HPGD* and *HPGDS* (Figure 7E and Supplementary Table 2). ILC2s were present in both the vascular and tissue compartment of the spleen (Figure 7C).

Two separate clusters of ILC3s were present in the spleen (Figure 7B) that differed in their anatomical location. ILC3s of cluster 0 predominantly occupied the intravascular compartment of the spleen (Figure 7C). Consistent with their ILC3 identity, cells in cluster 0 were characterized by transcripts that are expressed by ILC3s in human spleen and other secondary lymphoid organs, such as *TNFRSF25* (encoding DR3), *TYROBP*, *NFKBIA*, *ZFP36* (23, 34, 43). In addition, ILC3s in cluster 0 expressed genes involved in cell migration, such as the adhesion molecules *ITGB1* and *CD44*, as well as genes encoding S100A proteins (*S100A4, S100A6, S100A10*) (Figure 7F and Supplementary Table 2). Their gene signature suggested that intravascular ILC3s actively migrate into the extravascular space of the spleen. The second cluster (cluster 1) preferentially resided within the tissue compartment of the spleen (Figure 7C). ILC3s in cluster 1 expressed the transcription factor *ID2*, as well as the ILC3 signatures genes *LTB* and *TNFRSF4* (encoding OX40) that are involved in lymphoid tissue organogenesis and interaction of ILC3s with other cells (Figure 7F and Supplementary Table 2). Cluster 1 cells transcribed other genes that are expressed by human ILC3s in secondary lymphoid organs, such as *B2M, HLA-B, HLA-C, TNFRSF18* (encoding GITR), *TYROBP*, *IFITM1*, *IFITM2* (26, 34, 43).

ILCs in cluster 3 were characterized by expression of *ZBTB16* (Figure 7G Supplementary Table 2), encoding the transcription factor PLZF that is expressed by all human ILC subsets (34, 44, 45) and required for ILC development in mice (39, 46, 47). Otherwise, *ZBTB16*-ILCs expressed few distinctive genes (Supplementary Table 2), suggesting that they may be less differentiated. Finally, the frequency of *ZBTB16*-ILCs was greater in the spleen vasculature than in spleen tissue (Figure 7C). In conclusion, we found that not only known human ILC subsets are present in the spleen of HSPC-engrafted MISTRG mice, but also a distinct population of *ZBTB16*-ILCs which may represent an intermediate ILC differentiation stage.

Single-cell gene signature of proliferative *MKI67*-ILCs

Cluster 2 ILCs were distinguished by the expression of genes associated with cell proliferation, such as *MKI67*, *TOP2A*, *PCNA*, and *STMN1* as well as cyclin-dependent kinases (Figure 8A and Supplementary Table 2). Accordingly, gene ontology categories overrepresented in cluster 2 ILCs included "mitotic cell cycle" and "cell cycle process" (Figure 8B). Cell cycle scoring analysis confirmed that *MKI67*-ILCs were proliferative as most cells in this cluster were scored as in S or G2/M phase (Figure 8C). Furthermore *MKI67*-ILCs were present in both the intra- and extravascular compartment of the spleen (Figure 7C). *MKI67*-ILCs expressed low amounts of the transcription factors *EOMES*, *TBX21*, and *RORC* (Supplementary Figures 5B, C) and lower amounts of *GATA3* than ILC2s in cluster 6 (Figure 7E), suggesting that *MKI67*-ILCs did not correspond to NK cells, ILC1s, ILC2s, or ILC3s. However, *MKI67*-ILCs expressed *TCF7* (encoding TCF-1) (Supplementary Figures 5B, C), consistent with the TCF-1 protein expression determined by flow cytometry (Figure 4B). *MKI67*-ILCs also expressed several transcription factors, such as *LEF1, ID3, BCL11A*, and *BCL11B* (Figure 8D), that regulate the proliferative potential of lymphocytes. LEF1 is downstream of the WNT signaling pathway and is associated with the self-renewal capacity of T lymphocytes and NK cells (36). Moreover, *LEF1* has been reported to be more highly expressed by human $CD117^{-}CRTH2^{-}$ ILCs than by other ILC subsets and NK cells (34, 45). *ID3* is expressed by TCF-1^{+} CD8 T cells with stem cell-like features (48–50) and by human cord blood ILCs that are functionally immature (51). Finally, *BCL11B* is expressed by human ILC1-like cells in umbilical cord blood (52), while *BCL11A* expression is shared by $CD117^{-}CRTH2^{-}$ ILCs in human spleen and $CD34^{+}CD127^{+}$ common lymphoid progenitors from umbilical cord blood (23). In summary, these data support the notion that a distinct cluster of proliferative human ILCs resides in the spleen.

Discussion

The function of ILCs is tightly linked to their anatomical location and, like other tissue-resident immune cells, such as macrophages, the local microenvironment imprints tissue-specific features on ILCs (19, 53). However, the proliferative hierarchy and anatomical compartmentalization of human ILCs *in vivo* has not been determined. Here, we visualized proliferating ILCs within the vascular and tissue compartments using intravascular cell labeling

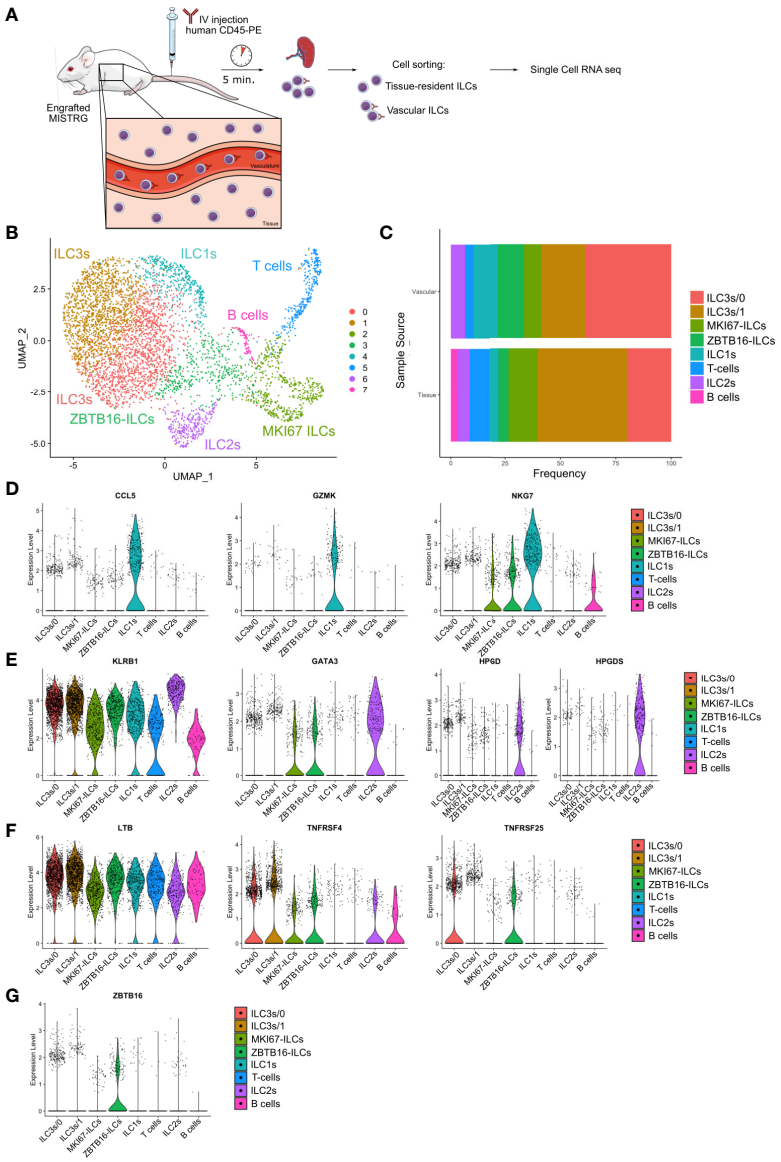

FIGURE 7
Heterogeneity of vascular and tissue ILCs in the spleen defined by single-cell RNA-sequencing. **(A)** Experimental outline. Human CD127$^+$CD94$^-$ ILCs were purified from both the intravascular and the extravascular (tissue) compartment of the spleen of HSPC-engrafted MISTRG mice and subjected to single-cell RNA-sequencing. **(B)** UMAP depicting human ILC clusters (4,935 cells) in the spleen of HSPC-engrafted MISTRG mice. **(C)** Frequency of ILC clusters within the vascular versus the tissue compartment of the spleen. **(D–G)** Violin plots showing expression of selected genes characteristic of ILC1 **(D)**, ILC2 **(E)**, ILC3 **(F)**, and *ZBTB16*-ILC **(G)** clusters. Data are from one single-cell RNA-sequencing experiment with spleen cells pooled from ten MISTRG mice engrafted with three pooled batches of human CD34$^+$ cells. **(A)** was created with Mind the Graph.

and single-cell RNA-sequencing in our MISTRG humanized mouse model. This allowed us to define the proliferative landscape of human ILCs within lymphoid and non-lymphoid organs (Supplementary Figure 6).

We found that proliferating ILCs occupied both the vascular and tissue space in various organs. Specifically, our approach allowed us to classify ILCs into four categories with distinct proliferative status and anatomical location (Supplementary Figure 6A). The first category corresponded to quiescent and intravascular ILCs. NK cells and ILC2s in spleen, lung, and liver as well as ILC3s in lung and liver belonged to this category. The second category of quiescent and tissue-resident ILCs was mainly represented by CD117$^+$CRTH2$^-$ ILC3s and ILCPs (24) in the spleen. The third category of proliferative and

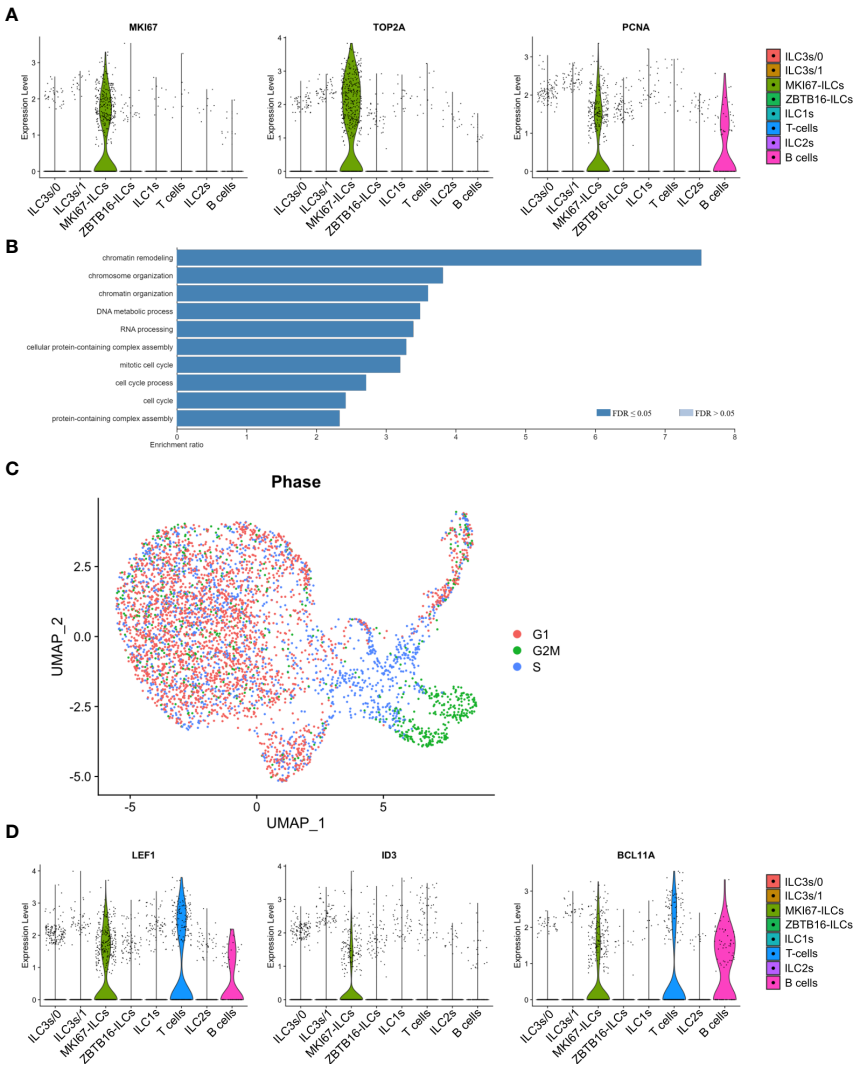

FIGURE 8
Single-cell gene signature of proliferative *MKI67*-ILCs. **(A)** Violin plots showing expression of proliferation-associated genes in the human ILC clusters from the UMAP in Figure 7B. **(B)** Gene Ontology over-representation analysis of genes differentially expressed by *MKI67*-ILCs. FDR, false-discovery rate. **(C)** Cell cycle scoring of ILCs superimposed on the UMAP from Figure 7B. **(D)** Violin plots showing expression of selected transcription factors in the human ILC clusters from the UMAP in Figure 7B. Data are from one single-cell RNA-sequencing experiment with spleen cells pooled from ten MISTRG mice engrafted with three pooled batches of human $CD34^+$ cells.

intravascular ILCs included lung and liver NK cells as well as the proliferative $CD117^-CRTH2^-CD45RA^+$ ILCs that we discovered in the spleen vasculature and in the systemic circulation. $CD117^-CRTH2^-CD45RA^+$ ILCs in the spleen also belonged to the fourth category of proliferative and tissue-resident ILCs.

The highly proliferative $CD117^-CRTH2^-$ human ILC population that we discovered had a naïve surface phenotype ($CD45RA^+$) and was characterized by the absence of transcription factors associated with mature ILCs. Despite having a surface phenotype ($CD117^-CRTH2^-$) that is normally associated with ILC1s, most $CD117^-CRTH2^-CD45RA^+$ ILCs lacked expression of the ILC1-defining transcription factor T-BET and did not produce IFNγ. Instead, this population expressed TCF-1, characteristic of lymphocytes with high proliferative capacity (54, 55). Therefore, proliferative $CD117^-CRTH2^-$ ILCs mostly represented $CD45RA^+T\text{-}BET^{lo}TCF\text{-}1^{hi}$ immature ILCs. Furthermore, this proliferative ILC population emerged early after transplantation of MISTRG mice with human $CD34^+$ HSPCs and was also present in human umbilical cord blood. Their "young" ontogeny supports the notion that proliferative $CD117^-CRTH2^-CD45RA^+$ ILCs may contribute to the ILC compartment in early life. Proliferative

$CD117^-CRTH2^-CD45RA^+$ ILCs were located in both the vascular and tissue compartment of lymphoid and non-lymphoid organs in HSPC-engrafted MISTRG mice but were most abundant in the spleen. Moreover, their spatial distribution is consistent with the idea that proliferative ILCs migrate from the local vasculature into the tissue compartment of the spleen. Overall, these observations suggest a link between ILC proliferation and migration in response to local cues leading to the establishment of tissue-resident ILCs.

We observed that $CD117^-CRTH2^-CD45RA^+$ ILCs were particularly abundant in the spleen, raising the idea that the spleen constitutes a proliferative niche for ILCs. It is therefore possible that ILC proliferation takes place in the spleen and $Ki67^+$ ILCs subsequently enter the circulation to disperse systemically. Alternatively, proliferating ILCs could egress from the bone marrow into the systemic circulation and thereby reach the local spleen vasculature. However, proliferating $CD117^-CRTH2^-CD45RA^+$ ILCs were almost absent from the bone marrow vasculature, arguing against this possibility. A previous study reported that the spleen environment promotes ILC1 differentiation in humanized mice (45). Furthermore, human $CD117^-CRTH2^-$ ILCs, described as ILC1s, show less transcriptional heterogeneity in lymphoid organs than at mucosal sites (23). ILCs in lymphoid tissues may receive less imprinting by local tissue cues than their counterparts in the mucosa because lymphoid organs are not directly exposed to the outside environment. Therefore, it seems plausible that "ILC1s" in lymphoid organs may be less differentiated. This is consistent with our observation that $CD117^-CRTH2^-$ ILCs in the spleen are highly proliferative and do not have features of mature ILC1s, such as T-BET expression and IFNγ production.

Unexpectedly, we detected a sizeable fraction of $Ki67^+$ ILCs within the vasculature in several organs of HSPC-engrafted MISTRG mice as well as in human blood during the neonatal period. In general, circulating (intravascular) immune cells, such as neutrophils, monocytes, and NK cells (36) are thought to represent mobile cells that do not proliferate in steady state. This raises the question whether $Ki67^+$ ILCs actively undergo cell division in the circulation because shear forces generated due to rapid blood flow likely make it difficult for cells to divide, at least in large blood vessels. However, the blood flow slows down in smaller vessels and capillaries, resulting in lower shear forces in the local vasculature of organs. Therefore, $Ki67^+$ ILCs could divide in the local vasculature when they adhere to the endothelium. Alternatively, intravascular $Ki67^+$ ILCs could represent cells that initiated cell division within tissues before entering the systemic circulation. This idea is supported by mouse studies showing that ILC proliferation occurs locally in the intestine before inter-organ trafficking of ILC2s to the lung *via* the circulation (10). Another possibility is that circulating $Ki67^+$ ILCs have entered the cell cycle and are primed to complete cell division when they enter tissues from the blood. Consistent with this concept, we found that $CD117^-CRTH2^-CD45RA^+$ ILCs that expressed intracellular Ki67 protein were mostly in the G1 phase of the cell cycle.

Due to their potent effector functions and strategic positioning, the expansion of ILCs needs to be tightly controlled to avoid tissue pathology and chronic inflammation (56–58). Therefore, understanding the mechanisms of ILC proliferation and migration are of importance in the context of human diseases, where ILCs play a role, such as infection, inflammation, and cancer.

Limitations of the study

MISTRG mice support human ILC-poiesis and the generation of all ILC subsets, thereby allowing to investigate the biology of human ILCs *in vivo* in a small animal model. One limitation is that human ILCs interact with the mouse tissue environment in MISTRG mice, such as the mouse endothelial cells. However, human ILCs distribute between the vascular and the tissue space within several organs in MISTRG mice, demonstrating that this model supports the migration of human ILCs across the mouse endothelium into tissues. Another limitation is that, besides the spleen, other lymphoid organs, especially lymph nodes, are not fully developed in MISTRG mice, which may affect ILC trafficking and proliferation. Finally, the relatively lymphopenic environment in MISTRG mice could potentially favor increased ILC proliferation. However, this situation is similar to the neonatal period when proliferating ILCs are more abundant in the circulation as shown in our study. Despite the limitations, studying human ILCs *in vivo* in the MISTRG model generates relevant knowledge beyond what is possible to obtain by analyzing ILCs from human blood and tissues *ex vivo*.

Data availability statement

The datasets presented in this study can be found in online repositories. The names of the repository/repositories and accession number(s) can be found below: https://www.ncbi.nlm.nih.gov/geo/, GSE199965.

Ethics statement

This study was reviewed and approved by Ethical Review Board at Karolinska Institutet. The patients/participants provided their written informed consent to participate in this study. The animal study was reviewed and approved by Linköping Animal Experimentation Ethics Committee.

Author contributions

YG and AA designed, performed, and analyzed most experiments. AA contributed to writing the paper. DB analyzed single-cell RNA-sequencing data. NS helped with mouse experiments. JD supervised single-cell RNA-sequencing analysis. TW conceived and supervised the study, acquired funding, designed experiments, analyzed data, and wrote the paper. All authors contributed to the article and approved the submitted version.

Funding

TW was supported by a faculty-funded career position at Karolinska Institutet (2-1060/2018), a KID grant from Karolinska Institutet (2018-00846), a Junior Investigator Grant from the Center for Innovative Medicine (CIMED) financed by Region Stockholm (2-538/2014), as well as a Project Grant from the Swedish Research Council (2015-02413). JD was supported by grants from the Swedish Research Council (2018-02070) and the Swedish Cancer Society.

Acknowledgments

We thank Regeneron Pharmaceuticals and Yale University for being able to use MISTRG mice.

Conflict of interest

The authors declare that the research was conducted in the absence of any commercial or financial relationships that could be construed as a potential conflict of interest.

Publisher's note

Supplementary material

The Supplementary Material for this article can be found online at: https://www.frontiersin.org/articles/10.3389/fimmu.2022.902881/full#supplementary-material

SUPPLEMENTARY TABLE 1
List of antibodies used for flow cytometry.

SUPPLEMENTARY TABLE 2
Genes in each human ILC cluster from the spleens of HSPC-engrafted MISTRG mice as defined by single-cell RNA-sequencing.

References

1. Artis D, Spits H. The biology of innate lymphoid cells. *Nature* (2015) 517 (7534):293–301. doi: 10.1038/nature14189

2. Eberl G, Colonna M, Di Santo JP, McKenzie AN. Innate lymphoid cells. innate lymphoid cells: a new paradigm in immunology. *Science* (2015) 348(6237): aaa6566. doi: 10.1126/science.aaa6566

3. Vivier E, Artis D, Colonna M, Diefenbach A, Di Santo JP, Eberl G, et al. Innate lymphoid cells: 10 years on. *Cell* (2018) 174(5):1054–66. doi: 10.1016/j.cell.2018.07.017

4. Colonna M. Innate lymphoid cells: Diversity, plasticity, and unique functions in immunity. *Immunity* (2018) 48(6):1104–17. doi: 10.1016/j.immuni.2018.05.013

5. Bal SM, Golebski K, Spits H. Plasticity of innate lymphoid cell subsets. *Nat Rev Immunol* (2020) 20(9):552–65. doi: 10.1038/s41577-020-0282-9

6. Kotas ME, Locksley RM. Why innate lymphoid cells? *Immunity* (2018) 48 (6):1081–90. doi: 10.1016/j.immuni.2018.06.002

7. Hazenberg MD, Spits H. Human innate lymphoid cells. *Blood* (2014) 124 (5):700–9. doi: 10.1182/blood-2013-11-427781

8. Gasteiger G, Fan X, Dikiy S, Lee SY, Rudensky AY. Tissue residency of innate lymphoid cells in lymphoid and nonlymphoid organs. *Science* (2015) 350(6263):981–5. doi: 10.1126/science.aac9593

9. Emgard J, Kammoun H, Garcia-Cassani B, Chesne J, Parigi SM, Jacob JM, et al. Oxysterol sensing through the receptor GPR183 promotes the lymphoid-Tissue-Inducing function of innate lymphoid cells and colonic inflammation. *Immunity* (2018) 48(1):120–32.e8. doi: 10.1016/j.immuni.2017.11.020

10. Huang Y, Mao K, Chen X, Sun MA, Kawabe T, Li W, et al. S1P-dependent interorgan trafficking of group 2 innate lymphoid cells supports host defense. *Science* (2018) 359(6371):114–9. doi: 10.1126/science.aam5809

11. Zeis P, Lian M, Fan X, Herman JS, Hernandez DC, Gentek R, et al. *In situ* maturation and tissue adaptation of type 2 innate lymphoid cell progenitors. *Immunity* (2020) 53(4):775–92.e9. doi: 10.1016/j.immuni.2020.09.002

12. Pearson C, Thornton EE, McKenzie B, Schaupp AL, Huskens N, Griseri T, et al. ILC3 GM-CSF production and mobilisation orchestrate acute intestinal inflammation. *Elife* (2016) 5:e10066. doi: 10.7554/eLife.10066

13. Puttur F, Denney L, Gregory LG, Vuononvirta J, Oliver R, Entwistle LJ, et al. Pulmonary environmental cues drive group 2 innate lymphoid cell dynamics in mice and humans. *Sci Immunol* (2019) 4(36):eaav7638. doi: 10.1126/sciimmunol.aav7638

14. Kim MH, Taparowsky EJ, Kim CH. Retinoic acid differentially regulates the migration of innate lymphoid cell subsets to the gut. *Immunity* (2015) 43(1):107–19. doi: 10.1016/j.immuni.2015.06.009

15. Kastele V, Mayer J, Lee ES, Papazian N, Cole JJ, Cerovic V, et al. Intestinal-derived ILCs migrating in lymph increase IFNgamma production in response to salmonella typhimurium infection. *Mucosal Immunol* (2021) 14(3):717–27. doi: 10.1038/s41385-020-00366-3

16. Dutton EE, Gajdasik DW, Willis C, Fiancette R, Bishop EL, Camelo A, et al. Peripheral lymph nodes contain migratory and resident innate lymphoid cell populations. *Sci Immunol* (2019) 4(35):eaau8082. doi: 10.1126/sciimmunol.aau8082

17. Ricardo-Gonzalez RR, Schneider C, Liao C, Lee J, Liang HE, Locksley RM. Tissue-specific pathways extrude activated ILC2s to disseminate type 2 immunity. *J Exp Med* (2020) 217(4):e20191172. doi: 10.1084/jem.20191172

18. Cautivo KM, Matatia PR, Lizama CO, Mroz NM, Dahlgren MW, Yu X, et al. Interferon gamma constrains type 2 lymphocyte niche boundaries during mixed inflammation. *Immunity* (2022) 55(2):254–71.e7. doi: 10.1016/j.immuni.2021.12.014

19. Ricardo-Gonzalez RR, Van Dyken SJ, Schneider C, Lee J, Nussbaum JC, Liang HE, et al. Tissue signals imprint ILC2 identity with anticipatory function. *Nat Immunol* (2018) 19(10):1093–9. doi: 10.1038/s41590-018-0201-4

20. Kim CH, Hashimoto-Hill S, Kim M. Migration and tissue tropism of innate lymphoid cells. *Trends Immunol* (2016) 37(1):68–79. doi: 10.1016/j.it.2015.11.003

21. Willinger T. Metabolic control of innate lymphoid cell migration. *Front Immunol* (2019) 10:2010. doi: 10.3389/fimmu.2019.02010

22. Simoni Y, Fehlings M, Kloverpris HN, McGovern N, Koo SL, Loh CY, et al. Human innate lymphoid cell subsets possess tissue-type based heterogeneity in phenotype and frequency. *Immunity* (2017) 46(1):148–61. doi: 10.1016/j.immuni.2016.11.005

23. Yudanin NA, Schmitz F, Flamar AL, Thome JJC, Tait Wojno E, Moeller JB, et al. Spatial and temporal mapping of human innate lymphoid cells reveals elements of tissue specificity. *Immunity* (2019) 50(2):505–19.e4. doi: 10.1016/j.immuni.2019.01.012

24. Lim AI, Li Y, Lopez-Lastra S, Stadhouders R, Paul F, Casrouge A, et al. Systemic human ILC precursors provide a substrate for tissue ILC differentiation. *Cell* (2017) 168(6):1086–100.e10. doi: 10.1016/j.cell.2017.02.021

25. Bar-Ephraim YE, Koning JJ, Burniol Ruiz E, Konijn T, Mourits VP, Lakeman KA, et al. CD62L is a functional and phenotypic marker for circulating innate lymphoid cell precursors. *J Immunol* (2019) 202(1):171–82. doi: 10.4049/jimmunol.1701153

26. Nagasawa M, Heesters BA, Kradolfer CMA, Krabbendam L, Martinez-Gonzalez I, de Bruijn MJW, et al. KLRG1 and NKp46 discriminate subpopulations of human CD117(+)CRTH2(-) ILCs biased toward ILC2 or ILC3. *J Exp Med* (2019) 216(8):1762–76. doi: 10.1084/jem.20190490

27. Rongvaux A, Willinger T, Martinek J, Strowig T, Gearty SV, Teichmann LL, et al. Development and function of human innate immune cells in a humanized mouse model. *Nat Biotechnol* (2014) 32(4):364–72. doi: 10.1038/nbt.2858

28. Willinger T, Rongvaux A, Strowig T, Manz MG, Flavell RA. Improving human hemato-lymphoid-system mice by cytokine knock-in gene replacement. *Trends Immunol* (2011) 32(7):321–7. doi: 10.1016/j.it.2011.04.005

29. Rongvaux A, Takizawa H, Strowig T, Willinger T, Eynon EE, Flavell RA, et al. Human hemato-lymphoid system mice: current use and future potential for medicine. *Annu Rev Immunol* (2013) 31:635–74. doi: 10.1146/annurev-immunol-032712-095921

30. Alisjahbana A, Mohammad I, Gao Y, Evren E, Ringqvist E, Willinger T. Human macrophages and innate lymphoid cells: Tissue-resident innate immunity in humanized mice. *Biochem Pharmacol* (2020) 174:113672. doi: 10.1016/j.bcp.2019.113672

31. Alisjahbana A, Gao Y, Sleiers N, Evren E, Brownlie D, von Kries A, et al. CD5 surface expression marks intravascular human innate lymphoid cells that have a distinct ontogeny and migrate to the lung. *Front Immunol* (2021) 12:752104. doi: 10.3389/fimmu.2021.752104

32. Deng K, Pertea M, Rongvaux A, Wang L, Durand CM, Ghiaur G, et al. Broad CTL response is required to clear latent HIV-1 due to dominance of escape mutations. *Nature* (2015) 517(7534):381–5. doi: 10.1038/nature14053

33. Evren E, Ringqvist E, Tripathi KP, Sleiers N, Rives IC, Alisjahbana A, et al. Distinct developmental pathways from blood monocytes generate human lung macrophage diversity. *Immunity* (2021) 54(2):259–75.e7. doi: 10.1016/j.immuni.2020.12.003

34. Bjorklund AK, Forkel M, Picelli S, Konya V, Theorell J, Friberg D, et al. The heterogeneity of human CD127(+) innate lymphoid cells revealed by single-cell RNA sequencing. *Nat Immunol* (2016) 17(4):451–60. doi: 10.1038/ni.3368

35. van der Ploeg EK, Golebski K, van Nimwegen M, Fergusson JR, Heesters BA, Martinez-Gonzalez I, et al. Steroid-resistant human inflammatory ILC2s are marked by CD45RO and elevated in type 2 respiratory diseases. *Sci Immunol* (2021) 6(55):eabd3489. doi: 10.1126/sciimmunol.abd3489

36. Collins PL, Cella M, Porter SI, Li S, Gurewitz GL, Hong HS, et al. Gene regulatory programs conferring phenotypic identities to human NK cells. *Cell* (2019) 176(1-2):348–60.e12. doi: 10.1016/j.cell.2018.11.045

37. Friedrich C, Taggenbrock R, Doucet-Ladeveze R, Golda G, Moenius R, Arampatzi P, et al. Effector differentiation downstream of lineage commitment in ILC1s is driven by hobit across tissues. *Nat Immunol* (2021) 22(10):1256–67. doi: 10.1038/s41590-021-01013-0

38. Cherrier DE, Serafini N, Di Santo JP. Innate lymphoid cell development: A T cell perspective. *Immunity* (2018) 48(6):1091–103. doi: 10.1016/j.immuni.2018.05.010

39. Constantinides MG, McDonald BD, Verhoef PA, Bendelac A. A committed precursor to innate lymphoid cells. *Nature* (2014) 508(7496):397–401. doi: 10.1038/nature13047

40. Juelke K, Romagnani C. Differentiation of human innate lymphoid cells (ILCs). *Curr Opin Immunol* (2016) 38:75–85. doi: 10.1016/j.coi.2015.11.005

41. Scoville SD, Freud AG, Caligiuri MA. Cellular pathways in the development of human and murine innate lymphoid cells. *Curr Opin Immunol* (2019) 56:100–6. doi: 10.1016/j.coi.2018.11.003

42. Vely F, Barlogis V, Vallentin B, Neven B, Piperoglou C, Ebbo M, et al. Evidence of innate lymphoid cell redundancy in humans. *Nat Immunol* (2016) 17(11):1291–9. doi: 10.1038/ni.3553

43. Bar-Ephraim YE, Cornelissen F, Papazian N, Konijn T, Hoogenboezem RM, Sanders MA, et al. Cross-tissue transcriptomic analysis of human secondary lymphoid organ-residing ILC3s reveals a quiescent state in the absence of inflammation. *Cell Rep* (2017) 21(3):823–33. doi: 10.1016/j.celrep.2017.09.070

44. Hernandez DC, Juelke K, Muller NC, Durek P, Ugursu B, Mashreghi MF, et al. An in vitro platform supports generation of human innate lymphoid cells from CD34(+) hematopoietic progenitors that recapitulate ex vivo identity. *Immunity* (2021) 54(10):2417–32.e5. doi: 10.1016/j.immuni.2021.07.019

45. Cella M, Gamini R, Secca C, Collins PL, Zhao S, Peng V, et al. Subsets of ILC3-ILC1-like cells generate a diversity spectrum of innate lymphoid cells in human mucosal tissues. *Nat Immunol* (2019) 20(8):980–91. doi: 10.1038/s41590-019-0425-y

46. Xu W, Cherrier DE, Chea S, Vosshenrich C, Serafini N, Petit M, et al. An Id2 (RFP)-reporter mouse redefines innate lymphoid cell precursor potentials. *Immunity* (2019) 50(4):1054–68.e3. doi: 10.1016/j.immuni.2019.02.022

47. Walker JA, Clark PA, Crisp A, Barlow JL, Szeto A, Ferreira ACF, et al. Polychromic reporter mice reveal unappreciated innate lymphoid cell progenitor heterogeneity and elusive ILC3 progenitors in bone marrow. *Immunity* (2019) 51(1):104–18.e7. doi: 10.1016/j.immuni.2019.05.002

48. Pais Ferreira D, Silva JG, Wyss T, Fuertes Marraco SA, Scarpellino L, Charmoy M, et al. Central memory CD8(+) T cells derive from stem-like Tcf7(hi) effector cells in the absence of cytotoxic differentiation. *Immunity* (2020) 53(5):985–1000.e11. doi: 10.1016/j.immuni.2020.09.005

49. Ji Y, Pos Z, Rao M, Klebanoff CA, Yu Z, Sukumar M, et al. Repression of the DNA-binding inhibitor Id3 by blimp-1 limits the formation of memory CD8+ T cells. *Nat Immunol* (2011) 12(12):1230–7. doi: 10.1038/ni.2153

50. Shan Q, Hu SS, Zhu S, Chen X, Badovinac VP, Peng W, et al. Tcf1 preprograms the mobilization of glycolysis in central memory CD8(+) T cells during recall responses. *Nat Immunol* (2022) 23(3):386–98. doi: 10.1038/s41590-022-01131-3

51. Bennstein SB, Scherenschlich N, Weinhold S, Manser AR, Noll A, Raba K, et al. Transcriptional and functional characterization of neonatal circulating innate lymphoid cells. *Stem Cells Transl Med* (2021) 10(6):867–82. doi: 10.1002/sctm.20-0300

52. Bennstein SB, Weinhold S, Manser AR, Scherenschlich N, Noll A, Raba K, et al. Umbilical cord blood-derived ILC1-like cells constitute a novel precursor for mature KIR(+)NKG2A(-) NK cells. *Elife* (2020) 9:e55232. doi: 10.7554/eLife.55232

53. Mazzurana L, Czarnewski P, Jonsson V, Wigge L, Ringner M, Williams TC, et al. Tissue-specific transcriptional imprinting and heterogeneity in human innate lymphoid cells revealed by full-length single-cell RNA-sequencing. *Cell Res* (2021) 31(5):554–68. doi: 10.1038/s41422-020-00445-x

54. Escobar G, Mangani D, Anderson AC. T Cell factor 1: A master regulator of the T cell response in disease. *Sci Immunol* (2020) 5(53):eabb9726. doi: 10.1126/sciimmunol.abb9726

55. Zhao X, Shan Q, Xue HH. TCF1 in T cell immunity: a broadened frontier. *Nat Rev Immunol* (2021) 22(3):147–57. doi: 10.1038/s41577-021-00563-6

56. Sonnenberg GF, Artis D. Innate lymphoid cells in the initiation, regulation and resolution of inflammation. *Nat Med* (2015) 21(7):698–708. doi: 10.1038/nm.3892

57. Branzk N, Gronke K, Diefenbach A. Innate lymphoid cells, mediators of tissue homeostasis, adaptation and disease tolerance. *Immunol Rev* (2018) 286(1):86–101. doi: 10.1111/imr.12718

58. Ebbo M, Crinier A, Vely F, Vivier E. Innate lymphoid cells: major players in inflammatory diseases. *Nat Rev Immunol* (2017) 17(11):665–78. doi: 10.1038/nri.2017.86

frontiers | Frontiers in Immunology

TYPE Review
PUBLISHED 16 August 2022
DOI 10.3389/fimmu.2022.946905

OPEN ACCESS

EDITED BY
Carolina Jancic,
Consejo Nacional de Investigaciones Científicas y Técnicas (CONICET), Argentina

REVIEWED BY
Hirohito Kita,
Mayo Clinic, United States
Bernd Heinrich,
National Institutes of Health (NIH), United States
Giuseppe Sciumè,
Sapienza University of Rome, Italy

*CORRESPONDENCE
Kelly M. McNagny
kelly@brc.ubc.ca

SPECIALTY SECTION
This article was submitted to NK and Innate Lymphoid Cell Biology, a section of the journal Frontiers in Immunology

RECEIVED 18 May 2022
ACCEPTED 26 July 2022
PUBLISHED 16 August 2022

CITATION
Kabil A, Shin SB, Hughes MR and McNagny KM (2022) "Just one word, plastic!": Controversies and caveats in innate lymphoid cell plasticity. *Front. Immunol.* 13:946905. doi: 10.3389/fimmu.2022.946905

"Just one word, plastic!": Controversies and caveats in innate lymphoid cell plasticity

Ahmed Kabil[1], Samuel B. Shin[1], Michael R. Hughes[1] and Kelly M. McNagny[1,2,3]*

[1]School of Biomedical Engineering, University of British Columbia, Vancouver, BC, Canada, [2]Department of Medical Genetics, University of British Columbia, Vancouver, BC, Canada, [3]Centre for Heart and Lung Innovation (HLI), St Paul's Hospital, University of British Columbia, Vancouver, BC, Canada

Innate lymphoid cells (ILCs) are frontline immune effectors involved in the early stages of host defense and maintenance of tissue homeostasis, particularly at mucosal surfaces such as the intestine, lung, and skin. Canonical ILCs are described as tissue-resident cells that populate peripheral tissues early in life and respond appropriately based on environmental exposure and their anatomical niche and tissue microenvironment. Intriguingly, there are accumulating reports of ILC "plasticity" that note the existence of non-canonical ILCs that exhibit distinct patterns of master transcription factor expression and cytokine production profiles in response to tissue inflammation. Yet this concept of ILC-plasticity is controversial due to several confounding caveats that include, among others, the independent large-scale recruitment of new ILC subsets from distal sites and the local, in situ, differentiation of uncommitted resident precursors. Nevertheless, the ability of ILCs to acquire unique characteristics and adapt to local environmental cues is an attractive paradigm because it would enable the rapid adaptation of innate responses to a wider array of pathogens even in the absence of pre-existing 'prototypical' ILC responder subsets. Despite the impressive recent progress in understanding ILC biology, the true contribution of ILC plasticity to tissue homeostasis and disease and how it is regulated remains obscure. Here, we detail current methodologies used to study ILC plasticity in mice and review the mechanisms that drive and regulate functional ILC plasticity in response to polarizing signals in their microenvironment and different cytokine milieus. Finally, we discuss the physiological relevance of ILC plasticity and its implications for potential therapeutics and treatments.

KEYWORDS

plasticity, migration, mucosal immunology, inflammation, innate lymphoid cell (ILC), controversy, transdifferentiation, local progenitors

Introduction

The innate lymphoid cell (ILC) family is a heterogeneous group of recently discovered immune-modulatory cells at the centre of extensive research. ILCs are now widely accepted to fulfill a similar set of biological functions to their more extensively studied relatives, $CD4^+$ helper (Th) and $CD8^+$ cytotoxic T cells (T_{CTL}). Yet, they perform these complementary roles in the absence of an antigen-specific receptor [i.e., functional T cell receptor (TCR)] and thus, represent an innate branch of this lymphocyte family (1). Besides the well-known and well-characterized cytotoxic innate lymphoid cells, namely natural killer (NK) cells, the more recently discovered groups of cytokine-producing "helper-like" ILC lineages were identified by several laboratories between 2008-2010 (2–16).

NK cells primarily function as cytotoxic cells that circulate in the bloodstream and can be thought of as an innate branch of lymphocytes serving parallel functions to $CD8^+$ T_{CTL} (17). "Helper-like" ILCs (ILC1, ILC2, and ILC3) are mainly tissue-resident with the capacity to migrate in response to inflammation (18, 19). Each ILC subset has distinct functional capabilities (20); ILC1s are activated in response to interleukin (IL)-12, IL-15, and IL-18 and primarily produce interferon gamma (IFNγ), which is associated with defence against viruses and intracellular bacteria. ILC2s are activated by IL-25, IL-33, or TSLP and, in response, produce type 2 cytokines, mainly IL-5 and IL-13, which are important in promoting allergic reactions but also serve as barrier surface defence mechanisms to eliminate parasitic infections. ILC3s are activated in response to IL-1β or IL-23 and produce IL-17 and IL-22, which are important for defence against extracellular pathogens, including bacteria and fungi. The principal activators and effector cytokines of different ILC subsets are of interest because accumulating evidence suggest that they are critical for tissue repair and homeostasis, metabolic regulation, and in neuroimmune circuits with enteric neurons (1). Despite the role of ILCs within the multi-layered regulation of barrier defenses, they have also been associated with tissue pathology in several inflammatory diseases, including allergic asthma, dermatitis, psoriasis, and intestinal inflammation (21).

ILCs populate the peripheral tissues very early in ontogeny (e.g., embryonic day (E) 12.5 – E13.5 in mice) and are postnatally activated at the time of birth, serving as an early guard against infection (22–24). ILCs are most frequently observed in tissues, particularly at barrier surfaces of tissues including the gut, skin, and lungs, and respond to various rapidly released damage-associated microenvironmental factors (collectively termed "alarmins"), neuropeptides, and cytokines (Figure 1) (25). Acting as danger signals, alarmins are typically secreted by local tissue epithelial cells and stroma in response to local epithelia insults or infection. As first responders, tissue-resident ILCs then interpret these immediate signals and orchestrate the subsequent, appropriate downstream immune effector cell response (26, 27). ILCs are poised to provide a rapid response because they acquire chromatin accessibility for critical effector cytokine genes in the early stages of cellular maturation and development, prior to activation (28). By contrast, naïve T cells need to be primed, activated, and appropriately polarized in lymph nodes prior to the subsequent

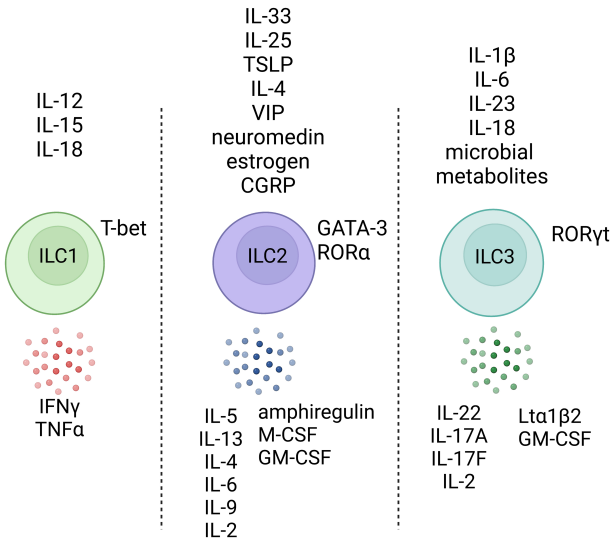

FIGURE 1
Helper-like innate lymphoid cells respond to various environmental factors. ILCs do not express an antigen-specific receptor but can respond to various environmental factors and, upon stimulation, produce effector cytokines that pattern the stereotype modules that the immune system has evolved to interact with tissues, the outside world, and organisms. Created with Biorender.org.

migration to effector sites, making their response relatively slow. Therefore, ILCs represent a local source of appropriate effector cytokines during the earliest stages of infection, providing a first innate response that allows critical time for the more targeted T cells to become instructed and recruited (29).

Mature ILCs are typically defined by T cell and NK cell lineage-determining transcription factors, and the lack of lineage-specific surface markers such as CD14 (myeloid cells), CD49b (NK cells), CD19 (B cells), CD3 (T-cells), among others (30). ILC1s are dependent on the canonical Th1-type transcriptional regulator, T-bet (*Tbx21*), but not the conventional NK (cNK) transcription factor EOMES (31, 32). ILC2s are characterized by the high expression of GATA3 and RAR-related orphan receptor alpha (RORα) (33–35). ILC3s express the Th17-associated transcription factor RAR-related orphan receptor gamma (RORγt). Although these properties initially guided the classification of ILCs into subsets and their placement within the hematopoietic phylogenetic tree, an influx of single cell studies has begun to reveal a complex network between different ILC subgroups as well as possible evidence of plasticity between specific subclasses of ILCs under certain conditions (36–40). Notably, these studies demonstrate that ILCs are likely much more heterogeneous than initially thought, even within subgroups that express the same "master" transcription factors, possibly reflecting more fine-tuned gene expression linked to their tissue microenvironment and rapid changes in response to the local inflammatory milieu (Table 1).

Increasing evidence suggests that ILC subsets are not intrinsically stable and can exhibit considerable plasticity *in vivo* and *in vitro*, most notably with the transdifferentiation of ILC3s into ILC1s through the upregulation of the canonical type 1 transcription factor T-bet and downregulation of RORγt (32, 53, 54, 61, 62). Nevertheless, other studies have reported that during inflammation, ILCs can acquire the ability to egress from the tissues of steady-state residence, enter the circulation, and travel to different anatomical locations and this can serve as a confounder in many studies examining apparent plasticity (48, 49, 63). Additionally, similar ILC subsets from distal tissues have distinctive patterns of tissue-specific gene signatures; for example, IL-33 receptor expression is largely limited to ILC2s in the lungs, whereas the IL-25 receptor is highly expressed by ILC2s in the small intestine and not by lung ILC2s (37). Therefore, the apparent upregulation of novel markers by resident cells, may, in fact, simply reflect the orchestrated recruitment of peripheral cells with a distinctive phenotype (48, 50). Thus, true evidence of plasticity is critically dependent on the use of a combination of epigenetic and transcriptional analyses at the single-cell level coupled with methods for lineage tracing. These key mechanistic details are critical to understanding ILC function in health and disease and their manipulation in designing new avenues for therapy.

In the current review, we focus on the phenomenon of ILC plasticity in mouse models which, through extrapolation to humans, could have significant clinical applications, specifically in the treatment of disease. Moreover, we discuss the heterogeneity and migratory responses of ILCs, and how these properties can impact immunity. As potent immune modulators, ILCs are a double-edged sword and, accordingly, understanding the mechanisms that regulate ILC maturation, recruitment to distal tissues, and plasticity is vital to progress in this field.

ILC2 plasticity in the lungs: A different perspective

ILC2s are the most studied ILC subset of the airways, likely because the healthy specific-pathogen free (SPF) mouse lung is almost entirely dominated by GATA3^{high} ILC2s and very few RORγt-expressing ILC3s (42, 64). The first functional

TABLE 1 Summary of cell surface phenotype, transcription factor/gene expression profiles of mouse ILC2 and ILC3 subsets.

ILC2 and ILC3 subsets	Transcription factor and gene expression profile*	References
Conventional ST2$^+$IL-18R$^-$ ILC2 (nILC2)	*Gata3*^{high}*Rora*$^+$	(34, 41, 42)
Resident ST2$^-$ IL-18R$^+$ ILC2 progenitors	*Gata3*^{int}*Tcf7*^{high}*Rora*$^+$	(43, 44)
Ex-ILC2/ILC1-like cells	*Gata3*^{int}*Tbx21*$^+$	(45, 46)
Mixed ILC2-ILC3 like cell	*Il5*$^+$*Il13*$^+$*Il17a*$^+$ *Il22*$^+$*Il23r*$^+$	(47)
Inflammatory ILC2 (iILC2)	*Gata3*^{high}RORγt^{int}*Il17rb*^{high}	(48–51)
Memory ILC2	*Gata3*^{high}*Il17rb*$^+$	(52)
CCR6$^-$NKp46$^-$ DN (precursor-like) ILC3	RORγt$^+$ T-bet$^-$	(53–56)
Transitional DN ILC3	RORγt$^+$T-bet$^+$	(53, 55)
NCR$^+$ ILC3	RORγt$^+$T-bet$^+$	(10, 57)
CCR6$^+$ LTi-like ILC3	RORγt$^+$T-bet$^-$	(58, 59)
Ex-ILC3/ILC1	RORγt$^-$T-bet$^+$	(32, 53, 54, 60)

int – intermediate expression level.
*evidence for transcript expression in italics.

10.3389/fimmu.2022.946905

assessments of lung-resident ILC2s through *ex vivo* pharmacological restimulation assays revealed them to be potent Th2 cytokine producing cells that failed to produce IFNγ or IL-17A (41). These C57BL/6 (B6) or B6-*Rag1*$^{-/-}$ lung-resident ILC2s (Lineage$^-$CD127$^+$CD90$^+$ cells) expressed the IL-33 receptor (IL-33R/T1-ST2) and were responsive to IL-33, a particularly potent alarmin that, *in vivo*, induces accumulation of ILC2s in the lung and the production of type 2 signature cytokines such as IL-13 and IL-5 (41, 42, 65). More recently, however, in the context of airway diseases and under certain context-dependent perturbations, ILC2s have been observed to undergo an apparent fate shift towards IFNγ-producing ex-ILC2/ILC1s or towards IL17-producing ILC3-like cells (Figure 2) (45, 46, 50, 66).

In a mouse model of influenza infection (A/FM/1/47: H_1N_1-adapted mouse strain), Silver and colleagues observed a striking increase in the proportion of lung T-bet$^+$ ILC1s and a corresponding decrease in the frequency of GATA3$^+$ ILC2s (46). To investigate whether the resident ILC2 pool converts into ILC1s, lung ILC2s (ST2$^+$IL-18Rα$^-$) were sorted from ST2-GFP reporter mice and adoptively transferred into lymphocyte-deficient *Rag2*$^{-/-}$*Il2rγ*$^{-/-}$ mice. Upon influenza infection of the recipients, GFP$^+$ ILC2s were found to have downregulated GATA3 expression and upregulated IL-12Rβ2 and IL-18Rα, becoming so-called ex-ILC2s that produced IFNγ upon *ex vivo* stimulation with IL-12 and IL-18. ST2$^-$IL-18Rα$^+$ ILC1s isolated from mice treated with IL-12, IL-18 and IL-33 had higher expression of *Tbx21*, *Ifng*, *Il12rb2*, and *Il18r1* and lower expression of ILC2-associated transcripts, including *Gata3, Il4, Il5*, and *Rora.*

In line with these findings, Ohne et al. demonstrated that mice treated with intranasal IL-12 or a combination of IL-1β and IL-12 induced a novel T-bet$^+$ IL-18Rα$^+$ subpopulation within the GATA3$^+$ ILC2 population (45). Their data suggest that, in the presence of IL-1β, IL-12 induces an ILC2 functional and phenotypic switch into IFNγ-producing ILC1-like cells that retain the ability to produce IL-13. Despite the co-induction of T-bet and IFNγ expression after *in vitro* stimulation with IL-12 and IL-18, the authors determined that T-bet was dispensable for this switch since similar phenotypic changes were observed in T-bet deficient mice during viral challenge (ie, IL-12Rβ and IL-18Rα upregulation and downregulation of GATA3) (46). T-bet did, however, prove essential for maximal production of IFNγ. Although reduced GATA3 expression was enough to drive ILC2 plasticity, this one-factor model may oversimplify ILC2 diversity given the different phenotypes and tissue-specific gene signatures in different tissues (37).

It is essential to bear in mind that apparent phenotypic and functional "plasticity" could, in fact, be due to the large-scale recruitment of new ILC subsets from distal sites or the differentiation of uncommitted, tissue-resident ILC precursors (67, 68). Indeed, recent work using *Rora*-YFP lineage tracer mice and scRNA-seq of all lung CD45$^{lo/+}$Lineage$^-$ cells demonstrated that ILC2s, expressing *Id2, Gata3, Rora, Il7r, Thy1* and lacking

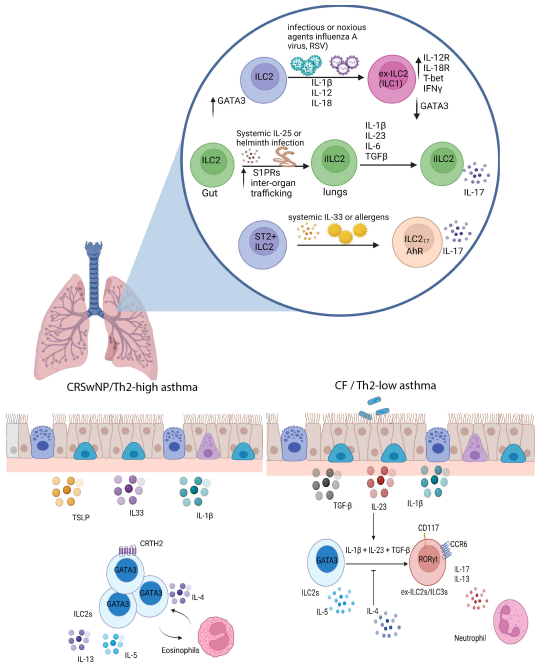

FIGURE 2
ILC2 plasticity in the lungs. In diseases like COPD and upon viral infections, ILC2s, in response to a combination of IL-12 and IL-1β, can transdifferentiate into IFNγ-producing ILC1-like cells. Infection with the migratory helminth, *Nippostrongylus brasiliensis*, or intraperitoneal IL-25 administration elicits the proliferation of IL-25-responsive intestinal iILC2s, which upregulate S1P receptors and can migrate to systemic sites such as the lungs. These iILC2s have the ability to produce IL-17 in response to Th17-like culture conditions, consisting of TGF-β, IL-1β, IL-23, and IL-6. Other mechanisms have been described by which ILC2s can produce IL-17 in a RORγt-independent manner under the influence of systemic IL-33 or allergen administration. In Th2-high asthma and CRSwNP, ILC2s are conventional players involved in IL-5 and IL-13 production and can interact with eosinophils. However, in cystic fibrosis and possibly Th2 low asthma, ILC2s have the ability, in response to IL-1β, IL-23, and TGF-β, to differentiate into ILC3-like cells that no longer produce IL-5 but retain the capacity to produce IL-13 and IL-17, and in this manner contributes to the neutrophilic inflammation observed in these types of diseases. Created with Biorender.org.

Rorc and *Tbx21*, can be segregated into two subsets: conventional IL-18Rα$^-$ST2$^+$ ILC2s and a small subset of IL18Rα$^+$ST2$^-$ cells that do not produce IL-5 and IL-13 in response to papain- or IL-18-induced mice (43). This latter IL18Rα$^+$ST2$^-$ ILC subset expresses *Tcf7*, like BM ILC progenitors (ILCps) (69, 70), and can give rise to multiple ILC lineages *in vivo* and *in vitro*. Therefore, instead of plasticity, it is likely that this local progenitor-like population undergoes tissue-specific adaptations *in situ* and differentiates into different effector ILC subsets, including ILC1s or ILC3s, depending on the class of alarmins they are exposed to and the downstream cell-to-cell interactions or signal transductions they detect upon inflammatory challenge.

Several other unanswered questions and caveats remain in the field of ILC2 plasticity in the lungs. Given that *in vitro* stimulation of gut ILC2s with IL-12 and IL-18 does not induce the upregulation of T-bet, there is the question of whether phenotypic changes in the lung represent a tissue-specific phenomenon (71). Indeed, different organs and tissues may be more permissive to induced plasticity or altered transcriptional profiles of a given ILC subset. In addition, different mouse strains with distinct genetic backgrounds may also underlie some variability observed in divergent phenotypes owing to their inherent genetic proclivity for Th1- or Th2- immunity. For example, the mouse-adapted influenza model PR8 induces a greater number of $CD90^+CD25^+$ ILC2s, which are essential in the amphiregulin-dependent reparative process following exposure to this cytopathic virus (41). This finding contradicts the phenotypic switch observed by Silver et al, in which lung resident ILC2s downregulate GATA3 and convert into IFNγ-producing ILC1-like populations in response to infection with PR8 influenza virus (46). Additionally, it is important to note that, in the study by Silver et al., $ST2^{+/GFP}$ mice on a BALB/c background, known to be genetically Th2-skewed, were used to survey the plastic behaviour of ILC2s instead of C57BL/6 mice which have a more balanced Th1/Th2 immune response (72). Thus, it remains unclear to what extent this phenotypic plasticity is a host strain-dependent phenomenon.

It is important to note that ILC2s are functionally heterogeneous. The notion of ILC2 functional plasticity was first demonstrated through intraperitoneal administration of IL-25 or infection with the migratory helminth *Nippostrongylus brasiliensis*. Both treatments in mice induce the expansion of an $ST2^-KLRG1^{high}$ ILC2 population in the lung termed "inflammatory ILC2s" (iILC2s) (50). This study revealed that these cells are absent during homeostasis in the lungs and are insensitive to both endogenous and exogenous IL-33. Instead, $ST2^-KLRG1^{high}$ iILC2s express IL-25R (*Il17rb*), low levels of CD90 (Thy-1) compared to $ST2^+$ lung-resident "natural" ILC2s (nILC2s) and intermediate amounts of RORγt accompanied by a robust expression of GATA3. The dual expression of RORγt and GATA3 hinted that these iILC2s may function both as type 2 and type 3 cytokine producing cells (50, 73). Predictably, under Th17-like culture conditions in the presence of TGF-β, IL-1β, IL-23 and IL-6, these iILC2s acquired the ability to produce IL-17 while maintaining the ability to produce IL-13, suggesting that lung iILC2s do indeed have the flexibility to become ILC3-like cells (Figure 2) (50).

To investigate the possibility that nILC2s can transition into IL-17-expressing iILC2s, nILC2s were exposed to various activating signals *in vitro* including the Notch activator, delta-like ligand (Dll1). Zhang et al. showed that the presence of the Notch ligand, Dll1, induces sorted nILC2s to downregulate *Il1rl1* and upregulate *Il17rb* and convert into IL-13 and IL-17 producing iILC2s. Without adequate Notch signaling, this transition is abolished (73). Although these studies further support the concept of ILC2 plasticity, the true extent of nILC2 to iILC2 conversion *in vivo* can only be addressed definitively by barcoding and fate-mapping approaches of lung resident nILC2s during conversion. Interestingly, IL-33-activated, or allergen-experienced nILC2s can upregulate *Il17rb* (IL-25R) upon re-exposure to papain or IL-33 and become potent $IL\text{-}5^+IL\text{-}13^+$ "memory" ILC2s, which are capable of responding more quickly and robustly during secondary exposures or after treatment with intranasal IL-25, unlike naïve nILC2s not previously exposed to IL-33 (52). It is less clear whether memory ILC2s can transition into cells that produce both type 2 cytokines and IL-17, especially in IL-17-dependent airway inflammatory models such as obesity-related airway hyperreactivity or oral *Candida albicans* infection model (50, 74).

In addition to IL-17 producing iILC2s, IL-17 producing $ST2^+$ ILC2s ($ILC2_{17}$s) have been documented as the main source of IL-17 in the context of papain challenge or IL-33 induced lung inflammation (75). Systemic administration of IL-33 into C57BL/6-wild-type or $Rag1^{-/-}$ mice resulted in the accumulation of IL-17-producing, $Lineage^-$ (CD3, B220, CD5, Gr-1), $GATA3^+$ ILC2s in the inflamed lung, which retain the ability to express IL-5 and IL-13. While these $ST2^+$ $ILC2_{17}$s are reminiscent of iILC2s in terms of their cytokine profile (50), the former was dependent on the aryl hydrocarbon receptor (AhR) and not RORγt for IL-17 production as they were not responsive in *Ahr*-deficient mice (75). Despite $Rag1^{-/-}Rorc^{gfp/gfp}$ mice exhibiting a lack of ILC3s (another source of IL-17) and having similar pathogenic outcomes in IL-33 induced lung inflammation (75), IL-17-producing ILC3s can still play an important role in different disease contexts such as obesity-induced asthma in which they can mediate the development of airway hyperreactivity and thus, should be at the forefront when considering IL-17-producing ILC populations (74). Moreover, the epigenetic circuits that control the conversion of resting ILC2s into IL-17 producing cells are not well understood and whether lung resident ILC2s are indeed poised to become IL-17 producing cells remains unknown. Certainly, future studies are needed to further clarify the relative contributions of the pool of IL-17-producing ILCs in response to tissue perturbation.

There are several possible approaches to address the extent of ILC2 plasticity in the lungs more adequately. Although ILCs do not express functional T cell receptors, we have previously shown that, surprisingly, lung ILC2s exhibit similar TCR rearrangement patterns to mature $V\gamma2^+$ γδ T cells but that these rearrangements are largely abortive Vγ2-Jγ1 locus rearrangements. This raises an interesting possibility that many lung-resident ILC2s are developmental relics of cells that failed to properly rearrange their TCR genes during neonatal γδ T cell development. This intriguing phenomenon aside, the TCR rearrangements may provide a convenient ontological "fingerprint" that allows tracking of lineage relationships between nILC2s, IL-17-producing ILC2s, and

lung ILC3s (76, 77). In short, these gene rearrangement patterns could be used as a genetic barcode to identify whether ILCs switch lineages. With this in mind, it would be of interest to evaluate whether ILC2s and ex-ILC2s (in response to influenza infection, chronic obstructive pulmonary disease (COPD) triggers, or other inflammatory perturbations) display the same genomic rearrangements. Future scRNA-seq analysis during inflammation may reveal the presence of an ILC1-ILC2 subset, ILC2-ILC3 subset, or occult intermediate subsets with mixed transcriptional phenotypes that may be revealed only with appropriate genomic or transcriptional analyses at the single-cell level. Future studies using computational models that better capture continuous variation in ILC transcriptional profiles and explicitly model dependencies among biological topics may help identify key relationships across heterogeneous samples. Finally, the transition potential of ILCs needs to be validated *in vivo* using fate-mapped mice and *in vitro* polarization experiments. While the role of "ex-ILC2s" and "IL-17 producing ILC2s" remains an active area of research, it is also important to investigate whether these populations provide a redundant or physiologically relevant source of IFNγ or IL-17 in inflammatory conditions such as viral infection, helminth infection and asthma.

Human ILC2s: A jack of all trades involved in immune tolerance and airway diseases

In humans, the three major groups of Lineage$^-$CD127$^+$ ILCs are conventionally defined based on differential expression of c-Kit (CD117) and CRTH2 (CD294): ILC1s are c-Kit$^-$CRTH2$^-$, ILC2s are CRTH2$^+$c-Kit$^{+/-}$, and ILC3s/ILCps are c-Kit$^+$CRTH2$^-$ (78, 79). However, the nature of these ILCs is still somewhat controversial and challenging to elucidate because commonly used surface markers (e.g. CRTH2 for ILC2s) may not capture all ILCs (80), and they can exhibit different functions and phenotypes depending on their tissue localization and activation state (81). For example, NKp44$^-$ ILC3s are the stereotypical players involved in IL-17 production, but recent reports indicate that human ILC2s are poised to become IL-17 producing cells in response to epithelium-derived cytokines that skew polarization of ILC subsets in the context of different pathologies.

A recent study by Golebski et al. examined the role of ILC2 plasticity in the pathology of chronic rhinosinusitis with nasal polyps (CRSwNP) in cystic fibrosis patients (66). In 2012, Mjosberg et al. previously demonstrated that CRTH2$^+$ ILC2s predominate in CRSwNP (16). However, IL-5-producing ILC2s are almost absent in nasal polyps from cystic fibrosis patients (CFwNP) (66). Instead, there is an enrichment of IL-17 producing NKp44$^-$ ILC3s in CFwNP. The changes in the accumulation of different ILC subtypes and cytokine profiles between CRSwNP and CFwNP were proposed to be mediated by the transdifferentiation of ILC2s into IL-17 producing ILC3s. The researchers isolated nasal epithelium and designed an air-liquid interface model in an attempt to test this hypothesis. When blood-derived ILC2s were added alongside *S. aureus* and *P. aeruginosa* (common opportunistic bacteria in patients with CF), they stopped producing IL-5 but instead produced significant amounts of IL-17. They found that Th17-polarizing cytokines (IL-1β, IL-23, and TGF-β), generated from the nasal epithelium, stimulated ILC2s to transdifferentiate into IL-17-producing cells. The establishment of a Th17-biased local tissue environment increased RORγt expression in IL-17 producing ILC2 clones. This plasticity was reversible because the addition of IL-4 was sufficient to recover the ILC2-like phenotype and inhibit IL-17 production due to a downregulation in the receptors (*IL1RL1* and *TGFBR1*) necessary for the induction of plasticity. In support of these findings, flow cytometry analysis revealed that blood-derived ILC2s produced IL-17 in response to stimulation with IL-1β, IL-23, and TGF-β (82). The functional plasticity of IL-17 producing ILC2s depended on the downregulation of *GATA3* and the induction of *RORC* given that RORγt blockade diminished IL-17 production *via* ILC2s. Of note, scRNA-seq and flow cytometry analysis revealed the presence of peripheral RORγt$^+$c-Kit$^+$ ILC2s that expressed CCR6, a marker also found on mouse LTi-like ILC3s, but expressed conventional ILC2-defining genes, including *RORA*, *IL17RB*, and *BCL11B* (82). However, c-Kit$^+$ ILC2s were unique because they contained RORγt$^+$CCR6$^+$ ILC2s and were able to produce IL-17 in response to IL-1β and IL-23 without the need for TGF-β. Conversely, c-Kit$^-$ ILC2s were somewhat refractory to the conversion into IL-17-producing ILC3-like cells but could be pushed towards the production of IL-17 with the additional presence of TGF-β. Therefore, the graded expression of c-Kit seems to correlate with the degree of ILC2 plasticity or their mature state.

Another potential mechanism is the recruitment of different ILC subsets from the blood to inflamed tissues. Chen et al. demonstrated that 24 hours after challenge with grass-pollen allergen, ILC2 numbers increased in the sputum but decreased in the blood, suggesting that ILC2s are recruited from the blood upon allergen challenge in asthmatic patients (83). Sputum ILC2s produced significantly more IL-13 post-allergen-challenge. On the other hand, in the periphery, there was no change in IL-13 producing ILC2s, which strongly suggests that ILC2s are recruited from the blood during allergic exacerbation, but the activation of ILC2s occurs in the lung tissue and not the periphery (83). This study illustrates one example of the phenotypic and functional differences between blood and tissue ILCs. Indeed, when ILC2s were isolated from nasal polyps and blood and cultured with IL-2, a cytokine that supports the survival and growth of these cells, only ILC2s derived from the nasal polyps could secrete IL-5 and IL-13,

suggesting that tissue-resident ILCs display a more activated or functionally mature state (84). Blood ILC2s display a relatively naive phenotype, and the majority of ILCs in the blood are ILC precursors that only upon migration to tissue may become more activated and differentiate towards a particular ILC subtype (79, 85). Therefore, plasticity may not be the sole mechanism by which ILCs contribute to disease exacerbation, and the recruitment of ILCs remains a possible source of the observed switches in effector ILC programs in human pathophysiology.

The modulation of ILC2 plasticity in humans and in immunotherapy will be beneficial only if plasticity is the causal cellular and molecular pathway by which ILCs regulate disease pathogenesis. While there is not much data on this yet, a recent report demonstrated that a combination of IL-33 and retinoic acid is able to induce IL-10 production by human GATA3$^+$ ILC2s, which upregulate Treg-associated genes, including *CTLA4* and *IL2RA* (CD25) (86). This makes these ILC2s resemble cells with a more regulatory phenotype that can potently inhibit both non-IL-10 producing ILC2s as well as Th2 cells. These IL-10-producing ILC2s (so-called regulatory ILCs or ILCregs) were detected in IL-10 reporter mice upon induction of house dust mite (HDM)-mediated lung allergy but were not present at steady state. Golebski et al. further demonstrated that in patients treated with grass pollen immunotherapy for 12 months, peripheral blood ILC2s have greater IL-10 production capacity (compared to blood ILC2s from placebo-treated patients), which indicates that this could be a way for the immune system to dampen the immune response (87).

ILC3 plasticity in the gut: Controversial players within a continuous spectrum in health and disease

The dominant cellular source of IL-22 in the intestine of humans and mice is RORγt$^+$ ILC3s (8, 12, 15, 58). ILC3s are functionally and phenotypically heterogeneous in nature and include a natural cytotoxicity receptor (NCR)$^+$ ILC3 subset that can co-express T-bet and RORγt as well as a subset that expresses high levels of CCR6 (originally defined as lymphoid tissue inducer cells that persist postnatally) termed LTi-like ILC3s. NCR$^+$ ILC3s are largely absent from intestinal cryptopatches and are, instead, localized primarily to the lamina propria, where they are tuned and poised for IL-22 production (10, 57). Conversely, LTi-like ILC3s are enriched in adult lymphoid tissues (53, 88).

Interestingly, despite a shared core ILC3 program (*Rorc, Il23r*, and *Il22* expression), NCR$^+$ ILC3s and LTi-like ILC3s are characterized by subset-specific transcriptional signatures. In fact, global gene expression analysis demonstrates that NCR$^+$ ILC3s exhibit a transcriptional profile more like that of ILC1s (*Ifng, Il12rb, Xcl1*, and *Tbx21*) than LTi-like ILC3s, which are T-bet *(Tbx21)* deficient (89). Despite the high level of *Ifng* expression, intestinal NCR$^+$ ILC3s produce minimal IFNγ at a steady state in WT mice or after *ex vivo* restimulation with IL-12, IL-18 and PMA/ionomycin with brefeldin A (55, 60, 90), but NCR$^+$T-bet$^+$ ILC3s appear poised for IFNγ production as part of the innate defense against infection (91). However, this type 1 functionality may also promote tissue inflammation reminiscent of pathogenic RORγt$^+$T-bet$^+$ Th17 cells that participate in autoimmune diseases and are dependent on IL-23 (92).

Initial fate-mapping studies in mice have demonstrated that a proportion of adoptively transferred RORγt-fate mapped (FM) intestinal NCR$^+$RORγt$^+$ ILC3s (isolated from RORγt-GFP reporter mice) can, over time, downregulate RORγt and further upregulate T-bet, thereby becoming so-called "ex-ILC3s" or "ILC1-like" cells, that express NK cell surface markers and transcriptional features associated with type 1 immunity (NK1.1, NKp46, NKG2D, IL-12Rβ2) (53, 54). These ex-ILC3s require IL-15 for their maintenance (32), and are capable of producing IFNγ under distinct inflammatory cytokine conditions (IL-12 and IL-15), implicating them as a major pathological source of IFNγ production. Accordingly, they exacerbate chronic intestinal inflammation in mouse models of CD40-triggered colitis or induce colitis-like pathologies in response to infection (53, 54). These results, only revealed through RORγt-Cre fate mapping strategies, highlight the plasticity of intestinal RORγt$^+$ ILC3 subsets and their ability to switch from "homeostatic" ILC3s to IFNγ-producing "inflammatory" ex-ILC3s/ILC1s. While the transition of NCR$^+$ ILC3s to ex-ILC3s/ILC1s can be pathogenic, this plasticity is dichotomous and may also be beneficial by evoking protective immunity to certain intracellular pathogens through the production of pro-inflammatory cytokines, namely IFNγ that enables the production of mucus-forming glycoproteins to protect the epithelial barrier (53, 93).

The overexpression of T-bet and progressive loss of RORγt causes a subset of NCR$^+$T-bet$^+$ ILC3s to transition into an ILC1-like/ex-ILC3 phenotype and display a surface marker phenotype that is akin to cNK cells (Lineage$^-$NK1.1$^+$NKp46$^+$ population), thus making it difficult to distinguish ex-ILC3s with a type 1 effector profile from *bona fide* ILC1s or NK cells (53, 56). Environmental cues such as IL-7R signalling or activation by the microbiota support RORγt expression within NCR$^+$ ILC3s and prevent the emergence of ex-ILC3s as seen by the reduced *Tbx21* and *Il22* expression in microbiota-perturbed mice (10, 36, 53, 54, 90). Early studies lacked high-resolution transcriptomic and epigenetic analyses, which are needed to reveal intermediate states and the sum of regulatory elements that dictate each subset's identity and function.

Adding to the diversity within the ILC3 compartment in the intestine, CCR6$^-$ ILC3s contain a subset of "double negative" (DN) precursor cells (CCR6$^-$NKp46$^-$) that upregulate T-bet and

give rise to NCR$^+$ ILC3s (NKp46$^+$RORγt$^+$T-bet$^+$) (53, 54, 56). Thus, NCR$^+$ ILC3s develop along a T-bet gradient (Figure 3). In addition, Notch signalling, microbial cues and IL-23 exposure instruct the upregulation of T-bet, thereby regulating the development of NCR$^+$ ILC3s and revealing the importance of environmental cues and the cytokine milieu in regulating the fate of ILC3 subsets (53, 56). However, the differential gene signatures defining these intestinal precursor-like DN ILC3s remain challenging, since DN ILC3s can exist in a transitional T-bet$^+$ state (between DN ILC3s and NCR$^+$ ILC3s) but NKp46$^-$ CCR6$^-$RORγt$^+$ DN ILC3s are still present in *Tbx21*$^{-/-}$ and germ-free mice, indicating that T-bet is dispensable for their development (53, 60). Therefore, there is a need to identify additional surface markers that distinguish DN ILC3s. Future unbiased scRNA-seq of RORγt-expressing cells using RORγt-reporter mice is required to fully define the role(s) and identity of DN ILC3s and their functional plasticity relative to other RORγt$^+$ ILC subsets.

Between the NCR$^+$ ILC3 and LTi-like subsets, there lies a range of transcriptional states that has not been previously appreciated. The first scRNA-seq analyses under homeostatic conditions revealed five unique transcriptional states among ILC3s (ILC3a-e) in the small intestinal lamina propria in mice that blurs the boundaries of the current ILC3 subset classification and the diversity within each subset (36). These transcriptional states indicate the possibility of dynamic functional plasticity in response to polarizing signals from the local environment or may represent discrete diversity (36, 40). This could explain the ability of the IL-23 responsive CCR6$^+$NCR$^-$CD4$^-$ LTi-like ILC3 population to co-produce IL-17 and IFNγ in response to *Helicobacter hepaticus* infection in 129SvEv-*Rag*$^{-/-}$mice (94). However, in the C57BL/6-*Rag*$^{-/-}$ strain, this functional plasticity is not induced, and no intestinal inflammation is observed (95). Given that CCR6 and NKp46 are used as mutually exclusive markers to discriminate LTi-like ILC3s and NCR$^+$ILC3s, it is unclear whether IL-17 producing LTi-like ILC3s do indeed have functional plasticity to produce IFNγ, seemingly in contrast to reports indicating that NCR$^+$T-bet$^+$ ILC3s represent the ILC3 subset with the capacity to produce IFNγ upon transition to ex-ILC3/ILC1-like cells under distinct inflammatory conditions (40, 53, 54).

NCR$^+$ ILC3s have an unconventional transcription factor profile that consists of master regulators, RORγt, T-bet, and GATA3 (53, 56, 96). Of note, although NKp46 is not stably expressed in ILC3s, fate-mapping studies using *R26*^{eYFP}*Ncr1*-iCre revealed a population of NCR$^-$ ILC3s (FM$^+$) that still expressed YFP, indicating that NKp46 expression has occurred in their life history (97). Using mice that could report and ablate IL-22 expression in NCR$^+$ ILCs, NCR$^-$ ILC3s (FM$^+$) were shown to produce IL-22. In line with this finding, conditional gene targeting in NKp46$^+$ ILCs using *Ncr1*^{creGFP} mice demonstrated that fate-mapped NKp46^{FM} ILC3s (ex-NKp46$^+$ ILC3s) in the small intestinal lamina propria produced more IL-22 than NCR$^+$ ILC3s at steady-state and expressed higher levels of c-Kit (CD117), reminiscent of DN ILC3s (98). Importantly, these ex-NKp46$^+$ ILC3s did not produce IL-17A or IFNγ, indicating that these murine 'ex-NKp46 ILC3s' revert to a DN ILC3 phenotype and are distinct from ex-ILC3s/ILC1s.

Although T-bet is important for the development of NCR$^+$ ILC3s, NCR$^-$ ILC3s (FM$^+$) are still present in a T-bet deficient

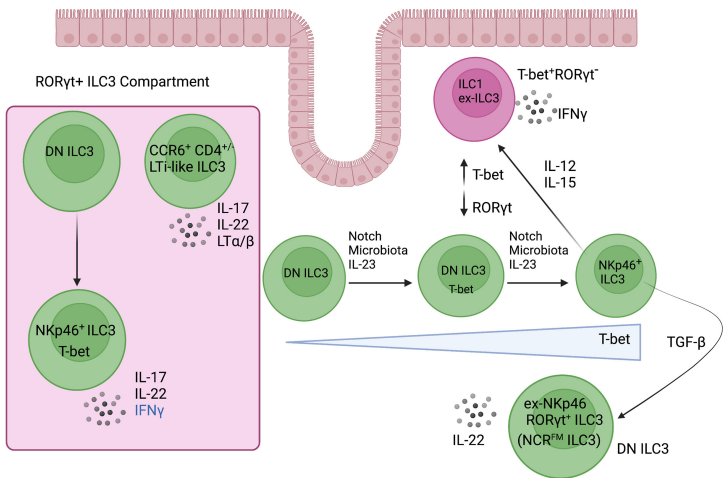

FIGURE 3
ILC3 plasticity and heterogeneity in the intestine. RORγt$^+$ ILC3s are enriched in the intestine where they are heterogeneous and consist of two major subsets. CCR6$^+$ ILC3s resemble the fetal lymphoid tissue inducer cells that are required for lymph node organogenesis. The CCR6$^-$ ILC3 compartment is distinguished mainly by its expression of the type 1 transcription factor, T-bet. DN (NKp46$^-$CCR6$^-$) ILC3-precursor cells give rise to NCR$^+$ ILC3s, which develop along a T-bet gradient that is controlled by Notch signalling, microbiota, and IL-23. Of note, NCR$^+$ ILC3s are poised to express IFNγ under distinct inflammatory cytokine conditions such as IL-12 and IL-15. Created with Biorender.org.

background (97). Therefore, T-bet is not required for the transition of NCR$^-$ ILC3s to NCR$^+$ ILC3s but may be required for the maintenance of NCR$^+$ ILC3s. In addition to T-bet, Notch signalling also plays an important role in the balance of NCR$^-$ ILC3s and NCR$^+$ ILC3s (97, 99). When pure NCR$^+$ ILC3s are sorted and cultured in the presence of Dll1 (Notch ligand), the majority of NCR$^+$ ILC3s retain NKp46 expression. In the absence of Notch, a substantial fraction of NCR$^+$ ILC3s lose NKp46 expression, which is associated with a downregulation of T-bet (97). Notch2 signals found in the tissue microenvironment are critically important in the transition of DN ILC3s into NCR$^+$ ILC3s by inducing the expression of T-bet and RORγt (99). Indeed, bone marrow reconstitution experiments and mouse models in which the Notch pathway was abrogated or constitutively activated revealed a direct, cell-intrinsic action whereby DN ILC3 precursor cells differentiate into NCR$^+$ ILC3s (Figure 3) (99). Of note, TGF-β plays an important role in regulating the balance between NCR$^-$ ILC3s and NCR$^+$ ILC3s because it antagonizes Notch signalling and suppresses the transition of DN ILC3s to NCR$^+$ ILC3s. This highlights the ability of ILC3 subsets to modulate their transcription factor profiles, effector functions, and phenotype in response to environmental signals (97).

What we know about the transcriptional regulatory circuits governing ILC3 functional phenotype and plasticity

ILC3s are critically dependent on the master transcription factor RORγt for their development, but the transient inhibition of RORγt expression in mature ILC3s does not affect core ILC3 functions, such as IL-22 production, likely because there are other key-ILC associated transcription factors regulating ILC function and phenotype (100). A recent study utilizing 5X polychromic reporter mice (*Id2*^{BFP}*Gata3*^{hCD2}*Rora*^{Teal}*Bcl11b*^{tdTom}*Rorc*^{Kat}) demonstrated that all ILC subsets express RORα, including small intestinal ILC1s/ex-ILC3s and this finding concurs with other gene expression analyses (89, 101). NK cells, however, failed to express RORα (101). Crucially, our previous findings revealed that RORα plays a key role in preserving ILC3 characteristics (102, 103). We demonstrated that dysregulated RORα expression reshapes the transcriptional spectrum of ILCs and attenuates expression of core ILC3-signature genes, including downregulation of *Rorc*, *Il23r*, and *Il1r* - an aberrant gene signature likely reflecting dysfunctional ILC3s that are unable to detect an inflammatory milieu. Moreover, in a *Salmonella*-driven model of Crohn's disease-like fibrosis, we showed that RORα-deficient mice were protected: RORα inactivation dampened Th17/ILC3-type cytokine production, including IL-17 and IL-22. The role of RORα in preserving ILC3 phenotype and function indicates that ILC fate and/or plasticity is dictated by an intricate balance and maintenance of transcription factor programs.

Another recent study investigated the roles of key-ILC associated transcription factors in regulating ILC3 heterogeneity, function, and phenotype using scRNA-seq of ILCs isolated from the small intestinal lamina propria from four inducible transgenic mouse models that allow combinatorial deletion of RORγt, RORα and T-bet in ILCs (60). Five ILC "superclusters" were identified from all genotypes: ILC1s/Ex-ILC3s, ILC2s, NCR$^+$ ILC3s, LTi-like ILC3s, and an "unknown" ILC cluster. Of note, RORγt depletion together with RORα led to the complete loss of NCR$^+$ ILC3s and a concomitant expansion of ex-ILC3s/ILC1s, which was associated with enhanced T-bet expression and a downregulated ILC3 program. Although the deletion of RORγt was associated with a loss in ILC3-related genes such as *Rorc, Il1r*, and *Il23r*, the full acquisition of a T-bet orchestrated type 1 immunity program and trans-differentiation towards an ex-ILC3/ILC1-like population required the deletion of RORα. These ex-ILC3s converge upon the same transcriptional and functional state as ILC1s (Figure 4).

Among ILC3s, c-Maf expression is highly correlated with that of T-bet, and conditional deletion of *Maf* along with fate mapping RORγt$^+$ ILC3s demonstrated that c-Maf regulates the balance of lineage-defining transcription factors, RORγt and T-bet (55). Specifically, c-Maf is downregulated with ILC3 to ILC1 conversion and deletion of c-Maf results in the upregulation of T-bet and concomitant downregulation of RORγt. *Rorc* fate-mapping approaches demonstrated that ex-ILC3s are increased in the *Maf* knockout, indicating increased conversion in the absence of c-Maf. Therefore, it appears that c-Maf functions to restrain this ILC3 to ILC1 cell plasticity, acting as a gatekeeper for the acquisition of type 1 features in ILC3s (55).

These regulatory circuits and co-expressed transcription factors appear to play a critical role in the identity and plasticity of ILC3s and possibly other ILC subsets and offer an exciting area for future research and manipulation.

The spectrum of ILC3-ILC1-like cells in humans

It is noteworthy that the ILC3 to ILC1 transitions identified in mouse models have also been observed in humans. At steady-state conditions, ILC3s represent the most abundant ILC subset in the human intestine, whereas the frequency of ILC1s is extremely low. When highly purified NKp44$^+$ ILC3s from fetal gut or tonsils are cultured with IL-2 and IL-12 in the presence of feeder cells, ILC3s stop producing IL-22 and lose expression of NKp44 and c-Kit (ILC3 phenotypic markers), but instead start producing large amounts of IFNγ, suggesting the differentiation of NKp44$^+$ ILC3s towards CD127$^+$ ILC1s (61, 62). This shift has

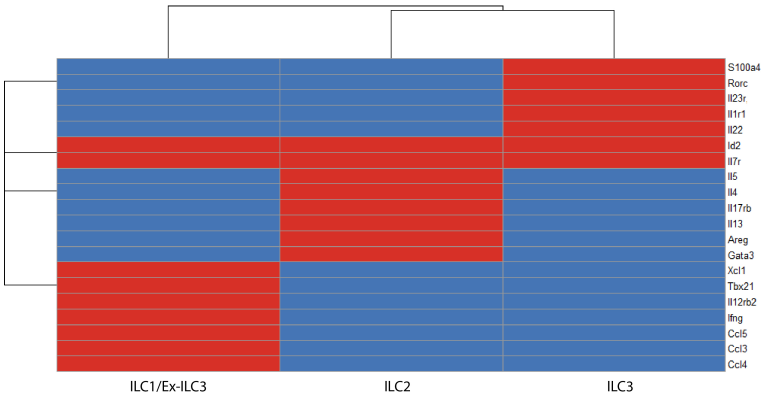

FIGURE 4
A binary matrix of ILC signature genes in the intestinal lamina propria (red = expressed, blue = not expressed). Common genes that distinguish ILC subsets in the intestinal lamina propria based on ScRNA-seq reports (36, 60, 103, 104). *Id2* and *Il7r* are core ILC genes. ILC1s/ex-ILC3s express *Tbx21*, *Ifng*, *Il12rb2*, *Ccl5*, *Gzmc*. ILC2s express high levels of *Gata3*, *Il17rb*, *Areg*, *Il5*, and *Il13*. ILC3s express *Rorc*, *Il1r1*, and *Il23r* (ILC3 program), which makes these cells exquisitely sensitive to stimulation with IL-23 and thus produce high levels of IL-22 on a per cell basis.

been proposed as a contributor to the observed changes between non-inflamed tissue versus inflamed regions of patients with Crohn's disease where there is a substantial increase in IFNγ-producing CD127$^+$ ILC1s at the cost of homeostatic IL-22 producing NKp44$^+$ ILC3s in the inflamed intestine (61).

Beyond the conventional IL-22 producing CD103$^-$NKp44$^+$ ILC3s (ILC3a) and IFNγ-producing CD103$^+$NKp44$^+$ ILC1s (ILC1a), two additional ILC subsets are detected in inflamed tonsils. These CD103$^+$NKp44$^+$ ILCs included CD196$^+$CD300LF$^+$ and CD300LF$^-$CD196$^+$ subsets referred to as ILC3b and ILC1b, respectively (105). Functional analysis of clones derived from these four ILC3-ILC1 subsets revealed a gradient in which the capacity to produce IFNγ increased from ILC3a to ILC3b to ILC1b, to ILC1a clones, which were exclusively IFNγ-producing cells. These four ILC3-ILC1 subsets were subjected to scRNA-seq and RNA velocity analysis to interrogate the whole spectrum of ILC3-ILC1-like cells and predict the future state of ILC3-ILC1 subsets in the human tonsils and lamina propria of ileal specimens (105). In this report, an intermediate cluster expressing *IL7R*, *CD300LF*, and *KLRD1* (CD94) manifested itself along the ILC3-ILC1 trajectory and appeared in a vector heading towards an IFNγ-producing ILC1 cluster that expressed *TBX21* and *IFNG*, indicative of plasticity. However, this work does not exclude the possibility that certain ILC subsets may directly derive from the differentiation of undetected rare progenitor cells. While there is strong evidence for ILC3s becoming more plastic and perhaps more ILC1-like cells in inflammatory bowel disease (61, 62), there could be other pathways regulating this shift in ILC composition, as discussed. Additionally, there certainly could be oxidative stress and cell death occurring in the context of ILC3s in inflammatory bowel disease (IBD) patients, which to the best of our knowledge, has not been carefully examined and warrants further investigation.

NK cells and ILC1s in the liver: A brief insight on the presence of locally maintained progenitors versus plasticity

NK cells and ILC1s are both defined as Lineage$^-$ NK1.1$^+$NKp46$^+$ IFNγ-producing cells that are driven by the transcription factor T-bet (106). Despite these similarities, the mouse liver represents one location in which one can clearly discriminate NK cells from ILC1s based on differential expression of CD49a and CD49b (107, 108). ILC1s are CD49a$^+$CD49b$^-$ whereas NK cells are CD49a$^-$ CD49b$^+$. Liver ILC1s are further defined by the expression of CD200R1, TRAIL, and CD69, which are all not found on NK cells. On the other hand, NK cells express the transcription factor EOMES, which distinguishes them from ILC1s. Surprisingly, in contrast to NK cells, liver ILC1s are not reconstituted by bone marrow cells (108). Instead, fetal liver cells are more efficient in reconstituting the liver ILC1 compartment. Intriguingly, fetal liver and adult liver contains a population of Lineage$^-$Sca-1$^+$Mac-1$^+$ cells with preferential ILC1 progenitor, over NK cell progenitor, activity. It is noteworthy that ablation of the capacity of NK cells and ILC1s to produce IFNγ attenuates the number of liver ILC1s, suggesting that IFNγ is a prerequisite for liver ILC1 development. A previous study using *Ncr1^{cre}Eomes^{floxed}* mice

showed that ablation of EOMES in NKp46^{+} cells depleted NK cells but had no impact on liver ILC1s (109). In aggregate, these results suggest that, like myeloid cells, which are derived in part from progenitors from embryonic life, a vanguard of fetal Lineage^{-}Sca-1^{+}Mac-1^{+} ILC1 precursors from the fetal liver seed this tissue and persist during adulthood. Thus, liver ILC1s develop locally *via* an IFNγ– dependent loop (108).

This, in turn, has led to speculation that NK cells can convert into ILC1-like cells (110, 111). For example, Cortez et al. demonstrated that ablation of SMAD4 in NKp46-expressing cells can induce NK cells to acquire an ILC1-like gene signature, including *Itga1* (CD49a) and *Tnfsf10* (TRAIL) expression (111). These ex-NK cells (ILC1-like) upregulate CD49a and were unable to control NK-cell-dependent containment of B16 lung metastasis. The presence of locally maintained ILC1 progenitors in the liver raises the question of whether the observed shift towards an ILC1-like phenotype by TGF-β imprinted SMAD4-deficient NK cells is in part due to a pathway that affects these progenitors, instead of plasticity.

Methodologies to ascertain ILC plasticity

ILC immune responses feature complex heterogeneity and transitions among cell states within what would be considered a single cell type. Therefore, to truly evaluate plasticity, there must be corroborative evidence that consists of techniques such as single-cell transcriptomic studies accompanied by lineage tracing, barcoding and epigenetic analyses.

For example, a recent study by Bielecki et al. conducted scRNA-seq of ILCs (CD45^{+}Lineage^{-}CD90^{+}) sorted from naïve and psoriatic skin of WT and *Rag1*$^{-/-}$ mice and identified a dense continuum of functional states and graded gene expression with overlapping expression of type 2 and type 3 genes (47). Due to the continuous variability in scRNA-seq data, this study used a probabilistic topic modelling to infer biological "topics", including "repressive/quiescent", "type2/ILC2-like", and "mixed type 3/pro-inflammatory ILC3-like", to describe the transcriptional profile in each cell. This revealed a spectrum of ILC states that was not previously anticipated. In fact, this spectrum shifted to a type 2/3 hybrid phenotype upon disease induction, hinting that classical IL-5 and IL-13 producing ILC2s transition to a new, pathology-associated mixed ILC2/ILC3-like subset. These mixed states and ILC2-ILC3 plasticity were experimentally validated *in vivo* by IL-5 fate-mapping and IL-22^{BFP}/IL-17A^{GFP} reporter mice that demonstrated a proportion of cells that expressed type 3 cytokines also previously expressed IL-5 (47). This suggests that some of the ILC3-like cells that arise after disease induction express the ILC2 program at an earlier point in their lifetime. Single-cell assay for transposase-accessible chromatin sequencing (scATAC-seq) of ILC populations from untreated skin showed open chromatin at transcription start sites for *Il5* and *Il13* alongside open chromatin at regulatory elements for *Il22*, *Il17a*, *Il17f*, and *Il13*, indicating that steady-state skin ILCs are epigenetically poised to become ILC3-like cells.

Discussion

Inflammatory diseases elicit a markedly different tissue environment compared to that of healthy, non-inflamed tissues, and these conditions can be remarkably disease-specific. At baseline, ILC subsets are present in characteristic frequencies in distinct anatomical locations, and they exhibit tissue-specific phenotypes and effector programs (81, 112). However, multiple studies suggest that different ILC subsets are expanded in the inflammatory environment and that ILCs can dramatically change their phenotype and function from that observed at homeostasis (39, 113). These perturbation-induced changes in mature effector ILC populations play a crucial role in the pathogenesis of upper and lower airway diseases as well as gut and skin inflammatory diseases. Thus, a critical question is how these shifts in frequency and phenotype occur mechanistically: *de novo* generation of cells *in situ* from precursors? Influx from a novel population from peripheral sites? Plastic reprogramming of local ILC populations? Ultimately, these mechanisms are key to understanding how inflammatory and repair functions are initiated, executed, and resolved and how they can be targeted to ameliorate inflammation or facilitate tissue repair. It is important to note that a combination of mechanisms might contribute to shifts in effector ILC populations. For instance, even if mature effector cells exist in a much more fluid state than as discrete entities, immature precursors may also directly contribute to the ILC compartment without the need for cell-state transitions.

The skewed ILC composition during chronic imbalances and inflammatory diseases in humans and mice has been proposed to be caused by "ILC plasticity". The concept of ILC plasticity suggests that the identity of ILC subsets is not set in stone and that, in response to potent local microenvironmental stimuli, these cells can transdifferentiate to produce different cytokines and adopt alternate cell-fates. However, as noted above, there are several confounders in many of these studies (Figure 5). We do not yet know to what extent the accumulation of different ILC subsets reflects *in situ* proliferation of tissue-resident ILCs, including expansion from rare undetected steady-state populations, versus recruitment of ILCs from the peripheral blood. Alternatively, these shifts in ILC subset numbers could result from the differentiation of locally-maintained precursor-like cells upon receiving appropriate localizing signals in tissue. Of note, each of those mechanisms has been shown to be relevant in different tissues or disease

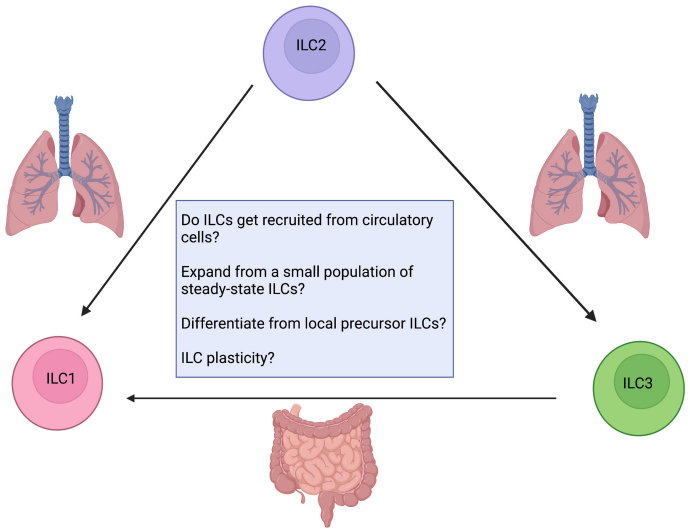

FIGURE 5
Confounding factors when addressing ILC plasticity. How do ILCs contribute to inflammation? Are they recruited from circulatory cells? Do they expand from a small undetected steady-state population or locally maintained ILC precursors? Are tissue-resident ILCs plastic? Future work aimed at developing critical animal models as reporter assays for fate mapping and lineage tracing will enable us to answer these questions. Created with Biorender.org.

contexts. For example, the lung contains a range of *Il18r1*$^{+}$ ILC progenitors (43), and when perturbed by *N. brasilinesis* infection, these precursors are pushed to transition from *Il18r1*^{high}*Tcf7*^{high} to *Gata3*^{high}*Il1rl1*^{high} through a proliferating transit-amplifying stage to give rise to a plethora of effector ILC2s (44). In terms of recruitment from circulatory cells, IL-25-activated ILC2s can upregulate S1P receptors and acquire the ability to enter the lymphatic vessels of villi (48). Once they enter the periphery, BATF-dependent iILC2 cells can accumulate in systemic sites of infection such as the lungs to contribute to tissue repair and orchestrate the re-establishment of barrier integrity (48, 49). Campbell et al. further found that *Trichinella spiralis*, an entirely gastrointestinal-dwelling mucosal parasite that never enters the lungs, caused intestinal iILC2s to proliferate and these effector IL-13-producing ILC2s moved into the blood to provide systemic innate protection in the lungs (51). Thus, there is evidence for dramatic local ILC differentiation and rapid influx from peripheral sites as a confounder to many studies of "plasticity".

Given the competing (or complementary) mechanistic explanations of current ILC plasticity studies, we advocate for a more critical approach that examines each case before inferring ILC plasticity and that, ideally, *bona fide* plasticity is confirmed through single-cell assays and cell tracking. Future studies are needed to further clarify lineage relationships, transition potential, and whether ILC plasticity can be manipulated for improved treatment of clinical disease. It is important to conduct appropriate epigenetic and transcriptional analysis at the single-cell level, along with functional assays and fate-mapping strategies to confidently claim "plasticity". While ILC plasticity may allow for flexible immunity to intracellular pathogens (beneficial), it has also been associated with autoimmunity (pathogenic), particularly inflammatory bowel disease in humans (61, 62, 113). Therefore, improved experimental rigour and the use of genomic rearrangements may offer additional insight into the extent of each subset's adaptability in response to the local tissue microenvironment and previous findings need to be revisited to avoid misleading interpretations.

Author contributions

AK contributed to conceptualization, topic curation, and wrote the review, and designed the figures and table. KM contributed to conceptualization, topic curation, writing, editing, and approved the manuscript. SS read, edited, and approved the manuscript. MH contributed to the elaboration of the figures and read, edited, and approved the manuscript. All authors contributed to the article and approved the submitted version.

Funding

This work was funded by grant numbers PJT-148681 and PJT-156235 from the Canadian Institutes of Health Research (CIHR). SS was supported by an AllerGen Network Centre of

Excellence and CIHR Frederick Banting & Charles Best Canada Graduate Scholarship–Master's Program (CGS-M) Scholarship.

Conflict of interest

The authors declare that the research was conducted in the absence of any commercial or financial relationships that could be construed as a potential conflict of interest.

Publisher's note

References

1. Vivier E, Artis D, Colonna M, Diefenbach A, di Santo JP, Eberl G, et al. Innate lymphoid cells: 10 years on. *Cell* (2018) 174:1054–66. doi: 10.1016/j.cell.2018.07.017

2. Kondo Y, Yoshimoto T, Yasuda K, Futatsugi-yumikura S, Morimoto M, Hayashi N, et al. Administration of IL-33 induces airway hyperresponsiveness and goblet cell hyperplasia in the lungs in the absence of adaptive immune system. *Int Immunol* (2008) 20(6):791–800. doi: 10.1093/intimm/dxn037

3. Fallon PG, Ballantyne SJ, Mangan NE, Barlow JL, Dasvarma A, Hewett DR, et al. Identification of an interleukin (IL)-25–dependent cell population that provides IL-4, IL-5, and IL-13 at the onset of helminth expulsion. *J Exp Med* (2006) 203(4):1105–16. doi: 10.1084/jem.20051615

4. Voehringer D, Reese TA, Huang X, Shinkai K, Locksley RM. Type 2 immunity is controlled by IL-4/IL-13 expression in hematopoietic non-eosinophil cells of the innate immune system. *J Exp Med* (2006) 203(6):1435–46. doi: 10.1084/jem.20052448

5. Neill DR, Wong SH, Bellosi A, Flynn RJ, Daly M, Langford TKA, et al. Nuocytes represent a new innate effector leukocyte that mediates type-2 immunity. *Nature* (2010) 464(7293):1367–70. doi: 10.1038/nature08900

6. Moro K, Yamada T, Tanabe M, Takeuchi T, Ikawa T, Kawamoto H, et al. Innate production of T(H)2 cytokines by adipose tissue-associated c-Kit(+)Sca-1(+) lymphoid cells. *Nature* (2010) 463(7280):540–44. doi: 10.1038/nature08636

7. Price AE, Liang HE, Sullivan BM, Reinhardt RL, Eisley CJ, Erle DJ, et al. Systemically dispersed innate IL-13-expressing cells in type 2 immunity. *Proc Natl Acad Sci U S A* (2010) 107(25):11489–94. doi: 10.1073/pnas.1003988107

8. Cella M, Fuchs A, Vermi W, Facchetti F, Otero K, Lennerz JKM, et al. A human natural killer cell subset provides an innate source of IL-22 for mucosal immunity. *Nature* (2008) 457(7230):722–5. doi: 10.1038/nature07537

9. Buonocore S, Ahern PP, Uhlig HH, Ivanov II, Littman DR, Maloy KJ, et al. Innate lymphoid cells drive IL-23 dependent innate intestinal pathology. *Nature* (2010) 464(7293):1371–5. doi: 10.1038/nature08949

10. Satoh-Takayama N, Vosshenrich CAJ, Lesjean-Pottier S, Sawa S, Lochner M, Rattis F, et al. Microbial flora drives interleukin 22 production in intestinal NKp46+ cells that provide innate mucosal immune defense. *Immunity* (2008) 29(6):958–70. doi: 10.1016/j.immuni.2008.11.001

11. Sanos SL, Bui VL, Mortha A, Oberle K, Heners C, Johner C, et al. RORgammat and commensal microflora are required for the differentiation of mucosal interleukin 22-producing NKp46+ cells. *Nat Immunol* (2009) 10(1):83–91. doi: 10.1038/ni.1684

12. Luci C, Reynders A, Ivanov II, Cognet C, Chiche L, Chasson L, et al. Influence of the transcription factor RORγt on the development of NKp46+ cell populations in gut and skin. *Nat Immunol* (2008) 10(1):75–82. doi: 10.1038/ni.1681

13. Cupedo T, Crellin NK, Papazian N, Rombouts EJ, Weijer K, Grogan JL, et al. Human fetal lymphoid tissue-inducer cells are interleukin 17-producing precursors to RORC+ CD127+ natural killer-like cells. *Nat Immunol* (2009) 10(1):66–74. doi: 10.1038/ni.1668

14. Luci C, Reynders A, Ivanov II, Cognet C, Chiche L, Chasson L, et al. Influence of the transcription factor RORgammat on the development of NKp46+ cell populations in gut and skin. *Nat Immunol* (2009) 10(1):75–82. doi: 10.1038/ni.1681

15. Sawa S, Lochner M, Satoh-Takayama N, Dulauroy S, Bérard M, Kleinschek M, et al. RORγt+ innate lymphoid cells regulate intestinal homeostasis by integrating negative signals from the symbiotic microbiota. *Nat Immunol* (2011) 12:4. doi: 10.1038/ni.2002

16. Sonnenberg GF, Monticelli LA, Alenghat T, Fung TC, Hutnick NA, Kunisawa J, et al. Innate lymphoid cells promote anatomical containment of lymphoid-resident commensal bacteria. *Science* (2012) 336(6086):1321–5. doi: 10.1126/science.1222551

17. Vivier E, Raulet DH, Moretta A, Caligiuri MA, Zitvogel L, Lanier LL, et al. Innate or adaptive immunity? The example of natural killer cells. *Science* (2012) 331(6013):1321–25. doi: 10.1126/science.1198687

18. Gasteiger G, Fan X, Dikiy S, Lee SY, Rudensky AY. Tissue residency of innate lymphoid cells in lymphoid and nonlymphoid organs. *Science* (2015) 350(6263):981–5. doi: 10.1126/science.aac9593

19. Mathä L, Takei F, Martinez-Gonzalez I. Tissue resident and migratory group 2 innate lymphoid cells. *Front Immunol* (2022) 13(2048):1321–25. doi: 10.3389/fimmu.2022.877005

20. Eberl G, Colonna M, Santo JPD, McKenzie ANJ. Innate lymphoid cells: A new paradigm in immunology. *Science* (2015) 348(6237):aaa6566. doi: 10.1126/science.aaa6566

21. Panda SK, Colonna M. Innate lymphoid cells in mucosal immunity. *Front Immunol* (2019) 10(MAY):861. doi: 10.3389/fimmu.2019.00861

22. Kotas ME, Locksley RM. Why innate lymphoid cells? *Immunity* (2018) 48(6):1081–90. doi: 10.1016/j.immuni.2018.06.002

23. Bando JK, Liang HE, Locksley RM. Identification and distribution of developing innate lymphoid cells in the fetal mouse intestine. *Nat Immunol* (2015) 16(2):153. doi: 10.1038/ni.3057

24. Simic M, Manosalva I, Spinelli L, Gentek R, Shayan RR, Siret C, et al. Distinct waves from the hemogenic endothelium give rise to layered lymphoid tissue inducer cell ontogeny. *Cell Rep* (2020) 32(6):108004. doi: 10.1016/j.celrep.2020.108004

25. Murphy JM, Ngai L, Mortha A, Crome SQ. Tissue-dependent adaptations and functions of innate lymphoid cells. *Front Immunol* (2022) 13:810. doi: 10.3389/fimmu.2022.836999

26. McKenzie ANJ, Spits H, Eberl G. Innate lymphoid cells in inflammation and immunity. *Immunity* (2014) 41(3):366–74. doi: 10.1016/j.immuni.2014.09.006

27. Diefenbach A, Colonna M, Koyasu S. Development, differentiation and diversity of innate lymphoid cells. *Immunity* (2014) 41(3):354. doi: 10.1016/j.immuni.2014.09.005

28. Shih HY, Sciumè G, Mikami Y, Guo L, Sun HW, Brooks SR, et al. Developmental acquisition of regulomes underlies innate lymphoid cell functionality. *Cell* (2016) 165(5):1120. doi: 10.1016/j.cell.2016.04.029

29. Weizman O, Adams NM, Schuster IS, Krishna C, Pritykin Y, Lau C, et al. ILC1 confer early host protection at initial sites of viral infection. *Cell* (2017) 171(4):795–808.e12. doi: 10.1016/j.cell.2017.09.052

30. Artis D, Spits H. The biology of innate lymphoid cells. *Nature* (2015) 517(7534):293–301. doi: 10.1038/nature14189

31. Spits H, Bernink JH, Lanier L. NK cells and type 1 innate lymphoid cells: partners in host defense. *Nat Immunol* (2016) 17(7):758–64. doi: 10.1038/ni.3482

32. Klose CSN, Flach M, Möhle L, Rogell L, Hoyler T, Ebert K, et al. Differentiation of type 1 ILCs from a common progenitor to all helper-like innate lymphoid cell lineages. *Cell* (2014) 157(2):340–56. doi: 10.1016/j.cell.2014.03.030

33. Gold MJ, Antignano F, Halim TYF, Hirota JA, Blanchet MR, Zaph C, et al. Group 2 innate lymphoid cells facilitate sensitization to local, but not systemic, TH2-inducing allergen exposures. *J Allergy Clin Immunol* (2014) 133(4):1142–1148.e5. doi: 10.1016/j.jaci.2014.02.033

34. Halim TYF, MacLaren A, Romanish MT, Gold MJ, McNagny KM, Takei F. Retinoic-acid-receptor-related orphan nuclear receptor alpha is required for

natural helper cell development and allergic inflammation. *Immunity* (2012) 37 (3):463–74. doi: 10.1016/j.immuni.2012.06.012

35. Mjösberg J, Bernink J, Golebski K, Karrich JJ, Peters CP, Blom B, et al. The transcription factor GATA3 is essential for the function of human type 2 innate lymphoid cells. *Immunity* (2012) 37(4):649–59. doi: 10.1016/j.immuni.2012.08.015

36. Gury-BenAri M, Thaiss CA, Serafini N, Winter DR, Giladi A, Lara-Astiaso D, et al. The spectrum and regulatory landscape of intestinal innate lymphoid cells are shaped by the microbiome. *Cell* (2016) 166(5):1231–46.e13. doi: 10.1016/j.cell.2016.07.043

37. Ricardo-Gonzalez RR, van Dyken SJ, Schneider C, Lee J, Nussbaum JC, Liang HE, et al. Tissue signals imprint ILC2 identity with anticipatory function. *Nat Immunol* (2018) 19:10. doi: 10.1038/s41590-018-0201-4

38. Wallrapp A, Riesenfeld SJ, Burkett PR, Abdulnour REE, Nyman J, Dionne D, et al. The neuropeptide NMU amplifies ILC2-driven allergic lung inflammation. *Nature* (2017) 549(7672):351–6. doi: 10.1038/nature24029

39. Colonna M. Innate lymphoid cells: Diversity, plasticity, and unique functions in immunity. *Immunity* (2018) 48(6):1104–17. doi: 10.1016/j.immuni.2018.05.013

40. Melo-Gonzalez F, Hepworth MR. Functional and phenotypic heterogeneity of group 3 innate lymphoid cells. *Immunology* (2017) 150(3):265–75. doi: 10.1111/imm.12697

41. Monticelli LA, Sonnenberg GF, Abt MC, Alenghat T, Ziegler CGK, Doering TA, et al. Innate lymphoid cells promote lung-tissue homeostasis after infection with influenza virus. *Nat Immunol* (2011) 12(11):1045–54. doi: 10.1038/ni.2131

42. Halim TYF, Krauß RH, Sun AC, Takei F. Lung natural helper cells are a critical source of Th2 cell-type cytokines in protease allergen-induced airway inflammation. *Immunity* (2012) 36(3):451–63. doi: 10.1016/j.immuni.2011.12.020

43. Ghaedi M, Shen ZY, Orangi M, Martinez-Gonzalez I, Wei L, Lu X, et al. Single-cell analysis of RORα tracer mouse lung reveals ILC progenitors and effector ILC2 subsets. *J Exp Med* (2020) 217(3):1–19. doi: 10.1084/jem.20182293

44. Zeis P, Lian M, Fan X, Herman JS, Hernandez DC, Gentek R, et al. *In situ* maturation and tissue adaptation of type 2 innate lymphoid cell progenitors. *Immunity* (2020) 53(4):775–792.e9. doi: 10.1016/j.immuni.2020.09.002

45. Ohne Y, Silver JS, Thompson-Snipes LA, Collet MA, Blanck JP, Cantarel BL, et al. IL-1 is a critical regulator of group 2 innate lymphoid cell function and plasticity. *Nat Immunol* (2016) 17(6):646–55. doi: 10.1038/ni.3447

46. Silver JS, Kearley J, Copenhaver AM, Sanden C, Mori M, Yu L, et al. Inflammatory triggers associated with exacerbations of COPD orchestrate plasticity of group 2 innate lymphoid cells in the lungs. *Nat Immunol* (2016) 17(6):626–35. doi: 10.1038/ni.3443

47. Bielecki P, Riesenfeld SJ, Hütter JC, Torlai Triglia E, Kowalczyk MS, Ricardo-Gonzalez RR, et al. Skin-resident innate lymphoid cells converge on a pathogenic effector state. *Nature* (2021) 592(7852):128–32. doi: 10.1038/s41586-021-03188-w

48. Huang Y, Mao K, Chen X, Sun MA, Kawabe T, Li W, et al. S1P-dependent interorgan trafficking of group 2 innate lymphoid cells supports host defense. *Science* (2018) 359(6371):114–9. doi: 10.1126/science.aam5809

49. Miller MM, Patel PS, Bao K, Danhorn T, O'Connor BP, Reinhardt RL. BATF acts as an essential regulator of IL-25-responsive migratory ILC2 cell fate and function. *Sci Immunol* (2020) 5(43):eaay3994. doi: 10.1126/sciimmunol.aay3994

50. Huang Y, Guo L, Qiu J, Chen X, Hu-Li J, Siebenlist U, et al. IL-25-responsive, lineage-negative KLRG1hi cells are multipotential "inflammatory" type 2 innate lymphoid cells. *Nat Immunol* (2015) 16(2):161. doi: 10.1038/ni.3078

51. Campbell L, Hepworth MR, Whittingham-Dowd J, Thompson S, Bancroft AJ, Hayes KS, et al. ILC2s mediate systemic innate protection by priming mucus production at distal mucosal sites. *J Exp Med* (2019) 216(12):2714–23. doi: 10.1084/jem.20180610

52. Martinez-Gonzalez I, Mathä L, Steer CA, Ghaedi M, Poon GFT, Takei F. Allergen-experienced group 2 innate lymphoid cells acquire memory-like properties and enhance allergic lung inflammation. *Immunity* (2016) 45(1):198–208. doi: 10.1016/j.immuni.2016.06.017

53. Klose CSN, Kiss EA, Schwierzeck V, Ebert K, Hoyler T, D'Hargues Y, et al. A T-bet gradient controls the fate and function of CCR6–RORγt+ innate lymphoid cells. *Nature* (2013) 494(7436):261–5. doi: 10.1038/nature11813

54. Vonarbourg C, Mortha A, Bui VL, Hernandez PP, Kiss EA, Hoyler T, et al. Regulated expression of nuclear receptor RORγt confers distinct functional fates to NK cell receptor-expressing RORγt(+) innate lymphocytes. *Immunity* (2010) 33 (5):736–51. doi: 10.1016/j.immuni.2010.10.017

55. Parker ME, Barrera A, Wheaton JD, Zuberbuehler MK, Allan DSJ, Carlyle JR, et al. C-maf regulates the plasticity of group 3 innate lymphoid cells by restraining the type 1 program. *J Exp Med* (2020) 217(1):e20191030. doi: 10.1084/jem.20191030

56. Rankin LC, Groom JR, Chopin M, Herold MJ, Walker JA, Mielke LA, et al. The transcription factor T-bet is essential for the development of NKp46+ innate lymphocytes via the notch pathway. *Nat Immunol* (2013) 14(4):389–95. doi: 10.1038/ni.2545

57. Satoh-Takayama N, Lesjean-Pottier S, Sawa S, Vosshenrich CAJ, Eberl G, di Santo JP. Lymphotoxin-β receptor-independent development of intestinal IL-22-producing NKp46+ innate lymphoid cells. *Eur J Immunol* (2011) 41(3):780–6. doi: 10.1002/eji.201040851

58. Sonnenberg GF, Monticelli LA, Elloso MM, Fouser LA, Artis D. CD4(+) lymphoid tissue-inducer cells promote innate immunity in the gut. *Immunity* (2011) 34(1):122–34. doi: 10.1016/j.immuni.2010.12.009

59. Eberl G, Marmon S, Sunshine MJ, Rennert PD, Choi Y, Littmann DR. An essential function for the nuclear receptor RORgamma(t) in the generation of fetal lymphoid tissue inducer cells. *Nat Immunol* (2004) 5(1):64–73. doi: 10.1038/ni1022

60. Fiancette R, Finlay CM, Willis C, Bevington SL, Soley J, Ng STH, et al. Reciprocal transcription factor networks govern tissue-resident ILC3 subset function and identity. *Nat Immunol* (2021) 22(10):1245–55. doi: 10.1038/s41590-021-01024-x

61. Bernink JH, Peters CP, Munneke M, te Velde AA, Meijer SL, Weijer K, et al. Human type 1 innate lymphoid cells accumulate in inflamed mucosal tissues. *Nat Immunol* (2013) 14(3):221–9. doi: 10.1038/ni.2534

62. Bernink JH, Krabbendam L, Germar K, de Jong E, Gronke K, Kofoed-Nielsen M, et al. Interleukin-12 and -23 control plasticity of CD127(+) group 1 and group 3 innate lymphoid cells in the intestinal lamina propria. *Immunity* (2015) 43 (1):146–60. doi: 10.1016/j.immuni.2015.06.019

63. Ardain A, Domingo-Gonzalez R, Das S, Kazer SW, Howard NC, Singh A, et al. Group 3 innate lymphoid cells mediate early protective immunity against tuberculosis. *Nature* (2019) 570(7762):528–32. doi: 10.1038/s41586-019-1276-2

64. Spencer SP, Wilhelm C, Yang Q, Hall JA, Bouladoux N, Boyd A, et al. Adaptation of innate lymphoid cells to a micronutrient deficiency promotes type 2 barrier immunity. *Science* (2014) 343(6169):432. doi: 10.1126/science.1247606

65. Halim TYF, Steer CA, Mathä L, Gold MJ, Martinez-Gonzalez I, McNagny KM, et al. Group 2 innate lymphoid cells are critical for the initiation of adaptive T helper 2 cell-mediated allergic lung inflammation. *Immunity* (2014) 40(3):425–35. doi: 10.1016/j.immuni.2014.01.011

66. Golebski K, Ros XR, Nagasawa M, van Tol S, Heesters BA, Aglmous H, et al. IL-1β, IL-23, and TGF-β drive plasticity of human ILC2s towards IL-17-producing ILCs in nasal inflammation. *Nat Commun* (2019) 10(1):1–15. doi: 10.1038s41467-019-09883-7

67. Willinger T. Metabolic control of innate lymphoid cell migration. *Front Immunol* (2019) 10(AUG). doi: 10.3389/fimmu.2019.02010

68. Lim AI, di Santo JP. ILC-poiesis: Ensuring tissue ILC differentiation at the right place and time. *Eur J Immunol* (2019) 49(1):11–8. doi: 10.1002/eji.201747294

69. Harly C, Cam M, Kaye J, Bhandoola A. Development and differentiation of early innate lymphoid progenitors. *J Exp Med* (2018) 215(1):249–62. doi: 10.1084/jem.20170832

70. Yang Q, Li F, Harly C, Xing S, Ye L, Xia X, et al. TCF-1 upregulation identifies early innate lymphoid progenitors in the bone marrow. *Nat Immunol* (2015) 16(10):1044–50. doi: 10.1038/ni.3248

71. Schroeder JH, Garrido-Mesa N, Zabinski T, Gallagher AL, Campbell L, Roberts LB, et al. T-Bet fate mapping identifies a novel ILC1-ILC2 subset *in vivo*. *bioRxiv* (2020), 261073. doi: 10.1101/2020.08.21.261073v1

72. Walsh ER, Sahu N, Kearley J, Benjamin E, Boo HK, Humbles A, et al. Strain-specific requirement for eosinophils in the recruitment of T cells to the lung during the development of allergic asthma. *J Exp Med* (2008) 205(6):1285–92. doi: 10.1084/jem.20071836

73. Zhang K, Xu X, Pasha MA, Siebel CW, Costello A, Haczku A, et al. Cutting edge: Notch signaling promotes the plasticity of group-2 innate lymphoid cells. *J Immunol* (2017) 198(5):1798–803. doi: 10.4049/jimmunol.1601421

74. Kim HY, Lee HJ, Chang YJ, Pichavant M, Shore SA, Fitzgerald KA, et al. Interleukin-17–producing innate lymphoid cells and the NLRP3 inflammasome facilitate obesity-associated airway hyperreactivity. *Nat Med* (2013) 20(1):54–61. doi: 10.1038/nm.3423

75. Cai T, Qiu J, Ji Y, Li W, Ding Z, Suo C, et al. IL-17–producing ST2+ group 2 innate lymphoid cells play a pathogenic role in lung inflammation. *J Allergy Clin Immunol* (2019) 143(1):229–244.e9. doi: 10.1016/j.jaci.2018.03.007

76. Shin SB, McNagny KM. ILC-you in the thymus: A fresh look at innate lymphoid cell development. *Front Immunol* (2021) 12. doi: 10.3389/fimmu.2021.681110/full

77. Shin SB, Lo BC, Ghaedi M, Wilder Scott R, Li Y, Messing M, et al. Abortive gdTCR rearrangements suggest ILC2s are derived from T-cell precursors. *Blood Advances* (2020) 4(21):5362–72. doi: 10.1182/bloodadvances.2020002758

78. Hazenberg MD, Spits H. Human innate lymphoid cells. *Blood* (2014) 124 (5):700–9. doi: 10.1182/blood-2013-11-427781

79. Lim AI, Li Y, Lopez-Lastra S, Stadhouders R, Paul F, Casrouge A, et al. Systemic human ILC precursors provide a substrate for tissue ILC differentiation. *Cell* (2017) 168(6):1086–100.e10. doi: 10.1016/j.cell.2017.02.021

80. Liu S, Sirohi K, Verma M, McKay J, Michalec L, Sripada A, et al. Optimal identification of human conventional and nonconventional (CRTH2–IL7Rα–) ILC2s using additional surface markers. *J Allergy Clin Immunol* (2020) 146 (2):390–405. doi: 10.1016/j.jaci.2020.01.038

81. Meininger I, Carrasco A, Rao A, Soini T, Kokkinou E, Mjösberg J. Tissue-specific features of innate lymphoid cells. *Trends Immunol* (2020) 41(10):902–17. doi: 10.1016/j.it.2020.08.009

82. Bernink JH, Ohne Y, Teunissen MBM, Wang J, Wu J, Krabbendam L, et al. C-kit-positive ILC2s exhibit an ILC3-like signature that may contribute to IL-17-mediated pathologies. *Nat Immunol* (2019) 20(8):992–1003. doi: 10.1038/s41590-019-0423-0

83. Chen R, Smith SG, Salter B, El-Gammal A, Oliveria JP, Obminski C, et al. Allergen-induced increases in sputum levels of group 2 innate lymphoid cells in subjects with asthma. *Am J Respir Crit Care Med* (2017) 196(6):700–12. doi: 10.1164/rccm.201612-2427OC

84. van der Ploeg EK, Golebski K, van Nimwegen M, Fergusson JR, Heesters BA, Martinez-Gonzalez I, et al. Steroid-resistant human inflammatory ILC2s are marked by CD45RO and elevated in type 2 respiratory diseases. *Sci Immunol* (2021) 6(55). doi: 10.1126/sciimmunol.abd3489

85. Nagasawa M, Heesters BA, Kradolfer CM, Krabbendam L, Martinez-Gonzalez I, de Bruijn MJ, et al. KLRG1 and NKp46 discriminate subpopulations of human CD117 + CRTH2 – ILCs biased toward ILC2 or ILC3. *J Exp Med* (2019) 213(8):1762–76. doi: 10.1084/jem.20190490

86. Morita H, Kubo T, Rückert B, Ravindran A, Soyka MB, Rinaldi AO, et al. Induction of human regulatory innate lymphoid cells from group 2 innate lymphoid cells by retinoic acid. *J Allergy Clin Immunol* (2019) 143(6):2190–201.e9. doi: 10.1016/j.jaci.2018.12.1018

87. Golebski K, Layhadi JA, Sahiner U, Steveling-Klein EH, Lenormand MM, Li RCY, et al. Induction of IL-10-producing type 2 innate lymphoid cells by allergen immunotherapy is associated with clinical response. *Immunity* (2021) 54(2):291–307.e7. doi: 10.1016/j.immuni.2020.12.013

88. Mackley EC, Houston S, Marriott CL, Halford EE, Lucas B, Cerovic V, et al. CCR7-dependent trafficking of RORγ+ ILCs creates a unique microenvironment within mucosal draining lymph nodes. *Nat Commun* (2015) 6(1):1–13. doi: 10.1038/ncomms6862

89. Robinette ML, Fuchs A, Cortez VS, Lee JS, Wang Y, Durum SK, et al. Transcriptional programs define molecular characteristics of innate lymphoid cell classes and subsets. *Nat Immunol* (2015) 16(3):306–17. doi: 10.1038/ni.3094

90. Sanos SL, Bui VL, Mortha A, Oberle K, Heners C, Johner C, et al. RORγt and commensal microflora are required for the differentiation of mucosal interleukin 22–producing NKp46+ cells. *Nat Immunol* (2008) 10(1):83–91. doi: 10.1038/ni.1684

91. Mikami Y, Scarno G, Zitti B, Shih HY, Kanno Y, Santoni A, et al. NCR+ ILC3 maintain larger STAT4 reservoir *via* T-BET to regulate type 1 features upon IL-23 stimulation in mice. *Eur J Immunol* (2018) 48(7):1174–80. doi: 10.1002/eji.201847480

92. Ghoreschi K, Laurence A, Yang XP, Tato CM, McGeachy MJ, Konkel JE, et al. Generation of pathogenic T(H)17 cells in the absence of TGF-β signalling. *Nature* (2010) 467(7318):967–71. doi: 10.1038/nature09447

93. Korchagina AA, Koroleva E, Tumanov AV. Innate lymphoid cells in response to intracellular pathogens: Protection versus immunopathology. *Front Cell Infection Microbiol* (2021) 11:1168. doi: 10.3389/fcimb.2021.775554

94. Buonocore S, Ahern PP, Uhlig HH, Ivanov II, Littman DR, Maloy KJ, et al. Innate lymphoid cells drive interleukin-23-dependent innate intestinal pathology. *Nature* (2010) 464(7293):1371–5. doi: 10.1038/nature08949

95. Boulard O, Kirchberger S, Royston DJ, Maloy KJ, Powrie FM. Identification of a genetic locus controlling bacteria-driven colitis and associated cancer through effects on innate inflammation. *J Exp Med* (2012) 209(7):1309–24. doi: 10.1084/jem.20120239

96. Zhong C, Cui K, Wilhelm C, Hu G, Mao K, Belkaid Y, et al. Group 3 innate lymphoid cells continuously require the transcription factor GATA-3 after commitment. *Nat Immunol* (2016) 17(2):169–78. doi: 10.1038/ni.3318

97. Viant C, Rankin LC, Girard-Madoux MJH, Seillet C, Shi W, Smyth MJ, et al. Transforming growth factor-β and notch ligands act as opposing environmental cues in regulating the plasticity of type 3 innate lymphoid cells. *Sci Signal* (2016) 9 (426). doi: 10.1126/scisignal.aaf2176

98. Verrier T, Satoh-Takayama N, Serafini N, Marie S, di Santo JP, Vosshenrich CAJ. Phenotypic and functional plasticity of murine intestinal NKp46+ group 3 innate lymphoid cells. *J Immunol* (2016) 196(11):4731–8. doi: 10.4049/jimmunol.1502673

99. Chea S, Perchet T, Petit M, Verrier T, Guy-Grand D, Banchi EG, et al. Notch signaling in group 3 innate lymphoid cells modulates their plasticity. *Sci Signal* (2016) 9(426). doi: 10.1126/scisignal.aaf2223

100. Withers DR, Hepworth MR, Wang X, Mackley EC, Halford EE, Dutton EE, et al. Transient inhibition of ROR-γt therapeutically limits intestinal inflammation by reducing TH17 cells and preserving group 3 innate lymphoid cells. *Nat Med* (2016) 22(3):319–23. doi: 10.1038/nm.4046

101. Walker JA, Clark PA, Crisp A, Barlow JL, Szeto A, Ferreira ACF, et al. Polychromic reporter mice reveal unappreciated innate lymphoid cell progenitor heterogeneity and elusive ILC3 progenitors in bone marrow. *Immunity* (2019) 51 (1):104–18.e7. doi: 10.1016/j.immuni.2019.05.002

102. Lo BC, Gold MJ, Hughes MR, Antignano F, Valdez Y, Zaph C, et al. Inflammatory bowel disease the orphan nuclear receptor RORa and group 3 innate lymphoid cells drive fibrosis in a mouse model of crohn's disease. *Sci Immunol* (2016) 1(3):eaaf8864. doi: 10.1126/sciimmunol.aaf8864

103. Lo BC, Canals Hernaez D, Scott RW, Hughes MR, Shin SB, Underhill TM, et al. The transcription factor RORα preserves ILC3 lineage identity and function during chronic intestinal infection. *J Immunol* (2019) 203(12):3209–15. doi: 10.4049/jimmunol.1900781

104. Nixon BG, Chou C, Krishna C, Dadi S, Michel AO, Cornish AE, et al. Cytotoxic granzyme c-expressing ILC1s contribute to antitumor immunity and neonatal autoimmunity. *Sci Immunol* (2022) 7(70). doi: 10.1126/sciimmunol.abi8642

105. Cella M, Gamini R, Sécca C, Collins PL, Zhao S, Peng V, et al. Subsets of ILC3–ILC1-like cells generate a diversity spectrum of innate lymphoid cells in human mucosal tissues. *Nat Immunol* (2019) 20(8):980–91. doi: 10.1038/s41590-019-0425-y

106. O'Sullivan TE, Sun JC, Lanier LL. Natural killer cell memory. *Vol 43 Immun* (2015) 43(4), 634–45. doi: 10.1016j.immuni.2015.09.013

107. O'sullivan TE, Rapp M, Walzer T, Dannenberg AJ, Sun JC. Adipose-resident group 1 innate lymphoid cells promote obesity-associated insulin resistance. *Immunity* (2016) 45:428–41. doi: 10.1016/j.immuni.2016.06.016

108. Bai L, Vienne M, Tang L, Kerdiles Y, Etiennot M, Escalière B, et al. Liver type 1 innate lymphoid cells develop locally via an interferon-γ-dependent loop. *Science* (2021) 371(6536). doi: 10.1126/science.aba4177

109. Pikovskaya O, Chaix J, Rothman NJ, Collins A, Chen YH, Scipioni AM, et al. Cutting edge: Eomesodermin is sufficient to direct type 1 innate lymphocyte development into the conventional NK lineage. *J Immunol* (2016) 196(4):1449–54. doi: 10.4049/jimmunol.1502396

110. Cuff AO, Sillito F, Dertschnig S, Hall A, Luong TV, Chakraverty R, et al. The obese liver environment mediates conversion of NK cells to a less cytotoxic ILC1-like phenotype. *Front Immunol* (2019) 10:2180. doi: 10.3389/fimmu.2019.02180

111. Cortez VS, Ulland TK, Cervantes-Barragan L, Bando JK, Robinette ML, Wang Q, et al. SMAD4 impedes the conversion of NK cells into ILC1-like cells by curtailing non-canonical TGF-β signaling. *Nat Immunol* (2017) 18(9):995–1003. doi: 10.1038/ni.3809

112. Murphy JM, Ngai L, Mortha A, Crome SQ. Tissue-dependent adaptations and functions of innate lymphoid cells. *Front Immunol* (2022) 0:836999/full. doi: 10.3389/fimmu.2022.836999/full

113. Bal SM, Golebski K, Spits H. Plasticity of innate lymphoid cell subsets. *Nat Rev Immunol* (2020) 20:9. doi: 10.1038/s41577-020-0282-9

frontiers | Frontiers in Immunology

TYPE Original Research
PUBLISHED 04 October 2022
DOI 10.3389/fimmu.2022.982827

OPEN ACCESS

EDITED BY
Carmelo Luci,
Institut National de la Santé et de la Recherche Médicale (INSERM), France

REVIEWED BY
Naoko Satoh-Takayama,
RIKEN Center for Integrative Medical Sciences (IMS), Japan
Nicolas Jacquelot,
University Health Network, Canada

*CORRESPONDENCE
Yohei Mikami
yoheimikami@keio.jp
Takanori Kanai
takagast@keio.jp

SPECIALTY SECTION
This article was submitted to NK and Innate Lymphoid Cell Biology, a section of the journal Frontiers in Immunology

RECEIVED 30 June 2022
ACCEPTED 12 September 2022
PUBLISHED 04 October 2022

CITATION
Irie E, Ishihara R, Mizushima I, Hatai S, Hagihara Y, Takada Y, Tsunoda J, Iwata K, Matsubara Y, Yoshimatsu Y, Kiyohara H, Taniki N, Sujino T, Takabayashi K, Hosoe N, Ogata H, Teratani T, Nakamoto N, Mikami Y and Kanai T (2022) Enrichment of type I interferon signaling in colonic group 2 innate lymphoid cells in experimental colitis.
Front. Immunol. 13:982827.
doi: 10.3389/fimmu.2022.982827

Enrichment of type I interferon signaling in colonic group 2 innate lymphoid cells in experimental colitis

Emi Irie[1], Rino Ishihara[1], Ichiro Mizushima[1], Shunya Hatai[2], Yuya Hagihara[1], Yoshiaki Takada[1], Junya Tsunoda[3], Kentaro Iwata[1], Yuta Matsubara[1], Yusuke Yoshimatsu[1], Hiroki Kiyohara[1], Nobuhito Taniki[1], Tomohisa Sujino[4], Kaoru Takabayashi[4], Naoki Hosoe[4], Haruhiko Ogata[4], Toshiaki Teratani[1], Nobuhiro Nakamoto[1], Yohei Mikami[1]* and Takanori Kanai[1,5]*

[1]Division of Gastroenterology and Hepatology, Department of Internal Medicine, School of Medicine, Keio University, Tokyo, Japan, [2]Laboratory for Innate Immune Systems, Department of Microbiology and Immunology, Graduate School of Medicine, Osaka University, Osaka, Japan, [3]Department of Surgery, School of Medicine, Keio University, Tokyo, Japan, [4]Center for Diagnostic and Therapeutic Endoscopy, School of Medicine, Keio University, Tokyo, Japan, [5]AMED-CREST, Japan Agency for Medical Research and Development, Tokyo, Japan

Group 2 innate lymphoid cells (ILC2s) serve as frontline defenses against parasites. However, excluding helminth infections, it is poorly understood how ILC2s function in intestinal inflammation, including inflammatory bowel disease. Here, we analyzed the global gene expression of ILC2s in healthy and colitic conditions and revealed that type I interferon (T1IFN)-stimulated genes were up-regulated in ILC2s in dextran sodium sulfate (DSS)-induced colitis. The enhancement of T1IFN signaling in ILC2s in DSS-induced colitis was correlated with the downregulation of cytokine production by ILC2s, such as interleukin-5. Blocking T1IFN signaling during colitis resulted in exaggeration of colitis in both wild-type and *Rag2*-deficient mice. The exacerbation of colitis induced by neutralization of T1IFN signaling was accompanied by reduction of amphiregulin (AREG) in ILC2s and was partially rescued by exogenous AREG treatment. Collectively, these findings show the potential roles of T1IFN in ILC2s that contribute to colitis manifestation.

KEYWORDS

ILC2 - group 2 innate lymphoid cell, type I interferon, IFNAR, colitis, IBD

Introduction

Innate lymphoid cells (ILCs) are a population of lymphocytes that lack an antigen-specific receptors. ILCs were initially classified into three subsets, group 1, 2, and 3 ILCs, based on the expression pattern of signature cytokines and lineage-determining transcription factors (1) and are now recognized as five subsets, natural killer cells, ILC1, ILC2, ILC3, and lymphoid tissue inducer cells, based on their development and function (2). ILCs are enriched at mucosal sites, including the gut, and play critical roles, particularly ILC3s, in the early immune response, tissue protection, and maintenance of intestinal integrity (2, 3). In line with its importance in the gut, the potential roles of ILCs in the context of intestinal inflammation in inflammatory bowel disease (IBD) and its animal models have been gradually recognized (4, 5). ILC3s are one of the most extensively studied classes of ILCs in the context of intestinal inflammation and are known to induce interleukin (IL)-22, which promotes epithelial regeneration and production of antimicrobial peptides (6). ILC2s provide an early source of Th2 cytokines, serve as a frontline defense against parasites such as helminths, and are important part of tumor immunity (7–9). Therefore, it is highly likely that ILC2s contribute to the manifestation of intestinal inflammation (4). However, the precise roles of ILC2s in intestinal inflammation and IBD are poorly understood.

Herein, we focused on the roles of colonic ILC2s and analyzed its transcriptome in healthy and diseased conditions to identify molecular networks chiefly regulated during murine experimental colitis. We demonstrated that ILC2s are the most abundant cells found in the small and large intestine than in the spleen and lymph nodes. In dextran sodium sulfate (DSS)-induced colitis, IL-5, the hallmark cytokine of ILC2s, was significantly reduced, while the type I interferon (T1IFN) signature was enriched. To investigate the role of T1IFN signaling in ILC2s, we assessed mice treated with anti-T1IFN receptor and observed reduced amphiregulin (AREG) production in ILC2s and exaggeration of colitis in wild-type (WT) and *Rag2*-deficient mice, which was rescued by supplementation with AREG. Our research highlights the potential protective mechanism of ILC2s through T1IFN signaling.

Methods

Mice

C57BL/6 WT mice were purchased from CLEA Japan (Tokyo, Japan). They were maintained in the germ-free (GF) facility of the Keio University School of Medicine. Sex (female)-matched mice aged 6 to 8 weeks were used in the experiments. *Rag2*-deficient mice were obtained from the Taconic Laboratory. All experiments were approved by the regional animal study committees (Keio University) and performed according to institutional guidelines and home office regulations.

DSS-induced colitis model

Colitis was induced in mice using 2.5% DSS solution in drinking water for 7 days. The mice were weighed daily and visually inspected for diarrhea and rectal bleeding. The disease activity index (DAI) was assessed in each mouse group (maximum total score, 12) (10).

Isolation of colonic lamina propria mononuclear cells in mice

Lamina propria mononuclear cells were isolated as described in the previous studies (11). The dissected colon mucosa was cut into 5mM pieces. Tissue was incubated with $Ca2^{+}$ and $Mg2^{+}$-free HBSS containing 1 mM dithiothreitol (DTT) and 5 μM Ethylenediaminetetraacetic acid (EDTA) at 37°C for 30 min, followed by further digestion with collagenase and DNase for 30 min. The cells were separated using a Percoll density gradient. The numbers of live cells was determined using the Countess II (Thermo Fisher Scientific).

Flow cytometry and cell sorting

After blocking with anti-mouse CD16/CD32 antibody for 20 min, the cells were incubated with the specific fluorescence-labelled monoclonal antibodies at 4°C for 30 min, followed by permeabilization with Foxp3/Transcription Factor Fixation/Permeabilization Concentrate and Diluent (eBioscience) and intracellular staining. The following monoclonal antibodies were used for the fluorescence-activated cell sorting (FACS) analysis: anti-mouse CD45.2, CD45, CD3e, CD5, CD19, NK1.1, B220, KLRG1, GATA3, IL-5, IL-13, IL-17A, IL-22, IFN-γ, amphiregulin, FOXP3, T-bet, and RORγt. Dead cells were excluded using the Fixable Viability Dye eFluor. Events were acquired with FACS Canto II or LSRFortessa (BD Biosciences) and analyzed using FlowJo software (BD Biosciences). Colonic ILC2s ($CD127^{+}NK1.1^{-}CD3^{-}CD5^{-}CD19^{-}B220^{-}KLRG^{+}$ cells) were stained after using EasySep Mouse ILC2 Enrichment Kit (STEMCELL Technologies) to remove other cells and sorted using BD FACSAria II (BD Biosciences). See Supplementary Table 1 for information on the antibodies.

RNA sequencing

RNA sequencing (RNA-seq) was performed and analyzed as described in the previous studies (12). Total RNA was prepared from approximately 10,000-50,000 cells by using the TRIzol reagent and was subsequently processed to generate an mRNA-seq library using the NEBNext Poly(A) mRNA Magnetic

Isolation Module (NEB, E7490S), NEBNext Ultra II Directional RNA Library Prep with Sample Purification Beads (NEB, E7765S), and NEBNext Multiplex Oligos for Illumina (Index Primers Set 1 and 2) (NEB, E7335S, and E7500S), according to the manufacturer's protocol. The libraries were sequenced for 150-bp paired-end read using Illumina HiSeq X Ten. To quantify transcript abundance, we pseudo-aligned RNA-seq reads to ENSEMBL transcripts (release 95 GRCm38), using Kallisto (v.0.44.0, options: -b 100) (13). Differentially expressed transcripts were identified using the sleuth R package. Transcript abundances were output by Kallisto in transcripts per million (TPM). Differentially expressed genes (DEGs) were calculated as genes with a sleuth q-value of < 0.05, fold change > 2, and expression > 10 TPM in at least one condition. Enrichment analyses of DEGs were performed using Metascape (http://metascape.org). Pathway analysis of DEGs were performed using Ingenuity pathway analysis (IPA) (Qiagen, Denmark).

Single-cell RNA sequencing

Colonic $CD45^+EpCAM^-$ live cells were sorted from the pooled colonic mononuclear cells and loaded into a chromium controller (10X Genomics). RNA-seq libraries were then prepared using the Chromium Single Cell 3′ Reagent Kit v2 according to the manufacturer's instructions (10X Genomics, CA, USA). The generated scRNA-seq libraries were sequenced using 150 cycles (paired-end reads) with a HiSeq X (Illumina, CA, USA).

In vitro culture

For *in vitro* experiments, 1.0×10^6 cells per well were cultured in a 24-well flat bottom plate in complete medium. Depending on the experiment, different combinations of 100 ng/mL IL-25 (R&D), 100 ng/mL IL-33 (Pepro Tech), or Phorbol-12-myristate-13-acetate (PMA) plus ionomycin were added and cultured for 4 h in a humidified incubator at 37°C. To stimulate *lamina propria* mononuclear cells (LPMC) for 24 h *in vitro*, 2.0×10^5 cells were cultured with 10 ng/ml IFN-β (PBL, NJ, USA) and 100ng/ml IL-33 or PMA plus ionomycin in complete medium in a 96-well plate.

In vivo cytokine treatment

To treat DSS-induced intestinal inflammation, mice were injected intraperitoneally (i.p.) with 1 mg of either IFN-alpha/beta receptor (IFNAR) blocking antibody (Ab), MAR1-5A3 (BioXCell, NH, USA),an isotype control Ab, MOPC-21 (BioXCell, NH, USA) or PBS on day 0 (14). Recombinant murine AREG (400 µg/kg; carrier-free, R &D) was administered i.p. on days 2, 4, and 6.

Histological assessment of intestinal inflammation

Colon samples were fixed in buffered 10% formalin and embedded in paraffin. Paraffin-embedded colon sections were stained with hematoxylin and eosin and then examined. The histological activity score (maximum total score, 40) was assessed as the sum of three parameters: extent, inflammation, and crypt damage related to the percentage of involvement of the mucosal surface in each slide (15).

Statistics

Prism (GraphPad Software) was used for statistical analyses. Data were tested using unpaired two-tailed Student's *t*-test or one-way ANOVA, as indicated. Data are presented as the mean ± SEM. Statistical significance was set at $P < 0.05$.

Result

ILC2s are the most frequent population among the colon ILCs

We first investigated the distribution of ILCs in the digestive and immune system organs of the peritoneal cavity, including the colon, small intestine, liver, spleen, and mesenteric lymph nodes (MLN). ILCs were gated on $CD45^+$ and $CD127\ (IL\text{-}7R)^+$ cells after removing lineage markers (Lin; CD3, CD5, CD19, and B220) with lymphoid morphology (1, 7, 16). In line with the roles of frontline defenses at the mucosal surface, ILCs are mainly populated in the colon and small intestine (Supplementary Figure 1A). Among the total ILCs, the proportion of ILC2s as transcription factor $GATA3^+$ cells among Lin^- $CD45^+$ $CD127^+$ cells (Figure 1A) (1) was significantly higher in the colon than in the small intestine, spleen, and MLN (Figure 1B). This finding is consistent with a previous study showing the predominance of ILC2s among total ILC subsets in rats (16). To confirm the profile of immune cells in the colonic *lamina propria*, we generated an scRNA-seq library of 4266 immune cells purified as $CD45^+$ $EpCAM^-$ live cells from the colonic *lamina propria* of healthy mice. The immune cells were unbiasedly clustered into 16 subsets, including T cells (cluster (Cl) 2, 6, 10, 11, and 12; *Cd3e*), B cells (Cl 0 and 1;*Cd19*), plasma cells (Cl 5 and 15; *Igha*), macrophages and dendritic cells (Cl 4, 8, and 9; *Csf1r*, *Itgam*), and ILCs (Cl 3, 7, and 13; *Il7r*) (Figure 1C and Supplementary Figure 1B). Substantial proportion of ILC2s were identified as $Cd3e^-$ $Il7r^+$ $Gata3^+$ (Cl 3 and 7) and expressed genes encoding signature cytokines and growth factors, such as *Il5*, *Il13*, *Calca*, and *Areg*, which is consistent with previous reports (17–20) (Figures 1D, E, Supplementary Figure 1B). These results

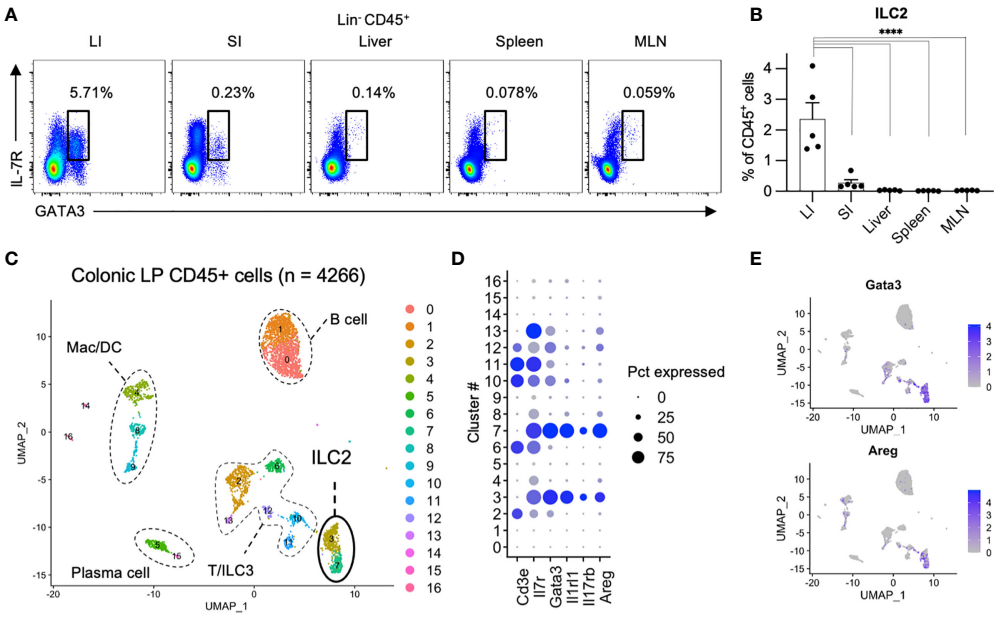

FIGURE 1
Comparison of ILC2s across digestive organs **(A, B)** Representative flow cytometry plots **(A)** and frequencies among CD45$^+$ lymphocytes **(B)** of Lin$^-$CD127$^+$GATA3$^+$ ILC2s in the colon (LI), small intestine (SI), liver, spleen, and mesenteric lymph nodes (MLN) of SPF (specific pathogen free) mice. n=5 for each tissue. Data are representative of two independent experiments (mean and SEM in B). **(C–E)** ScRNA-seq analysis of colonic CD45$^+$ cells. **(C)** Uniform manifold approximation and projection (UMAP) of CD45$^+$ cells (n = 4266) derived from pooled 5 SPF mice, showing the formation of 16 main clusters represented by different colors. The functional description of each cluster is determined by the gene expression characteristics of each. **(D)** Dot plot visualizing the expression of representative genes of ILC2s. The color represents the average expression level, and the circle size represents the proportion of cells expressing each gene. **(E)** Expression levels of the specified marker genes on the UMAP plots. ****P < 0.0001.

highlight that ILC2s are the dominant ILC subset in colonic tissues.

Type I interferon-stimulated genes were up-regulated in ILC2s in DSS-induced colitis

To investigate the phenotype of ILC2s in colitis, we fed mice with 2.5% DSS to induce acute colonic inflammation. DSS-induced colitis is a commonly used mouse model for investigating the pathology of IBD (21). DSS-treated mice showed significantly more sever body weight loss, shorter colon length, and higher DAI than that of the control mice (Figure 2A). Post 7 days of DSS treatment, the frequency of colonic ILC2s among lymphocytes decreased; however, the numbers of ILC2s were comparable in DSS-induced colitis and control mice (Figure 2B). We next assessed the cytokine production in ILC2s and observed that production of IL-5, but not IL-13, was significantly reduced in DSS-induced colitis when stimulated by PMA plus ionomycin (Supplementary Figures 2A, B). We also confirmed that colonic ILC2s obtained from DSS-induced colitis mice showed significantly reduced IL-5 production only when stimulated with IL-25 and IL-33 alone or in combination (Supplementary Figure 2C).

Given that the phenotype of colonic ILC2s is altered in DSS-induced colitis, we assessed the global gene expression of ILC2s under healthy and colitic conditions (sorting strategy is shown in Supplementary Figure 2D). First, we analyzed the signature genes of ILC2s (22). As expected, substantial levels of ILC2s' signature genes, such as *Gata3*, *Klrg1*, *Rora*, *Il1rl1*, *Areg*, *Il5*, and *Il13*, were detected in ILC2s in both groups, while signature genes for ILC1 and ILC3 were at marginal levels (Supplementary Figures 2E, F). To elucidate the phenotypic changes of ILC2s during colitis, we used DEGs as shown in the heatmap (Figure 2C) and performed gene ontology (GO) analysis (Figure 2D). GO analysis indicated that genes related to T1IFN and IFN-γ signaling or response to viruses were significantly enriched in ILC2s in DSS-induced colitis. Consistently, pathway analysis also showed the upregulation of genes related to T1IFN signaling, such as interferon-stimulated genes (ISGs) and IFN-stimulated gene factor3 (ISGF3) in ILC2s in DSS-induced colitis (Figures 2E, F). These data suggest that T1IFN signaling is enhanced in colonic ILC2s during colitis.

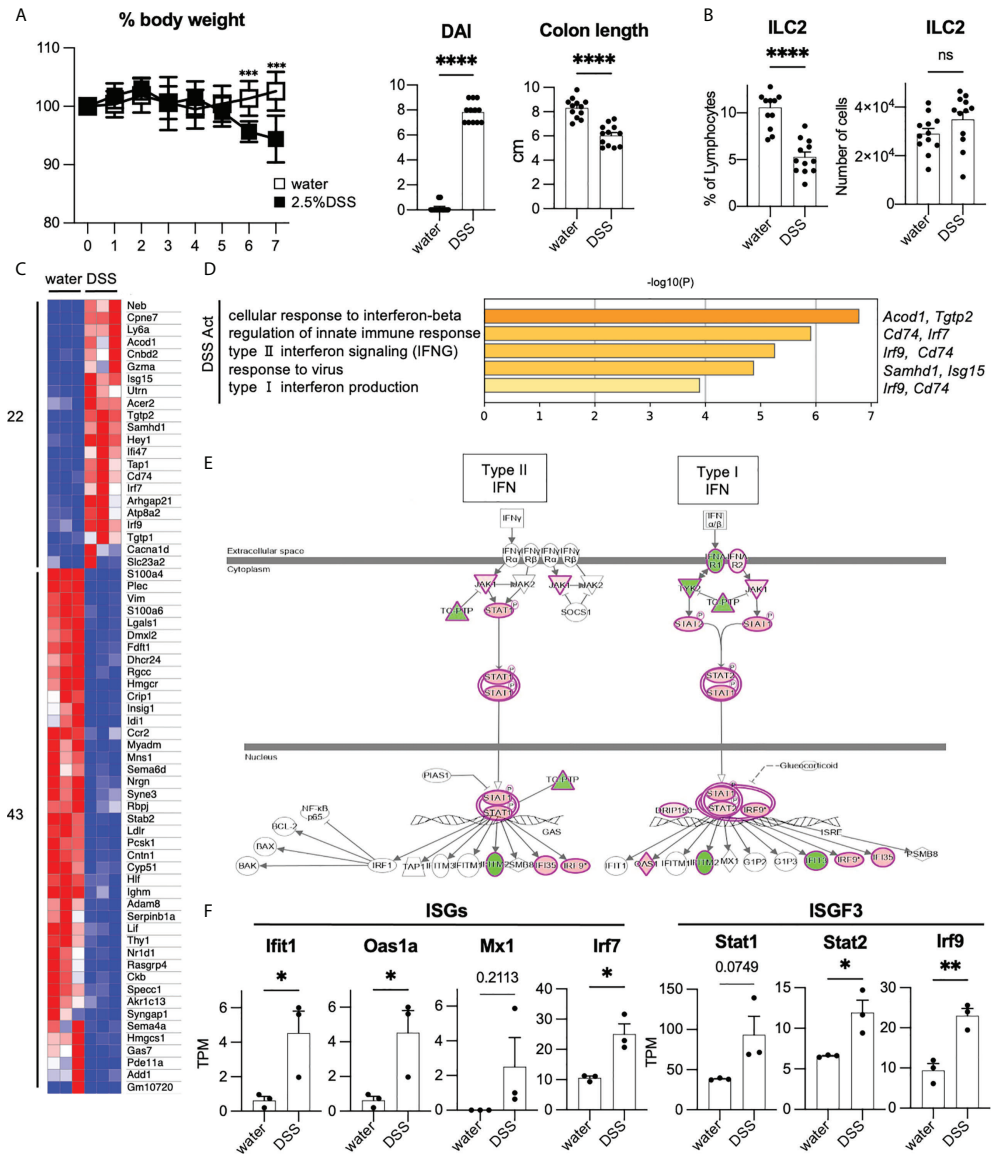

FIGURE 2
Enhancement of T1IFN signaling in ILC2s in DSS-induced colitis **(A, B)** WT mice were administered DSS for 7 days. Graphs show pooled data from three independent experiments (n=12 for each group). **(A)** Change in % body weight relative to initial body weight of control mice (drinking water) and DSS-treated mice in two representative experiments (n=8 for each group). Disease activity index (DAI) score on day 7 and colon length of mice of each group (n=12 for each group). **(B)** % lymphocyte and absolute number of colonic ILC2s in each group (n=12 for each group). **(C)** Heatmap showing relative gene expression of highly expressed differentially expressed (DE) genes (max TPM>10, log2FC>1, log2FC<-1) and the number of upregulated (22 genes) and downregulated genes (43 genes) in DSS treated (n=3) compared to that of control mice (n=3). **(D)** Gene Ontology (GO) analysis of the DSS-activated genes defined in panel C including names of representative genes. **(E)** Ingenuity pathway analysis (IPA) of interferon signaling pathway of genes differentially expressed in DSS-induced colitis. **(F)** Absolute gene expression (TPM) of Type I IFN related genes. Data are mean and SEM in **(A, B, F)** ns, not significant; *$P < 0.05$, **$P < 0.01$, ***$P < 0.001$, ****$P < 0.0001$.

Neutralization of T1IFN signaling reduced amphiregulin in ILC2s in DSS-induced colitis

T1IFN acts as an anti-inflammatory immunomodulator with protective effects against colitis (23, 24). T1IFN may be associated with the phenotypic changes that occur in ILC2s to impart protection against colitis. To analyze the effects of T1IFN signaling on ILC2s during colitis, we blocked T1IFN signaling in mice by i.p. injecting anti-IFNAR1 antibody to mice on day 0 and administered DSS. Although no significant reduction in body weight was observed (Figure 3A), injection of anti-IFNAR1

antibody resulted in increased DAI and shortened colon length (Figure 3B) compared with that in control DSS mice. Histology also showed exacerbation of colitis in anti-IFNAR1 treated mice compared with that in control mice (Figures 3C, D). Consistent with WT mice (Figures 3A–D), neutralizing T1IFN signaling resulted in a more sever colitis histology in *Rag2*-deficient mice (Supplementary Figures 3A–D).

We next investigated the potential contribution of ILC2s in exacerbating colitis. Blocking of IFNAR1 reduced AREG-expressing ILC2s in WT and *Rag2*-deficient mice (Figure 3E, Supplementary Figure 3E), which have been reported to play critical roles in DSS-induced colitis (20). In addition, ILC2s are a major source of AREG in hematopoietic cells in the colon (Figures 1D, E). Eosinophils and mast cells produce AREG in some allergic models challenged by specific antigens; however, there are very few eosinophils and mast cells in the colon of healthy and colitis C57BL/6 WT mice (Supplementary Figure 3F). Next, we evaluated the colonic ILC2-derived AREG expression following type I IFN stimulation *in vitro* and observed that IFN stimulation significantly increased AREG expression in colonic ILC2s (Supplementary Figure 3G). We also reanalyzed publicly available RNA-seq data (GSE73272) (25) and found that IFN-γ, another STAT1-activating cytokine, induced *Areg* expression in ILC2s (Supplementary Figure 3H). These data suggest that T1IFN signaling is important for AREG production in colonic ILC2s and protection of the host from intestinal inflammation.

Exogenous AREG rescued severity of DSS-induced colitis exacerbated by neutralization of T1IFN signaling

To confirm the protective role of AREG in intestinal inflammation by neutralizing T1IFN signaling, WT mice were treated with exogenous recombinant AREG (rAREG) over the course of DSS exposure. Administration of rAREG significantly ameliorated body weight loss (Figure 4A) and DAI (Figure 4B) in the anti-IFNAR1 treated DSS mice. Shortened colon length in anti-IFNAR1 treated DSS mice was diminished in rAREG-treated DSS mice (Figure 4B). Histological scoring confirmed the improvement owing to rAREG treatment (Figures 4C, D). Unlike lung ILC2s in allergic inflammations (26), IRF7 expressing ILC2s in the colon were reduced in anti-IFNAR1 treated mice compared to that of control mice, regardless of rAREG treatment (Figure 4E, Supplementary Figure 4), which indicates that exogenous rAREG does not recover the downregulation of T1IFN signaling in ILC2s. Collectively, these results demonstrate that the T1IFN signaling exacerbation of colitis was partly due to AREG in an ILC2-dependent manner.

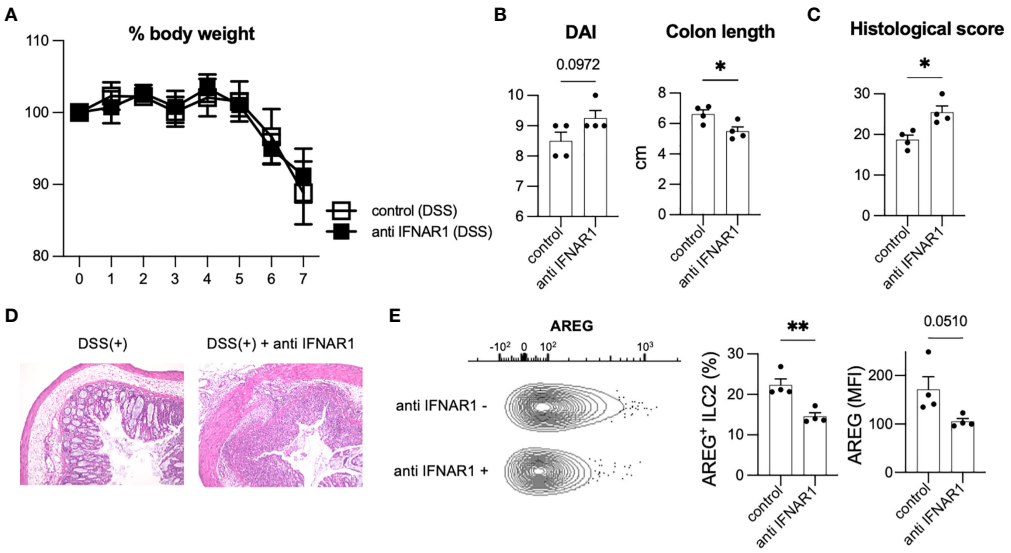

FIGURE 3
Inhibition of T1IFN signaling exacerbated DSS-induced colitis. WT mice were injected anti-IFN-alpha/beta receptor1 (IFNAR1) antibody intraperitoneally (i.p.) on day 0 and administered DSS (n=4 for each group). **(A)** Change in % body weight relative to initial body weight of control (DSS treated) mice (n=4) and anti IFNAR1 i.p. injected (DSS treated) mice (n=4). **(B)** Disease activity index (DAI) score on day 7 and colon length of mice of each group (n=4 for each group). **(C, D)** Histological score (n=4 for each group) and histopathology of distal colon. **(E)** Amphiregulin (AREG) expression in ILC2s of control mice and anti-IFNAR1 treated mice. Representative contour plots showing AREG expressing ILC2s in control mice (DSS treated) and anti IFNAR1 i.p. injected mice (DSS treated). Frequency of AREG expressing ILC2s among all ILC2s and mean fluorescence intensity (MFI) of AREG in ILC2s (n=4 for each group). Data are mean and SEM. $^*P < 0.05$, $^{**}P < 0.01$.

10.3389/fimmu.2022.982827

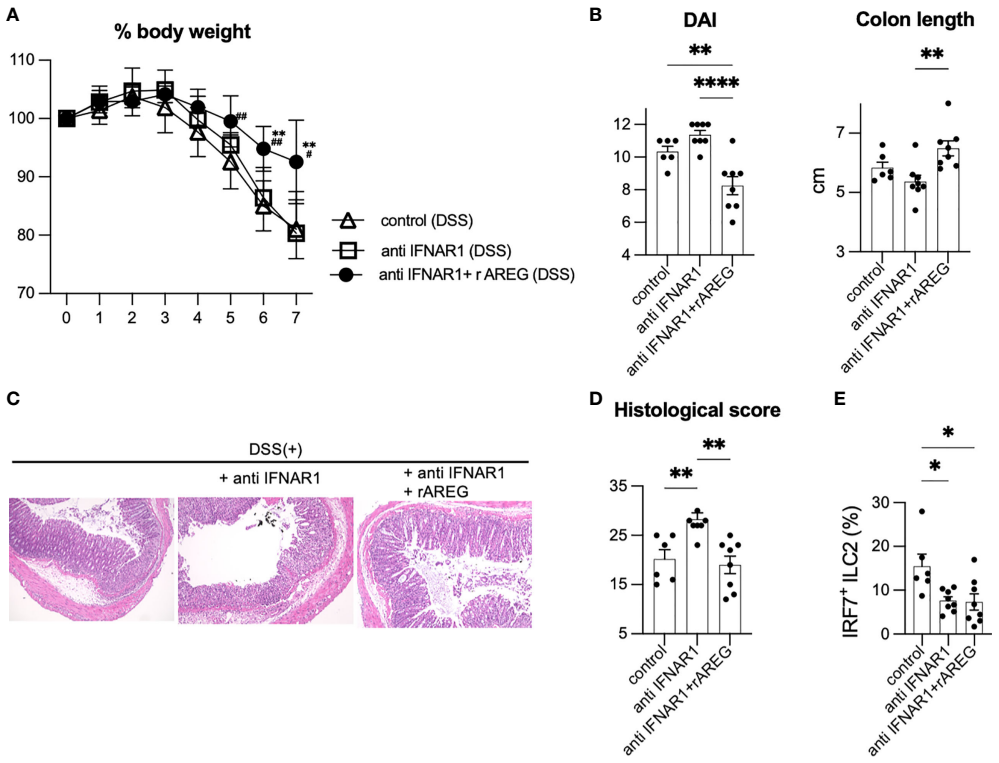

FIGURE 4
Amphiregulin treatment partially rescued severity of DSS-induced colitis in anti-IFNAR treated mice. WT mice were injected exogenous recombinant AREG (rAREG) over the course of DSS exposure with anti-IFNAR1 i.p. injection. Data are representative of two independent experiments (n=6 for control group, n=8 for anti IFNAR1 only and anti IFNAR1 plus rAREG injected group). **(A)** Change in % body weight relative to initial body weight of control mice (DSS treated) (n=6), anti IFNAR1 i.p. injected mice (DSS treated) (n=8) and anti IFNAR1 plus rAREG i.p. injected mice (DSS treated) (n=8). $^{**}P<0.01$ vs anti IFNAR1 group, $^{\#}P<0.05$, $^{\#\#}P<0.01$ vs control group. **(B)** Disease activity index (DAI) score on day 7 and colon length of mice of each group. **(C, D)** Histological score and histopathology of distal colon. **(E)** Frequency of IRF7^{+} ILC2s in each group. Data are mean and SEM. $^{*}P < 0.05$, $^{**}P < 0.01$, $^{****}P < 0.0001$.

Discussion

The roles of ILC2s in the intestinal tract have been extensively studied in the context of helminth infections (7, 18, 27). These studies have revealed the critical roles of ILC2s during type 2 immune responses and mainly focused on type 2 cytokines, such as IL-5 and IL-13, which induce eosinophilia and goblet cell hyperplasia. However, the roles of ILC2s in intestinal inflammation, except for type 2 inflammation, remains unclear. Herein, we revealed a previously unrecognized role of ILC2s in controlling the pathogenesis of acute intestinal inflammation. ILC2s are the most abundant cells in the colon among visceral organs, and ILC2s obtained from the colonic mucosa under inflammatory conditions showed significant enrichment of T1IFN signaling. Neutralization of T1IFN signaling exacerbated colitis severity accompanied by a reduction in AREG-producing ILC2s in DSS-induced colitis, which was ameliorated by exogenous treatment with AREG.

ILC2s play a central role in the formation of type 2 immune responses during infections by parasites and fungi and allergic conditions in the lungs and other organs. Multiple factors contribute to the activation and repression of ILC2s. ILC2s proliferate and produce IL-5 and IL-13 upon IL-25 and IL-33 stimulation, which are suppressed by STAT1-dependent cytokines such as T1IFN, IFN-γ, and IL-27 (25, 28). Transcriptomic analysis unbiasedly revealed the enrichment of genes related to T1IFN signaling in ILC2s during colitis. Our data suggests that ILC2s show enhanced production of genes related to T1IFN responses and a reduction in IL-5 production in colitis. Our findings indicate that upregulation of T1IFN alters the ILC2 phenotype.

AREG plays a critical role in wound repair and tissue remodeling by promoting epithelial cell proliferation (29). Despite the importance of AREG production by hematopoietic cells in the context of mucosal damage, regulation of AREG expression in ILC2s is not yet fully understood, and the roles of STAT1 dependent cytokines, including IFN-β, IFN-γ, and IL-27, show inconclusive results for AREG production in ILC2s (25, 28). A recent report suggested that long-term stimulation with IFN-β enhanced AREG production (30). Consistently, GO analysis

showed enrichment of genes related to T1IFN signaling and a decrease in AREG expression in ILC2s upon neutralization of T1IFN signaling, providing an additional aspect of the protective roles of ILC2s through T1IFN signaling *in vivo*. Consistently, adoptive transfer of ILC2s expanded in mice treated with IL-33 into mice with DSS-induced colitis, resulting in a significant improvement in the severity of colitis compared to mice without ILC2 transfer (31). Although both pro- and anti-inflammatory roles of T1IFN in intestinal inflammation have been reported (32), and clinical trials have shown inconclusive results for T1IFN in IBD patients (33), tissue- or cell type- specific manipulation of T1IFN signaling or AREG supplementation might be a potential therapeutic option for treating IBD or other intestinal inflammatory diseases.

ILC2s have been reported to exacerbate colitis (34, 35) and promote wound healing (20, 36). Recent reports suggest that cytokines known to activate ILC2s, such as IL-33 and thymic stromal lymphopoietin (TSLP), have protective effects against DSS-induced colitis (20, 37). It was unexpected that T1IFN, known to repress type 2 cytokine production in ILC2s, enhances AREG production in ILC2s *in vivo*. AREG is expressed by intestinal epithelial cells (29); however, type III IFN, rather than type I IFN, induces the nuclear translocation of STAT1 in colonic epithelial cells (38). Therefore, it is possible that T1IFN and AREG act on both colonic epithelial cells and hematopoietic cells. In addition to epithelial cells and ILC2s, there are several hematopoietic cell types that are known to produce AREG, such as eosinophils, mast cells, and T cells (39–42). However, we detected a minimal number of eosinophils and mast cells in colitic *Rag2*-deficient mice, in which blocking T1IFN worsened colitis. In addition, scRNA-seq analysis showed that ILC2s are a major source of AREG among hematopoietic cells, suggesting that ILC2s are a major producer of AREG upon T1IFN signaling in hematopoietic cell populations in the colon. A limitation of this study is the lack of evidence regarding the importance of ILC2-derived AREG in colitis. Although the generation of ILC2-specific deletions of AREG is technically challenging, future studies are expected to reveal an ILC2-specific role of AREG in intestinal homeostasis. Another issue that remains to be clarified is that although colonic ILC2s produce AREG upon T1IFN stimulation *in vitro*, colitis itself does not induce AREG. We speculate that AREG production is induced or repressed by multifactorial cytokine networks during colitis; however, leastwise, "tonic T1IFN signaling" (43, 44) is important in maintaining AREG production; thus, blocking T1IFN signaling significantly reduced AREG production in colonic ILC2s.

In summary, this study is the first to demonstrate the anticolitic role of T1IFN signaling in ILC2s during acute intestinal damage. AREG production mediates the anticolitic phenotype of ILC2s. However, the effect of the neutralization of T1IFN signaling in the chronic phase has not been clarified because the functions of ILC2s are different in the acute and chronic phases of inflammation (45). The role of T1IFN in colonic ILC2s found in a murine colitis model is expected to be further explored in human diseases.

Data availability statement

RNA sequencing data have been deposited to Gene Expression Omnibus under the accession number GSE212939.

Ethics statement

The animal study was reviewed and approved by Animal study committees (Keio University).

Author contributions

EI and YoM designed the experiments and interpreted data. EI, RI, SH, IM, YH, YT, JT, KI, YuM, YY, HK, TS, and TT performed the experiments. EI, IM, and YoM analyzed the genomic data and generated the figures. KT, NH, HO, NN, and TK supervised and supported this study. EI drafted the manuscript. YoM wrote the manuscript with input from other authors. All authors contributed to the article and approved the submitted version.

Funding

This study was funded by the Japan Society for the Promotion of Science (JSPS) KAKENHI (B) 20H03666 to YoM, and (A) 20H00536 to TK; JSPS Grant-in-Aid for Transformative Research Areas(B): 21H05123 to YoM.; Advanced Research and Development Programs for Medical Innovation (AMED-CREST: 21gm1510002h0001to TK, and 20gm1210001h0001 to YM; the Practical Research Project for Rare/Intractable Disease: 21ek0109556h0001 to YM); the Japan Foundation for Applied Enzymology; and Keio University Medical Fund.

Acknowledgments

We thank R. Sakakibara, S Suzuki, Y. Kaieda, H. Suzuki, K. Ono, S. Tanemoto, M. Ichikawa, K. Miyamoto, and Y. Harada (Keio University) for technical assistance. We thank C. Ido and the animal facility staff (Keio University) for their technical support in handling mice. We thank Kazuyo Moro (Osaka University), Giuseppe Sciumè (Sapienza University of Rome), Hiroki Kabata (Keio University), and the members of the Kanai laboratory for their helpful suggestions. We would like to thank Editage (www.editage.com) for English language editing.

Conflict of interest

The authors declare that the research was conducted in the absence of any commercial or financial relationships that could be construed as a potential conflict of interest.

Publisher's note

Supplementary material

The Supplementary Material for this article can be found online at: https://www.frontiersin.org/articles/10.3389/fimmu.2022.982827/full#supplementary-material

SUPPLEMENTARY FIGURE 1
(A) Frequency of $Lin^{-}CD127^{+}$ total ILCs among $CD45^{+}$ lymphocytes in the colon (LI), small intestine (SI), liver, spleen, and MLN of SPF mice. n=5 for each tissue. Data are representative of two independent experiments (mean and SEM). ****P < 0.0001. **(B)** UMAP (Uniform Manifold Approximation and Projection) of representative gene expression for T cells *(Cd3e)*, B cells *(Cd19)*, plasma cells *(Igha)*, macrophages and dendritic cells *(Csf1r, Itgam, Itgae)*, T cells and ILCs *(Il7r)*, and ILC2s *(Rora, Il5, Il13, Calca)*. (n=5 SPF mice).

SUPPLEMENTARY FIGURE 2
(A) Representative flow cytometry plots of cytokine production by ILC2s in the control and DSS-treated groups stimulated with PMA plus ionomycin. **(B)** Frequency of IL-5 and IL-13 producing colonic ILC2s in each group among all ILC2s. Graphs show pooled data from three independent experiments (n=12 for each group). **(C)** Frequencies of IL-5 producing colonic ILC2s among all ILC2s of each group stimulated with PMA plus ionomycin, IL-25, IL-33, and IL-25 plus IL-33 for 4h (n=4 for each group). **(D)** Gating strategy for the enrichment of colonic ILC2s. **(E)** Heatmap showing the relative expression of signature genes of ILC2s (22) and the number of upregulated (12 genes) and downregulated genes (20 genes) in DSS-treated mice compared to that in control mice (n=3 for each group). **(F)** TPM values of signature genes of ILC2s and other groups of ILCs. *P<0.05, **P<0.01, ***P<0.001.

SUPPLEMENTARY FIGURE 3
Rag2-deficient mice were injected anti IFNAR1 antibody i.p. on day 0 and administered DSS (n=4 for control group and n=5 for anti IFNAR1 i.p. injected group). **(A)** Change in % body weight relative to initial body weight of control mice (DSS treated) (n=4) and anti IFNAR1 i.p. injected mice (DSS treated) (n=5). **(B)** Disease activity index (DAI) score on day 7 and colon length of the mice in each group. **(C, D)** Histological score and histopathology of the distal colon. **(E)** Frequency of AREG expressing ILC2s among all ILC2s in each group. **(F)** The number of colonic ILC2s, eosinophil, and mast cells in control and DSS-treated *Rag2*-deficient mice (n=3 for each group). **(G)** Frequency of AREG expressing ILC2s among all ILC2s following 4h *in vitro* stimulation with or without IFNβ. 12 mice were used and 2 mice were pooled in one sample. n=3 for each group. **(H)** FPKM (fragments per kilobase million) values of *Il5, Areg, and Stat2* of ILC2s treated with IL-33 or IL-33 plus IFN-γ. Data are mean and SEM.

SUPPLEMENTARY FIGURE 4
(A) Representative contour plots showing IRF7 expressing ILC2s in control mice (DSS treated), anti IFNAR1 i.p. injected mice (DSS treated), and anti IFNAR1 plus rAREG i.p. injected mice (DSS treated). **(B)** MFI of IRF7 in ILC2s (n=4 per group from one experiment). **(C)** Absolute number of $IRF7^{+}$ ILC2s in each group. Graphs show pooled data from two independent experiments (n=6 for control mice, n=8 for anti IFNAR1 i.p. injected mice and anti IFNAR1 plus rAREG i.p. injected mice). Data are mean and SEM.

References

1. Spits H, Artis D, Colonna M, Diefenbach A, Di Santo JP, Eberl G, et al. Innate lymphoid cells–a proposal for uniform nomenclature. *Nat Rev Immunol* (2013) 13 (2):145–9. doi: 10.1038/nri3365

2. Vivier E, Artis D, Colonna M, Diefenbach A, Di Santo JP, Eberl G, et al. Innate lymphoid cells: 10 years on. *Cell* (2018) 174(5):1054–66. doi: 10.1016/j.cell.2018.07.017

3. Mizuno S, Mikami Y, Kamada N, Handa T, Hayashi A, Sato T, et al. Cross-talk between rorγt+ innate lymphoid cells and intestinal macrophages induces mucosal il-22 production in crohn's disease. *Inflammation Bowel Dis* (2014) 20 (8):1426–34. doi: 10.1097/MIB.0000000000000105

4. Goldberg R, Prescott N, Lord GM, MacDonald TT, Powell N. The unusual suspects–innate lymphoid cells as novel therapeutic targets in ibd. *Nat Rev Gastroenterol Hepatol* (2015) 12(5):271–83. doi: 10.1038/nrgastro.2015.52

5. Friedrich M, Pohin M, Powrie F. Cytokine networks in the pathophysiology of inflammatory bowel disease. *Immunity* (2019) 50(4):992–1006. doi: 10.1016/j.immuni.2019.03.017

6. Aujla SJ, Chan YR, Zheng M, Fei M, Askew DJ, Pociask DA, et al. Il-22 mediates mucosal host defense against gram-negative bacterial pneumonia. *Nat Med* (2008) 14(3):275–81. doi: 10.1038/nm1710

7. Moro K, Yamada T, Tanabe M, Takeuchi T, Ikawa T, Kawamoto H, et al. Innate production of T(H)2 cytokines by adipose tissue-associated c-Kit(+)Sca-1 (+) lymphoid cells. *Nature* (2010) 463(7280):540–4. doi: 10.1038/nature08636

8. Wilhelm C, Harrison OJ, Schmitt V, Pelletier M, Spencer SP, Urban JF, et al. Critical role of fatty acid metabolism in Ilc2-mediated barrier protection during malnutrition and helminth infection. *J Exp Med* (2016) 213(8):1409–18. doi: 10.1084/jem.20151448

9. Jacquelot N, Seillet C, Wang M, Pizzolla A, Liao Y, Hediyeh-Zadeh S, et al. Blockade of the Co-inhibitory molecule pd-1 unleashes Ilc2-dependent antitumor immunity in melanoma. *Nat Immunol* (2021) 22(7):851–64. doi: 10.1038/s41590-021-00943-z

10. Hidalgo-Cantabrana C, Algieri F, Rodriguez-Nogales A, Vezza T, Martínez-Camblor P, Margolles A, et al. Effect of a ropy exopolysaccharide-producing bifidobacterium animalis subsp. lactis strain orally administered on dss-induced colitis mice model. *Front Microbiol* (2016) 7:868. doi: 10.3389/fmicb.2016.00868

11. Honda K, Littman DR. The microbiota in adaptive immune homeostasis and disease. *Nature* (2016) 535(7610):75–84. doi: 10.1038/nature18848

12. Iwata S, Mikami Y, Sun HW, Brooks SR, Jankovic D, Hirahara K, et al. The transcription factor T-bet limits amplification of type I ifn transcriptome and

circuitry in T helper 1 cells. *Immunity* (2017) 46(6):983–91.e4. doi: 10.1016/j.immuni.2017.05.005

13. Bray NL, Pimentel H, Melsted P, Pachter L. Erratum: Near-optimal probabilistic rna-seq quantification. *Nat Biotechnol* (2016) 34(8):888. doi: 10.1038/nbt0816-888d

14. Calame DG, Mueller-Ortiz SL, Morales JE, Wetsel RA. The C5a anaphylatoxin receptor (C5ar1) protects against listeria monocytogenes infection by inhibiting type 1 ifn expression. *J Immunol* (2014) 193(10):5099–107. doi: 10.4049/jimmunol.1401750

15. Mennigen R, Nolte K, Rijcken E, Utech M, Loeffler B, Senninger N, et al. Probiotic mixture Vsl3 protects the epithelial barrier by maintaining tight junction protein expression and preventing apoptosis in a murine model of colitis. *Am J Physiol Gastrointest Liver Physiol* (2009) 296(5):G1140–9. doi: 10.1152/ajpgi.90534.2008

16. Abidi A, Laurent T, Bériou G, Bouchet-Delbos L, Fourgeux C, Louvet C, et al. Characterization of rat ilcs reveals Ilc2 as the dominant intestinal subset. *Front Immunol* (2020) 11:255. doi: 10.3389/fimmu.2020.00255

17. Hoyler T, Klose CS, Souabni A, Turqueti-Neves A, Pfeifer D, Rawlins EL, et al. The transcription factor gata-3 controls cell fate and maintenance of type 2 innate lymphoid cells. *Immunity* (2012) 37(4):634–48. doi: 10.1016/j.immuni.2012.06.020

18. Nussbaum JC, Van Dyken SJ, von Moltke J, Cheng LE, Mohapatra A, Molofsky AB, et al. Type 2 innate lymphoid cells control eosinophil homeostasis. *Nature* (2013) 502(7470):245–8. doi: 10.1038/nature12526

19. Xu H, Ding J, Porter CBM, Wallrapp A, Tabaka M, Ma S, et al. Transcriptional atlas of intestinal immune cells reveals that neuropeptide A-cgrp modulates group 2 innate lymphoid cell responses. *Immunity* (2019) 51(4):696–708.e9. doi: 10.1016/j.immuni.2019.09.004

20. Monticelli LA, Osborne LC, Noti M, Tran SV, Zaiss DM, Artis D. Il-33 promotes an innate immune pathway of intestinal tissue protection dependent on amphiregulin-egfr interactions. *Proc Natl Acad Sci USA* (2015) 112(34):10762–7. doi: 10.1073/pnas.1509070112

21. Strober W, Fuss IJ, Blumberg RS. The immunology of mucosal models of inflammation. *Annu Rev Immunol* (2002) 20:495–549. doi: 10.1146/annurev.immunol.20.100301.064816

22. Robinette ML, Fuchs A, Cortez VS, Lee JS, Wang Y, Durum SK, et al. Transcriptional programs define molecular characteristics of innate lymphoid cell classes and subsets. *Nat Immunol* (2015) 16(3):306–17. doi: 10.1038/ni.3094

23. González-Navajas JM, Lee J, David M, Raz E. Immunomodulatory functions of type I interferons. *Nat Rev Immunol* (2012) 12(2):125–35. doi: 10.1038/nri3133

24. Kotredes KP, Thomas B, Gamero AM. The protective role of type I interferons in the gastrointestinal tract. *Front Immunol* (2017) 8:410. doi: 10.3389/fimmu.2017.00410

25. Moro K, Kabata H, Tanabe M, Koga S, Takeno N, Mochizuki M, et al. Interferon and il-27 antagonize the function of group 2 innate lymphoid cells and type 2 innate immune responses. *Nat Immunol* (2016) 17(1):76–86. doi: 10.1038/ni.3309

26. He J, Yang Q, Xiao Q, Lei A, Li X, Zhou P, et al. Irf-7 is a critical regulator of type 2 innate lymphoid cells in allergic airway inflammation. *Cell Rep* (2019) 29 (9):2718–30 e6. doi: 10.1016/j.celrep.2019.10.077

27. Neill DR, Wong SH, Bellosi A, Flynn RJ, Daly M, Langford TK, et al. Nuocytes represent a new innate effector leukocyte that mediates type-2 immunity. *Nature* (2010) 464(7293):1367–70. doi: 10.1038/nature08900

28. Duerr CU, McCarthy CD, Mindt BC, Rubio M, Meli AP, Pothlichet J, et al. Type I interferon restricts type 2 immunopathology through the regulation of group 2 innate lymphoid cells. *Nat Immunol* (2016) 17(1):65–75. doi: 10.1038/ni.3308

29. Zaiss DMW, Gause WC, Osborne LC, Artis D. Emerging functions of amphiregulin in orchestrating immunity, inflammation, and tissue repair. *Immunity* (2015) 42(2):216–26. doi: 10.1016/j.immuni.2015.01.020

30. Feng X, Bao R, Li L, Deisenhammer F, Arnason BGW, Reder AT. Interferon-B corrects massive gene dysregulation in multiple sclerosis: Short-term and long-term effects on immune regulation and neuroprotection. *EBioMedicine* (2019) 49:269–83. doi: 10.1016/j.ebiom.2019.09.059

31. Ngo Thi Phuong N, Palmieri V, Adamczyk A, Klopfleisch R, Langhorst J, Hansen W, et al. Il-33 drives expansion of type 2 innate lymphoid cells and regulatory T cells and protects mice from severe, acute colitis. *Front Immunol* (2021) 12:669787. doi: 10.3389/fimmu.2021.669787

32. Rauch I, Hainzl E, Rosebrock F, Heider S, Schwab C, Berry D, et al. Type I interferons have opposing effects during the emergence and recovery phases of colitis. *Eur J Immunol* (2014) 44(9):2749–60. doi: 10.1002/eji.201344401

33. Mannon PJ, Hornung RL, Yang Z, Yi C, Groden C, Friend J, et al. Suppression of inflammation in ulcerative colitis by interferon-B-1a is accompanied by inhibition of il-13 production. *Gut* (2011) 60(4):449–55. doi: 10.1136/gut.2010.226860

34. Qiu X, Qi C, Li X, Fang D, Fang M. Il-33 deficiency protects mice from dss-induced experimental colitis by suppressing Ilc2 and Th17 cell responses. *Inflammation Res* (2020) 69(11):1111–22. doi: 10.1007/s00011-020-01384-4

35. Camelo A, Barlow JL, Drynan LF, Neill DR, Ballantyne SJ, Wong SH, et al. Blocking il-25 signalling protects against gut inflammation in a type-2 model of colitis by suppressing nuocyte and nkt derived il-13. *J Gastroenterol* (2012) 47 (11):1198–211. doi: 10.1007/s00535-012-0591-2

36. Frisbee AL, Saleh MM, Young MK, Leslie JL, Simpson ME, Abhyankar MM, et al. Il-33 drives group 2 innate lymphoid cell-mediated protection during clostridium difficile infection. *Nat Commun* (2019) 10(1):2712. doi: 10.1038/s41467-019-10733-9

37. Negishi H, Miki S, Sarashina H, Taguchi-Atarashi N, Nakajima A, Matsuki K, et al. Essential contribution of Irf3 to intestinal homeostasis and microbiota-mediated tslp gene induction. *Proc Natl Acad Sci USA* (2012) 109(51):21016–21. doi: 10.1073/pnas.1219482110

38. McElrath C, Espinosa V, Lin JD, Peng J, Sridhar R, Dutta O, et al. Critical role of interferons in gastrointestinal injury repair. *Nat Commun* (2021) 12 (1):2624. doi: 10.1038/s41467-021-22928-0

39. Arpaia N, Green JA, Moltedo B, Arvey A, Hemmers S, Yuan S, et al. A distinct function of regulatory T cells in tissue protection. *Cell* (2015) 162(5):1078–89. doi: 10.1016/j.cell.2015.08.021

40. Burzyn D, Kuswanto W, Kolodin D, Shadrach JL, Cerletti M, Jang Y, et al. A special population of regulatory T cells potentiates muscle repair. *Cell* (2013) 155 (6):1282–95. doi: 10.1016/j.cell.2013.10.054

41. Okumura S, Sagara H, Fukuda T, Saito H, Okayama Y. Fcepsilonri-mediated amphiregulin production by human mast cells increases mucin gene expression in epithelial cells. *J Allergy Clin Immunol* (2005) 115(2):272–9. doi: 10.1016/j.jaci.2004.10.004

42. Morimoto Y, Hirahara K, Kiuchi M, Wada T, Ichikawa T, Kanno T, et al. Amphiregulin-producing pathogenic memory T helper 2 cells instruct eosinophils to secrete osteopontin and facilitate airway fibrosis. *Immunity* (2018) 49 (1):134–50.e6. doi: 10.1016/j.immuni.2018.04.023

43. Mostafavi S, Yoshida H, Moodley D, LeBoite H, Rothamel K, Raj T, et al. Parsing the interferon transcriptional network and its disease associations. *Cell* (2016) 164(3):564–78. doi: 10.1016/j.cell.2015.12.032

44. Gough DJ, Messina NL, Clarke CJ, Johnstone RW, Levy DE. Constitutive type I interferon modulates homeostatic balance through tonic signaling. *Immunity* (2012) 36(2):166–74. doi: 10.1016/j.immuni.2012.01.011

45. Gieseck RL, Wilson MS, Wynn TA. Type 2 immunity in tissue repair and fibrosis. *Nat Rev Immunol* (2018) 18(1):62–76. doi: 10.1038/nri.2017.90

frontiers | Frontiers in Immunology

TYPE Original Research
PUBLISHED 07 March 2023
DOI 10.3389/fimmu.2023.1127413

OPEN ACCESS

EDITED BY
Carmelo Luci,
Institut National de la Santé et de la Recherche Médicale (INSERM), France

REVIEWED BY
Christoph Siegfried Niki Klose,
Charité Universitätsmedizin Berlin, Germany
Lisa Anna Mielke,
Olivia Newton-John Cancer Research Institute, Australia

*CORRESPONDENCE
Xiaofei Shen
dg1535058@smail.nju.edu.cn
Wenxian Guan
wenxian_guan@126.com
Xiaofeng Lu
lxf_doctor@sina.com

†These authors have contributed equally to this work

SPECIALTY SECTION
This article was submitted to NK and Innate Lymphoid Cell Biology, a section of the journal Frontiers in Immunology

RECEIVED 19 December 2022
ACCEPTED 20 February 2023
PUBLISHED 07 March 2023

CITATION
Song P, Cao K, Mao Y, Ai S, Sun F, Hu Q, Liu S, Wang M, Lu X, Guan W and Shen X (2023) Tissue specific imprinting on innate lymphoid cells during homeostasis and disease process revealed by integrative inference of single-cell transcriptomics. *Front. Immunol.* 14:1127413. doi: 10.3389/fimmu.2023.1127413

Tissue specific imprinting on innate lymphoid cells during homeostasis and disease process revealed by integrative inference of single-cell transcriptomics

Peng Song[1,2†], Ke Cao[3†], Yonghuan Mao[1,2†], Shichao Ai[1], Feng Sun[1], Qiongyuan Hu[1], Song Liu[1], Meng Wang[1], Xiaofeng Lu[1*], Wenxian Guan[1*] and Xiaofei Shen[1,2*]

[1]Department of Gastrointestinal Surgery, Nanjing Drum Tower Hospital, The Affiliated Hospital of Nanjing University Medical School, Nanjing, China, [2]Department of Gastrointestinal Surgery, Nanjing Drum Tower Hospital, Drum Tower Clinical Medical College of Nanjing Medical University, Nanjing, China, [3]Department of Critical Care Medicine, Nanjing Drum Tower Hospital, The Affiliated Hospital of Nanjing University Medical School, Nanjing, China

Introduction: Innate lymphoid cells (ILCs) are key components of the immune system, yet the similarity and distinction of the properties across tissues under homeostasis, inflammation and tumor process remain elusive.

Methods: Here we performed integrative inference of ILCs to reveal their transcriptional profiles and heterogeneity from single-cell genomics. We collected a large number of ILCs from human six different tissues which can represent unique immune niches (circulation, lymphoid tissue, normal and inflamed mucosa, tumor microenvironment), to systematically address the transcriptional imprinting.

Results: ILCs are profoundly imprinted by their organ of residence, and tissue-specific distinctions are apparent under pathological conditions. In the hepatocellular carcinoma microenvironment, we identified intermediate c-kit$^+$ ILC2 population, and lin$^-$CD127$^-$ NK-like cells that expressed markers of cytotoxicity including *CCL5* and *IFNG*. Additionally, CD127$^+$CD94$^+$ ILC1s were preferentially enriched in inflamed ileum from patients with Crohn's disease.

Discussion: These analyses depicted a comprehensive characterization of ILC anatomical distribution and subset heterogeneity, and provided a base line for future temporal or spatial studies focused on tissue-specific ILC-mediated immunity.

KEYWORDS

innate lymphoid cells, single-cell transcriptomics, tissue imprinting, cell heterogeneity, integrative inference

Introduction

Innate lymphoid cells (ILCs) are newly discovered lymphocytes which are functionally analogous to polarized $CD4^+$ T helper (Th) cells, acting as important contributors to the regulation of immunity, inflammation, and tissue homeostasis (1). ILCs lack antigen-specific receptors on their surface, making them distinct from dendritic cells (DCs), macrophages, B and T lymphocytes (termed Lineage negative, Lin^-) (1, 2). ILCs have the capacity to adjust to tissue-specific environments and respond to shocks or infections by producing cytokines, which direct and enhance immune responses on the front line of attack (2–4). Currently, ILCs are well characterized into five categories: NK cells, lymphoid-tissue inducer (LTi) cells together with group 1, 2 and 3 ILCs (ILC1s, ILC2s and ILC3s, respectively). ILC1s ($CD127^+CD117^-CRTH2^-$) and NK cells ($CD127^-$) share several common features, including their expression of the transcription factor T-bet (encoded by *TBX21*), the responsiveness to IL-15, IL-12 and IL-18, and the capacity to secrete interferon-γ (IFN-γ). Most NK cells are also dependent on EOMES for lineage specification, and it appears the characteristics of killer cells in immunosurveillance, whereas ILC1s are innate helper cells with weaker cytotoxic activity (5–7). With regard to ILC2s ($CD127^+CD117^{\pm}CRTH2^+$), GATA3 is the master transcriptional regulator for their development, as well as their capacity of producing IL-5 and IL-13 that govern a wide spectrum of features, including type 2 immune response, helminth infection and tissue fibrosis (8). ILC3s ($CD127^+CD117^+CRTH2^-$) are defined by RORγt (encoded by *RORC*) expression, produce IL-17and IL-22, which have important functions in lymphoid tissue development and protection against extracellular bacteria and fungi (9, 10).

Recently, the single-cell RNA sequencing (scRNA-seq) technologies have been increasingly applied to characterize tissue-specific imprinting of ILCs, which improved our knowledge of the human immune system's diversity. For example, Mazzurana et al. identified a novel unconventional ILC2 subpopulation ($CRTH2^-$ ILC2) in the lung, expressing receptors for IL-33 and IL-25, by full-length Smart-seq2 scRNA-seq (11). Heinrich et al. discovered c-Kit^+ ILC2s increased in frequency from non-tumor liver to tumor tissue in contrast to $NKp44^-$ ILC3s (12). Among the ILC3s, Rethacker et al. identified a $CD56^+$ILC3 subset expressed cytotoxicity genes (such as *PRF1*, *GZMA* and *GZMB*) shared with NK cells, which infiltrated metastatic breast cancer lymph nodes (13). Besides, combination of measurements of many cellular properties by flow cytometry and unbiased cell type identification by scRNA-seq allowed us to find the best cellular parameters to purify any cell type of interest (14).

In this study, using a combination of published scRNA-seq data, we painted the landscapes of ILCs across six human tissues including blood, colon, lung, tonsil, inflamed ileum from Crohn's disease patients and hepatocellular carcinoma (HCC). By characterizing the degree of commonalities and differences of those subsets in different tissues, we aim to reveal the diversity and plasticity of human ILCs, and extend understanding of innate immune system.

Methods

Single-cell RNA-seq datasets collected in this study

We searched PubMed databases through September 2022 using the following search terms: single-cell RNA sequencing OR scRNA-seq AND ILC. In order to find any relevant studies, the manual search was augmented by carefully reading the reference lists from those retrieved publications. For inclusion, the study must meet the following criteria: (1) human tissue samples were obtained from adult or pediatric donors (excluding fetal tissues); (2) for the scRNA-seq characterization, ILCs were purified by flow cytometry ($CD45^+$ $Lineage^-$); (3) raw sequencing reads or count matrix could be obtained. When study populations were overlapped or duplicated in some studies, we chose the most complete and suitable research.

Single-cell RNA-seq data processing and integration

For collected scRNA-seq datasets, cell annotation tables (ILC types) were obtained from the original publications; otherwise, we applied Seurat (version 4) with default parameters to filter and identify ILC types. Briefly, cells with fewer than 200 genes detected or > 40% mitochondrial counts or > 50% ribosomal counts were filtered out; genes detected in > 3 cells and UMI count > 1000 were kept. The GSE179795 dataset was run *via* Scrublet to eliminate any potential doublets, setting the expected doublet rate to 0.05 (15).

Considering the heterogeneity from different platforms and different studies, we applied "computesumFactors" function from scran R package to compute the size factor of each cell, which in turn was used to normalized the counts (16). A log2 transformation was also performed on normalized counts. Next, we used the "modelGeneVar" function to compute the biological variation for each gene, and the top 2000 genes were identified as highly variable features (HVGs). Mitochondrion, ribosomal and cell cycle genes were not interesting in our research, and thus were excluded in HVGs. Then gene expression matrix was scaled to z-score which could remove much of the batch effect caused by differences in platforms. To further handle more batches, "harmony" (17) or "LIGER" (18) was applied immediately after PCA. For visualization, the dimensionality of this combined dataset was further reduced using Uniform Manifold Approximation and Projection (UMAP).

In order to quantitatively evaluate the performance on integration, the Local Inverse Simpson Index (LISI) that defines the effective number of datasets in a neighborhood of a cell was calculated (17). LISI represents the local neighborhood of a sample with respect to the batch (integration LISI, iLISI) or accuracy (cell-type LISI, cLISI), respectively. While in good and accurate integration, higher iLISI value indicated that neighborhoods presented by more datasets and lower batch effect; lower cLISI value reflected a separation of unique cell types throughout the embedding and thus accurate integration.

Tissue distribution of clusters

To quantify the tissue preference of ILC subsets, odds ratios (OR) were calculated. As Zheng et al. described, the OR is a disproportional measure based on the ratio of the odds of one ILC subset in a specifical tissue, compared to the odds of remaining ILC subsets in the other tissues (19). One subset was identified as being enriched in a specific tissue if OR > 1.5.

Differential expression analysis

To identify differentially expressed genes for cluster demarcation, "FindAllMarkers" function in Seurat was used. GO enrichment analysis was performed using the clusterProfiler R package separately for differentially upregulated genes (adjusted p-value < 0.05) for each cluster (20). The functional gene sets belonging to biological process were focused and selected with an adjusted p-value cutoff of 0.05. Cytokines were annotated according to the "KEGG_CYTOKINE_CYTOKINE_RECEPTOR_INTERACTION" gene set. Only the cytokine genes that were detected in at least 0.25 percent of cells in either of the two populations were retained.

Pseudo-bulk differential expression analysis across different tissues

Given that our samples are from different tissues, it was crucial to consider sample-to-sample variation. Therefore, pseudo-bulk samples were created for differential expression testing based on the subpopulation-stratified scRNA-Seq data (21, 22). Specifically, we summed counts transcript per gene for each subpopulation per sample, and then performed DESeq2 differential analysis (21). Pseudo-bulk samples consisting of fewer than 10 cells were removed.

Results

Integration of multiple scRNA-seq datasets

We compiled an integration of single-cell transcriptomics of ILC across six human tissues (Supplementary Table 1). As Mazzurana et al. described, one minor cluster of cells lacking expression of *PTPRC* (encoding CD45) and another minor cluster of cells coordinating antigen-presenting function (e.g., high expression of *HLA-DQA1*, *HLA-DRA* and *HLA-DPA1*) were identified and removed (11). After stringent quality-control filtering, we obtained 6670 ILCs from 20 samples, derived from three single-cell RNA-seq datasets [GSE150050 (11), GSE179795 (12) and GSE173642 (23)]. As shown in Figures 1A, B, we used Harmony and LIGER to integrate the above three datasets, respectively. Both Harmony and LIGER successfully removed batch effects from different platforms, whereas Harmony exhibited low bio-conservation score (Figures 1C, D). Thus, we used LIGER to integrate the above three scRNA-seq datasets for further analysis.

Single-cell transcriptional landscape of ILCs in different tissues

To characterize the subsets of 6670 ILCs among different tissues (blood, colon, lung, tonsil, ileum and HCC), we performed unsupervised graph-based clustering and then identified 10 clusters based on canonical cell markers (Figures 2A, B). Two clusters expressed *NKG7*, *EOMES*, *GZMA/B*, *NCAM1* (CD56), *KLRF1* and *KLRD1* (CD94) but lacking *IL7R* were annotated as NK cells (NK_c1 and NK_c2). One cluster lacked expression of *IL7R*, *NCAM1* and *KLRD1*, but expressed IL1 related genes (*IKZF3*), which shared characteristics of both NK cells and ILC1s, and thus named "NK_like" subset (12). One cluster was identified as ILC1_c1 subset, with higher levels of expression of specific transcription factor (*IKZF3*), and T cell markers (*CD3D*, *CD3G* and *CD3E*). One ILC2 subset (ILC2_c1) shared common ILC2s markers (*GATA3*, *MAF* and *RORA*). The ILC2-specialized gene *PTGDR2* (encoding CRTH2) was not examined because it was absent in GSE173642 dataset. Four clusters were characterized as ILC3s (ILC3_c1, ILC3_c2, ILC3_c3 and ILC3_c4) on the basis of uniquely high *RORC*, *IL23R*, *IL1R1*, *KIT*, *AHR*, *TOX* and *TTN* expression. We discovered c-Kit$^+$ ILC2 specific clusters in the GSE179795 dataset and CD127$^+$CD94$^+$ ILC1 subset in GSE173642 dataset as a result of independent analysis of the included datasets (Supplementary Figure 1). Therefore, one cluster in this integrated graph with both *GATA3* and *KIT* high expressing, was annotated as CD127$^+$c-Kit$^{-/+}$CD94$^{-/+}$ ILC subset for further analysis. The proportion of cells in these lineages varied highly among different tissues, indicating a heterogeneous cellular condition (Figure 2C). To further dissect in variability within the CD127$^+$c-Kit$^{-/+}$CD94$^{-/+}$ ILC subset, 1537 aligned cells were re-clustered. Intriguingly, we found 5 clusters: one CD94$^+$ ILC1 subset (ILC1_c2), two c-Kit$^+$ ILC2 subsets, one c-Kit$^-$ ILC2 subset (ILC2_c2) and one ILC3 subset (ILC3_c5) using above cell markers (Figures 2D, E; Supplementary Figure 2). Interestingly, ILC1_c2 subset consisted primarily of CD127$^+$CD94$^+$ ILCs from inflamed ileum in GSE173642 dataset (Supplementary Figure 2). Moreover, Krabbendam et al. reported that no IL-22 expression was detected when IL-23, IL-1, or IL-15 were used to cultivate with ex vivo isolated CD127$^+$CD94$^+$ ILCs; whereas IFN-γ expression was clearly detected in response to IL-15 or IL-12+IL-1β stimulation, which confirming that CD127$^+$CD94$^+$ cells belong to the group 1 ILCs (23). We also assigned each cluster to a cell type using gating strategy base on gene expression, which validated the clustering strategy is considerably accurate (Supplementary Figure 3).

Transcriptome analysis of ILC1s

As shown in Figure 3A, we identified two ILC1 subsets: ILC1_c1 and ILC1_c2 (CD94$^+$). ILC1_c1 population were mainly distributed

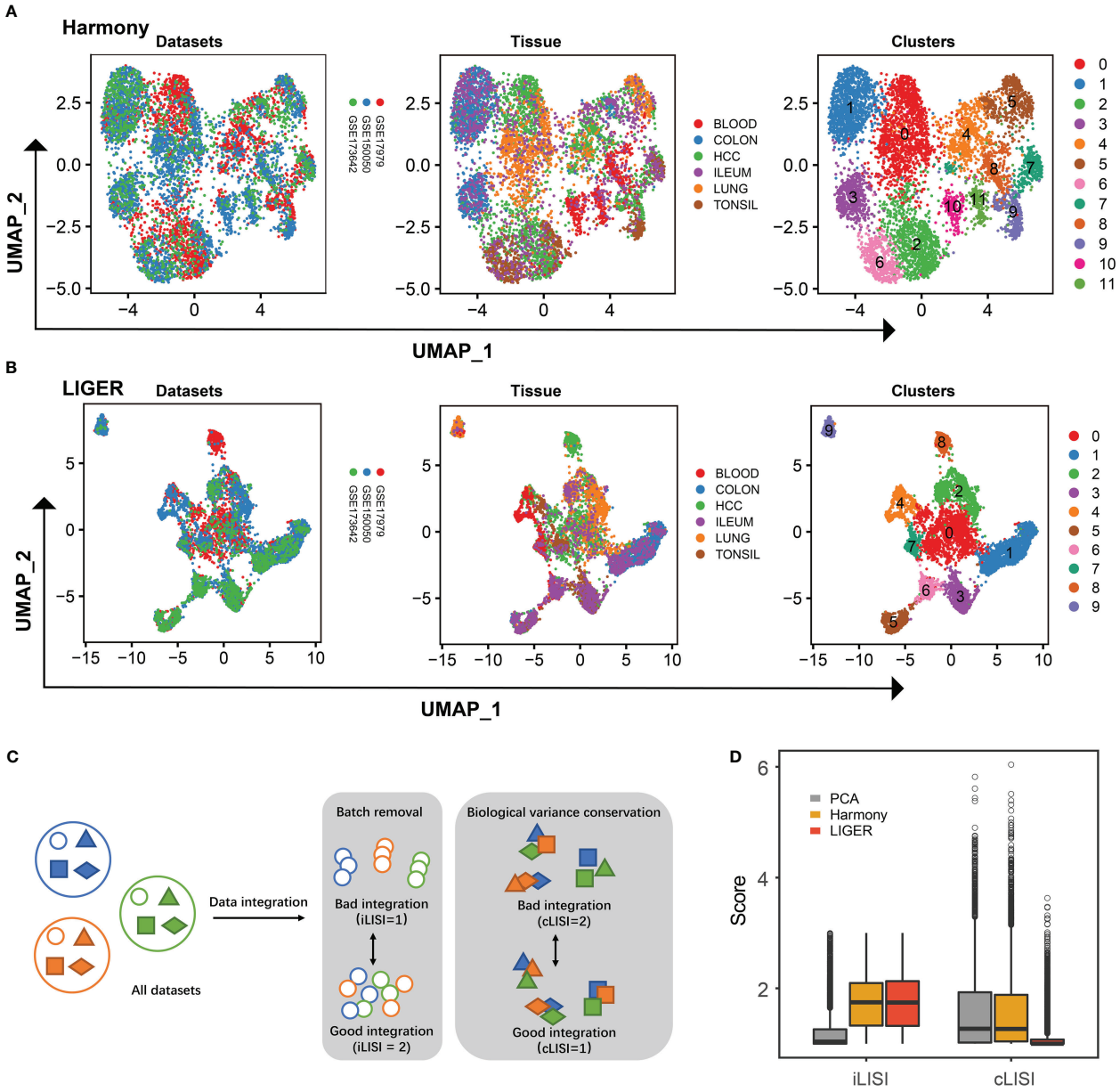

FIGURE 1
Integration of ILCs from three scRNA-seq datasets. **(A)** UMAP plots showing the integration of three scRNA-seq datasets by Harmony. **(B)** UMAP plots showing the integration of three scRNA-seq datasets by LIGER. **(C)** Schematic workflow to the quantitative assessment of data integration and batch-correction fidelity. iLISI metrics and cLISI provide measures of the degree of mixing among datasets and integration accuracy on cell types, respectively. **(D)** Boxplot showing the iLISI and cLISI distribution of data integrated by PCA, Harmony and LIGER.

in blood and tonsil. To identify unique profiles to the ILC1 populations, we compared the gene expression of ILC1s with the combined expression profile of genes in the other populations pooled together. Notably, ILC1_c1 cells had significantly higher expression of *CD3D*, *CD3E*, CD3G and *CD8A*, as previously described (11, 24), which were involved in T-cell development and signal transduction. Among these markers, *CD3D* was most strongly transcribed. This subset also expressed TCR-associated signaling molecules such as *LCK*, which has previously been regarded as T-cell specific gene, and glycolysis-associated transcript *LDHB* (Figure 3B). Furthermore, ILC1_c1 cells displayed differential expression of genes encoding transcription factors (*LEF1*, *BCL11B*, *IKZF3*, *GTF3A* and *ARID5B*) and secreted effectors (*TNFSF8* and *CCL5*). ILC1_c2 populations ($CD127^{+}CD94^{+}$ ILC1) co-expressed *IL7R*, *KLRD1*, *GNLY*, and shared characteristics of both NK cells and conventional ILCs. Theses ILC1s accumulated within inflamed ileum, and were proposed to contribute to inflammation. The ILC1_c2 subset also specifically expressed genes encoding *JUND* and *FOSB* (Figure 3B; Supplementary Table 2), belonging to functional component of the AP1 transcription factor complex, which appeared to have distinct effects on cell proliferation and transformation (25). By performing GO analysis, we noted the upregulation of functions associated with regulation of T cell activation and cellular homeostasis related to

10.3389/fimmu.2023.1127413

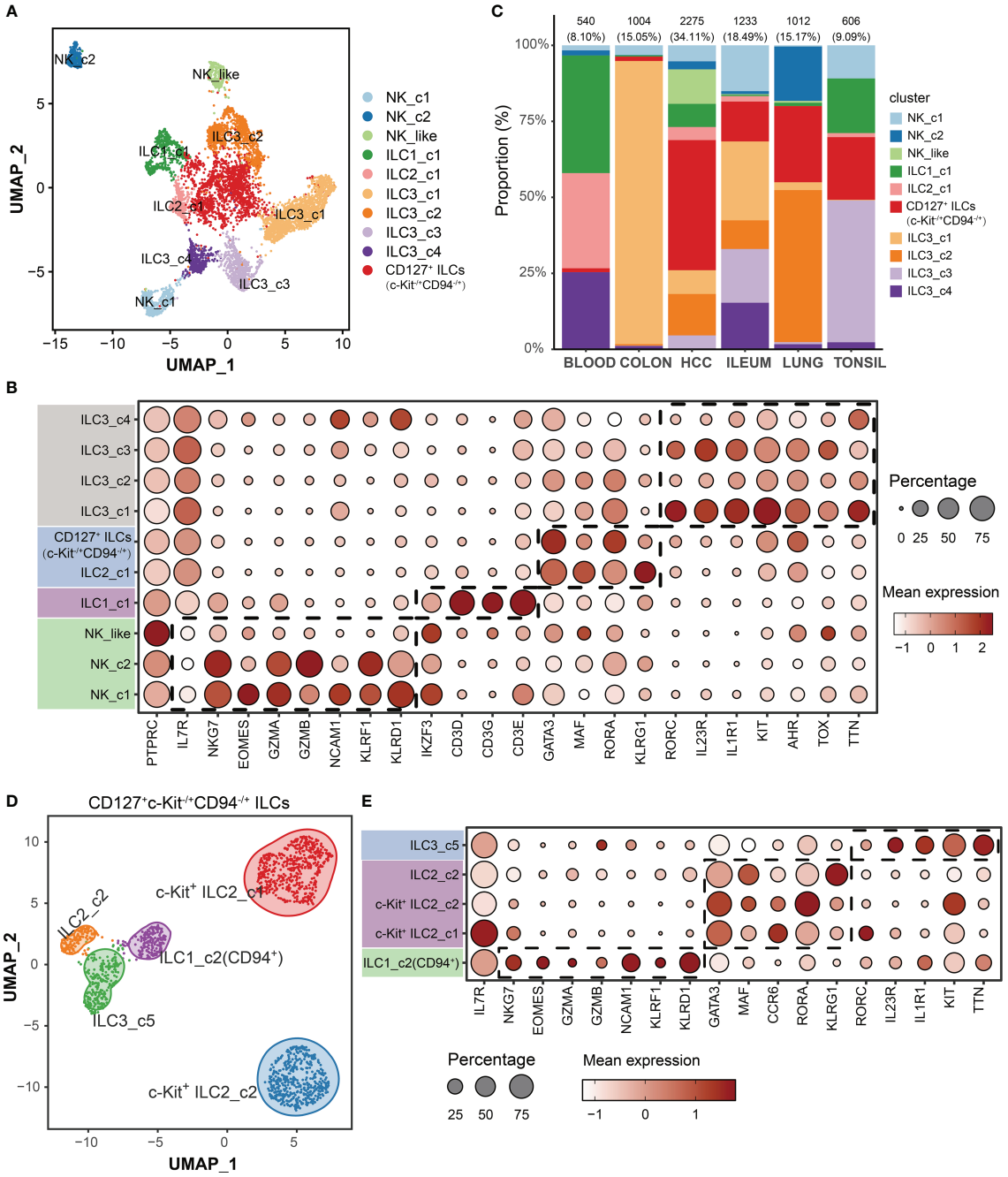

FIGURE 2
Single-cell transcriptome profiles of ILCs among different tissues. **(A)** UMAP visualization of all cells (6670) color-coded on the basis of annotated clusters. **(B)** Dot plot displaying average and percent expression of marker genes across ten ILC clusters. **(C)** Proportion of each cell type among different tissues. **(D)** UMAP visualization of c-Kit$^{-/+}$ ILC2/ILC3 subset (1537 cells). **(E)** Dot plot displaying average and percent expression of marker genes for c-Kit$^{-/+}$ ILC2/ILC3 subset across five clusters.

focal/cell adhesion. Besides, the ILC1_c2 subset of genes were enriched for cytoplasmic translation and ribosome biogenesis. (Figure 3C; Supplementary Table 3).

Transcriptome analysis of ILC2s

The distribution of ILC2s exhibited obvious cross-group differences, indicating surprising levels of heterogeneity among cells. We totally identified four subsets of ILC2s, and ILC2_c1 (KLRG1^{+}) and ILC2_c2 (CD69^{+}) were major ILC populations in the blood and tonsil, respectively. The other two subsets (c-Kit^{+} ILC2_c1 and c-Kit^{+} ILC2_c2) were only detected in HCC (Figure 4A). All subsets had high expression of transcription factor *GATA3* required for ILC2 development (Figure 4B; Supplementary Table 2). The TNF family-related transcripts *TNFSF10* (encoding TRAIL, also known as APO-2 ligand) were also highly expressed by ILC2_c1 and ILC2_c2 subsets, acting as a

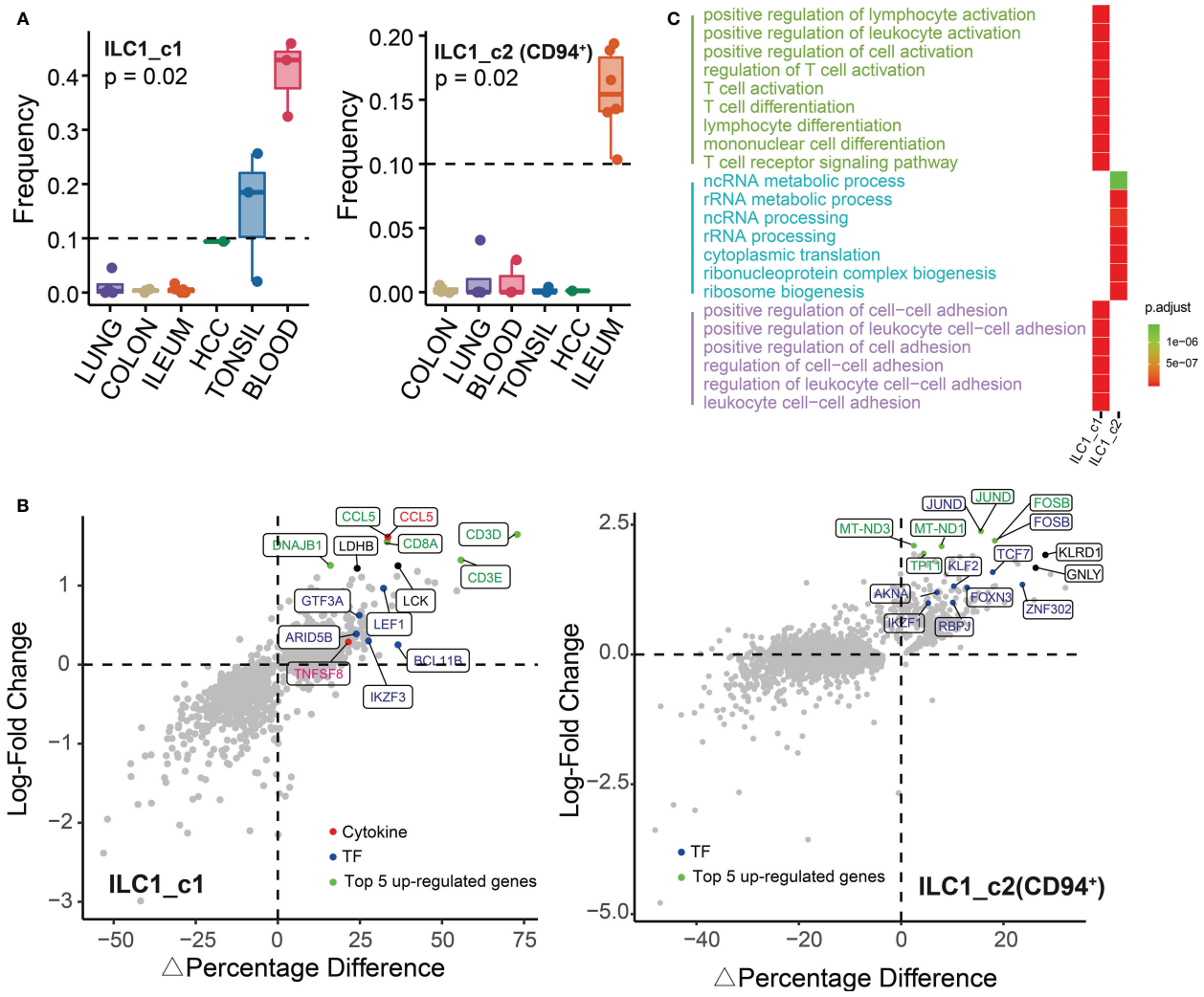

FIGURE 3
Characterization of ILC1s in different tissues. **(A)** Box plots showing the frequencies of ILC1s (divided by the total CD127$^+$ ILC number) in lung, colon, ileum, tonsil, blood and HCC. P value were calculated from Kruskal-Wallis test. **(B)** The percentage of differentially expressed transcripts (△Percent of Cells and log-fold change) in ILC1s is shown. **(C)** Gene ontology analysis (biological processes) of differentially expressed genes showing top 15 GO terms in each ILC1 subset.

cytotoxic protein which activates rapid apoptosis in tumor cells, but not in normal cells (26). In addition, early differentiation markers, including *SELL*, *IL10RA*, and *KLRG1*, were expressed differentially in ILC2_c1 subset, that appeared to be in an immune quiescence state (27). Interestingly, circulating KLRG1$^+$ ILC2s from individuals with allergic disease were unable to generate IL-10, but this ability was recovered after effective allergen immunotherapy (8, 28). CD200R1 encoding a receptor for the OX-2 membrane glycoprotein was also shown to be expressed most highly on ILC2_c1 subset (Supplementary Table 2). The tissue-residency marker CD69 was mostly expressed in ILC2_c2 subset. Within the ILC2_c2 population, several endogenous regulators of the anti-inflammatory response (*DUSP1* and *EGR1*) were identified (28). Specifically, one study analyzed the nasal epithelium exposed to grass-pollen allergen, and found IL-10-producing ILC2s reduced the expression of pro-inflammatory genes *NFKB1* and *MYC* in an IL-10-dependent manner and increased the expression of the anti-inflammatory transcription factor *EGR1* (28).

A strong enrichment of ribosomal protein encoding genes (starting with RPL- or RPS-) and metabolism-related gene (*FTH1*) in c-Kit$^+$ ILC2_c1 subset, indicating a higher level of oxidative phosphorylation and metabolic changes which was similar with our previous work (29). Among the genes encoding secreted proteins, the c-Kit$^+$ ILC2_c1 population expressed *XCL1* that involved in the recruitment of dendritic cells (30), and fibrosis-associated gene *TGFB1* with either tumor-suppressing or tumor-promoting effects (31, 32). The c-Kit$^+$ ILC2_c2 population highly expressed *TLE4*, which belongs to Groucho family members function as transcription co-repressors within the context of Wnt signaling (33). We next performed GO analysis on all populations, leading us to note that the pathways mainly involved in T cell activation (typical associated genes: *LEF1*, *PAG1*, *TESPA1*, *B2M*,

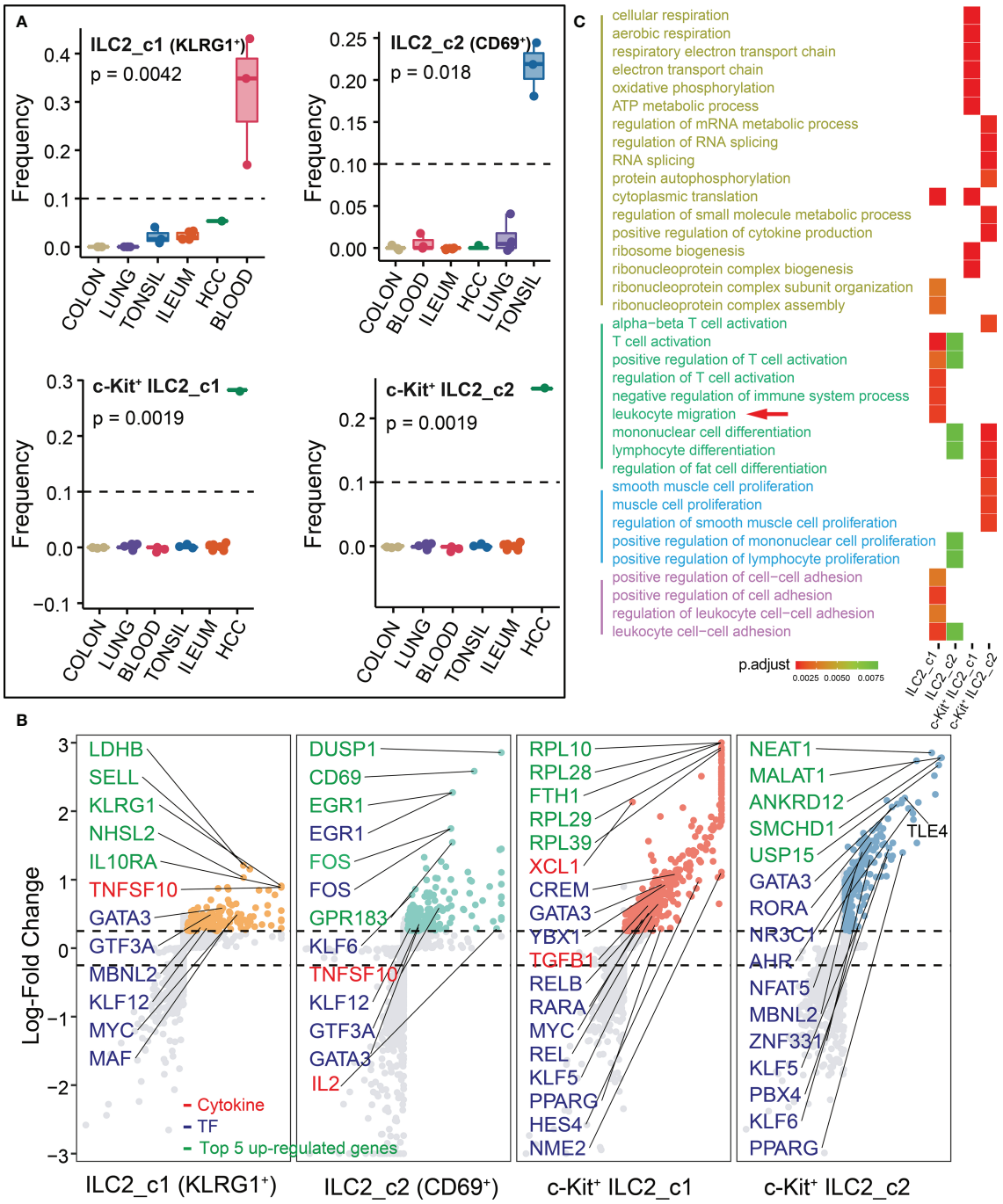

FIGURE 4
Characterization of ILC2s in different tissues. **(A)** Box plots showing the frequencies of four ILC2 subsets (divided by the total CD127$^+$ ILC number) in lung, colon, ileum, tonsil, blood and HCC. P values were calculated from Kruskal-Wallis test. **(B)** Differential gene expression analysis showing up- and down-regulated transcripts across four ILC2 subsets. **(C)** Functional enrichment analysis showing top 15 GO terms in each ILC2 subset of biological process.

IL2; ILC2_c1 and c2 subsets), leukocyte migration (*S1PR1*, *SELL*, *CD200R1*, *ANXA1*, *SELPLG*; ILC2_c1 subset), metabolic process (cytoplasmic translation, *RPS26*, *RPL36A*, *RPL10*; ATP metabolic process, *ALDOA*, *CHCHD10*, *TMSB4X*; c-Kit$^+$ ILC2_c1 subset), and regulation of RNA splicing (*AHNAK*, *FUS*, *RBM39*, *PIK3R*; c-Kit$^+$ ILC2_c2 subset; Figure 4C; Supplementary Table 3).

Transcriptome analysis of ILC3s

Each tissue has its unique ILC3 subsets distribution. For instance, in the colon ILC3_c1 subset is the most predominant; the lung is populated by ILC3_c2 and ILC3_c5 (CD69$^+$) subsets; ILC3_c3 (CD74$^+$) subset is most relevant in tonsil; while ILC3_c4 (CD94$^+$)

10.3389/fimmu.2023.1127413

are widely localized in blood and ileum, respectively (Figure 5A). To further reveal the features of these ILC3 clusters, we next examined the top five highly expressed genes, transcriptional factors, cytokines, respectively (Figure 5B; Supplementary Table 2). The ILC3_c1 populations expressed high levels of transcription factors including Fos gene family (*FOS*, *FOSB* and *FOSL2*), steroid-thyroid hormone-retinoid receptor superfamily (*NR4A1*, *NR4A2* and *NR4A3*), indicating that Fos/Jun signaling and calcineurin/NFAT might be important for this subset differentiation (34, 35). In addition to the cytokines, this subset also expressed *LIF*, *CSF2*, *TNFSF11* and *TNFSF13B*, resulting in strong intestinal inflammation. In all this subset shared a common transcriptomic signature characteristic of

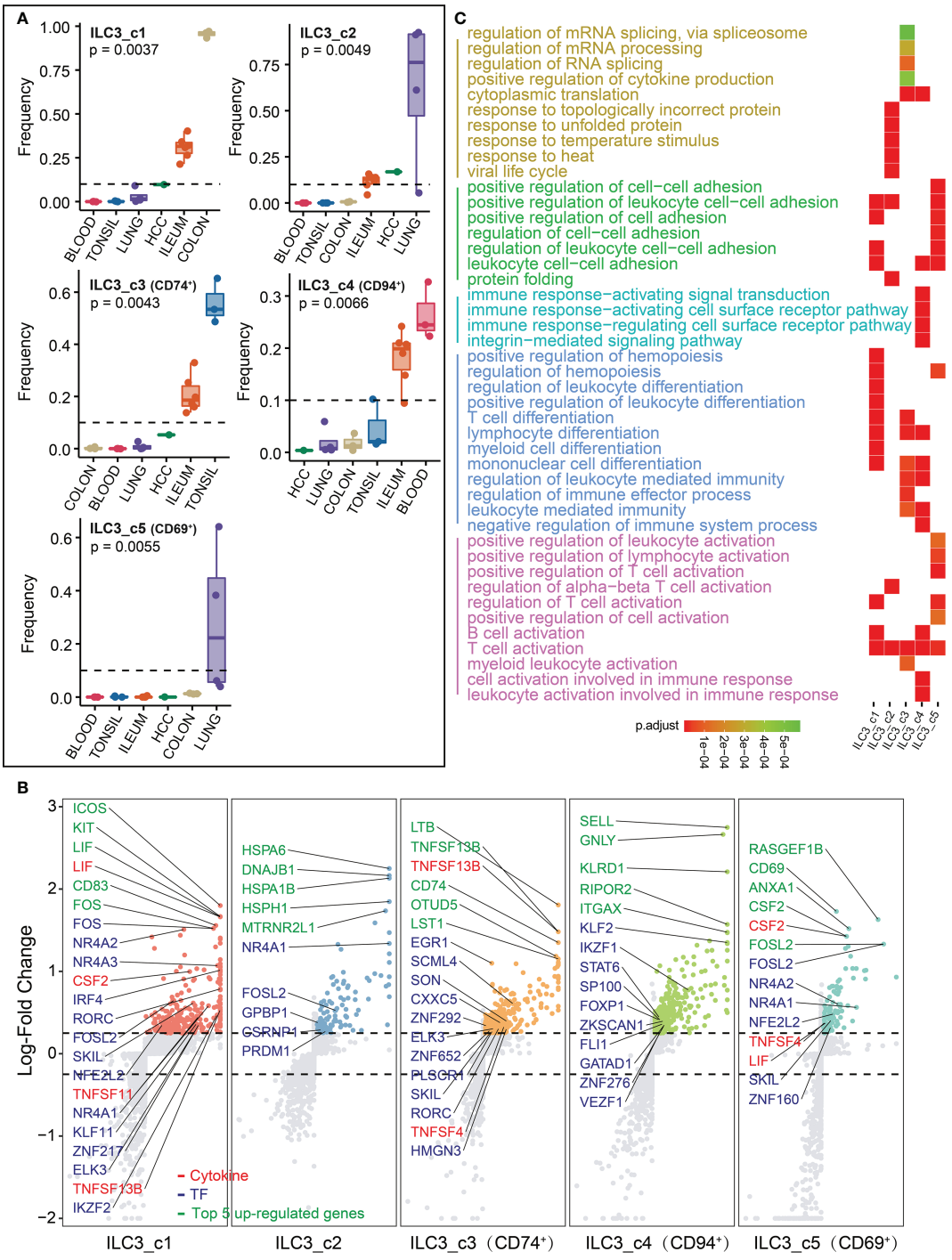

FIGURE 5
Characterization of ILC3s in different tissues. **(A)** Box plots showing the frequencies of four ILC3 subsets (divided by the total CD127$^+$ ILC number) in lung, colon, ileum, tonsil, blood and HCC. P values were calculated from Kruskal-Wallis test. **(B)** Differential gene expression analysis showing up- and down-regulated transcripts across six ILC3 subsets. **(C)** Functional enrichment analysis showing top 15 GO terms in each ILC3 subset of biological process.

typical ILC3s. The ILC3_c2 subset was enriched for heat shock proteins (*HSPA6*, *HSPA1B*, *HSPH1* and *DNAJB1*), suggesting that the unfolded protein response best distinguishes this population. The ILC3_c3 subset showed abundant amounts of *LTB* and *CD74* which have been demonstrated to have *in vivo* significance in murine models (36, 37), and *OTUD5* that also been shown to regulate RORγt stability (38). Nagasawa et al. reported that NKp46$^+$ ILCs and tonsillar ILC3 populations shared the expression of CD74 that associated with antigen presentation for immune response, suggesting it as a distinctive marker for ILC3 (39). *LST1* was specifically upregulated in this subcluster, which can inhibit the proliferation of lymphocytes (Supplementary Table 2). The ILC3_c4 subset was transcriptionally less active, and could be characterized by expression of *SELL* and *ITGAX*, involved in cell adhesion and migration, and *KLRD1* with *GNLY*, expressed in T and NK cells, might correspond to cytotoxic ILC3s. The residency marker CD69 was strongly expressed in ILC3_c5 subset. Strikingly, consistent with ILC3_c1 subset, the high expression of proliferation genes *NR4A1*, *NR4A2* and *FOSL2*, cytokine genes *CSF2* and *LIF* were also highly expressed in the ILC3_c5 subset, further indicating colon and lung might share associated transcriptional imprinting of ILC3. ILC3-derived CSF2 controlled macrophages and dendritic cells to maintain colonic Treg homeostasis (40). Besides, high expression of *TNFSF4* (encoding OX40 ligand) was observed in ILC3_c3 and c5 subsets. Deng et al. revealed the importance of OX40-OX40L signaling for intestinal homeostasis by the crosstalk between Tregs (OX40) and ILC3s (OX40L) (41). Consistently, we found that the enriched GO terms were in line with the function of aforementioned genes (such as regulation of immune effector processes and responses, Figure 5C; Supplementary Table 3).

Transcriptome analysis of NK and NK_like cells

We next explored the transcriptome changes for NK and NK_like cells, and found that differentiated NK cells predominated in tonsil, ileum (NK_c1) and lung (NK_c2), and NK_like cells distributed in HCC (Figure 6A). Differential expression analysis showed that NK cell subsets shared relatively high expression of cytokines (*CCL3*, *CCL4*, *CCL5*, *CCL4L2*, *FASLG* and *IFNG*, Figure 6B; Supplementary Table 2). The NK_c1 population highly expressed *EOMES* that are related T-box transcription factors that control NK cell development (7). The NK_c2 and NK_like population uniquely expressed *ZEB2* encoding a transcriptional regulator involved in terminal NK cell maturation (42). Biological process enrichment analysis demonstrated that the transcriptome of NK and NK_like cells was specifically enriched in cell cytotoxicity and immune response (Figure 6C; Supplementary Table 3).

Characteristics and pseudotemporal analysis of ILCs

To explore the profile of ILC subsets across different tissues, we continued the analysis of pseudo-bulk samples. As shown in Figure 7, the specificity of ILC distribution was also observed in pseudobulk data (Supplementary Table 4). ILC1_c2, ILC2_c2, c-Kit$^+$ ILC2_c1/2, ILC3_c5 and NK-like subsets were the predominant ILC populations in the corresponding tissues, since the number of related ILCs within the other tissues was less than 10. Several encoding transcription factors (*KLF4*, *FOS*, *JUN* and *JUND*) and early activation markers (*CD69* and *DUSP1*) were unregulated in unique tissues or different disease state (43). We further used OR values to quantified tissue enrichment of ILC subsets across different tissues (Figure 8A). The compositions of ILCs from different tissues displayed prominent differences, especially to c-Kit$^+$ ILC2 groups that appeared to be tumor-enriched. The proximity in UMAP coordinates of ILCs (excluding NK and NK_like cells) indicated that their transcriptomes might be connected continuously. Next, we searched for a potential developmental path by applying the pseudotime algorithm. As shown in Figure 8B, the trajectory evinced a pseudotemporal order of ILCs, and placed individual ILCs into different states with striking fidelity to our annotations. The root of the trajectory was mainly populated by ILC1s, and the two termini of the tree were populated mainly by ILC3_c1 and ILC3_c2. This pseudotemporal analysis further helped identify genes associated ILC1s from the root to both fates such as *CD27*, *CD3D*, *CD3G*, and also genes related with ILC3s that were up-regulated in cells differentiating into both fates such as *IL1R1*, *IL23R* and *KIT* (Figure 8C). Additionally, ILC2-associated genes *LMNA* (highly expressed in c-Kit$^+$ ILC2_c1 subset), *MTRNR2L12* (highly expressed in c-Kit$^+$ ILC2_c2 subset) were mostly expressed in the intermediate state, indicating the plasticity of ILC2s (44) (Figure 8D).

Discussion

Recent studies of ILCs have focused on their subsets' specific roles in these processes like tissue remodeling and repair, immune-mediated disease, lymphoid tissue production, intestinal and mucosal defense, and epithelial homeostasis (2, 9). We collected a large number of ILCs from human six different tissues which can represent unique immune niches (circulation, lymphoid tissue, normal and inflamed mucosa, tumor microenvironment), to systematically address the transcriptional imprinting. Through this approach, we have identified tissue-specific ILC subsets with the potential to remodel the local environment.

Two subpopulations of ILC1 cells were characterized in our study. ILC1_subset showed a strong distribution preference in blood and tonsil, and exhibited high levels of *IKZF3*, followed the regulation pattern of T-bet and EOMES, being predominantly expressed by ILC1 and NK cells (45). ILC1_c2 subset (CD94$^+$) exhibited distinct phenotypic profile, tended to be enriched in inflamed ileum, and highly expressed *GNLY*, encoding for the cytotoxic protein granulysin that is linked to chemotaxis or fugetaxis of monocytes and bacterial lysis. While exploring the heterogeneity of NK cells, we identified two "conventional" NK subsets (CD127$^-$CD56$^+$CD94$^+$), and a NK-like subset (CD127$^-$CD56$^-$CD94$^-$IKZF3$^+$) that expressed markers of cytotoxicity including *IFNG* and *CCL5*. The CD127$^-$NK_like cell population

10.3389/fimmu.2023.1127413

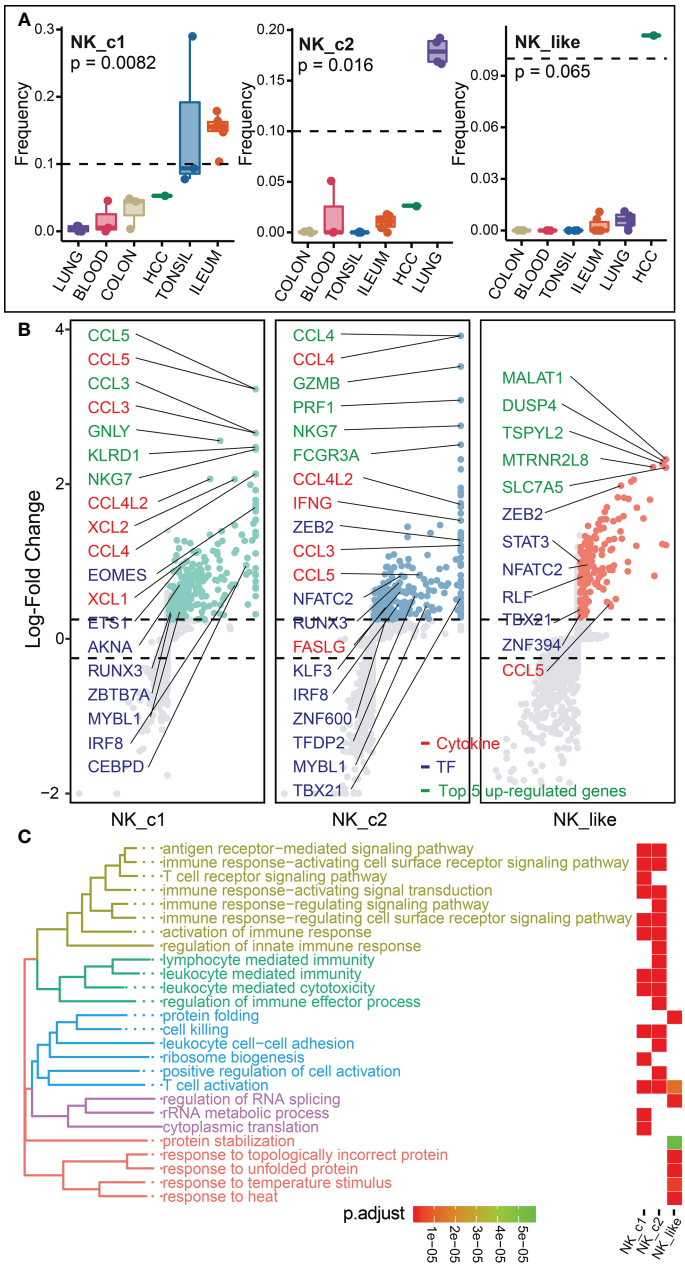

FIGURE 6
Characterization of NK and NK_like cells in different tissues. **(A)** Box plots showing the frequencies of four NK subsets (divided by the total ILC number) in lung, colon, ileum, tonsil, blood and HCC. P values were calculated from Kruskal-Wallis test. **(B)** Differential gene expression analysis showing up- and down-regulated transcripts across three NK subsets. **(C)** Functional enrichment analysis showing top 15 GO terms in each NK subset of biological process.

mainly presented in the HCC microenvironment, which was in accord with the results Heinrich et al. described (12).

ILC2s concentrate at barrier surfaces, such as the skin, lung and intestine, where they are phenotypically and functionally adapted to the tissue specific environment (46). Recent discoveries have generated profound insights into ILCs biology of circulating between different organs upon activation, as they are readily detectable in healthy human peripheral blood (8, 47). Notably, the ILC2_c1 cells identified within multiple tissues were preferentially enriched in blood, resembling the reported migratory ILC2s. These ILC2s increased expression of genes involved in cell migration such as *SELL*, *S1PR1* and *CD200R1*. Although distinct subsets of ILCs can be identified in blood, the precursor ILC (ILCp), which has the ability to home to peripheral tissues and differentiate into mature ILC subsets, makes up the majority of the circulating ILC population (48). For example, Winkler et al. observed that ILC2s accumulate in bronchoalveolar lavage fluid after allergen challenge in asthmatic patients, whereas circulating ILC2 numbers decrease at the same time, suggesting ILC2s are recruited from the blood into the lung during inflammation (49). Liu et al. have identified two migratory colon ILC2 subsets (IL-17A$^+$ ILC2s and CD27$^+$ ILC2s) with potential to

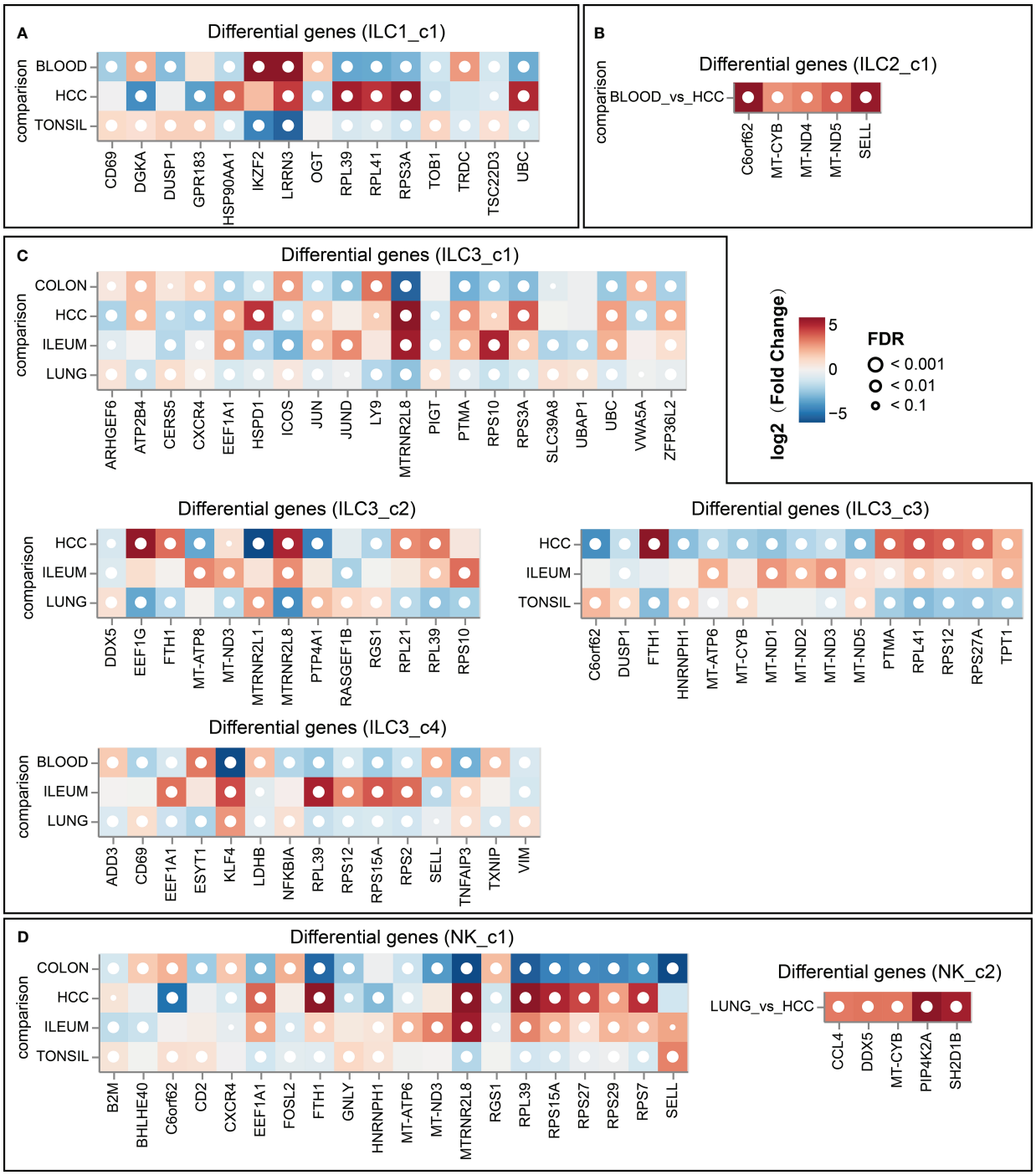

FIGURE 7
Top 5 differentially expressed genes in ILC subsets (**A**, for ILC1_c1 subset; **B**, for ILC2_c1 subset; **C**, for ILC3 subsets; **D**, for NK subsets) across different tissues (DESeq2 on pseudo-bulk).

migrate to the mouse lung in response to IL-25 stimulation (35). As mentioned above, *SELL* is also highly expressed in ILC3_c4 subset, which was preferentially enriched in blood and inflamed ileum. Krabbendam et al. revealed that co-expression of *SELL* and *CCR7* in CD127$^+$CD94$^+$ granulysin-expressing ILCs are capable of traveling to the lymph node *via* high endothelial venules (23). Additionally, we observed two unique c-Kit$^+$ ILC2 subsets in HCC, reflecting plasticity as induced by the tumor environment. Heinrich et al. reported that supernatant derived from HCC tissue with high IL-6 and TGF-β induced an increase in c-Kit$^+$ ILC2s. In parallel, the frequency of NKp44$^-$ ILC3s and ILC1s was reduced (12). Bernink et al. similarly observed that TGF-β regulates the transition of c-Kit$^-$ ILC2s into IL-17 producing c-Kit$^+$ ILC2 cells, and this switch was reliant on RORγt and the downregulation of GATA3 (50).

Analysis of human tissue samples shows that diversity spectrum of ILC3s is dependent on the local environment. ILC3s were

10.3389/fimmu.2023.1127413

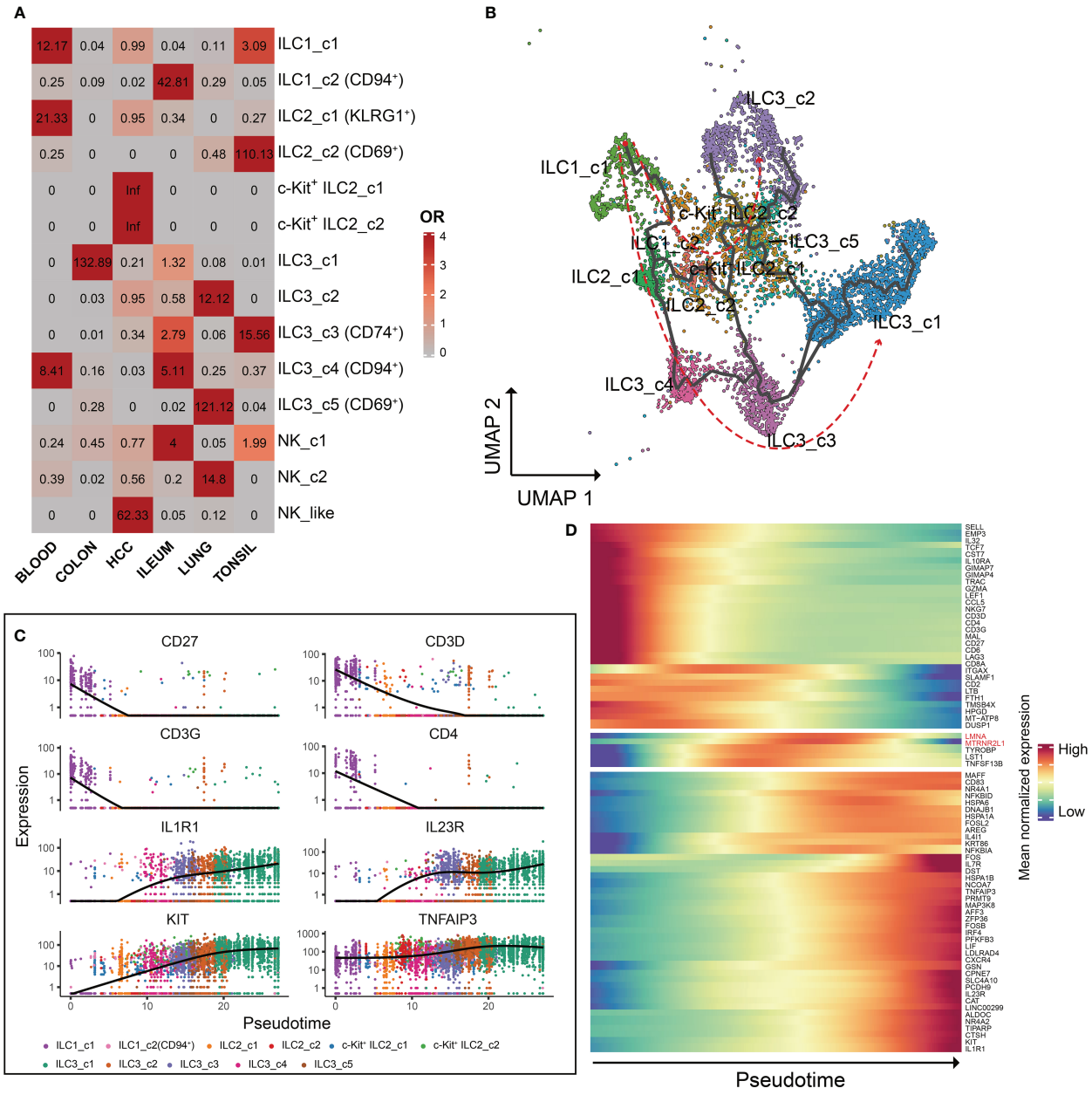

FIGURE 8
Characteristics and pseudotemporal gene expression analysis of the ILCs across different tissues. **(A)** Tissue prevalence of ILC clusters estimated by OR values. OR > 1.5 indicates that this ILC cluster is preferred to distribute in the corresponding tissue. **(B)** Pseudotime inference of the ILCs (excluding NK cells) trajectory with cells color-coded according to the corresponding ILC subsets identified by UMAP. **(C)** Monocle analysis reveals the kinetics of indicated genes (*CD27*, *CD3D*, *CD3G*, *CD4*, *IL1R1*, *IL23R*, *KIT* and *TNFAIP3*) across pseudotime. **(D)** Heatmap of gene expression analysis associated with ILC specification in Monocle.

previously further subdivided according to the expression of CD56 and especially of NKp44. Human NKp44$^+$ ILC3s are the most prevalent cells in adult tonsil and gut, and represent an exclusive source of IL-22 (51). We also observed *NCR2* (NKp44) highly expressed in ILC3_c1 and ILC3_c3 subsets that were enriched in colon and tonsil, respectively (Supplementary Figure 4). We further found these two subsets also expressed *ENTPD1* (CD39), an ectoenzyme related to suppression of inflammation (Supplementary Figure 4). Strictly, CD39 was mainly restricted to NKp44$^+$ ILC3 cells in mucosal tissues (52). ILC3_c1 subset is the predominant source of intestinal ILC-derived LIF, which belongs to IL-6 family cytokines, and restricts inflammation by blocking Th17-cell differentiation (53). ILC3s (except ILC3_c2 subset) demonstrated high levels of histocompatibility complex class II (MHCII) associated transcripts including *HLA-DQB1*, *HLA-E*, *HLA-F* and *HLA-DRA*. Goc et al. reported that a dialog between ILC3s and CD4 T cells *via* major MHCII is disrupted in colon cancer, resulting in destruction

of immunologic homeostasis in the gut and tumor microenvironment (54). Interestingly, we also found ILC3_c4 subset abundantly expressed high levels of *GNLY* and *KLRD1*, that mediate cellular cytotoxicity. ILC3s can be harnessed for cytotoxic responses *via* differentiation with IL-12 and IL-15 stimulation as described previously (55, 56). In healthy gut mucosa, Qi et al. similarly found a population of ILC3/NK cells that had transcriptomic features in common with both ILC3 and NK cells (24). This population expressed *NKG7*, *KLRD1*, *GNLY*, *XCL2* and *CCL4* similar to NK cells, but differed from conventional ILC3s. However, Björklund et al. has described a subset with high *SELL* expressing as naive ILC3 cells in tonsil (57). CD62L^{+} (*SELL*) ILC3s didn't respond to IL-23 plus IL-1β stimulation, and neither IL-22 nor IL-17F was detected, but produced IL-2 relatively infrequently. The biological role of this ILC3 subset remained to be addressed. Using scRNA-seq technology, clusters in the UMAP plot expressed helper ILC-related genes (*IL7R* and *KIT*), but lacked transcripts that encode for effector functions, were usually annotated as naïve ILCs (nILCs) (11, 23). In ILC-poiesis, nILCs may represent the functional equivalent of ILC precursors. In our joint analysis, we did not discover this cluster, which might be caused by the simultaneous integration across donors and technologies. Regarding the activation state, ILC3_c5 (CD69^{+}) subset was preferentially enriched in lung and expressed high levels of *CSF2* (GM-CSF), which plays an important role in antimicrobial pulmonary host defense function and is essential for surfactant homeostasis (58).

The past decade has witnessed an explosion of knowledge of innate immune cell, owing to the definition of many additional subsets. In this study, we found several ILC subsets across six tissues, that exhibited tissue-adapted phenotypes and functions. The typical ILC clusters with specific markers could be distinguished easily, whereas some cells had transcriptomic features in common, rendering their identification complicated. Therefore, we defined a population of CD127^{+}c-Kit$^{-/+}$CD94$^{-/+}$ cells, and further divided it into five clusters, indicating the plasticity between ILC subsets, which can be induced by changes in the tissue microenvironment. However, we defined theses subsets based an unbiased transcriptome-wide perspective, *ex vivo* co-culture experiments were not performed to confirm their functions.

Overall, the main objective of this study was to characterize the heterogeneity of ILCs in human tissues under physiological and pathological conditions. Integrative inference of these single-cell transcriptomics unveiled the diversity and plasticity of ILCs, and generated a comprehensive map of human ILC composition, which provided insights into ILC-mediated tissue-specific immunity.

Data availability statement

Three single-cell RNA-seq datasets (GSE150050, GSE179795 and GSE173642) used in this study can be obtained from the GEO database (https://www.ncbi.nlm.nih.gov/geo/). The original contributions presented in the study are included in the article. Further inquiries can be directed to the corresponding authors.

Author contributions

Conception and design: PS, XS and WG. Collection and assembly of data: PS, KC, YM and XL. Data analysis and interpretation: PS, XS, KC, YM, SA, FS, QH, SL and MW. Manuscript writing: PS. Manuscript revision: KC, YM, XS and WG. All authors read and approved the final manuscript.

Funding

This work was supported by National Natural Science Foundation of China (81970500 XS, 82172645 WG, 82002082 KC), Start-up funding for the introduction of talents in Nanjing Drum Tower Hospital (RC2022-015, XS).

Conflict of interest

The authors declare that the research was conducted in the absence of any commercial or financial relationships that could be construed as a potential conflict of interest.

Publisher's note

Supplementary material

The Supplementary Material for this article can be found online at: https://www.frontiersin.org/articles/10.3389/fimmu.2023.1127413/full#supplementary-material

SUPPLEMENTARY FIGURE 1
Single-cell RNA sequencing of HCC for GSE179795 dataset. **(A)** UMAP of single-cell transcriptomes color-coded by ILC clusters. **(B)** Dot plot displaying average and percent expression of marker genes across seven ILC clusters.

SUPPLEMENTARY FIGURE 2
Single-cell transcriptome profiles of CD127^{+}c-Kit$^{-/+}$CD94$^{-/+}$ ILC subset among different tissues. **(A)** Heatmap of top 3 signature genes for indicated cell types were shown. **(B)** Expression of *KLRD1* (CD94) plotted in purple on the UMAP clustering. **(C)** Proportion of each indicated cell type among different tissues.

SUPPLEMENTARY FIGURE 3
Gating strategy to identify ILCs using multi-omics single-cell sequencing data. Representative gates were generated to assign ILCs (ILC1, ILC2, ILC3 and NK+NK_like cells) based on identified specific population markers.

SUPPLEMENTARY FIGURE 4
Single-cell transcriptome profiles of ILC3 subset among different tissues. **(A)**: Dot plot displaying average and percent expression of representative genes across five ILC3 clusters. **(B)** Expression of *NCR2* (NKp44) and *ENTPD1* (CD39) in purple on the UMAP clustering.

References

1. Yudanin NA, Schmitz F, Flamar AL, Thome JJC, Tait Wojno E, Moeller JB, et al. Spatial and temporal mapping of human innate lymphoid cells reveals elements of tissue specificity. *Immunity* (2019) 50(2):505–19.e4. doi: 10.1016/j.immuni.2019.01.012

2. Jacquelot N, Seillet C, Vivier E, Belz GT. Innate lymphoid cells and cancer. *Nat Immunol* (2022) 23(3):371–9. doi: 10.1038/s41590-022-01127-z

3. Bando JK, Gilfillan S, Di Luccia B, Fachi JL, Sécca C, Cella M, et al. Ilc2s are the predominant source of intestinal ilc-derived il-10. *J Exp Med* (2020) 217(2):e20191520. doi: 10.1084/jem.20191520

4. Muraoka WT, Korchagina AA, Xia Q, Shein SA, Jing X, Lai Z, et al. Campylobacter infection promotes ifnγ-dependent intestinal pathology *Via* Ilc3 to Ilc1 conversion. *Mucosal Immunol* (2021) 14(3):703–16. doi: 10.1038/s41385-020-00353-8

5. Gao Y, Souza-Fonseca-Guimaraes F, Bald T, Ng SS, Young A, Ngiow SF, et al. Tumor immunoevasion by the conversion of effector nk cells into type 1 innate lymphoid cells. *Nat Immunol* (2017) 18(9):1004–15. doi: 10.1038/ni.3800

6. Gordon SM, Chaix J, Rupp LJ, Wu J, Madera S, Sun JC, et al. The transcription factors T-bet and eomes control key checkpoints of natural killer cell maturation. *Immunity* (2012) 36(1):55–67. doi: 10.1016/j.immuni.2011.11.016

7. Zhang J, Le Gras S, Pouxvielh K, Faure F, Fallone L, Kern N, et al. Sequential actions of eomes and T-bet promote stepwise maturation of natural killer cells. *Nat Commun* (2021) 12(1):5446. doi: 10.1038/s41467-021-25758-2

8. Spits H, Mjösberg J. Heterogeneity of type 2 innate lymphoid cells. *Nat Rev Immunol* (2022), 22(11)701–12. doi: 10.1038/s41577-022-00704-5

9. Sanos SL, Diefenbach A. Innate lymphoid cells: From border protection to the initiation of inflammatory diseases. *Immunol Cell Biol* (2013) 91(3):215–24. doi: 10.1038/icb.2013.3

10. Zeng B, Shi S, Ashworth G, Dong C, Liu J, Xing F. Ilc3 function as a double-edged sword in inflammatory bowel diseases. *Cell Death Dis* (2019) 10(4):315. doi: 10.1038/s41419-019-1540-2

11. Mazzurana L, Czarnewski P, Jonsson V, Wigge L, Ringnér M, Williams TC, et al. Tissue-specific transcriptional imprinting and heterogeneity in human innate lymphoid cells revealed by full-length single-cell rna-sequencing. *Cell Res* (2021) 31 (5):554–68. doi: 10.1038/s41422-020-00445-x

12. Heinrich B, Gertz EM, Schäffer AA, Craig A, Ruf B, Subramanyam V, et al. The tumour microenvironment shapes innate lymphoid cells in patients with hepatocellular carcinoma. *Gut* (2022) 71(6):1161–75. doi: 10.1136/gutjnl-2021-325288

13. Rethacker L, Boy M, Bisio V, Roussin F, Denizeau J, Vincent-Salomon A, et al. Innate lymphoid cells: Nk and cytotoxic Ilc3 subsets infiltrate metastatic breast cancer lymph nodes. *Oncoimmunology* (2022) 11(1):2057396. doi: 10.1080/2162402x.2022.2057396

14. Baron CS, Barve A, Muraro MJ, van der Linden R, Dharmadhikari G, Lyubimova A, et al. Cell type purification by single-cell transcriptome-trained sorting. *Cell* (2019) 179(2):527–42.e19. doi: 10.1016/j.cell.2019.08.006

15. Wolock SL, Lopez R, Klein AM. Scrublet: Computational identification of cell doublets in single-cell transcriptomic data. *Cell Syst* (2019) 8(4):281–91.e9. doi: 10.1016/j.cels.2018.11.005

16. Yip SH, Sham PC, Wang J. Evaluation of tools for highly variable gene discovery from single-cell rna-seq data. *Brief Bioinform* (2019) 20(4):1583–9. doi: 10.1093/bib/bby011

17. Korsunsky I, Millard N, Fan J, Slowikowski K, Zhang F, Wei K, et al. Fast, sensitive and accurate integration of single-cell data with harmony. *Nat Methods* (2019) 16(12):1289–96. doi: 10.1038/s41592-019-0619-0

18. Welch JD, Kozareva V, Ferreira A, Vanderburg C, Martin C, Macosko EZ. Single-cell multi-omic integration compares and contrasts features of brain cell identity. *Cell* (2019) 177(7):1873–87.e17. doi: 10.1016/j.cell.2019.05.006

19. Zheng L, Qin S, Si W, Wang A, Xing B, Gao R, et al. Pan-cancer single-cell landscape of tumor-infiltrating T cells. *Science* (2021) 374(6574):abe6474. doi: 10.1126/science.abe6474

20. Wu T, Hu E, Xu S, Chen M, Guo P, Dai Z, et al. Clusterprofiler 4.0: A universal enrichment tool for interpreting omics data. *Innovation (Camb)* (2021) 2(3):100141. doi: 10.1016/j.xinn.2021.100141

21. Salcher S, Sturm G, Horvath L, Untergasser G, Kuempers C, Fotakis G, et al. High-resolution single-cell atlas reveals diversity and plasticity of tissue-resident neutrophils in non-small cell lung cancer. *Cancer Cell* (2022) 40(12):1503–20.e8. doi: 10.1016/j.ccell.2022.10.008

22. Squair JW, Gautier M, Kathe C, Anderson MA, James ND, Hutson TH, et al. Confronting false discoveries in single-cell differential expression. *Nat Commun* (2021) 12(1):5692. doi: 10.1038/s41467-021-25960-2

23. Krabbendam L, Heesters BA, Kradolfer CMA, Haverkate NJE, Becker MAJ, Buskens CJ, et al. Cd127+ Cd94+ innate lymphoid cells expressing granulysin and perforin are expanded in patients with crohn's disease. *Nat Commun* (2021) 12(1):5841. doi: 10.1038/s41467-021-26187-x

24. Qi J, Crinier A, Escalière B, Ye Y, Wang Z, Zhang T, et al. Single-cell transcriptomic landscape reveals tumor specific innate lymphoid cells associated with colorectal cancer progression. *Cell Rep Med* (2021) 2(8):100353. doi: 10.1016/j.xcrm.2021.100353

25. Agarwal SK, Novotny EA, Crabtree JS, Weitzman JB, Yaniv M, Burns AL, et al. Transcription factor jund, deprived of menin, switches from growth suppressor to growth promoter. *Proc Natl Acad Sci U S A* (2003) 100(19):10770–5. doi: 10.1073/pnas.1834524100

26. Höfle J, Trenkner T, Kleist N, Schwane V, Vollmers S, Barcelona B, et al. Engagement of trail triggers degranulation and ifnγ production in human natural killer cells. *EMBO Rep* (2022) 23(8):e54133. doi: 10.15252/embr.202154133

27. He Y, Luo J, Zhang G, Jin Y, Wang N, Lu J, et al. Single-cell profiling of human Cd127(+) innate lymphoid cells reveals diverse immune phenotypes in hepatocellular carcinoma. *Hepatology* (2022) 76(4):1013–29. doi: 10.1002/hep.32444

28. Golebski K, Layhadi JA, Sahiner U, Steveling-Klein EH, Lenormand MM, Li RCY, et al. Induction of il-10-Producing type 2 innate lymphoid cells by allergen immunotherapy is associated with clinical response. *Immunity* (2021) 54(2):291–307.e7. doi: 10.1016/j.immuni.2020.12.013

29. Shen X, Liang M, Chen X, Pasha MA, D'Souza SS, Hidde K, et al. Cutting edge: Core binding factor B is required for group 2 innate lymphoid cell activation. *J Immunol* (2019) 202(6):1669–73. doi: 10.4049/jimmunol.1800852

30. Mattiola I. Immune circuits to shape natural killer cells in cancer. *Cancers* (2021) 13(13):3225. doi: 10.3390/cancers13133225

31. Katz LH, Li Y, Chen JS, Muñoz NM, Majumdar A, Chen J, et al. Targeting tgf-B signaling in cancer. *Expert Opin Ther Targets* (2013) 17(7):743–60. doi: 10.1517/14728222.2013.782287

32. Nakatsuka Y, Yaku A, Handa T, Vandenbon A, Hikichi Y, Motomura Y, et al. Profibrotic function of pulmonary group 2 innate lymphoid cells is controlled by regnase-1. *Eur Respir J* (2021) 57(3):2000018. doi: 10.1183/13993003.00018-2020

33. Wu J, Bowe DB, Sadlonova A, Whisenhunt TR, Hu Y, Rustgi AK, et al. O-Glcnac transferase is critical for transducin-like enhancer of split (Tle)-mediated repression of canonical wnt signaling. *J Biol Chem* (2014) 289(17):12168–76. doi: 10.1074/jbc.M114.553859

34. Jennings E, Elliot TAE, Thawait N, Kanabar S, Yam-Puc JC, Ono M, et al. Nr4a1 and Nr4a3 reporter mice are differentially sensitive to T cell receptor signal strength and duration. *Cell Rep* (2020) 33(5):108328. doi: 10.1016/j.celrep.2020.108328

35. Liu H, Li L, Hao Y, Li J, Liu Z, Qi J, et al. Identification of two migratory colon Ilc2 populations differentially expressing il-17a and il-5/Il-13. *Sci China Life Sci* (2023) 66(1): 67–80. doi: 10.1007/s11427-022-2127-2

36. Chea S, Schmutz S, Berthault C, Perchet T, Petit M, Burlen-Defranoux O, et al. Single-cell gene expression analyses reveal heterogeneous responsiveness of fetal innate lymphoid progenitors to notch signaling. *Cell Rep* (2016) 14(6):1500–16. doi: 10.1016/j.celrep.2016.01.015

37. Ghaedi M, Shen ZY, Orangi M, Martinez-Gonzalez I, Wei L, Lu X, et al. Single-cell analysis of rorα tracer mouse lung reveals ilc progenitors and effector Ilc2 subsets. *J Exp Med* (2020) 217(3):jem.20182293. doi: 10.1084/jem.20182293

38. Rutz S, Kayagaki N, Phung QT, Eidenschenk C, Noubade R, Wang X, et al. Deubiquitinase duba is a post-translational brake on interleukin-17 production in T cells. *Nature* (2015) 518(7539):417–21. doi: 10.1038/nature13979

39. Nagasawa M, Heesters BA, Kradolfer CMA, Krabbendam L, Martinez-Gonzalez I, de Bruijn MJW, et al. Klrg1 and Nkp46 discriminate subpopulations of human Cd117 (+)Crth2(-) ilcs biased toward Ilc2 or Ilc3. *J Exp Med* (2019) 216(8):1762–76. doi: 10.1084/jem.20190490

40. Mortha A, Chudnovskiy A, Hashimoto D, Bogunovic M, Spencer SP, Belkaid Y, et al. Microbiota-dependent crosstalk between macrophages and Ilc3 promotes intestinal homeostasis. *Science* (2014) 343(6178):1249288. doi: 10.1126/science.1249288

41. Deng T, Suo C, Chang J, Yang R, Li J, Cai T, et al. Ilc3-derived Ox40l is essential for homeostasis of intestinal tregs in immunodeficient mice. *Cell Mol Immunol* (2020) 17(2):163–77. doi: 10.1038/s41423-019-0200-x

42. Crinier A, Dumas PY, Escalière B, Piperoglou C, Gil L, Villacreces A, et al. Single-cell profiling reveals the trajectories of natural killer cell differentiation in bone marrow and a stress signature induced by acute myeloid leukemia. *Cell Mol Immunol* (2021) 18(5):1290–304. doi: 10.1038/s41423-020-00574-8

43. Smith SL, Kennedy PR, Stacey KB, Worboys JD, Yarwood A, Seo S, et al. Diversity of peripheral blood human nk cells identified by single-cell rna sequencing. *Blood Adv* (2020) 4(7):1388–406. doi: 10.1182/bloodadvances.2019000699

44. Lim AI, Menegatti S, Bustamante J, Le Bourhis L, Allez M, Rogge L, et al. Il-12 drives functional plasticity of human group 2 innate lymphoid cells. *J Exp Med* (2016) 213(4):569–83. doi: 10.1084/jem.20151750

45. Mazzurana L, Forkel M, Rao A, Van Acker A, Kokkinou E, Ichiya T, et al. Suppression of aiolos and ikaros expression by lenalidomide reduces human Ilc3-Ilc1/Nk cell transdifferentiation. *Eur J Immunol* (2019) 49(9):1344–55. doi: 10.1002/eji.201848075

46. Ricardo-Gonzalez RR, Van Dyken SJ, Schneider C, Lee J, Nussbaum JC, Liang HE, et al. Tissue signals imprint Ilc2 identity with anticipatory function. *Nat Immunol* (2018) 19(10):1093–9. doi: 10.1038/s41590-018-0201-4

47. Mathä L, Takei F, Martinez-Gonzalez I. Tissue resident and migratory group 2 innate lymphoid cells. *Front Immunol* (2022) 13:877005. doi: 10.3389/fimmu.2022.877005

48. Lim AI, Li Y, Lopez-Lastra S, Stadhouders R, Paul F, Casrouge A, et al. Systemic human ilc precursors provide a substrate for tissue ilc differentiation. *Cell* (2017) 168 (6):1086–100.e10. doi: 10.1016/j.cell.2017.02.021

49. Winkler C, Hochdörfer T, Israelsson E, Hasselberg A, Cavallin A, Thörn K, et al. Activation of group 2 innate lymphoid cells after allergen challenge in asthmatic patients. *J Allergy Clin Immunol* (2019) 144(1):61–9.e7. doi: 10.1016/j.jaci.2019.01.027

50. Bernink JH, Ohne Y, Teunissen MBM, Wang J, Wu J, Krabbendam L, et al. C-Kit-Positive Ilc2s exhibit an Ilc3-like signature that may contribute to il-17-Mediated pathologies. *Nat Immunol* (2019) 20(8):992–1003. doi: 10.1038/s41590-019-0423-0

51. Montaldo E, Juelke K, Romagnani C. Group 3 innate lymphoid cells (Ilc3s): Origin, differentiation, and plasticity in humans and mice. *Eur J Immunol* (2015) 45 (8):2171–82. doi: 10.1002/eji.201545598

52. Simoni Y, Fehlings M, Kløverpris HN, McGovern N, Koo SL, Loh CY, et al. Human innate lymphoid cell subsets possess tissue-type based heterogeneity in phenotype and frequency. *Immunity* (2018) 48(5):1060. doi: 10.1016/j.immuni.2018.04.028

53. Zhang YS, Xin DE, Wang Z, Song X, Sun Y, Zou QC, et al. Stat4 activation by leukemia inhibitory factor confers a therapeutic effect on intestinal inflammation. *EMBO J* (2019) 38(6):e99595. doi: 10.15252/embj.201899595

54. Goc J, Lv M, Bessman NJ, Flamar AL, Sahota S, Suzuki H, et al. Dysregulation of Ilc3s unleashes progression and immunotherapy resistance in colon cancer. *Cell* (2021) 184(19):5015–30.e16. doi: 10.1016/j.cell.2021.07.029

55. Krabbendam L, Heesters BA, Kradolfer CMA, Spits H, Bernink JH. Identification of human cytotoxic Ilc3s. *Eur J Immunol* (2021) 51(4):811–23. doi: 10.1002/eji.202048696

56. Raykova A, Carrega P, Lehmann FM, Ivanek R, Landtwing V, Quast I, et al. Interleukins 12 and 15 induce cytotoxicity and early nk-cell differentiation in type 3 innate lymphoid cells. *Blood Adv* (2017) 1(27):2679–91. doi: 10.1182/bloodadvances.2017008839

57. Björklund ÅK, Forkel M, Picelli S, Konya V, Theorell J, Friberg D, et al. The heterogeneity of human Cd127(+) innate lymphoid cells revealed by single-cell rna sequencing. *Nat Immunol* (2016) 17(4):451–60. doi: 10.1038/ni.3368

58. Rösler B, Herold S. Lung epithelial gm-csf improves host defense function and epithelial repair in influenza virus pneumonia-a new therapeutic strategy? *Mol Cell Pediatr* (2016) 3(1):29. doi: 10.1186/s40348-016-0055-5

frontiers | Frontiers in Immunology

TYPE Original Research
PUBLISHED 09 March 2023
DOI 10.3389/fimmu.2023.1105145

OPEN ACCESS

EDITED BY
Carolina Jancic,
National Scientific and Technical Research Council (CONICET), Argentina

REVIEWED BY
Christoph Siegfried Niki Klose,
Charité Universitätsmedizin Berlin, Germany
Xiaofei Yu,
Fudan University, China
Liang Zhou,
University of Florida, United States

*CORRESPONDENCE
Chen Dong
chendong@tsinghua.edu.cn
Xiaohu Wang
wangxhu@tsinghua.edu.cn

†Lead contact

SPECIALTY SECTION
This article was submitted to NK and Innate Lymphoid Cell Biology, a section of the journal Frontiers in Immunology

RECEIVED 22 November 2022
ACCEPTED 22 February 2023
PUBLISHED 09 March 2023

CITATION
Chang D, Zhang H, Ge J, Xing Q, Guo X, Wang X and Dong C (2023) A *cis*-element at the *Rorc* locus regulates the development of type 3 innate lymphoid cells.
Front. Immunol. 14:1105145.
doi: 10.3389/fimmu.2023.1105145

A *cis*-element at the *Rorc* locus regulates the development of type 3 innate lymphoid cells

Dehui Chang[1], Hao Zhang[1], Jing Ge[2], Qi Xing[1], Xinyi Guo[1], Xiaohu Wang[1]* and Chen Dong[1,2,3,4]*†

[1]Institute for Immunology and School of Medicine, Tsinghua University, Beijing, China, [2]Shanghai Immune Therapy Institute, Shanghai Jiao Tong University School of Medicine Affiliated Renji Hospital, Shanghai, China, [3]Tsinghua University-Peking University Center for Life Sciences, Tsinghua University, Beijing, China, [4]Research Unit of Immune Regulation and Immune Diseases of Chinese Academy of Medical Sciences, Shanghai Jiao Tong University School of Medicine-Affiliated Renji Hospital, Shanghai, China

Background: As an important early source of IL-17A and IL-22 in immune responses, type 3 innate lymphoid cells (ILC3s) are critically regulated by the transcription factor retinoic-acid-receptor-related orphan receptor gamma t (RORγt). Previously, we have identified a crucial role of the conserved non-coding sequence 9 (CNS9), located at +5,802 to +7,963 bp of the *Rorc* gene, in directing T helper 17 differentiation and related autoimmune disease. However, whether *cis*-acting elements regulate RORγt expression in ILC3s is unknown.

Results: Here we show that CNS9 deficiency in mice not only decreases ILC3 signature gene expression and increases ILC1-gene expression features in total ILC3s, but also leads to generation of a distinct $CD4^+NKp46^+$ ILC3 population, though the overall numbers and frequencies of $ROR\gamma t^+$ ILC3s are not affected. Mechanistically, CNS9 deficiency selectively decreases RORγt expression in ILC3s, which thus alters ILC3 gene expression features and promotes cell-intrinsic generation of $CD4^+NKp46^+$ ILC3 subset.

Conclusion: Our study thus identifies CNS9 as an essential *cis*-regulatory element controlling the lineage stability and plasticity of ILC3s through modulating expression levels of RORγt protein.

KEYWORDS

ILC3s, RORγt, CNS9, cis-element, plasticity

Introduction

Innate lymphoid cells (ILCs), important in defense against invading pathogens at the mucosal surface, contain three major subpopulations depending on their distinct gene expression patterns. Group 3 ILCs (ILC3s), similar to T helper 17 (Th17) cells, express transcription factor RORγt and secrete interleukin-17A (IL-17A) and/or IL-22 (1, 2). ILC3s

play important roles in controlling extracellular bacteria and fungi, as well as tissue repair following mucosal barrier damage (3).

ILC3s are generally divided into three major subsets in mice, based on expression of chemokine receptor CCR6 and natural cytotoxicity receptor NKp46. $CCR6^+(NKp46^-)$ ILC3s include lymphoid tissue inducer (LTi) and LTi-like cells, are heterogenous in CD4 expression, which are indispensable for lymphoid tissue formation (4). $CCR6^+(NKp46^-)$ ILC3s have been reported to facilitate $CD4^+/CD8^+$ T cells in anti-tumor response (5). $NKp46^+(CCR6^-)$ ILC3s are pathogenic in anti-CD40-induced innate colitis model, through recruiting inflammatory monocytes (6). However, the role of $CCR6^-$ $NKp46^-$ double-negative ILC3s has not been extensively characterized. Intestinal $NKp46^+(CCR6^-)$ ILC3s, developed from $NKp46^-CCR6^-$ ILC3s upon up-regulating T-bet expression, have mixed features of both ILC3s and ILC1s, with expression of NKp46, T-bet and interferon γ (IFN-γ), and can convert to ILC1-like cell or even ILC1s (7–11). ILC3s are thus highly plastic, readily in response to continuously changing microenvironments.

As the lineage-specific transcription factor of both Th17 cells and ILC3s, RORγt (encoded by *Rorc*) is essential for their development and effector functions. Conserved non-coding sequences (CNSs) are regulatory *cis*-acting elements critically controlling gene expression *via* interaction with various *trans*-acting factors. A number of CNSs have been identified at the *Rorc* locus. CNS9 and CNS6 are required for IL-6-STAT3 and TGF-β-SMAD&c-MAF signaling, respectively (12). Interestingly, deletion of CNS6 or CNS9 did not affect the development of γδT cells or ILC3s. Therefore, the *cis*-regulatory mechanisms controlling *Rorc* transcription in ILC3s remain unclear. Comparative transposase-accessible chromatin using sequencing (ATAC-seq) and RNA-seq analysis revealed many potentially active *cis*-elements in ILCs (13), but none of them have been functionally and genetically analyzed.

In this study, we discovered that CNS9 deficiency altered ILC3 features in intestine, associated with increased ILC1 but decreased ILC3 signature gene expression. Moreover, loss of CNS9 reduced RORγt expression at per cell level and causes induction of specific $CD4^+NKp46^+$ ILC3 subset that is not found in healthy WT mice. Our results thus indicate that *cis*-regulatory element CNS9 is important in maintaining the lineage stability or development of ILC3s.

Materials and methods

Mice

C57BL/6J and $CD45.1^+$ mice were obtained from Jackson Laboratory, and were crossed to generate $CD45.1^+CD45.2^+$ mice. CNS9-deficient mice were generated on C57BL/6J background by using CRISPR-Cas9 system in our previous study (12). $ROR\gamma t^{GFP}$ mice were generated by the laboratory of Prof. Dan R. Littman (4).

All mice were housed in specific pathogen-free (SPF) conditions and in isolated ventilated cages in the animal facility at Tsinghua University, which has been accredited by AAALAC (Association for Assessment and Accreditation of Laboratory Animal Care International). All the animal protocols used in this study has been approved by IACUC (Institutional Animal Care and Use Committee) of Tsinghua University. All mice used in this study were at 6-15 weeks, age and sex matched.

Isolation of immune cells

Lamina propria lymphocytes (LPLs) were isolated from small intestine or large intestine. The intestine was collected by removing mesenteric lymph nodes and Peyer's patches and cut into 2-3 cm pieces longitudinally, then digested at 37°C for 30 mins in RPMI 1640 medium containing 5 mM EDTA, 20 mM HEPES, 1 mM DTT and Penicillin/Streptomycin. The tissues were washed twice using RPMI 1640 medium containing 2mM EDTA, 20mM HEPES and Penicillin/Streptomycin. The remaining tissues were chopped into small pieces and digested in digestion buffer (RPMI 1640 medium with 20 mM HEPES, 0.5 mg/ml collagenase D, 1 mg/ml Dispase and 2 mg/ml DNase I and Penicillin/Streptomycin) at 37°C for 30 min. Then the tissues were meshed through 100 μm cell strainer for cells suspension. LPLs were obtained from the interface of 70% and 40% Percoll after centrifuging at 2500 rpm, 25°C for 30 min.

Spleen, mesenteric and inguinal lymph nodes were taken out, ground and passed through 100 μm cell strainer (spleen needed additional lysing to remove red blood cells).

C. rodentium infection model

Mice were fasted for 7-8 hours and then orally gavaged with $2*10^9$ CFU *C. rodentium*/mouse. The body weight and fecal bacterial load were monitored. If indicated, the mice were sacrificed and intestinal LPLs were analyzed 8 days post-infection.

Ex vivo stimulation

To measure IFN-γ expression, ILC3s were stimulated at 37°C for 4 hours with 25 ng/ml IL-12, 50 ng/ml IL-15 and 5 ng/ml IL-23 in the presence of GolgiStop™. While for measuring IL-22 and IL-17A, cells were stimulated at 37°C for 4 hours with 5 ng/ml IL-23 in the presence of GolgiStop™. As specifically indicated, IL-22 production in Figure S2B was measured with IL-12 and IL-15 stimulation.

Generation of RORγt overexpression chimeric mice

On day 0, bone marrow cells were isolated from CNS9-deficient mice, depleted red blood cells and then cultured in 6-well plates (4×10^6 cell for each well) in RPMI 1640 medium (20 ng/mL IL-3, 50 ng/mL IL-6 and 50 ng/mL SCF with Penicillin/Streptomycin) at 37°C in a CO_2 incubator. On day 2, polybrene was added into the cell mixture at a final concentration of 8 μg/mL. Bone marrow cells were infected with RVKM control or RVKM-RORγt retrovirus, centrifuged at 1800 rpm for 2 hours at 35°C. This infection was repeated on day 3. On day 4, the virus infected GFP^+ bone marrow cells were sorted, and then intravenously injected into lethally irradiated (2 rounds of 5Gy irradiation, an interval

of 2 hours) CD45.1$^+$ recipient mice at 2 x 10^6/mouse. Seven weeks later, the recipient mice were sacrificed and analyzed.

Antibiotic treatment

CNS9-deficient mice were treated with antibiotics (ampicillin: 1 g/L, vancomycin: 500 mg/L, neomycin: 1 mg/mL and metronidazole: 1 mg/mL) starting from 3 to 6 weeks old. The antibiotics were supplied in drinking water and changed every two days to keep fresh.

ScRNA-seq library construction and data processing

ILC3 (CD45^{mid} CD3$^-$ CD90.2^{high}) cells were sorted from small intestine LPLs using flow cytometry. Single-cell RNA libraries were generated using 10X Genomics chromium according to the manufacturer's instructions. The quality of libraries was determined by Agilent 2100 bioanalyzer and sequenced with NovaSeq 6000 PE150(Illumina).

To generate single cell feature counts, the clean data of each sample were mapped to mouse reference genome (mm10) by the command "cell ranger count" within cell ranger toolkit (version 6.0.1) provided by 10X genomics. For each sample, cells as outliers in feature count matrix (proportion of mitochondrial genes > 10% and ncount_feature < 300 or ncount_feature > 4700) were removed from further analysis. To remove impure cells, we first filtered the cells by *Ptprc*$^+$ *Cd3e*$^-$ *Thy1*$^+$ according to sorting strategy, and then exclude non-ILC3 based on signature gene expression, including T cells (*Cd3g, Cd3e*), B cells (Cd79a, IgIv1, Jchain), macrophages (*Cd68, Apoe, C1qb, Csf1r*), endothelial cells (*Fabp4, Id3, Lyve1* (14)), ILC1/NK (*Ccl5, Klrd1, Klrc2, Eomes*) and ILC2s (*Klrg1, Il4, Il5, Il13*) (15). Finally, we obtained 6860 cells and 4517 cells from WT and CNS9KO samples respectively.

Clustering of single cell data matrix

The Seurat R package (version 4.0.3) was conducted for further analysis of feature count matrix. For each sample, about 2,000 genes with the highest variance based on a variance stabilizing transformation data were selected to compute a PCA dimensionality reduction. Integration of two samples was conducted by RunHarmony() function in Seurat R package. The 30 principal components (PCs) of the integrated Seurat object were used for further nonlinear dimensional reduction analysis. The integrated data were clustered using Seurat's FindClusters() function (resolution parameters was set to 0.8), then visualized by UMAP. The different expression of the selected marker genes in each cluster were visualized by DotPlot() function.

RNA velocity analysis

For each sample, a.loom file with counts divided in spliced/unspliced/ambiguous was generated by velocyto.py toolkit (version 0.17). Then, the data were pre-processed by scVelo python toolkit (version 0.2.4). Genes that are detected in less than 20 counts were filtered out and 2000 genes with the highest variability were selected. After normalization and logarithmization, the first and second order moments (means and uncentered variances) were computed among nearest neighbors in PCA space under default parameters. Then, the RNA velocity was estimated by scVelo's scv.tl.velocity() function, and visualized by scv.pl.velocity_embedding_stream() function.

Generation of bone marrow chimeric mice

Bone marrow cells from C57BL/6J, CNS9-deficient and CD45.1$^+$CD45.2$^+$ mice were isolated and depleted red blood cells. C57BL/6J or CNS9-deficient bone marrow cells were mixed with the ones from CD45.1$^+$CD45.2$^+$ mice at 1:1 ratio, and 4×10^6 mixed bone marrow cells were injected intravenously into lethally irradiated (2 rounds of 5Gy irradiation, an interval of 2 hours) CD45.1$^+$ recipient mice. The reconstituted mice were then sacrificed and analyzed 7 weeks later.

Flow cytometry analysis

The antibodies and corresponding dilutions listed below were used for staining: CD45.2 (104, 109824, BioLegend; 104, 56-0454, eBioscience; 1:400), CD45.1 (A20, 558701, BD BioSciences; 1:400), CD3 (17A2, 48-0032-82, eBioscience; 1:400), CD3e (145-2C11, 45-0031-82, eBioscience; 1:200), CD90.2(53-2.1, 25-0902-82/17-0902-83, eBioscience; 1:400), CD4(RM4-5, 562314/557956, BD BioSciences; RM4-5, 25-0042-81, eBioscience; 1:400), CCR6 (29-2L17, 129819, BioLegend; 1:200), NKp46 (29A1.4, 137606, BioLegend; 29A1.4, 25-3351-82, eBioscience; 1:400), RORγt (Q31-378, 562607/562682, BD BioSciences; 1:400), T-bet (4B10, 644814, BioLegend: 1:400), IL-17a (eBio17B7, 48-7177-82, eBioscience; 1:200), IL-22(IL22JOP, 17-7222-82, eBioscience; 1:200), IFN-γ (XMG1.2, 557998, BD BioSciences; 1:200).

Quantification and statistical analysis

Data were analyzed using Graphpad Prism 6 or Graphpad Prism 8 and preformed as mean ± SD. Statistical significance was calculated using unpaired Student's t test and shown as (*$p < 0.05$; **$p < 0.01$; ***$p < 0.001$, ****$p < 0.0001$).

Results

CNS9 deficiency alters intestinal ILC3 subsets

We have previously identified CNS9, located at +5,802 to +7,963 bp of the *Rorc* gene, whose deficiency in mice caused a profound defect in *Rorc* expression and RORγt-directed IL-17A expression in Th17 cells (12). In contrast, CNS9 deficiency had little

effect on development of total RORγt$^+$ ILC3s (gated on CD45$^+$CD3$^-$ CD90$^+$) in small intestine under steady state, as examinbed in both percentages and numbers (Figure 1A). In addition, under *C. rodentium* infection state, CNS9-deficient mice showed comparable degrees of weight loss and bacterial loads at the early stage of infection to control WT mice (Figures S1A, B). These data suggest that the general development and function of ILC3s were largely unaffected by CNS9 deficiency.

However, a careful examination revealed that CNS9 deficiency significantly increased expression of both CD4 and NKp46 in ILC3s in the LPLs of small intestine under steady state, resulting in a clear population of CD4$^+$NKp46$^+$ double positive cells (Figure 1B). As introduced previously, CD4 only expressed by part of CCR6$^+$ ILC3s but not NKp46$^+$ ILC3s, suggesting the CD4$^+$NKp46$^+$ ILC3 subset in CNS9-deficient mice is a distinct population compared with WT mice. In addition, the expression of CCR6 was found decreased in CNS9-deficient ILC3s (Figure 1C), suggesting the composition of ILC3 subsets was significantly altered in CNS9-deficient mice, despite their overall function may not be affected. Consistently, CD4$^+$NKp46$^+$ ILC3s were also present in the lamina propria of both small and large intestines in CNS9-deficient mice 8 days after *C. rodentium* infection (Figures S1C, D), as well as in other lymphoid tissues including mesenteric lymph nodes (mLN), inguinal lymph nodes (iLN) and spleen under steady status (Figure S1E), though less prominent than in gut-associated mucosal tissues.

At cytokine levels, CNS9-deficient ILC3s secreted 50% to 80% less IL-22 and IL-17A, but about 3-fold increase of IFN-γ, compared with WT ILC3s (Figure 2A). The CD4$^+$NKp46$^+$ ILC3s showed similar cytokine producing abilities to CD4$^-$NKp46$^+$ ILC3s in CNS9-deficient mice, with reduced IL-22 and increased IFN-γ but no IL-17A expression, compared with other subsets (Figure 2B). Moreover, associated with increased IFN-γ secretion, an obvious population of IFN-γ and IL-22 double positive cells was detected in NKp46$^+$ ILC3s in CNS9-deficient mice (Figure 2C). These results indicate that CNS9-deficient ILC3s gained increased ILC1-related cytokine secretion potential at the expense of reduced ILC3 effector function.

Notably, there was no defect in IL-22 production in CNS9-deficient ILC3s under stimulation with IL-12, IL-15 and IL-23 condition (Figure S2A), which was different from cells stimulated with IL-23 alone (Figure 2A). Interestingly, IL-12 and IL-15 treatment could also induce IL-22 production in ILC3s, in the absence of IL-23 (Figure S2B), suggesting distinct mechanisms involved in IL-23- and IL-12/15-stimulated conditions.

We further measured IL-22 production in ILC3s after *C.rodentium* infection, but with only a slightly decreased trend in CNS9-deficient ILC3s compared with WT cells (Figure S2C), indicating a compensatory mechanism or context-dependent regulation of IL-22 production in ILC3s by CNS9 as revealed in Figures 2A, S2A. In line with this, CNS9-deficient mice showed comparable weight loss and fecal bacterial loads after *C. rodentium* infection (Figures S1A, B).

CNS9 deficiency promotes cell-intrinsic induction of CD4$^+$NKp46$^+$ ILC3s

Since RORγt and its isoform RORγ can be expressed by a number of cell subsets, including Th17 cells, γδT cells, NKT cells and even non-immune cells, CNS9 deficiency may affect ILC3 development through an indirect manner. To test this possibility, mixed bone marrow chimeric mice were generated by reconstituting lethally irradiated

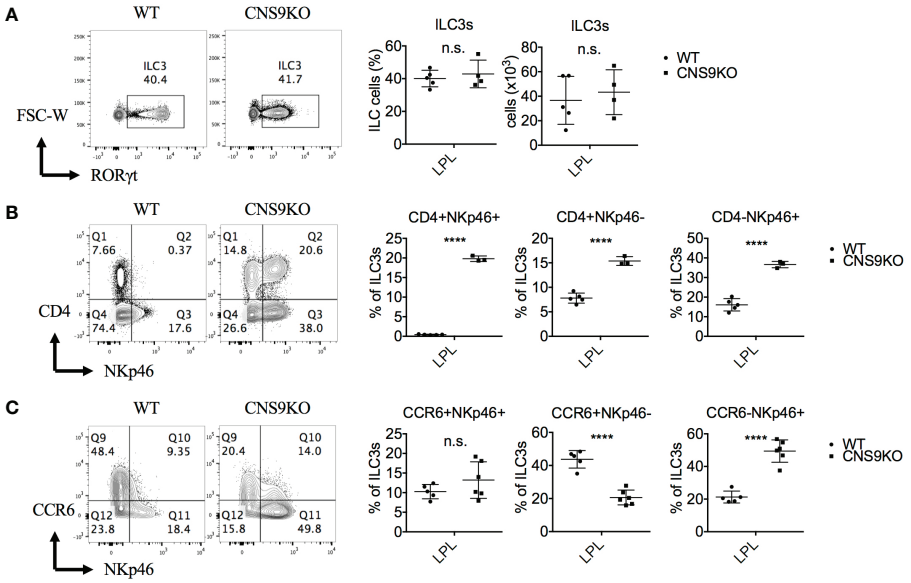

FIGURE 1
CNS9 deficiency alters the composition of ILC3s. ILC3s were isolated from the small intestine lamina propria lymphocytes (LPLs) of age- and sex-matched WT and CNS9-deficient (CNS9KO in figure) mice under steady state, directly stained with indicated surface markers and RORγt, and then analyzed by flow cytometry. **(A)** Left: intracellular staining of RORγt (pre-gated on Live CD45$^+$ CD3$^-$ CD90$^+$); right: statistic of the staining data and cell number of ILC3s. Staining (left) and statistic (right) of the surface marker CD4 and NKp46 **(B)** or CD4 and CCR6 **(C)** on ILC3s (pre-gated on ILC3: Live CD45$^+$ CD3$^-$ CD90$^+$ RORγt$^+$). The data shown are a representative of two to three independent experiments and presented as mean ± SD. Also see Figure S1. Statistical significance was calculated using unpaired Student's t test and shown as ****$p < 0.0001$ or n.s. (non-significant) $p > 0.05$.

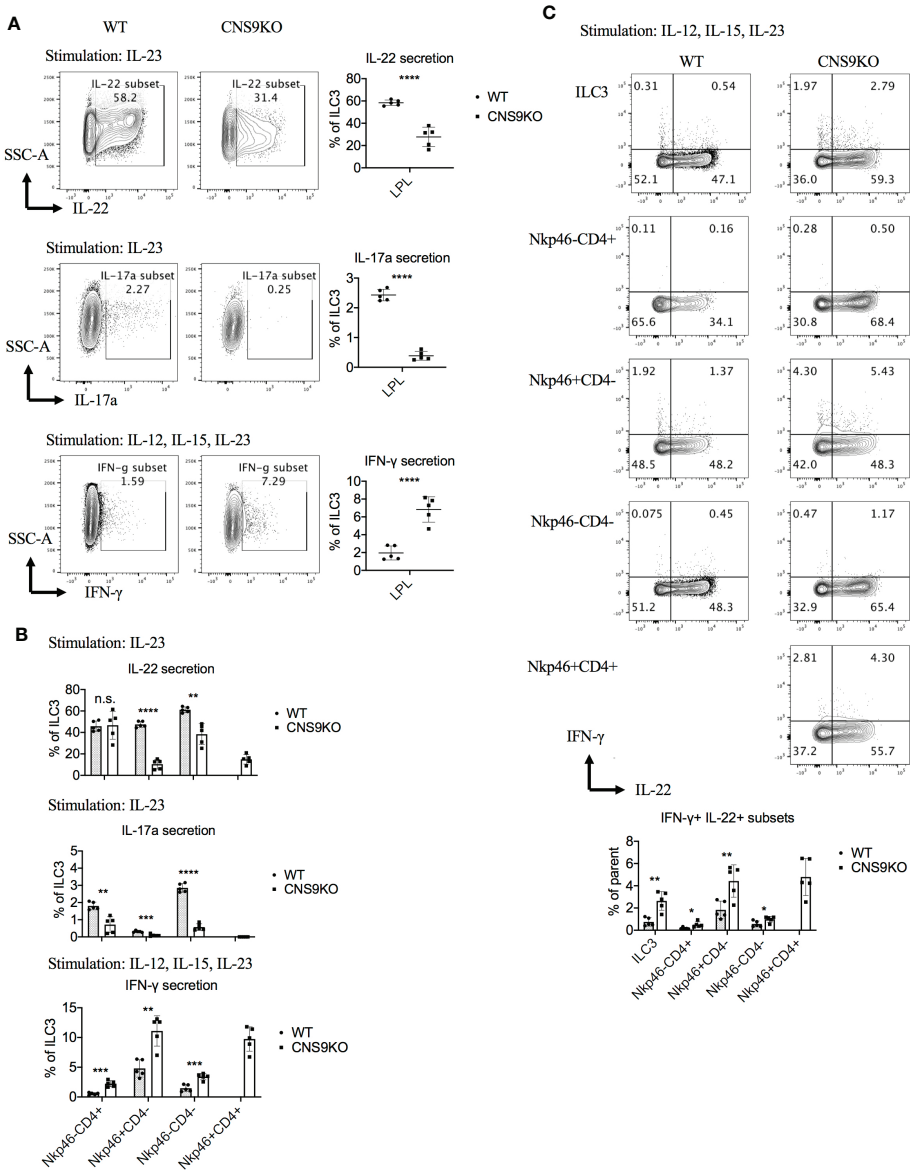

FIGURE 2
CNS9 deficiency modulates the cytokine production of ILC3s. ILC3s were isolated from the small intestine lamina propria lymphocytes (LPLs) of age- and sex-matched WT and CNS9-deficient mice under steady state. Stimulated *ex vivo* for 4 hours before staining with surface markers, RORγt and cytokines, and then analyzed by flow cytometry. **(A)** Left: intracellular staining of IL-22, IL-17A and IFN-γ single positive cells in total ILC3s; right: statistic of the staining data. **(B)** Statistic analysis of IL-22, IL-17A and IFN-γ in different ILC3 subsets. **(C)** Up: intracellular staining of IL-22 and IFN-γ; down: statistic analysis of IL-22$^+$IFN-γ$^+$ double positive cells in total ILC3s and different subsets. The data shown are a representative of two to three independent experiments and presented as mean ± SD. Also see Figure S2. Statistical significance wascalculated using unpaired Student's t test and shown as *p < 0.05; **p < 0.01; ***p < 0.001, ****p < 0.0001 or n.s. (non-significant) p > 0.05.

CD45.1$^+$ mice with WT CD45.1$^+$CD45.2$^+$ bone marrow cells and CD45.2$^+$ WT or CNS9-deficient bone marrow cells at a 1:1 ratio (Figure 3A). 7 weeks after reconstitution, a distinct group of CD4$^+$NKp46$^+$ ILC3s was developed from CNS9-deficient but not WT bone marrow cells (Figure 3B), similar to CNS9 germline knockout mice. In addition, CNS9 deficiency led to significantly increased NKp46$^+$ but decreased CCR6$^+$ ILC3 populations, similar to unmanipulated mice at steady state, but the overall frequencies of CD4-expressing ILC3s were largely not affected in the chimeric animals (Figure 3B and Figure 1B). Similar to those from CNS9-deficient mice, ILC3s developed from CNS9-deficient bone marrow cells in the chimeric mice showed reduced RORγt expression level compared with those from WT bone marrow cells (Figure 3C). These results thus demonstrate that CNS9 functions in a cell-intrinsic manner in constraining the development of CD4$^+$NKp46$^+$ ILC3 subset. However, unlike CNS9-deficient mice, CNS9-deficient bone marrow cells showed a severe defect in development towards ILC3s but not ILC1s, compared with WT bone marrow cells, suggesting their apparent disadvantage in ILC3 development under competitive microenvironments (Figure 3D).

ILCs, abundant at mucosal barriers, are regulated by microbiota in development, maintenance and function (15, 16). To examine whether the development of CD4$^+$NKp46$^+$ ILC3s in CNS9-deficient mice was regulated by intestinal microbiota, we treated 3-week old mice with antibiotics (ampicillin, vancomycin, neomycin and metronidazole)

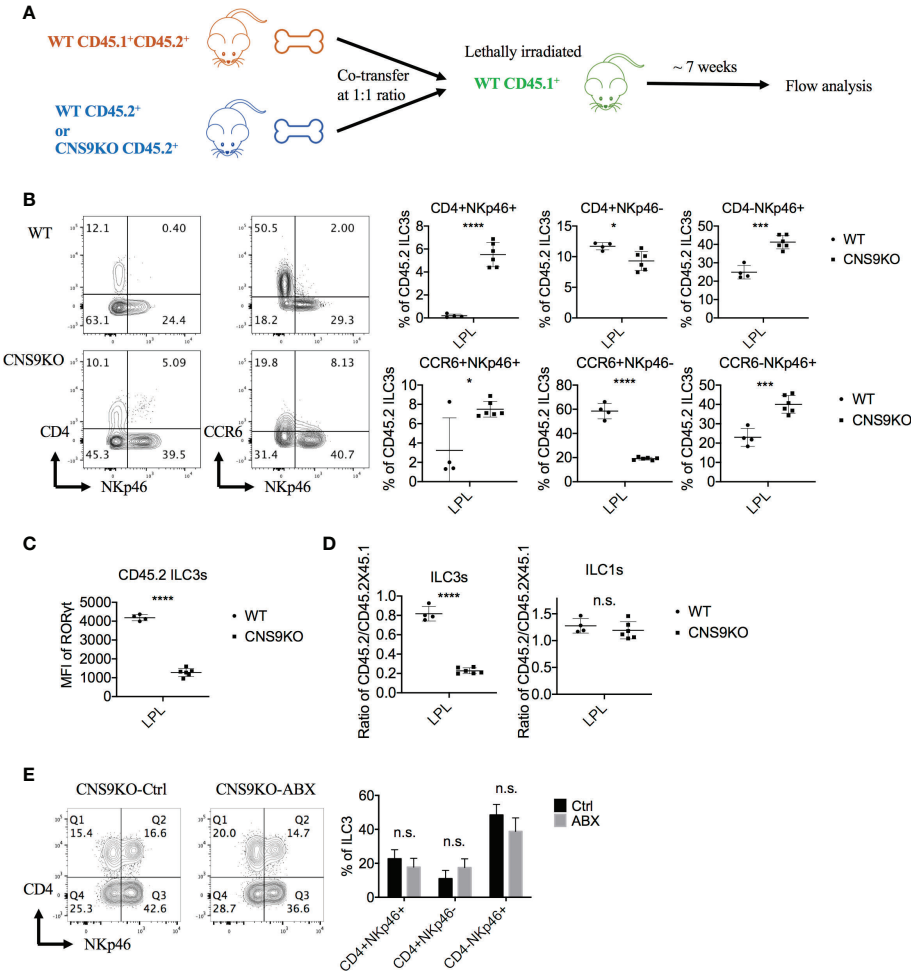

FIGURE 3
CNS9 deficiency promotes the generation of CD4$^+$NKp46$^+$ ILC3 subset *via* a cell-intrinsic manner. **(A)** Experiment protocol: The CD45.1$^+$CD45.2$^+$ WT BM cells and CD45.2$^+$ CNS9-deifient BM cells were transferred to irradiated CD45.1$^+$ mice at a 1:1 ratio. Seven weeks later, the recipient mice were sacificed and the small intestine LPLs were collected and analyzed by flow cytometry. **(B)** The ILC3s were gated as Live CD3$^-$ CD90$^+$ RORγt$^+$ CD45.2$^+$ cells. Left: surface staining of CD4, NKp46, CCR6 of ILC3s; right: statistic of the staining data. **(C)** MFI of RORγt in CD45.2$^+$ WT and CNS9-deficient ILC3s. **(D)** The ratios of CD45.2$^+$ WT/CNS9-deficient *versus* CD45.1$^+$CD45.2$^+$ WT ILC3s or ILC1s. The data shown are a representative of two independent experiments and presented as mean ± SD. **(E)** CNS9-deficient mice were treated with ABX or water (as control) continuously started from 3 weeks after wean. The LPLs of small intestine were isolated and analyzed at the age of 6 weeks old. Left: surface staining of CD4 and NKp46 (gated on ILC3s); right: statistic of the staining data. The flow data shown are a representative of two independent experiments and the statistical analysis was performed by combining two experiments and presented as mean ± SD (n=4 for both Ctrl and ABX group). Statistical significance was calculated using unpaired Student's t test and shown as *p < 0.05; ***p < 0.001, ****p < 0.0001 or n.s. (non-significant) p > 0.05.

supplied in drinking water for 3 weeks to remove gut microbiota. Compared with water-treated control group, antibiotic treatment did not affect the population of CD4$^+$NKp46$^+$ ILC3s in CNS9-deficient mice (Figure 3E), suggesting their generation in CNS9-deficient mice were independent of gut-associated microbiota.

CNS9-deficient ILC3s exhibit increased ILC1 gene expression features

To further understand the function of CNS9, total ILC3s (gated on CD45^{mid} CD3$^-$ CD90.2^{high}) were sorted from the LPLs of small intestine in WT and CNS9-deficient mice and analyzed by single-cell RNA sequencing. In total, 10 distinct clusters were identified after removing contaminated cells (Figures 4A, B). A previous study from Ido Amit lab (15) has defined a set of uniquely expressed genes in ILC1, ILC2 and ILC3, based on the RNA-seq data of intestinal ILC1s (CD45$^+$ Lin$^-$ CD127$^+$ RORγt$^-$ NKp46$^+$), ILC2s (CD45$^+$ Lin$^-$ CD127$^+$ RORγt$^-$ KLRG-1$^+$) and ILC3s (CD45$^+$ Lin$^-$ CD127$^+$ RORγt$^+$) in mice, which were used as different ILC signature genes in this study. Clusters 0, 1, 2, 7 and 9 were characterized as NKp46$^+$ ILC3s due to high expression of *Ncr1* (encoding NKp46) and *Tbx21* (encoding T-bet). Cluster 2 also expressed ILC1-related signature genes, such as *Ccl5* and *Xcl1*, and may represent ILC1-like ILC3s. Clusters 4, 5 and 6 had the highest *Ccr6* expression, thus representing CCR6$^+$ ILC3s (Figures 4A, S3A). Consistently, cluster 5 also had the highest expression of *Ltb* (encoding lymphotoxin beta), a gene involved in lymphoid tissue development. Cluster 4 had high H2-Aa expression, indicating a MHCII-dependent antigen presentation potential. Cluster 6 expressed high levels of *Il17a, Il17f*

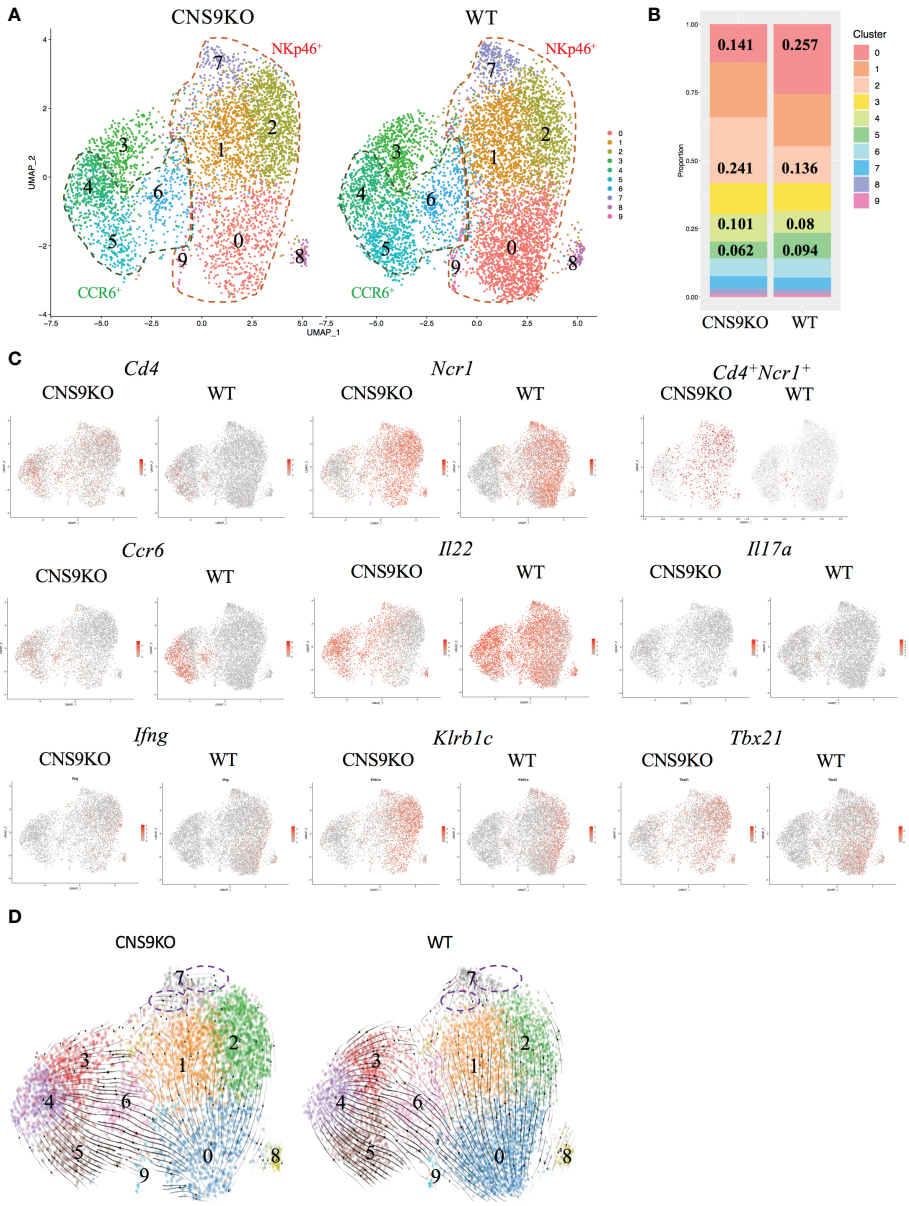

FIGURE 4
Single cell RNA-seq analysis of ILC3s isolated from CNS9-deficient mice and WT mice. The ILC3s ($CD3^-CD90.2^{high}CD45^{mid}$) were sorted from small intestine LPLs of WT and CNS9-deficient mice, and single-cell RNA libraries were constructed using 10x Genomics. **(A)** UMAP plots of CNS9-deficient and WT ILC3s. **(B)** Statistic quantification of individual clusters between WT and CNS9-deficient ILC3s. **(C)** Selected gene expression of UMAP plots. **(D)** RNA velocity analysis among clusters. Purple dotted circle indicating RNA velocity direction from Cluster 7 to other clusters. Also see Figure S3.

and *Il22*, representing mature or effector ILC3s. Cluster 3 expressed neither CCR6 nor NKp46 and was characterized as IL-22 producing $CCR6^-NKp46^-$ ILC3s. Clusters 0 and 5 expressed high amount of *Zfp36*, a negative regulator for TNF-α and GM-CSF (17). Cluster 7 highly expressed *Tnfrsf9* (encoding CD137 or 4-1BB). Cluster 8 highly expressed *Ifit1*, a gene involved in induction of type I interferons. Cluster 9 was identified as actively proliferating ILC3s due to high expression of *Mki67* and *Stmn1* (Figure S3A).

In the UMAP plots analysis, CNS9-deficient ILC3s contained clearly more single *Cd4* or *Ncr1* expressing and co-expressing cell populations, with reduced *Ccr6*-expressing population (Figure 4C). For effector cytokines secreted by ILC3s, CNS9 deficiency resulted in decreased *Il22* and *Il17a* but increased *Ifng* transcription, consistent with the results obtained by flow cytometry in CNS9-deficient mice (Figures 4C, 2A). In addition, CNS9-deficient ILC3s contained cells with increased expression of *Klrb1c* (encoding NK1.1), *Tbx21* (encoding T-bet), *Ccl5* and *Xcl1*, at both population and per cell levels (Figures 4C, S3B), indicating CNS9-deficient ILC3s acquired an ILC1-gene expression feature, when compared with WT ILC3s. Gene set variation analysis (GSVA) further confirmed our hypothesis that CNS9 deficiency increased expression of ILC1 signature genes but decreased expression of ILC3 signature genes (15) (Figure S3C).

We further analyzed the relationships of cell clusters by RNA velocity. Increased frequency of cluster 2 and decreased frequency of cluster 0 (Figure 4B), along with the velocity direction from cluster 0 to cluster 1 and cluster 2 (Figure 4D), indicated a strong conversion potential from cluster 0 to cluster 2 in CNS9-deficient NKp46$^+$ ILC3s. Similarly, decreased cluster 5 and increased cluster 4 represented a more flexible change from cluster 5 to cluster 4 in CCR6$^+$ ILC3 subset after CNS9 deficiency (Figures 4B, D). Moreover, cluster 7, ending with all velocity arrows, represented as a fully differentiated cluster in WT ILC3s, but still had a transition potential towards other clusters in CNS9-deficient ILC3s (Figure 4D). Taken together, these results suggest that genetic ablation of CNS9 in ILC3s increased their plasticity and conversion potentials towards ILC1-like cells.

Decreased cellular RORγt expression causes induction of CD4$^+$NKp46$^+$ ILC3 subset

Our scRNA-seq data showed that *Rorc* transcription was decreased in CNS9-deficient ILC3s compared with WT ILC3s, also with a trend following velocity directions (cluster 0 -> cluster 1&2 and cluster 5 -> cluster 4) (Figure S4A), suggesting an internal link between *Rorc* expression levels with cluster variability. CNS9-deficient ILC3s showed increased *Cd4* transcription (Figure S4B). Of note, cluster 4 had lower *Rorc* but higher *Cd4* expression, compared with cluster 5, in both WT and CNS9-deficient ILC3s (Figures S4A, B), suggesting a potential negative regulation of *Cd4* by RORγt in ILC3s. Consistently, CNS9-deficient ILC3s had reduced RORγt protein expression at per cell levels, as examined by flow cytometry, compared with WT ILC3s (Figure 5A). Specifically, the subset of CD4$^+$NKp46$^+$ cells in CNS9-deficient ILC3s showed the lowest RORγt expression (Figure S4C), indicating CNS9-directed RORγt expression plays a critical role in restricting induction of CD4$^+$NKp46$^+$ ILC3s, likely in a dosage-dependent manner.

To test the above possibility, we examined ILC3s in the heterozygous RORγt^{GFP} mice, in which the *Gfp* gene was inserted into the first exon of *Rorc* and thus disrupted ~50% of RORγt expression at per cell levels (Figure 5B). Similar to CNS9-deficient mice, RORγt^{GFP} mice contained a distinct CD4$^+$NKp46$^+$ ILC3 subset (Figure 5C), and showed increased NKp46 and IFN-γ expression in total ILC3s, but a reciprocal decrease of CCR6, IL-22 and IL-17A, though CD4 expression was normal, compared with control WT mice (Figures 5C, D).

To further confirm the dosage effect of RORγt protein, *Rorc* was retrovirally overexpressed in CNS9-deficient bone marrow cells (CD45.2$^+$) *in vitro*, then transferred into irradiated CD45.1$^+$ mice. 7 weeks after reconstitution, the mice were sacrificed and analyzed. Overall, *Rorc* overexpression reduced ~70% of CD4$^+$NKp46$^+$ ILC3s compared with control empty vector (Figure 6A), suggesting that decreased RORγt expression indeed contributes to the generation of CD4$^+$NKp46$^+$ ILC3s in CNS9-deficient mice. For unknown reasons, control retro-virus infection also promoted overall cellular RORγt expression (Figure 6B) and decreased the frequency of CD4$^+$NKp46$^+$ ILC3s compared with mice under steady state.

It has been reported previously that T-bet is critical for generation of NKp46$^+$ ILC3s *via* inducing IFN-γ and NKp46 expression (8–10). We further confirmed our scRNA-seq data with flow cytometry, and found that CNS9-deficient ILC3s, including ILC3 subsets, had increased T-bet protein expression compared with WT cells (Figure S5). Thus, this result suggests the decreased RORγt expression directly promoted T-bet expression, and further resulted in upregulation of IFN-γ and NKp46.

CNS9-deficient ILC3s showed gain of ILC1-like gene expression feature (Figures 4C and S3B, C), increased T-bet (Figure S5) and IFN-γ expression (Figure 2A), suggesting that RORγt may regulate the balance between ILC3s and ILC1s, *via* its dosage expression. However, the percentages and cell numbers of ILC1s were only slightly increased, whereas the ratio of ILC3s to ILC1s was not significantly altered in CNS9-deficient mice, compared with WT control mice (Figure S6). These suggest that CNS9-directed *Rorc* transcription is not involved in transition between ILC3s and ILC1s, and CD4$^+$NKp46$^+$ ILC3s represent a transient state fixed by reduced but not abolished RORγt expression in CNS9-deficient mice.

Discussion

Cis-regulatory mechanisms have been extensively investigated in different T helper cell subsets, such as Th1, Th2 and Th17 cells, but remain largely unclear in their corresponding counterparts of innate immune cells. In previous studies, we showed that CNS9 deficiency abolished RORγt expression and Th17 cell differentiation *in vitro* and *in vivo*. However, this study reveals that CNS9 deficiency did not affect the generation of RORγt$^+$ ILC3s at both frequencies and numbers, but decreased RORγt expression at per cell level, which not only caused acquiring ILC1-like gene expression feature in ILC3 cells but also led to generation of a specific CD4$^+$NKp46$^+$ ILC3 subset. These findings thus characterize CNS9 as an essential regulator controlling the development, stability or plasticity of ILC3s, through fine tuning dose expression of RORγt.

As the master transcription factor of ILC3s, RORγt inhibits ILC1/2-related gene expression. The trans-differentiation from ILC3s to ILC1s, requires down-regulation of RORγt and up-regulation of T-bet expression (18). Previous reports showed that T-bet directly instructed IFN-γ and NKp46 expression (8–10). Therefore, the increased T-bet expression, as a result of decreased RORγt expression, could contribute to the induction of CD4$^+$NKp46$^+$ ILC3s in CNS9-deficient mice. Consistently, decreased RORγt expression in CNS9-deficient ILC3s resulted in decreased IL-22 and IL-17A secretion and increased IFN-γ production (Figures 2, 5A). Moreover CD4$^+$NKp46$^+$ ILC3s are likely induced by decreased dose of RORγt expression, as evidenced in both CNS9-deficient and RORγt^{GFP} mice (Figures 5A–C). This speculation was further confirmed by the findings that the development of CD4$^+$NKp46$^+$ ILC3s can be largely prevented by RORγt-overexpression in the bone marrow stage

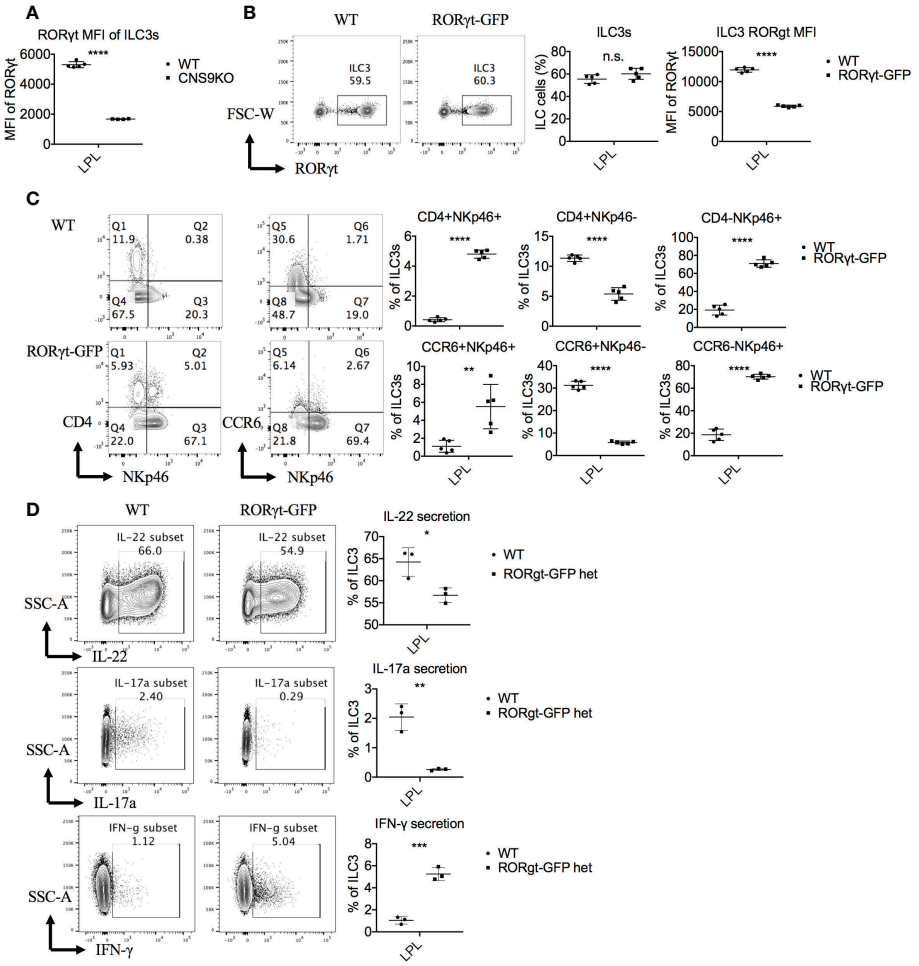

FIGURE 5
RORγt expression levels regulate the generation of the CD4$^+$NKp46$^+$ ILC3 subset. ILC3s were isolated from small intestine LPLs of age- and sex-matched WT and CNS9-deficient mice **(A)** or RORγt^{GFP} mice **(B–D)** under steady state. Stimulated *ex vivo* for 4 hours before staining with surface markers, RORγt and cytokines, and then analyzed by flow cytometry. **(A)** MFI of RORγt in WT and CNS9-deficient ILC3s. **(B)** Left: intracellular staining of RORγt (pre-gated on Live CD45$^+$ CD3$^-$ CD90$^+$); right: statistic of the staining data and MFI of RORγt. **(C)** Left: surface staining of CD4, NKp46 and CCR6 of ILC3s; right: statistic of the staining data. **(D)** Left: intracellular staining of IL-22, IL-17A and IFN-γ after stimulation (pre-gated on ILC3s: Live CD45$^+$ CD3$^-$ CD90$^+$ RORγt$^+$); right: statistic of the staining data. The data shown are a representative of three independent experiments and presented as mean ± SD. Also see Figures S4 and S5. Statistical significance was calculated using unpaired Student's t test and shown as *p < 0.05; **p < 0.01; ***p < 0.001, ****p < 0.0001 or n.s. (non-significant) p > 0.05.

(Figure 6). Previously, a small population of CD4$^+$NKR$^-$LTi cells was reported in adult RORγt^{fm} mice (*Rorc*-Cre^{Tg} heterozygous) (7), and also increased population of NKp46$^+$ILC3s observed in RORγt^{GFP} mice compared with WT mice (19), which supports our hypothesis that CNS9 regulates ILC3 subsets development or plasticity through modulating RORγt expression levels.

However, in the mixed bone-marrow reconstituted mice, CNS9 deficiency led to about 75% less frequency of CD4$^+$NKp46$^+$ ILC3s compared with mice under steady state (Figures 3B, 1B), despite this population was also clearly detected. The difference could be caused by different ages of mice analyzed or altered healthy status in the BM-chimeric mice in the course of experiments. Of note, CNS9-deficient mice had less RORγt expression than RORγt^{GFP} mice, but contained noticeably more abundant CD4$^+$NKp46$^+$ ILC3s (Figures 5A–C, 1B), further confirmed a dosage-sensitive role of RORγt in control of the development of ILC3s.

Interestingly, we noticed an inverse correlation between *Cd4* and RORγt expression levels in CNS9-deficient ILC3s (Figures S4A, B). Considering upregulation of CD4$^+$ ILC3s was not found in CNS9-deficent BM-chimeric mice (Figure 3B), neither in RORγt^{GFP} mice (Figure 5C), suggesting additional mechanism(s) is involved in regulating *Cd4* expression in CNS9-deficient ILC3s, possibly independent on relative dosages of RORγt expression.

In Th17 cells, deletion of CNS9 completely abolishes IL-6 induced RORγt expression and RORγt-directed Th17 cell differentiation, and is thus identified as the dominant *cis*-element in the *Rorc* locus in response to IL-6-STAT3 signaling, with a particularly important role in activating the chromatin structures across the *Rorc* gene locus (12). In contrast to Th17 cells, it has been reported that STAT3 deficiency does not affect RORγt expression in the development of ILC3s (20). Accordingly, CNS9-deficienct mice had normal number and frequency of RORγt$^+$ ILC3s compared with WT mice (Figure 1A). However, CNS9 deficiency reduced the

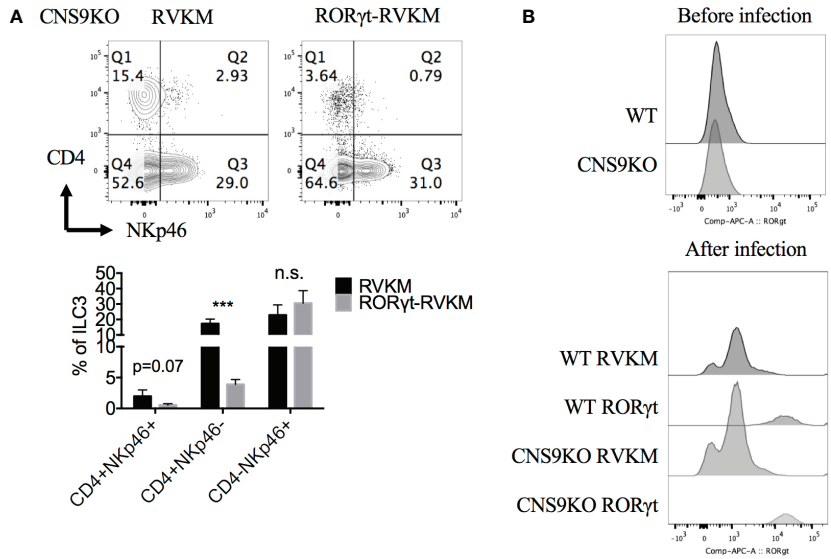

FIGURE 6
Reduced RORγt expression after CNS9 deficiency are the cause of altered ILC3 subsets. RV-GFP control or RORγt-expressing plasmids were transduced into CNS9-deficient BM cells by retro-virus infection. The infected GFP$^+$ cells were sorted and transferred into irradiated CD45.1$^+$ mice introveneously. ILC3s from small intestine LPLs were gated as Live CD45$^+$ CD3$^-$ CD90$^+$ RORγt$^+$ cells. **(A)** Up: surface staining of CD4, NKp46 in ILC3s; down: statistic of the staining data (n=4 for RVKM group and n=3 for RORγt -RVKM group). **(B)** RORγt protein staining in WT or CNS9-deficient BM cells before (up) and after (down) retro-virus infection (after retro-virus infection, BM cells were pre-gated on live GFP$^+$ cells). The flow data shown are a representative of two independent experiments and the statistical analysis was performed by combining two experiments and presented as mean ± SD. Also see Figure S6. Statistical significance was calculated using unpaired Student's t test and shown as ***p < 0.001 or n.s. (non-significant) p > 0.05.

amounts of RORγt protein in individual ILC3 cells (Figure 5A) and altered their composition, inducing a population of CD4$^+$NKp46$^+$ ILC3s that is not present in normal health mice (Figure 1B). These findings thus highlight a distinct role of the same *cis*-acting element between adaptive and innate immune cells.

In this study, defective IL-22 production was observed in mature CNS9-deficient ILC3s stimulated with IL-23 only, but not in the presence of IL-12 and IL-15 (Figures 2A, S2A). It is known that IL-12 and IL-23 share a common subunit p40, and a common receptor subunit IL-12Rβ1, so the difference is possibly caused by competition or compensation between IL-23 and IL-12 signaling in ILC3s. Interestingly, our scRNA-seq data showed that the mRNA levels of *Il12rb2* (encoding the unique receptor for IL-12) were ~10 times higher in CNS9-deficient than in WT ILC3s (data not shown). Considering the concentration of IL-12 (25 ng/ml) used was 5 fold of IL-23 (5 ng/ml) in *ex vivo* culture, increased IL-12 signaling strength was expected in CNS9-deficient ILC3s, compared to WT ILC3s, which may confer different phenotypes under different stimulation conditions. Since CNS9 functions in a context-dependent manner, whether it regulates fetal or early stage ILC3 development needs further investigation.

In summary, this study, for the first time, investigated the *cis*-regulatory mechanism in ILC3s *via* a genetic approach. Further discovered a distinct essential role of *cis*-element CNS9 in controlling the development or plasticity of ILC3s, through modulating dosing expression of its master transcription factor RORγt. These findings could be useful for understanding the physiological relevance in response to dynamically changing gut-associated microenvironments.

Data availability statement

The data presented in the study are deposited in the GEO DataSets, accession number is GSE225928.

Ethics statement

The animal study was reviewed and approved by Ethics Statement All the animal experiments were performed with the use of protocols approved by the Institutional Animal Care and Use Committee of Tsinghua University.

Author contributions

DC and CD designed the project. DC and HZ performed the experiments and analyzed the data. JG analyzed the bioinformatics data of scRNA-seq. QX helped with the experiments especially overexpress genes in BM cells. XG constructed single cell library. DC, H Z, XW, and CD prepared the manuscript. All authors contributed to the article and approved the submitted version.

Funding

This work was supported by grants from National Natural Science Foundation of China (31630022, 31821003 and 31991170 to C. Dong, 32070889 to X. Wang), Beijing Natural Science Foundation (5222011

to X. Wang) and Shanghai Science and Technology Commission (21JC1404200 to C. Dong.).

Acknowledgments

We thank the Immunology Core Facility for FACS support, the animal facility at Tsinghua University for mouse support, and all Dong lab members for help.

Conflict of interest

C. Dong is a FViL Investigator.

The authors declare that the research was conducted in the absence of any commercial or financial relationships that could be construed as a potential conflict of interest.

Publisher's note

Supplementary material

The Supplementary Material for this article can be found online at: https://www.frontiersin.org/articles/10.3389/fimmu.2023.1105145/full#supplementary-material

References

1. Satoh-Takayama N, Vosshenrich CAJ, Lesjean-Pottier S, Sawa S, Lochner M, Rattis F, et al. Microbial flora drives interleukin 22 production in intestinal NKp46+ cells that provide innate mucosal immune defense. *Immunity* (2008) 29(6):958–70. doi: 10.1016/j.immuni.2008.11.001

2. Buonocore S, Ahern PP, Uhlig HH, Ivanov II, Littman DR, Maloy KJ, et al. Innate lymphoid cells drive interleukin-23-dependent innate intestinal pathology. *Nature* (2010) 464(7293):1371–5. doi: 10.1038/nature08949

3. Sonnenberg GF, Artis D. Innate lymphoid cells in the initiation, regulation and resolution of inflammation. *Nat Med* (2015) 21(7):698–708. doi: 10.1038/nm.3892

4. Eberl G, Marmon S, Sunshine MJ, Rennert PD, Choi Y, Littmann DR. An essential function for the nuclear receptor RORγt in the generation of fetal lymphoid tissue inducer cells. *Nat Immunol* (2004) 5(1):64–73. doi: 10.1038/ni1022

5. Bruchard M, Geindreau M, Perrichet A, Truntzer C, Ballot E, Boidot R, et al. Recruitment and activation of type 3 innate lymphoid cells promote antitumor immune responses. *Nat Immunol* (2022) 23(2):262–74. doi: 10.1038/s41590-021-01120-y

6. Song C, Lee JS, Gilfillan S, Robinette ML, Newberry RD, Stappenbeck TS, et al. Unique and redundant functions of NKp46+ ILC3s in models of intestinal inflammation. *J Exp Med* (2015) 212(11):1869–82. doi: 10.1084/jem.20151403

7. Vonarbourg C, Mortha A, Bui VL, Hernandez PP, Kiss EA, Hoyler T, et al. Regulated expression of nuclear receptor RORγt confers distinct functional fates to NK cell receptor-expressing RORγt+ innate lymphocytes. *Immunity* (2010) 33(5):736–51. doi: 10.1016/j.immuni.2010.10.017

8. Sciumè G, Hirahara K, Takahashi H, Laurence A, Villarino AA, Singleton KL, et al. Distinct requirements for t-bet in gut innate lymphoid cells. *J Exp Med* (2012) 209 (13):2331–8. doi: 10.1084/jem.20122097

9. Klose CSN, Kiss EA, Schwierzeck V, Ebert K, Hoyler T, D'Hargues Y, et al. A t-bet gradient controls the fate and function of CCR6-RORγt + innate lymphoid cells. *Nature* (2013) 494(7436):261–5. doi: 10.1038/nature11813

10. Rankin L, Groom JR, Chopin M, Herold M, Walker JA, Mielke LA, et al. T-bet is essential for NKp46+ innate lymphocyte development through the notch pathway. *Nat Immunol* (2013) 14(4):389–95. doi: 10.1038/ni.2545

11. Krzywinska E, Sobecki M, Nagarajan S, Zacharjasz J, Tambuwala MM, Pelletier A, et al. The transcription factor HIF-1α mediates plasticity of NKp46+ innate lymphoid cells in the gut. *J Exp Med* (2022) 219(2):1–23. doi: 10.1084/jem.20210909

12. Chang D, Xing Q, Su Y, Zhao X, Xu W, Wang X, et al. The conserved non-coding sequences CNS6 and CNS9 control cytokine-induced rorc transcription during t helper 17 cell differentiation. *Immunity* (2020) 53(3):614–26. doi: 10.1016/j.immuni.2020.07.012

13. Yoshida H, Lareau CA, Ramirez RN, Buenrostro JD, Benoist C, Yoshida H, et al. The cis -regulatory atlas of the mouse immune resource. *Cell* (2019) 176(4):897–912. doi: 10.1016/j.cell.2018.12.036

14. Goncharov NV, Nadeev AD, Jenkins RO, Avdonin PV. Markers and biomarkers of endothelium: When something is rotten in the state. *Oxid Med Cell Longevity* (2017). doi: 10.1155/2017/9759735

15. Gury-BenAri M, Thaiss CA, Serafini N, Winter DR, Giladi A, Lara-Astiaso D, et al. The spectrum and regulatory landscape of intestinal innate lymphoid cells are shaped by the microbiome. *Cell* (2016) 5(166):1231–46. doi: 10.1016/j.cell.2016.07.043

16. Ganal-Vonarburg SC, Duerr CU. The interaction of intestinal microbiota and innate lymphoid cells in health and disease throughout life. *Immunology* (2020) 159 (1):39–51. doi: 10.1111/imm.13138

17. Brooks SA, Blackshear PJ. Tristetraprolin (TTP): Interactions with mRNA and proteins, and current thoughts on mechanisms of action. *Biochim Biophys Acta - Gene Regul Mech* (2013) 1829(0):666–79. doi: 10.1016/j.bbagrm.2013.02.003

18. Bal SM, Golebski K, Spits H. Plasticity of innate lymphoid cell subsets. *Nat Rev Immunol* (2020) 20(9):552–65. doi: 10.1038/s41577-020-0282-9

19. Zhong C, Cui K, Wilhelm C, Hu G, Mao K, Belkaid Y, et al. Group 3 innate lymphoid cells continuously require the transcription factor GATA-3 after commitment. *Nat Immunol* (2016) 17(2):169–78. doi: 10.1038/ni.3318

20. Guo X, Qiu J, Tu T, Yang X, Deng L, Anders RA, et al. Induction of innate lymphoid cell-derived interleukin-22 by the transcription factor STAT3 mediates protection against intestinal infection. *Immunity* (2014) 40(1):25–39. doi: 10.1016/j.immuni.2013.10.021

frontiers | Frontiers in Immunology

TYPE Original Research
PUBLISHED 11 April 2023
DOI 10.3389/fimmu.2023.1113735

OPEN ACCESS

EDITED BY
Carolina Jancic,
National Scientific and Technical Research Council (CONICET), Argentina

REVIEWED BY
Adam Savage,
Allen Institute for Immunology, United States
Itziar Martinez Gonzalez,
Karolinska Institutet (KI), Sweden

*CORRESPONDENCE
Graham M. Lord
graham.lord@manchester.ac.uk

†PRESENT ADDRESS
Joana F. Neves,
Centre for Host-Microbiome Interactions, King's College London, London, United Kingdom

SPECIALTY SECTION
This article was submitted to NK and Innate Lymphoid Cell Biology, a section of the journal Frontiers in Immunology

RECEIVED 01 December 2022
ACCEPTED 28 February 2023
PUBLISHED 11 April 2023

CITATION
Schroeder J-H, Beattie G, Lo JW, Zabinski T, Powell N, Neves JF, Jenner RG and Lord GM (2023) CD90 is not constitutively expressed in functional innate lymphoid cells.
Front. Immunol. 14:1113735.
doi: 10.3389/fimmu.2023.1113735

CD90 is not constitutively expressed in functional innate lymphoid cells

Jan-Hendrik Schroeder[1], Gordon Beattie[2,3], Jonathan W. Lo[1,4], Tomasz Zabinski[1], Nick Powell[4], Joana F. Neves[1†], Richard G. Jenner[5] and Graham M. Lord[1,6*]

[1]School of Immunology and Microbial Sciences, King's College London, London, United Kingdom, [2]Cancer Research UK (CRUK) City of London Centre Single Cell Genomics Facility, University College London Cancer Institute, University College London (UCL), London, United Kingdom, [3]Genomics Translational Technology Platform, University College London (UCL) Cancer Institute, University College London, London, United Kingdom, [4]Division of Digestive Diseases, Faculty of Medicine, Imperial College London, London, United Kingdom, [5]University College London (UCL) Cancer Institute, University College London, London, United Kingdom, [6]School of Biological Sciences, Faculty of Biology, Medicine and Health, Division of Infection, Immunity and Respiratory Medicine, University of Manchester, Manchester, United Kingdom

Huge progress has been made in understanding the biology of innate lymphoid cells (ILC) by adopting several well-known concepts in T cell biology. As such, flow cytometry gating strategies and markers, such as CD90, have been applied to indentify ILC. Here, we report that most non-NK intestinal ILC have a high expression of CD90 as expected, but surprisingly a sub-population of cells exhibit low or even no expression of this marker. CD90-negative and CD90-low CD127$^+$ ILC were present amongst all ILC subsets in the gut. The frequency of CD90-negative and CD90-low CD127$^+$ ILC was dependent on stimulatory cues *in vitro* and enhanced by dysbiosis *in vivo*. CD90-negative and CD90-low CD127$^+$ ILC were a potential source of IL-13, IFNγ and IL-17A at steady state and upon dysbiosis- and dextran sulphate sodium-elicited colitis. Hence, this study reveals that, contrary to expectations, CD90 is not constitutively expressed by functional ILC in the gut.

KEYWORDS

innate lymphoid cell (ILC), CD90, intestine, DSS-colitis, fecal microbial transplant (FMT)

Introduction

Resident leukocytes play an important role in maintaining mucosal surfaces at steady state and early during an infection (1, 2). Since the discovery of innate lymphoid cells (ILC) about a decade ago, it has become increasingly apparent that these cells play a significant role in mucosal homeostasis. However, the role for ILC is far from being fully characterized, and much of the current knowledge has been gained from testing concepts that had previously been established for T and NK cell biology. As such, group 1, 2 and 3 ILC (ILC1, ILC2 and ILC3) express T-bet, GATA3 and RORγt, respectively, as characteristic

transcription factors as well as cytokines associated with Th1, Th2 and Th17 cells (1, 3). Due to the absence of T cell receptor (TCR) expression in ILC, these cells elicit immune functions in response to cytokines, chemokines and neurotransmitters, as has been well described for NK cells (1, 2).

Similarly to T and NK cells, ILC express the glycophosphatidylinositol (GPI) anchored protein CD90 in diverse tissues, and CD90 has often been used as a key marker to identify ILC (4–24) or as key target to deplete ILC in Rag-deficient mice using a specific antibody (e.g. 25–32). Despite the presence of CD90 on T and NK cells, very little is known regarding its functionality (5). In NK cells, CD90 downregulation was associated with successful differentiation, but its presence has also been linked to an activation phenotype (33–35). IL-17A-producing inflammatory ILC2 in lungs and small intestinal lamina propria (SI LP) have been observed to have lower expression of CD90 in comparison to natural ILC2, but the implications of this are not known (36–38). In relation to this, transition of $CD90^{low}$ to $CD90^{high}$ ILC2 precursors has been described using an *in vitro* model in which CLP were seeded, but again the role of the gain in CD90 is unknown (39). Furthermore, IL-10 expressing intestinal ILC2 have a characteristic lack of CD90 expression (40). ILC3 from the intestinal lamina propria of naïve mice were reported to have a characteristic $CD90^{high}$ $CD45^{low}$ phenotype, however, ILC3 were also found among $CD90^{low}$ $CD45^{high}$ ILC from the small intestine (41). Recently, it was reported that in the murine liver $Ly49E^{+}$ ILC1 have a lower expression of CD90 than $Ly49E^{-}$ ILC1 (42, 43).

Here, we report for the first time that cytokine-producing intestinal lamina propria ILC exhibit varied expression of CD90, and strikingly some ILC show no expression of this marker. These $CD90^{-}$ and $CD90^{low}$ ILC are a significant source of IFNγ, IL-13 and IL-17A upon dysbiosis and dextran sulphate sodium (DSS)-elicited colitis. However, in naïve mice, $CD90^{-}$ ILC have a dominant type 2 cytokine expression profile. Furthermore, stimulation with IL-25/IL-33 promotes the frequency of $CD90^{-/low}$ ILC2 *in vitro*. Conversely, IL-12/IL-18 stimulation results in a lower prevalence of $CD90^{-/low}$ $NKp46^{+}$ ILC. These data suggest that CD90 expression in intestinal ILC is regulated by cytokines and has a limited suitability as a constitutive marker of the ILC lineage.

Results

CD90-negative colonic lamina propria $CD127^{+}$ ILC produce cytokines upon induced colitis

CD90 expression in ILC was tested in a mouse model of DSS-induced colitis. BALB/c *Rag2*$^{-/-}$ mice were treated with 5% DSS in the drinking water for 5 days after which the animals showed clinical signs of colitis like weight loss (44), and the cytokine expression profile of colonic lamina propria (cLP) ILC was analyzed at day 10. Analyses of $CD45^{+}$ Lin^{-} (CD3, CD5, B220, CD19, CD11b, TER-119, Gr-1, FcεRI) $CD127^{+}$ cLP ILC re-stimulated with PMA and ionomycin (PMA Iono) *in vitro* revealed that in addition to $CD90^{high}$ ILC there were $CD90^{-}$ and $CD90^{low}$ ILC populations (Figure 1A; Supplementary Figures 1A, B).

The abundance of $CD90^{high}$ ILC was greater than that of $CD90^{-}$ and $CD90^{low}$ ILC, but these populations represented ~30% and 20%, respectively, of the total $CD127^{+}$ ILC population. In order to determine whether $CD90^{-}$ and $CD90^{low}$ ILC were associated with a T-bet-expressing ILC subset, we analyzed $CD90^{-}$ and $CD90^{low}$ ILC in *Tbx21*$^{-/-}$ x *Rag2*$^{-/-}$ non-ulcerative colitis (TRnUC) mice. This revealed that the presence of these cells was not dependent on T-bet, and their frequency was not affected. $CD90^{-}$ and $CD90^{low}$ ILC were a relevant source of IFNγ, IL-13 and IL-17A, but still significantly less potent than $CD90^{high}$ ILC in these DSS-treated *Rag2*-deficient mice (Figures 1C, D). DSS-treated TRnUC mice did not have altered frequencies of $CD90^{-}$ and $CD90^{low}$ ILC or IL-13 production in these cells in comparison to DSS-treated *Rag2*$^{-/-}$ mice (Figures 1B–D). However, TRnUC mice had a greater frequency of IL-17A expressing $CD90^{-}$ and $CD90^{high}$ ILC than *Rag2*$^{-/-}$ mice. This could be explained by the far greater cellularity of ILC3 in *Rag2*$^{-/-}$ mice driven by the deficiency of *Tbx21* (45).

ILC2 expressing RORγt were reported to have no or lower expression of CD90 in comparison to RORγt-negative natural ILC2 (36, 37). We detected $CD90^{-}$ and $CD90^{+}$ ILC co-expressing IL-13 and IL-17A (Figures 1E, F). We also detected more $CD90^{+}$ than $CD90^{-}$ inflammatory $IL\text{-}13^{+}$ $IL\text{-}17A^{+}$ ILC2 (Figures 1E, F), supporting the notion that inflammatory ILC2 have a $CD90^{-}$ and $CD90^{+}$ phenotype. We also noted that $CD90^{-}$ ILC can express IL-17A independently of IL-13 (Figure 1F). Interestingly, T-bet-deficiency appears to promote the frequency of $CD90^{-}$ $IL\text{-}17^{+}$ among $IL\text{-}13^{+}$ ILC2 in these *Rag2*$^{-/-}$ mice.

Functional $CD90^{-}$ and $CD90^{low}$ ILC were also observed in DSS-treated wild-type BALB/c mice (Supplementary Figures 2A, B). In these DSS-treated mice, $CD90^{high}$ ILC were a vastly more significant source of IFNγ, IL-13 and IL-17A in comparison to $CD90^{-}$ and $CD90^{low}$ ILC (Supplementary Figures 2C, D). As observed in Rag2-deficient mice, $CD90^{-}$ and $CD90^{low}$ ILC were able to produce IL-17A and IL-13, but the proportion of $CD90^{-}$ and $CD90^{low}$ ILC producing these cytokines was increased in DSS-treated BALB/c-background *Tbx21*$^{-/-}$ mice (Supplementary Figures 2C, D). These *Tbx21*$^{-/-}$ mice also had an enhanced frequency of $IL\text{-}17A^{+}$ $CD90^{high}$ ILC (Supplementary Figures 2C, D). $CD90^{-}$ and $CD90^{low}$ ILC were also detected in DSS-treated WT C57BL/6 mice (Supplementary Figures 3A, B). As observed in the other mouse strains, $CD90^{-}$ and $CD90^{low}$ ILC produced IFNγ, IL-13 and IL-17A, although $CD90^{high}$ ILC appeared to be a greater source of these cytokines (Supplementary Figures 3C, D). In contrast to BALB/c background mice, C57BL/6 background *Tbx21*$^{-/-}$ mice did not have a greater prevalence of IL-17A- and IL-13-producing $CD90^{-}$, $CD90^{low}$ or $CD90^{high}$ ILC than WT mice, however, the frequency of $CD90^{low}$ ILC was reduced significantly (Supplementary Figures 3A–D).

Furthermore, we did not detect any IFNγ producing $IL\text{-}13^{+}$ ILC in contrast to IL-17A production among $CD90^{+}$ and $CD90^{-}$ $IL\text{-}13^{+}$ ILC2 in DSS-treated BALB/c *Rag2*$^{-/-}$ mice and C57BL/6 WT mice (Figures 1E, F; Supplementary Figure 3E). These data indicate that low expression of CD90 is not a simple marker of inflammatory ILC2 in these mice.

CD90-negative $CD127^{+}$ ILC have a predominant type 2 phenotype at steady state

Similar to DSS-treated mice (Figure 1; Supplementary Figures 2, 3), most ILC were $CD90^{high}$ in naïve untreated C57BL6 mice.

10.3389/fimmu.2023.1113735

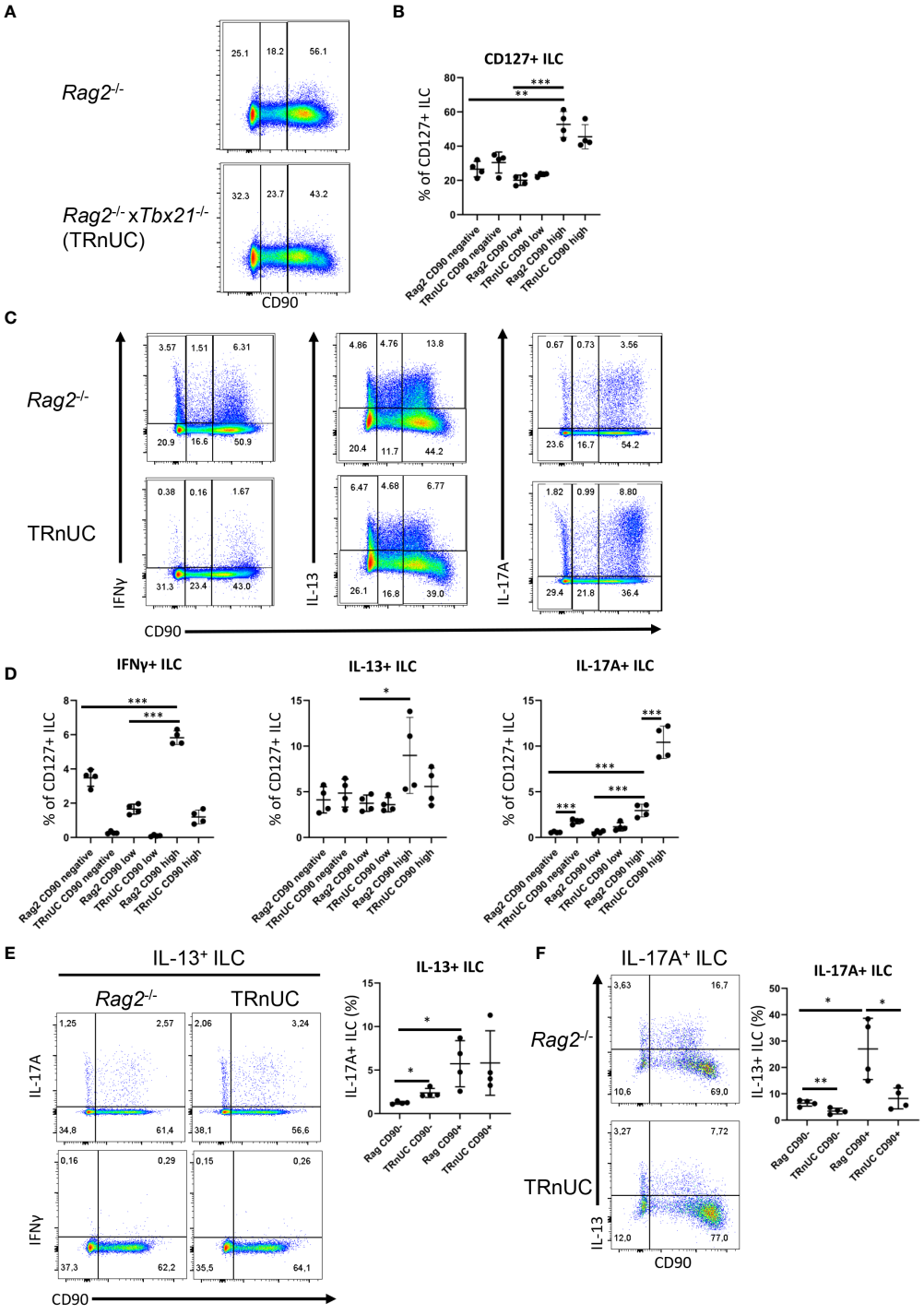

FIGURE 1
CD90-negative Rag2-deficient ILC are a substantial source of IFNγ and IL-13 during DSS colitis. cLP ILC from 5% DSS-treated *Rag2*$^{-/-}$ and TRnUC mice were isolated and stimulated with PMA and ionomycin (3 hours) prior to flow cytometry analysis. **(A)** Frequencies of CD90^{hi}, CD90^{low} and CD90^{-} in total CD127^{+} ILC and **(B)** statistical analyses are shown. **(C)** IFNγ, IL-13 and IL-17A expression in CD90^{hi}, CD90^{low} and CD90^{-} total CD127^{+} ILC and **(D)** corresponding statistical analyses are outlined. **(E)** CD90 co-expression with IL-17A or IFNγ in IL-13^{+} ILC and corresponding statistical analyses are shown. **(F)** Flow cytometry and statistical analysis of CD90 and IL-13 expression in IL-17A^{+} ILC are presented. Data shown are representative of 4 biological replicates. *p < 0.05; **p< 0.01; ***p<0.001.

However, CD90^{-} and CD90^{low} ILC populations were also detected in these mice (Supplementary Figures 4A, B). Interestingly, both CD90^{-} and CD90^{low} ILC produced predominately IL-13 and IL-5 and fewer of these cells produced IFNγ and IL-17A (Supplementary Figures 4B–G). Although moderately low, CD90^{-} and CD90^{low} ILC had a significantly greater frequency of IFNγ positivity than CD90^{high} ILC (Supplementary Figure 4C). A similar trend was not observed for IL-17A (Supplementary Figure 4D). IFNγ and IL-

17A production was also driven mostly by distinct populations of cells (Supplementary Figure 4B). Further analyses revealed that the prevalence of IL-13$^+$ and IL-5$^+$ ILC was greater among CD90^{high} and CD90^{low} ILC in comparison to CD90$^-$ ILC (Supplementary Figures 4B–G, 5A). *Tbx21*$^{-/-}$ CD90$^-$, CD90^{low} and CD90^{high} ILC exhibit greater expression of IL-5 than ILC in WT mice (Supplementary Figures 4B–G), which could be explained by one of our previous reports indicating increased cLP ILC2 abundance in *Tbx21*$^{-/-}$ mice (46). Since CD90$^-$ and CD90^{low} ILC appeared to be predominately functional ILC2, we sought to determine whether these cells were able to adopt functional characteristics of ILC1 and ILC3. Plasticity of ILC2 allowing expression of T-bet and RORγt is a well-known phenomenon (1). Similar to the observations in DSS-treated WT C57BL/6 and *Rag2*-deficient mice, we detected minimal co-expression of IL-13 and IL-17A in CD90$^-$ and CD90^{low} cLP ILC from naïve WT and *Tbx21*$^{-/-}$ mice indicating the presence of a minor inflammatory ILC2 population (Supplementary Figure 5A). However, we could also find IL-13 and IL-17A co-expressing CD90^{high} ILC. In contrast, virtually no IL-13 and IFNγ co-expressing CD90$^-$ and CD90^{low} ILC were detected in these mice (Supplementary Figure 5B).

CD90 expression in CD127$^+$ ILC is controlled by stimulatory cues

Overall, we detected CD90$^-$ and CD90^{low} ILC in both untreated and DSS-treated mice. This suggests that CD90 is not a reliable marker for detection of all ILC in the gut. When we analyzed CD127 and CD90 co-expression in lineage-negative cLP leukocytes, we noticed that almost all CD90$^+$ cLP ILC had a detectable surface expression of CD127 in naïve C57BL/6 WT and DSS-treated C57BL/6 WT, BALB/c WT and BALB/c *Rag2*$^{-/-}$ mice (Supplementary Figure 6). For further analyses, KLRG1 was used as a marker of intestinal ILC2 in line with recent publications (37, 45–47). The use of KLRG1 as a marker for intestinal ILC2 has an advantage over GATA3 as intestinal ILC3 have a low expression of GATA3 and the expression of this transcription factor is variable within the ILC2 population (48–50). KLRG1^{hi} intestinal ILC as gated in this study require GATA3 for post-developmental maintenance, supporting the notion these cells are ILC2 (51). We found that CD90$^-$ and CD90^{low} ILC can be detected among both KLRG1^{hi} and KLRG1$^-$ cLP ILC from C57BL/6 background mice, demonstrating that CD90$^-$ and CD90^{low} ILC are also components of the non-ILC2 compartment (Figure 2A).

Next, following an established method to develop ILC2 *in vitro*, we seeded bone marrow-derived ILC2 precursors (ILC2p; defined as Lin$^-$ CD127$^+$ α4β7^{hi} Flt3$^-$ CD25$^+$) in a 6-day culture on OP9-DL1 stromal cells in the presence of IL-7, SCF and IL-33 (52). Strikingly, the Lin$^-$ cell population that was generated also exhibited variable levels of CD90 (Figure 2B). Most of the ILC were CD90^{high}, but there were also substantial CD90$^-$ and CD90^{low} subpopulations.

In order to determine whether CD90 expression can be altered by immunological stimulations, we isolated KLRG1$^+$ cLP ILC2 and KLRG1$^-$ cLP ILC for *in vitro* culture with OP9-DL1 cells in the presence of distinct cytokines. Strikingly, ILC2 stimulation with IL-25 and IL-33 induced the presence of CD90$^{-/low}$ ILC2 (Figures 2C, D; Supplementary Figure 7). A similar but less potent effect was observed when IL-12 and IL-18 were added to the culture medium. Additional IL-6/IL-1β/TNFα/IL-27 stimulation did not further alter IL-12/IL-18-mediated CD90$^{-/low}$ ILC2 frequency, while IL-1β/IL-23 stimulation also had no effect. Conversely to ILC2, IL-12/IL-18 stimulation of non-ILC2 in the presence or absence of IL-6/IL-1β/TNFα/IL-27 resulted in fewer CD90$^{-/low}$ NKp46$^+$ ILC (Figures 2C, D). IL-1β/IL-23 and IL-25/IL-33 stimulation of these cells had no effect in terms of CD90 expression. Stimulation with PMA and ionomycin or a soluble agonistic anti-CD28 antibody [chosen due to reports of its expression in human ILC (53, 54)] also had no effect on the frequency of CD90 expressing ILC2 or NKp46$^+$ non-ILC2.

All ILC subset populations in the intestine exhibit variable levels of CD90

In order to investigate CD90 variation in ILC more closely, we analyzed single-cell (sc)RNA-seq data sets from three recent publications: ILC2 from gut, skin, lung, fat and bone marrow (BM) (Ricardo-Gonzalez et al. (49)), intestinal ILC2, LTi-like ILC3, NKp46 (NCR)$^+$ ILC3 and ex-ILC3/ILC1 (47), and intestinal NK cells, ILC1 and NKp46$^+$ ILC3 (55) (Figures 3A–C; Supplementary Figure 8A). Visualising clusters of cells that have similar transcriptional profiles using uniform manifold approximation and projection (UMAP) dimensionality reduction and overlaying expression levels of *Thy1* (encoding CD90), we found that *Thy1* expression could be detected across all of the ILC subsets in each dataset (Figure 3C; Supplementary Figure 8A). A pseudotime trajectory analysis of these ILC subsets did not uncover a specific developmental direction from either *Thy1* high to low expression or vice versa (Figure 3C; Supplementary Figure 8A). Identification of genes up and downregulated in cells positive for CD90 mRNA vs negative/low for CD90 mRNA within each dataset only identified a limited set of genes (Figure 3D; Supplementary Figure 8B). Together with the expression of CD90 across the various cell clusters, this indicates that CD90$^{-/low}$ ILC are not a novel ILC population with their own expression profile. In terms of ILC2, the Fiancette et al. data set indicated a higher expression of *Nkg7* in CD90 mRNA-high cells, but no genes specific for CD90 mRNA-negative/low ILC2 were detected in this data set. In contrast, in the Ricardo Gonzalez et al. data set intestinal CD90 mRNA-negative/low ILC2 exhibited greater expression of *Gzma* (encoding granzyme A) and *Gdd45a*, *Scin* and *Ctla4*, while intestinal CD90 mRNA-high ILC2 were characterized by *S100a4*, *S100a6*, *Cd3d*, *Cd3g*, *Furin* and *Cxcl2* expression. *S100a4* and *S100a6* expression was also detected in CD90 mRNA-high ILC2 from fat, while *S100a4* and *S100a6* was exhibited in cutaneous and pulmonary CD90 mRNA-high ILC2, respectively. *Lgals1* expression was detected in CD90 mRNA-high ILC2 from lungs, skin and fat tissue. As observed in the Fiancette et al. data on intestinal ILC2, *Nkg7* expression is also associated with CD90 mRNA-high ILC2 from skin and bone marrow, in addition to *Cd7*, *Ncr1*, *Klrk1*, *Ms4a4b* and *Ccl5* in BM CD90 mRNA-high ILC2. No genes showed consistently higher expression in CD90 mRNA-negative/low cells across all the tissue types but, in the bone marrow, CD90 mRNA-negative/low ILC2 were

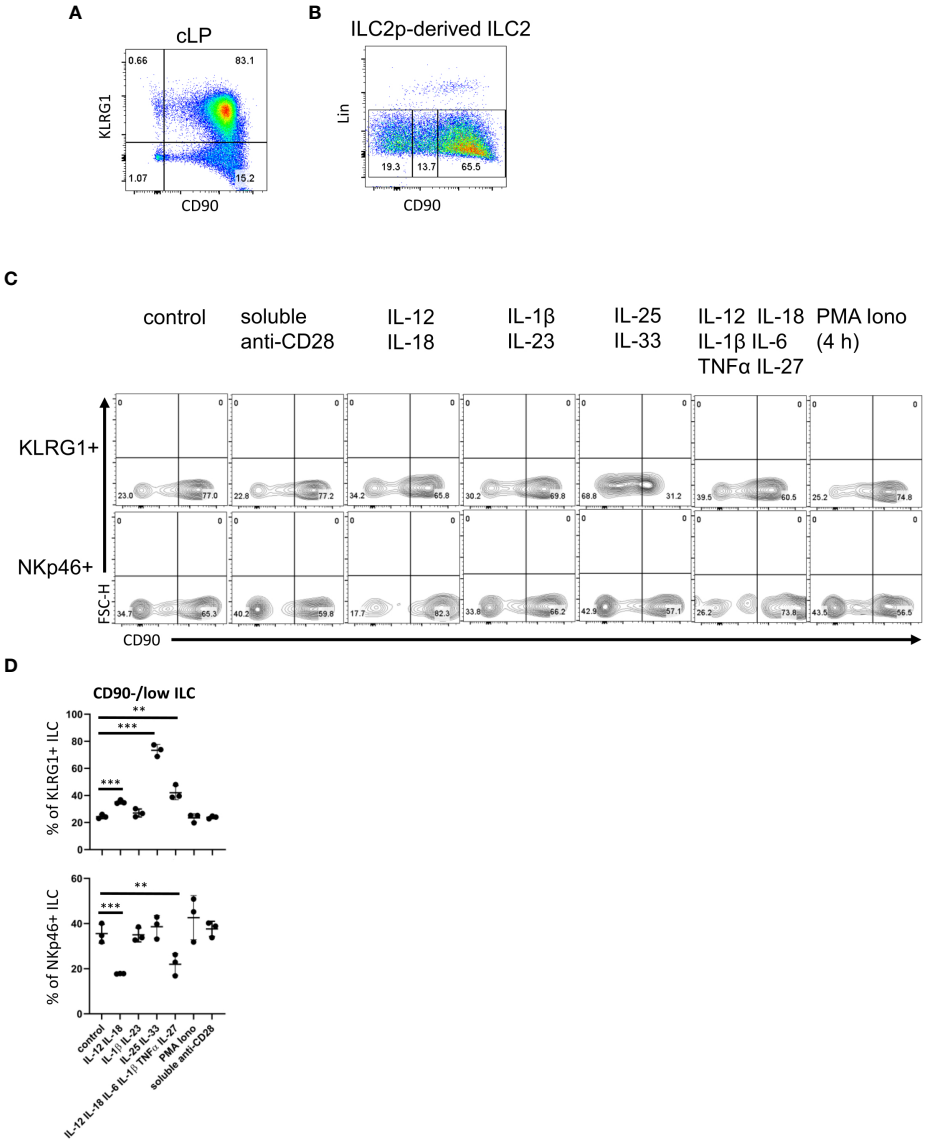

FIGURE 2
cLP ILC have a variable expression of CD90 depending on stimulatory cues. **(A)** KLRG1 and CD90 co-expression in cLP CD127$^+$ ILC was demonstrated by flow cytometry (n=12). **(B)** ILC2 were generated from ILC2p stimulated with IL-7, SCF and IL-33, and seeded onto OP9-DL1. CD90^{hi}, CD90^{low} and CD90$^-$ ILC2 are shown. **(C, D)** KLRG1$^+$ or KLRG1$^-$ CD127$^+$ ILC were isolated and stimulated *in vitro* for 48 hours prior to harvest and flow cytometry analyses of KLRG1$^+$ or NKp46$^+$ ILC, respectively. In addition to a control condition, soluble agonistic anti-CD28 antibodies, IL-12&IL-18, IL-1β&IL23, IL-25&IL-33 or IL-12&IL-18& IL-1β&IL-6&TNFα &IL-27 were used as stimuli. In a separate condition designated as "PMA Iono", sorted cells were stimulated with PMA and ionomycin in the presence of monensin for the final 4 hours prior to harvesting. **(D)** Flow cytometry analyses of CD90^{hi} and CD90$^{low/neg}$ CD127$^+$ ILC and statistical analyses of CD90$^{low/neg}$ ILC frequencies among KLRG1$^+$ or NKp46$^+$ cLP ILC are outlined. Data shown are representative of 3 biological replicates. **p< 0.01; ***p<0.001.

associated with the expression of *Hbb-bs*, *Hbb-b7*, *Hba-a1*, *Hba-a2* and *S100a8*. The Fiancette et al. data set revealed a characteristic expression of *S100a4*, *S100a6*, *Pm29* and *Arg1* in CD90 mRNA-high LTi-like ILC3, while genes specific for CD90 mRNA-negative/low LTi-like ILC3 were not detected. Both the Fiancette et al. and Krzywinska et al. data sets highlight a specific expression of *Pcp4* in CD90 mRNA-high NKp46$^+$ ILC3, while the latter data set also indicate an expression of *Nrgn* in CD90 mRNA-high NKp46$^+$ ILC3 and *Cd74* in CD90$^{-/low}$ NKp46$^+$ ILC3. In terms of the ex-ILC3/ILC1 cluster *Tmem176a*, *Rorc* and *Gda* expression was enhanced in CD90 mRNA-high cells, while *Ccl5* expression was more common in cells in which CD90 mRNA was absent or low. In the Krzywinska et al. data, CD90 mRNA-high ILC1 exhibited a characteristic expression of *Il22*, *Cd83* and *Pxdc1*, while CD90 mRNA-negative/low ILC1 were not defined by specific genes. No genes were found to be upregulated in CD90 mRNA-high NK cells but *Prf1* and *Gzma* expression was enhanced in CD90 mRNA-negative/low NK cells. Further analyses demonstrated that also only a very few genes were specific for CD90 mRNA-negative/low and CD90 mRNA-high in total ILC and NKp46$^+$ ILC (Figure 3E). As similar sets of genes were associated between CD90 mRNA-negative/low and CD90 mRNA-high ILC subsets, it appears that these respective populations may be related.

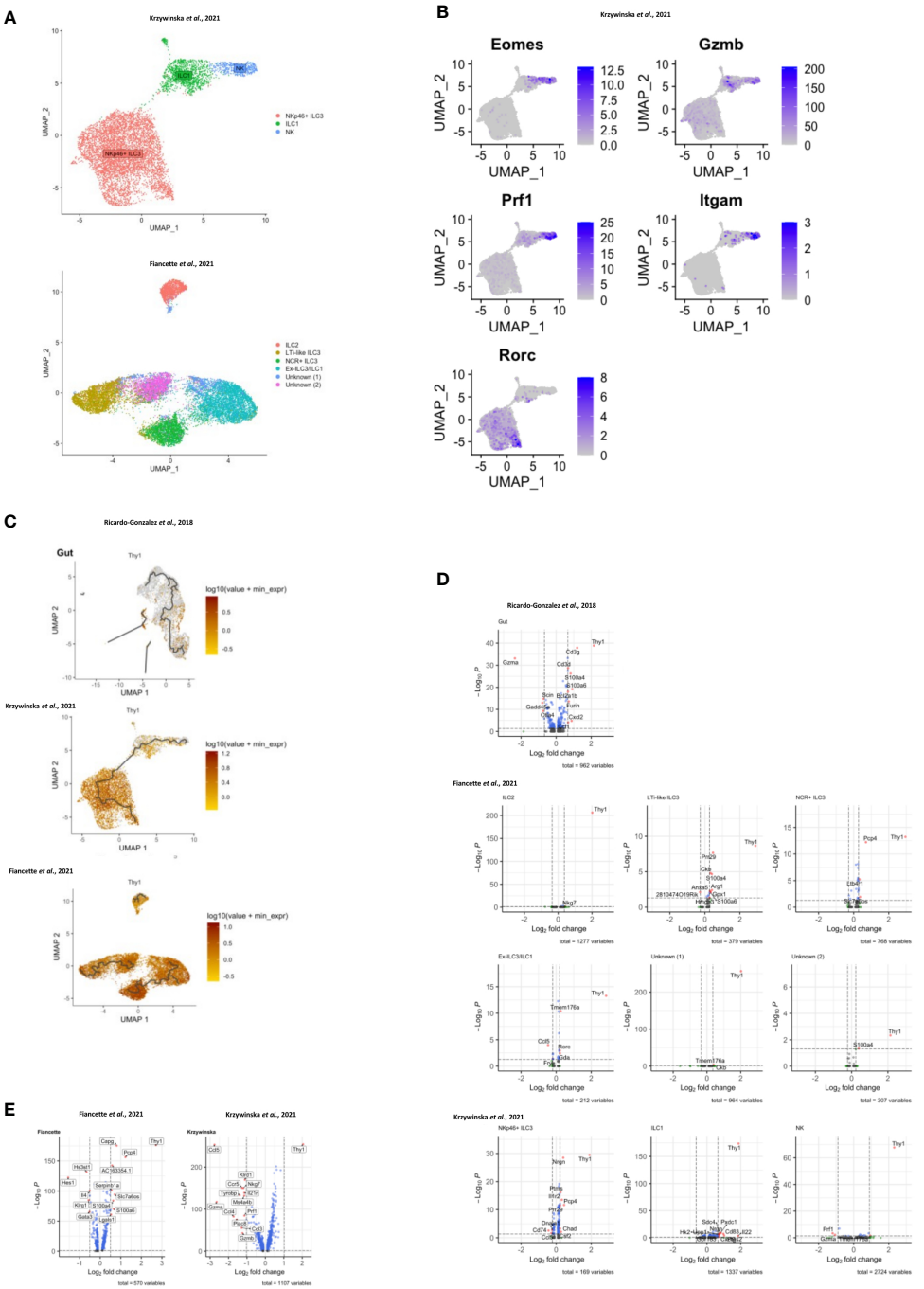

FIGURE 3
Transcriptomic analyses of CD90 expression in intestinal ILC. scRNA-seq data sets of intestinal ILC from published studies (47, 49, 55) were employed to analyze expression of *Thy1* (encoding CD90) across ILC subsets and its role on the global transcriptional profile. **(A)** UMAP plots of ILC subset annotation from the scRNA-seq data sets of the (47, 55) studies. **(B)** UMAP analyses of gene expression in the ILC subset clusters in the data set obtained from (55). **(C)** UMAP analysis of *Thy1* expression intensity in ILC subsets in the respective studies. A trajectory analysis along the *Thy1* expression intensity was performed in the indicated ILC subsets. **(D, E)** Volcano plots comparing gene expression (log2 fold change and p_{adj}) between $Thy1^{high}$ ILC versus $Thy1^{low/negative}$ **(D)** ILC subsets, as annotated in the respective published data set, and **(E)** total ILC. The most differentially expressed genes are labelled. In order to generate the volcano plots the median normalized *Thy1* expression across all datasets was calculated and used to delineate $Thy1^{high}$ and $Thy1^{low/negative}$ cells.

Dysbiosis correlates ILC1 and ILC3 lymphopenia and altered CD90 expression in ILC

Next, we sought to further analyze CD90 expression dynamics in a model of dysbiosis-driven spontaneous colitis in *Rag2*$^{-/-}$ mice. We have previously shown that spontaneous colitis in *Tbx21*$^{-/-}$ x *Rag2*$^{-/-}$ ulcerative colitis (TRUC) mice is partially driven by IL-17A-producing CD90^{+} ILC (25, 56). Hence, it was anticipated that these ILC would also promote inflammation in *Rag2*$^{-/-}$ mice receiving a transfer of feces derived from TRUC mice. These mice developed colitis with decreased body weight and increased colon weight (data not shown). However, in contrast, we detected reduced frequency of DN ILC3, CCR6^{+} ILC3, NKp46^{+} ILC3 and ILC1 (Figures 4A, B; Supplementary Figure 1A). Hence, ILC2 formed a large proportion of the cLP ILC upon fecal microbial transfer (FMT). In addition to these ILC subset frequency alterations, we detected fewer CD90^{high} and more CD90^{low} cells among the ILC population upon FMT treatment, but the frequency of CD90^{-} ILC was not altered in these mice (Figures 4C, D). Consistent with a greater frequency of ILC2 in FMT-treated mice, cLP ILC production of IL-13 was enhanced, while a significant alteration in IFNγ or IL-17A production was not detected (Figure 4E). However, the frequency of IFNγ producing CD90^{high}, CD90^{low} and CD90^{-} ILC was much reduced upon the enforced dysbiosis (Figures 4F, G). Furthermore, pathogenic FMT also resulted in a lower frequency of IL-17A^{+} CD90^{high} ILC, while IL-17A production in CD90^{low} and CD90^{-} ILC was not affected. When comparing CD90^{high}, CD90^{low} and CD90^{-} ILC that produced IFNγ and IL-17A, only a reduction in IFNγ production in CD90^{-} ILC was observed. In contrast to IFNγ and IL-17A, FMT appeared to promote IL-13 production in CD90^{high}, CD90^{low} and CD90^{-} ILC subsets.

Discussion

Ever since the discovery of ILC around a decade ago, there have been refinements to the ILC analysis strategy by flow cytometry. This is still an active process, as an increasing number of functional states within the ILC subsets are being reported. In the past, many groups have used CD90 as a marker for ILC and CD90-specific antibodies are often employed to deplete ILC *in vivo* (e.g. 25, 27–32). However, our results demonstrate that the use of CD90 to detect and purify ILC has limitations when analyzing intestinal populations. In contrast to the notion that CD90 is a pan-ILC marker, the data presented in this study reveal that intestinal ILC can be separated into CD90^{-} and CD90^{high} ILC in addition to CD90^{low} ILC, which are most likely transitional cells. CD90^{-} ILC2 were also detected in the lungs indicating that the findings in our study are applicable to ILC from diverse tissues (57). In our hands, CD127 is a far more reliable marker of ILC than CD90. Virtually all CD90^{+} cLP ILC express CD127, however other reports indicate that pulmonary ILC can lose CD127 *in vivo* and IL-7 downregulates CD127 expression in ILC *in vitro* (27, 58). Hence, in the absence of better ILC markers, we advise using a combination of CD127 and CD90 to detect ILC.

In BALB/c background mice, CD90^{-} ILC accounted for about a fifth to a third of cLP ILC, and we detected a substantial amount of IFNγ, IL-13 and IL-17A production by these cells in the context of DSS- or dysbiosis-elicited colitis. Hence, we believe these findings support the notion that these cells play a relevant role in the ILC response in intestinal tissue. It is out of the scope of this report to define a functionality of CD90 in ILCs, but it was striking to note that whilst ILC2 accounted for most cytokine-producing cLP CD90^{-} ILC in C57BL/6 at steady state, the lack of CD90 expression was not restricted to ILC2. The combination of IL-33 and IL-25, known to activate ILC2, was a potent stimulus for CD90 downregulation in cLP ILC2 *in vitro*, suggesting that low CD90 expression may be an indicator of intestinal ILC2 activity. In this experiment CD90 in sorted ILC2 was reduced within a relatively short culture period of 48 hours indicating that CD90 expression is dynamic. Interestingly, CD90 expression in pulmonary ILC2 was also shown to drop upon stimulation with IL-33 (59). Furthermore, distinct ILC2 clusters from adult and neonate lungs with high and low expression of CD90 were detected by scRNAseq analysis (60). This publication also presents a trajectory analysis predicting transformation of adult pulmonary ILC2 along these clusters which may also indicate a dynamic expression of CD90 in ILC2. In our report cLP ILC2 stimulation with IL-12 and IL-18 also enhanced the frequency of CD90$^{-/low}$ cells. It has been reported that IL-12/IL-18 and IL-25/IL-33 can induce ILC2 to express T-bet and RORγt, respectively (37, 61). In a model of DSS-induced colitis, we could not associate either IFNγ or IL-17A production by cLP ILC2 with loss of CD90 expression. In contrast to ILC2, CD90 expression was enhanced by IL-12/IL-18-mediated stimulation in NKp46^{+} cLP ILC, which may further indicate that CD90 plays a functional role. Furthermore, in dysbiotic mice we noticed a reduced expression of CD90 in IL-13-producing ILC indicating that CD90 downregulation occurs in activated ILC2 in these mice. Such modified expression of CD90 upon exposure to pathogens is not without precedent. The frequency of intestinal CD90^{-} ILC2 was enhanced in *Hoil1*$^{-/-}$ mice, a mouse model defined by microbe-driven intestinal inflammation (62). In comparison, an alteration of CD90^{+} ILC2 prevalence was not observed in these mice (62). Furthermore, *Aspergillus fumigatus*-induced inflammation also leads to the promoted occurrence of pulmonary CD4^{+} T cells with low expression of CD90 (63). In the intestine, variable expression of CD90 can be observed in Vγ7^{+} intraepithelial lymphocytes in addition to conventional CD4^{+} and CD8^{+} T cells (64, 65).

The functional role of CD90 expression on murine ILC is unknown and is also ill-defined in other lymphocytes, while CD90 expression in human ILC appears to be lacking. Known ligands of CD90 are integrins αvβ3, αxβ2, $\alpha_M\beta2$, $\alpha_5\beta1$, $\alpha_V\beta5$, syndecan-4 and CD97, and interactions with binding partners have reported to occur either *in cis* or *in trans* (4, 66–69). *In vitro* studies in unpolarized and polarized CD4^{+} T cells suggested that CD90 activation with a specific antibody can promote proliferation as well as IFNγ, IL-17A and IL-13 production, in particular in the case of co-stimulation with an agonistic anti-CD28 antibody in the absence of TCR stimulation (70, 71). Further work is required to determine the significance of this signaling axis, but, strikingly, scRNA-seq analysis in germinal center (GC) T follicular helper (T_{FH}) cells showed distinct transcriptional differences between cells with high

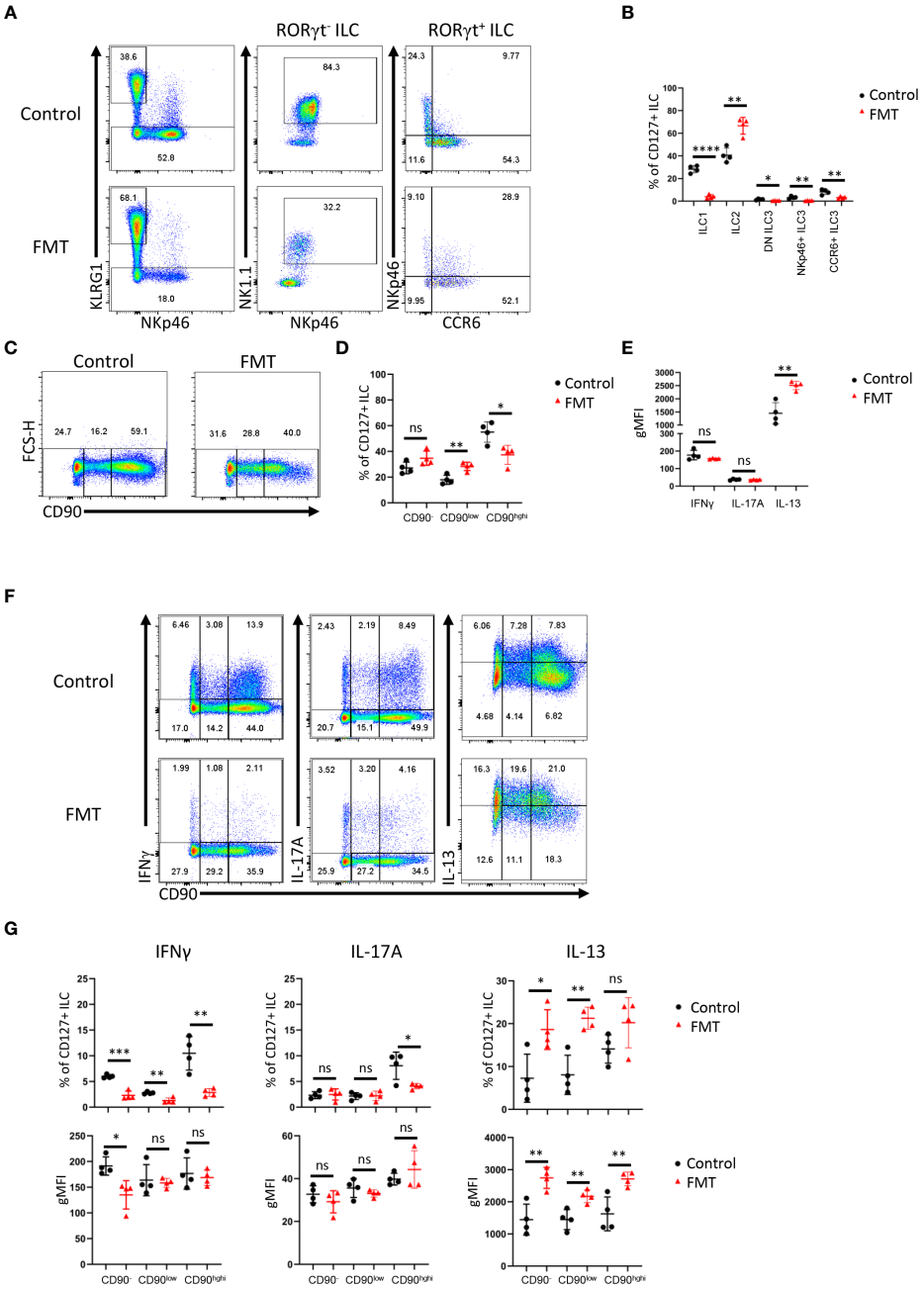

FIGURE 4
Dysbiosis-triggered appearance of functional cLP ILC with a low expression of CD90. Feces from TRUC mice were transferred into *Rag2*$^{-/-}$ mice and cLP leukocytes were isolated 21 days later from treated and untreated mice. **(A)** KLRG1^{+} ILC2, KLRG1^{-} RORγt^{-} NKp46^{+} NK1.1^{+} ILC1, KLRG1^{-} RORγt^{+} ILC3 subsets from FMT-treated and untreated control mice were analyzed by flow cytometry. ILC3 subsets were defined as NKp46^{+} CCR6^{-}, CCR6^{+} NKp46^{-} or DN ('double negative') in these analyses. **(B)** A statistical analysis of ILC subset frequency among the whole cLP ILC population is outlined. **(C)** ILC with no or a low or high expression of CD90 were analyzed by flow cytometry and **(D)** a statistical analysis of the frequency of these ILC among the whole ILC population is presented. **(E)** The per cell expression of IFNγ, IL-17A and IL-13 in ILC was analyzed statistically. **(F)** IFNγ, IL-17A and IL-13 expression in CD90^{-}, CD90^{low} and CD90^{high} ILC was determined by flow cytometry. **(G)** Related statistical analyses investigating the frequency of respective ILC and the per cell expression of IFNγ, IL-17A and IL-13 in the CD90^{-}, CD90^{low} and CD90^{high} ILC populations are shown. Data are representative of 4 biological replicates. ns, non-significant; *p < 0.05; **p< 0.01; ***p<0.001; ****p<0.0001.

expression of CD90 versus cells with low or no expression of CD90 (72). These differences included high expression of genes indicative of exocytosis/degranulation in CD90$^{-/low}$ GC T_{FH} cells, and genes relating to chemokine receptors and proliferation in CD90^{high} GC T_{FH} (72). Moreover, in addition to CD90^{high} CD8^{+} T cells, splenic CD90^{-} and CD90^{low} CD8^{+} T cells are also a relevant source of IFNγ in a mouse model of LCMV infection (73). The CD90 extracellular domain has binding sites for αvβ3 and syndecan-4, which may be the basis of a reported *in trans* interaction of CD90 with αvβ3 and syndecan-4 expressed on other cells (4, 74). Indeed, the interaction between CD90 and αvβ3 was functional in CD4 T cells in terms of promoting the differentiation of Th2 cells (74). Binding sites for the

in trans interaction with other integrins or CD97 are yet to be characterized. In addition to *in trans* interactions, αvβ5 is inactivated by binding CD90 *in cis*, preventing activation of latent TGF-β1 (4, 75). Cis CD90-CD90 interactions have been suggested to promote cluster formation in lipid rafts, which may play a critical role for RhoA-dependent signaling, as reported downstream of CD90 (4, 69). Due to its numerous known ligands, CD90 may equip ILC for intercellular interactions with several hematopoietic or non-hematopoietic cell types, but the functional role of CD90 for ILC has still to be defined (5). Interestingly, CD90 was demonstrated to regulate PPARγ expression in adipocytes (76), and other groups have reported previously that PPARγ plays an important role in ILC2 functionality (77, 78). Our study marks the first step to defining CD90 function in ILC by revealing that intestinal ILC can be separated into $CD90^+$ and $CD90^-$ populations. These data have critical implications for the analysis procedures through which ILC functionality will be uncovered in intestinal tissue.

Methods

Animals

C57BL/6 WT, *Tbx21*$^{-/-}$ (both C57BL/6 and BALB/c background) and *Rag2*$^{-/-}$ (BALB/c background) mice were sourced commercially (Charles River). A colony of colitis-free BALB/c *Rag2*$^{-/-}$ x *Tbx21*$^{-/-}$ (TRnUC) mice was generated from a descendant of the TRUC colony described previously (25, 56, 79). All mice were housed in specific pathogen–free facilities at King's College London Biological Services Unit or at Charles River Laboratories.

Isolation of cells

cLP leukocytes were isolated using a published method (80). Briefly, the epithelium was removed by incubation in HBSS lacking Mg^{2+} or Ca^{2+} (Invitrogen) supplemented with EDTA and HEPES. The tissue was further digested in 2% of fetal calf serum (FCS Gold, PAA Laboratories) supplemented in 0.5 mg/ml collagenase D, 10 µg/ml DNase I and 1.5 mg/ml dispase II (all Roche). The LP lymphocyte-enriched population was harvested from a 40%-80% Percoll (GE Healthcare) gradient.

Flow cytometry

Flow cytometry was performed using a standard protocol. Fc receptor blocking was carried out with anti-CD16/32 specific antibodies. A lineage cocktail of antibodies specific for CD3, CD45R, CD19, CD11b, TER-119, Gr-1, CD5 and FcεRI was used for cLP ILC analyses. Live/Dead Fixable Blue Cell Stain Kit (Invitrogen) stain was used to exclude dead cells from the analysis. The cLP ILC gating strategy is outlined in our recent publications (44, 45). For a complete list of the antibodies used see Table 1. A FoxP3 staining kit (ebioscience) was used for intracellular staining of cytokines and transcription factors. In case of cytokine expression analyses, cells were pre-stimulated with 100 ng/ml PMA and 2 µM ionomycin in the presence of 6 µM monensin for 3-4 hours prior to flow cytometry analysis. Samples were acquired using an LSRFortessa™ cell analyser (Becton Dickinson, USA), and all the data were analyzed using FlowJo software (Tree Star, USA).

ILC2 generation in OP9-DL1 system

ILC2p were seeded on OP9-DL1 to generate ILC2 using an established method (52). Briefly, 7,500 cells were co-cultured with mitomycin pre-treated OP9-DL1 in presence of rmIL-7, rmSCF and rmIL-33 (all 20 ng/ml) for 6 days prior to FACS analysis.

TABLE 1 Antibody clones and distributors.

Antibody	Clone	Company
α4β7	DATK32	eBioscience
CD25	PC61.5	eBioscience
CD3	17A2	eBioscience
CD5	53-7.3	eBioscience
CD19	1D3	eBioscience
B220	RA3-6B2	eBioscience
CD11b	M1/70	eBioscience/Biolegend
Gr-1	RB6-8C5	eBioscience
Flt3	A2F10	eBioscience
Ter119	TER-119	eBioscience
FcεRI	MAR-1	eBioscience
CD127	A7R34	eBioscience
NKp46	29A1.4	eBioscience
IL-13	eBio13A	eBioscience
IFNγ	XMG1.2	eBioscience
CD45	30-F11	Invitrogen
CD90.2	5a-8 30-H12	eBioscience BD
IL-5	TRFK5	BD
IL-17A	eBio17B7	eBioscience
KLRG1	2F1	eBioscience
CCR6	29-2L17	eBioscience
NKp46	29A1.4	eBioscience
RORγt	AFKJS-9	eBioscience
NK1.1	PK136	Biolegend

cLP ILC sorting and *in vitro* culture

Single-cell suspensions from colonic lamina propria were stained with fluorescently labelled antibodies and isolated using a BD FACSAria III cell sorter (BD Biosciences). Live $CD45^+$ Lin^- $CD127^+$ ILC FACS sorted as $KLRG1^+$ and $KLRG1^-$ were cultured in DMEM supplemented with 10% FCS, 1xGlutaMax (Gibco), 50 U/ml penicillin, 50 µg/ml streptomycin, 10 mM HEPES, 1x non-essential amino acids (Gibco), 1 mM sodium pyruvate and 50 µM β-mercaptoethanol (Gibco). 20,000 cells were plated per well of a 96-well plate pre-seeded with OP9-DL1 using an established method (52, 81). The medium was further supplemented with rmIL-7 and rhIL-2 (both at 10 µg/ml) and further recombinant mouse cytokines or anti-CD28 antibody (2µg/ml; clone 37.51) as indicated (all cytokines were used at a final concentration of 10 µg/ml unless indicated otherwise). Cells were harvested and analyzed by flow cytometry after 2 days in culture. FACS sort-derived cells from these conditions were harvested and analyzed without additional pre-stimulation.

In vivo models

DSS-elicted colitis was induced by adding 3 or 5% DSS (36-50 KDa, MP Biomedicals, Ontario, USA) to the drinking water for 5 days and mice were sacrificed 10 days after the beginning of the treatment. To establish a non-colitic control condition, mice were administered sterile drinking water. Regarding all *in vivo* models, body weights and clinical abnormalities were monitored on a daily basis.

For dysbiosis-induced colitis models TRUC mice cecal feces were administered to colitis-free *Rag2*$^{-/-}$ mice *via* the oral route using a published method and sacrificed 21 days after FMT (45). Regarding all *in vivo* models, body weights and clinical abnormalities were monitored on a daily basis.

Single-cell RNA-seq analysis

Raw expression matrices were obtained from GEO accession GSE117567 (49) and raw sequencing data were obtained from ArrayExpress accessions E-MTAB-9795 (47) and E-MTAB-11238, (55). Raw reads were mapped to mm10 using CellRanger 6.0.1. UMAP co-ordinates and clustering metadata was obtained from correspondence with the authors of (47, 55), therefore downstream processing steps can be considered identical to those carried out by the respective authors. For the matrices obtained from 49, cells with over 10% reads mapping to mitochondrial genes and cells with less than 400 genes detected were removed. Each matrix was then normalized using SCTransform (82), followed by RunPCA (PCs = 30) and RunUMAP (dims = 30). Shared nearest neighbor and clustering were carried out using FindNeighbours (dims = 30) and FindClusters respectively. NormalizeData was then ran, and this assay was used for downstream visualization and differential expression analysis using the MAST algorithm (83). Pseudotime/trajectory analyses were carried out using monocle3 (84, 85).

Statistics

Results are expressed as mean ± SEM. Data were analyzed using Student's t-test using GraphPad Prism 5.0 (GraphPad Inc., USA). ns: non-significant; *p < 0.05; **p< 0.01; ***p<0.001; ****p<0.0001.

Study approval

All animal experiments were performed in accredited facilities in accordance with the UK Animals (Scientific Procedures) Act 1986 (Home Office Licence Numbers PPL: 70/6792, 70/8127 and 70/7869).

Data availability statement

The datasets presented in this study can be found in online repositories. The names of the repository/repositories and accession number(s) can be found below: https://www.ebi.ac.uk/arrayexpress/, E-MTAB-9795. https://www.ebi.ac.uk/arrayexpress/, E-MTAB-11213. https://www.ebi.ac.uk/arrayexpress/, E-MTAB-11212.

Ethics statement

All animal experiments were performed in accredited facilities in accordance with the UK Animals (Scientific Procedures) Act 1986 (Home Office Licence Numbers PPL: 70/6792, 70/8127 and 70/7869). Written informed consent was obtained from the owners for the participation of their animals in this study.

Author contributions

Study concept and design: J-HS, GL, JN, and NP. Acquisition of data: J-HS, JL, and TZ. Bioinformatics analysis: GB. Data analysis and interpretation: J-HS, GL, RJ, JN, and NP. Obtained funding: GL, NP, and JN. Drafting of manuscript: J-HS. Editing of manuscript: RJ. Study supervision: GL, RJ.

Funding

This study was supported by grants awarded by the Wellcome Trust (091009), the Medical Research Council (MR/M003493/1; MR/K002996/1, all to GL) and RCUK/UKRI Rutherford Fund fellowship (MR/R024812/1) to JN. Research was also supported by the National Institute for Health Research (NIHR) Biomedical Research Centre at Guy's and St Thomas and King's College London. The views expressed are those of the author(s) and not necessarily those of the NHS, the NIHR, or the Department of Health. Work at the CRUK City of London Centre Single Cell Genomics Facility and Cancer Institute Genomics Translational Technology Platform was supported by the CRUK City of London Centre Award [C7893/A26233].

Acknowledgments

We thank the BRC flow cytometry core team for technical help, and acknowledge financial support from the Department of Health *via* the NIHR comprehensive Biomedical Research Centre award to Guy's and St. Thomas' NHS Foundation Trust in partnership with King's College London and King's College Hospital NHS Foundation Trust. We also thank Professor Zúñiga-Pflücker (Sunnybrook Research Institute, University of Toronto) for contributing OP9-DL1 cells. Furthermore, we thank Professor Richard Locksley (University of California San Francisco), Professor Christian Stockmann (University of Zurich), Dr Matthew Hepworth (University of Manchester), Zheng Fan (University of Zurich) and Syed Murtuza Baker (University of Manchester) for providing scRNA-seq data. We also thank Luke Roberts (The University of Manchester) for critical feedback and Ian Jackson (King's College London) for technical assistance.

Conflict of interest

The authors declare that the research was conducted in the absence of any commercial or financial relationships that could be construed as a potential conflict of interest.

Publisher's note

Supplementary material

The Supplementary Material for this article can be found online at: https://www.frontiersin.org/articles/10.3389/fimmu.2023.1113735/full#supplementary-material

SUPPLEMENTARY FIGURE 1
Gating strategy for cLP ILC. Murine cLP ILC were isolated from *Rag2*-deficient mice for flow cytometry analysis. **(A)** ILC were gated as live single CD45$^+$ Lin$^-$ CD127$^+$ leukocytes. The lineage cocktail contained CD3, CD5, CD19, B220, CD11b, Gr-1, FcεR1 and Ter119. **(B)** CD90 expression intensity in cLP ILC was evaluated using an FMO control sample.

SUPPLEMENTARY FIGURE 2
CD90-negative WT cLP CD127$^+$ ILC are a source of IFNγ, IL-13 and IL-17A upon DSS treatment of BALB/c mice. cLP ILC from 3% DSS-treated BALB/c WT and *Tbx21*$^{-/-}$ mice were isolated and stimulated with PMA and ionomycin (3 hours) prior to flow cytometry analysis. **(A)** Frequencies of CD90^{hi}, CD90^{low} and CD90$^-$ in total CD127$^+$ ILC and **(B)** statistical analyses are outlined. **(C)** IFNγ, IL-13 and IL-17A expression in CD90^{hi}, CD90^{low} and CD90$^-$ CD127$^+$ ILC and **(D)** corresponding statistical analyses are shown. Data shown are representative of 4 biological replicates. *p < 0.05; **p < 0.01; ***p<0.001.

SUPPLEMENTARY FIGURE 3
CD90-negative WT cLP CD127$^+$ ILC are a minor source of IFNγ, IL-13 and IL-17A during DSS colitis in C57BL/6 mice. cLP ILC from 3% DSS-treated C57BL/6 WT and *Tbx21*$^{-/-}$ mice were isolated and stimulated with PMA and ionomycin (3 hours) prior to flow cytometry analysis. **(A)** Frequencies of CD90^{hi}, CD90^{low} and CD90$^-$ in total CD127$^+$ ILC and **(B)** statistical analyses are outlined. **(C)** IFNγ, IL-13 and IL-17A expression in CD90^{hi}, CD90^{low} and CD90$^-$ CD127$^+$ ILC and **(D)** corresponding statistical analyses are shown. **(E)** CD90 co-expression with IL-17A or IFNγ in IL-13$^+$ ILC is demonstrated. Data shown are representative of 4 biological replicates.*p< 0.05; **p< 0.01; ***p<0.001.

SUPPLEMENTARY FIGURE 4
Intestinal CD90-negative CD127$^+$ ILC have a predominant type 2 phenotype. cLP CD127$^+$ ILC were isolated from untreated C57BL/6 WT and *Tbx21*$^{-/-}$ mice and stimulated with PMA and ionomycin (4 hours) prior to flow cytometry analysis. **(A)** Frequencies of CD90^{hi}, CD90^{low} and CD90$^-$ in CD127$^+$ ILC and statistical analyses are outlined. **(B)** IL-13, IL-5, IFNγ and IL-17A expression in CD90^{hi}, CD90^{low} and CD90$^-$ total CD127$^+$ ILC and statistical analyses of **(C)** IFNγ and **(D)** IL-17A, **(E)** IL-13 and **(F)** IL-5 expression flow cytometry analyses in CD90^{hi}, CD90^{low} and CD90$^-$ CD127$^+$ ILC are illustrated. **(G)** Statistical analysis of IL-5$^+$ IL-13$^-$ CD90^{hi}, CD90^{low} and CD90$^-$ CD127$^+$ ILC. Data shown are representative of 3 biological replicates. *p < 0.05; **p< 0.01; ***p<0.001.

SUPPLEMENTARY FIGURE 5
Characterization of CD90 expression in inflammatory ILC2. cLP CD127$^+$ ILC were isolated from untreated C57BL/6 WT and *Tbx21*$^{-/-}$ mice and stimulated with PMA and ionomycin (4 hours) prior to flow cytometry analysis. Flow cytometry analyses of IL-13 co-expression with **(A)** IL-17A and **(B)** IFNγ in CD90^{hi}, CD90^{low} and CD90$^-$ CD127$^+$ ILC are outlined. Data shown are representative of 3 biological replicates.

SUPPLEMENTARY FIGURE 6
CD90 and CD127 co-expression in cLP ILC. cLP leukocytes were isolated from untreated C57BL/6 and DSS-treated C57BL/6, BALB/c and Rag2-deficient BALB/c mice. CD127 and CD90 co-expression in lineage-negative leukocytes are shown.

SUPPLEMENTARY FIGURE 7
Gating strategy for cLP ILC for *in vitro* assay analysis. KLRG1$^+$ or KLRG1$^-$ CD127$^+$ ILC were isolated and stimulated *in vitro* for 48 hours prior to harvest and flow cytometry analyses of KLRG1$^+$ or NKp46$^+$ ILC, respectively. ILC from these cultures were gated as live single CD45$^+$ Lin$^-$ leukocytes. The lineage cocktail contained CD3, CD5, CD19, B220, CD11b, Gr-1, FcεR1 and Ter119.

SUPPLEMENTARY FIGURE 8
Transcriptome analyses of CD90 expression in intestinal ILC2. A scRNA-seq data set from a published study (49) was employed to analyze CD90 expression across ILC2 isolated from lungs, skin, fat and bone marrow (BM) and its role on the global transcriptional profile. **(A)** A UMAP plot of *Thy1* expression intensity in ILC2 and a trajectory analysis along the CD90 expression intensity was performed in these ILC2. **(B)** Volcano plots comparing gene expression (log2 fold-change and p_{adj}) between CD90^{high} ILC versus CD90$^{low/negative}$ ILC2, as annotated in the published data set. The most differentially expressed genes are labelled.

References

1. Bal SM, Golebski K, Spits H. Plasticity of innate lymphoid cell subsets. *Nat Rev Immunol* (2020) 20(9):552–65. doi: 10.1038/s41577-020-0282-9

2. Klose CSN, Artis D. Innate lymphoid cells control signaling circuits to regulate tissue-specific immunity. *Cell Res* (2020) 30(6):475–91. doi: 10.1038/s41422-020-0323-8

3. Schroeder JH, Howard JK, Lord GM. Transcription factor-driven regulation of ILC1 and ILC3. *Trends Immunol* (2022) 43(7):564–79. doi: 10.1016/j.it.2022.04.009

4. Leyton L, Díaz J, Martínez S, Palacios E, Pérez LA, Pérez RD. Thy-1/CD90 a bidirectional and lateral signaling scaffold. *Front Cell Dev Biol* (2019) 7:132. doi: 10.3389/fcell.2019.00132

5. Sauzay C, Voutetakis K, Chatziioannou A, Chevet E, Avril T. CD90/Thy-1, a cancer-associated cell surface signaling molecule. *Front Cell Dev Biol* (2019) 7:66. doi: 10.3389/fcell.2019.00066

6. Barman TK, Huber VC, Bonin JL, Califano D, Salmon SL, McKenzie ANJ, et al. Viral PB1-F2 and host IFN-γ guide ILC2 and T cell activity during influenza virus infection. *Proc Natl Acad Sci USA.* (2022) 119(8):e2118535119. doi: 10.1073/pnas.2118535119

7. Cox CB, Storm EE, Kapoor VN, Chavarria-Smith J, Lin DL, Wang L, et al. IL-1R1-dependent signaling coordinates epithelial regeneration in response to intestinal damage. *Sci Immunol* (2021) 6(59):eabe8856. doi: 10.1126/sciimmunol.abe8856

8. Fachi JL, Pral LP, Dos Santos JAC, Codo AC, de Oliveira S, Felipe JS, et al. Hypoxia enhances ILC3 responses through HIF-1α-dependent mechanism. *Mucosal Immunol* (2021) 14(4):828–41. doi: 10.1038/s41385-020-00371-6

9. He Y, Xu H, Song C, Koprivsek JJ, Arulanandam B, Yang H, et al. Adoptive transfer of group 3-like innate lymphoid cells restores mouse colon resistance to colonization of a gamma interferon-susceptible chlamydia muridarum mutant. *Infect Immun* (2021) 89(2):e00533–20. doi: 10.1128/IAI.00533-20

10. Ualiyeva S, Lemire E, Aviles EC, Wong C, Boyd AA, Lai J, et al. Tuft cell-produced cysteinyl leukotrienes and IL-25 synergistically initiate lung type 2 inflammation. *Sci Immunol* (2021) 6(66):eabj0474. doi: 10.1126/sciimmunol.abj0474

11. Bruchard M, Geindreau M, Perrichet A, Truntzer C, Ballot E, Boidot R, et al. Recruitment and activation of type 3 innate lymphoid cells promote antitumor immune responses. *Nat Immunol* (2022) 23(2):262–74. doi: 10.1038/s41590-021-01120-y

12. Chen W, Chen S, Yan C, Zhang Y, Zhang R, Chen M, et al. Allergen protease-activated stress granule assembly and gasdermin d fragmentation control interleukin-33 secretion. *Nat Immunol* (2022) 23(7):1021–30. doi: 10.1038/s41590-022-01255-6

13. Glaubitz J, Wilden A, Golchert J, Homuth G, Völker U, Bröker BM, et al. In mouse chronic pancreatitis $CD25^{+}FOXP3^{+}$ regulatory T cells control pancreatic fibrosis by suppression of the type 2 immune response. *Nat Commun* (2022) 13 (1):4502. doi: 10.1038/s41467-022-32195-2

14. Han J, Wan Q, Seo GY, Kim K, El Baghdady S, Lee JH, et al. Hypoxia induces adrenomedullin from lung epithelia, stimulating ILC2 inflammation and immunity. *J Exp Med* (2022) 219(6):e20211985. doi: 10.1084/jem.20211985

15. He J, Jiang G, Li X, Xiao Q, Chen Y, Xu H, et al. Bilirubin represents a negative regulator of ILC2 in allergic airway inflammation. *Mucosal Immunol* (2022) 15(2):314–26. doi: 10.1038/s41385-021-00460-0

16. Liu N, He J, Fan D, Gu Y, Wang J, Li H, et al. Circular RNA circTmem241 drives group III innate lymphoid cell differentiation *via* initiation of Elk3 transcription. *Nat Commun* (2022) 13(1):4711. doi: 10.1038/s41467-022-32322-z

17. Peng V, Xing X, Bando JK, Trsan T, Di Luccia B, Collins PL, et al. Whole-genome profiling of DNA methylation and hydroxymethylation identifies distinct regulatory programs among innate lymphocytes. *Nat Immunol* (2022) 23(4):619–31. doi: 10.1038/s41590-022-01164-8

18. Peng V, Cao S, Trsan T, Bando JK, Avila-Pacheco J, Cleveland JL, et al. Ornithine decarboxylase supports ILC3 responses in infectious and autoimmune colitis through positive regulation of IL-22 transcription. *Proc Natl Acad Sci U S A.* (2022) 119(45):e2214900119. doi: 10.1073/pnas.2214900119

19. Riding AM, Loudon KW, Guo A, Ferdinand JR, Lok LSC, Richoz N, et al. Group 3 innate lymphocytes make a distinct contribution to type 17 immunity in bladder defence. *iScience* (2022) 25(7):104660. doi: 10.1016/j.isci.2022.104660

20. Schmalzl A, Leupold T, Kreiss L, Waldner M, Schürmann S, Neurath MF, et al. Interferon regulatory factor 1 (IRF-1) promotes intestinal group 3 innate lymphoid responses during citrobacter rodentium infection. *Nat Commun* (2022) 13(1):5730. doi: 10.1038/s41467-022-33326-5

21. Sheikh A, Lu J, Melese E, Seo JH, Abraham N. IL-7 induces type 2 cytokine response in lung ILC2s and regulates GATA3 and CD25 expression. *J Leukoc Biol* (2022) 112(5):1105–13. doi: 10.1002/JLB.3AB1220-819RRR

22. Xiao Q, Han X, Liu G, Zhou D, Zhang L, He J, et al. Adenosine restrains ILC2-driven allergic airway inflammation vi A2A receptor. *Mucosal Immunol* (2022) 15 (2):338–50. doi: 10.1038/s41385-021-00475-7

23. Wu X, Kasmani MY, Zheng S, Khatun A, Chen Y, Winkler W, et al. BATF promotes group 2 innate lymphoid cell-mediated lung tissue protection during acute respiratory virus infection. *Sci Immunol* (2022) 7(67):eabc9934. doi: 10.1126/sciimmunol.abc9934

24. Wu X, Khatun A, Kasmani MY, Chen Y, Zheng S, Atkinson S, et al. Group 3 innate lymphoid cells require BATF to regulate gut homeostasis in mice. *J Exp Med* (2022) 219(11):e20211861. doi: 10.1084/jem.20211861

25. Powell N, Walker AW, Stolarczyk E, Canavan JB, Gökmen MR, Marks E, et al. The transcription factor T-bet regulates intestinal inflammation mediated by interleukin-7 receptor+ innate lymphoid cells. *Immunity* (2012) 37(4):674–84. doi: 10.1016/j.immuni.2012.09.008

26. Mortha A, Chudnovskiy A, Hashimoto D, Bogunovic M, Spencer SP, Belkaid Y, et al. Microbiota-dependent crosstalk between macrophages and ILC3 promotes intestinal homeostasis. *Science* (2014) 343(6178):1249288. doi: 10.1126/science.1249288

27. Martin CE, Spasova DS, Frimpong-Boateng K, Kim HO, Lee M, Kim KS, et al. Interleukin-7 availability is maintained by a hematopoietic cytokine sink comprising innate lymphoid cells and T cells. *Immunity* (2017) 47(1):171–182.e4. doi: 10.1016/j.immuni.2017.07.005

28. Rafei-Shamsabadi DA, van de Poel S, Dorn B, Kunz S, Martin SF, Klose CSN, et al. Lack of type 2 innate lymphoid cells promotes a type I-driven enhanced immune response in contact hypersensitivity. *J Invest Dermatol* (2018) 138(9):1962–72. doi: 10.1016/j.jid.2018.03.001

29. Castro-Dopico T, Fleming A, Dennison TW, Ferdinand JR, Harcourt K, Stewart BJ, et al. GM-CSF calibrates macrophage defense and wound healing programs during intestinal infection and inflammation. *Cell Rep* (2020) 32(1):107857. doi: 10.1016/j.celrep.2020.107857

30. Dobeš J, Ben-Nun O, Binyamin A, Stoler-Barak L, Oftedal BE, Goldfarb Y, et al. Extrathymic expression of aire controls the induction of effective T_H17 cell-mediated immune response to candida albicans. *Nat Immunol* (2022) 23(7):1098–108. doi: 10.1038/s41590-022-01247-6

31. Ray JL, Shaw PK, Postma B, Beamer CA, Holian A. Nanoparticle-induced airway eosinophilia is independent of ILC2 signaling but associated with sex differences in macrophage phenotype development. *J Immunol* (2022) 208(1):110–20. doi: 10.4049/jimmunol.2100769

32. Zhou L, Zhou W, Joseph AM, Chu C, Putzel GG, Fang B, et al. Group 3 innate lymphoid cells produce the growth factor HB-EGF to protect the intestine from TNF-mediated inflammation. *Nat Immunol* (2022) 23(2):251–61. doi: 10.1038/s41590-021-01110-0

33. Gillard GO, Bivas-Benita M, Hovav AH, Grandpre LE, Panas MW, Seaman MS, et al. Thy1+ NK cells from vaccinia virus-primed mice confer protection against vaccinia virus challenge in the absence of adaptive lymphocytes. *PloS Pathog* (2011) 7 (8):e1002141. doi: 10.1371/journal.ppat.1002141

34. Alvarez M, Simonetta F, Baker J, Pierini A, Wenokur AS, Morrison AR, et al. Regulation of murine NK cell exhaustion through the activation of the DNA damage repair pathway. *JCI Insight* (2019) 5(14):e127729. doi: 10.1172/jci.insight.127729

35. Potempa M, Aguilar OA, Gonzalez-Hinojosa MDR, Tenvooren I, Marquez DM, Spitzer MH, et al. Influence of self-MHC class I recognition on the dynamics of NK cell responses to cytomegalovirus infection. *J Immunol* (2022) 208(7):1742–54. doi: 10.4049/jimmunol.2100768

36. Huang Y, Guo L, Qiu J, Chen X, Hu-Li J, Siebenlist U, et al. IL-25-responsive, lineage-negative KLRG1(hi) cells are multipotential 'inflammatory' type 2 innate lymphoid cells. *Nat Immunol* (2015) 16(2):161–9. doi: 10.1038/ni.3078

37. Flamar AL, Klose CSN, Moeller JB, Mahlakõiv T, Bessman NJ, Zhang W, et al. Interleukin-33 induces the enzyme tryptophan hydroxylase 1 to promote inflammatory group 2 innate lymphoid cell-mediated immunity. *Immunity* (2020) 52(4):606–619.e6. doi: 10.1016/j.immuni.2020.02.009

38. Roberts LB, Schnoeller C, Berkachy R, Darby M, Pillaye J, Oudhoff MJ, et al. Acetylcholine production by group 2 innate lymphoid cells promotes mucosal immunity to helminths. *Sci Immunol* (2021) 6(57):eabd0359. doi: 10.1126/sciimmunol.abd0359

39. Seehus CR, Aliahmad P, de la Torre B, Iliev ID, Spurka L, Funari VA. The development of innate lymphoid cells requires TOX-dependent generation of a common innate lymphoid cell progenitor. *J.Nat Immunol* (2015) 16(6):599–608. doi: 10.1038/ni.3168

40. Bando JK, Gilfillan S, Di Luccia B, Fachi JL, Sécca C, Cella M, et al. ILC2s are the predominant source of intestinal ILC-derived IL-10. *J Exp Med* (2020) 217(2):e20191520. doi: 10.1084/jem.20191520

41. Guo X, Qiu J, Tu T, Yang X, Deng L, Anders RA, et al. Induction of innate lymphoid cell-derived interleukin-22 by the transcription factor STAT3 mediates protection against intestinal infection. *Immunity* (2014) 40(1):25–39. doi: 10.1016/j.immuni.2013.10.021

42. Chen Y, Wang X, Hao X, Li B, Tao W, Zhu S, et al. Ly49E separates liver ILC1s into embryo-derived and postnatal subsets with different functions. *J Exp Med* (2022) 219(5):e20211805. doi: 10.1084/jem.20211805

43. Sparano C, Solís-Sayago D, Vijaykumar A, Rickenbach C, Vermeer M, Ingelfinger F, et al. Embryonic and neonatal waves generate distinct populations of hepatic ILC1s. *Sci Immunol* (2022) 7(75):eabo6641. doi: 10.1126/sciimmunol.abo6641

44. Schroeder JH, Roberts LB, Meissl K, Lo JW, Hromadová D, Hayes K, et al. Sustained post-developmental T-bet expression is critical for the maintenance of type one innate lymphoid cells *in vivo*. *Front Immunol* (2021) 12:760198. doi: 10.3389/fimmu.2021.760198

45. Schroeder JH, Meissl K, Hromadová D, Lo JW, Neves JF, Helmby H, et al. T-Bet controls cellularity of intestinal group 3 innate lymphoid cells. *Front Immunol* (2021) 11:623324. doi: 10.3389/fimmu.2020.623324

46. Garrido-Mesa N, Schroeder JH, Stolarczyk E, Gallagher AL, Lo JW, Bailey C, et al. T-Bet controls intestinal mucosa immune responses *via* repression of type 2 innate lymphoid cell function. *Mucosal Immunol* (2019) 12(1):51–63. doi: 10.1038/s41385-018-0092-6

47. Fiancette R, Finlay CM, Willis C, Bevington SL, Soley J, Ng STH, et al. Reciprocal transcription factor networks govern tissue-resident ILC3 subset function and identity. *Nat Immunol* (2021) 22(10):1245–55. doi: 10.1038/s41590-021-01024-x

48. Zhong C, Cui K, Wilhelm C, Hu G, Mao K, Belkaid Y, et al. Group 3 innate lymphoid cells continuously require the transcription factor GATA-3 after commitment. *Nat Immunol* (2016) 17(2):169–78. doi: 10.1038/ni.3318

49. Ricardo-Gonzalez RR, Van Dyken SJ, Schneider C, Lee J, Nussbaum JC, Liang HE, et al. Tissue signals imprint ILC2 identity with anticipatory function. *Nat Immunol* (2018) 19(10):1093–9. doi: 10.1038/s41590-018-0201-4

50. Zhong C, Zheng M, Cui K, Martins AJ, Hu G, Li D, et al. Differential expression of the transcription factor GATA3 specifies lineage and functions of innate lymphoid cells. *Immunity* (2020) 52(1):83–95.e4. doi: 10.1016/j.immuni.2019.12.001

51. Yagi R, Zhong C, Northrup DL, Yu F, Bouladoux N, Spencer S, et al. The transcription factor GATA3 is critical for the development of all IL-7Rα-expressing innate lymphoid cells. *Immunity* (2014) 40(3):378–88. doi: 10.1016/j.immuni.2014.01.012

52. Seehus C, Kaye J. *In vitro* differentiation of murine innate lymphoid cells from common lymphoid progenitor cells. *Bio Protoc* (2016) 6(6):e1770. doi: 10.21769/BioProtoc.1770

53. Björklund ÅK, Forkel M, Picelli S, Konya V, Theorell J, Friberg D, et al. The heterogeneity of human CD127(+) innate lymphoid cells revealed by single-cell RNA sequencing. *Nat Immunol* (2016) 17(4):451–60. doi: 10.1038/ni.3368

54. Roan F, Stoklasek TA, Whalen E, Molitor JA, Bluestone JA, Buckner JH, et al. CD4+ group 1 innate lymphoid cells (ILC) form a functionally distinct ILC subset that is increased in systemic sclerosis. *J Immunol* (2016) 196(5):2051–62. doi: 10.4049/jimmunol.1501491

55. Krzywinska E, Sobecki M, Nagarajan S, Zacharjasz J, Tambuwala MM, Pelletier A, et al. The transcription factor HIF-1α mediates plasticity of NKp46+ innate lymphoid cells in the gut. *J Exp Med* (2022) 219(2):e20210909. doi: 10.1084/jem.20210909

56. Powell N, Lo JW, Biancheri P, Vossenkämper A, Pantazi E, Walker AW, et al. Interleukin 6 increases production of cytokines by colonic innate lymphoid cells in mice and patients with chronic intestinal inflammation. *Gastroenterology* (2015) 149(2):456–67.e15. doi: 10.1053/j.gastro.2015.04.017

57. Loering S, Cameron GJ, Bhatt NP, Belz GT, Foster PS, Hansbro PM, et al. Differences in pulmonary group 2 innate lymphoid cells are dependent on mouse age, sex and strain. *Immunol Cell Biol* (2021) 99(5):542–51. doi: 10.1111/imcb.12430

58. Cavagnero KJ, Badrani JH, Naji LH, Amadeo MB, Shah VS, Gasparian S, et al. Unconventional ST2- and CD127-negative lung ILC2 populations are induced by the fungal allergen alternaria alternata. *J Allergy Clin Immunol* (2019) 144(5):1432–1435.e9. doi: 10.1016/j.jaci.2019.07.018

59. Entwistle LJ, Gregory LG, Oliver RA, Branchett WJ, Puttur F, Lloyd CM. Pulmonary group 2 innate lymphoid cell phenotype is context specific: Determining the effect of strain, location, and stimuli. *Front Immunol* (2020) 10:3114. doi: 10.3389/fimmu.2019.03114

60. Zeis P, Lian M, Fan X, Herman JS, Hernandez DC, Gentek R, et al. *In situ* maturation and tissue adaptation of type 2 innate lymphoid cell progenitors. *Immunity* (2020) 53(4):775–792.e9. doi: 10.1016/j.immuni.2020.09.002

61. Silver JS, Kearley J, Copenhaver AM, Sanden C, Mori M, Yu L, et al. Inflammatory triggers associated with exacerbations of COPD orchestrate plasticity of group 2 innate lymphoid cells in the lungs. *Nat Immunol* (2016) 17(6):626–35. doi: 10.1038/ni.3443

62. Wood MJ, Marshall JN, Hartley VL, Liu TC, Iwai K, Stappenbeck TS, et al. HOIL1 regulates group 2 innate lymphoid cell numbers and type 2 inflammation in the small intestine. *Mucosal Immunol* (2022) 15(4):642–55. doi: 10.1038/s41385-022-00520-z

63. Ulrich BJ, Kharwadkar R, Chu M, Pajulas A, Muralidharan C, Koh B, et al. Allergic airway recall responses require IL-9 from resident memory $CD4^+$ T cells. *Sci Immunol* (2022) 7(69):eabg9296. doi: 10.1126/sciimmunol.abg9296

64. Lei X, Ketelut-Carneiro N, Shmuel-Galia L, Xu W, Wilson R, Vierbuchen T, et al. Epithelial HNF4A shapes the intraepithelial lymphocyte compartment *via* direct regulation of immune signaling molecules. *J Exp Med* (2022) 219(8):e20212563. doi: 10.1084/jem.20212563

65. Lo JW, Cozzetto D, Liu Z, Ibraheim H, Sieh J, Olbei M, et al. Immune checkpoint inhibitor-induced colitis is mediated by $CXCR6^+$ polyfunctional lymphocytes and is dependent on the IL23/IFNγ axis. *Res Square* (2022). doi: 10.21203/rs.3.rs-1249584/v1

66. Wandel E, Saalbach A, Sittig D, Gebhardt C, Aust G. Thy-1 (CD90) is an interacting partner for CD97 on activated endothelial cells. *J Immunol* (2012) 188(3):1442–50. doi: 10.4049/jimmunol.1003944

67. Kong M, Muñoz N, Valdivia A, Alvarez A, Herrera-Molina R, Cárdenas A, et al. Thy-1-mediated cell-cell contact induces astrocyte migration through the engagement of αVβ3 integrin and syndecan-4. *Biochim Biophys Acta* (2013) 1833(6):1409–20. doi: 10.1016/j.bbamcr.2013.02.013

68. Leyton L, Hagood JS. Thy-1 modulates neurological cell-cell and cell-matrix interactions through multiple molecular interactions. *Adv Neurobiol* (2014) 8:3–20. doi: 10.1007/978-1-4614-8090-7_1

69. Pérez LA, Leyton L, Valdivia A. Thy-1 (CD90), Integrins and syndecan 4 are key regulators of skin wound healing. *Front Cell Dev Biol* (2022) 10:810474. doi: 10.3389/fcell.2022.810474

70. Haeryfar SM, Al-Alwan MM, Mader JS, Rowden G, West KA, Hoskin DW. Thy-1 signaling in the context of costimulation provided by dendritic cells provides signal 1 for T cell proliferation and cytotoxic effector molecule expression, but fails to trigger delivery of the lethal hit. *J Immunol* (2003) 171(1):69–77. doi: 10.4049/jimmunol.171.1.69

71. Furlong S, Coombs MRP, Ghassemi-Rad J, Hoskin DW. Thy-1 (CD90) signaling preferentially promotes RORγt expression and a Th17 response. *Front Cell Dev Biol* (2018) 6:158. doi: 10.3389/fcell.2018.00158

72. Yeh CH, Finney J, Okada T, Kurosaki T, Kelsoe G. Primary germinal center-resident T follicular helper cells are a physiologically distinct subset of $CXCR5^{hi}PD\text{-}1^{hi}$ T follicular helper cells. *Immunity* (2022) 55(2):272–289.e7. doi: 10.1016/j.immuni.2021.12.015

73. Gather R, Aichele P, Goos N, Rohr J, Pircher H, Kögl T, et al. Trigger-dependent differences determine therapeutic outcome in murine primary hemophagocytic lymphohistiocytosis. *Eur J Immunol* (2020) 50(11):1770–82. doi: 10.1002/eji.201948123

74. Szeto ACH, Ferreira ACF, Mannion J, Clark PA, Sivasubramaniam M, Heycock MWD, et al. An αvβ3 integrin checkpoint is critical for efficient T_H2 cell cytokine polarization and potentiation of antigen-specific immunity. *Nat Immunol* (2023) 24(1):123–35. doi: 10.1038/s41590-022-01378-w

75. Zhou Y, Hagood JS, Lu B, Merryman WD, Murphy-Ullrich JE. Thy-1-integrin alphav beta5 interactions inhibit lung fibroblast contraction-induced latent transforming growth factor-beta1 activation and myofibroblast differentiation. *J Biol Chem* (2010) 285(29):22382–93. doi: 10.1074/jbc.M110.126227

76. Woeller CF, O'Loughlin CW, Pollock SJ, Thatcher TH, Feldon SE, Phipps RP. Thy1 (CD90) controls adipogenesis by regulating activity of the src family kinase, fyn. *FASEB J* (2015) 29(3):920–31. doi: 10.1096/fj.14-257121

77. Karagiannis F, Masouleh SK, Wunderling K, Surendar J, Schmitt V, Kazakov A, et al. Lipid-droplet formation drives pathogenic group 2 innate lymphoid cells in airway inflammation. *Immunity* (2020) 52(4):620–634.e6. doi: 10.1016/j.immuni.2020.03.003

78. Xiao Q, He J, Lei A, Xu H, Zhang L, Zhou P, et al. PPARγ enhances ILC2 function during allergic airway inflammation *via* transcription regulation of ST2. *Mucosal Immunol* (2021) 14(2):468–78. doi: 10.1038/s41385-020-00339-6

79. Garrett WS, Lord GM, Punit S, Lugo-Villarino G, Mazmanian SK, Ito S, et al. Communicable ulcerative colitis induced by T-bet deficiency in the innate immune system. *Cell* (2007) 131(1):33–45. doi: 10.1016/j.cell.2007.08.017

80. Gronke K, Kofoed-Nielsen M, Diefenbach A. Isolation and flow cytometry analysis of innate lymphoid cells from the intestinal lamina propria. *Methods Mol Biol* (2017) 1559:255–65. doi: 10.1007/978-1-4939-6786-5_17

81. Schroeder JH, Bell LS, Janas ML, Turner M. Pharmacological inhibition of glycogen synthase kinase 3 regulates T cell development *in vitro*. *PloS One* (2013) 8(3):e58501. doi: 10.1371/journal.pone.0058501

82. Hafemeister C, Satija R. Normalization and variance stabilization of single-cell RNA-seq data using regularized negative binomial regression. *Genome Biol* (2019) 20(1):296. doi: 10.1186/s13059-019-1874-1

83. Finak G, McDavid A, Yajima M, Deng J, Gersuk V, Shalek AK, et al. MAST: a flexible statistical framework for assessing transcriptional changes and characterizing heterogeneity in single-cell RNA sequencing data. *Genome Biol* (2015) 16:278. doi: 10.1186/s13059-015-0844-5

84. Trapnell C, Cacchiarelli D, Grimsby J, Pokharel P, Li S, Morse M, et al. The dynamics and regulators of cell fate decisions are revealed by pseudotemporal ordering of single cells. *Nat Biotechnol* (2014) 32(4):381–6. doi: 10.1038/nbt.2859

85. Qiu X, Mao Q, Tang Y, Wang L, Chawla R, Pliner HA, et al. Reversed graph embedding resolves complex single-cell trajectories. *Nat Methods* (2017) 14(10):979–82. doi: 10.1038/nmeth.4402

frontiers | Frontiers in Immunology

TYPE Review
PUBLISHED 17 October 2023
DOI 10.3389/fimmu.2023.1271699

OPEN ACCESS

EDITED BY
Carolina Jancic,
National Scientific and Technical Research Council (CONICET), Argentina

REVIEWED BY
Mohamad El-Zaatari,
University of Michigan, United States
Luke Roberts,
The University of Manchester, United Kingdom

*CORRESPONDENCE
Đorđe Miljković
djordjem@ibiss.bg.ac.rs

†These authors have contributed equally to this work

RECEIVED 02 August 2023
ACCEPTED 02 October 2023
PUBLISHED 17 October 2023

CITATION
Koprivica I, Stanisavljević S, Mićanović D, Jevtić B, Stojanović I and Miljković Đ (2023) ILC3: a case of conflicted identity. *Front. Immunol.* 14:1271699. doi: 10.3389/fimmu.2023.1271699

ILC3: a case of conflicted identity

Ivan Koprivica†, Suzana Stanisavljević†, Dragica Mićanović, Bojan Jevtić, Ivana Stojanović and Đorđe Miljković*

Department of Immunology, Institute for Biological Research "Siniša Stanković" - National Institute of Republic of Serbia, University of Belgrade, Belgrade, Serbia

Innate lymphoid cells type 3 (ILC3s) are the first line sentinels at the mucous tissues, where they contribute to the homeostatic immune response in a major way. Also, they have been increasingly appreciated as important modulators of chronic inflammatory and autoimmune responses, both locally and systemically. The proper identification of ILC3 is of utmost importance for meaningful studies on their role in immunity. Flow cytometry is the method of choice for the detection and characterization of ILC3. However, the analysis of ILC3-related papers shows inconsistency in ILC3 phenotypic definition, as different inclusion and exclusion markers are used for their identification. Here, we present these discrepancies in the phenotypic characterization of human and mouse ILC3s. We discuss the pros and cons of using various markers for ILC3 identification. Furthermore, we consider the possibilities for the efficient isolation and propagation of ILC3 from different organs and tissues for *in-vitro* and *in-vivo* studies. This paper calls upon uniformity in ILC3 definition, isolation, and propagation for the increased possibility of confluent interpretation of ILC3's role in immunity.

KEYWORDS

innate lymphoid cells, phenotype, flow cytometry, humans, mice

1 Introduction

Group 3 innate lymphoid cells (ILC3s) have been identified as critical regulators of intestinal homeostasis and immune responses to both commensal and pathogenic bacteria in the gut. Subsequent studies showed that ILC3s are present in a variety of tissues and organs, including the lungs, skin, and lymphoid tissues. ILC3s are now recognized as important players in the immune response against different pathogens and are suggested to interfere with the development of inflammatory and autoimmune diseases (1, 2). The discovery of ILC3 has opened new avenues for the study of the role of the innate immune system in health and disease. Overall, the discovery of these cells represents a significant milestone in our understanding of the innate immune system.

ILCs were first identified in the early 2010s by researchers studying the immune system in the intestinal mucosa. Before being classified as a distinct cell population, they had been identified in mice and humans as cells that lack antigen-specific T-cell or B-cell receptors

(TCR or BCR), expressing natural killer (NK) cell markers and producing various cytokines in response to stimulation. There are three populations of ILCs, namely, ILC1, ILC2, and ILC3, broadly corresponding to Th1, Th2, and Th17/Treg cells, respectively. Initially, ILC3s were described as RORγt-dependent NKp46$^+$ NK cells that produce IL-22 and provide mucosal immune defense in the intestine of mice (3–5). At the same time, IL-2-producing NKp44$^+$ NK cells were detected in human mucosa-associated lymphoid tissues, such as tonsils and Peyer's patches (6). Due to the almost simultaneous discovery by several research groups, IL-22-producing natural cytotoxicity receptor-expressing (NCR$^+$) cells have been referred to as NK22 (6, 7), NCR22 (8), NKR-Lti (9), or ILC22 (10). Given the similarities between IL-22-producing NCR$^+$ ILC and NK cells, researchers sought to elucidate their developmental pathways. Although RORγt$^+$ ILCs were originally thought to be a subpopulation of NK cells, cell fate-mapping studies showed that their developmental pathways were distinct. This conclusion is supported by the fact that NK cells do not express RORγt during development (8, 9). Further distinctions between ILC3 and NK cells are observed at the mature stage. Like T helper (Th) 17 cells, ILC3s express RORγt and aryl hydrocarbon receptor (AhR) and produce a high amount of IL-22 in response to IL-23. On the other hand, NK cells from peripheral or cord blood cultured under Th17 conditions with or without AhR ligands are unable to produce IL-22 (6). Additionally, under Th17-polarizing conditions, IL-22-producing NCR$^+$ ILC cells do not produce IL-17 (6). In light of this, it has been suggested that ILC3s and NK cells undergo distinct differentiation pathways.

Since ILC3s express RORγt, another explanation was that they may develop from lymphoid tissue inducer (LTi) cells, previously known to also express RORγt (9). LTi cells are involved in the formation of lymphoid tissue during fetal development in mice and humans. While LTi cells express IL-17 and IL-22, NKp46$^+$ ILCs express only IL-22 (11, 12). Moreover, LTi cells are distinguished from (NKp46$^{+/-}$) ILCs by expressing markers such as CD4, CD25, and CCR6 on their surface (13, 14). In contrast to LTi, which are only found during fetal development, "adult LTi," called LTi-like cells, can be found in the lamina propria of the intestine and in the tonsils, and they arise from bone marrow precursors (15). Although LTi-like cells and LTi are very similar in their expression profile, only the former express OX40L and CD30L (16). Evidence that NCR$^+$ ILCs are a distinct lineage from LTi was provided by studies showing that RORγt$^+$α4β7$^+$ cells develop into CD4$^+$ and CD4$^-$ LTi, whereas RORγt$^+$α4β7$^-$ give rise to IL-22-producing NKp46$^+$ cells in mice (12). Therefore, the term ILC3 was introduced by Spits and colleagues to describe the group 3 ILCs which are distinct from LTi (17). However, it is still not clear if NCR$^+$ ILC3s have a different developmental pathway from LTi. It is generally presumed that LTi cells arise in the fetal liver and are primarily involved in developing lymphoid tissues, while NCR$^+$ ILC3s develop from bone marrow lymphoid progenitors in the gut and lymphoid tissue. Accordingly, RORγt$^+$CD34$^+$α4β7$^+$ hematopoietic progenitor cells have been defined in humans as IL-22$^+$ ILC3-specific precursors (18). Still, there was a report that LTi cells gave rise to ILC3 in fetal lymph nodes (11), thus suggesting that the development of LTi and ILC3 is not strictly divergent. Furthermore, NCR$^+$ ILC3 can be generated from RORγt$^+$ precursors stemming from LTi-like cells. Indeed, in a study on mice, it was shown that NKp46$^+$RORγt$^+$ cells differentiate directly from LTi-like cells (NKp46$^-$RORγt$^+$) (9). Along the same line, it was demonstrated that human RORγt$^+$NKp46$^+$ cells can be generated *in vitro* from LTi-like cells obtained from adult tonsils (19).

As in mice, the development of ILC in humans begins with the common lymphoid progenitor (CLP), characterized as lineage (Lin)$^-$CD34$^+$CD45RA$^+$CD10$^+$KIT$^-$, from which all lymphocyte subsets, including ILC, T, and B cells can develop. Intermediate stages of NK development are also thought to differentiate from this progenitor, at least in secondary lymphoid tissues, such as tonsils and lymph nodes (20). ILC differentiation further leads to the early tonsil progenitor cells (EToP), with two distinct phenotypes, EToP1 (Lin$^-$CD34$^+$CD10$^+$KIT$^-$) or EToP2 (Lin$^-$CD34$^+$CD10$^+$KIT$^+$) (21, 22). EToP2 can be divided into two groups based on ST2 (IL-33R, IL1r1) expression and on their ability to form ILC (21). Unlike ST2$^-$ EToP, which can give rise to T cells and dendritic cells (DCs) *in vitro*, ST2$^+$ EToPs give rise exclusively to ILC, both *in vitro* and *in vivo*, when isolated from pediatric tonsils and injected into immunodeficient NGS mice (22), and cannot give rise to non-ILC cells. Thus, these cells are the earliest human common ILC progenitors identified to date (22). Two other restricted progenitors were identified, one of which is a Lin$^-$CD34$^-$CD7$^+$IL-7R$^+$KIT$^+$ ILC progenitor (ILCP), found in cord blood, fetal liver, peripheral blood, and other human tissues (23). This progenitor is common for ILC3, LTi, and ILC2 cells. Another progenitor, identified downstream of the ILCP, is CD34$^-$KIT$^+$CD56$^+$, termed restricted ILCP (rILCP) (24), and can give rise to NK cells, ILC1, and ILC3, but not to ILC2 cells (25). This may partially explain the ILC plasticity observed in different tissues and under different conditions. Single-cell RNA sequencing of human ILC3 and ILC1 from the tonsils and intestine and bioinformatics analysis (RNA velocity) recently enabled the identification of a cluster of cells that represent a spectrum of cell conversions between ILC3 and ILC1, with a pronounced bias toward ILC1. Cell transfers into humanized mice demonstrated *in-vivo* conversion of ILC3 to ILC1, which occurred preferentially in TGF-β-expressing tissues, such as the spleen (26). As observed in mice, the formation of mature human ILC3 subsets not only occurs during fetal development but can also occur after birth locally in tissues, such as adult tonsils and intestine (19). Different developmental pathways and marked plasticity even in adult ILC complicate their classification into subtypes.

2 Literature survey results

A detailed survey of papers on ILC3 was performed using the PubMed database (https://pubmed.ncbi.nlm.nih.gov/) until 15 June 2023. Searching for "ILC3 mouse" and "ILC3 human" retrieved more than 300 articles each. Papers containing data on ILC3 identification by flow cytometry (121 and 226 for human and mouse ILC3, respectively) were analyzed for the following information: phenotypic markers used for the definition of ILC3, lineage markers used for excluding immune cells other than ILC3, and organ/tissue of ILC3 origin. The obtained information was

compiled in Tables 1, 2, dedicated to human and mouse ILC3, respectively. The overview of the tables shows inconsistency in the markers used for the identification of ILC3, as well as of those used in lineage cocktails for the exclusion of non-ILC3 cells. The most commonly used inclusion markers for human ILC3 are CD117, CD127, and CD161, while CD294 is the most frequently used exclusion marker (Figure 1A). The most frequently used marker combinations for the identification of human ILC3 are 1) $CD127^+CD117^+CD294^-$, 2) $CD127^+CD117^+CD161^+CD294^-$, and 3) $CD127^+CD117^+$ (Figure 1B). The most commonly used markers for mouse ILC3 are RORγt, CD127, and CD90 (Figure 1C), while the prevalent combinations are $CD127^+$RORγt$^+$ and $CD90^+$RORγt$^+$ (Figure 1D). A detailed list of the markers and their combinations is given in Table 3. Interestingly, RORγt is frequently used as a single marker for ILC3 identification in mice and is by far the predominantly used marker for ILC3 in mouse, but not in human samples (*vide infra*). The adequacy of the phenotypic markers used for defining ILC3 in relation to the tissue/organ of their origin is discussed in the following chapters.

3 Lineage cocktails

CD3 is a marker that is targeted by almost all lineage cocktails. Additionally, in some of the mouse studies, CD3 is the only negative marker used for ILC3 identification. The logic behind this strategy is clear when RORγt is used as the key positive ILC3 marker. As RORγt is expressed by T cells and ILC3 (346), the latter can be identified as $CD3^-$RORγt$^+$ cells. It is known that human bone marrow and blood neutrophils, as well as mouse lung neutrophils, can express RORγt (347, 348). However, neutrophils are easily distinguished from the lymphocytic populations by flow cytometry using forward and side scatter. Also, there is a report on a RORγt-expressing DC subset in the spleen (349), while the existence of a similar subset was not confirmed in the intestine (98). Thus, CD3 and RORγt can be used as the basic discriminators of ILC3 in the murine intestine, but not the spleen. As for human samples, it seems that RORγt can be expressed by all ILC subsets, as well as by NK cells (24), thus making it an unsuitable marker for ILC3 discrimination.

Other T-cell markers can be used instead of CD3, such as TCRαβ and TCRγδ. Lineage cocktails used in some studies contained both CD3- and TCR-specific antibodies, even though this combination seems redundant having in mind that CD3 already defines all TCR-positive cells. Additionally, CD4 and CD8a were used as lineage markers in some studies. While there are no data on the expression of CD8 in ILC3, there are studies showing that the LTi ILC3 subset can express CD4 (160, 350), thus making CD4 inadequate as a lineage marker. Also, there are data on the expression of RORγt by $CD3^+CD4^-CD8^-$ cells in patients with systemic lupus erythematosus and psoriasis (351, 352), which contribute to the view that CD3, and not CD4 and CD8, should be used in lineage cocktails. CD5-specific antibodies are also frequently used in mice, as this marker is specific for T cells and a subset of B cells.

The second most commonly used lineage markers are B-cell markers, including B220 (CD45RA) and CD19. CD45RA is an isoform of CD45, a molecule expressed on all types of hematopoietic cells except mature erythrocytes and platelets (353). Although it is expressed in mouse DC (354), naive T cells (355), and T cells undergoing apoptosis (356, 357), it is considered a pan-B-cell marker in mice, present on pre-B cells and at all stages of B-cell maturation (358), making it a suitable negative marker for phenotyping ILC. CD19 is a molecule belonging to the immunoglobulin superfamily, and its expression is specific to normal and neoplastic B cells, as well as follicular DC (359). Both B220 and CD19 molecules are suitable B-cell markers in mice, whereas in humans, B220 is detected on ILC3 in the blood and cord blood, with heterogeneous expression in tonsillar, intestinal, and lung ILC3 (360). Therefore, CD19, and not B220, should be used as a B-cell-related lineage component for human ILC detection.

The most challenging distinction is the one between NK and ILC3 cells. NK cells and ILC share the same progenitor, while the mature forms of ILC also share some markers with NK cells. For instance, ILC1, some ILC3, and NK cells express T-bet. Therefore, it is important to distinguish these cells when detecting ILC3. NK1.1-specific antibodies are frequently used in mice lineage cocktails, while CD94 (Klrd1) is preferentially used in human samples to exclude NK cells, although the use of NKG2A has also been reported in some studies. Additionally, CD56 is used to exclude NK cells and other immune cells able to express this molecule, such as T cells, DC, and monocytes (361). Some researchers also use markers specific for lymphocyte subpopulations, such as CD49b for some T cells (Tr1, NKT), Klrg1 for effector memory $CD8^+$ T and NK cells, or CD27 for activated effector T cells, NK cells, and activated B cells. One important issue is that different mouse strains carry different NK-related markers. For example, the Balb/c strain lacks NK1.1 (362), so CD49b can be used for the determination of NK cells.

CD11b, CD11c, Gr1, Ly6G, Ly6C, and Ly6B are markers that are used in lineage cocktails to eliminate monocytes, DC, granulocytes, macrophages, NK cells, and subsets of T and B cells. Additionally, F4/80 is a relevant marker of murine macrophages. FcεRIα is also used to detect epidermal Langerhans cells, eosinophils, mast cells, basophils, and various antigen-presenting cells. However, there are reports on ILC3 expressing CD11b and CD11c (27), thus compromising their use in lineage cocktails. Finally, Ter119 is routinely used to exclude erythrocytes from analyses.

Different lineage cocktails can be used while studying ILC3. It is on the researchers to make the best choice for a particular species and tissue in which ILC3s are being detected. It seems that the uncritical use of redundant markers in the lineage cocktails does not improve the efficacy of ILC3 detection, while the use of markers that are potentially expressed by ILC3 increases the risk of excluding some ILC3 subpopulations from the analysis. So, the advice on lineage cocktails might be the following: keep it simple and efficient.

4 Markers used for the discrimination of ILC3

Various markers are used, alone or in combination, to identify ILC3. CD45 is a marker of hematopoietic cells and is, therefore,

TABLE 1 Phenotypic characterization of human ILC3.

Phenotype	Lineage	Tissue/organ	Reference
$CD103^-$	CD3, CD19	Tonsils	(27)
$CD117^+$	CD3, CD19, CD34, CD94	Tonsils	(28)
$CD117^+$	CD94/NKG2A	UCB	(29)
$CD117^+CD294^-$	CD3, CD19, CD16, CD62L	Ileum	(30)
$CD117^+CD294^-$	CD3, CD1a, CD11c, CD14, CD19, CD34, CD123, TCRαβ, TCRγδ, CD303, FcεR1α, CD94	PB	(31)
$CD117^+ROR\gamma t^+$	$CD94/NKG2A^-$	UCB	(32)
$CD117^+ROR\gamma t^+$	CD14, CD19, CD3, CD11b, CD11c, TCRγδ	Colon	(33)
$CD127^+$	CD3	Intestine	(34)
$CD127^+$	CD3	Colon LP	(35)
$CD127^+CD117^+$	CD1a, CD3, CD14, CD19, CD94, CD34, CD123, TCRαβ, TCRγδ, CD303, FcεR1α	Tonsils, intestine, mLN	(36)
$CD127^+CD117^+$	CD3, CD5, CD14, CD19, CD11c	Colon	(37)
$CD127^+CD117^+$	Data not found	Colon	(38)
$CD127^+CD117^+$	CD3, CD19, CD14, CD28, CD11c	PBMC	(39)
$CD127^+CD117^+$	CD19, CD11b, CD11c, CD3, CD5, CD14, FcεR1α,	Colon	(40)
$CD127^+CD117^+$	CD1a, CD3, CD14, CD19, CD20, CD203c	Nasal epithelium	(41)
$CD127^+CD117^+$	CD3, CD4, CD5, TCRαβ, TCRγδ, CD33, CD14, CD19, CD235a	mLN	(42)
$CD127^+CD117^+CD294^-$	CD3, CD20, CD13, CD123, CD303, CD34, FcεR1α, CD11c	Colon LP, tonsils	(43)
$CD127^+CD117^+CD161^+$	CD3, TCRαβ, TCRγδ, CD34, CD123, CD94, CD14, CD303, FcεR1α, CD1a, CD11c, CD19, B220	PB, UCB, tonsils	(44)
$CD127^+CD117^+CD161^+$	CD3, CD4, CD19, CD20, CD14, CD34, CD11c, CD94	Tonsils, PB	(45)
$CD127^+CD117^+CD161^+CD294^-$	CD3, CD14, CD16, CD20, CD56	PB	(46)
$CD127^+CD117^+CD161^+CD294^-$	CD1a, CD3, CD14, CD19, CD34, CD94, CD123, FcεR1α, TCRαβ, TCRγδ, CD303	PBMC, tonsils	(47)
$CD127^+CD117^+CD161^+CD294^-$	CD1a, CD34, CD3, TCRαβ, TCRγδ, CD14, CD19, CD16, CD94, CD123, CD303, FcεR1α	PB	(48)
$CD127^+CD117^+CD161^+CD294^-$	CD3, CD4, CD14, CD16, CD19, CD21, CD94, CD11c, CD123, CD303	PBMC	(49)
$CD127^+CD117^+CD161^+CD294^-$	CD3, TCRαβ, TCRγδ, CD34, CD123, CD94, CD14, CD303, FcεR1α, CD1a, CD11c, CD19, B220	PBMC	(50)
$CD127^+CD117^+CD161^+CD294^-$	CD3, TCRαβ, TCRγδ, CD34, CD123, CD94, CD14, CD303, FcεR1α, CD1a, CD11c, CD19, B220	UCB	(51)
$CD127^+CD117^+CD161^+CD294^-$	CD3, CD19, CD20, CD14, CD11c	PB	(52)
$CD127^+CD117^+CD161^+CD294^-$	CD1a, CD3, CD4, CD8, CD14, CD16, CD19, CD34, CD94, CD303, TCRαβ, TCRγδ, FcεR1α	Thymus	(53)

(Continued)

10.3389/fimmu.2023.1271699

TABLE 1 Continued

Phenotype	Lineage	Tissue/organ	Reference
$CD127^+CD117^+CD161^+CD294^-$	CD3, CD14, CD19, CD20, CD94, FcεR1α, TCRαβ, TCRγδ, CD123, CD34	Spleen, PBMC	(54)
$CD127^+CD117^+CD161^+CD294^-$	CD3	PBMC	(55)
$CD127^+CD117^+CD294^-$	CD1a, CD3, CD11c, CD14, CD19, CD34, CD94, CD123, CD303, FcεR1α, TCRαβ, TCRγδ	PBMC, skin	(56)
$CD127^+CD117^+CD294^-$	CD1a, CD3, CD4, CD5, CD14, CD19, CD16, CD34, CD94, CD123, CD303, TCRαβ, TCRγδ, FcεR1α	PB, UCB	(57)
$CD127^+CD117^+CD294^-$	CD3, CD19, CD11b, CD11c	Bladder	(58)
$CD127^+CD117^+CD294^-$	CD3, CD14, CD16, CD19, CD20, CD56	Abdominal fat, PBMC	(59)
$CD127^+CD117^+CD294^-$	CD3, CD19	Distal ileum	(60)
$CD127^+CD117^+CD294^-$	CD3, CD19, CD94, CD14, CD34, CD303	PB, tonsils	(61)
$CD127^+CD117^+CD294^-$	CD3, CD4, CD14, CD16, CD19, CD8, CD15CD20, CD33, CD34, CD203c, FcεR1α	Lip tissue	(62)
$CD127^+CD117^+CD294^-$	CD1a, CD8, CD19, CD3, CD4, CD14, CD16, CD34, CD123, TCRαβ, TCRγδ,	PB	(63)
$CD127^+CD117^+CD294^-$	CD1a, CD3, CD14, CD11c, CD19, CD34, CD94, CD123, CD303, FcεR1α, TCRαβ, TCRγδ	Entheseal tissue	(64)
$CD127^+CD117^+CD294^-$	CD34, CD3, CD19, FcεR1α, CD123, CD94, CD14, CD11c, CD1a, CD303	PBMC	(65)
$CD127^+CD117^+CD294^-$	CD3, CD19, CD14, TCRαβ, TCRγδ, CD94, CD16, FcεR1α, CD34, CD123, CD303	PBMC	(66)
$CD127^+CD117^+CD294^-$	CD34, CD3, CD19, FcεR1α, CD123, CD94, CD14, CD11c, CD1a, CD303	PB	(67)
$CD127^+CD117^+CD294^-$	CD3, CD1a, CD14, CD19, TCRαβ, TCRγδ, CD1, CD303, FcεR1α, CD235α, CD66b, CD34, CD20, CD94	UCB, tonsils	(68)
$CD127^+CD117^+CD294^-$	Data not found	PB	(69)
$CD127^+CD117^+CD294^-$	CD3, CD14, CD19, CD11c, CD303a, CD15, CD203c, FcεR1α	PBMC	(70)
$CD127^+CD117^+CD294^-$	CD1a, CD34, CD3, TCRαβ, TCRγδ, CD14, CD19, CD16, CD94, CD123, CD303, FcεR1α	PB	(71)
$CD127^+CD117^+CD294^-$	CD3, CD4, CD8, CD14, CD15, CD16, CD19, CD20, CD33, CD34, CD203c, FcεR1α	PBMC	(72)
$CD127^+CD117^+CD294^-$	CD3, CD19, CD94, CD1a, CD11c, CD123, CD303, CD14, FcεR1α, CD34	Tonsils	(73)
$CD127^+CD117^+CD294^-$	CD1a, CD3, CD4, CD56, CD16, CD11c, CD14, CD19, CD94, CD34, CD123, TCRαβ, TCRγδ, CD303, FcεR1α	PB	(74)
$CD127^+CD117^+CD294^-$	CD3	PB	(75)
$CD127^+CD294^-$	CD3, CD19, CD14, CD94	Tonsils	(19)
$CD127^+IL\text{-}23R^+$	CD2, CD3, CD14, CD16, CD19, CD56, CD235a	PBMC	(76)
$CD127^+ROR\gamma t^+$	CD15, CD14, CD3, CD19, CD56, CD11b	Decidua	(77)
$CD300LF^+CD196^+$	CD3, CD19	Tonsils	(26)
$CD336^+$	CD3, CD14, CD19, CD20, CD94	UCB	(78)

(Continued)

10.3389/fimmu.2023.1271699

TABLE 1 Continued

Phenotype	Lineage	Tissue/organ	Reference
$CD336^+CD56^+$	CD3, CD1a, CD14, CD19, TCRαβ, TCRγδ, CD123, CD303, FcεR1α, CD235a, CD66b, NKG2A	UCB	(79)
$CD45^+$	CD3, CD4, CD8, CD56, CD14, CD19, TCRγδ	Ileum	(80)
$CD45^+CD117^+$	CD3, CD5, CD14, FcεR1α, CD11b, CD11c, CD19	Colon LP	(13)
$CD45^+CD117^+$	CD3, CD14, CD19, CD56, CD34, CD11a, CD94	UCB	(81)
$CD45^+CD117^+CD294^-$	TCRαβ, TCRγδ, CD19, CD94, CD1a, CD123, CD14, CD303, FcεR1α, CD34	PBMC, ileum/colon	(82)
$CD45^+CD117^+CD294^-$	CD3, CD19, CD20	PB, skin	(83)
$CD45^+CD127^+$	CD19, CD14, CD3	Decidua, tonsils, PBMC	(84)
$CD45^+CD127^+$	CD3, CD14, CD19, CD20, CD123, CD141, FcεR1α	Tonsils, colon	(85)
$CD45^+CD127^+$	CD3, CD14, CD16, CD19, CD20, CD56	PBMC	(86)
$CD45^+CD127^+$ $CD117^+CD294^-$	CD3, CD5, CD11c, CD16, CD19, TCRαβ	PBMC	(87)
$CD45^+CD127^+CD117^+CD294^-$	CD3, CD5, CD11b, CD11c, CD14, CD16, CD19, CD34, CD123, FcεR1α	PBMC	(88)
$CD45^+CD127^+$ $CD117^+CD294^-$	CD1a, CD3, CD4, CD14, CD16, CD19, CD34, CD303, FcεR1α	PB	(89)
$CD45^+CD127^+CD117^+$	CD3, CD14, CD19, CD34	Inguinal LN	(90)
$CD45^+CD127^+CD117^+$	CD3ε, CD11c, CD11b, CD14, CD19, CD49b, FcεR1α	Sputum, PB	(91)
$CD45^+CD127^+CD117^+$	CD34, CD19, CD20, CD3, CD16, CD14, CD11c, CD123	PB	(92)
$CD45^+CD127^+CD117^+$	CD3, CD19, CD11c, CD11b	Lung	(93)
$CD45^+CD127^+CD117^+$	CD3, CD14, CD19, CD20	Duodenum	(94)
$CD45^+CD127^+CD117^+$	CD19, CD3, CD1a, CD11b, CD34, FcεR1α, CD14, CD11c, CD94	Distal ileum	(95)
$CD45^+CD127^+CD117^+$	CD3, CD11b, CD11c, CD14, CD19, CD34, CD94, CD123, FcεR1α	Tonsils, intestine	(96)
$CD45^+CD127^+CD117^+$	CD3, CD19, CD94, CD14, CD16, CD1a, CD303, CD123, FcεR1α, CD34	Periodontal ligament tissues	(97)
$CD45^+CD127^+CD117^+$	CD3, CD11c, CD14, CD19, CD34, CD94, CD123, FcεR1α	Colon	(98)
$CD45^+CD127^+CD117^+$	CD1a, CD3, CD11c, CD14, CD19, CD94, CD34, CD123, TCRαβ, TCRγδ, CD303, FcεR1α	Tonsils, LP	(99)
$CD45^+CD127^+CD117^+$	CD11b, CD11c, B220, CD3ε, CD5, CD8α	Terminal ileum	(100)
$CD45^+CD127^+CD117^+$	CD34, CD19, CD14, CD3, CD94	Decidua	(101)
$CD45^+CD127^+CD117^+$	CD34, CD14, CD19, CD3, CD94	Decidua	(102)
$CD45^+CD127^+CD117^+$	CD19, CD14, CD3, CD94	Decidua	(103)
$CD45^+CD127^+CD117^+$	CD3, CD4, CD5, CD14 CD16, CD19, TCRαβ, TCRγδ, CD94, NKG2A	PB	(104)

(Continued)

10.3389/fimmu.2023.1271699

TABLE 1 Continued

Phenotype	Lineage	Tissue/organ	Reference
$CD45^+CD127^+CD117^+CD161^+$	CD3, TCRαβ, TCRγδ, CD14, CD16, CD19, CD94, FcεR1α, CD123, CD303	Tonsils	(105)
$CD45^+CD127^+CD117^+CD161^+$	CD3, CD19	Colonic mucosa, PBMC	(106)
$CD45^+CD127^+CD117^+CD161^+CD294^-$	CD14, CD1a, CD3, CD34, CD123, FcεR1α, TCRαβ, TCRγδ, CD303, CD19	Tonsils, ileum/colon	(107)
$CD45^+CD127^+CD117^+CD161^+CD294^-$	CD3	PB	(108)
$CD45^+CD127^+CD117^+CD161^+CD294^-$	CD3, CD14, FcR1α, CD34, CD123, CD1a, TCRαβ, TCRγδ, CD94, CD303, CD19	Tonsils	(109)
$CD45^+CD127^+CD117^+CD161^+CD294^-$	CD1a, CD3, CD14, CD16, CD19, CD34, CD94, CD123, CD303, FcεR1α, TCRαβ, TCRγδ,	Skin, PBMC	(110)
$CD45^+CD127^+CD117^+CD161^+CD294^-$	CD1a, CD3, CD4, CD8, CD14, CD16, CD19, CD34, CD94, CD123, CD303, FcεR1α, TCRαβ, TCRγδ	PBMC, tonsils, UCB, bone marrow	(111)
$CD45^+CD127^+CD117^+CD161^+CD294^-$	CD1a, CD3, CD14, CD19, FcεR1α, CD34, CD123, CD94, CD303, TCRαβ, TCRγδ	Tonsils, PBMC	(112)
$CD45^+CD127^+CD117^+CD161^+CD294^-$	CD1a, CD3, CD11c, CD14, CD16, CD19, CD34, CD123, FcεR1α, NKp80, CD303, TCRαβ, TCRγδ	Intestine, colon, PB	(113)
$CD45^+CD127^+CD117^+CD161^+CD294^-$	CD1a, CD4, TCRαβ, TCRγδ, CD3, CD11c, CD14, CD94, CD19, CD123, CD303, CD34, FcεR1α, CD16	PB	(114)
$CD45^+CD127^+CD117^+CD161^+CD294^-$	CD3, CD4, CD19, CD94, CD1a, CD11c, CD123, BDAC2, CD14, CD34, FcεR1α	PBMC	(115)
$CD45^+CD127^+CD117^+CD161^+CD294^-$	CD11c, CD123, CD14, CD19, CD1a, CD3, CD303a, CD94, FcεR1α, TCRαβ, TCRγδ, CD34	Colon, PBMC	(116)
$CD45^+CD127^+CD117^+CD161^+CD294^-$	Without	PB	(117)
$CD45^+CD127^+CD117^+CD161^+CD294^-$	CD3, CD4, CD19, CD11b	PBMC	(118)
$CD45^+CD127^+CD117^+CD161^+CD294^-$	CD3, CD45CD19, CD14, CD1a, CD94, CD34	PB	(119)
$CD45^+CD127^+CD117^+CD161^+CD294^-$	CD3, CD1CD11c, CD34, CD123, TCRγδ, TCRαδ, CD303, FcεR1α, CD19, CD14, CD94	PB, UCB, placenta	(120)
$CD45^+CD127^+CD117^+CD294^-$	CD3, CD4, CD8, CD11c, CD14, CD19, CD34, CD94, CD123, FcεR1α	Ileum, colon	(121)
$CD45^+CD127^+CD117^+CD294^-$	CD3, CD14, CD19, CD11b, CD11c, CD49b, FcεR1α	Terminal ileum, colon	(122)
$CD45^+CD127^+CD117^+CD294^-$	CD3, CD16, CD19, CD20, CD14, CD56	Thymus, PB	(123)
$CD45^+CD127^+CD117^+CD294^-$	CD3, CD11c, CD14, CD16, CD19, CD20, CD34, CD56, CD94, FcεR1α	PB	(124)
$CD45^+CD127^+CD117^+CD294^-$	CD3, CD19, CD11c, CD11b, CD14	Ileal LP, PBMC	(125)
$CD45^+CD127^+CD117^+CD294^-$	CD3, CD11c, CD14, CD16, CD19, CD34	PBMC	(126)
$CD45^+CD127^+CD117^+CD294^-$	CD3, CD5, CD11b, CD11c, CD19, FcεR1α	Intestine	(127)
$CD45^+CD127^+CD117^+CD294^-$	CD3, CD14, CD16, CD19, CD20, CD56	PB	(128)
$CD45^+CD127^+CD117^+CD294^-$	CD3, CD14, CD19, CD303, CD123, CD1a, TCRαβ, TCRγδ, CD34, FcεR1α,	PB	(129)
$CD45^+CD127^+CD117^+CD294^-$	CD3, CD19, CD14, CD34, CD94, CD123, TCRαβ, TCRγδ, FcεR1α	Liver, PB	(130)
$CD45^+CD127^+CD117^+CD294^-$	CD3, CD14, CD16, CD19, CD20, CD56	PB	(131)

(Continued)

10.3389/fimmu.2023.1271699

TABLE 1 Continued

Phenotype	Lineage	Tissue/organ	Reference
$CD45^+CD127^+CD117^+CD294^-$	TCRγδ, TCRαβ, CD3, CD19, CD14, CD16, CD94, CD123, CD34, CD303, FcεR1α	Intestine, PB	(132)
$CD45^+CD127^+CD117^+CD294^-$	Data not found	PBMC	(133)
$CD45^+CD127^+CD117^+CD294^-$	CD3, CD14, CD19, CD20	Terminal ileum LP, PBMC	(134)
$CD45^+CD127^+CD117^+CD294^-$	CD3, CD14, CD19, CD94	PB	(135)
$CD45^+CD127^+CD117^+CD294^-$	CD3, CD14, CD16, CD19, CD20, CD56	PBMC	(136)
$CD45^+CD127^+CD117^+CD294^-$	CD3, CD11c, CD14, CD16, CD19, CD20, CD34, CD56, CD94, FcεR1α	PBMC	(137)
$CD45^+CD127^+CD117^+CD294^-$	CD14, CD16, CD19, FcεR1α, CD3, CD34, CD123, CD1a, CD303, TCRαβ, TCRγδ, CD94	Tonsils	(138)
$CD45^+CD127^+CD117^+CD294^-$	CD11b, CD14, CD16, CD303a, TCRαβ, TCRγδ, CD19, CD123, CD34, FcεR1α, CD1a, CD94, CD3, CD20, CD11c	PB	(139)
$CD45^+CD127^+CD117^+CD294^-$	CD3, CD19, CD14, CD34, CD94	LN, spleen, tonsils, PB	(140)
$CD45^+CD127^+CD117^+CD294^-$	CD1a, CD3, CD4, CD11c, CD14, CD19, CD34, CD123, TCRαβ, TCRγδ, CD303, FcεR1α, CD94	PB, skin	(141)
$CD45^+CD127^+CD117^+$ $CD294^-$	CD3, CD19, CD14, CD11c, CD123, CD34, FcεR1α, CD94, TCRαβ	PB	(142)
$CD45^+CD127^+CD117^+CD294^-$	CD3, CD19, CD14, CD11c, CD123, CD34, FcεR1α, TCRαβ, CD94	PB	(143)
$CD45^+CD127^+CD117^+CD294^-$	CD3, CD11c, CD14, CD19, CD34, CD94, CD123, FcεR1α	PB, peritoneal fluid, endometrium	(144)
$CD45^+CD127^+CD294^-$	CD3, TCRαβ, TCRγδ, CD14, CD19, CD20, CD94, NKp80, CD16, CD1a, CD12, FcεR1α, $BDCA^-2$	Liver, tonsils, colon, blood	(145)
$CD45^+CD127^+ROR\gamma t^+$	CD3, TCRαβ, CD20, CD11c, CD11b, CD123, CD303, CD14, FcεR1α, CD31, CD34.	Endomyocardium	(146)
$CD45^+CD127^+ROR\gamma t^+$	CD3, CD5, CD19	Cerebrospinal fluid	(147)
$CD45^+CD127^+ROR\gamma t^+$	CD3, CD5, CD11b, CD11c, CD14, FcεR1α	BALF, lungs	(148)
$ROR\gamma t^+$	CD3, CD14, CD16, CD19, CD20, CD56	PB	(149)

BALF, bronchoalveolar fluid; LN, lymph node; LP, lamina propria; mLN, mesenteric lymph node; PB, peripheral blood; PBMC, peripheral blood mononuclear cell; UCB, umbilical cord blood.

10.3389/fimmu.2023.1271699

TABLE 2 Phenotypic characterization of mouse ILC3.

Phenotype	Lineage	Tissue/organ	Reference
CD117$^+$CD4$^+$	CD3, CD19	PBMC	(150)
CD117$^+$RORγt$^+$	Data not found	SI LP	(151)
CD117$^+$RORγt$^+$	CD3, CD8α, CD11c, CD19, B220, Ly6G/6C, TCRβ, TCRγδ, NK1.1	Spleen	(152)
CD127$^+$CD117$^+$	CD3, B220, CD11b, Ter119, Ly6G	Aorta, spleen	(153)
CD127$^+$CD117$^+$RORγt$^+$	Data not found	Fetal spleen	(154)
CD127$^+$CD117$^+$RORγt$^+$	CD3	Neonatal SI LP	(155)
CD127$^+$CD117$^+$RORγt$^+$	NK1.1	PL	(156)
CD127$^+$Id2$^+$	CD3, CD19, CD4, CD5, CD8, TCRβ, TCRγδ, NK1.1, CD11b, Ly6G/6C, CD11c, Ter119, NK1.1, Bcl11b	Lung	(157)
CD127$^+$IL-22$^+$	CD3	SI LP	(158)
CD127$^+$KLRG$^-$	CD19, CD3, CD11c, CD25, Ly6G/6C	Lung	(159)
CD127$^+$RORγt$^+$	CD3	SI LP	(160)
CD127$^+$RORγt$^+$	CD3ε, CD5, CD19, B220, Ly6G/6C	SI LP	(161)
CD127$^+$RORγt$^+$	CD3, B220, CD5, NK1.1, CD11b, CD11c	Colon, mLN	(40)
CD127$^+$RORγt$^+$	CD3, B220, CD11b, Ly6G, Ter119	Skin	(162)
CD127$^+$RORγt$^+$	CD3, B220, CD11c, CD11b, CD5	Ear skin, auricular LN, SI LP, lung, mLN	(163)
CD127$^+$RORγt$^+$	CD3ε, CD5, CD19, B220, CD11b, CD11c, Ter119, F4/80, Ly6G/6C, CD49b, FcεR1α	Liver, spleen	(65)
CD127$^+$RORγt$^+$	Data not found	SI LP	(164)
CD127$^+$RORγt$^+$	CD3ε, CD8α, CD19, B220, CD11c, CD11b, Ter119, Ly6G/6C, TCRβ, TCRγδ, NK1.1	Blood	(165)
CD127$^+$RORγt$^+$	TCRγδ, CD3ε, CD19, CD5, Ly6G/6C, Ter119	SI LP	(166)
CD127$^+$RORγt$^+$	CD3, CD19	SI	(167)
CD127$^+$RORγt$^+$	CD3, B220, CD11b, Ter119, Ly6G/6C, CD11c, NK1.1, CD8α, CD4	Spleen	(168)
CD127$^+$RORγt$^+$	Data not found	Blood, spleen, kidney	(169)
CD127$^+$RORγt$^+$	B220, CD3, CD5, CD11b, CD11c, CD19, CD49b, CD123, F4/80, FcεR1α, Ly6G/6C, Ter119, CD8α, CD3i	Thymus, mLN	(170)
CD127$^+$RORγt$^+$	Data not found	Lung	(171)
CD127$^+$RORγt$^+$KLRG1$^-$	CD3, CD5, CD11b, CD11c, B220	SI	(172)
CD127$^+$RORγt$^+$	CD3, CD8α, CD19, Ly6G/6C	SI LP	(173)
CD45$^+$CD117$^+$RORγt$^+$	CD3, Ly6G/6C, CD11b, B220, Ter119	Colon	(174)
CD45$^+$CD117$^+$RORγt$^+$	CD3, CD8, CD11b, CD19, MHC II, F4/80, CD161, Ly6G, F4/80	Neonatal lung	(175)
CD45$^+$CD127$^+$	CD3, NK1.1	SI LP	(176)
CD45$^+$CD127$^+$	CD3, CD19, CD8α, CD11b, CD4, NK1.1	SI	(177)
CD45$^+$CD127$^+$	Data not found	Colon LP	(178)
CD45$^+$CD127$^+$	NK1.1, other data not found	SI LP	(179)
CD45$^+$CD127$^+$CD117$^+$	CD3, CD19, CD11c, CD11b, Ly6G/6C, NK1.1	SI LP	(180)
CD45$^+$CD127$^+$CD117$^+$	Data not found	Colon, SI	(181)
CD45$^+$CD127$^+$CD117$^+$	CD3, CD19, B220, CD11b, Ly6G/6C, CD11c, TCRβ, TCRγδ	Colon LP	(182)
CD45$^+$CD127$^+$CD117$^+$RORγt$^+$	CD3ε, CD11b, B220, Ter119, Ly6G/6C, ICOS	Lung	(183)
CD45$^+$CD127$^+$CD117$^+$RORγt$^+$	CD3ε, CD11b, B220, Ter119, Ly6G/6C	SI LP	(184)
CD45$^+$CD127$^+$CD117$^+$CD4$^+$RORγt$^+$	CD3, other data not found	LP	(185)
CD45$^+$CD127$^+$CD117$^+$RORγt$^+$IL-23R$^+$	CD3, CD19, CD11c, Ly6G, F4/80, CD14, NK1.1	PL, LP, spleen	(186)
CD45$^+$CD127$^+$CD25$^+$	CD3, CD5, CD8, NK1.1, B220, CD11c, CD11b	mLN	(13)
CD45$^+$CD127$^+$CD4$^+$	CD3	Spleen	(187)

(Continued)

10.3389/fimmu.2023.1271699

TABLE 2 Continued

Phenotype	Lineage	Tissue/organ	Reference
CD45$^+$CD127$^+$RORγ$^+$	NK1.1, other data not found	Pooled spleen, lung, intestine, peripheral LN	(188)
CD45$^+$CD127$^+$RORγt	CD3, Ly6G/6C, CD11b, B220, Ter119	Lungs	(189)
CD45$^+$CD127$^+$RORγt$^+$	CD8, CD3ε, TCRβ, TCRγδ, B220, Ter119, Ly6G/6C, NK1.1	Bladder, kidney, SI	(190)
CD45$^+$CD127$^+$RORγt$^+$	CD3, B220, CD11b, Ter119, Ly6G/6C	SI	(191)
CD45$^+$CD127$^+$RORγt$^+$	ICOS, other data not found	Lung	(192)
CD45$^+$CD127$^+$RORγt$^+$	Data not found	Colon LP	(193)
CD45$^+$CD127$^+$RORγt$^+$	CD3ε, TCRβ, CD19	Colon	(194)
CD45$^+$CD127$^+$RORγt$^+$	CD19, CD3, CD5, F4/80, FcεR1α, Ly6G/6C	SI	(195)
CD45$^+$CD127$^+$RORγt$^+$	CD3ε, B220, Ly6G/6C, CD11c, CD11b, Ter119, FcεR1α	Liver	(196)
CD45$^+$CD127$^+$RORγt$^+$	CD3, CD11b, CD11c, B220, Ter119, FcεR1α, T-bet	SI	(197)
CD45$^+$CD127$^+$RORγt$^+$	Data not found	Colon LP	(198)
CD45$^+$CD127$^+$RORγt$^+$	CD3, NK1.1, CD11b, Ter119, Ly6G/6C, CD11c, B220	Colon LP	(199)
CD45$^+$CD127$^+$RORγt$^+$	CD3ε, CD5, CD8α, NK1.1, CD11c, CD11b, B220	SI LP	(127)
CD45$^+$CD127$^+$RORγt$^+$	CD3, CD19, Ly6G/6C	Meninges	(200)
CD45$^+$CD127$^+$RORγt$^+$	CD3, CD19	Colon LP, SI LP PP	(201)
CD45$^+$CD127$^+$RORγt$^+$	CD3	SI LP	(202)
CD45$^+$CD127$^+$RORγt$^+$	Data not found	SI LP	(203)
CD45$^+$CD127$^+$RORγt$^+$	CD3, CD4, CD19, NK1.1, CD11b, CD11c, Ly6G/6C, F4/80, Ter119	SI LP	(204)
CD45$^+$CD127$^+$RORγt$^+$	TCRβ, TCRδ, CD19, CD11c, CD11b, Ly6G/6C, Ter119	SI LP	(205)
CD45$^+$CD127$^+$RORγt$^+$	B220, CD3, CD5, CD11b, CD11c	mLN	(206)
CD45$^+$CD127$^+$RORγt$^+$	CD3, CD19	SI LP	(207)
CD45$^+$CD127$^+$RORγt$^+$	CD3	SI LP	(100)
CD45$^+$CD127$^+$RORγt$^+$	CD3ε, CD5, F4/80, CD11b, CD19, Ly6G	Lung, bone marrow, SI LP	(148)
CD45$^+$CD127$^+$RORγt$^+$	CD3	SI LP, colon LP	(208)
CD45$^+$CD127$^+$RORγt$^+$	CD3, CD4, CD5, CD11b, CD11c, CD19, B220, F4/80, FcεR1α, Ly6G/6C, TCRβ, TCRγδ, Ter119	Lung, intestine	(209)
CD45$^+$CD127$^+$RORγt$^+$	CD3, B220, CD11b, Ter119, Ly6G/6C	SI LP	(210)
CD45$^+$CD127$^+$RORγt$^+$	CD3, CD19, CD11c	Spleen	(210)
CD45$^+$CD127$^+$RORγt$^+$	CD3, B220, CD19, CD11b, Ter119, Ly6G/6C, CD5, FcεR1α	Colon LP, SI LP	(211)
CD45$^+$CD127$^+$RORγt$^+$	CD3, B220, CD19, CD11b, Ter119, Ly6G/6C, CD5, FcεR1α	Colon LP, SI LP	(212)
CD45$^+$CD127$^+$RORγt$^+$	CD3, Ly6G/6C, CD11b, B220, Ter119	Lung	(213)
CD45$^+$CD127$^+$RORγt$^+$	CD3, CD4, CD14, CD16, CD19, CD8, CD15, CD20, CD34, CD203	Meninges	(147)
CD45$^+$CD127$^+$RORγt$^+$	CD3, CD19	SI	(214)
CD45$^+$CD127$^+$RORγt$^+$	CD3, CD19, NK1.1, CD11b	Liver	(215)
CD45$^+$CD127$^+$RORγt$^+$	CD3	SI	(216)
CD45$^+$CD127$^+$RORγt$^+$	CD11b, CD3ε, B220, SiglecF, FcεR1α	Lung	(217)
CD45$^+$CD127$^+$RORγt$^+$	CD3, CD4, CD11b, CD11c, CD19, CD49b, F4/80, FcεR1α	Colon	(122)
CD45$^+$CD127$^+$RORγt$^+$	Data not found	mLN, inguinal LN	(218)
CD45$^+$CD127$^+$RORγt$^+$KLRG1$^-$	CD5, CD8α, CD3, Ly6G/6C, TCRγδ, FcεR1α, CD19, CD11c, NK1.1	SI LP	(219)
CD45$^+$CD127$^+$RORγt$^+$	CD3, CD4, CD19, CD11b, CD11c, Ly6G/6C, F4/80, Ter119	SI LP	(220)
CD45$^+$CD127$^+$RORγt$^+$	CD3, CD19	Colon LP, SI LP	(221)
CD45$^+$CD127$^+$RORγt$^+$	CD3, CD11b, B220, Ly6G/6C, Ter119	SI LP	(222)
CD45$^+$CD127$^+$RORγt$^+$	CD3ε, CD11b, B220, Ly6G/6C, Ter119	Colon LP	(223)

(Continued)

10.3389/fimmu.2023.1271699

TABLE 2 Continued

Phenotype	Lineage	Tissue/organ	Reference
$CD45^+CD127^+ROR\gamma t^+$	CD3ε, CD11b, B220, Ter119, Ly6G/6C, CD49b	LN, spleen, lung	(224)
$CD45^+CD90^+$	CD11b, CD11c, B220, Ly6G/6C, FcεR1α, Ter119	Skin	(225)
$CD45^+CD90^+$	CD3, CD5, CD19, B220	SI LP, colon LP	(226)
$CD45^+CD90^+$	CD3ε, CD5, CD19, CD11b, CD11c, NK1.1, KLRG1	SI	(227)
$CD45^+CD90^+$	NK1.1	SI LP	(202)
$CD45^+CD90^+$	CD3ε, CD11b, CD45R, TER119, Ly6GLy6C	PP	(228)
$CD45^+CD90^+$	CD3, CD5, CD19, B220, Ly6G, FcεR1α, CD11c, CD11b, Ter119, NK1.1, CD16/CD32	SI LP, colon LP	(229)
$CD45^+CD90^+$	CD3	Colon LP	(230)
$CD45^+CD90^+$	CD3ε, CD5, CD19	SI LP	(231)
$CD45^+CD90^+KLRG1^-$	CD8, CD11b, CD11c, CD19, NK1.1, Ly6G/6C, Ter119, CD3ε	mLN	(232)
$CD45^+CD90^+CD127^+$	Data not found	mLN, inguinal LN	(218)
$CD45^+CD90^+CD127^+$	CD11b, CD3ε, CD5, CD11c, CD19, NK1.1, Ly6G/6C, Ter119, TCRγδ	Lung	(233)
$CD45^+CD90^+CD127^+$	CD3, CD4, CD5, CD8, CD11b, CD11c, CD19, CD49b, Ly6G/6C, NK1.1	Spleen, mLN, PP, SI, colon	(234)
$CD45^+CD90^+CD127^+$	CD3, CD19	SI LP	(235)
$CD45^+CD90^+CD127^+KLRG1^-$	CD3ε, CD5, CD8α, NK1.1, CD11c, CD11b, B220, CD27	SI LP	(127)
$CD45^+CD90^+CD127^+ROR\gamma t^+$	CD3ε, CD4, CD8, TCRγδ, CD11b, CD11c, CD19, B220, Ly6G/6C, NK1.1, Ter119.	Spleen, mLN, SI LP, colon, lung, liver, bone marrow	(236)
$CD45^+CD90^+CD127^+ROR\gamma t^+$	CD19, CD3, CD11b, Ly6G/6C, CD11c	Spleen	(237)
$CD45^+CD90^+CD127^+ROR\gamma t^+$	CD11b, CD11c, B220, CD3ε, CD5, CD8α	SI LP, colon LP	(100)
$CD45^+CD90^+CD127^+ROR\gamma t^+$	CD11b, CD11c, CD19, CD3ε, CD5, CD8α	mLN, spleen, PP	(238)
$CD45^+CD90^+CD127^+ROR\gamma t^+KLRG1^-$	CD3, CD5, CD19, B220, Ly6G/6C, NK1.1, CD11b, CD11c	Intestine, mLN	(98)
$CD45^+CD90^+CD127^+ROR\gamma t^+KLRG1^-$	CD3ε, CD49b, CD11b, CD94, CD5, TCRγδ, CD19, Ter119, Ly6G/6C, CD45RB, Ly6G	Lung	(239)
$CD45^+CD90^+CD127^+ROR\gamma t^+KLRG1^-$	CD3ε, CD5, CD8α, NK1.1, TCRγδ, CD11b, CD11c, B220	SI, colon	(240)
$CD45^+CD90^+CD127^+CD117^+ROR\gamma t^+KLRG1^-$	CD3ε, TCRβ, CD19, B220, Ly6G/6C, CD11b	SI LP, lung, mLN	(241)
$CD45^+CD90^+CD127^+KLRG1^-$	B220, CD11c, NK1.1	Spleen, colon LP	(242)
$CD45^+CD90^+CD127^+ROR\gamma t^+$	CD3, CD5, NKK1.1, B220, CD11b, CD11c	mLN, SI LP	(243)
$CD45^+CD90^+CD127^+ROR\gamma t^+$	Ter119, F4/80, CD11b, CD11c, FcεR1α, Ly6G/6C, CD19, CD3, TCRβ, TCRγδ	SI LP, skin	(244)
$CD45^+CD90^+CD127^+ROR\gamma t^+$	CD3, B220, CD11b, CD11c Ter119, Ly6G/6C, TCRγδ	Bladder	(58)
$CD45^+CD90^+CD127^+ROR\gamma t^+$	CD3ε, CD5, FcεR1α, F4/80, CD11b, CD11c, B220	mLN, SI LP, PP	(125)
$CD45^+CD90^+CD127^+ROR\gamma t^+$	CD3e, CD11b, Ter119, B220, Ly6G/6C	Colon LP	(245)
$CD45^+CD90^+CD127^+ROR\gamma t^+$	CD3ε, CD8α, TCRβ, TCRγδ, CD19, Ly6G/6C, CD11c, Ter119	Colon LP	(246)
$CD45^+CD90^+CD127^+ROR\gamma t^+KLRG1^-$	CD3, CD19, NK1.1	SI LP	(247)
$CD45^+CD90^+IL\text{-}17^+$	B220, CD11b, CD11c, Ly6G/6C, NK1.1	Skin	(248)
$CD45^+CD90^+IL\text{-}23R^+$	CD3, NK1.1, CD11b	Ileum LP	(50)
$CD45^+CD90^+KLRG1^-$	CD3ε, CD8α, CD19, B220, CD11c, CD11b, Ter119, Ly6G/6C, TCRβ, TCRγδ, NK1.1	SI LP, mLN, spleen, lung	(165)
$CD45^+CD90^+KLRG1^-$	CD3, Ly6G/6C, CD11b, B220, Ter119, NK1.1	Ileum LP, colon LP, mLN, spleen	(249)
$CD45^+CD90^+ROR\gamma t^+$	CD4, CD8, CD11b, CD11c, CD19, B220, NK1.1, Ter119, Ly6G/6C, FcεR1α, TCRβ, TCRγ, CD3ε	Skin	(250)
$CD45^+CD90^+ROR\gamma t^+$	CD3, Ly6G/6C, CD11b, B220, Ter119	SI LP	(251)
$CD45^+CD90^+ROR\gamma t^+$	CD3, B220, CD11c, CD11b, NK1.1	Colon LP, spleen, SI LP	(252)
$CD45^+CD90^+ROR\gamma t^+$	CD3, other data not found	SI LP, ileal LP	(253)
$CD45^+CD90^+ROR\gamma t^+$	B220, CD3, NK1.1, CD11b	SI LP, blood, inguinal LN, spleen	(44)

(Continued)

10.3389/fimmu.2023.1271699

TABLE 2 Continued

Phenotype	Lineage	Tissue/organ	Reference
CD45$^+$CD90$^+$RORγt$^+$	CD3	Colon, SI, skin, lung	(254)
CD45$^+$CD90$^+$RORγt$^+$	CD3, CD19	SI LP, colon LP	(255)
CD45$^+$CD90$^+$RORγt$^+$	Data not found	SI LP, colon LP, cecum	(256)
CD45$^+$CD90$^+$RORγt$^+$	CD11b, CD11c, CD19	SI LP	(257)
CD45$^+$CD90$^+$RORγt$^+$	CD3, CD5, CD8α, CD11b, B220, NK1.1	mLN, PP, SI LP	(258)
CD45$^+$CD90$^+$RORγt$^+$	CD3, CD49b, TCRβ, TCRγδ, CD5, F4/80, CD11c, Ly6G/6C, CD19, FcεR1α, B220, CD27	Lung	(259)
CD45$^+$CD90$^+$RORγt$^+$	CD3ε, CD11b, CD11c, F4/80, Ly6G/6C, Ter119, B220	SI LP	(260)
CD45$^+$CD90$^+$RORγt$^+$	NK1.1	Bone marrow	(235)
CD45$^+$CD90$^+$RORγt$^+$	CD3, TCRβ, CD5, CD19, CD11b, CD11c, Ly6G/6C, FcεR1α, CD31, Ter119	Heart	(146)
CD45$^+$CD90$^+$RORγt$^+$	CD11b, CD11c, B220, CD4, TCRβ	Lung	(261)
CD45$^+$CD90$^+$RORγt$^+$	Without	SI LP, colon LP, mLN	(262)
CD45$^+$CD90$^+$RORγt$^+$	Data not found	Colon LP	(262)
CD45$^+$CD90$^+$RORγt$^+$	Ter119, CD11b, Ly6G/6C, CD3ε, B220, TCRβ, NK1.1	Colon LP	(263)
CD45$^+$CD90$^+$RORγt$^+$	CD4, TCRβ, TCRγδ, CD8α, CD8β, CD19, CD11b, CD11c, DX5, Ly6G/6C, Ter119, NK1.1	SI LP, colon LP	(264)
CD45$^+$CD90$^+$RORγt$^+$	Without	SI LP	(265)
CD45$^+$CD90$^+$RORγt$^+$	CD11c, CD11b, NK1.1, B220, CD3	Colon LP	(266)
CD45$^+$CD90$^+$RORγt$^+$	CD3, CD19, B220, CD11c, Ly6G/6C	SI LP	(267)
CD45$^+$CD90$^+$RORγt$^+$	CD3	Colon LP	(268)
CD45$^+$CD90$^+$RORγt$^+$	CD3, CD5, CD19, CD11c, CD11b	SI	(269)
CD45$^+$CD90$^+$RORγt$^+$	CD3ε, Ly6G/6C, CD11b, B220, Ter119	SI LP, colon LP, lung, liver, PP, skin	(270)
CD45$^+$CD90$^+$RORγt$^+$	Data not found	Colon, SI	(271)
CD45$^+$CD90$^+$RORγt$^+$	CD3ε, CD5, CD19	SI	(272)
CD45$^+$CD90$^+$RORγt$^+$	CD3	SI LP	(273)
CD45$^+$CD90$^+$RORγt$^+$ KLRG1$^-$	Ly6G/6C, CD3ε, CD11b, B220	Liver	(274)
CD45$^+$CD90$^+$RORγt$^+$	Data not found	SI	(275)
CD45$^+$CD90$^+$RORγt$^+$KLRG1$^-$	CD3, B220, CD49a, CD11b, CD11c, NK1.1	SI	(128)
CD45$^+$CD90$^+$RORγt$^+$KLRG1$^-$	CD11c	Colon LP, SI	(242)
CD45$^+$CD90$^+$RORγt$^+$KLRG1$^-$	CD3, Ly6G/6C, CD11b, B220, Ter119, NK1.1	Colon LP, SI LP, mLN, spleen, PP	(276)
CD45$^+$CD90$^+$Sca-1^{hi}	CD3, B220, CD11b, Ly6G/6C, Ter119	Neonatal SI, colon, mLN, spleen	(277)
CD45$^+$CD90^{hi}RORγt$^+$	CD3, Ly6G/6C, CD11b, B220, Ter119	SI, colon	(278)
CD45$^+$IL-17$^+$	CD3, CD19, CD11b, CD11c, CD49b, F4/80, FcεR1α	Lung	(279)
CD45$^+$IL-17$^+$	TCRγδ, TCRβ	Spleen	(280)
CD45$^+$IL-17$^+$IL-22$^+$	CD5, CD11b, B220, Ly6G/6C, Ter119, CD3	Colon LP	(281)
CD45$^+$RORγt$^+$	CD3ε, CD19	Liver	(282)
CD45$^+$RORγt$^+$	TCRαβ, TCRγδ, CD5, CD3ε, CD19, Ly6G/6C, F4/80	Colon LP, SI LP	(283)
CD45$^+$RORγt$^+$	CD3, CD11b, B220, Ly6G, Ter119	Colon LP	(284)
CD45$^+$RORγt$^+$	Data not found	Colon LP	(285)
CD45$^+$RORγt$^+$	CD3, CD19	SI LP	(286)
CD45$^+$RORγt$^+$	CD3, CD11b, B220, Ly6G, Ter119	Colon, mLN	(287)
CD45$^+$RORγt$^+$	CD3, CD19	SI LP	(288)
CD45$^+$RORγt$^+$	CD3, CD19	SI, colon, cecum	(289)
CD45$^+$RORγt$^+$	CD3, CD19	SI LP	(290)

(Continued)

TABLE 2 Continued

Phenotype	Lineage	Tissue/organ	Reference
CD45$^+$RORγt$^+$	CD3	SI LP	(291)
CD45$^+$RORγt$^+$	CD3, CD19	SI LP, colon LP	(292)
CD45$^+$RORγt$^+$	CD3, B220, Ter119, Ly6G/6C, CD11b, CD19, NK1.1	SI LP	(293)
CD45$^+$RORγt$^+$	CD3, CD19	SI LP	(294)
CD45$^+$RORγt$^+$	TCRβ, B220, TCRγd	mLN, jejunum LP, colon LP, cecum	(295)
CD45$^+$RORγt$^+$	Data not found	SI LP, colon LP	(296)
CD45$^+$RORγt$^+$	NK1.1, other data not found	Colon LP	(297)
CD45$^+$RORγt$^+$	CD3, CD19, B220, Ly6G/6C, CD11c, CD11b	Pooled axillary, brachial, inguinal and cervical LN, mLN	(298)
CD45$^+$RORγt$^+$	Data not found	Ileum, colon	(299)
CD45$^+$RORγt$^+$	CD3ε, CD19	SI LP	(300)
CD45$^+$RORγt$^+$	CD3ε, CD11b, B220, Ly6G/6C	SI LP	(301)
CD45$^+$RORγt$^+$	CD3ε, CD5, CD19	SI LP, colon LP, mLN	(302)
CD45$^+$RORγt$^+$	CD19, CD3	SI LP	(303)
CD45$^+$RORγt$^+$	CD3, CD4, CD8, CD19, Ly6G/6C, Ter119	SI LP	(304)
CD45$^+$RORγt$^+$	CD3, CD11b, B220, Ly6G, Ter119	Colon LP	(190)
CD45$^+$RORγt$^+$	CD3, Ly6G/6C, CD11b, B220, Ter119	Colon, mLN	(305)
CD45$^+$RORγt$^+$	CD3ε, CD11b, B220, Ter119, Ly6G/6C	Colon LP	(306)
CD45$^+$RORγt$^+$	CD3	Lung	(307)
CD45$^+$RORγt$^+$	CD3ε, NK1.1, Ly6G/6C, CD11b, B220, Ter119	Cornea, conjunctiva, lacrimal gland	(308)
CD45$^+$RORγt$^+$KLRG1$^-$	CD3, CD5, B220, CD11c, NK1.1	SI, Colon, cecum LP	(242)
CD90$^+$	CD3e, CD8α, B220, CD11b, CD11c	Neonatal SI LP	(309)
CD90$^+$CD117$^+$KLRG1$^-$	CD3ε, CD8α, CD11b, CD11c, CD19, B220, Ly6G/6C, TCRβ, TCRγ/δ, Ter119, NK1.1	Spleen, SI	(310)
CD90$^+$CD127$^+$	CD3, CD11c, B220	Spleen	(311)
CD90$^+$CD127$^+$CD117$^+$	CD3, B220, CD11c, Ly6G/6C, NK1.1	Spleen	(312)
CD90$^+$CD127$^+$CD25$^+$	CD3, CD19, CD11c, NK1.1	mLN	(313)
CD90$^+$CD127$^+$KLRG1$^-$	CD3, CD11b, CD11c, CD14, CD19, TCRβ, TCRγ, NK1.1	SI LP, colon LP	(314)
CD90$^+$CD127$^+$KLRG1$^-$Sca-1^{lo}	CD3ε, CD4, CD8α, CD5, NK1.1, B220, CD11b, CD11c, Gr-1, FcεRIα, Ter119	SI LP	(315)
CD90$^+$CD127$^+$RORγt$^+$	CD5, CD3, CD11b, CD11c, B220, Ly6G/6C, Ter119	Colon	(316)
CD90$^+$CD127$^+$RORγt$^+$	CD3, CD5, B220, NK1.1, F4/80, Ly6G/6C	Colon LP	(317)
CD90$^+$CD127$^+$RORγt$^+$	CD3, Ly6C/6G, CD11b, B220, Ter119	SI	(318)
CD90$^+$CD127$^+$RORγt$^+$	CD3, CD11b, Ly6G/6C, B220, NK1.1, CD11c, Ter119	Lung	(319)
CD90$^+$CD127$^+$RORγt$^+$	Data not found	Cecum, mLN	(320)
CD90$^+$CD127$^+$RORγt$^+$	CD3, CD5, B220, CD11b, Ly6G/6C, Ly6B, Ter119	Lung	(321)
CD90$^+$CD127$^+$RORγt$^+$	CD3ε, TCRβ, GL3, CD19, Ly6G/6C, CD11b, F4/80, Ter119, NK1.1, CD49b, CD11c	LN, spleen	(322)
CD90$^+$CD127$^+$RORγt$^+$	CD3ε, CD11b, B220, Ter119, Ly6G/6C	SI LP	(323)
CD90$^+$CD127$^+$RORγt$^+$KLRG1$^-$	CD3, CD5, CD19, CD11b, TCRγδ	Colon LP, SI LP	(37)
CD90$^+$IL-23R$^+$	CD3	SI LP	(324)
CD90$^+$RORγt$^+$	CD3, CD8α, TCRβ, TCRγδ, CD11b, CD11c, B220, Ly6G/6C, NK1.1, Ter119	SI	(325)
CD90$^+$RORγt$^+$	CD3, TCRγδ, CD11b, NK1.1	Colon LP	(33)
CD90$^+$RORγt$^+$	TCRβ, TCRγδ, CD19, Ly6G/6C, Ter119, NK1.1, CD11c, CD11b	Colon LP	(326)
CD90$^+$RORγt$^+$	Data not found	Colon LP	(327)
CD90$^+$RORγt$^+$	CD5, CD8, CD3, B220, CD11c, CD11b, T-bet	SI	(328)

(Continued)

TABLE 2 Continued

Phenotype	Lineage	Tissue/organ	Reference
CD90$^+$RORγt$^+$	CD3	Colon LP, SI LP	(329)
CD90$^+$RORγt$^+$KLRG1$^-$	CD3, CD8, CD11c, CD19, B220, Ly6G/6C, TCRβ, TCRγδ, Ter119	SI, colon	(330)
RORγt$^+$	CD3ε, CD5, CD8α, CD19, Ter119, Ly6G/6C, TCRβ, TCRδ	Spleen, bone marrow, SI LP	(331)
RORγt$^+$	CD3, CD19, B220, CD11b, CD11c, Ter119	SI LP	(332)
RORγt$^+$	CD3e, CD11b, B220, Ter119, Ly6G/6C	PP	(228)
RORγt$^+$	CD3	Colon LP	(333)
RORγt$^+$	CD3, CD4, CD8, CD16, CD19, CD11c, FcεR1α	Colon LP	(334)
RORγt$^+$	CD3ε	SI LP	(335)
RORγt$^+$	CD3ε, CD5, CD19	SI LP	(231)
RORγt$^+$	CD3, CD19	SI LP I IE	(336)
RORγt$^+$	CD3, CD5, CD19, B220, Ly6G, CD11b, CD11c, Ter119	SI LP, colon LP	(229)
RORγt$^+$	CD3, B220, CD11b, CD11c	Spleen, colon LP, SI LP	(337)
RORγt$^+$	CD3, B220, CD11b, CD11c	Colon LP	(338)
RORγt$^+$	CD3ε	SI LP	(339)
RORγt$^+$	CD11b, CD11c, Ter119, B220, CD3ε, Ly6G/6C, TCRβ	SI LP	(340)
RORγt$^+$	CD3ε, B220, CD11b, CD11c	SI, colon	(341)
RORγt$^+$CD161$^+$KLRG1$^-$	CD3, TCRβ, CD11b, CD14, CD19, B220, TCRγδ, NK1.1	SI LP	(342)
RORγt$^+$IL-22$^+$	Without	SI LP	(343)
RORγt$^+$MHC II$^+$	Without	SI LP	(344)
RORγt$^+$MHC II$^+$	CD3, CD19, NK1.1, CD11b, B220, F4/80, CD11c, Ly6G/6C, FcεR1α	Spleen, mLN	(345)

LP, lamina propria; PL, peritoneal lavage; PP, Peyer's patches; SI, small intestine; LN, lymph node; mLN, mesenteric lymph node.

expressed by ILC3. The use of anti-CD45 antibodies is essential when identifying ILC3 in the intestine, lungs, and other organs and tissues where there is plenty of non-hematopoietic cells. There, gating on CD45$^+$ cells as one of the first steps in flow cytometry analysis is a prerequisite to prevent contamination with non-hematopoietic cells and to get precise data on ILC3. On the other hand, identification of ILC3 in the peripheral blood, spleen, tonsils, or lymph nodes does not require the use of anti-CD45 antibodies, as there are few non-hematopoietic cells, if any. Still, it is clear from Tables 1, 2 that some authors do not use CD45-specific antibodies where necessary, and the results of such studies should be carefully considered.

Table 4 presents the most common markers used in ILC3-related studies. Both CD nomenclature and alternative names are used in research papers, thus confusing readers who are not specialized in the ILC3 field. While alternative names have the advantage of functional comprehension and historical connotation, CD designation offers a more systematic approach. Thus, it seems productive to use CD nomenclature as much as possible, or at least to provide information on CD designation in the papers that use alternative names.

4.1 CD127

According to the literature (Figure 1; Table 3), CD127 is the most commonly used ILC3 marker in humans and the second most common in mice. This marker is an α subunit of the IL-7 receptor. IL-7 is important for the early development of T and B cells from bone marrow precursors and for the development of T cells in the thymus (363). As IL-7 is the major growth factor of ILC, but not NK cells, CD127 is expressed by the former (364), but not by the latter, and is thus a valuable marker for the distinction of these two cell types. In addition to ILC, CD127 is expressed in naive (365), memory (366), and regulatory T cells (367). Therefore, using T-cell-specific antibodies in the lineage cocktail is necessary to be able to use CD127 as a reliable marker of ILC. This marker is of particular interest for discriminating between NK and ILC1 cells, as both cell types are known to express T-bet. Still, keeping in mind that NK cells do not express RORγt, CD127 does not appear to be essential for the discrimination between ILC3 and NK cells. It seems that it is reasonable to use CD127 in ILC3 research when analyzing all ILC subsets, while it is not essential for ILC3 subset identification.

4.2 CD117

This marker is used in ILC3 studies in humans almost as frequently as CD127 is, yet its use in mouse studies is not so frequent (Figure 1; Table 3). CD117 is a tyrosine kinase, also known as c-Kit, and it is the receptor for the SCF. CD117 plays an important role in early hematopoiesis and its expression is lost during cellular differentiation (368). However, in addition to mature

mast cells and melanocytes, CD117 is also expressed on recently activated human $CD8^+$ T cells (369) and circulating B cells (370). Within the ILC, CD117 is expressed on ILC2 and ILC3 (17). Since CD117 is not exclusively expressed on ILC3, additional markers should be used to distinguish between ILC2 and ILC3, and its use may not be crucial for detecting ILC3.

4.3 CD294

This marker is frequently used in human but not in mouse studies. CD294, also known as CRTH2, is a prostaglandin D2 receptor expressed on Th2 cells and ILC2 in humans, but not in mice. It is also present in both human and mouse eosinophils and basophils (371), while it is not expressed on ILC3 (17). Thus, when phenotyping ILC3, it serves to exclude the ILC2 population. CD294 is most often used in combination with CD127 and CD117, as based on the expression of these three markers in lineage-negative cells, all three ILC subsets can be distinguished. However, when only detecting the ILC3 population, it does not seem necessary to use all of these markers.

4.4 CD90

This marker is very frequently used in mouse but not in human studies, although the mouse and human CD90 proteins are highly similar. Despite this, CD90 expression is negligible in human cells and, thus, cannot be used as a marker for ILC (372). CD90 is a glycophosphatidylinositol-anchored cell surface protein and a member of the immunoglobulin superfamily. While its function is still not fully elucidated, it has been shown to interact with integrins and is therefore presumably important for cell adhesion (274). Within immune cells, CD90 is expressed in T cells, NK cells, and ILCs. It is found on the surface of all subtypes of ILC (373). In $Rag1^{-/-}$ mice, the anti-CD90 antibody is commonly used to deplete ILC (374). Although CD90 is considered a pan-ILC marker, a recent study showed that CD90 is not constitutively expressed in intestinal ILC (375). Additionally, having in mind that CD90 is expressed in all ILC subsets, CD90 does not appear to be the best choice for the detection of ILC3. Furthermore, based on their results of different expressions of CD90 on ILC, Schroeder et al. (375) suggested that CD127 is a much more reliable ILC marker than CD90.

4.5 CD161

CD161 is used as an additional marker to determine ILC3 in humans, but not in mice. CD161 is a human homolog of NK1.1 and is expressed in NK cells, T cells, NKT cells, monocytes, and DCs (376). It is used in combination with CD127 and CD117, with or without CD294 (Figure 1; Table 3). Aside from ILC3, CD161 is also expressed on ILC2 (377). Therefore, this molecule cannot be used as a basic, but only as a supplementary marker for ILC3 phenotyping.

4.6 RORγt

RORγt is by far the most frequently used marker for the discrimination of ILC3 in mouse studies, but not in humans. This molecule is expressed by T cells and ILC3 (346). Human bone marrow and blood neutrophils, as well as mouse lung neutrophils and splenic DCs, can also express RORγt, as previously mentioned (347–349). However, in human secondary lymphoid tissues, including the tonsils, lymph nodes, and spleen, RORγt is expressed in all ILC subsets, as well as in NK cells. In these tissues, a novel $Lin^-CD34^+CD45RA^+CD117^+IL\text{-}1R1^+ROR\gamma t^+$ cell population was found, capable of differentiating into all major ILC populations (24). The expression of RORγt was also found in human fetal gut and adult peripheral blood ILC2 cells (377). Although there are no data showing the expression of RORγt in adult human intestinal ILC1 and ILC2, Cogswell et al. (378) have demonstrated the expression of RORγt in ILC1, ILC3, and NK cells in the colon of rhesus macaques, which additionally compromises the use of RORγt in the identification of ILC3 in humans. However, in all of the abovementioned studies, the expression of RORγt was much higher in ILC3 than in other ILC subsets. Thus, RORγt is the crucial marker for the identification of ILC3 in mice and a supplementary one in humans.

5 Molecules important for the identification of ILC3 subsets

5.1 CD196

CD196 or CCR6 is a G protein-coupled receptor expressed on DCs, $CD4^+$ T cells, B cells, and ILCs. CCL20 is a high-affinity ligand for CCR6, and pro-inflammatory cytokines have been shown to induce its expression (379). CCL20 is highly present in inflamed tissues and drives the recruitment of CCR6-expressing immune cells (380). Within ILC3, CCR6 is expressed on LTi and LTi-like cells (381) and is an important marker for identifying these cells. While CCR6-expressing ILC3s are important for the formation of lymphoid organs during development, in adult mice, these cells are usually aggregated with DCs, B cells, and stromal cells in cryptopatches and isolated lymphoid follicles (382). Thus, CD196 is a valuable marker for the identification of ILC3 subpopulations.

5.2 CD335

CD335 or NKp46 is a member of the immunoglobulin superfamily and one of the NCRs of NK cells. While there are three NCRs in humans, namely, NKp30, NKp44, and NKp46, the only NCR described in mice is NKp46 (383). It is expressed on the surface of non-activated and activated NK cells (384), a small population of T lymphocytes, ILC1, and a subset of ILC3, called NCR^+ ILC3 (385). Although the functional role of NKp46 on ILC3 is poorly understood, this molecule is essential for the identification of ILC3 subsets.

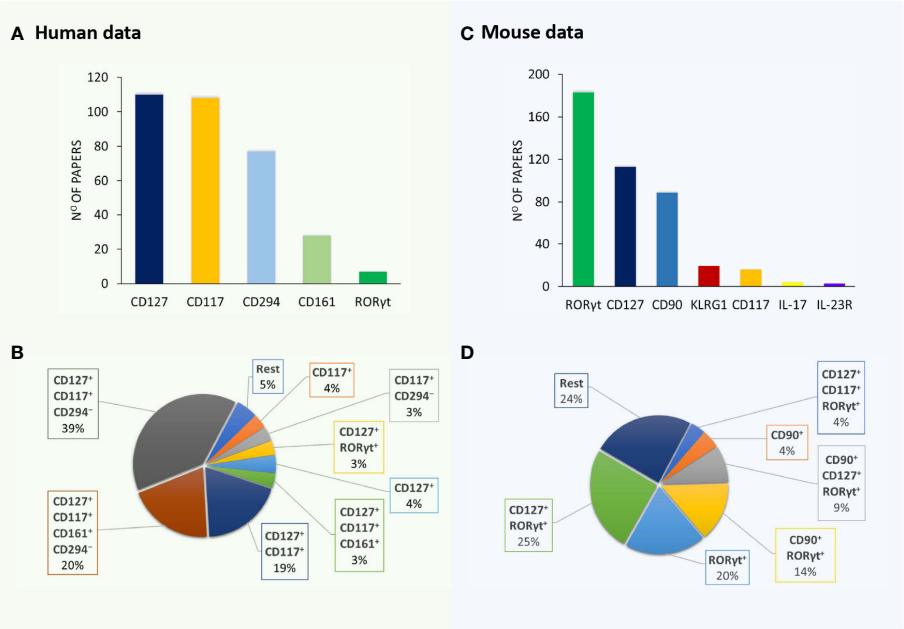

FIGURE 1
Markers and their combinations used for the identification of ILC3. Visual representation of data from Tables 1, 2. The number of papers in which specific markers were used for the identification of human **(A)** and mouse **(B)** ILC3s. The most frequently used marker combinations for the identification of human **(C)** and mouse **(D)** ILC3s (% of all papers examined).

5.3 CD336

CD336 or NKp44 is another NCR and is expressed only in humans. Like NKp46, it belongs to the immunoglobulin superfamily, but there is no homology between these two molecules (386). While NKp30 and NKp46 are constitutively expressed in human NK cells, NKp44 is expressed only upon activation (384), and the use of anti-NKp44 antibodies has been shown to stimulate cytokine production by human ILC3 (387). In addition to NK cells, NKp44 is also expressed on ILC1 and ILC3 (388) and is thus helpful in defining ILC3 subsets.

TABLE 3 Markers used for the identification of human and mouse ILC3.

Human				Mouse			
Markers	*n*	Combinations	*n*	Markers	*n*	Combinations	*n*
CD127	114	$CD127^+CD117^+CD294^-$	48	RORγt	189	$CD127^+ROR\gamma t^+$	60
CD117	112	$CD127^+CD117^+CD161^+CD294^-$	25	CD127	117	$ROR\gamma t^+$	48
CD294	79	$CD127^+CD117^+$	24	CD90	89	$CD90^+ROR\gamma t^+$	32
CD161	30	$CD127^+CD117^+CD161^+$	5	KLRG1	19	$CD90^+CD127^+ROR\gamma t^+$	20
RORγt	7	$CD127^+$	5	CD117	16	CD90	10
IL-23R	1	$CD117^+CD294^-$	4	IL-17	4	$CD127^+CD117^+ROR\gamma t^+$	8
		$CD127^+ROR\gamma t^+$	4	IL-23R	3	$CD90^+ROR\gamma t^+KLRG1^-$	5
		$CD117^+$	4			$CD90^+CD127^+$	5
		$CD117^+ROR\gamma t^+$	2			$CD127^+$	5
		$ROR\gamma t^+$	2			$CD127^+CD117^+$	4
		$CD127^+IL\text{-}23R^+$	1			$CD90^+CD127^+ROR\gamma t^+KLRG1^-$	4
		$CD127^+CD294^-$	1			$CD117^+ROR\gamma t^+$	3
						Rest	30

n, number of studies.

6 ILC3 subsets in humans

Three different ILC3 subtypes can be distinguished in humans (Figure 2). LTi cells are the subtype that is most distinct by their developmental pathway and functional properties, and some even consider them to be a separate cell population (385). However, when it comes to their identification by flow cytometry, there is a clear lack of appropriate markers (385). Two other important subtypes are distinguished in humans based on the expression of CD336 (NKp44) and are referred to as NKp44$^-$ ILC3 and NKp44$^+$ ILC3 (38, 48, 387, 389). Still, LTi cells are also defined as NKp44$^-$. The distinction between NKp44$^-$ ILC3 and LTi in humans can only be performed through analysis of CD45 expression. While NKp44$^-$ ILC3s have high CD45 expression, LTi cells express intermediate levels of CD45 (385). Thus, we are in need of a novel marker that would make a clear distinction between NKp44$^-$ ILC3 and LTi. An additional subpopulation of NKp44$^+$ ILC3 that loses the ability to express RORγt but keeps the expression of T-bet, and thus becomes closer to the ILC1 phenotype, can be identified as "ex-ILC3" cells (390).

ILC3s in humans are most often found in mucosal tissue and are most abundant in the intestine, where they exhibit several functions (30). For instance, it was shown that after gastrointestinal transplantation, the recipients' ILC rapidly infiltrated the graft (95). Increased frequencies of human NKp44$^+$ ILC3 were observed in the graft, which has been associated with successful intestinal transplants as it reduces the risk of rejection (99). A similar observation was made in leukemic patients after hematopoietic stem cell transplantation (95). These observations have further strengthened the hypothesis that NKp44$^+$ ILC3s are essential for maintaining homeostasis and protecting the gastrointestinal tract. However, there are conflicting data from some cancer studies that the role of IL-22-producing NKp44$^+$ ILC3 may be detrimental to patients. For example, patients with hepatocarcinoma had more NKp44$^+$ ILC3s than healthy controls (48). On the other hand, NKp44$^-$ ILC3s have been described to exacerbate inflammation, especially in inflammatory bowel disease, due to their secretion of IFN-γ and IL-17A (122, 390, 391). Additionally, it was shown that upon activation, human ILC3s were able to induce antigen-specific CD4$^+$ memory T-cell responses (392). Both NKp44$^+$ ILC3 and NKp44$^-$ cells can produce IL-17, but the ability to produce IL-22 is mainly restricted to NKp44$^+$ ILC3 (387). By producing IL-22, NKp44$^+$ ILC3s promote tissue integrity, maintain barrier functions, and promote homeostasis (238), particularly in the gastrointestinal tract. IL-22 secretion by NKp44$^+$ ILC3 is activated after various stimuli such as food intake (241, 314), danger signals (111, 393), and changes in the cytokine milieu (6, 7). In addition, NKp44$^+$ ILC3 can interact with other cells through the expression of neuroregulatory receptors which allows them to directly interact with glial cells (246) and goblet cells (394).

TABLE 4 Cluster of differentiation (CD) and alternative nomenclature of common ILC3 markers.

CD nomenclature	Alternative names	Function
CD90	Thy-1	Not elucidated, cell adhesion
CD117	c-kit, SCFR	Receptor tyrosine kinase
CD127	IL-7Rα	IL-7 receptor
CD161	Klrb1b, NKRP1A	Negative regulator of cytotoxicity
CD196	CCR6	Chemokine receptor for CXCL20
CD294	CRTH2, DP-2	Prostaglandin D2 receptor 2
CD335	NCR1, NKp46	Cytotoxicity triggering receptor
CD336	NCR2, NKp44	Cytotoxicity triggering receptor

CCR6, C-C motif chemokine receptor 6; CRTH2, chemoattractant receptor-homologous molecule expressed on TH2 cells; IL-7R-α, interleukin-7 receptor subunit alpha; Klrb1b, killer cell lectin-like receptor subfamily B, member 1; Klrd1, killer cell lectin-like receptor subfamily D, member 1; NCR, natural cytotoxicity triggering receptor; SCFR, mast/stem cell growth factor receptor; Thy-1, thymocyte differentiation antigen 1.

The attempt to classify ILC3 subgroups becomes more complex when different tissues are observed. For example, single-cell RNA sequencing analysis has shown that three populations can be identified in the tonsils based on the expression of NKp44, human leukocyte antigen D-related (HLA-DR), and CD62L, and each of these subpopulations has a different cytokine profile (395). HLA-DR$^+$ ILC3s have also been observed in the human intestine (138, 396). Apart from this, NKp44$^+$ ILC3s can be further divided into two populations based on the expression of neuropilin-1 (NRP-1). NRP-1$^+$ ILC3s produce more cytokines than NRP-1$^-$ ILC3, and these cells have been detected only in lymphoid tissues and inflamed lung tissue (105). Overall, these data make it necessary to find a consensus in identifying and classifying ILC3s into specific subtypes.

It was generally presumed that all human ILC3s express a common transcription factor RORγt, which implied that RORγt is essential for their functions. However, in patients with RORγt deficiency, IL-22$^+$ but not IL-17$^+$ ILC3s were found. Similarly, *in-vitro* experiments showed that chemical inhibition of RORγt did not affect the ability of ILC3 to produce IL-22 (40). This suggests that other transcription factors such as AhR or GATA3 may regulate IL-22$^+$ ILC3, as studies in mice have found that these transcription factors are implicated in the regulation of IL-22 production by ILC3 (161, 397).

7 ILC3 subsets in mice

Discrimination among ILC3 subgroups in mice is mainly based on the expression of two cell markers: CD196 (CCR6) and CD335 (NKp46) (Figure 2). There are three basic populations of murine ILC3: NCR$^+$ ILC3 (CCR6$^-$NKp46$^+$), NCR$^-$ ILC3 (CCR6$^-$NKp46$^+$), and LTi cells (CCR6$^+$NKp46$^-$). LTi cells identified postnatally are referred to as LTi-like. Additionally, there is a subpopulation of NCR$^+$ ILC3 that is called "ex-ILC3," which is characterized by diminished RORγt and upregulated T-bet expression.

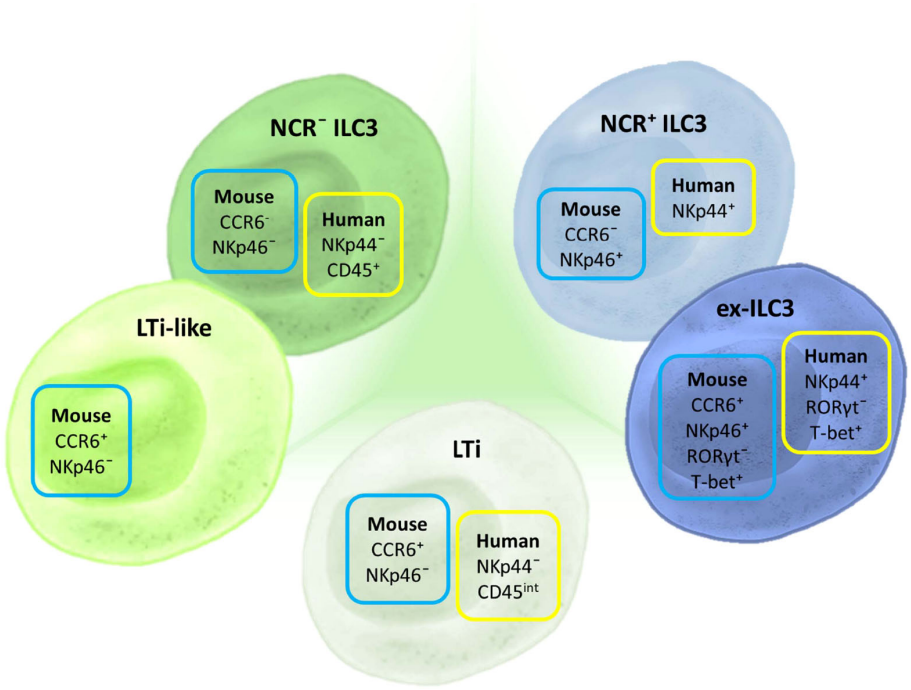

FIGURE 2
Markers for ILC3 subset discrimination in humans and mice. The basic classification of ILC3 includes three subtypes in humans and mice: LTi, NCR$^+$, and NCR$^-$ ILC3. In mice, an additional subpopulation can be identified—LTi-like cells, although it is still not clear if this subpopulation is distinct from NCR$^-$ ILC3. Different NCRs are used for characterizing human and mouse ILC3s: NKp44 and NKp46, respectively. CCR6 is an additional marker used for ILC3 classification in mice. Aside from these basic subtypes, there is a defined group of ILCs that shares certain markers and properties of both ILC3 and ILC1. These cells are considered to have converted from ILC3 toward ILC1 and are thus termed "ex-ILC3." They are distinguished from NCR$^+$ ILC3 by the expression of RORγt and T-bet.

LTi cells are vital for the formation of secondary lymphoid organs throughout the prenatal period as they produce lymphotoxin-α1β2, which activates lymphoid tissue organizer cells in future lymph node and Peyer's patch (PP) sites (15, 398). Post-birth, LTi-like cells also play a role in the development of cryptopatches, small lymphoid aggregates in the gut, which can grow into isolated lymphoid follicles (ILFs) in response to microbial signals (398). CCL20, the major CCR6 ligand, is constitutively expressed within the intestinal PP, ILF, and mesenteric lymph nodes (mLNs), confirming the importance of CCR6-mediated signals for secondary lymphoid organogenesis. These signals also help keep leukocytes at sites critical for immune surveillance (399). Accordingly, CCR6$^+$ LTi-like ILC3s are the prevailing ILC3 subset in the PP, mLN, and colon lamina propria (243). In the intestine, LTi-like cells are also important for maintaining local gut homeostasis, through their interactions with both the innate and adaptive immune responses. For instance, LTi-like cells can produce IL-22 and IL-17, which are able to increase the expression of intestinal antimicrobial peptides (350, 400).

Additionally, LTi-like cells, unlike CCR6$^-$ ILC3, constitutively express MHC II in the gut while lacking the expression of co-stimulatory molecules CD40, CD80, and CD86, compared with DCs (369). This is one of the features that allows them to play a part in maintaining tolerance through the suppression of commensal antigen-specific T effector cells, enhanced generation of memory T cells, and promotion of mucosal antibody responses [reviewed by Zhong et al. (14)]. LTi-like cells can also be separated into CD4$^+$ and CD4$^-$ subsets, even though gene expression analysis showed that there were minimal differences between the two groups—probably not enough to allow functional significance (288). Aside from confirming that CCR6 transcripts were expressed at higher levels in LTi-like cells compared with other ILC3s, the same was shown for an additional chemokine receptor, CXCR5 (288). Finally, fate-mapping studies have demonstrated that while the LTi lineages develop from ILC progenitors that have never expressed the transcription factor PLZF, all other ILC3 subtypes are generated from progenitors that do express it (401). GATA3 is another transcription factor that was shown to be necessary for the development of non-LTi ILCs, while it was not required for the generation of LTi-like cells (402). Additional precursor single-cell analyses (403) and the use of multitranscription factor reporter mice (404) confirmed the distinct origins of ILC and LTi lineages. Based on the differences in gene expression needed for their development, LTi-like cells could be considered a separate group of ILCs, despite sharing similarities in phenotype and function with NKp46$^+$ ILC3.

NKp46$^+$CCR6$^-$ ILC3, unlike CCR6$^+$ LTi-like cells, are marked by T-bet expression. Their postnatal development from NKp46$^-$CCR6$^-$RORγt$^+$ progenitors, often labeled as double negative (DN) ILC3, is in part guided by commensal microbiota signals and IL-23, while c-Maf-controlled graded T-bet expression ensures the expression of NKp46 (247, 405). To maintain their

phenotype, NKp46$^+$ ILC3s also require Notch signaling, which can be regulated by both AhR (406) and T-bet (407), while it was shown that TGF-β impairs their development (290).

In the gut, NKp46$^+$ ILC3s are predominantly found in the small intestine lamina propria (243), and their localization within the lamina propria villi is influenced by CXCR6 (160). NKp46$^+$ ILC3s also make up most of the ILC3s in the cecum and are necessary for its homeostasis (289). NKp46 has mostly been studied as one of the NCRs that are expressed by NK cells and whose activation by various pathogen-derived ligands can trigger NK cell-mediated cytotoxicity accomplished by the secretion of perforin or proinflammatory cytokines such as IFN-γ and TNF or through activation-induced cell death. Unlike NK cells, it seems that intestinal NKp46$^+$ ILC3s are not able to perform these functions, while they do produce IL-22 to fight intestinal inflammation (3), similar to LTi-like cells. Interestingly, questions about the redundancy of the NKp46$^+$ subgroup of ILC3s have been brought up in some experimental settings. For instance, NKp46$^+$ ILC3s were shown to be inessential in the fight with a *Citrobacter rodentium* infection, when compared with LTi-like ILC3s (256). More specifically, IL-22 was necessary for the resistance to *C. rodentium*, but IL-22 production by NKp46$^+$ ILC3 was not (289). However, NKp46$^+$ ILC3s also have the potential to secrete GM-CSF and were crucial in promoting the accumulation and activation of inflammatory monocytes in an anti-CD40-induced colitis model (256).

A fate-mapping study by Viant et al. (290) demonstrated a notable proportion of NKp46$^-$ ILC3 used to express NKp46, and this phenomenon was predominantly observed in mucosal tissues but not in the bone marrow. Furthermore, an RORγt fate-mapping study revealed that, in some inflammatory conditions, NKp46$^+$ ILC3 can significantly lower or lose RORγt expression, while T-bet expression increases. At the same time, these "ex-ILC3s" start producing IFN-γ and upregulate perforin and granzyme B expression, becoming more akin to ILC1 (9). Following *Salmonella typhimurium* infection, these cells were the main source of IFN-γ in the small intestine (405), which implies an adaptive role in microbial defense. On the other hand, NKp46$^+$ ILC3 plasticity is regulated by c-Maf, which suppresses their conversion into the ILC1-like state by restraining T-bet expression and supporting RORγt activity (219, 247). Finally, the transcriptional profile of NKp46$^+$ ILC3 was shown to have features in between those of NKp46$^-$ LTi-like ILC3 and NKp46$^+$ ILC1 (while sharing more transcripts with NKp46$^+$ ILC1). This might be the basis of their plasticity potential, which is probably shaped by their specific microenvironment (288).

8 ILC3 sorting and culture

Our literature survey shows that a consensus about the minimal or optimal panel of surface markers for ILC3 sorting is still missing. However, in most sorting protocols, the live/dead discrimination and doublet exclusion seem to be mandatory. Some authors suggest that before cell sorting, enrichment of CD90$^+$ (233) or Lin$^-$ cells (408) should take place. The most efficient sorting of mouse ILC3 occurs in samples obtained from mice that carry a fluorescently labeled reporter RORγt. In this case, the sorting protocol might include only a CD3 staining, after which ILC3s are sorted as CD3$^-$RORγt$^+$ cells (the exclusion of Th17 cells is achieved). However, most of the protocols include additional surface markers—ILC3 can be sorted as CD45^{int}CD90^{high}RORγt$^+$ (275) or as Lin$^-$CD45$^+$CD90.2$^+$RORγt$^+$ (270). In the studies not using RORγt reporter mice, investigators tend to use as many markers as they can for the determination of ILC3. For example, Zhou et al. (96) sorted an enriched population of ILC3 as Lin$^-$CD45^{low}CD90.2^{high}CD127$^+$KLRG1$^-$. However, other groups used fewer denominators for the enrichment of ILC3, for example, the CD3$^-$ and CD90^{high}CD45^{low} gating (254) or complete lineage-negative population coupled with CD90^{high} and CD45^{low} markers (238, 269). Some groups use KLRG1 as an additional discriminative factor for ILC3 enrichment in the following panel Lin$^-$CD90.2$^+$KLRG1$^-$ (330) or Lin$^-$CD45$^+$CD90.2$^+$KLRG1$^-$ (128). As recent data indicate that surface CD90 can be downregulated when ILC3s are functionally active, the usage of CD90 for ILC3 sorting is questionable (375). CD127 and ST2 are also used to determine ILC3 for sorting in addition to Lin$^-$CD45$^+$CD4$^-$. The same study uses the NKp46 marker to sort-purify NCR$^+$ and NCR$^-$ ILC3s (122). In all articles that we have analyzed so far, the percentage of acquired RORγt$^+$ cells after ILC3 sorting (without the use of knock-in fluorescent labeling of RORγt) was not determined. Therefore, cells sorted in such a way can be referred to as enriched ILC3s, or just ILCs (as they are composed out of all three ILC types). The recommendation for future studies where these cells are used *in vitro* would be to evaluate the ILC distribution in post-sorted samples before engaging in any treatment or stimulation.

Human ILC3 cell sorting tends to be more difficult, as their surface markers may be different in peripheral blood mononuclear cells (PBMCs) and within the tissues. Also, unlike in mice, human ILC2 and ILC3 cannot exclusively be defined by transcription factors GATA3 and RORγt (409); therefore, there is no need for confirmation in post-sort samples. In general, ILC3 sorting from the PBMC or colon was performed according to the surface markers Lin$^-$CD45$^+$CD127$^+$CRTH2$^-$CD117$^+$ (410, 411). However, when ILC3s are sorted from the lungs, additional markers were included such as CD16$^-$NKG2A$^-$ and CD161$^+$ (411).

ILC3 sorting is usually done in order to perform single-cell RNA sequencing, *in-vitro* culture, or cell transfer. *In-vitro* culture of enriched human ILC3 is a prolonged process that requires several growth factors (SCF, IL-7, Flt-3L, IL-2, IL-15). The success of ILC3 propagation *in vitro* can depend upon a layer of cells to support ILC3 proliferation (such as mesenchymal stem cells) (79). Mouse-enriched ILC3s are usually cultured with SCF and IL-7 and on occasion with the addition of IL-1β, IL-12, or IL-23. *In-vitro* culture and stimulation of ILC3 with PMA/ionomycin/brefeldin is done in order to detect ILC3-derived cytokines. However, this can lead to the downregulation of ILC3-specific surface markers, thus interfering with flow cytometry analysis of post-treatment ILC3 (412). For performing a cell transfer, ILC3s are usually used freshly sorted from cell suspension derived from intestinal lamina propria or the lungs. Lamina propria is most often chosen as the source of

ILC3 because of the abundance of ILC3s in the innate immune cell compartment. As the numbers of obtained ILC3 from tissues are very low, researchers use from 100,000 to 500,000 cells per transfer (233, 267). Having in mind the required precision in ILC3 phenotyping, sorting, and culture conditions and the paucity of tissue ILC3, as well as the limited availability of organs/tissues for their isolation, the use of ILC3 for human cell therapy seems to be complex and unrealistic. Still, alternative strategies, such as propagating tissue-like ILC3 from $CD34^+$ hematopoietic progenitors (79), could overcome the above-stated obstacles on the road toward ILC3-based therapy.

9 Conclusions

The ILC3 research field is still relatively novel, and ILC3 identification by flow cytometry is not yet standardized. The expanding complexity of phenotypic determinants of ILC3 and the tissue specificities of ILC3 contribute to the discrepancies in protocols used by different research groups. Through analysis of the current state of phenotypic characterization of ILC3 by flow cytometry, we conclude that markers for the identification of ILC3 should be chosen in relation to the study species and design, as well as to the tissue of origin. The following are our suggestions for the identification of ILC3 by flow cytometry.

9.1 Mice: $CD3^-ROR\gamma t^+$

RORγt is the most reliable marker for ILC3 in mice. It is enough to use CD3 as the lineage marker in combination with RORγt in most of the studies. Additional lineage markers seem redundant as long as samples are not obtained from the lungs or spleen when neutrophil or myeloid/DC exclusion is needed. CD127 is required as an additional positive marker only if ILC1 and ILC2 are identified in parallel. CD90 should not be used as an exclusive ILC3 marker.

9.2 Humans: $CD3^-CD127^+CD117^+CD294^-$

CD127 in combination with T-cell-specific lineage markers is a proper way to distinguish human ILC from NK cells. CD294 is an ILC2-specific marker and is a good marker to discriminate between ILC2 and ILC3. As for the distinction of ILC1, CD117 is expressed on ILC2 and ILC3, but not on ILC1. The addition of CD161 is not necessary. It can be used instead of CD127, but in that case, additional lineage markers for myeloid cells are required. RORγt cannot be used for distinguishing ILC3 from other innate lymphocytes in humans.

9.3 General

There is no need to use CD45 when analyzing cells isolated from the blood, lymph nodes, spleen, or tonsils, but it is necessary to use it in quantitative analysis of tissue-residing ILC3.

In a number of studies analyzed in this review, we observe a superfluous use of lineage cocktail markers. Although unnecessary, such overapplication of markers does not jeopardize proper ILC3 identification. On the other hand, there are studies in which ILC3 is identified by an insufficient number of markers or inappropriate marker combinations. This raises the question of the accuracy of the results and the conclusions of such studies. We hope that this paper will help researchers interested in ILC3-related studies to tailor their research design to the best of their specific needs.

Author contributions

ĐMil: Conceptualization, Funding acquisition, Writing – original draft, Writing – review & editing. IK: Visualization, Writing – original draft, Writing – review & editing. SS: Visualization, Writing – original draft. BJ: Writing – original draft, Writing – review & editing. DMic: Writing – original draft, Writing – review & editing. IS: Conceptualization, Writing – original draft, Writing – review & editing.

Funding

The author(s) declare financial support was received for the research, authorship, and/or publication of this article. This work was supported by the Ministry of Science, Technological Development, and Innovations, Republic of Serbia, contract No. 451-03-47/2023-01/200007, and Science Fund, Republic of Serbia, Ideas Program, project GUTtoAID, contract No. 7742898.

Conflict of interest

The authors declare that the research was conducted in the absence of any commercial or financial relationships that could be construed as a potential conflict of interest.

Publisher's note

References

1. Miljković Đ, Jevtić B, Stojanović I, Dimitrijević M. ILC3, a central innate immune component of the gut-brain axis in multiple sclerosis. *Front Immunol* (2021) 12:657622. doi: 10.3389/fimmu.2021.657622

2. Stojanović I, Saksida T, Miljković Đ, Pejnović N. Modulation of intestinal ILC3 for the treatment of type 1 diabetes. *Front Immunol* (2021) 12:653560. doi: 10.3389/fimmu.2021.653560

3. Satoh-Takayama N, Vosshenrich CA, Lesjean-Pottier S, Sawa S, Lochner M, Rattis F, et al. Microbial flora drives interleukin 22 production in intestinal NKp46+ cells that provide innate mucosal immune defense. *Immunity* (2008) 29(6):958–70. doi: 10.1016/j.immuni.2008.11.001

4. Luci C, Reynders A, Ivanov II, Cognet C, Chiche L, Chasson L, et al. Influence of the transcription factor RORgammat on the development of NKp46+ cell populations in gut and skin. *Nat Immunol* (2009) 10(1):75–82. doi: 10.1038/ni.1681

5. Sanos SL, Bui VL, Mortha A, Oberle K, Heners C, Johner C, et al. RORgammat and commensal microflora are required for the differentiation of mucosal interleukin 22-producing NKp46+ cells. *Nat Immunol* (2009) 10(1):83–91. doi: 10.1038/ni.1684

6. Cella M, Fuchs A, Vermi W, Facchetti F, Otero K, Lennerz JK, et al. A human natural killer cell subset provides an innate source of IL-22 for mucosal immunity. *Nature* (2009) 457(7230):722–5. doi: 10.1038/nature07537

7. Cella M, Otero K, Colonna M. Expansion of human NK-22 cells with IL-7, IL-2, and IL-1beta reveals intrinsic functional plasticity. *Proc Natl Acad Sci U.S.A.* (2010) 107 (24):10961–6. doi: 10.1073/pnas.1005641107

8. Satoh-Takayama N, Lesjean-Pottier S, Vieira P, Sawa S, Eberl G, Vosshenrich CA, et al. IL-7 and IL-15 independently program the differentiation of intestinal CD3-NKp46+ cell subsets from Id2-dependent precursors. *J Exp Med* (2010) 207(2):273–80. doi: 10.1084/jem.20092029

9. Vonarbourg C, Mortha A, Bui VL, Hernandez PP, Kiss EA, Hoyler T, et al. Regulated expression of nuclear receptor RORγt confers distinct functional fates to NK cell receptor-expressing RORγt(+) innate lymphocytes. *Immunity* (2010) 33(5):736–51. doi: 10.1016/j.immuni.2010.10.017

10. Spits H, Di Santo JP. The expanding family of innate lymphoid cells: regulators and effectors of immunity and tissue remodeling. *Nat Immunol* (2011) 12(1):21–7. doi: 10.1038/ni.1962

11. Cupedo T, Crellin NK, Papazian N, Rombouts EJ, Weijer K, Grogan JL, et al. Human fetal lymphoid tissue-inducer cells are interleukin 17-producing precursors to RORC+ CD127+ natural killer-like cells. *Nat Immunol* (2009) 10(1):66–74. doi: 10.1038/ni.1668

12. Sawa S, Lochner M, Satoh-Takayama N, Dulauroy S, Bérard M, Kleinschek M, et al. RORγt+ innate lymphoid cells regulate intestinal homeostasis by integrating negative signals from the symbiotic microbiota. *Nat Immunol* (2011) 12(4):320–6. doi: 10.1038/ni.2002

13. Hepworth MR, Fung TC, Masur SH, Kelsen JR, McConnell FM, Dubrot J, et al. Immune tolerance. Group 3 innate lymphoid cells mediate intestinal selection of commensal bacteria-specific $CD4^+$ T cells. *Science* (2015) 348(6238):1031–5. doi: 10.1126/science.aaa4812

14. Zhong C, Zheng M, Zhu J. Lymphoid tissue inducer-A divergent member of the ILC family. *Cytokine Growth Factor Rev* (2018) 42:5–12. doi: 10.1016/j.cytogfr.2018.02.004

15. van de Pavert SA. Lymphoid Tissue inducer (LTi) cell ontogeny and functioning in embryo and adult. *BioMed J* (2021) 44(2):123–32. doi: 10.1016/j.bj.2020.12.003

16. Kim MY, Anderson G, White A, Jenkinson E, Arlt W, Martensson IL, et al. OX40 ligand and CD30 ligand are expressed on adult but not neonatal CD4+CD3- inducer cells: evidence that IL-7 signals regulate CD30 ligand but not OX40 ligand expression. *J Immunol* (2005) 174(11):6686–91. doi: 10.4049/jimmunol.174.11.6686

17. Spits H, Artis D, Colonna M, Diefenbach A, Di Santo JP, Eberl G, et al. Innate lymphoid cells–a proposal for uniform nomenclature. *Nat Rev Immunol* (2013) 13 (2):145–9. doi: 10.1038/nri3365

18. Montaldo E, Teixeira-Alves LG, Glatzer T, Durek P, Stervbo U, Hamann W, et al. Human RORγt(+)CD34(+) cells are lineage-specified progenitors of group 3 RORγt(+) innate lymphoid cells. *Immunity* (2014) 41(6):988–1000. doi: 10.1016/j.immuni.2014.11.010

19. Crellin NK, Trifari S, Kaplan CD, Cupedo T, Spits H. Human NKp44+IL-22+ cells and LTi-like cells constitute a stable RORC+ lineage distinct from conventional natural killer cells. *J Exp Med* (2010) 207(2):281–90. doi: 10.1084/jem.20091509

20. Scoville SD, Freud AG, Caligiuri MA. Modeling human natural killer cell development in the era of innate lymphoid cells. *Front Immunol* (2017) 8:360. doi: 10.3389/fimmu.2017.00360

21. Freud AG, Yokohama A, Becknell B, Lee MT, Mao HC, Ferketich AK, et al. Evidence for discrete stages of human natural killer cell differentiation *in vivo*. *J Exp Med* (2006) 203(4):1033–43. doi: 10.1084/jem.20052507

22. Scoville SD, Freud AG, Caligiuri MA. Cellular pathways in the development of human and murine innate lymphoid cells. *Curr Opin Immunol* (2019) 56:100–6. doi: 10.1016/j.coi.2018.11.003

23. Lim AI, Li Y, Lopez-Lastra S, Stadhouders R, Paul F, Casrouge A, et al. Systemic human ILC precursors provide a substrate for tissue ILC differentiation. *Cell* (2017) 168 (6):1086–1100.e10. doi: 10.1016/j.cell.2017.02.021

24. Scoville SD, Mundy-Bosse BL, Zhang MH, Chen L, Zhang X, Keller KA, et al. A progenitor cell expressing transcription factor RORγt generates all human innate lymphoid cell subsets. *Immunity* (2016) 44(5):1140–50. doi: 10.1016/j.immuni.2016.04.007

25. Chen L, Youssef Y, Robinson C, Ernst GF, Carson MY, Young KA, et al. CD56 expression marks human group 2 innate lymphoid cell divergence from a shared NK cell and group 3 innate lymphoid cell developmental pathway. *Immunity* (2018) 49 (3):464–476.e4. doi: 10.1016/j.immuni.2018.08.010

26. Cella M, Gamini R, Sécca C, Collins PL, Zhao S, Peng V, et al. Subsets of ILC3-ILC1-like cells generate a diversity spectrum of innate lymphoid cells in human mucosal tissues. *Nat Immunol* (2019) 20(8):980–91. doi: 10.1038/s41590-019-0425-y

27. Fuchs A, Vermi W, Lee JS, Lonardi S, Gilfillan S, Newberry RD, et al. Intraepithelial type 1 innate lymphoid cells are a unique subset of IL-12- and IL-15-responsive IFN-γ-producing cells. *Immunity* (2013) 38(4):769–81. doi: 10.1016/j.immuni.2013.02.010

28. Victor AR, Nalin AP, Dong W, McClory S, Wei M, Mao C, et al. IL-18 drives ILC3 proliferation and promotes IL-22 production via NF-κB. *J Immunol* (2017) 199 (7):2333–42. doi: 10.4049/jimmunol.1601554

29. Damele L, Amaro A, Serio A, Luchetti S, Pfeffer U, Mingari MC, et al. EZH1/2 inhibitors favor ILC3 development from human HSPC-CD34+ Cells. *Cancers (Basel)* (2021) 13(2):319. doi: 10.3390/cancers13020319

30. Hoorweg K, Peters CP, Cornelissen F, Aparicio-Domingo P, Papazian N, Kazemier G, et al. Functional differences between human NKp44(-) and NKp44(+) RORC(+) innate lymphoid cells. *Front Immunol* (2012) 3:72. doi: 10.3389/fimmu.2012.00072

31. Munneke JM, Björklund AT, Mjösberg JM, Garming-Legert K, Bernink JH, Blom B, et al. Activated innate lymphoid cells are associated with a reduced susceptibility to graft-versus-host disease. *Blood* (2014) 124(5):812–21. doi: 10.1182/blood-2013-11-536888

32. Damele L, Montaldo E, Moretta L, Vitale C, Mingari MC. Effect of tyrosin kinase inhibitors on NK cell and ILC3 development and function. *Front Immunol* (2018) 9:2433. doi: 10.3389/fimmu.2018.02433

33. Longman RS, Diehl GE, Victorio DA, Huh JR, Galan C, Miraldi ER, et al. CX_3CR1^+ mononuclear phagocytes support colitis-associated innate lymphoid cell production of IL-22. *J Exp Med* (2014) 211(8):1571–83. doi: 10.1084/jem.20140678

34. Talayero P, Mancebo E, Calvo-Pulido J, Rodríguez-Muñoz S, Bernardo I, Laguna-Goya R, et al. Innate lymphoid cells groups 1 and 3 in the epithelial compartment of functional human intestinal allografts. *Am J Transplant* (2016) 16 (1):72–82. doi: 10.1111/ajt.13435

35. Powell N, Lo JW, Biancheri P, Vossenkämper A, Pantazi E, Walker AW, et al. Interleukin 6 increases production of cytokines by colonic innate lymphoid cells in mice and patients with chronic intestinal inflammation. *Gastroenterology* (2015) 149 (2):456–67.e15. doi: 10.1053/j.gastro.2015.04.017

36. Bernink JH, Krabbendam L, Germar K, de Jong E, Gronke K, Kofoed-Nielsen M, et al. Interleukin-12 and -23 control plasticity of CD127(+) group 1 and group 3 innate lymphoid cells in the intestinal lamina propria. *Immunity* (2015) 43(1):146–60. doi: 10.1016/j.immuni.2015.06.019

37. Castellanos JG, Woo V, Viladomiu M, Putzel G, Lima S, Diehl GE, et al. Microbiota-induced TNF-like ligand 1A drives group 3 innate lymphoid cell-mediated barrier protection and intestinal T cell activation during colitis. *Immunity* (2018) 49 (6):1077–1089.e5. doi: 10.1016/j.immuni.2018.10.014

38. Seidelin JB, Bahl MI, Licht TR, Mead BE, Karp JM, Johansen JV, et al. Acute experimental barrier injury triggers ulcerative colitis-specific innate hyperresponsiveness and ulcerative colitis-type microbiome changes in humans. *Cell Mol Gastroenterol Hepatol* (2021) 12(4):1281–96. doi: 10.1016/j.jcmgh.2021.06.002

39. Le Coz C, Nolan BE, Trofa M, Kamsheh AM, Khokha MK, Lakhani SA, et al. Cytotoxic T-lymphocyte-associated protein 4 haploinsufficiency-associated inflammation can occur independently of T-cell hyperproliferation. *Front Immunol* (2018) 9:1715. doi: 10.3389/fimmu.2018.01715

40. Withers DR, Hepworth MR, Wang X, Mackley EC, Halford EE, Dutton EE, et al. Transient inhibition of RORγt therapeutically limits intestinal inflammation by reducing TH17 cells and preserving group 3 innate lymphoid cells. *Nat Med* (2016) 22(3):319–23. doi: 10.1038/nm.4046

41. Latek M, Lacwik P, Molinska K, Blauz A, Lach J, Rychlik B, et al. Effect of an intranasal corticosteroid on quality of life and local microbiome in young children with chronic rhinosinusitis: A randomized clinical trial. *JAMA Pediatr* (2023) 177(4):345–52. doi: 10.1001/jamapediatrics.2022.6172

42. Rethacker L, Boy M, Bisio V, Roussin F, Denizeau J, Vincent-Salomon A, et al. Innate lymphoid cells: NK and cytotoxic ILC3 subsets infiltrate metastatic breast cancer lymph nodes. *Oncoimmunology* (2022) 11(1):2057396. doi: 10.1080/2162402X.2022.2057396

43. Castleman MJ, Dillon SM, Purba CM, Cogswell AC, Kibbie JJ, McCarter MD, et al. Commensal and Pathogenic Bacteria Indirectly Induce IL-22 but Not IFNγ Production From Human Colonic ILC3 via Multiple Mechanisms. *Front Immunol* (2019) 10:649. doi: 10.3389/fimmu.2019.00649

44. Eken A, Yetkin MF, Vural A, Okus FZ, Erdem S, Azizoglu ZB, et al. Fingolimod alters tissue distribution and cytokine production of human and murine innate lymphoid cells. *Front Immunol* (2019) 10:217. doi: 10.3389/fimmu.2019.00217

45. Komlósi ZI, Kovács N, van de Veen W, Kirsch AI, FAhRner HB, Wawrzyniak M, et al. Human CD40 ligand-expressing type 3 innate lymphoid cells induce IL-10-producing immature transitional regulatory B cells. *J Allergy Clin Immunol* (2018) 142 (1):178–194.e11. doi: 10.1016/j.jaci.2017.07.046

46. Ssekamatte P, Nakibuule M, Nabatanzi R, Egesa M, Musubika C, Bbuye M, et al. Type 2 diabetes mellitus and latent tuberculosis infection moderately influence innate lymphoid cell immune responses in Uganda. *Front Immunol* (2021) 12:716819. doi: 10.3389/fimmu.2021.716819

47. Kindstedt E, Koskinen Holm C, Palmqvist P, Sjöström M, Lejon K, Lundberg P. Innate lymphoid cells are present in gingivitis and periodontitis. *J Periodontol* (2019) 90 (2):200–7. doi: 10.1002/JPER.17-0750

48. Heinrich B, Ruf B, Subramanyam V, Myojin Y, Lai CW, Craig AJ, et al. Checkpoint inhibitors modulate plasticity of innate lymphoid cells in peripheral blood of patients with hepatocellular carcinoma. *Front Immunol* (2022) 13:849958. doi: 10.3389/fimmu.2022.849958

49. Darboe A, Nielsen CM, Wolf AS, Wildfire J, Danso E, Sonko B, et al. Age-related dynamics of circulating innate lymphoid cells in an african population. *Front Immunol* (2020) 11:594107. doi: 10.3389/fimmu.2020.594107

50. Eken A, Cansever M, Somekh I, Mizoguchi Y, Zietara N, Okus FZ, et al. Genetic deficiency and biochemical inhibition of ITK affect human th17, treg, and innate lymphoid cells. *J Clin Immunol* (2019) 39(4):391–400. doi: 10.1007/s10875-019-00632-5

51. Haliloglu Y, Ozcan A, Erdem S, Azizoglu ZB, Bicer A, Ozarslan OY, et al. Characterization of cord blood CD3+ TCRVα7.2+ CD161high T and innate lymphoid cells in the pregnancies with gestational diabetes, morbidly adherent placenta, and pregnancy hypertension diseases. *Am J Reprod Immunol* (2022) 88(1):e13555. doi: 10.1111/aji.13555

52. Geier CB, Kraupp S, Bra D, Eibl MM, Farmer JR, Csomos K, et al. Reduced numbers of circulating group 2 innate lymphoid cells in patients with common variable immunodeficiency. *Eur J Immunol* (2017) 47(11):1959–69. doi: 10.1002/eji.201746961

53. Nagasawa M, Germar K, Blom B, Spits H. Human CD5+ Innate lymphoid cells are functionally immature and their development from CD34+ Progenitor cells is regulated by id2. *Front Immunol* (2017) 8:1047. doi: 10.3389/fimmu.2017.01047

54. Audia S, Moulinet T, Ciudad-Bonté M, Samson M, Facy O, Ortega-Deballon P, et al. Altered distribution and function of splenic innate lymphoid cells in adult chronic immune thrombocytopenia. *J Autoimmun* (2018) 93:139–44. doi: 10.1016/j.jaut.2018.07.015

55. Eken A, Cansever M, Okus FZ, Erdem S, Nain E, Azizoglu ZB, et al. ILC3 deficiency and generalized ILC abnormalities in DOCK8-deficient patients. *Allergy* (2020) 75(4):921–32. doi: 10.1111/all.14081

56. Petrasca A, Hambly R, Molloy O, Kearns S, Moran B, Smith CM, et al. Innate lymphoid cell (ILC) subsets are enriched in the skin of patients with hidradenitis suppurativa. *PloS One* (2023) 18(2):e0281688. doi: 10.1371/journal.pone.0281688

57. Nagasawa M, Heesters BA, Kradolfer CMA, Krabbendam L, Martinez-Gonzalez I, de Bruijn MJW, et al. KLRG1 and NKp46 discriminate subpopulations of human CD117+CRTH2- ILC biased toward ILC2 or ILC3. *J Exp Med* (2019) 216(8):1762–76. doi: 10.1084/jem.20190490

58. Riding AM, Loudon KW, Guo A, Ferdinand JR, Lok LSC, Richoz N, et al. Group 3 innate lymphocytes make a distinct contribution to type 17 immunity in bladder defence. *iScience* (2022) 25(7):104660. doi: 10.1016/j.isci.2022.104660

59. Sattler FR, Mert M, Sankaranarayanan I, Mack WJ, Galle-Treger L, Gonzalez E, et al. Feasibility of quantifying change in immune white cells in abdominal adipose tissue in response to an immune modulator in clinical obesity. *PloS One* (2020) 15(9): e0237496. doi: 10.1371/journal.pone.0237496

60. Pucci Molineris M, González Polo V, Rumbo C, Fuxman C, Lowestein C, Nachman F, et al. Acute cellular rejection in small-bowel transplantation impairs NCR + innate lymphoid cell subpopulation 3/interleukin 22 axis. *Transpl Immunol* (2020) 60:101288. doi: 10.1016/j.trim.2020.101288

61. Campana S, De Pasquale C, Barberi C, Oliveri D, Sidoti Migliore G, Galletti B, et al. Circulating ILC precursors expressing CD62L exhibit a type 2 signature distinctly decreased in psoriatic patients. *Eur J Immunol* (2021) 51(7):1792–8. doi: 10.1002/eji.202048893

62. Simmerman E, Qin X, Marshall B, Perry L, Cai L, Wang T, et al. Innate lymphoid cells: a paradigm for low SSI in cleft lip repair. *J Surg Res* (2016) 205(2):312–7. doi: 10.1016/j.jss.2016.06.081

63. Pearson C, Thornton EE, McKenzie B, Schaupp AL, Huskens N, Griseri T, et al. ILC3 GM-CSF production and mobilisation orchestrate acute intestinal inflammation. *Elife* (2016) 5:e10066. doi: 10.7554/eLife.10066

64. Cuthbert RJ, Fragkakis EM, Dunsmuir R, Li Z, Coles M, Marzo-Ortega H, et al. Brief report: group 3 innate lymphoid cells in human enthesis. *Arthritis Rheumatol* (2017) 69(9):1816–22. doi: 10.1002/art.40150

65. Wang S, Li J, Wu S, Cheng L, Shen Y, Ma W, et al. Type 3 innate lymphoid cell: a new player in liver fibrosis progression. *Clin Sci (Lond)* (2018) 132(24):2565–82. doi: 10.1042/CS20180482

66. Carvelli J, Piperoglou C, Bourenne J, Farnarier C, Banzet N, Demerlé C, et al. Imbalance of circulating innate lymphoid cell subpopulations in patients with septic shock. *Front Immunol* (2019) 10:2179. doi: 10.3389/fimmu.2019.02179

67. Wang SQ, Shen Y, Li J, Liu Y, Cheng LS, Wu SD, et al. Entecavir-induced interferon-λ1 suppresses type 2 innate lymphoid cells in patients with hepatitis B virus-related liver cirrhosis. *J Viral Hepat* (2021) 28(5):795–808. doi: 10.1111/jvh.13476

68. Bennstein SB, Scherenschlich N, Weinhold S, Manser AR, Noll A, Raba K, et al. Transcriptional and functional characterization of neonatal circulating Innate Lymphoid Cells. *Stem Cells Transl Med* (2021) 10(6):867–82. doi: 10.1002/sctm.20-0300

69. Braudeau C, Amouriaux K, Néel A, Herbreteau G, Salabert N, Rimbert M, et al. Persistent deficiency of circulating mucosal-associated invariant T (MAIT) cells in ANCA-associated vasculitis. *J Autoimmun* (2016) 70:73–9. doi: 10.1016/j.jaut.2016.03.015

70. Xuan X, Zhou J, Tian Z, Lin Y, Song J, Ruan Z, et al. ILC3 cells promote the proliferation and invasion of pancreatic cancer cells through IL-22/AKT signaling. *Clin Transl Oncol* (2020) 22(4):563–75. doi: 10.1007/s12094-019-02160-5

71. Heinrich B, Gertz EM, Schäffer AA, Craig A, Ruf B, Subramanyam V, et al. The tumour microenvironment shapes innate lymphoid cells in patients with hepatocellular carcinoma. *Gut* (2022) 71(6):1161–75. doi: 10.1136/gutjnl-2021-325288

72. Ercolano G, Wyss T, Salomé B, Romero P, Trabanelli S, Jandus C. Distinct and shared gene expression for human innate versus adaptive helper lymphoid cells. *J Leukoc Biol* (2020) 108(2):723–37. doi: 10.1002/JLB.5MA0120-209R

73. Ahn YO, Weeres MA, Neulen ML, Choi J, Kang SH, Heo DS, et al. Human group3 innate lymphoid cells express DR3 and respond to TL1A with enhanced IL-22 production and IL-2-dependent proliferation. *Eur J Immunol* (2015) 45(8):2335–42. doi: 10.1002/eji.201445213

74. Ruiter B, Patil SU, Shreffler WG. Vitamins A and D have antagonistic effects on expression of effector cytokines and gut-homing integrin in human innate lymphoid cells. *Clin Exp Allergy* (2015) 45(7):1214–25. doi: 10.1111/cea.12568

75. Min HK, Moon J, Lee SY, Lee AR, Lee CR, Lee J, et al. Expanded IL-22+ Group 3 innate lymphoid cells and role of oxidized LDL-C in the pathogenesis of axial spondyloarthritis with dyslipidaemia. *Immune Netw* (2021) 21(6):e43. doi: 10.4110/in.2021.21.e43

76. Wu Y, Yue J, Wu J, Zhou W, Li D, Ding K, et al. Obesity may provide pro-ILC3 development inflammatory environment in asthmatic children. *J Immunol Res* (2018) 2018:1628620. doi: 10.1155/2018/1628620

77. Xu Y, Romero R, Miller D, Silva P, Panaitescu B, Theis KR, et al. Innate lymphoid cells at the human maternal-fetal interface in spontaneous preterm labor. *Am J Reprod Immunol* (2018) 79(6):e12820. doi: 10.1111/aji.12820

78. Einenkel R, Ehrhardt J, Zygmunt M, Muzzio DO. Oxygen regulates ILC3 antigen presentation potential and pregnancy-related hormone actions. *Reprod Biol Endocrinol* (2022) 20(1):109. doi: 10.1186/s12958-022-00979-2

79. Bennstein SB, Weinhold S, Degistirici Ö, Oostendorp RAJ, Raba K, Kögler G, et al. Efficient *in vitro* generation of IL-22-secreting ILC3 from CD34+ Hematopoietic progenitors in a human mesenchymal stem cell niche. *Front Immunol* (2021) 12:797432. doi: 10.3389/fimmu.2021.797432

80. Ciccia F, Guggino G, Rizzo A, Saieva L, Peralta S, Giardina A, et al. Type 3 innate lymphoid cells producing IL-17 and IL-22 are expanded in the gut, in the peripheral blood, synovial fluid and bone marrow of patients with ankylosing spondylitis. *Ann Rheum Dis* (2015) 74(9):1739–47. doi: 10.1136/annrheumdis-2014-206323

81. Kiekens L, Wahlen S, Persyn E, De Vos Z, Taghon T, Vandekerckhove B, et al. T-BET drives the conversion of human type 3 innate lymphoid cells into functional NK cells. *Front Immunol* (2022) 13:975778. doi: 10.3389/fimmu.2022.975778

82. Forkel M, van Tol S, Höög C, Michaëlsson J, Almer S, Mjösberg J. Distinct alterations in the composition of mucosal innate lymphoid cells in newly diagnosed and established crohn's disease and ulcerative colitis. *J Crohns Colitis* (2019) 13(1):67–78. doi: 10.1093/ecco-jcc/jjy119

83. Villanova F, Flutter B, Tosi I, Grys K, Sreeneebus H, Perera GK, et al. Characterization of innate lymphoid cells in human skin and blood demonstrates increase of NKp44+ ILC3 in psoriasis. *J Invest Dermatol* (2014) 134(4):984–91. doi: 10.1038/jid.2013.477

84. Pelosi A, Alicata C, Tumino N, Ingegnere T, Loiacono F, Mingari MC, et al. An anti-inflammatory microRNA signature distinguishes group 3 innate lymphoid cells from natural killer cells in human decidua. *Front Immunol* (2020) 11:133. doi: 10.3389/fimmu.2020.00133

85. Pascual-Reguant A, Köhler R, Mothes R, Bauherr S, Hernández DC, Uecker R, et al. Multiplexed histology analyses for the phenotypic and spatial characterization of human innate lymphoid cells. *Nat Commun* (2021) 12(1):1737. doi: 10.1038/s41467-021-21994-8

86. Wang SC, Yang KD, Lin CY, Huang AY, Hsiao CC, Lin MT, et al. Intravenous immunoglobulin therapy enhances suppressive regulatory T cells and decreases innate lymphoid cells in children with immune thrombocytopenia. *Pediatr Blood Cancer* (2020) 67(2):e28075. doi: 10.1002/pbc.28075

87. Chen ZX, Liu HQ, Wu ZH, He JL, Zhong HJ. Type 3 innate lymphoid cells as an indicator of renal dysfunction and serum uric acid in hyperuricemia. *Adv Clin Exp Med* (2023) 32(3):307–13. doi: 10.17219/acem/154625

88. Huang JC, Schleisman M, Choi D, Mitchell C, Watson L, Asquith M, et al. Preliminary report on interleukin-22, GM-CSF, and IL-17F in the pathogenesis of acute anterior uveitis. *Ocul Immunol Inflammation* (2021) 29(3):558–65. doi: 10.1080/09273948.2019.1686156

89. Kawka L, Felten R, Schleiss C, Fauny JD, Le Van Quyen P, Dumortier H, et al. Alteration of innate lymphoid cell homeostasis mainly concerns salivary glands in primary Sjögren's syndrome. *RMD Open* (2023) 9(2):e003051. doi: 10.1136/rmdopen-2023-003051

90. Rodríguez-Carrio J, Hähnlein JS, Ramwadhdoebe TH, Semmelink JF, Choi IY, van Lienden KP, et al. Brief report: altered innate lymphoid cell subsets in human lymph node biopsy specimens obtained during the at-risk and earliest phases of rheumatoid arthritis. *Arthritis Rheumatol* (2017) 69(1):70–6. doi: 10.1002/art.39811

91. Ham J, Kim J, Sohn KH, Park IW, Choi BW, Chung DH, et al. Cigarette smoke aggravates asthma by inducing memory-like type 3 innate lymphoid cells. *Nat Commun* (2022) 13(1):3852. doi: 10.1038/s41467-022-31491-1

92. Zhang Z, Cheng L, Zhao J, Li G, Zhang L, Chen W, et al. Plasmacytoid dendritic cells promote HIV-1-induced group 3 innate lymphoid cell depletion. *J Clin Invest* (2015) 125(9):3692–703. doi: 10.1172/JCI82124

93. De Grove KC, Provoost S, Verhamme FM, Bracke KR, Joos GF, Maes T, et al. Characterization and quantification of innate lymphoid cell subsets in human lung. *PloS One* (2016) 11(1):e0145961. doi: 10.1371/journal.pone.0145961

94. Graves CL, Li J, LaPato M, Shapiro MR, Glover SC, Wallet MA, et al. Intestinal epithelial cell regulation of adaptive immune dysfunction in human type 1 diabetes. *Front Immunol* (2017) 7:679. doi: 10.3389/fimmu.2016.00679

95. Gómez-Massa E, Lasa-Lázaro M, Gil-Etayo FJ, Ulloa-Márquez E, Justo I, Loinaz C, et al. Donor helper innate lymphoid cells are replaced earlier than lineage positive cells and persist long-term in human intestinal grafts - a descriptive study. *Transpl Int* (2020) 33(9):1016–29. doi: 10.1111/tri.13609

96. Zhou L, Zhou W, Joseph AM, Chu C, Putzel GG, Fang B, et al. Group 3 innate lymphoid cells produce the growth factor HB-EGF to protect the intestine from TNF-mediated inflammation. *Nat Immunol* (2022) 23(2):251–61. doi: 10.1038/s41590-021-01110-0

97. Li C, Liu J, Pan J, Wang Y, Shen L, Xu Y. ILC1s and ILC3 exhibit inflammatory phenotype in periodontal ligament of periodontitis patients. *Front Immunol* (2021) 12:708678. doi: 10.3389/fimmu.2021.708678

98. Lyu M, Suzuki H, Kang L, Gaspal F, Zhou W, Goc J, et al. ILC3 select microbiota-specific regulatory T cells to establish tolerance in the gut. *Nature* (2022) 610 (7933):744–51. doi: 10.1038/s41586-022-05141-x

99. Kang J, Loh K, Belyayev L, Cha P, Sadat M, Khan K, et al. Type 3 innate lymphoid cells are associated with a successful intestinal transplant. *Am J Transplant* (2021) 21(2):787–97. doi: 10.1111/ajt.16163

100. Zhou L, Chu C, Teng F, Bessman NJ, Goc J, Santosa EK, et al. Innate lymphoid cells support regulatory T cells in the intestine through interleukin-2. *Nature* (2019) 568(7752):405–9. doi: 10.1038/s41586-019-1082-x

101. Vacca P, Montaldo E, Croxatto D, Loiacono F, Canegallo F, Venturini PL, et al. Identification of diverse innate lymphoid cells in human decidua. *Mucosal Immunol* (2015) 8(2):254–64. doi: 10.1038/mi.2014.63

102. Croxatto D, Micheletti A, Montaldo E, Orecchia P, Loiacono F, Canegallo F, et al. Group 3 innate lymphoid cells regulate neutrophil migration and function in human decidua. *Mucosal Immunol* (2016) 9(6):1372–83. doi: 10.1038/mi.2016.10

103. Vacca P, Pesce S, Greppi M, Fulcheri E, Munari E, Olive D, et al. PD-1 is expressed by and regulates human group 3 innate lymphoid cells in human decidua. *Mucosal Immunol* (2019) 12(3):624–31. doi: 10.1038/s41385-019-0141-9

104. Croft CA, Thaller A, Marie S, Doisne JM, Surace L, Yang R, et al. Notch, RORC and IL-23 signals cooperate to promote multi-lineage human innate lymphoid cell differentiation. *Nat Commun* (2022) 13(1):4344. doi: 10.1038/s41467-022-32089-3

105. Shikhagaie MM, Björklund ÅK, Mjösberg J, Erjefält JS, Cornelissen AS, Ros XR, et al. Neuropilin-1 is expressed on lymphoid tissue residing LTi-like group 3 innate lymphoid cells and associated with ectopic lymphoid aggregates. *Cell Rep* (2017) 18 (7):1761–73. doi: 10.1016/j.celrep.2017.01.063

106. Mitsialis V, Wall S, Liu P, Ordovas-Montanes J, Parmet T, Vukovic M, et al. Single-cell analyses of colon and blood reveal distinct immune cell signatures of ulcerative colitis and crohn's disease. *Gastroenterology* (2020) 159(2):591–608.e10. doi: 10.1053/j.gastro.2020.04.074

107. Konya V, Czarnewski P, Forkel M, Rao A, Kokkinou E, Villablanca EJ, et al. Vitamin D downregulates the IL-23 receptor pathway in human mucosal group 3 innate lymphoid cells. *J Allergy Clin Immunol* (2018) 141(1):279–92. doi: 10.1016/j.jaci.2017.01.045

108. Kroeze A, van Hoeven V, Verheij MW, Turksma AW, Weterings N, van Gassen S, et al. Presence of innate lymphoid cells in allogeneic hematopoietic grafts correlates with reduced graft-versus-host disease. *Cytotherapy* (2022) 24(3):302–10. doi: 10.1016/j.jcyt.2021.10.011

109. Coorens M, Rao A, Gräfe SK, Unelius D, Lindforss U, Agerberth B, et al. Innate lymphoid cell type 3-derived interleukin-22 boosts lipocalin-2 production in intestinal epithelial cells via synergy between STAT3 and NF-κB. *J Biol Chem* (2019) 294 (15):6027–41. doi: 10.1074/jbc.RA118.007290

110. Bernink JH, Ohne Y, Teunissen MBM, Wang J, Wu J, Krabbendam L, et al. c-Kit-positive ILC2s exhibit an ILC3-like signature that may contribute to IL-17-mediated pathologies. *Nat Immunol* (2019) 20(8):992–1003. doi: 10.1038/s41590-019-0423-0

111. Hazenberg MD, Haverkate NJE, van Lier YF, Spits H, Krabbendam L, Bemelman WA, et al. Human ectoenzyme-expressing ILC3: immunosuppressive innate cells that are depleted in graft-versus-host disease. *Blood Adv* (2019) 3 (22):3650–60. doi: 10.1182/bloodadvances.2019000176

112. Mazzurana L, Forkel M, Rao A, Van Acker A, Kokkinou E, Ichiya T, et al. Suppression of Aiolos and Ikaros expression by lenalidomide reduces human ILC3-ILC1/NK cell transdifferentiation. *Eur J Immunol* (2019) 49(9):1344–55. doi: 10.1002/eji.201848075

113. Krämer B, Goeser F, Lutz P, Glässner A, Boesecke C, Schwarze-Zander C, et al. Compartment-specific distribution of human intestinal innate lymphoid cells is altered in HIV patients under effective therapy. *PloS Pathog* (2017) 13(5):e1006373. doi: 10.1371/journal.ppat.1006373

114. Gelmez MY, Cinar S, Cetin EA, Ozcit-Gürel G, Babuna-Kobaner G, Erdugan M, et al. Inflammatory status might direct ILC and NK cells to IL-17 expressing ILC3 and NK subsets in Behcet's disease. *Immunol Lett* (2021) 235:1–8. doi: 10.1016/j.imlet.2021.04.008

115. Cole S, Murray J, Simpson C, Okoye R, Tyson K, Griffiths M, et al. Interleukin (IL)-12 and IL-18 synergize to promote MAIT cell IL-17A and IL-17F production independently of IL-23 signaling. *Front Immunol* (2020) 11:585134. doi: 10.3389/fimmu.2020.585134

116. Creyns B, Jacobs I, Verstockt B, Cremer J, Ballet V, Vandecasteele R, et al. Biological therapy in inflammatory bowel disease patients partly restores intestinal innate lymphoid cell subtype equilibrium. *Front Immunol* (2020) 11:1847. doi: 10.3389/fimmu.2020.01847

117. Yu H, Wei Y, Dong Y, Chen P. Regulation of notch signaling pathway to innate lymphoid cells in patients with acute myocardial infarction. *Immunol Invest* (2023) 52 (2):241–55. doi: 10.1080/08820139.2022.2158856

118. Mohr A, Trésallet C, Monot N, Bauvois A, Abiven D, Atif M, et al. Tissue infiltrating LTi-like group 3 innate lymphoid cells and T follicular helper cells in graves' and hashimoto's thyroiditis. *Front Immunol* (2020) 11:601. doi: 10.3389/fimmu.2020.00601

119. Zhang L, Lin Q, Jiang L, Wu M, Huang L, Quan W, et al. Increased circulating innate lymphoid cell (ILC)1 and decreased circulating ILC3 are involved in the pathogenesis of Henoch-Schonlein purpura. *BMC Pediatr* (2022) 22(1):201. doi: 10.1186/s12887-022-03262-w

120. Mendes J, Rodrigues-Santos P, Areia AL, Almeida JS, Alves V, Santos-Rosa M, et al. Type 2 and type 3 innate lymphoid cells at the maternal-fetal interface: implications in preterm birth. *BMC Immunol* (2021) 22(1):28. doi: 10.1186/s12865-021-00423-x

121. Goc J, Lv M, Bessman NJ, Flamar AL, Sahota S, Suzuki H, et al. Dysregulation of ILC3 unleashes progression and immunotherapy resistance in colon cancer. *Cell* (2021) 184(19):5015–5030.e16. doi: 10.1016/j.cell.2021.07.029

122. Chang Y, Kim JW, Yang S, Chung DH, Ko JS, Moon JS, et al. Increased GM-CSF-producing NCR- ILC3s and neutrophils in the intestinal mucosa exacerbate inflammatory bowel disease. *Clin Transl Immunol* (2021) 10(7):e1311. doi: 10.1002/cti2.1311

123. de Sousa TR, Sgnotto FDR, Fagundes BO, Duarte AJDS, Victor JR. Non-atopic neonatal thymic innate lymphoid cell subsets (ILC1, ILC2, and ILC3) identification and the modulatory effect of igG from dermatophagoides pteronyssinus (Derp)-atopic individuals. *Front Allergy* (2021) 2:650235. doi: 10.3389/falgy.2021.650235

124. Schielke L, Zimmermann N, Hobelsberger S, Steininger J, Strunk A, Blau K, et al. Metabolic syndrome in psoriasis is associated with upregulation of CXCL16 on monocytes and a dysbalance in innate lymphoid cells. *Front Immunol* (2022) 13:916701. doi: 10.3389/fimmu.2022.916701

125. Chu C, Moriyama S, Li Z, Zhou L, Flamar AL, Klose CSN, et al. Anti-microbial functions of group 3 innate lymphoid cells in gut-associated lymphoid tissues are regulated by G-protein-coupled receptor 183. *Cell Rep* (2018) 23(13):3750–8. doi: 10.1016/j.celrep.2018.05.099

126. Cruz-Zárate D, Cabrera-Rivera GL, Ruiz-Sánchez BP, Serafín-López J, Chacón-Salinas R, López-Macías C, et al. Innate Lymphoid Cells Have Decreased HLA-DR Expression but Retain Their Responsiveness to TLR Ligands during Sepsis. *J Immunol* (2018) 201(11):3401–10. doi: 10.4049/jimmunol.1800735

127. Teng F, Goc J, Zhou L, Chu C, Shah MA, Eberl G, et al. A circadian clock is essential for homeostasis of group 3 innate lymphoid cells in the gut. *Sci Immunol* (2019) 4(40):eaax1215. doi: 10.1126/sciimmunol.aax1215

128. Wang X, Cai J, Lin B, Ma M, Tao Y, Zhou Y, et al. GPR34-mediated sensing of lysophosphatidylserine released by apoptotic neutrophils activates type 3 innate lymphoid cells to mediate tissue repair. *Immunity* (2021) 54(6):1123–1136.e8. doi: 10.1016/j.immuni.2021.05.007

129. Hu C, Xu B, Wang X, Wan WH, Lu J, Kong D, et al. Gut microbiota-derived short-chain fatty acids regulate group 3 innate lymphoid cells in HCC. *Hepatology* (2023) 77(1):48–64. doi: 10.1002/hep.32449

130. Siegler JJ, Correia MP, Hofman T, Prager I, Birgin E, Rahbari NN, et al. Human ILC3 exert TRAIL-mediated cytotoxicity towards cancer cells. *Front Immunol* (2022) 13:742571. doi: 10.3389/fimmu.2022.742571

131. Pan L, Chen X, Liu X, Qiu W, Liu Y, Jiang W, et al. Innate lymphoid cells exhibited IL-17-expressing phenotype in active tuberculosis disease. *BMC Pulm Med* (2021) 21(1):318. doi: 10.1186/s12890-021-01678-1

132. Qi J, Crinier A, Escalière B, Ye Y, Wang Z, Zhang T, et al. Single-cell transcriptomic landscape reveals tumor specific innate lymphoid cells associated with colorectal cancer progression. *Cell Rep Med* (2021) 2(8):100353. doi: 10.1016/j.xcrm.2021.100353

133. Hou M, Liu S. Innate lymphoid cells are increased in systemic lupus erythematosus. *Clin Exp Rheumatol* (2019) 37(4):676–9.

134. Tang Y, Tan SA, Iqbal A, Li J, Glover SC. STAT3 Genotypic Variant rs744166 and Increased Tyrosine Phosphorylation of STAT3 in IL-23 Responsive Innate Lymphoid Cells during Pathogenesis of Crohn's Disease. *J Immunol Res* (2019) 2019:9406146. doi: 10.1155/2019/9406146

135. Fu W, Wang W, Zhang J, Zhao Y, Chen K, Wang Y, et al. Dynamic change of circulating innate and adaptive lymphocytes subtypes during a cascade of gastric lesions. *J Leukoc Biol* (2022) 112(4):931–8. doi: 10.1002/JLB.5MA0422-505R

136. Guo C, Zhou M, Zhao S, Huang Y, Wang S, Fu R, et al. Innate lymphoid cell disturbance with increase in ILC1 in systemic lupus erythematosus. *Clin Immunol* (2019) 202:49–58. doi: 10.1016/j.clim.2019.03.008

137. Soare A, Weber S, Maul L, Rauber S, Gheorghiu AM, Luber M, et al. Cutting edge: homeostasis of innate lymphoid cells is imbalanced in psoriatic arthritis. *J Immunol* (2018) 200(4):1249–54. doi: 10.4049/jimmunol.1700596

138. Björklund ÅK, Forkel M, Picelli S, Konya V, Theorell J, Friberg D, et al. The heterogeneity of human CD127(+) innate lymphoid cells revealed by single-cell RNA sequencing. *Nat Immunol* (2016) 17(4):451–60. doi: 10.1038/ni.3368

139. Camelo A, Rosignoli G, Ohne Y, Stewart RA, Overed-Sayer C, Sleeman MA, et al. IL-33, IL-25, and TSLP induce a distinct phenotypic and activation profile in human type 2 innate lymphoid cells. *Blood Adv* (2017) 1(10):577–89. doi: 10.1182/bloodadvances.2016002352

140. Bar-Ephraim YE, Cornelissen F, Papazian N, Konijn T, Hoogenboezem RM, Sanders MA, et al. Cross-tissue transcriptomic analysis of human secondary lymphoid organ-residing ILC3 reveals a quiescent state in the absence of inflammation. *Cell Rep* (2017) 21(3):823–33. doi: 10.1016/j.celrep.2017.09.070

141. Teunissen MBM, Munneke JM, Bernink JH, Spuls PI, Res PCM, Te Velde A, et al. Composition of innate lymphoid cell subsets in the human skin: enrichment of NCR(+) ILC3 in lesional skin and blood of psoriasis patients. *J Invest Dermatol* (2014) 134(9):2351–60. doi: 10.1038/jid.2014.146

142. Aglas-Leitner F, Juillard P, Juillard A, Byrne SN, Hawke S, Grau GE, et al. Circulating CCR6+ILC proportions are lower in multiple sclerosis patients. *Clin Transl Immunol* (2022) 11(12):e1426. doi: 10.1002/cti2.1426

143. Aglas-Leitner FT, Juillard P, Juillard A, Byrne SN, Hawke S, Grau GE, et al. Mass cytometry reveals cladribine-induced resets among innate lymphoid cells in multiple sclerosis. *Sci Rep* (2022) 12(1):20411. doi: 10.1038/s41598-022-24617-4

144. Sugahara T, Tanaka Y, Hamaguchi M, Fujii M, Shimura K, Ogawa K, et al. Reduced innate lymphoid cells in the endometrium of women with endometriosis. *Am J Reprod Immunol* (2022) 87(1):e13502. doi: 10.1111/aji.13502

145. Raabe J, Kaiser KM, ToVinh M, Finnemann C, Lutz P, Hoffmeister C, et al. Identification and characterisation of a hepatic IL-13 producing ILC3-like population potentially involved in liver fibrosis. *Hepatology* (2023) 78(3):787–802. doi: 10.1097/HEP.0000000000000350

146. Bracamonte-Baran W, Chen G, Hou X, Talor MV, Choi HS, Davogustto G, et al. Non-cytotoxic cardiac innate lymphoid cells are a resident and quiescent type 2-commited population. *Front Immunol* (2019) 10:634. doi: 10.3389/fimmu.2019.00634

147. Baban B, Braun M, Khodadadi H, Ward A, Alverson K, Malik A, et al. AMPK induces regulatory innate lymphoid cells after traumatic brain injury. *JCI Insight* (2021) 6(1):e126766. doi: 10.1172/jci.insight.126766

148. Oherle K, Acker E, Bonfield M, Wang T, Gray J, Lang I, et al. Insulin-like growth factor 1 supports a pulmonary niche that promotes type 3 innate lymphoid cell development in newborn lungs. *Immunity* (2020) 52(2):275–294.e9. doi: 10.1016/j.immuni.2020.01.005

149. Rodríguez OL, Lugo DA, Cabrera M, Sánchez MA, Zerpa O, Tapia FJ. Innate lymphoid cells in peripheral blood of patients with American Cutaneous Leishmaniasis. *Exp Dermatol* (2021) 30(7):982–7. doi: 10.1111/exd.14351

150. Mxinwa V, Dludla PV, Nyambuya TM, Nkambule BB. Circulating innate lymphoid cell subtypes and altered cytokine profiles following an atherogenic high-fat diet. *Innate Immun* (2021) 27(7-8):525–32. doi: 10.1177/17534259211053634

151. Kawano Y, Edwards M, Huang Y, Bilate AM, Araujo LP, Tanoue T, et al. Microbiota imbalance induced by dietary sugar disrupts immune-mediated protection from metabolic syndrome. *Cell* (2022) 185(19):3501–3519.e20. doi: 10.1016/j.cell.2022.08.005

152. von Burg N, Chappaz S, Baerenwaldt A, Horvath E, Bose Dasgupta S, Ashok D, et al. Activated group 3 innate lymphoid cells promote T-cell-mediated immune responses. *Proc Natl Acad Sci U.S.A.* (2014) 111(35):12835–40. doi: 10.1073/pnas.1406908111

153. Wu C, He S, Liu J, Wang B, Lin J, Duan Y, et al. Type 1 innate lymphoid cell aggravation of atherosclerosis is mediated through TLR4. *Scand J Immunol* (2018) 87(5):e12661. doi: 10.1111/sji.12661

154. Hoorweg K, Narang P, Li Z, Thuery A, Papazian N, Withers DR, et al. A stromal cell niche for human and mouse type 3 innate lymphoid cells. *J Immunol* (2015) 195(9):4257–63. doi: 10.4049/jimmunol.1402584

155. Niu X, Daniel S, Kumar D, Ding EY, Savani RC, Koh AY, et al. Transient neonatal antibiotic exposure increases susceptibility to late-onset sepsis driven by microbiota-dependent suppression of type 3 innate lymphoid cells. *Sci Rep* (2020) 10(1):12974. doi: 10.1038/s41598-020-69797-z

156. Zhao D, Yang B, Ye C, Zhang S, Lv X, Chen Q. Enteral nutrition ameliorates the symptoms of Crohn's disease in mice via activating special pro-resolving mediators through innate lymphoid cells. *Innate Immun* (2021) 27(7-8):533–42. doi: 10.1177/17534259211057038

157. Yu Y, Tsang JC, Wang C, Clare S, Wang J, Chen X, et al. Single-cell RNA-seq identifies a PD-1hi ILC progenitor and defines its development pathway. *Nature* (2016) 539(7627):102–6. doi: 10.1038/nature20105

158. Shen W, Hixon JA, McLean MH, Li WQ, Durum SK. IL-22-expressing murine lymphocytes display plasticity and pathogenicity in reporter mice. *Front Immunol* (2016) 6:662. doi: 10.3389/fimmu.2015.00662

159. Warren KJ, Poole JA, Sweeter JM, DeVasure JM, Dickinson JD, Peebles RS Jr, et al. Neutralization of IL-33 modifies the type 2 and type 3 inflammatory signature of viral induced asthma exacerbation. *Respir Res* (2021) 22(1):206. doi: 10.1186/s12931-021-01799-5

160. Satoh-Takayama N, Serafini N, Verrier T, Rekiki A, Renauld JC, Frankel G, et al. The chemokine receptor CXCR6 controls the functional topography of interleukin-22 producing intestinal innate lymphoid cells. *Immunity* (2014) 41(5):776–88. doi: 10.1016/j.immuni.2014.10.007

161. Zhong C, Cui K, Wilhelm C, Hu G, Mao K, Belkaid Y, et al. Group 3 innate lymphoid cells continuously require the transcription factor GATA-3 after commitment. *Nat Immunol* (2016) 17(2):169–78. doi: 10.1038/ni.3318

162. Li Z, Hodgkinson T, Gothard EJ, Boroumand S, Lamb R, Cummins I, et al. Epidermal Notch1 recruits RORγ(+) group 3 innate lymphoid cells to orchestrate normal skin repair. *Nat Commun* (2016) 7:11394. doi: 10.1038/ncomms11394

163. Dutton EE, Camelo A, Sleeman M, Herbst R, Carlesso G, Belz GT, et al. Characterisation of innate lymphoid cell populations at different sites in mice with defective T cell immunity. *Wellcome Open Res* (2017) 2:117. doi: 10.12688/wellcomeopenres.13199.3

164. Miranda MCG, Oliveira RP, Torres L, Aguiar SLF, Pinheiro-Rosa N, Lemos L, et al. Frontline Science: Abnormalities in the gut mucosa of non-obese diabetic mice precede the onset of type 1 diabetes. *J Leukoc Biol* (2019) 106(3):513–29. doi: 10.1002/JLB.3HI0119-024RR

165. Godinho-Silva C, Domingues RG, Rendas M, Raposo B, Ribeiro H, da Silva JA, et al. Light-entrained and brain-tuned circadian circuits regulate ILC3 and gut homeostasis. *Nature* (2019) 574(7777):254–8. doi: 10.1038/s41586-019-1579-3

166. Gao X, Shen X, Liu K, Lu C, Fan Y, Xu Q, et al. The transcription factor thPOK regulates ILC3 lineage homeostasis and function during intestinal infection. *Front Immunol* (2022) 13:939033. doi: 10.3389/fimmu.2022.939033

167. Fuchs A, Ghosh S, Chang SW, Bochicchio GV, Turnbull IR. Pseudomonas aeruginosa pneumonia causes a loss of type-3 and an increase in type-1 innate lymphoid cells in the gut. *J Surg Res* (2021) 265:212–22. doi: 10.1016/j.jss.2021.03.043

168. Yan J, Yu J, Yuan S, Tang W, Ma W, Yang X, et al. Musculin is highly enriched in Th17 and IL-22-producing ILC3 and restrains pro-inflammatory cytokines in murine colitis. *Eur J Immunol* (2021) 51(4):995–8. doi: 10.1002/eji.202048573

169. Hu L, Hu J, Chen L, Zhang Y, Wang Q, Yang X. Interleukin-22 from type 3 innate lymphoid cells aggravates lupus nephritis by promoting macrophage infiltration in lupus-prone mice. *Front Immunol* (2021) 12:584414. doi: 10.3389/fimmu.2021.584414

170. Jones R, Cosway EJ, Willis C, White AJ, Jenkinson WE, Fehling HJ, et al. Dynamic changes in intrathymic ILC populations during murine neonatal development. *Eur J Immunol* (2018) 48(9):1481–91. doi: 10.1002/eji.201847511

171. Cai J, Lu H, Su Z, Mi L, Xu S, Xue Z. Dynamic changes of NCR- type 3 innate lymphoid cells and their role in mice with bronchopulmonary dysplasia. *Inflammation* (2022) 45(2):497–508. doi: 10.1007/s10753-021-01543-7

172. Fiancette R, Finlay CM, Willis C, Bevington SL, Soley J, Ng STH, et al. Reciprocal transcription factor networks govern tissue-resident ILC3 subset function and identity. *Nat Immunol* (2021) 22(10):1245–55. doi: 10.1038/s41590-021-01024-x

173. Cuff AO, Male V. Conventional NK cells and ILC1 are partially ablated in the livers of Ncr1 iCreTbx21 fl/fl mice. *Wellcome Open Res* (2017) 2:39. doi: 10.12688/wellcomeopenres.11741.2

174. Javadzadeh SM, Keykhosravi M, Tehrani M, Asgarian-Omran H, Rashidi M, Hossein-Nattaj H, et al. Evaluation of innate lymphoid cells (ILC) population in the mouse model of colorectal cancer. *Iran J Immunol* (2022) 19(4):339–48. doi: 10.22034/IJI.2022.92467.2152

175. Gray J, Oehrle K, Worthen G, Alenghat T, Whitsett J, Deshmukh H. Intestinal commensal bacteria mediate lung mucosal immunity and promote resistance of newborn mice to infection. *Sci Transl Med* (2017) 9(376):eaaf9412. doi: 10.1126/scitranslmed.aaf9412

176. Okubo Y, Tokumaru S, Yamamoto Y, Miyagawa SI, Sanjo H, Taki S. Generation of a common innate lymphoid cell progenitor requires interferon regulatory factor 2. *Int Immunol* (2019) 31(8):489–98. doi: 10.1093/intimm/dxz019

177. Yamamoto Y, Yoshizawa K, Takamoto M, Soejima Y, Sanjo H, Taki S. Circulating T cells and resident non-T cells restrict type 2 innate lymphoid cell expansion in the small intestine. *Biochem Biophys Res Commun* (2022) 618:93–9. doi: 10.1016/j.bbrc.2022.06.007

178. Leon-Coria A, Kumar M, Workentine M, Moreau F, Surette M, Chadee K. Muc2 mucin and nonmucin microbiota confer distinct innate host defense in disease susceptibility and colonic injury. *Cell Mol Gastroenterol Hepatol* (2021) 11(1):77–98. doi: 10.1016/j.jcmgh.2020.07.003

179. Walker JA, Clark PA, Crisp A, Barlow JL, Szeto A, Ferreira ACF, et al. Polychromic reporter mice reveal unappreciated innate lymphoid cell progenitor heterogeneity and elusive ILC3 progenitors in bone marrow. *Immunity* (2019) 51(1):104–118.e7. doi: 10.1016/j.immuni.2019.05.002

180. Aparicio-Domingo P, Romera-Hernandez M, Karrich JJ, Cornelissen F, Papazian N, Lindenbergh-Kortleve DJ, et al. Type 3 innate lymphoid cells maintain intestinal epithelial stem cells after tissue damage. *J Exp Med* (2015) 212(11):1783–91. doi: 10.1084/jem.20150318

181. Wanke F, Tang Y, Gronke K, Klebow S, Moos S, Hauptmann J, et al. Expression of IL-17F is associated with non-pathogenic Th17 cells. *J Mol Med (Berl)* (2018) 96(8):819–29. doi: 10.1007/s00109-018-1662-5

182. Castro-Dopico T, Fleming A, Dennison TW, Ferdinand JR, Harcourt K, Stewart BJ, et al. GM-CSF calibrates macrophage defense and wound healing programs during intestinal infection and inflammation. *Cell Rep* (2020) 32 (1):107857. doi: 10.1016/j.celrep.2020.107857

183. Sim S, Lee DH, Kim KS, Park HJ, Kim YK, Choi Y, et al. Micrococcus luteus-derived extracellular vesicles attenuate neutrophilic asthma by regulating miRNAs in airway epithelial cells. *Exp Mol Med* (2023) 55(1):196–204. doi: 10.1038/s12276-022-00910-0

184. Deng F, Hu JJ, Lin ZB, Sun QS, Min Y, Zhao BC, et al. Gut microbe-derived milnacipran enhances tolerance to gut ischemia/reperfusion injury. *Cell Rep Med* (2023) 4(3):100979. doi: 10.1016/j.xcrm.2023.100979

185. Frascoli M, Jeanty C, Fleck S, Moradi PW, Keating S, Mattis AN, et al. Heightened immune activation in fetuses with gastroschisis may be blocked by targeting IL-5. *J Immunol* (2016) 196(12):4957–66. doi: 10.4049/jimmunol.1502587

186. Dalli J, Colas RA, Arnardottir H, Serhan CN. Vagal regulation of group 3 innate lymphoid cells and the immunoresolvent PCTR1 controls infection resolution. *Immunity* (2017) 46(1):92–105. doi: 10.1016/j.immuni.2016.12.009

187. Schaeuble K, Britschgi MR, Scarpellino L, Favre S, Xu Y, Koroleva E, et al. Perivascular fibroblasts of the developing spleen act as LTα1β2-dependent precursors of both T and B zone organizer cells. *Cell Rep* (2017) 21(9):2500–14. doi: 10.1016/j.celrep.2017.10.119

188. Tripathi D, Radhakrishnan RK, Sivangala Thandi R, Paidipally P, Devalraju KP, Neela VSK, et al. IL-22 produced by type 3 innate lymphoid cells (ILC3) reduces the mortality of type 2 diabetes mellitus (T2DM) mice infected with Mycobacterium tuberculosis. *PloS Pathog* (2019) 15(12):e1008140. doi: 10.1371/journal.ppat.1008140

189. de Araújo EF, Preite NW, Veldhoen M, Loures FV, Calich VLG. Pulmonary paracoccidioidomycosis in AhR deficient hosts is severe and associated with defective Treg and Th22 responses. *Sci Rep* (2020) 10(1):11312. doi: 10.1038/s41598-020-68322-6

190. Huang J, Fu L, Huang J, Zhao J, Zhang X, Wang W, et al. Group 3 innate lymphoid cells protect the host from the uropathogenic escherichia coli infection in the bladder. *Adv Sci (Weinh)* (2022) 9(6):e2103303. doi: 10.1002/advs.202103303

191. Liu N, He J, Fan D, Gu Y, Wang J, Li H, et al. Circular RNA circTmem241 drives group III /innate lymphoid cell differentiation via initiation of Elk3 transcription. *Nat Commun* (2022) 13(1):4711. doi: 10.1038/s41467-022-32322-z

192. Darby M, Roberts LB, Mackowiak C, Chetty A, Tinelli S, Schnoeller C, et al. ILC3-derived acetylcholine promotes protease-driven allergic lung pathology. *J Allergy Clin Immunol* (2021) 147(4):1513–1516.e4. doi: 10.1016/j.jaci.2020.10.038

193. Zhao D, Cai C, Zheng Q, Jin S, Song D, Shen J, et al. Vancomycin pre-treatment impairs tissue healing in experimental colitis: Importance of innate lymphoid cells. *Biochem Biophys Res Commun* (2017) 483(1):237–44. doi: 10.1016/j.bbrc.2016.12.160

194. Shi Z, Takeuchi T, Nakanishi Y, Kato T, Beck K, Nagata R, et al. A Japanese herbal formula, daikenchuto, alleviates experimental colitis by reshaping microbial profiles and enhancing group 3 innate lymphoid cells. *Front Immunol* (2022) 13:903459. doi: 10.3389/fimmu.2022.903459

195. Stehle C, Rückert T, Fiancette R, Gajdasik DW, Willis C, Ulbricht C, et al. T-bet and RORα control lymph node formation by regulating embryonic innate lymphoid cell differentiation. *Nat Immunol* (2021) 22(10):1231–44. doi: 10.1038/s41590-021-01029-6

196. Hamaguchi M, Okamura T, Fukuda T, Nishida K, Yoshimura Y, Hashimoto Y, et al. Group 3 innate lymphoid cells protect steatohepatitis from high-fat diet induced toxicity. *Front Immunol* (2021) 12:648754. doi: 10.3389/fimmu.2021.648754

197. Kawano R, Okamura T, Hashimoto Y, Majima S, Senmaru T, Ushigome E, et al. Erythritol ameliorates small intestinal inflammation induced by high-fat diets and improves glucose tolerance. *Int J Mol Sci* (2021) 22(11):5558. doi: 10.3390/ijms22115558

198. Canesso MCC, Lemos L, Neves TC, Marim FM, Castro TBR, Veloso ÉS, et al. The cytosolic sensor STING is required for intestinal homeostasis and control of inflammation. *Mucosal Immunol* (2018) 11(3):820–34. doi: 10.1038/mi.2017.88

199. Dong Y, Fan H, Zhang Z, Jiang F, Li M, Zhou H, et al. Berberine ameliorates DSS-induced intestinal mucosal barrier dysfunction through microbiota-dependence and Wnt/β-catenin pathway. *Int J Biol Sci* (2022) 18(4):1381–97. doi: 10.7150/ijbs.65476

200. Hatfield JK, Brown MA. Group 3 innate lymphoid cells accumulate and exhibit disease-induced activation in the meninges in EAE. *Cell Immunol* (2015) 297(2):69–79. doi: 10.1016/j.cellimm.2015.06.006

201. Ebihara T, Song C, Ryu SH, Plougastel-Douglas B, Yang L, Levanon D, et al. Runx3 specifies lineage commitment of innate lymphoid cells. *Nat Immunol* (2015) 16 (11):1124–33. doi: 10.1038/ni.3272

202. Verrier T, Satoh-Takayama N, Serafini N, Marie S, Di Santo JP, Vosshenrich CA. Phenotypic and functional plasticity of murine intestinal NKp46+ Group 3 innate lymphoid cells. *J Immunol* (2016) 196(11):4731–8. doi: 10.4049/jimmunol.1502673

203. Saez de Guinoa J, Jimeno R, Farhadi N, Jervis PJ, Cox LR, Besra GS, et al. CD1d-mediated activation of group 3 innate lymphoid cells drives IL-22 production. *EMBO Rep* (2017) 18(1):39–47. doi: 10.15252/embr.201642412

204. Liu B, Ye B, Yang L, Zhu X, Huang G, Zhu P, et al. Long noncoding RNA lncKdm2b is required for ILC3 maintenance by initiation of Zfp292 expression. *Nat Immunol* (2017) 18(5):499–508. doi: 10.1038/ni.3712

205. Lu Y, Zhang X, Bouladoux N, Kaul SN, Jin K, Sant'Angelo D, et al. Zbtb1 controls NKp46+ ROR-gamma-T+ innate lymphoid cell (ILC3) development. *Oncotarget* (2017) 8(34):55877–88. doi: 10.18632/oncotarget.19645

206. Li Z, Buttó LF, Buela KA, Jia LG, Lam M, Ward JD, et al. Death receptor 3 signaling controls the balance between regulatory and effector lymphocytes in SAMP1/yitFc mice with crohn's disease-like ileitis. *Front Immunol* (2018) 9:362. doi: 10.3389/fimmu.2018.00362

207. Yin S, Yu J, Hu B, Lu C, Liu X, Gao X, et al. Runx3 mediates resistance to intracellular bacterial infection by promoting IL12 signaling in group 1 ILC and NCR +ILC3. *Front Immunol* (2018) 9:2101. doi: 10.3389/fimmu.2018.02101

208. Hou P, Zhou X, Yu L, Yao Y, Zhang Y, Huang Y, et al. Exhaustive exercise induces gastrointestinal syndrome through reduced ILC3 and IL-22 in mouse model. *Med Sci Sports Exerc* (2020) 52(8):1710–8. doi: 10.1249/MSS.0000000000002298

209. Mincham KT, Snelgrove RJ. OMIP-086: Full spectrum flow cytometry for high-dimensional immunophenotyping of mouse innate lymphoid cells. *Cytometry A* (2022) 103(2):110–6. doi: 10.1002/cyto.a.24702

210. Gogoleva VS, Kuprash DV, Grivennikov SI, Tumanov AV, Kruglov AA, Nedospasov SA. LTα, TNF, and ILC3 in peyer's patch organogenesis. *Cells* (2022) 11 (12):1970. doi: 10.3390/cells11121970

211. Schroeder JH, Meissl K, Hromadová D, Lo JW, Neves JF, Howard JK, et al. T-bet controls cellularity of intestinal group 3 innate lymphoid cells. *Front Immunol* (2021) 11:623324. doi: 10.3389/fimmu.2020.623324

212. Schroeder JH, Roberts LB, Meissl K, Lo JW, Hromadová D, Hayes K, et al. Sustained post-developmental T-bet expression is critical for the maintenance of type one innate lymphoid cells *in vivo*. *Front Immunol* (2021) 12:760198. doi: 10.3389/fimmu.2021.760198

213. de Araújo EF, Loures FV, Preite NW, Feriotti C, Galdino NA, Costa TA, et al. AhR ligands modulate the differentiation of innate lymphoid cells and T helper cell subsets that control the severity of a pulmonary fungal infection. *Front Immunol* (2021) 12:630938. doi: 10.3389/fimmu.2021.630938

214. Liu B, Liu N, Zhu X, Yang L, Ye B, Li H, et al. Circular RNA circZbtb20 maintains ILC3 homeostasis and function via Alkbh5-dependent m6A demethylation of Nr4a1 mRNA. *Cell Mol Immunol* (2021) 18(6):1412–24. doi: 10.1038/s41423-021-00680-1

215. Liu Y, Song Y, Lin D, Lei L, Mei Y, Jin Z, et al. NCR- group 3 innate lymphoid cells orchestrate IL-23/IL-17 axis to promote hepatocellular carcinoma development. *EBioMedicine* (2019) 41:333–44. doi: 10.1016/j.ebiom.2019.02.050

216. Serafini N, Jarade A, Surace L, Goncalves P, Sismeiro O, Varet H, et al. Trained ILC3 responses promote intestinal defense. *Science* (2022) 375(6583):859–63. doi: 10.1126/science.aaz8777

217. Michaudel C, Bataille F, Maillet I, Fauconnier L, Colas C, Sokol H, et al. Ozone-induced aryl hydrocarbon receptor activation controls lung inflammation via interleukin-22 modulation. *Front Immunol* (2020) 11:144. doi: 10.3389/fimmu.2020.00144

218. Melo-Gonzalez F, Kammoun H, Evren E, Dutton EE, Papadopoulou M, Bradford BM, et al. Antigen-presenting ILC3 regulate T cell-dependent IgA responses to colonic mucosal bacteria. *J Exp Med* (2019) 216(4):728–42. doi: 10.1084/jem.20180871

219. Tizian C, Lahmann A, Hölsken O, Cosovanu C, Kofoed-Branzk M, Heinrich F, et al. c-Maf restrains T-bet-driven programming of CCR6-negative group 3 innate lymphoid cells. *Elife* (2020) 9:e52549. doi: 10.7554/eLife.52549

220. Xia P, Liu J, Wang S, Ye B, Du Y, Xiong Z, et al. WASH maintains NKp46+ ILC3 cells by promoting AHR expression. *Nat Commun* (2017) 8:15685. doi: 10.1038/ncomms15685

221. Bergmann H, Roth S, Pechloff K, Kiss EA, Kuhn S, Heikenwälder M, et al. Card9-dependent IL-1β regulates IL-22 production from group 3 innate lymphoid cells and promotes colitis-associated cancer. *Eur J Immunol* (2017) 47(8):1342–53. doi: 10.1002/eji.201646765

222. Saksida T, Paunović V, Koprivica I, Mićanović D, Jevtić B, Jonić N, et al. Development of type 1 diabetes in mice is associated with a decrease in IL-2-producing ILC3 and foxP3+ Treg in the small intestine. *Molecules* (2023) 28(8):3366. doi: 10.3390/molecules28083366

223. Xie J, Tian S, Liu J, Huang S, Yang M, Yang X, et al. Combination therapy with indigo and indirubin for ulcerative colitis via reinforcing intestinal barrier function. *Oxid Med Cell Longev* (2023) 2023:2894695. doi: 10.1155/2023/2894695

224. Chan L, Mehrani Y, Minott JA, Bridle BW, Karimi K. The potential of dendritic-cell-based vaccines to modulate type 3 innate lymphoid cell populations. *Int J Mol Sci* (2023) 24(3):2403. doi: 10.3390/ijms24032403

225. Lewis JM, Monico PF, Mirza FN, Xu S, Yumeen S, Turban JL, et al. Chronic UV radiation-induced RORγt+ IL-22-producing lymphoid cells are associated with mutant KC clonal expansion. *Proc Natl Acad Sci U.S.A.* (2021) 118(37):e2016963118. doi: 10.1073/pnas.2016963118

226. Fachi JL, Sécca C, Rodrigues PB, Mato FCP, Di Luccia B, Felipe JS, et al. Acetate coordinates neutrophil and ILC3 responses against C. difficile through FFAR2. *J Exp Med* (2020) 217(3):e20190489. doi: 10.1084/jem.20190489

227. Peng V, Cao S, Trsan T, Bando JK, Avila-Pacheco J, Cleveland JL, et al. Ornithine decarboxylase supports ILC3 responses in infectious and autoimmune colitis through positive regulation of IL-22 transcription. *Proc Natl Acad Sci U.S.A.* (2022) 119 (45):e2214900119. doi: 10.1073/pnas.2214900119

228. Kim SH, Cho BH, Kiyono H, Jang YS. Microbiota-derived butyrate suppresses group 3 innate lymphoid cells in terminal ileal Peyer's patches. *Sci Rep* (2017) 7(1):3980. doi: 10.1038/s41598-017-02729-6

229. Li S, Bostick JW, Ye J, Qiu J, Zhang B, Urban JF Jr, et al. Aryl hydrocarbon receptor signaling cell intrinsically inhibits intestinal group 2 innate lymphoid cell function. *Immunity* (2018) 49(5):915–928.e5. doi: 10.1016/j.immuni.2018.09.015

230. Kang L, Zhang X, Ji L, Kou T, Smith SM, Zhao B, et al. The colonic macrophage transcription factor RBP-J orchestrates intestinal immunity against bacterial pathogens. *J Exp Med* (2020) 217(4):e20190762. doi: 10.1084/jem.20190762

231. Bando JK, Gilfillan S, Song C, McDonald KG, Huang SC, Newberry RD, et al. The tumor necrosis factor superfamily member RANKL suppresses effector cytokine production in group 3 innate lymphoid cells. *Immunity* (2018) 48(6):1208–1219.e4. doi: 10.1016/j.immuni.2018.04.012

232. Lo BC, Gold MJ, Hughes MR, Antignano F, Valdez Y, Zaph C, et al. The orphan nuclear receptor RORα and group 3 innate lymphoid cells drive fibrosis in a mouse model of Crohn's disease. *Sci Immunol* (2016) 1(3):eaaf8864. doi: 10.1126/sciimmunol.aaf8864

233. Tait Wojno ED, Beamer CA. Isolation and identification of innate lymphoid cells (ILCs) for immunotoxicity testing. *Methods Mol Biol* (2018) 1803:353–70. doi: 10.1007/978-1-4939-8549-4_21

234. Geiger TL, Abt MC, Gasteiger G, Firth MA, O'Connor MH, Geary CD, et al. Nfil3 is crucial for development of innate lymphoid cells and host protection against intestinal pathogens. *J Exp Med* (2014) 211(9):1723–31. doi: 10.1084/jem.20140212

235. Xu W, Cherrier DE, Chea S, Vosshenrich C, Serafini N, Petit M, et al. An id2RFP-reporter mouse redefines innate lymphoid cell precursor potentials. *Immunity* (2019) 50(4):1054–1068.e3. doi: 10.1016/j.immuni.2019.02.022

236. Liu Q, Kim MH, Friesen L, Kim CH. BATF regulates innate lymphoid cell hematopoiesis and homeostasis. *Sci Immunol* (2020) 5(54):eaaz8154. doi: 10.1126/sciimmunol.aaz8154

237. Sepahi A, Liu Q, Friesen L, Kim CH. Dietary fiber metabolites regulate innate lymphoid cell responses. *Mucosal Immunol* (2021) 14(2):317–30. doi: 10.1038/s41385-020-0312-8

238. Yu HB, Yang H, Allaire JM, Ma C, Graef FA, Mortha A, et al. Vasoactive intestinal peptide promotes host defense against enteric pathogens by modulating the recruitment of group 3 innate lymphoid cells. *Proc Natl Acad Sci U.S.A.* (2021) 118(41):e2106634118. doi: 10.1073/pnas.2106634118

239. Jonckheere AC, Seys SF, Steelant B, Decaesteker T, Dekoster K, Cremer J, et al. Innate lymphoid cells are required to induce airway hyperreactivity in a murine neutrophilic asthma model. *Front Immunol* (2022) 13:849155. doi: 10.3389/fimmu.2022.849155

240. Zhou J, Hou P, Yao Y, Yue J, Zhang Q, Yi L, et al. Dihydromyricetin Improves High-Fat Diet-Induced Hyperglycemia through ILC3 Activation via a SIRT3-Dependent Mechanism. *Mol Nutr Food Res* (2022) 66(16):e2101093. doi: 10.1002/mnfr.202101093

241. Seillet C, Luong K, Tellier J, Jacquelot N, Shen RD, Hickey P, et al. The neuropeptide VIP confers anticipatory mucosal immunity by regulating ILC3 activity. *Nat Immunol* (2020) 21(2):168–77. doi: 10.1038/s41590-019-0567-y

242. Emgård J, Kammoun H, García-Cassani B, Chesné J, Parigi SM, Jacob JM, et al. Oxysterol sensing through the receptor GPR183 promotes the lymphoid-tissue-inducing function of innate lymphoid cells and colonic inflammation. *Immunity* (2018) 48(1):120–132.e8. doi: 10.1016/j.immuni.2017.11.020

243. Melo-Gonzalez F, Hepworth MR. Identification and functional characterization of murine group 3 innate lymphoid cell (ILC3) subsets in the intestinal tract and associated lymphoid tissues. *Methods Mol Biol* (2020) 2121:37–49. doi: 10.1007/978-1-0716-0338-3_4

244. Linley H, Ogden A, Jaigirdar S, Buckingham L, Cox J, Priestley M, et al. CD200R1 promotes IL-17 production by ILC3, by enhancing STAT3 activation. *Mucosal Immunol* (2023) 16(2):167–79. doi: 10.1016/j.mucimm.2023.01.001

245. Sudan R, Fernandes S, Srivastava N, Pedicone C, Meyer ST, Chisholm JD, et al. LRBA deficiency can lead to lethal colitis that is diminished by SHIP1 agonism. *Front Immunol* (2022) 13:830961. doi: 10.3389/fimmu.2022.830961

246. Ibiza S, García-Cassani B, Ribeiro H, Carvalho T, Almeida L, Marques R, et al. Glial-cell-derived neuroregulators control type 3 innate lymphoid cells and gut defence. *Nature* (2016) 535(7612):440–3. doi: 10.1038/nature18644

247. Parker ME, Barrera A, Wheaton JD, Zuberbuehler MK, Allan DSJ, Carlyle JR, et al. c-Maf regulates the plasticity of group 3 innate lymphoid cells by restraining the type 1 program. *J Exp Med* (2020) 217(1):e20191030. doi: 10.1084/jem.20191030

248. Nakagawa S, Matsumoto M, Katayama Y, Oguma R, Wakabayashi S, Nygaard T, et al. Staphylococcus aureus virulent PSMα Peptides induce keratinocyte alarmin release to orchestrate IL-17-dependent skin inflammation. *Cell Host Microbe* (2017) 22(5):667–677.e5. doi: 10.1016/j.chom.2017.10.008

249. Chun E, Lavoie S, Fonseca-Pereira D, Bae S, Michaud M, Hoveyda HR, et al. Metabolite-sensing receptor ffar2 regulates colonic group 3 innate lymphoid cells and gut immunity. *Immunity* (2019) 51(5):871–884.e6. doi: 10.1016/j.immuni.2019.09.014

250. Bielecki P, Riesenfeld SJ, Hütter JC, Torlai Triglia E, Kowalczyk MS, Ricardo-Gonzalez RR, et al. Skin-resident innate lymphoid cells converge on a pathogenic effector state. *Nature* (2021) 592(7852):128–32. doi: 10.1038/s41586-021-03188-w

251. Zhou J, Yue J, Yao Y, Hou P, Zhang T, Zhang Q, et al. Dihydromyricetin protects intestinal barrier integrity by promoting IL-22 expression in ILC3 through the AMPK/SIRT3/STAT3 signaling pathway. *Nutrients* (2023) 15(2):355. doi: 10.3390/nu15020355

252. Crittenden S, Cheyne A, Adams A, Forster T, Robb CT, Felton J, et al. Purine metabolism controls innate lymphoid cell function and protects against intestinal injury. *Immunol Cell Biol* (2018) 96(10):1049–59. doi: 10.1111/imcb.12167

253. Seo GY, Shui JW, Takahashi D, Song C, Wang Q, Kim K, et al. LIGHT-HVEM signaling in innate lymphoid cell subsets protects against enteric bacterial infection. *Cell Host Microbe* (2018) 24(2):249–260.e4. doi: 10.1016/j.chom.2018.07.008

254. Huang J, Lee HY, Zhao X, Han J, Su Y, Sun Q, et al. Interleukin-17D regulates group 3 innate lymphoid cell function through its receptor CD93. *Immunity* (2021) 54(4):673–686.e4. doi: 10.1016/j.immuni.2021.03.018

255. Vojkovics D, Kellermayer Z, Gábris F, Schippers A, Wagner N, Berta G, et al. Differential effects of the absence of nkx2-3 and MAdCAM-1 on the distribution of intestinal type 3 innate lymphoid cells and postnatal SILT formation in mice. *Front Immunol* (2019) 10:366. doi: 10.3389/fimmu.2019.00366

256. Song C, Lee JS, Gilfillan S, Robinette ML, Newberry RD, Stappenbeck TS, et al. Unique and redundant functions of NKp46+ ILC3 in models of intestinal inflammation. *J Exp Med* (2015) 212(11):1869–82. doi: 10.1084/jem.20151403

257. Goto Y, Obata T, Kunisawa J, Sato S, Ivanov II, Lamichhane A, et al. Innate lymphoid cells regulate intestinal epithelial cell glycosylation. *Science* (2014) 345(6202):1254009. doi: 10.1126/science.1254009

258. Fung TC, Bessman NJ, Hepworth MR, Kumar N, Shibata N, Kobuley D, et al. Lymphoid-tissue-resident commensal bacteria promote members of the IL-10 cytokine family to establish mutualism. *Immunity* (2016) 44(3):634–46. doi: 10.1016/j.immuni.2016.02.019

259. Silver JS, Kearley J, Copenhaver AM, Sanden C, Mori M, Yu L, et al. Inflammatory triggers associated with exacerbations of COPD orchestrate plasticity of group 2 innate lymphoid cells in the lungs. *Nat Immunol* (2016) 17(6):626–35. doi: 10.1038/ni.3443

260. Paustian AMS, Paez-Cortez J, Bryant S, Westmoreland S, Waegell W, Kingsbury G. Continuous IL-23 stimulation drives ILC3 depletion in the upper GI tract and, in combination with TNFα, induces robust activation and a phenotypic switch of ILC3. *PloS One* (2017) 12(8):e0182841. doi: 10.1371/journal.pone.0182841

261. Yang C, Kwon DI, Kim M, Im SH, Lee YJ. Commensal microbiome expands Tγδ17 cells in the lung and promotes particulate matter-induced acute neutrophilia. *Front Immunol* (2021) 12:645741. doi: 10.3389/fimmu.2021.645741

262. Bhatt B, Zeng P, Zhu H, Sivaprakasam S, Li S, Xiao H, et al. Gpr109a limits microbiota-induced IL-23 production to constrain ILC3-mediated colonic inflammation. *J Immunol* (2018) 200(8):2905–14. doi: 10.4049/jimmunol.1701625

263. Yang FC, Chiu PY, Chen Y, Mak TW, Chen NJ. TREM-1-dependent M1 macrophage polarization restores intestinal epithelium damaged by DSS-induced colitis by activating IL-22-producing innate lymphoid cells. *J BioMed Sci* (2019) 26(1):46. doi: 10.1186/s12929-019-0539-4

264. Poholek CH, Dulson SJ, Zajac AJ, Harrington LE. IL-21 controls ILC3 cytokine production and promotes a protective phenotype in a mouse model of colitis. *Immunohorizons* (2019) 3(6):194–202. doi: 10.4049/immunohorizons.1900005

265. Di Luccia B, Gilfillan S, Cella M, Colonna M, Huang SC. ILC3 integrate glycolysis and mitochondrial production of reactive oxygen species to fulfill activation demands. *J Exp Med* (2019) 216(10):2231–41. doi: 10.1084/jem.20180549

266. Bauché D, Joyce-Shaikh B, Jain R, Grein J, Ku KS, Blumenschein WM, et al. LAG3+ Regulatory T cells restrain interleukin-23-producing CX3CR1+ Gut-resident macrophages during group 3 innate lymphoid cell-driven colitis. *Immunity* (2018) 49(2):342–352.e5. doi: 10.1016/j.immuni.2018.07.007

267. Seo GY, Giles DA, Kronenberg M. Bacterial infection allows for functional examination of adoptively transferred mouse innate lymphoid cell subsets. *Methods Mol Biol* (2020) 2121:129–40. doi: 10.1007/978-1-0716-0338-3_12

268. He L, Zhou M, Li YC. Vitamin D/vitamin D receptor signaling is required for normal development and function of group 3 innate lymphoid cells in the gut. *iScience* (2019) 17:119–31. doi: 10.1016/j.isci.2019.06.026

269. Fachi JL, Pral LP, Dos Santos JAC, Codo AC, de Oliveira S, Felipe JS, et al. Hypoxia enhances ILC3 responses through HIF-1α-dependent mechanism. *Mucosal Immunol* (2021) 14(4):828–41. doi: 10.1038/s41385-020-00371-6

270. Li Y, Ge J, Zhao X, Xu M, Gou M, Xie B, et al. Cell autonomous expression of BCL6 is required to maintain lineage identity of mouse CCR6+ ILC3s. *J Exp Med* (2023) 220(4):e20220440. doi: 10.1084/jem.20220440

271. Xiong L, Wang S, Dean JW, Oliff KN, Jobin C, Curtiss R 3rd, et al. Group 3 innate lymphoid cell pyroptosis represents a host defence mechanism against Salmonella infection. *Nat Microbiol* (2022) 7(7):1087–99. doi: 10.1038/s41564-022-01142-8

272. Peng V, Xing X, Bando JK, Trsan T, Di Luccia B, Collins PL, et al. Whole-genome profiling of DNA methylation and hydroxymethylation identifies distinct regulatory programs among innate lymphocytes. *Nat Immunol* (2022) 23(4):619–31. doi: 10.1038/s41590-022-01164-8

273. Chang D, Zhang H, Ge J, Xing Q, Guo X, Wang X, et al. A cis-element at the Rorc locus regulates the development of type 3 innate lymphoid cells. *Front Immunol* (2023) 14:1105145. doi: 10.3389/fimmu.2023.1105145

274. Hu P, Leyton L, Hagood JS, Barker TH. Thy-1-integrin interactions in cis and trans mediate distinctive signaling. *Front Cell Dev Biol* (2022) 10:928510. doi: 10.3389/fcell.2022.928510

275. Krzywinska E, Sobecki M, Nagarajan S, Zacharjasz J, Tambuwala MM, Pelletier A, et al. The transcription factor HIF-1α mediates plasticity of NKp46+ innate lymphoid cells in the gut. *J Exp Med* (2022) 219(2):e20210909. doi: 10.1084/jem.20210909

276. Hou Q, Huang J, Xiong X, Guo Y, Zhang B. Role of nutrient-sensing receptor GPRC6A in regulating colonic group 3 innate lymphoid cells and inflamed mucosal healing. *J Crohns Colitis* (2022) 16(8):1293–305. doi: 10.1093/ecco-jcc/jjac020

277. Chen L, He Z, Slinger E, Bongers G, Lapenda TLS, Pacer ME, et al. IL-23 activates innate lymphoid cells to promote neonatal intestinal pathology. *Mucosal Immunol* (2015) 8(2):390–402. doi: 10.1038/mi.2014.77

278. Ma Z, Li C, Xue L, Zhang S, Yang Y, Zhang H, et al. Linggan Wuwei Jiangxin formula ameliorates airway hyperresponsiveness through suppression of IL-1β and IL-17A expression in allergic asthmatic mice especially with diet-induced obesity. *Ann Transl Med* (2021) 9(8):682. doi: 10.21037/atm-21-1189

279. Kim HY, Lee HJ, Chang YJ, Pichavant M, Shore SA, Fitzgerald KA, et al. Interleukin-17-producing innate lymphoid cells and the NLRP3 inflammasome facilitate obesity-associated airway hyperreactivity. *Nat Med* (2014) 20(1):54–61. doi: 10.1038/nm.3423

280. He J, Shen X, Fu D, Yang Y, Xiong K, Zhao L, et al. Human periodontitis-associated salivary microbiome affects the immune response of diabetic mice. *J Oral Microbiol* (2022) 14(1):2107814. doi: 10.1080/20002297.2022.2107814

281. Nettleford SK, Zhao L, Qian F, Herold M, Arner B, Desai D, et al. The essential role of selenoproteins in the resolution of citrobacter rodentium-induced intestinal inflammation. *Front Nutr* (2020) 7:96. doi: 10.3389/fnut.2020.00096

282. Di Censo C, Marotel M, Mattiola I, Müller L, Scarno G, Pietropaolo G, et al. Granzyme A and CD160 expression delineates ILC1 with graded functions in the mouse liver. *Eur J Immunol* (2021) 51(11):2568–75. doi: 10.1002/eji.202149209

283. Valle-Noguera A, Gómez-Sánchez MJ, Girard-Madoux MJH, Cruz-Adalia A. Optimized protocol for characterization of mouse gut innate lymphoid cells. *Front Immunol* (2020) 11:563414. doi: 10.3389/fimmu.2020.563414

284. Huang S, Wang X, Xie X, Su Y, Pan Z, Li Y, et al. Dahuang Mudan decoction repairs intestinal barrier in chronic colitic mice by regulating the function of ILC3. *J Ethnopharmacol* (2022) 299:115652. doi: 10.1016/j.jep.2022.115652

285. Chen MJ, Feng Y, Gao L, Lin MX, Wang SD, Tong ZQ. Composite sophora colon-soluble capsule ameliorates DSS-induced ulcerative colitis in mice via gut microbiota-derived butyric acid and NCR+ ILC3. *Chin J Integr Med* (2023) 29 (5):424–33. doi: 10.1007/s11655-022-3317-1

286. Mielke LA, Groom JR, Rankin LC, Seillet C, Masson F, Putoczki T, et al. TCF-1 controls ILC2 and NKp46+RORγt+ innate lymphocyte differentiation and protection in intestinal inflammation. *J Immunol* (2013) 191(8):4383–91. doi: 10.4049/jimmunol.1301228

287. Xie X, Zhao M, Huang S, Li P, Chen P, Luo X, et al. Luteolin alleviates ulcerative colitis by restoring the balance of NCR-ILC3/NCR+ILC3 to repairing impaired intestinal barrier. *Int Immunopharmacol* (2022) 112:109251. doi: 10.1016/j.intimp.2022.109251

288. Robinette ML, Fuchs A, Cortez VS, Lee JS, Wang Y, Durum SK, et al. Transcriptional programs define molecular characteristics of innate lymphoid cell classes and subsets. *Nat Immunol* (2015) 16(3):306–17. doi: 10.1038/ni.3094

289. Rankin LC, Girard-Madoux MJ, Seillet C, Mielke LA, Kerdiles Y, Fenis A, et al. Complementarity and redundancy of IL-22-producing innate lymphoid cells. *Nat Immunol* (2016) 17(2):179–86. doi: 10.1038/ni.3332

290. Viant C, Rankin LC, Girard-Madoux MJ, Seillet C, Shi W, Smyth MJ, et al. Transforming growth factor-β and Notch ligands act as opposing environmental cues in regulating the plasticity of type 3 innate lymphoid cells. *Sci Signal* (2016) 9(426):ra46. doi: 10.1126/scisignal.aaf2176

291. Goverse G, Labao-Almeida C, Ferreira M, Molenaar R, Wahlen S, Konijn T, et al. Vitamin A controls the presence of RORγ+ Innate lymphoid cells and lymphoid tissue in the small intestine. *J Immunol* (2016) 196(12):5148–55. doi: 10.4049/jimmunol.1501106

292. Robinette ML, Bando JK, Song W, Ulland TK, Gilfillan S, Colonna M. IL-15 sustains IL-7R-independent ILC2 and ILC3 development. *Nat Commun* (2017) 8:14601. doi: 10.1038/ncomms14601

293. Liu B, Ye B, Zhu X, Huang G, Yang L, Zhu P, et al. IL-7Rα glutamylation and activation of transcription factor Sall3 promote group 3 ILC development. *Nat Commun* (2017) 8(1):231. doi: 10.1038/s41467-017-00235-x

294. Robinette ML, Cella M, Telliez JB, Ulland TK, Barrow AD, Capuder K, et al. Jak3 deficiency blocks innate lymphoid cell development. *Mucosal Immunol* (2018) 11 (1):50–60. doi: 10.1038/mi.2017.38

295. Abou-Samra E, Hickey Z, Aguilar OA, Scur M, Mahmoud AB, Pyatibrat S, et al. NKR-P1B expression in gut-associated innate lymphoid cells is required for the control of gastrointestinal tract infections. *Cell Mol Immunol* (2019) 16(11):868–77. doi: 10.1038/s41423-018-0169-x

296. Gronke K, Hernández PP, Zimmermann J, Klose CSN, Kofoed-Branzk M, Guendel F, et al. Interleukin-22 protects intestinal stem cells against genotoxic stress. *Nature* (2019) 566(7743):249–53. doi: 10.1038/s41586-019-0899-7

297. Li Y, Xie HQ, Zhang W, Wei Y, Sha R, Xu L, et al. Type 3 innate lymphoid cells are altered in colons of C57BL/6 mice with dioxin exposure. *Sci Total Environ* (2019) 662:639–45. doi: 10.1016/j.scitotenv.2019.01.139

298. Yamano T, Dobeš J, Vobořil M, Steinert M, Brabec T, Ziętara N, et al. Aire-expressing ILC3-like cells in the lymph node display potent APC features. *J Exp Med* (2019) 216(5):1027–37. doi: 10.1084/jem.20181430

299. Qi H, Li Y, Yun H, Zhang T, Huang Y, Zhou J, et al. Lactobacillus maintains healthy gut mucosa by producing L-Ornithine. *Commun Biol* (2019) 2:171. doi: 10.1038/s42003-019-0424-4

300. Ke K, Chen TH, Arra M, Mbalaviele G, Swarnkar G, Abu-Amer Y. Attenuation of NF-κB in intestinal epithelial cells is sufficient to mitigate the bone loss comorbidity of experimental mouse colitis. *J Bone Miner Res* (2019) 34(10):1880–93. doi: 10.1002/jbmr.3759

301. Gao Y, Bian Z, Xue W, Li Q, Zeng Y, Wang Y, et al. Human IL-23R cytokine-binding homology region-fc fusion protein ameliorates psoriasis via the decrease of systemic th17 and ILC3 cell responses. *Int J Mol Sci* (2019) 20(17):4170. doi: 10.3390/ijms20174170

302. Wang Q, Robinette ML, Billon C, Collins PL, Bando JK, Fachi JL, et al. Circadian rhythm-dependent and circadian rhythm-independent impacts of the molecular clock on type 3 innate lymphoid cells. *Sci Immunol* (2019) 4(40):eaay7501. doi: 10.1126/sciimmunol.aay7501

303. Kim HJ, Lee SH, Hong SJ. Antibiotics-induced dysbiosis of intestinal microbiota aggravates atopic dermatitis in mice by altered short-chain fatty acids. *Allergy Asthma Immunol Res* (2020) 12(1):137–48. doi: 10.4168/aair.2020.12.1.137

304. Bank U, Deiser K, Plaza-Sirvent C, Osbelt L, Witte A, Knop L, et al. c-FLIP is crucial for IL-7/IL-15-dependent NKp46+ ILC development and protection from intestinal inflammation in mice. *Nat Commun* (2020) 11(1):1056. doi: 10.1038/s41467-020-14782-3

305. Zhu Y, Shi T, Lu X, Xu Z, Qu J, Zhang Z, et al. Fungal-induced glycolysis in macrophages promotes colon cancer by enhancing innate lymphoid cell secretion of IL-22. *EMBO J* (2021) 40(11):e105320. doi: 10.15252/embj.2020105320

306. Zhang W, Zhou Q, Liu H, Xu J, Huang R, Shen B, et al. Bacteroides fragilis strain ZY-312 facilitates colonic mucosa regeneration in colitis via motivating STAT3 signaling pathway induced by IL-22 from ILC3 secretion. *Front Immunol* (2023) 14:1156762. doi: 10.3389/fimmu.2023.1156762

307. Chu S, Ma L, Yang X, Xiao B, Liang Y, Zheng S, et al. NCR negative group 3 innate lymphoid cell (NCR- ILC3) participates in abnormal pathology of lung in cigarette smoking-induced COPD mice. *Immun Inflammation Dis* (2023) 11(3):e816. doi: 10.1002/iid3.816

308. Ma B, Zhou Y, Hu Y, Duan H, Sun Z, Wang P, et al. Mapping resident immune cells in the murine ocular surface and lacrimal gland by flow cytometry. *Ocul Immunol Inflammation* (2023) 31(4):748–59. doi: 10.1080/09273948.2023.2182327

309. Zhao X, Liang W, Wang Y, Yi R, Luo L, Wang W, et al. Ontogeny of RORγt+ cells in the intestine of newborns and its role in the development of experimental necrotizing enterocolitis. *Cell Biosci* (2022) 12(1):3. doi: 10.1186/s13578-021-00739-6

310. Lehmann FM, von Burg N, Ivanek R, Teufel C, Horvath E, Peter A, et al. Microbiota-induced tissue signals regulate ILC3-mediated antigen presentation. *Nat Commun* (2020) 11(1):1794. doi: 10.1038/s41467-020-15612-2

311. Irshad S, Flores-Borja F, Lawler K, Monypenny J, Evans R, Male V, et al. RORγt + Innate lymphoid cells promote lymph node metastasis of breast cancers. *Cancer Res* (2017) 77(5):1083–96. doi: 10.1158/0008-5472.CAN-16-0598

312. Seshadri S, Allan DSJ, Carlyle JR, Zenewicz LA. Bacillus anthracis lethal toxin negatively modulates ILC3 function through perturbation of IL-23-mediated MAPK signaling. *PloS Pathog* (2017) 13(10):e1006690. doi: 10.1371/journal.ppat.1006690

313. Giacomin PR, Moy RH, Noti M, Osborne LC, Siracusa MC, Alenghat T, et al. Epithelial-intrinsic IKKα expression regulates group 3 innate lymphoid cell responses and antibacterial immunity. *J Exp Med* (2015) 212(10):1513–28. doi: 10.1084/jem.20141831

314. Talbot J, Hahn P, Kroehling L, Nguyen H, Li D, Littman DR. Feeding-dependent VIP neuron-ILC3 circuit regulates the intestinal barrier. *Nature* (2020) 579(7800):575–80. doi: 10.1038/s41586-020-2039-9

315. Sasaki T, Moro K, Kubota T, Kubota N, Kato T, Ohno H, et al. Innate lymphoid cells in the induction of obesity. *Cell Rep* (2019) 28(1):202–217.e7. doi: 10.1016/j.celrep.2019.06.016

316. Muraoka WT, Korchagina AA, Xia Q, Shein SA, Jing X, Lai Z, et al. Campylobacter infection promotes IFNγ-dependent intestinal pathology via ILC3 to ILC1 conversion. *Mucosal Immunol* (2021) 14(3):703–16. doi: 10.1038/s41385-020-00353-8

317. Wang B, Lim JH, Kajikawa T, Li X, Vallance BA, Moutsopoulos NM, et al. Macrophage β2-integrins regulate IL-22 by ILC3 and protect from lethal citrobacter rodentium-induced colitis. *Cell Rep* (2019) 26(6):1614–1626.e5. doi: 10.1016/j.celrep.2019.01.054

318. Snyder LM, Doherty CM, Mercer HL, Denkers EY. Induction of IL-12p40 and type 1 immunity by Toxoplasma gondii in the absence of the TLR-MyD88 signaling cascade. *PloS Pathog* (2021) 17(10):e1009970. doi: 10.1371/journal.ppat.1009970

319. Van Maele L, Carnoy C, Cayet D, Ivanov S, Porte R, Deruy E, et al. Activation of Type 3 innate lymphoid cells and interleukin 22 secretion in the lungs during Streptococcus pneumoniae infection. *J Infect Dis* (2014) 210(3):493–503. doi: 10.1093/infdis/jiu106

320. Lo BC, Canals Hernaez D, Scott RW, Hughes MR, Shin SB, Underhill TM, et al. The transcription factor RORα Preserves ILC3 lineage identity and function during chronic intestinal infection. *J Immunol* (2019) 203(12):3209–15. doi: 10.4049/jimmunol.1900781

321. Stier MT, Goleniewska K, Cephus JY, Newcomb DC, Sherrill TP, Boyd KL, et al. STAT1 represses cytokine-producing group 2 and group 3 innate lymphoid cells during viral infection. *J Immunol* (2017) 199(2):510–9. doi: 10.4049/jimmunol.1601984

322. Yang J, Cornelissen F, Papazian N, Reijmers RM, Llorian M, Cupedo T, et al. IL-7-dependent maintenance of ILC3s is required for normal entry of lymphocytes into lymph nodes. *J Exp Med* (2018) 215(4):1069–77. doi: 10.1084/jem.20170518

323. Liébana-García R, Olivares M, Francés-Cuesta C, Rubio T, Rossini V, Quintas G, et al. Intestinal group 1 innate lymphoid cells drive macrophage-induced inflammation and endocrine defects in obesity and promote insulinemia. *Gut Microbes* (2023) 15(1):2181928. doi: 10.1080/19490976.2023.2181928

324. Chan IH, Jain R, Tessmer MS, Gorman D, Mangadu R, Sathe M, et al. Interleukin-23 is sufficient to induce rapid *de novo* gut tumorigenesis, independent of carcinogens, through activation of innate lymphoid cells. *Mucosal Immunol* (2014) 7 (4):842–56. doi: 10.1038/mi.2013.101

325. Wu X, Khatun A, Kasmani MY, Chen Y, Zheng S, Atkinson S, et al. Group 3 innate lymphoid cells require BATF to regulate gut homeostasis in mice. *J Exp Med* (2022) 219(11):e20211861. doi: 10.1084/jem.20211861

326. Friedrich C, Mamareli P, Thiemann S, Kruse F, Wang Z, Holzmann B, et al. MyD88 signaling in dendritic cells and the intestinal epithelium controls immunity against intestinal infection with C. *rodentium. PloS Pathog* (2017) 13(5):e1006357. doi: 10.1371/journal.ppat.1006357

327. Kim M, Gu B, Madison MC, Song HW, Norwood K, Hill AA, et al. Cigarette smoke induces intestinal inflammation via a th17 cell-neutrophil axis. *Front Immunol* (2019) 10:75. doi: 10.3389/fimmu.2019.00075

328. Snyder LM, Belmares-Ortega J, Doherty CM, Denkers EY. Impact of MyD88, Microbiota, and Location on Type 1 and Type 3 Innate Lymphoid Cells during Toxoplasma gondii Infection. *Immunohorizons* (2022) 6(9):660–70. doi: 10.4049/immunohorizons.2200070

329. Lin YD, Arora J, Diehl K, Bora SA, Cantorna MT. Vitamin D is required for ILC3 derived IL-22 and protection from citrobacter rodentium infection. *Front Immunol* (2019) 10:1. doi: 10.3389/fimmu.2019.00001

330. Teufel C, Horvath E, Peter A, Ercan C, Piscuoglio S, Hall MN, et al. mTOR signaling mediates ILC3-driven immunopathology. *Mucosal Immunol* (2021) 14 (6):1323–34. doi: 10.1038/s41385-021-00432-4

331. Chea S, Perchet T, Petit M, Verrier T, Guy-Grand D, Banchi EG, et al. Notch signaling in group 3 innate lymphoid cells modulates their plasticity. *Sci Signal* (2016) 9 (426):ra45. doi: 10.1126/scisignal.aaf2223

332. Li S, Heller JJ, Bostick JW, Lee A, Schjerven H, Kastner P, et al. Ikaros inhibits group 3 innate lymphoid cell development and function by suppressing the aryl hydrocarbon receptor pathway. *Immunity* (2016) 45(1):185–97. doi: 10.1016/j.immuni.2016.06.027

333. Suo C, Fan Z, Zhou L, Qiu J. Perfluorooctane sulfonate affects intestinal immunity against bacterial infection. *Sci Rep* (2017) 7(1):5166. doi: 10.1038/s41598-017-04091-z

334. Aguiar SLF, Miranda MCG, Guimarães MAF, Santiago HC, Queiroz CP, Cunha PDS, et al. High-salt diet induces IL-17-dependent gut inflammation and exacerbates colitis in mice. *Front Immunol* (2018) 8:1969. doi: 10.3389/fimmu.2017.01969

335. Mikami Y, Scarno G, Zitti B, Shih HY, Kanno Y, Santoni A, et al. NCR+ ILC3 maintain larger STAT4 reservoir via T-BET to regulate type 1 features upon IL-23 stimulation in mice. *Eur J Immunol* (2018) 48(7):1174–80. doi: 10.1002/eji.201847480

336. Almeida FF, Tognarelli S, Marçais A, Kueh AJ, Friede ME, Liao Y, et al. A point mutation in the Ncr1 signal peptide impairs the development of innate lymphoid cell subsets. *Oncoimmunology* (2018) 7(10):e1475875. doi: 10.1080/2162402X.2018.1475875

337. Deng T, Suo C, Chang J, Yang R, Li J, Cai T, et al. ILC3-derived OX40L is essential for homeostasis of intestinal Tregs in immunodeficient mice. *Cell Mol Immunol* (2020) 17(2):163–77. doi: 10.1038/s41423-019-0200-x

338. Li J, Shi W, Sun H, Ji Y, Chen Y, Guo X, et al. Activation of DR3 signaling causes loss of ILC3 and exacerbates intestinal inflammation. *Nat Commun* (2019) 10 (1):3371. doi: 10.1038/s41467-019-11304-8

339. Yordanova IA, Lamatsch M, Kühl AA, Hartmann S, Rausch S. Eosinophils are dispensable for the regulation of IgA and Th17 responses in Giardia muris infection. *Parasite Immunol* (2021) 43(3):e12791. doi: 10.1111/pim.12791

340. Cho SX, Rudloff I, Lao JC, Pang MA, Goldberg R, Bui CB, et al. Characterization of the pathoimmunology of necrotizing enterocolitis reveals novel therapeutic opportunities. *Nat Commun* (2020) 11(1):5794. doi: 10.1038/s41467-020-19400-w

341. Chang J, Ji X, Deng T, Qiu J, Ding Z, Li Z, et al. Setd2 determines distinct properties of intestinal ILC3 subsets to regulate intestinal immunity. *Cell Rep* (2022) 38 (11):110530. doi: 10.1016/j.celrep.2022.110530

342. Sano T, Huang W, Hall JA, Yang Y, Chen A, Gavzy SJ, et al. An IL-23R/IL-22 circuit regulates epithelial serum amyloid A to promote local effector th17 responses. *Cell* (2015) 163(2):381–93. doi: 10.1016/j.cell.2015.08.061

343. Tan C, Hong G, Wang Z, Duan C, Hou L, Wu J, et al. Promoting effect of L-fucose on the regeneration of intestinal stem cells through AHR/IL-22 pathway of intestinal lamina propria monocytes. *Nutrients* (2022) 14(22):4789. doi: 10.3390/nu14224789

344. Riba A, Olier M, Lacroix-Lamandé S, Lencina C, Bacquié V, Harkat C, et al. Early life stress in mice is a suitable model for Irritable Bowel Syndrome but does not predispose to colitis nor increase susceptibility to enteric infections. *Brain Behav Immun* (2018) 73:403–15. doi: 10.1016/j.bbi.2018.05.024

345. Park HJ, Lee SW, Van Kaer L, Hong S. CD1d-dependent iNKT cells control DSS-induced colitis in a mouse model of IFNγ-mediated hyperinflammation by increasing IL22-secreting ILC3 cells. *Int J Mol Sci* (2021) 22(3):1250. doi: 10.3390/ijms22031250

346. Eberl G. RORγt, a multitask nuclear receptor at mucosal surfaces. *Mucosal Immunol* (2017) 10(1):27–34. doi: 10.1038/mi.2016.86

347. Taylor PR, Roy S, Leal SM Jr, Sun Y, Howell SJ, Cobb BA, et al. Activation of neutrophils by autocrine IL-17A-IL-17RC interactions during fungal infection is regulated by IL-6, IL-23, RORγt and dectin-2. *Nat Immunol* (2014) 15(2):143–51. doi: 10.1038/ni.2797

348. Savers A, Rasid O, Parlato M, Brock M, Jouvion G, Ryffel B, et al. Infection-Mediated Priming of Phagocytes Protects against Lethal Secondary Aspergillus fumigatus Challenge. *PloS One* (2016) 11(4):e0153829. doi: 10.1371/journal.pone.0153829

349. Brown CC, Gudjonson H, Pritykin Y, Deep D, Lavallée VP, Mendoza A, et al. Transcriptional basis of mouse and human dendritic cell heterogeneity. *Cell* (2019) 179 (4):846–863.e24. doi: 10.1016/j.cell.2019.09.035

350. Sonnenberg GF, Monticelli LA, Elloso MM, Fouser LA, Artis D. CD4(+) lymphoid tissue-inducer cells promote innate immunity in the gut. *Immunity* (2011) 34(1):122–34. doi: 10.1016/j.immuni.2010.12.009

351. Crispín JC, Oukka M, Bayliss G, Cohen RA, Van Beek CA, Stillman IE, et al. Expanded double negative T cells in patients with systemic lupus erythematosus produce IL-17 and infiltrate the kidneys. *J Immunol* (2008) 181(12):8761–6. doi: 10.4049/jimmunol.181.12.8761

352. Ueyama A, Imura C, Fusamae Y, Tsujii K, Furue Y, Aoki M, et al. Potential role of IL-17-producing CD4/CD8 double negative αβ T cells in psoriatic skin inflammation in a TPA-induced STAT3C transgenic mouse model. *J Dermatol Sci* (2017) 85(1):27–35. doi: 10.1016/j.jdermsci.2016.10.007

353. Thomas ML. The leukocyte common antigen family. *Annu Rev Immunol* (1989) 7:339–69. doi: 10.1146/annurev.iy.07.040189.002011

354. Nakano H, Yanagita M, Gunn MD. CD11c(+)B220(+)Gr-1(+) cells in mouse lymph nodes and spleen display characteristics of plasmacytoid dendritic cells. *J Exp Med* (2001) 194(8):1171–8. doi: 10.1084/jem.194.8.1171

355. Merkenschlager M, Fisher AG. CD45 isoform switching precedes the activation-driven death of human thymocytes by apoptosis. *Int Immunol* (1991) 3 (1):1–7. doi: 10.1093/intimm/3.1.1

356. Renno T, Attinger A, Rimoldi D, Hahne M, Tschopp J, MacDonald HR. Expression of B220 on activated T cell blasts precedes apoptosis. *Eur J Immunol* (1998) 28(2):540–7. doi: 10.1002/(SICI)1521-4141(199802)28:02<540::AID-IMMU540>3.0.CO;2-Y

357. Oka S, Mori N, Matsuyama S, Takamori Y, Kubo K. Presence of B220 within thymocytes and its expression on the cell surface during apoptosis. *Immunology* (2000) 100(4):417–23. doi: 10.1046/j.1365-2567.2000.00063.x

358. Melchers F, ten Boekel E, Seidl T, Kong XC, Yamagami T, Onishi K, et al. Repertoire selection by pre-B-cell receptors and B-cell receptors, and genetic control of B-cell development from immature to mature B cells. *Immunol Rev* (2000) 175:33–46. doi: 10.1111/j.1600-065X.2000.imr017510.x

359. Wang K, Wei G, Liu D. CD19: a biomarker for B cell development, lymphoma diagnosis and therapy. *Exp Hematol Oncol* (2012) 1(1):36. doi: 10.1186/2162-3619-1-36

360. Meininger I, Carrasco A, Rao A, Soini T, Kokkinou E, Mjösberg J. Tissue-specific features of innate lymphoid cells. *Trends Immunol* (2020) 41(10):902–17. doi: 10.1016/j.it.2020.08.009

361. Van Acker HH, Capsomidis A, Smits EL, Van Tendeloo VF. CD56 in the immune system: more than a marker for cytotoxicity? *Front Immunol* (2017) 8:892. doi: 10.3389/fimmu.2017.00892

362. Carlyle JR, Mesci A, Ljutic B, Belanger S, Tai LH, Rousselle E, et al. Molecular and genetic basis for strain-dependent NK1.1 alloreactivity of mouse NK cells. *J Immunol* (2006) 176(12):7511–24. doi: 10.4049/jimmunol.176.12.7511

363. Sheikh A, Abraham N. Interleukin-7 receptor alpha in innate lymphoid cells: more than a marker. *Front Immunol* (2019) 10:2897. doi: 10.3389/fimmu.2019.02897

364. Artis D, Spits H. The biology of innate lymphoid cells. *Nature* (2015) 517 (7534):293–301. doi: 10.1038/nature14189

365. Alves NL, van Leeuwen EM, Remmerswaal EB, Vrisekoop N, Tesselaar K, Roosnek E, et al. A new subset of human naive CD8+ T cells defined by low expression of IL-7R alpha. *J Immunol* (2007) 179(1):221–8. doi: 10.4049/jimmunol.179.1.221

366. Huster KM, Busch V, Schiemann M, Linkemann K, Kerksiek KM, Wagner H, et al. Selective expression of IL-7 receptor on memory T cells identifies early CD40L-dependent generation of distinct CD8+ memory T cell subsets. *Proc Natl Acad Sci U.S.A.* (2004) 101(15):5610–5. doi: 10.1073/pnas.0308054101

367. Liu W, Putnam AL, Xu-Yu Z, Szot GL, Lee MR, Zhu S, et al. CD127 expression inversely correlates with FoxP3 and suppressive function of human CD4+ T reg cells. *J Exp Med* (2006) 203(7):1701–11. doi: 10.1084/jem.20060772

368. Lennartsson J, Rönnstrand L. Stem cell factor receptor/c-Kit: from basic science to clinical implications. *Physiol Rev* (2012) 92(4):1619–49. doi: 10.1152/physrev.00046.2011

369. Frumento G, Zuo J, Verma K, Croft W, Ramagiri P, Chen FE, et al. CD117 (c-kit) is expressed during CD8+ T cell priming and stratifies sensitivity to apoptosis according to strength of TCR engagement. *Front Immunol* (2019) 10:468. doi: 10.3389/fimmu.2019.00468

370. Onkanga IO, Hamilton R, Mwinzi PNM, Schneider T, Ondigo BN, Sang H, et al. Expression of CD117 (c-kit) on circulating B cells in pediatric schistosomiasis. *Infect Immun* (2022) 90(8):e0016022. doi: 10.1128/iai.00160-22

371. Oliver ET, Chichester K, Devine K, Sterba PM, Wegner C, Vonakis BM, et al. Effects of an oral CRTh2 antagonist (AZD1981) on eosinophil activity and symptoms in chronic spontaneous urticaria. *Int Arch Allergy Immunol* (2019) 179(1):21–30. doi: 10.1159/000496162

372. Sauzay C, Voutetakis K, Chatziioannou A, Chevet E, Avril T. CD90/thy-1, a cancer-associated cell surface signaling molecule. *Front Cell Dev Biol* (2019) 7:66. doi: 10.3389/fcell.2019.00066

373. Corral D, Charton A, Krauss MZ, Blanquart E, Levillain F, Lefrançais E, et al. ILC precursors differentiate into metabolically distinct ILC1-like cells during Mycobacterium tuberculosis infection. *Cell Rep* (2022) 39(3):110715. doi: 10.1016/j.celrep.2022.110715

374. Sonnenberg GF, Monticelli LA, Alenghat T, Fung TC, Hutnick NA, Kunisawa J, et al. Innate lymphoid cells promote anatomical containment of lymphoid-resident commensal bacteria. *Science* (2012) 336(6086):1321–5. doi: 10.1126/science.1222551

375. Schroeder JH, Beattie G, Lo JW, Zabinski T, Powell N, Neves JF, et al. CD90 is not constitutively expressed in functional innate lymphoid cells. *Front Immunol* (2023) 14:1113735. doi: 10.3389/fimmu.2023.1113735

376. Poggi A, Rubartelli A, Moretta L, Zocchi MR. Expression and function of NKRP1A molecule on human monocytes and dendritic cells. *Eur J Immunol* (1997) 27 (11):2965–70. doi: 10.1002/eji.1830271132

377. Mjösberg JM, Trifari S, Crellin NK, Peters CP, van Drunen CM, Piet B, et al. Human IL-25- and IL-33-responsive type 2 innate lymphoid cells are defined by expression of CRTH2 and CD161. *Nat Immunol* (2011) 12(11):1055–62. doi: 10.1038/ni.2104

378. Cogswell A, Ferguson N, Barker E. Presence of inflammatory group I and III innate lymphoid cells in the colon of simian immunodeficiency virus-infected rhesus macaques. *J Virol* (2020) 94(9):e01914–19. doi: 10.1128/JVI.01914-19

379. Starner TD, Barker CK, Jia HP, Kang Y, McCray PB Jr. CCL20 is an inducible product of human airway epithelia with innate immune properties. *Am J Respir Cell Mol Biol* (2003) 29(5):627–33. doi: 10.1165/rcmb.2002-0272OC

380. Kulkarni N, Pathak M, Lal G. Role of chemokine receptors and intestinal epithelial cells in the mucosal inflammation and tolerance. *J Leukoc Biol* (2017) 101 (2):377–94. doi: 10.1189/jlb.1RU0716-327R

381. Ignacio A, Breda CNS, Camara NOS. Innate lymphoid cells in tissue homeostasis and diseases. *World J Hepatol* (2017) 9(23):979–89. doi: 10.4254/wjh.v9.i23.979

382. Eberl G, Marmon S, Sunshine MJ, Rennert PD, Choi Y, Littman DR. An essential function for the nuclear receptor RORgamma(t) in the generation of fetal lymphoid tissue inducer cells. *Nat Immunol* (2004) 5(1):64–73. doi: 10.1038/ni1022

383. Glasner A, Isaacson B, Viukov S, Neuman T, Friedman N, Mandelboim M, et al. Increased NK cell immunity in a transgenic mouse model of NKp46 overexpression. *Sci Rep* (2017) 7(1):13090. doi: 10.1038/s41598-017-12998-w

384. Sivori S, Vitale M, Morelli L, Sanseverino L, Augugliaro R, Bottino C, et al. p46, a novel natural killer cell-specific surface molecule that mediates cell activation. *J Exp Med* (1997) 186(7):1129–36. doi: 10.1084/jem.186.7.1129

385. Vivier E, Artis D, Colonna M, Diefenbach A, Di Santo JP, Eberl G, et al. Innate lymphoid cells: 10 years on. *Cell* (2018) 174(5):1054–66. doi: 10.1016/j.cell.2018.07.017

386. Bottino C, Biassoni R, Millo R, Moretta L, Moretta A. The human natural cytotoxicity receptors (NCR) that induce HLA class I-independent NK cell triggering. *Hum Immunol* (2000) 61(1):1–6. doi: 10.1016/s0198-8859(99)00162-7

387. Glatzer T, Killig M, Meisig J, Ommert I, Luetke-Eversloh M, Babic M, et al. RORγt$^+$ innate lymphoid cells acquire a proinflammatory program upon engagement of the activating receptor NKp44. *Immunity* (2013) 38(6):1223–35. doi: 10.1016/j.immuni.2013.05.013

388. Cella M, Miller H, Song C. Beyond NK cells: the expanding universe of innate lymphoid cells. *Front Immunol* (2014) 5:282. doi: 10.3389/fimmu.2014.00282

389. Simoni Y, Fehlings M, Kløverpris HN, McGovern N, Koo SL, Loh CY, et al. Human innate lymphoid cell subsets possess tissue-type based heterogeneity in phenotype and frequency. *Immunity* (2017) 46(1):148–61. doi: 10.1016/j.immuni.2016.11.005

390. Bernink JH, Peters CP, Munneke M, te Velde AA, Meijer SL, Weijer K, et al. Human type 1 innate lymphoid cells accumulate in inflamed mucosal tissues. *Nat Immunol* (2013) 14(3):221–9. doi: 10.1038/ni.2534

391. Geremia A, Arancibia-Cárcamo CV, Fleming MP, Rust N, Singh B, Mortensen NJ, et al. IL-23-responsive innate lymphoid cells are increased in inflammatory bowel disease. *J Exp Med* (2011) 208(6):1127–33. doi: 10.1084/jem.20101712

392. Rao A, Strauss O, Kokkinou E, Bruchard M, Tripathi KP, Schlums H, et al. Cytokines regulate the antigen-presenting characteristics of human circulating and tissue-resident intestinal ILCs. *Nat Commun* (2020) 11(1):2049. doi: 10.1038/s41467-020-15695-x

393. Jarade A, Di Santo JP, Serafini N. Group 3 innate lymphoid cells mediate host defense against attaching and effacing pathogens. *Curr Opin Microbiol* (2021) 63:83–91. doi: 10.1016/j.mib.2021.06.005

394. Pian Y, Chai Q, Ren B, Wang Y, Lv M, Qiu J, et al. Type 3 Innate Lymphoid Cells Direct Goblet Cell Differentiation via the LT-LTβR Pathway during Listeria Infection. *J Immunol* (2020) 205(3):853–63. doi: 10.4049/jimmunol.2000197

395. Simoni Y, Newell EW. Dissecting human ILC heterogeneity: more than just three subsets. *Immunology* (2018) 153(3):297–303. doi: 10.1111/imm.12862

396. Hepworth MR, Monticelli LA, Fung TC, Ziegler CG, Grunberg S, Sinha R, et al. Innate lymphoid cells regulate CD4+ T-cell responses to intestinal commensal bacteria. *Nature* (2013) 498(7452):113–7. doi: 10.1038/nature12240

397. Kiss EA, Diefenbach A. Role of the aryl hydrocarbon receptor in controlling maintenance and functional programs of RORγt(+) innate lymphoid cells and intraepithelial lymphocytes. *Front Immunol* (2012) 3:124. doi: 10.3389/fimmu.2012.00124

398. Sécca C, Bando JK, Fachi JL, Gilfillan S, Peng V, Di Luccia B, et al. Spatial distribution of LTi-like cells in intestinal mucosa regulates type 3 innate immunity. *Proc Natl Acad Sci U.S.A.* (2021) 118(23):e2101668118. doi: 10.1073/pnas.2101668118

399. Ito T, Carson WF4, Cavassani KA, Connett JM, Kunkel SL. CCR6 as a mediator of immunity in the lung and gut. *Exp Cell Res* (2011) 317(5):613–9. doi: 10.1016/j.yexcr.2010.12.018

400. Takatori H, Kanno Y, Watford WT, Tato CM, Weiss G, Ivanov II, et al. Lymphoid tissue inducer-like cells are an innate source of IL-17 and IL-22. *J Exp Med* (2009) 206(1):35–41. doi: 10.1084/jem.20072713

401. Constantinides MG, McDonald BD, Verhoef PA, Bendelac A. A committed precursor to innate lymphoid cells. *Nature* (2014) 508(7496):397–401. doi: 10.1038/nature13047

402. Zhong C, Zheng M, Cui K, Martins AJ, Hu G, Li D, et al. Differential expression of the transcription factor GATA3 specifies lineage and functions of innate lymphoid cells. *Immunity* (2020) 52(1):83–95.e4. doi: 10.1016/j.immuni.2019.12.001

403. Ishizuka IE, Chea S, Gudjonson H, Constantinides MG, Dinner AR, Bendelac A, et al. Single-cell analysis defines the divergence between the innate lymphoid cell lineage and lymphoid tissue-inducer cell lineage. *Nat Immunol* (2016) 17(3):269–76. doi: 10.1038/ni.3344

404. Kasal DN, Bendelac A. Multi-transcription factor reporter mice delineate early precursors to the ILC and LTi lineages. *J Exp Med* (2021) 218(2):e20200487. doi: 10.1084/jem.20200487

405. Klose CS, Kiss EA, Schwierzeck V, Ebert K, Hoyler T, d'Hargues Y, et al. A T-bet gradient controls the fate and function of CCR6-RORγt+ innate lymphoid cells. *Nature* (2013) 494(7436):261–5. doi: 10.1038/nature11813

406. Lee JS, Cella M, McDonald KG, Garlanda C, Kennedy GD, Nukaya M, et al. AHR drives the development of gut ILC22 cells and postnatal lymphoid tissues via pathways dependent on and independent of Notch. *Nat Immunol* (2011) 13(2):144–51. doi: 10.1038/ni.2187

407. Rankin LC, Groom JR, Chopin M, Herold MJ, Walker JA, Mielke LA, et al. The transcription factor T-bet is essential for the development of NKp46+ innate lymphocytes via the Notch pathway. *Nat Immunol* (2013) 14(4):389–95. doi: 10.1038/ni.2545

408. Cossarizza A, Chang HD, Radbruch A, Abrignani S, Addo R, Akdis M, et al. Guidelines for the use of flow cytometry and cell sorting in immunological studies (third edition). *Eur J Immunol* (2021) 51(12):2708–3145. doi: 10.1002/eji.202170126

409. Simoni Y, Fehlings M, Kløverpris HN, McGovern N, Koo SL, Loh CY, et al. Human innate lymphoid cell subsets possess tissue-type based heterogeneity in phenotype and frequency. *Immunity* (2018) 48(5):1060. doi: 10.1016/j.immuni.2018.04.028

410. Bonne-Année S, Bush MC, Nutman TB. Differential modulation of human innate lymphoid cell (ILC) subsets by IL-10 and TGF-β. *Sci Rep* (2019) 9(1):14305. doi: 10.1038/s41598-019-50308-8

411. Mazzurana L, Czarnewski P, Jonsson V, Wigge L, Ringnér M, Williams TC, et al. Tissue-specific transcriptional imprinting and heterogeneity in human innate lymphoid cells revealed by full-length single-cell RNA-sequencing. *Cell Res* (2021) 31 (5):554–68. doi: 10.1038/s41422-020-00445-x

412. Del Zotto G, Vacca P, Moretta L, Quatrini L. CPHEN-15: Comprehensive phenotyping of human peripheral blood helper-ILCs by flow cytometry. *Cytometry A* (2023) 103(5):378–82. doi: 10.1002/cyto.a.24717

frontiers | Frontiers in Immunology

TYPE Original Research
PUBLISHED 01 December 2023
DOI 10.3389/fimmu.2023.1271879

OPEN ACCESS

EDITED BY
Carolina Jancic,
National Scientific and Technical Research Council (CONICET), Argentina

REVIEWED BY
Han-Yu Shih,
National Eye Institute (NIH), United States
Jan-Hendrik Schroeder,
King's College London, United Kingdom

*CORRESPONDENCE
Chao Zhong
zhongc@pku.edu.cn

†These authors have contributed equally to this work

RECEIVED 03 August 2023
ACCEPTED 13 November 2023
PUBLISHED 01 December 2023

CITATION
Zhang Y, Hu L, Ren G, Zeng Y, Zhao X and Zhong C (2023) Distinct regulatory machineries underlying divergent chromatin landscapes distinguish innate lymphoid cells from T helper cells. *Front. Immunol.* 14:1271879. doi: 10.3389/fimmu.2023.1271879

Distinct regulatory machineries underlying divergent chromatin landscapes distinguish innate lymphoid cells from T helper cells

Yime Zhang[1,2†], Luni Hu[3,4†], Guanqun Ren[3,4], Yanyu Zeng[1,2], Xingyu Zhao[1,2] and Chao Zhong[1,2,3,4*]

[1]Department of Immunology, School of Basic Medical Sciences, Peking University Health Science Center, Beijing, China, [2]Key National Health Commission Laboratory of Medical Immunology, Peking University, Beijing, China, [3]Institute of Systems Biomedicine, School of Basic Medical Sciences, Peking University Health Science Center, Beijing, China, [4]Beijing Key Laboratory of Tumor Systems Biology, Peking University, Beijing, China

Innate lymphoid cells (ILCs), as the innate counterpart of $CD4^+$ T helper (Th) cells, play crucial roles in maintaining tissue homeostasis. While the ILC subsets and their corresponding Th subsets demonstrate significant similarities in core programming related to effector function and regulatory mechanisms, their principal distinctions, given their innate and adaptive lymphocyte nature, remain largely unknown. In this study, we have employed an integrative analysis of 294 bulk RNA-sequencing results across all ILC and Th subsets, using scRNA-seq algorithms. Consequently, we identify two genesets that predominantly differentiate ILCs from Th cells, as well as three genesets that distinguish various immune responses. Furthermore, through chromatin accessibility analysis, we find that the ILC geneset tends to rely on specific transcriptional regulation at promoter regions compared with the Th geneset. Additionally, we observe that ILCs and Th cells are under differential transcriptional regulation. For example, ILCs are under stronger regulation by multiple transcription factors, including RORα, GATA3, and NF-κB. Otherwise, Th cells are under stronger regulation by AP-1. Thus, our findings suggest that, despite the acknowledged similarities in effector functions between ILC subsets and corresponding Th subsets, the underlying regulatory machineries still exhibit substantial distinctions. These insights provide a comprehensive understanding of the unique roles played by each cell type during immune responses.

KEYWORDS

innate lymphoid cells, T helper cells, transcriptome, chromatin accessibility, transcription factor

Introduction

In recent years, innate lymphoid cells (ILCs) have garnered increasing attention owing to their functional parallels with $CD4^+$ T helper (Th) cells of the adaptive immune system (1–3). Both ILCs and Th cells play pivotal roles by secreting effector cytokines, sharing similarities in their effector functions and regulatory mechanisms. These shared characteristics lead to the categorization of both cell types into distinct subsets based on the expression of signature effector cytokines and master transcription factors (4–7). For instance, type 1 ILCs (ILC1s) and Th1 cells mainly produce IFN-γ and TNF-α, regulated by the master transcription factor T-bet (8, 9). Likewise, ILC2s and Th2 cells predominantly express IL-5 and IL-13, controlled by the transcription factor GATA3 (10–12). Furthermore, ILC3s, encompassing natural killer receptor expressing (NCR^+) ILC3s, double-negative (DN) ILC3s, and lymphoid tissue-inducer (LTi) cells, mirror Th17 cells as they primarily secrete IL-22 and IL-17, under the regulation of the transcription factor RORγt (13, 14).

Although the ILC subsets and their corresponding Th subsets share functional and regulatory similarities, it remains imperative to acknowledge their fundamental differences as innate and adaptive lymphocytes, respectively. One notable distinction lies in the role of T-cell receptor (TCR) signaling, which is crucial for the activation, differentiation, and effector functions of Th cells (15). TCR signaling triggers downstream transcription factors like AP-1, NF-AT, and NF-κB (16). In contrast, ILCs, lacking TCR expression, rely on cytokines, neuropeptides, eicosanoids, and other environmental signal for activation (17–21). Additionally, ILCs are characterized by their tissue residency, meaning that their activation and functions are regulated by local environmental cues and they exert crucial regulatory roles in maintaining tissue homeostasis (22, 23). Th cells, however, are primarily circulatory, undergoing initially activated and differentiated in secondary lymphoid organs before migrating to exert effector functions in peripheral tissues (24). This distinction underscores that despite parallels, there exist key functional and regulatory differences between ILCs and Th cells intrinsic to their identities as innate versus adaptive lymphocytes.

The transcriptomic differences between ILC subsets and their corresponding Th cells should, to varying degrees, reflect their functional and regulatory differences. Previous studies have attempted transcriptional comparison between these cell types (25–27). For instance, in a study examining *Nippostrongylus brasiliensis* infection, lung ILC2s and Th2 cells isolated on day 14 were subjected to bulk RNA-sequencing (RNA-seq) analysis. The resulting differentially expressed genes between the two cell types were indeed substantial (25). However, the core programing of lung ILC2 and Th2 cells, including cell-surface receptors, cytokines, and transcription factors, exhibited significant shared properties (26, 28). Furthermore, other studies have demonstrated that differentiated Th2 cells and memory Th2 cells can produce effector cytokines independently of TCR signaling, similar to innate lymphocytes (29, 30). These findings may partially explain the resemblance between lung Th2 cells and ILC2s after *N. brasiliensis* infection. Nevertheless, it remains unclear whether all ILC subsets and their corresponding Th cells exhibit such comparable features under different conditions. Moreover, ILCs primarily reside in local tissues, where they participate in maintaining tissue homeostasis. Conversely, Th cells typically undergo activation and differentiation in secondary lymphoid organs, specializing in cytokine production to facilitate immune responses. Therefore, further investigation into the fundamental difference between ILCs and Th cells is still imperative.

Results

Integrated transcriptome analysis uncovers distinct gene expression signatures between ILC and Th subsets

ILCs and Th cells exhibited parallel effector functions in innate and adaptive immunity, respectively (31). However, the transcriptomic differences between these cell types had remained largely unclear. To comprehensively compare their transcriptomes and minimize variations from a single data source, we performed an integrative analysis leveraging publicly available bulk RNA-sequencing (RNA-seq) datasets. In total, we collected bulk RNA-seq datasets from 52 published studies, comprising 294 samples, including 21 ILC1, 64 ILC2, 41 ILC3, 61 Th1 cell, 49 Th2 cell, and 58 Th17 cell samples (Figure 1A, Supplementary Table 1). Subsequently, we applied a series of data processing steps to the bulk RNA-seq datasets, including normalization of data, filtration of genes with low expression, and removal of batch effect (Figure 1B, Supplementary Figure 1A). Through these steps, we identified 8,393 genes with significantly high expression levels (transcripts per million or TPM >10) in at least one ILC or Th subset (expressed in more than 80% of the samples for each respective subset) (Figure 1C, Supplementary Figure 1B). Following the removal of batch effects, the RNA-seq samples underwent UMAP classification, a commonly used algorithm frequently used for single-cell RNA-seq (scRNA-seq) analysis, based on the gene expression profiles of the samples (Figure 1D, Supplementary Figure 1C). The UMAP analysis accurately assigned the samples to their respective cell type categories, indicating that the gene expression profiles effectively captured the cellular heterogeneity within the dataset. To further validate the accuracy of the RNA-seq dataset processing, we examined the expression of expected signature genes in ILC and Th subsets. Specifically, all three ILC subsets exhibited enriched expression of the ILC marker *Kit*, whereas the three Th subsets showed specific expression of the T-cell marker *Cd3e* (Figure 1E). Moreover, the master transcriptional factors *Tbx21*, *Gata3*, and *Rorc*, associated with different immune cell types, were accurately and highly expressed by their respective ILC or Th subsets (Figure 1E).

The successful classification allowed us to further investigate the distinct transcriptional features present in each ILC and Th subset by employing algorithms specifically designed for scRNA-seq analysis. Despite sharing similarities in effector functions, we anticipated significant transcriptional differences between ILC subsets and their corresponding Th subsets, reflecting their

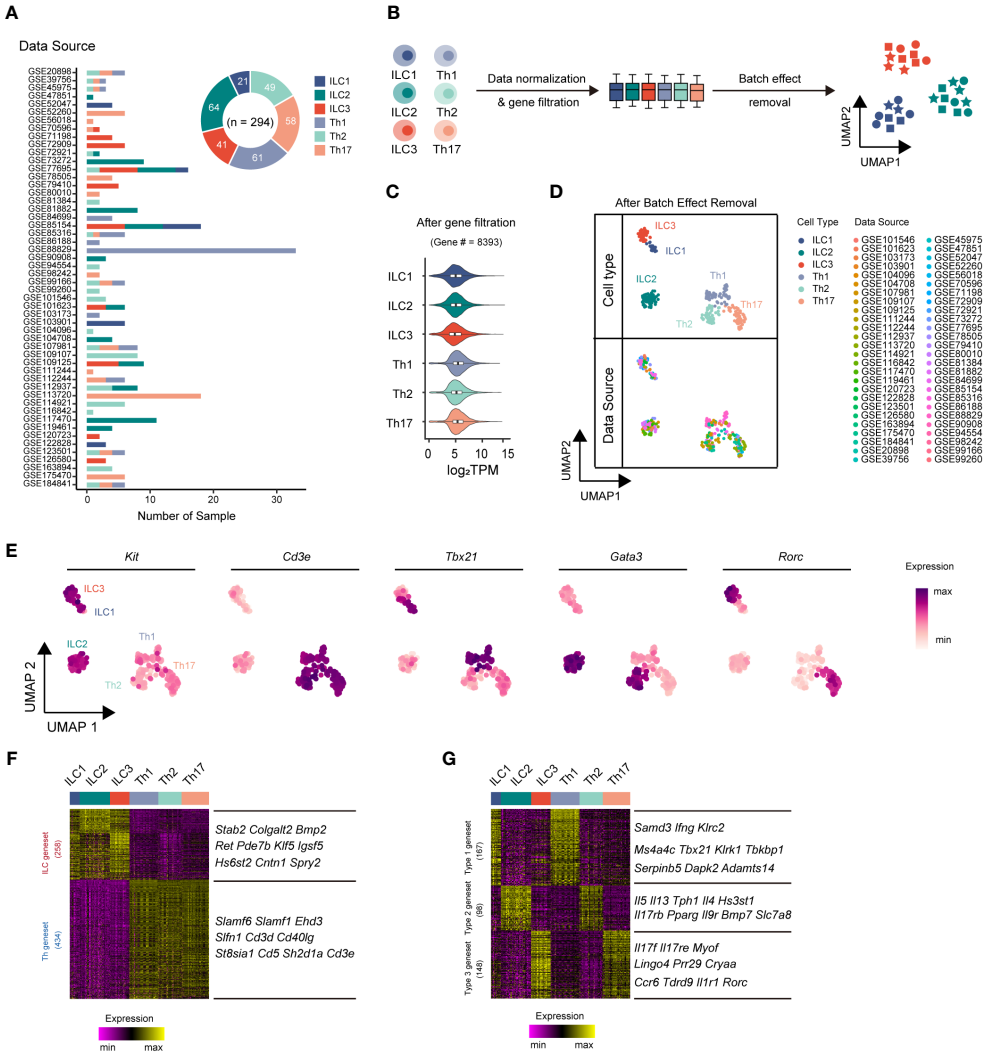

FIGURE 1
Integrative RNA-seq analysis uncovers principal genesets distinguishing ILC and Th subsets. **(A)** Bar chart showing the sources and numbers of bulk RNA-seq datasets across different ILC and Th subsets, and donut plot showing the numbers of bulk RNA-seq datasets collected for each cell type. **(B)** Schematics of the RNA-seq data preprocessing strategy. RNA-seq datasets of ILCs and Th cells are normalized into TPM, and then low-expression genes are filtered out, followed by batch effect removal using the limma package. **(C)** Violin plot showing average gene expression (log_2 TPM) in each cell type after low expression gene filtering. **(D)** UMAP plot showing distribution of ILC and Th RNA-seq samples after batch effect removal. Cell types and data sources are annotated. **(E)** Scatter plot showing the expression of *Kit*, *Cd3e*, *Tbx21*, *Gata3*, and *Rorc* across ILC and Th subsets. **(F)** Heatmap showing differentially expressed genes between ILC and Th (log_2 fold-change > 0.25, P. value < 0.01). The top 10 ILC-specific and Th-specific genes ranked by fold change are listed. **(G)** Heatmap showing conserved genes in ILC and Th subsets of each immune response (log_2 fold change > 0.25, P. value < 0.01). The top 10 genes with minimum fold change among ILC and Th subset are listed. UMAP, Uniform Manifold Approximation and Projection. TPM, transcripts per million mapped reads.

inherent differentiation as innate and adaptive immune cells, respectively. To elucidate such transcriptional differences, we conducted paired transcriptome comparisons between ILC subsets and their parallel Th subsets (ILC1 versus Th1, ILC2 versus Th2, and ILC3 versus Th17). This analysis revealed 258 ILC-specific genes and 434 Th-specific genes, referred to as the ILC geneset and Th geneset, respectively (Figure 1F, Supplementary Table 2). To further verify the reliability of the geneset and eliminate the interference of the tissue environment, we conducted a comparison of the expression levels of the ILC geneset and the Th geneset between ILC and Th subsets originating from the same source (25, 32, 33). As we anticipated, most genes in the ILC geneset exhibit a higher expression level in ILC subsets, whereas most genes in the Th geneset exhibit a higher expression level in Th subsets from the same source (Supplementary Figure 2). Overall, the ILC geneset and Th geneset represent fundamental distinctions between ILC and Th cells and are minimally affected by environmental factors.

The different subsets of ILCs, along with their corresponding Th subsets, play distinct roles in immune responses. Therefore, we next conducted a screening process to identify genes that underlay specific immune responses, exhibiting conserved, subset-specific expression patterns in individual ILC subsets and their corresponding Th counterparts, aiming to identify genes

underlying specific immune responses. As a result, we defined 167 genes as the type 1 geneset, which included *Ifng* and *Tbx21*, specifically expressed in both ILC1s and Th1 cells. We also defined 98 genes as the type 2 geneset, such as *Il4*, *Il5*, *Il13*, and *Gata3*, which were preferentially upregulated in both ILC2s and Th2 cells. Additionally, we defined 148 genes as the type 3 geneset, like *Il17a*, *Il17f*, *Il22*, and *Rorc*, exhibiting significant increases in both ILC3s and Th17 cells (Figure 1G, Supplementary Table 3).

Collectively, by conducting an integrated analysis of 294 bulk RNA-seq datasets across ILC and Th subsets using scRNA-seq algorithms, we have successfully identified genesets that highlight the key transcriptional differences between ILCs and Th cells, as well as the variations in immune response programs.

GO enrichment analysis reveals fundamental functional and regulatory disparities across ILC and Th subsets

These genesets identified in our analysis provided valuable insights into the fundamental transcriptional characteristics underlying the functional properties of the ILC and Th subsets. To further elucidate the functional differences between ILCs and Th cells, as well as between distinct immune response programs, we performed gene ontology (GO) enrichment analysis on these genesets. The analysis revealed the top 100 enriched GO terms in the ILC and Th genesets, highlighting the significant overrepresentation of pathways related to "lymphocyte activation and chemotaxis" in both ILCs and Th cells. This finding underscored the critical role of these processes in shaping the functional properties of ILCs and Th cells in the immune system (Figure 2A, Supplementary Tables 4, 5). To validate this observation, we examined the expression profile of representative genes within these GO terms across different ILC and Th subsets (Supplementary Figure 3A). Additionally, GO terms associated with pathways of "cell migration", "epithelium development", "mesenchyme development", "blood vessel development", and "nervous system process" were specifically enriched in the ILC geneset (Figure 2A, Supplementary Table 4), consistent with the known role of ILCs as tissue-resident immune cells involved in maintaining tissue homeostasis (22, 23). Specifically, GO terms related to "cytokine production", "MAPK-ERK pathway" and "SMAD pathway" were also enriched in the ILC geneset, suggesting distinct regulation machineries underlying the immune

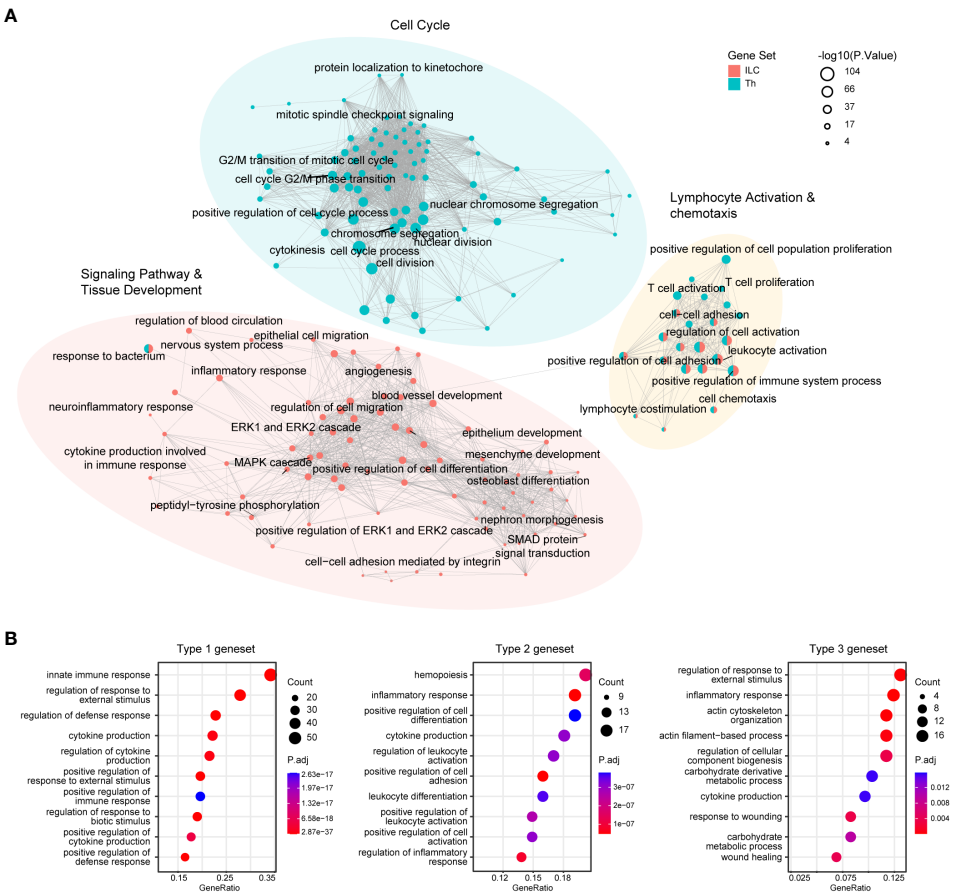

FIGURE 2
GO enrichment analysis reveals fundamental functional and regulatory differences between ILCs and Th cells. **(A)** GO analysis of the ILC and Th genesets. Enrichment map shows the top100 terms enriched in the ILC or Th genesets. **(B)** Dot plot showing the top10 terms enriched in immune response-specific genesets. GO, gene ontology.

effects of ILCs compared with Th cells (Figure 2A). In contrast, GO terms associated with "cell cycle" were highly enriched in the Th geneset, indicating fundamental disparities between Th cells and ILCs in terms of proliferation (Figure 2A, Supplementary Table 5). This observation aligned with the knowledge that T cells underwent clonal expansion during activation and differentiation, resulting in a significant increase in cell number (34). Furthermore, the expression profiles of representative genes within the specifically enriched GO terms in the ILC and Th genesets confirmed the functional distinctions between ILCs and Th cells (Supplementary Figures 3B–D).

In addition, we examined the enriched GO terms in the three immune response-related genesets. Although there were discernible differences between these immune response programs, it was noted that GO terms associated with cytokine production, defense response, and inflammatory response were consistently enriched across all three genesets (Figure 2B, Supplementary Figures 3E–G, Supplementary Tables 6–8). This suggested a similarity in their helper-like functionalities and their contribution to immune responses.

Together, the combined GO enrichment analysis of the predefined ILC and Th genesets, as well as the immune response-related genesets, provides a comprehensive understanding of the functional and regulatory similarities and differences between the different ILC and Th subsets.

Expression-concordant opening chromatin regions associated with the ILC geneset tend to distribute in close proximity to the transcription start sites

Gene expression levels often exhibited correlation with the accessibility of corresponding chromatin loci (35, 36). To further understand the transcriptional disparities between ILCs and Th cells, we compared the chromatin accessibility across the ILC and Th genesets using publicly available sequencing of DNase I hypersensitive sites (DNase-seq) data (GSE172358) (37) (Figure 3A). Through this analysis, we identified 3,292 opening chromatin regions (OCRs) across the ILC genesets and 4,293 OCRs across the Th geneset (within 50 kb to the transcriptional start site or TSS). The accessibility of these OCRs was then compared between ILCs and Th cells. OCRs that exhibited accessibility changes consistent with the expression changes of their associated genes when comparing ILCs and Th cells were referred to as expression-concordant OCRs (Figures 3A, B). Conversely, OCRs showing discord accessibility and expression changes between ILC and Th subsets were categorized as expression-non-concordant OCRs. As a result, we identified 1,022 concordant OCRs across the ILC genesets, which we termed as ILC concordant OCRs (Figure 3C). These OCRs corresponded to majority (79.5%) of the genes in the ILC geneset (Figure 3D). Additionally, we identified 2,270 ILC non-concordant OCRs, encompassing 94.2% of the genes in the ILC geneset (Supplementary Figures 4A, B). Similarly, we discovered 1,559 concordant OCRs across the Th genesets, named as Th concordant OCRs (Figure 3E). These OCRs accounted for 72.4% in the genes in the Th geneset (Figure 3F). We also identified 2,734 Th non-concordant OCRs, corresponding to 92.6% of the genes in the Th geneset (Supplementary Figure 4C, D). Similar to RNA-seq, Th subsets for DNase-seq are differentiated *in vitro* whereas ILC subsets are isolated *in vivo*. For eliminating the interference of the tissue environment and differentiation method, we validated chromatin accessibility of ILC concordant OCRs and Th concordant OCRs in ATAC-seq data of ILC and Th subsets *in vivo* (25). As we anticipated, most of ILC concordant OCRs are specifically opened in ILC subsets, whereas most of Th concordant OCRs are specifically opened in Th subsets *in vivo* (Supplementary Figure 5). This confirmed that the specific regulatory regions of ILC geneset and Th geneset are not affected by environmental factors.

Furthermore, we performed a detailed characterization of the ILC and Th concordant and non-concordant OCRs associated with the ILC and Th genesets. Notably, we observed that the peak widths of the ILC concordant OCRs in all ILC subsets were broader compared with the peak widths of the Th concordant OCRs in the Th subsets (Figures 3C, E). To statistically confirm this difference, we quantified the peak widths of the ILC and Th concordant and non-concordant OCRs (Figure 3G). The ILC concordant OCRs exhibited a significant increase in width compared with the Th concordant OCRs (Figure 3G). Conversely, the width of the ILC non-concordant OCRs showed some variation and even reduction when compared with the width of the Th non-concordant OCRs (Supplementary Figure 4E). Previous studies had suggested that wider OCRs might result from the merging of multiple accessible regions and were more likely to be located in the promoter and super-enhancer regions of the associated genes (38). Therefore, we also investigated the genomic distribution of these ILC and Th concordant and non-concordant OCRs. Consistent with the previous studies (39–41), ILC concordant OCRs demonstrated a preferential distribution within 1 kilobase pair (kb) around TSSs compared with the Th concordant OCRs (Figure 3H). However, the distribution of ILC non-concordant OCRs did not show such a tendency (Supplementary Figure 4F). Overall, these findings suggest that the transcriptional regulation of the ILC geneset tends to heavily rely on promoter regions compared with the transcriptional regulation of the Th geneset.

Different transcription factors are involved in distinguishing the functionalities of ILCs from Th cells

The observed differences in chromatin landscapes between the ILC and Th genesets suggested that they might be regulated by distinct transcriptional control mechanisms mediated by unique regulators. To explore this further, we conducted an analysis to identify enriched transcription factor binding motifs within the ILC and Th concordant OCRs. Indeed, we found that the ILC concordant OCRs displayed enriched binding motifs for transcription factors including RORα, GATA3, GABPA, and c-Rel (Figure 4A), whereas differentially enriched binding motifs were observed for transcription factors such as BATF, AP-1, and ELK4 in the Th concordant OCRs (Figure 4A). Subsequently, we considered

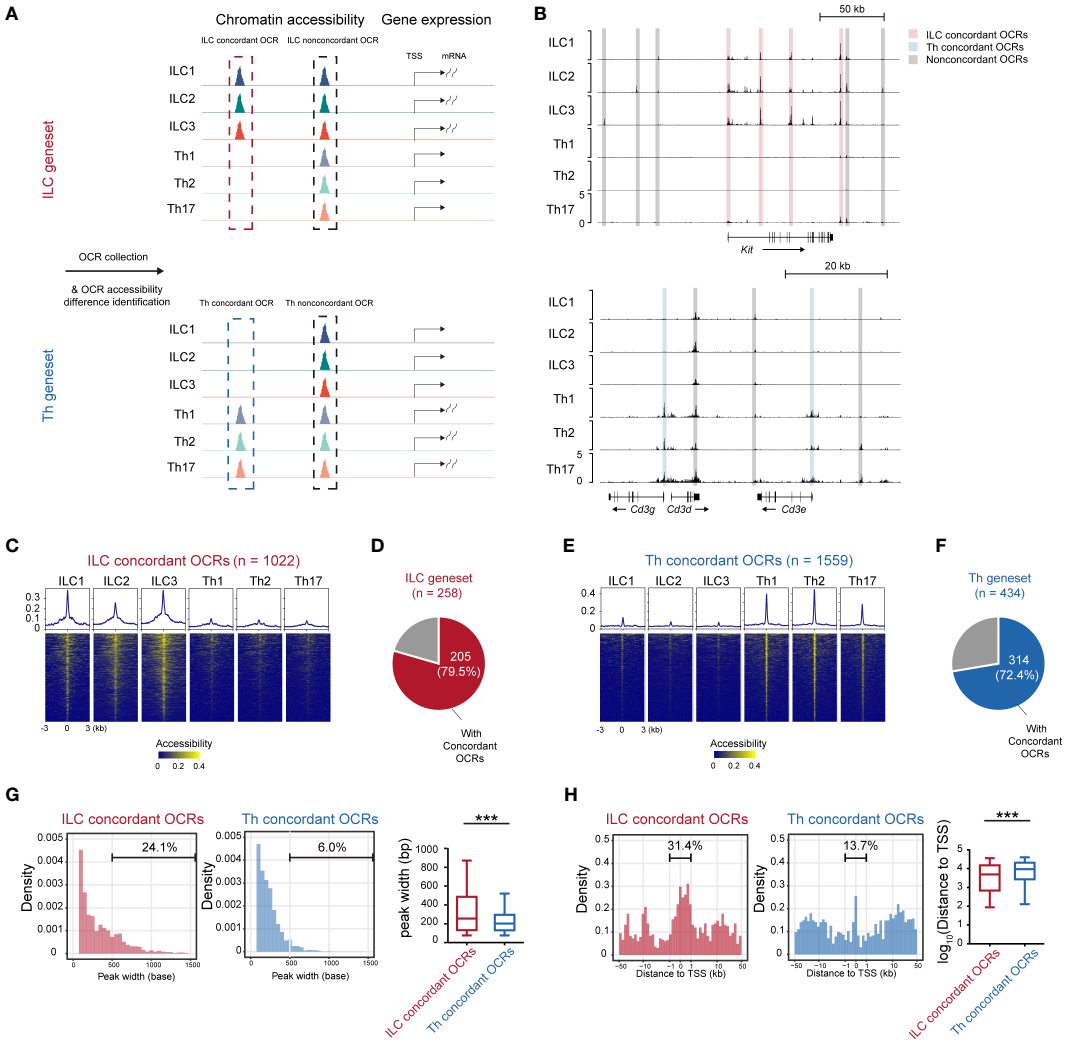

FIGURE 3
Expression-concordant opening chromatin regions associated with the ILC geneset tend to distribute in close proximity to the transcription start sites. **(A)** Schematics of identifying all OCRs associated with the genes in the ILC and Th genesets. **(B)** DNase-seq tracks at the *Kit* locus and *Cd3g*, *Cd3d*, and *Cd3e* loci in ILC and Th subsets. Expression-concordant OCRs (fold change > 1.5 between ILC and Th, minimum BPM in both repeats of each ILC subset > maximum BPM in both repeats of each Th subset, BPM in all ILC/Th sample > 0.5, red in ILC and blue in Th) and expression-non-concordant OCRs (gray) are signed. **(C)** Heatmap showing chromatin accessibility of ILC concordant OCRs in the ILC and Th subsets. Profile plot illustrates the average chromatin accessibility of corresponding regions. **(D)** Pie chart showing the number and proportion of genes in the ILC geneset with ILC concordant OCRs at their gene loci. **(E)** Heatmap showing chromatin accessibility of Th concordant OCRs in ILC and Th subsets. **(F)** Pie chart showing the number and proportion of genes in the Th geneset with Th concordant OCRs at their gene loci. **(G)** Histogram showing peak size distribution of expression-concordant OCRs in ILCs and in Th cells. The percentage of OCRs broader than 500 bp are calculated. **(H)** Histogram showing distances of expression-concordant OCRs to transcription start sites (TSSs) of their neighboring genes in ILC and in Th. Percentage of OCRs within 1 kb of TSS is calculated. For box plots, the three horizontal lines of the box represent the third quartile, median, and first quartile, respectively, from top to bottom. The whiskers below and above the box show 5 and 95 percentiles. Statistical significance of peak size and distance of OCRs to their associated TSSs are calculated by two-sided Mann–Whitney U test. P. value above 0.05 is considered not significant, ***P < 0.001. OCRs, open chromatin regions. BPM, bins per million mapped reads.

the average expression levels of these predicted transcription factors across ILC or Th subsets, providing further evidence of their potential roles in driving the divergence of gene expression programs between ILCs and Th cells (Figure 4B). Importantly, the motifs for BATF and AP-1, both belonging to the bZIP family, were notably enriched in the Th concordant OCRs (Figures 4A, B). This observation aligned with the notion that these transcription factors could form the AP-1-BATF transcriptional complex, exerting crucial regulatory functions downstream of TCR signaling to promote the activation and function of Th cells (16, 42). In contrast, the transcriptional regulation of the ILC geneset appeared to rely on a distinct set of transcription factors, primarily belonging to different transcription factor families rather than the bZIP family (Figure 4B). On the other hand, a diverse range of transcription factors were enriched in the expression-non-concordant OCRs in both ILCs and Th cells, indicating their unlikely involvement in regulating the gene expression in the ILC or Th geneset (Supplementary Figures 6A, B).

In our analysis of the ILC concordant OCRs, we identified 10 potential transcription factors with highly enriched binding motifs

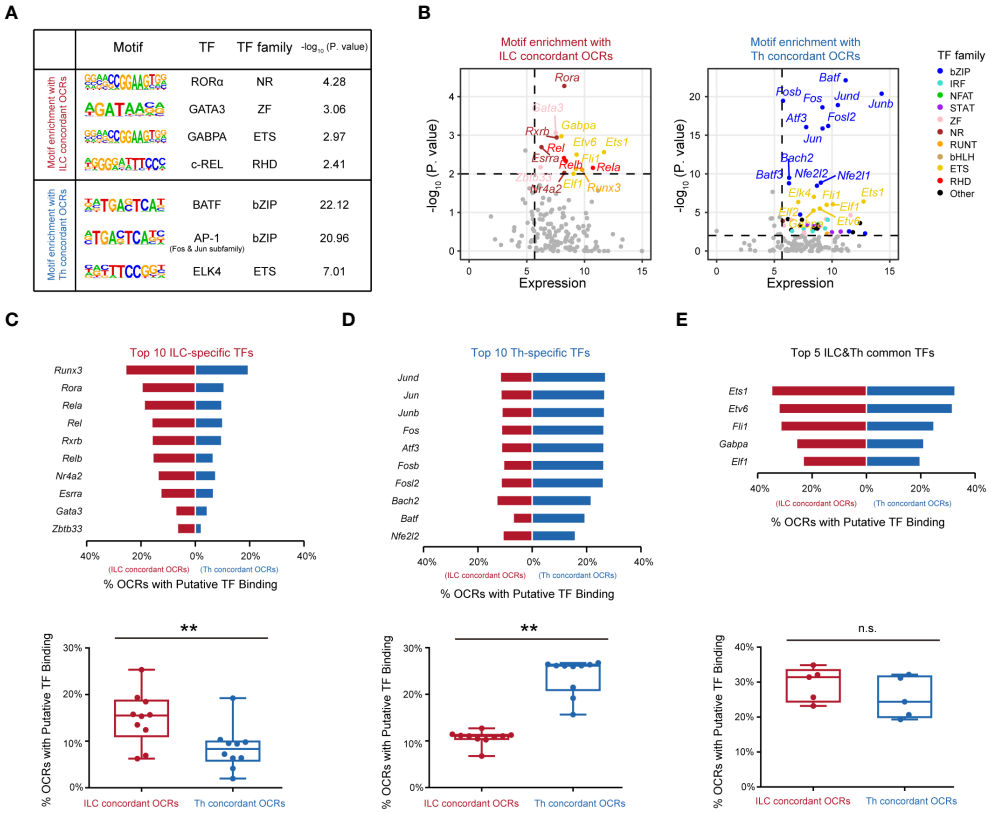

FIGURE 4
Distinct transcription factors are involved in distinguishing the functionalities of ILCs from Th cells. **(A)** Motif enrichment of expression-concordant OCRs in ILCs and in Th cells. The top significantly enriched motifs and the associated P. value are shown. TF and the TF family are annotated in the HOCOMOCO database and Homer software. Similar transcription factors in the same TF family are not shown. **(B)** Scatter plot of potential transcription factors that may bind to expression-concordant OCRs in ILCs and in Th cells. TF expression (X axis) and enrichment score (Y axis) are shown. Potential TFs in ILCs and Th cells are identified by TPM >50 in ILCs or Th cells, and P. value < 0.01. Colors indicate TF families as in (4A). **(C)** Bar chart showing percentage of OCRs with binding motifs of the top 10 ILC-specific TFs within the ILC concordant OCRs and within the Th concordant OCRs (top). The percentages of OCRs with binding motifs of the top 10 ILC-specific TFs within the ILC concordant OCRs and within the Th concordant OCRs are analyzed by the two-sided Wilcoxon test (bottom). **(D)** Bar chart showing percentage of OCRs with binding motifs of the top 10 putative TFs in Th cells, within the ILC concordant OCRs and within the Th concordant OCRs (top). The average percentages of OCRs with binding motifs of the top 10 Th-specific TFs within the ILC concordant OCRs and within the Th concordant OCRs are analyzed by the two-sided Wilcoxon test (bottom). **(E)** Bar chart showing percentage of OCRs with binding motifs of the top five ILC and Th common TFs, within the ILC concordant OCRs and within the Th concordant OCRs (top). The top 10 TFs in Th cells (TPM >50 in all three Th subsets) are ordered by P. value. The percentages of OCRs with binding motifs of the top five ILCs and Th common TFs within the ILC concordant OCRs and within the Th concordant OCRs are analyzed by two-sided Wilcoxon test (bottom). For box plots, the three horizontal lines of the box represent the third quartile, median, and first quartile, respectively, from top to bottom. The whiskers below and above the box show the 5th and 95th percentile. P. value above 0.05 is considered not significant, **P < 0.01. ns, no significance.

and significant expression levels, namely, RORα, GATA3, RXRβ, c-REL, REL-B, REL-A, ERRα, ZBTB33, NR4A2, and RUNX3. Notably, RORα, a member of the nuclear receptor family, displayed the highest enrichment in the ILC concordant OCRs. This finding aligned with previous studies that highlighted the crucial roles of RORα in the development, maintenance, and immune activation of ILC2s and ILC3s (43–45). Similarly, we observed significant enrichment of GATA3 binding motifs, supporting the notion that GATA3 played a regulatory role in the development, expansion, and activation of both ILC2s and ILC3s in our previous studies (12, 46, 47). Thus, these results validated the accuracy of our analysis. Furthermore, we observed substantial enrichment of binding motifs for REL-A, REL-B, and c-Rel in the ILC concordant OCRs. Their transcription factors, belonging to the RHD family, formed complexes with the NF-κB subunits (p50 for REL-A and c-Rel, and p52 for REL-B) (48). This suggested a potential involvement of NF-κB in the transcriptional regulation of the ILC geneset. In contrast, in the Th concordant OCRs, all of the top 10 enriched potential transcription factors with significant expression levels belonged to the bZIP family. This highlighted the critical role of AP-1 in regulating T-cell function under TCR signaling (49). Additionally, we discovered substantial enrichment of potential transcription factors from the ETS family in both the ILC and Th concordant OCRs. For example, ETS1 was identified as occupying a significant number of expression-concordant OCRs in both cell types. Based on literature, ETS1 had been reported to play crucial regulatory roles in both the expansion of ILC2s and the activation of Th cells (50, 51). Overall, our analysis identified the top 10 highly enriched potential transcription factors in ILCs or Th cells based on their expression-concordant OCRs, as well as five

potential transcription factors that were commonly enriched in both cell types.

Subsequently, we investigated the frequencies of binding motifs associated with these potential transcription factors in the expression-concordant OCRs of ILCs and Th cells. The top 10 potential transcription factors specific to ILCs displayed enhanced regulation of the ILC geneset in ILCs compared with the Th geneset in Th cells, indicating their importance in distinguishing the functionalities of ILC and Th cells (Figure 4C). Moreover, the top 10 Th-specific transcription factors from the bZIP family exhibited significant regulation of the Th geneset specifically in Th cells, whereas their impact on the ILC geneset in ILCs was relatively limited (Figure 4D). This underscored the essential role of AP-1 in distinguishing the functionalities of Th cells from ILCs. Additionally, the five potential transcription factors commonly enriched in the expression-concordant OCRs of ILCs and Th cells demonstrated comparable regulation of the ILC geneset in ILCs and the Th geneset in Th cells (Figure 4E). However, these transcription factors regulated a relatively high frequency of genes within both the ILC and Th genesets, suggesting their critical roles. In contrast, the distribution patterns of these potential transcription factors in the expression-non-concordant OCRs of ILCs and Th cells did not align with the gene expression patterns (Supplementary Figures 6C–E). Collectively, these findings indicate that distinct functionalities of ILCs and Th cells are regulated by different transcription factors.

Similar effector roles of ILCs and Th cells are operated by distinct regulatory machineries

Given the presence of distinct regulatory machineries for the ILC and Th genesets, we further wondered whether the immune response-related genesets, which exhibited similar expression in both ILC subsets and their corresponding Th subsets, were differentially regulated. Remarkably, we found that chromatin regions of signature effector genes associated with different immune responses, such as the *Ifng* locus in ILC1s and Th1 cells, the *Il4*, *Il5*, and *Il13* loci in ILC2s and Th2 cells, and the *Il17a* and *Il17f* loci in ILC3s and Th17 cells, all displayed variant accessibility between ILC subsets and their corresponding Th subsets (Figure 5A). Therefore, we defined the ILC and Th subset-specific OCRs based on their differential chromatin accessibility between ILC subsets and their corresponding Th subsets (Figure 5B, Supplementary Figure 7A). ILC3- and Th17-specific OCRs displayed exclusive chromatin accessibility in ILC3 and Th17 subsets *in vivo*, respectively (Supplementary Figure 7B). In addition, ILC2- and Th2-specific OCRs displayed higher accessibility in ILC2 and Th2 subsets *in vivo*, respectively (Supplementary Figure 7C). Notably, the overall width of ILC subset-specific OCRs exceeded that of the corresponding Th subset-specific OCRs, with the former preferentially located in close proximity to TSSs, suggesting distinct regulation of these genesets between the two cell types (Figures 5C, D, Supplementary Figures 7D, E). Consequently, we conducted an analysis of potential transcription factors inferred from these subset-specific OCRs in ILCs and Th cells. As expected, different sets of potential transcription factors with significant expression were enriched by the subset-specific OCRs in ILC subsets and the corresponding Th subsets, respectively (Figure 5E). Interestingly, these potential transcription factors exhibited considerable consistency with those we inferred from the expression-concordant OCRs to the ILC or Th genesets, indicating the utilization of the same regulatory machinery to govern effector functions in each subset. Notably, the master transcription factors *Tbx21*, *Gata3*, and *Rorc* displayed the highest enrichment by the ILC subset-specific OCRs, underscoring their indispensable regulatory roles in the effector functions of ILC subsets. Additionally, upon assessing the distribution patterns of binding motifs linked to these potential transcription factors in the ILC or Th subset-specific OCRs, we confirmed the preferential binding of potential transcription factors specific to ILC subsets to the ILC subset-specific OCRs, whereas those specific to Th subsets tended to interact with the Th subset-specific OCRs (Figure 5F). Therefore, despite the striking similarity in effector roles between ILC subsets and their corresponding Th subsets, the underlying regulatory mechanisms remain distinctive.

Discussion

ILCs are often regarded as the innate counterparts to Th cells in the adaptive immune system due to their shared functionalities and regulatory mechanisms (3, 31). However, it is important to recognize the fundamental differences between these two cell types as innate and adaptive lymphocytes, respectively. In this study, we have demonstrated the presence of significant distinctions in functionalities and underlying regulatory mechanisms between ILCs and Th cells by conducting integrative transcriptome and chromatin landscape analyses.

Bulk RNA-seq has been widely used as a mature approach for transcriptome analysis for many years. More recently, single-cell transcriptome analysis, or scRNA-seq, has emerged as a highly valuable tool in the field (52, 53). While scRNA-seq offers several advantages over bulk RNA-seq, it also comes with certain limitations (54). One noticeable drawback is the higher cost associated with scRNA-seq, resulting in smaller sample sizes for each cell type. In contrast, bulk RNA-seq is comparatively more cost-effective, and thus researchers can easily access numerous publicly available datasets, particularly for the ILC and Th transcriptomes that are relevant to our study (55). Furthermore, due to technological differences, scRNA-seq typically captures fewer genes compared with bulk RNA-seq (52). In our study, we sought to harness the advantages of both technologies. Therefore, we compiled and processed a collection of 294 publicly available bulk RNA-seq datasets for ILCs and Th cells, which were subsequently analyzed using algorithms designed for scRNA-seq. Through this integrated approach, we successfully identified two genesets specific to all ILCs or Th cells, as well as three genesets specific to different types of immune responses. Although for bulk RNA-seq data, most of Th cell datasets are derived from *in vitro* differentiated lineages, and most ILCs are isolated from mucosal tissue *in vivo*, we observed

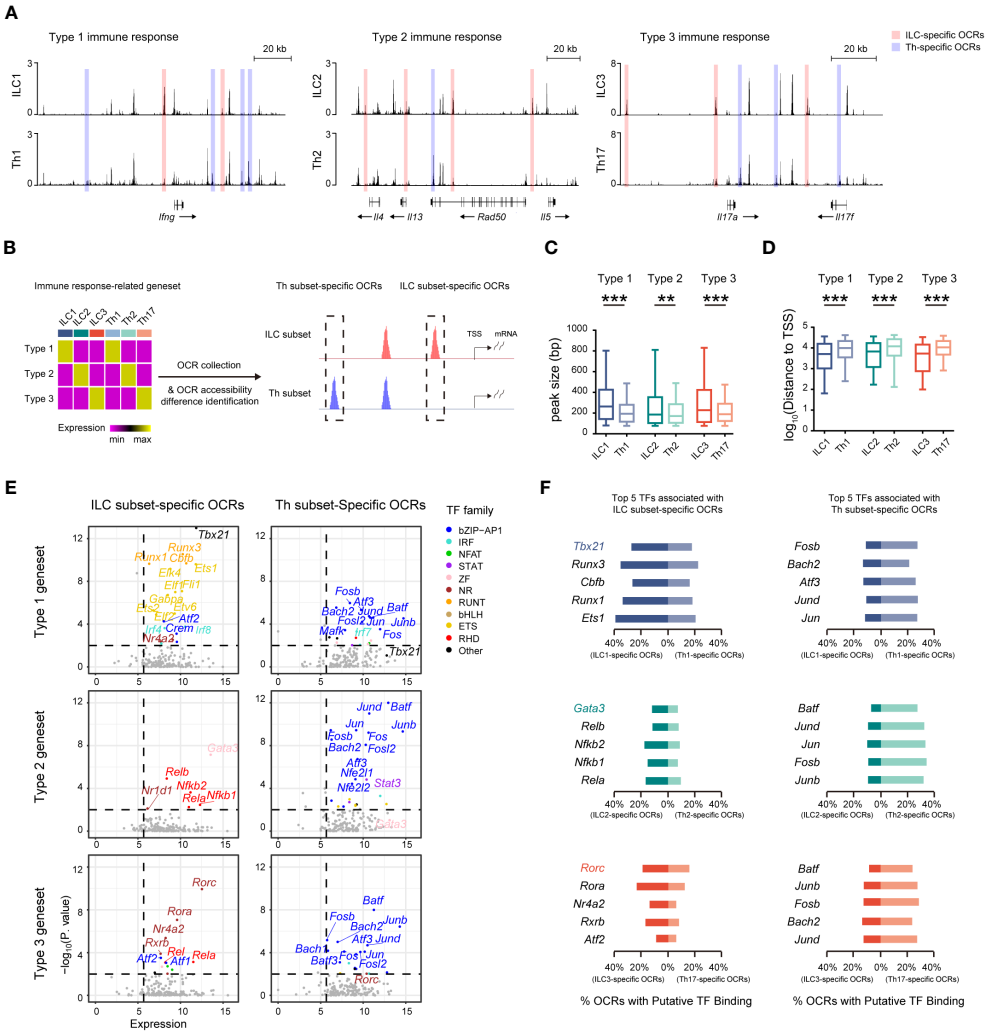

FIGURE 5
Similar effector roles of ILCs and Th cells are operated by distinct regulatory machineries. **(A)** DNase-seq tracks at the *Ifng* locus, *Il4*, *Il13*, and *Il5* loci, and *Il17a* and *Il17f* loci in the indicated ILC and Th subsets. ILC-specific OCRs in corresponding ILC and Th subsets are defined as, for example, accessibility ILC1/Th1 >1.5, minimum accessibility of ILC1 > maximum accessibility of Th1, and minimum accessibility of ILC1 >0.5 (chromatin accessibility of OCRs are calculated to BPM). Similarly, Th-specific OCRs are defined as, for example, accessibility Th1/ILC1 >1.5, minimum accessibility of Th1 > maximum accessibility of ILC1, and minimum accessibility of ILC1 >0.5. **(B)** Schematics of identifying ILC-specific OCRs and Th-specific OCRs associated with each respective immune response-specific geneset. **(C)** Box plot showing peak size of ILC-specific and Th-specific OCRs related to the type 1, type 2, and type 3 genesets. Statistical significance is calculated using two-sided Mann–Whitney U test. **(D)** Box plot showing distances of ILC-specific and Th-specific OCRs related to the type 1, type 2, and type 3 genesets to TSSs of neighboring genes. Statistical significance is calculated using two-sided Mann–Whitney U test. **(E)** Scatter plot of potential transcription factors that may bind to ILC-specific OCRs or Th-specific OCRs related to the type 1, type 2, and type 3 genesets. Expression levels of TFs (X axis) and their enrichment score (Y axis) are shown. Potential TFs in ILCs versus Th cells are identified by TPM >50 in corresponding ILC and Th subsets, and P. value <0.01. Colors indicate TF families as in Figure 4A. **(F)** Bar chart showing percentage of putative binding of OCRs by the top five TFs enriched in ILCs and Th cells within OCRs associated with the type 1, type 2, or type 3 geneset. For box plots, the three horizontal lines of the box represent the third quartile, median, and first quartile, respectively, from top to bottom. The whiskers below and above the box show the 5th and 95th percentiles. A P. value above 0.05 is considered not significant, **P < 0.01, ***P < 0.001.

that our defined ILC geneset and Th geneset still represent difference between ILC and Th subsets *in vivo*, suggesting that these genesets represent fundamental distinctions between ILC and Th cells.

The accuracy and reliability of the genesets we defined are ensured by their generation from a large number of bulk RNA-seq datasets derived from various experiments conducted in different laboratories. This comprehensive approach guarantees that the genesets should accurately capture the fundamental differences between ILCs and Th cells, as well as between different types of immune responses. Consequently, we performed GO enrichment analysis to gain further insights into the functional disparities underlying the transcriptional differences. While there are some shared features between the ILC and Th genesets, they are predominantly enriched in distinct pathways. Consistent with our understanding of T-cell expansion following activation, we observed a preferential enrichment of cell cycle-related pathways in the Th geneset. On the other hand, the ILC geneset exhibited specific enrichment in pathways associated with their role in maintaining tissue homeostasis. Moreover, despite ILC and Th

subsets being involved in diverse immune responses, we identified a similarity in pathway enrichment for immune response-related genesets, indicating the existence of certain fundamental similarities in their T helper cell functions through cytokine secretion.

The differential enrichment of pathways in the ILC and Th genesets suggests that the functionalities of these two cell types may be regulated by distinct mechanisms. Notably, the expression-concordant OCRs associated with the ILC geneset are generally broader in width compared with those associated with the Th genesets. ILC concordant regions preferentially localize around TSSs, which correspond to the promoter regions of genes. Interestingly, the OCRs specific to the immune response-related genesets in ILCs also exhibit a similar distribution pattern as compared with distribution of the Th-specific OCRs in Th cells. This characteristic may confer an advantage for multiple transcription factors to bind to the promoter regions in ILCs, thereby facilitating rapid transcription initiation upon cell activation.

We have conducted further analysis on the expression-associated OCRs for the ILC and Th genesets, as well as on the ILC- and Th-specific OCRs for the immune response-related genesets, to infer the potential involvement of transcription factors. It is noteworthy that Th cells exhibit a heightened tendency to specifically utilize AP-1-mediated regulation, which occurs downstream of TCR signaling. In contrast, ILCs do not favor AP-1 and exhibit enhanced utilization of master transcription factors specific to their respective subsets. Additionally, our findings indicate a preferential reliance on NF-κB for regulatory processes in ILCs. Furthermore, despite the similar effector functions of ILC subsets and their corresponding Th subsets, the underlying regulatory mechanisms are also largely distinct, aligning with their innate and adaptive lymphocyte properties, respectively (56). Consequently, our study provides valuable insights into the functional and regulatory differences between ILCs and Th cells, contributing to a comprehensive understanding of their unique roles during immune responses.

Materials and methods

Data acquisition

Raw data for gene expression profiles (RNA-seq) of ILC and Th subsets were retrieved from Sequence Read Archive (SRA); accession numbers are given in Figure 1A and Supplementary Table 1. Raw data for RNA-seq of ILC and Th subsets *in vivo* were retrieved from SRA under accession numbers SRP060453, SRP069783, and SRP337230. Chromatin accessibility profiles (DNase-seq) of ILC and Th subsets were retrieved from SRP315389, and ATAC-seq of ILC and Th subsets *in vivo* were retrieved from SRP069783.

RNA-seq data processing

The RNA-seq reads were aligned to the GRCm38/mm10 assembly of mouse genome using HISAT2 (v 2.2.1), and quantified by featureCounts. The gene expression level was counted by featureCounts (v 2.0.3) against mouse GRCm38 genome assembly (v 94). Transcripts per million mapped reads (TPM) were calculated using R package scuttle (v1.4.0). Genes with significantly high expression levels were filtered by TPM >10 in at least one ILC or Th subset. Batch effect removal was performed by the "removeBatchEffect" function in the limma package (v3.50.3) (57). Dimension reduction of the gene expression matrix before or after batch effect removal by the Uniform Manifold Approximation and Projection (UMAP) algorithm was performed by R package Seurat (v4.3.0) (58). "ScaleData", "RunPCA", and "RunUMAP" were sequentially executed, and top20 principle components (PCs) were used for UMAP analysis. GSEA was performed by GSEA software (v3.0).

Differential expression analysis and gene ontology enrichment

For differential expression analysis between ILCs and Th cells and among three types of immune responses, the FindConservedMarkers function in the Seurat package was performed (minimum of $\log_2$ fold change >0.25 and maximum of P. value <0.01). The FindMarkers function was used in differential expression analysis in each ILC and Th subsets ($\log_2$ fold-change >0.25 and P value < 0.01). GO analysis was performed by overrepresentation test with R package clusterProfiler (v4.2.2). Function "compareCluster" was performed for GO enrichment of ILC - and Th-specific genesets (q value < 0.05), and the top 100 GO terms in q value are shown in enrichment map by the "emapplot" function in the "enrichplot" package. Function enrichGO was performed for GO enrichment of immune response-specific genesets.

DNase-seq data processing

DNase-seq reads were mapped to the mm10 genome with Bowtie2 (v2.4.4). Non-redundant reads with MAPQ ≥10 were remained. The remaining reads were sorted using Samtools (v 1.13). DNase-seq peaks (OCRs) were called by MACS2 (v2.2.7.1) with settings of –nomodel –extsize 75, based on a q-value threshold of 0.01. DNase-seq reads in each OCR were quantified using bedtools (v2.27.1). Bins per million mapped reads (BPM) values of OCRs were calculated with R-package scuttle as TPM in RNA-seq data.

Peak annotation and differential OCR analysis

Annotation of OCRs to their neighboring genes were performed by the annotatePeak function in R package ChIPseeker (v1.30.3). OCRs within 50 kb to TSS of neighboring genes were defined as OCRs related to these genes. For OCRs related to genes in the ILC and Th genesets, concordant OCRs were defined as OCRs exhibiting concordant accessibility changes with the expression changes of their related genes; the residual OCRs were defined as non-concordant OCRs. For example, in OCRs related to the ILC

geneset, the ILC concordant OCRs were defined as OCRs with a fold change of ILC/Th >1.5, minimum BPM in both repeats of each ILC subset > maximum BPM in both repeats of each Th subset, and BPM of both repeats in all ILC subsets >0.5. The residual OCRs related to the ILC geneset are defined as ILC non-concordant OCRs. Similar criteria are used to define Th concordant and non-concordant OCRs.

For OCRs related to immune response-related genesets, ILC-specific OCRs are defined as OCRs with fold change between ILC subsets and the corresponding Th subsets >1.5, minimum BPM in both repeats of the ILC subset > maximum BPM in both repeats of the corresponding Th subset, and BPM of both repeats in the ILC subset >0.5. A similar criterion is used to define Th concordant OCRs.

Motif enrichment

Transcription factor motif enrichment was performed by the findMotifsGenome function in Homer software (v4.10), using the HOCOMOCO database and the database included in HOMER. For each OCR, transcription factor binding sites were annotated by FIMO software in MEME Suite (v5.0.5), using a p-value threshold of 0.0001.

Data visualization and statistics

Data were analyzed by R version 4.1.2. Bar charts, pie charts, box plots, scatter plots, and histograms were operated by ggplot2 (v3.4.2). Heatmaps in schematic illustration were performed by pheatmap (v1.0.12). Heatmaps of OCRs in DNase-seq were visualized by deepTools (v3.5.1). DNase-Seq tracks were visualized using UCSC Genome Browser. The statistical significance of GO enrichment and motif enrichment were calculated by a two-sided hypergeometric test. P values above 0.05 were considered not significant, *P < 0.05 **P < 0.01, ***P < 0.001.

Data availability statement

The original contributions presented in the study are included in the article/Supplementary Material. Further inquiries can be directed to the corresponding author.

Author contributions

YZ: Conceptualization, Data curation, Formal Analysis, Investigation, Methodology, Software, Visualization, Writing – original draft. LH: Data curation, Formal Analysis, Methodology, Software, Visualization, Writing – original draft. GR: Data curation, Methodology, Writing – original draft. YYZ: Data curation, Methodology, Writing – original draft. XZ: Data curation, Methodology, Writing – original draft. CZ: Conceptualization, Funding acquisition, Methodology, Project administration, Supervision, Writing – review & editing.

Funding

The author(s) declare financial support was received for the research, authorship, and/or publication of this article. The work was supported by the National Key R&D program of China (2022YFA1103602 and 2022YFA0806400 to CZ), the National Natural Science Foundation of China (32170896, 31770957 and 91842102 to CZ), the Shenzhen Innovation Committee of Science and Technology (JCYJ20220818100401003 to CZ), and the Natural Science Foundation of Beijing (18G10645 to CZ).

Acknowledgments

We thank all the members of the Zhong laboratory for their valuable assistance.

Conflict of interest

The authors declare that the research was conducted in the absence of any commercial or financial relationships that could be construed as a potential conflict of interest.

Publisher's note

Supplementary material

The Supplementary Material for this article can be found online at: https://www.frontiersin.org/articles/10.3389/fimmu.2023.1271879/full#supplementary-material

References

1. Spits H, Artis D, Colonna M, Diefenbach A, Di Santo JP, Eberl G, et al. Innate lymphoid cells–a proposal for uniform nomenclature. *Nat Rev Immunol* (2013) 13:145–9. doi: 10.1038/nri3365

2. Artis D, Spits H. The biology of innate lymphoid cells. *Nature* (2015) 517:293–301. doi: 10.1038/nature14189

3. Vivier E, Artis D, Colonna M, Diefenbach A, Di Santo JP, Eberl G, et al. Innate lymphoid cells: 10 years on. *Cell* (2018) 174:1054–66. doi: 10.1016/j.cell.2018.07.017

4. Guo L, Junttila IS, Paul WE. Cytokine-induced cytokine production by conventional and innate lymphoid cells. *Trends Immunol* (2012) 33:598–606. doi: 10.1016/j.it.2012.07.006

5. Fang D, Zhu J. Dynamic balance between master transcription factors determines the fates and functions of CD4 T cell and innate lymphoid cell subsets. *J Exp Med* (2017) 214:1861–76. doi: 10.1084/jem.20170494

6. Zhong C, Zhu J. Transcriptional regulatory network for the development of innate lymphoid cells. *Mediators Inflammation* (2015) 2015:264502. doi: 10.1155/2015/264502

7. Spinner CA, Lazarevic V. Transcriptional regulation of adaptive and innate lymphoid lineage specification. *Immunol Rev* (2020) 300:65–81. doi: 10.1111/imr.12935

8. Fuchs A, Vermi W, Lee JS, Lonardi S, Gilfillan S, Newberry RD, et al. Intraepithelial type 1 innate lymphoid cells are a unique subset of IL-12- and IL-15-responsive IFN-gamma-producing cells. *Immunity* (2013) 38:769–81. doi: 10.1016/j.immuni.2013.02.010

9. Bernink JH, Peters CP, Munneke M, te Velde AA, Meijer SL, Weijer K, et al. Human type 1 innate lymphoid cells accumulate in inflamed mucosal tissues. *Nat Immunol* (2013) 14:221–9. doi: 10.1038/ni.2534

10. Hoyler T, Klose CS, Souabni A, Turqueti-Neves A, Pfeifer D, Rawlins EL, et al. The transcription factor GATA-3 controls cell fate and maintenance of type 2 innate lymphoid cells. *Immunity* (2012) 37:634–48. doi: 10.1016/j.immuni.2012.06.020

11. Liang HE, Reinhardt RL, Bando JK, Sullivan BM, Ho IC, Locksley RM. Divergent expression patterns of IL-4 and IL-13 define unique functions in allergic immunity. *Nat Immunol* (2011) 13:58–66. doi: 10.1038/ni.2182

12. Yagi R, Zhong C, Northrup DL, Yu F, Bouladoux N, Spencer S, et al. The transcription factor GATA3 is critical for the development of all IL-7Rα-expressing innate lymphoid cells. *Immunity* (2014) 40:378–88. doi: 10.1016/j.immuni.2014.01.012

13. Ciccia F, Guggino G, Rizzo A, Saieva L, Peralta S, Giardina A, et al. Type 3 innate lymphoid cells producing IL-17 and IL-22 are expanded in the gut, in the peripheral blood, synovial fluid and bone marrow of patients with ankylosing spondylitis. *Ann Rheum Dis* (2015) 74:1739–47. doi: 10.1136/annrheumdis-2014-206323

14. Sawa S, Cherrier M, Lochner M, Satoh-Takayama N, Fehling HJ, Langa F, et al. Lineage relationship analysis of RORgammat+ innate lymphoid cells. *Science* (2010) 330:665–9. doi: 10.1126/science.1194597

15. Li MO, Rudensky AY. T cell receptor signalling in the control of regulatory T cell differentiation and function. *Nat Rev Immunol* (2016) 16:220–33. doi: 10.1038/nri.2016.26

16. Gaud G, Lesourne R, Love PE. Regulatory mechanisms in T cell receptor signalling. *Nat Rev Immunol* (2018) 18:485–97. doi: 10.1038/s41577-018-0020-8

17. McGinty JW, von Moltke J. A three course menu for ILC and bystander T cell activation. *Curr Opin Immunol* (2020) 62:15–21. doi: 10.1016/j.coi.2019.11.005

18. Klose CSN, Mahlakõiv T, Moeller JB, Rankin LC, Flamar AL, Kabata H, et al. The neuropeptide neuromedin U stimulates innate lymphoid cells and type 2 inflammation. *Nature* (2017) 549:282–6. doi: 10.1038/nature23676

19. Xue L, Salimi M, Panse I, Mjösberg JM, McKenzie AN, Spits H, et al. Prostaglandin D2 activates group 2 innate lymphoid cells through chemoattractant receptor-homologous molecule expressed on TH2 cells. *J Allergy Clin Immunol* (2014) 133:1184–94. doi: 10.1016/j.jaci.2013.10.056

20. Wu D, Hu L, Han M, Deng Y, Zhang Y, Ren G, et al. PD-1 signaling facilitates activation of lymphoid tissue inducer cells by restraining fatty acid oxidation. *Nat Metab* (2022) 4:867–82. doi: 10.1038/s42255-022-00595-9

21. Wu D, Li Z, Zhang Y, Zhang Y, Ren G, Zeng Y, et al. Proline uptake promotes activation of lymphoid tissue inducer cells to maintain gut homeostasis. *Nat Metab* (2023) 5:1953–68. doi: 10.1038/s42255-023-00908-6

22. Gasteiger G, Fan X, Dikiy S, Lee SY, Rudensky AY. Tissue residency of innate lymphoid cells in lymphoid and nonlymphoid organs. *Science* (2015) 350:981–5. doi: 10.1126/science.aac9593

23. Meininger I, Carrasco A, Rao A, Soini T, Kokkinou E, Mjosberg J. Tissue-specific features of innate lymphoid cells. *Trends Immunol* (2020) 41:902–17. doi: 10.1016/j.it.2020.08.009

24. Schenkel JM, Pauken KE. Localization, tissue biology and T cell state - implications for cancer immunotherapy. *Nat Rev Immunol* (2023) 23:807–23. doi: 10.1038/s41577-023-00884-8

25. Shih HY, Sciume G, Mikami Y, Guo L, Sun HW, Brooks SR, et al. Developmental acquisition of regulomes underlies innate lymphoid cell functionality. *Cell* (2016) 165:1120–33. doi: 10.1016/j.cell.2016.04.029

26. Nagashima H, Mahlakoiv T, Shih HY, Davis FP, Meylan F, Huang Y, et al. Neuropeptide CGRP limits group 2 innate lymphoid cell responses and constrains type 2 inflammation. *Immunity* (2019) 51:682–695 e6. doi: 10.1016/j.immuni.2019.06.009

27. Koues OI, Collins PL, Cella M, Robinette ML, Porter SI, Pyfrom SC, et al. Distinct gene regulatory pathways for human innate versus adaptive lymphoid cells. *Cell* (2016) 165:1134–46. doi: 10.1016/j.cell.2016.04.014

28. Van Dyken SJ, Nussbaum JC, Lee J, Molofsky AB, Liang HE, Pollack JL, et al. A tissue checkpoint regulates type 2 immunity. *Nat Immunol* (2016) 17:1381–7. doi: 10.1038/ni.3582

29. Rahimi RA, Nepal K, Cetinbas M, Sadreyev RI, Luster AD. Distinct functions of tissue-resident and circulating memory Th2 cells in allergic airway disease. *J Exp Med* (2020) 217(9):e20190865. doi: 10.1164/ajrccm-conference.2020.201.1_MeetingAbstracts.A1303

30. Steinfelder S, Rausch S, Michael D, Kuhl AA, Hartmann S. Intestinal helminth infection induces highly functional resident memory CD4(+) T cells in mice. *Eur J Immunol* (2017) 47:353–63. doi: 10.1002/eji.201646575

31. Bando JK, Colonna M. Innate lymphoid cell function in the context of adaptive immunity. *Nat Immunol* (2016) 17:783–9. doi: 10.1038/ni.3484

32. Sano T, Huang W, Hall JA, Yang Y, Chen A, Gavzy SJ, et al. An IL-23R/IL-22 circuit regulates epithelial serum amyloid A to promote local effector th17 responses. *Cell* (2015) 163:381–93. doi: 10.1016/j.cell.2015.08.061

33. Lyu M, Suzuki H, Kang L, Gaspal F, Zhou W, Goc J, et al. ILC3s select microbiota-specific regulatory T cells to establish tolerance in the gut. *Nature* (2022) 610:744–51. doi: 10.1038/s41586-022-05141-x

34. Mayer A, Zhang Y, Perelson AS, Wingreen NS. Regulation of T cell expansion by antigen presentation dynamics. *Proc Natl Acad Sci U.S.A.* (2019) 116:5914–9. doi: 10.1073/pnas.1812800116.

35. Cao J, Cusanovich DA, Ramani V, Aghamirzaie D, Pliner HA, Hill AJ, et al. Joint profiling of chromatin accessibility and gene expression in thousands of single cells. *Science* (2018) 361:1380–5. doi: 10.1126/science.aau0730

36. Klemm SL, Shipony Z, Greenleaf WJ. Chromatin accessibility and the regulatory epigenome. *Nat Rev Genet* (2019) 20:207–20. doi: 10.1038/s41576-018-0089-8

37. Fang D, Cui K, Cao Y, Zheng M, Kawabe T, Hu G, et al. Differential regulation of transcription factor T-bet induction during NK cell development and T helper-1 cell differentiation. *Immunity* (2022) 55:639–655 e7. doi: 10.1016/j.immuni.2022.03.005

38. Pott S, Lieb JD. What are super-enhancers? *Nat Genet* (2015) 47:8–12. doi: 10.1038/ng.3167

39. Boyle AP, Davis S, Shulha HP, Meltzer P, Margulies EH, Weng Z, et al. High-resolution mapping and characterization of open chromatin across the genome. *Cell* (2008) 132:311–22. doi: 10.1016/j.cell.2007.12.014

40. Kellis M, Wold B, Snyder MP, Bernstein BE, Kundaje A, Marinov GK, et al. Defining functional DNA elements in the human genome. *Proc Natl Acad Sci U.S.A.* (2014) 111:6131–8. doi: 10.1073/pnas.1318948111

41. Hu L, Zhao X, Li P, Zeng Y, Zhang Y, Shen Y, et al. Proximal and distal regions of pathogenic th17 related chromatin loci are sequentially accessible during pathogenicity of th17. *Front Immunol* (2022) 13:864314. doi: 10.3389/fimmu.2022.864314

42. Li P, Spolski R, Liao W, Wang L, Murphy TL, Murphy KM, et al. BATF-JUN is critical for IRF4-mediated transcription in T cells. *Nature* (2012) 490:543–6. doi: 10.1038/nature11530

43. Halim TY, MacLaren A, Romanish MT, Gold MJ, McNagny KM, Takei F. Retinoic-acid-receptor-related orphan nuclear receptor alpha is required for natural helper cell development and allergic inflammation. *Immunity* (2012) 37:463–74. doi: 10.1016/j.immuni.2012.06.012

44. Fiancette R, Finlay CM, Willis C, Bevington SL, Soley J, Ng STH, et al. Reciprocal transcription factor networks govern tissue-resident ILC3 subset function and identity. *Nat Immunol* (2021) 22:1245–55. doi: 10.1038/s41590-021-01024-x

45. Lo BC, Canals Hernaez D, Scott RW, Hughes MR, Shin SB, Underhill TM, et al. The transcription factor RORα Preserves ILC3 lineage identity and function during chronic intestinal infection. *J Immunol* (2019) 203:3209–15. doi: 10.4049/jimmunol.1900781

46. Zhong C, Cui K, Wilhelm C, Hu G, Mao K, Belkaid Y, et al. Group 3 innate lymphoid cells continuously require the transcription factor GATA-3 after commitment. *Nat Immunol* (2016) 17:169–78. doi: 10.1038/ni.3318

47. Zhong C, Zheng M, Cui K, Martins AJ, Hu G, Li D, et al. Differential expression of the transcription factor GATA3 specifies lineage and functions of innate lymphoid cells. *Immunity* (2020) 52:83–95 e4. doi: 10.1016/j.immuni.2019.12.001

48. Dolcet X, Llobet D, Pallares J, Matias-Guiu X. NF-kB in development and progression of human cancer. *Virchows Arch* (2005) 446:475–82. doi: 10.1007/s00428-005-1264-9

49. Yukawa M, Jagannathan S, Vallabh S, Kartashov AV, Chen X, Weirauch MT, et al. AP-1 activity induced by co-stimulation is required for chromatin opening during T cell activation. *J Exp Med* (2020) 217(1):e20182009. doi: 10.1084/jem.20182009

50. Zook EC, Ramirez K, Guo X, van der Voort G, Sigvardsson M, Svensson EC, et al. The ETS1 transcription factor is required for the development and cytokine-induced expansion of ILC2. *J Exp Med* (2016) 213:687–96. doi: 10.1084/jem.20150851

51. Zhong Y, Walker SK, Pritykin Y, Leslie CS, Rudensky AY, van der Veeken J. Hierarchical regulation of the resting and activated T cell epigenome by major transcription factor families. *Nat Immunol* (2022) 23:122–34. doi: 10.1038/s41590-021-01086-x

52. Chen G, Ning B, Shi T. Single-cell RNA-seq technologies and related computational data analysis. *Front Genet* (2019) 10:317. doi: 10.3389/fgene.2019.00317

53. Saliba AE, Westermann AJ, Gorski SA, Vogel J. Single-cell RNA-seq: advances and future challenges. *Nucleic Acids Res* (2014) 42:8845–60. doi: 10.1093/nar/gku555

54. Svensson V, Vento-Tormo R, Teichmann SA. Exponential scaling of single-cell RNA-seq in the past decade. *Nat Protoc* (2018) 13:599–604. doi: 10.1038/nprot.2017.149

55. Thind AS, Monga I, Thakur PK, Kumari P, Dindhoria K, Krzak M, et al. Demystifying emerging bulk RNA-Seq applications: the application and utility of bioinformatic methodology. *Brief Bioinform* (2021) 22(6):bbab259. doi: 10.1093/bib/bbab259

56. Fang D, Healy A, Zhu J. Differential regulation of lineage-determining transcription factor expression in innate lymphoid cell and adaptive T helper cell subsets. *Front Immunol* (2022) 13:1081153. doi: 10.3389/fimmu.2022.1081153

57. Ritchie ME, Phipson B, Wu D, Hu Y, Law CW, Shi W, et al. limma powers differential expression analyses for RNA-sequencing and microarray studies. *Nucleic Acids Res* (2015) 43:e47. doi: 10.1093/nar/gkv007

58. Hao Y, Hao S, Andersen-Nissen E, Mauck WM 3rd, Zheng S, Butler A, et al. Integrated analysis of multimodal single-cell data. *Cell* (2021) 184:3573–3587 e29. doi: 10.1016/j.cell.2021.04.048

Frontiers in Immunology

Explores novel approaches and diagnoses to treat immune disorders.

The official journal of the International Union of Immunological Societies (IUIS) and the most cited in its field, leading the way for research across basic, translational and clinical immunology.

Discover the latest Research Topics

See more →

Frontiers

Avenue du Tribunal-Fédéral 34
1005 Lausanne, Switzerland
frontiersin.org

Contact us

+41 (0)21 510 17 00
frontiersin.org/about/contact